

**Università degli Studi di Milano**

**Department of Chemistry**



**Doctorate School in Chemical Science and Technologies**

**Ph.D Course in Chemical Science - XXX Cycle**

**Metal Porphyrin Complexes: Smart Catalysts to  
Promote Eco-Friendly C-C and C-N Bond  
Formations**

**Ph.D Thesis of:**

**Daniela Maria Carminati**

**Matr. n. R10957-R12**

**Tutor: Prof. Emma Gallo**

**Coordinator: Prof. Emanuela Licandro**

**Academic Year 2016/2017**



<b>Chapter I General introduction</b>	<b>5</b>
1. The porphyrin ligand	6
1.1. Structure of porphyrin ring	6
1.2. Synthesis of porphyrins	7
2. Porphyrin complexes	9
2.1. Synthesis of metal porphyrin complexes	9
2.2. Catalytic activity of metal porphyrin complexes in Nature	10
3. Aim and outline of the thesis	13
4. References	14
<b>Chapter II C-C bond formations: Cyclopropanes</b>	<b>15</b>
1. Introduction	16
1.1. Chiral porphyrin ligands	17
1.2. Group 8 chiral porphyrin-catalysed cyclopropanation reactions	19
1.2.1. D <sub>4</sub> -symmetric metal porphyrin complexes	19
1.2.2. D <sub>2</sub> -symmetric metal porphyrin complexes	23
1.2.3. C <sub>2</sub> -symmetric metal porphyrin complexes	24
2. Discussion	25
2.1. Cyclopropanation reactions catalysed by Fe( <b>17</b> )OMe	25
2.1.1. Recycling and recovery of Fe( <b>17</b> )OMe	26
2.1.2. Study of the steric effects of the Fe( <b>17</b> )OMe chiral bulk	27
2.1.3. DFT theoretical studies	29
2.2. Synthesis of amino ester and glycoside conjugates porphyrin ligands	31
2.2.1. Synthesis of glycoside and amino ester conjugates porphyrins	31
2.2.2. DFT theoretical studies	34
2.2.3. Synthesis of new 'Totem' porphyrins	35
2.3. Synthesis of hydrophilic 'Totem' porphyrin	37
3. Experimental section	38
3.1. Synthesis of organic precursors	38
3.2. Synthesis of porphyrin ligands	40
3.3. Synthesis of iron porphyrin complexes	52
3.4. Synthesis of cyclopropanes catalysed by chiral iron(III) porphyrin complexes	57
3.4.1. Synthesis of diazo compounds	57
3.4.2. Synthesis of cyclopropanes	58
3.5. NMR spectra	65
4. References	81
<b>Chapter III C-N bond formations: Aziridines</b>	<b>83</b>
1. Introduction	84
1.1. Aziridination reactions	85
1.1.1. Group 8 porphyrin-catalysed aziridination reactions	86
1.2. Reactivity of aziridines with carbon dioxide	89
2. Discussion	93
2.1. Aziridination reaction under continuous flow conditions	93

2.2. Aziridines reactivity: synthesis of oxazolidinones	95
3. Experimental Section	100
3.1. Synthesis of porphyrin ligands	100
3.2. Synthesis of ruthenium porphyrin complexes	104
3.3. Synthesis of metal porphyrin complexes	110
3.4. Synthesis of azides	112
3.5. Aziridination reactions catalysed by Ru(TPP)(CO)	116
3.6. Synthesis of oxazolidinones	120
3.6.1 Synthesis of <i>N</i> -alkyl-phenylaziridines	120
3.6.2 Synthesis of oxazolidinones	125
3.7. NMR spectra	132
4. References	147
<b>Chapter IV C-N bond formations: Indoles</b>	<b>149</b>
1. Introduction	150
1.1. Synthesis of indoles	150
1.1.1. Larock indole synthesis	150
1.1.2. Cyclization of 2-alkynylanilines	152
1.1.3. Synthesis of indole via metal-catalysed nitrene insertions	152
1.1.4. C-H functionalisation by oxidative coupling	153
1.1.5. Reductive cyclization of nitroarenes	154
2. Discussion	156
3. Experimental Section	160
3.1. Synthesis of ruthenium porphyrin complexes	160
3.2. Synthesis of aryl azides	161
3.3. Synthesis of indoles catalysed by ruthenium porphyrin complexes	163
3.3.1. Synthesis of indoles	163
3.3.2. Kinetic studies	166
3.4. NMR spectra	168
4. References	175
<b>Chapter V C-N bond formations: Amines</b>	<b>177</b>
1. Introduction	178
1.1. Group 8 porphyrin-catalysed amination reactions by organic azides	178
1.1.1. Proposed mechanism for the ruthenium porphyrin-catalysed amination reaction of hydrocarbons by aryl azides	183
2. Discussion	185
3. Experimental Section	188
3.1. Synthesis of ruthenium porphyrin complexes	188
3.2. Amination reaction catalysed by Ru(TPP)(py) <sub>2</sub>	189
4. References	192
<b>Summary</b>	<b>193</b>
<b>List of publications</b>	<b>199</b>

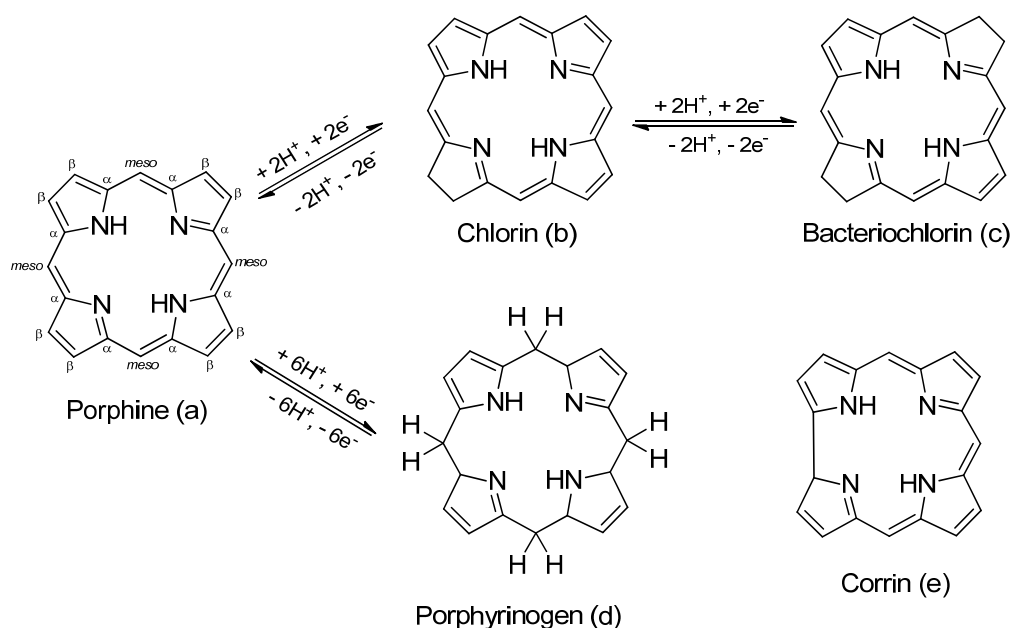
# **Chapter I**

## **General introduction**

# 1. The porphyrin ligand

## 1.1. Structure of porphyrin ring

Porphyrin ligands are a class of heterocyclic macrocycles composed of four pyrrole units interconnected at the  $\alpha$  carbon atoms by methine bridges, thus having 11 conjugate double bonds and 26  $\pi$ -electrons delocalized all over the macrocyclic ring respecting the Huckel rule ( $4n+2$ ). Porphine is the parent porphyrin compound and its structure is represented in Scheme 1 along with the classification of the porphyrin carbon atoms ( $\alpha$ ,  $\beta$  and *meso*).



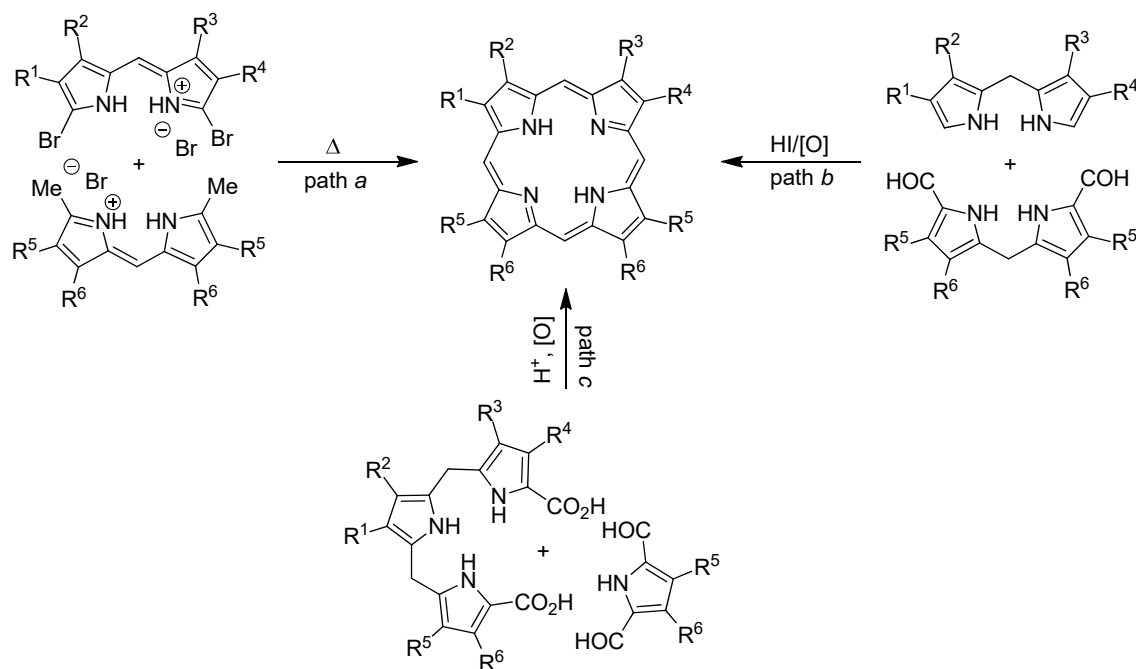
**Scheme 1.** Porphine and other related tetrapyrrolic macrocycles.

Porphyrins and metal porphyrin complexes, with their reduced-aromatic forms (Scheme 1), are fundamental molecules which play a vital role for all organisms. Thanks to their biological and chemical properties, porphyrin ligands, also named ‘the pigment of life’, are contained in a large number of biological compounds such as hemoglobin, myoglobin, chlorophyll, catalase and peroxidases. They also play a very important role in chemical, industrial and technological fields as biosensors, semiconductors and catalysts.

## 1.2. Synthesis of porphyrins

The isolation of porphyrins from natural sources in pure and significant amounts often requires time-consuming synthesis and/or extensive purification steps; for these reasons, a great effort has been dedicated in developing efficient synthetic procedures to obtain porphyrins.<sup>1</sup> The choice of the most suitable synthetic route to synthesis a specific porphyrin depends on the nature of the substituents on the porphyrin scaffold which also influence the ligand symmetry.

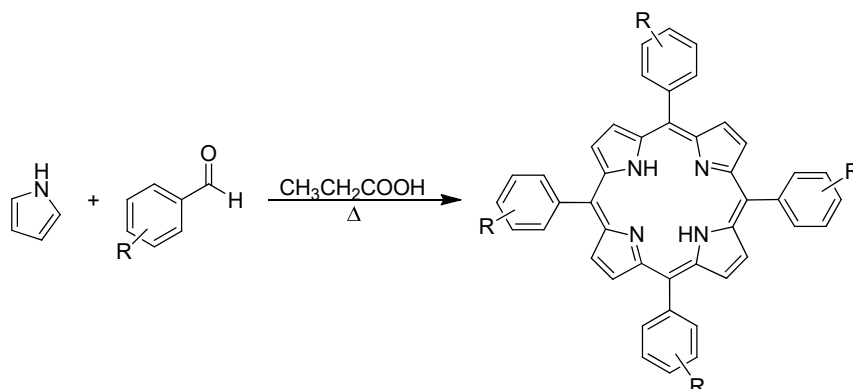
The first synthesis of  $\beta$ -substituted porphyrin was reported by Hans Fischer in 1926 using dipyrromethene salts in an organic melt (Scheme 2, path *a*).<sup>2</sup> He reported the synthesis of the natural compound Protoporphyrin IX that was pivotal for Fischer's 1930 Nobel Prize award. The major limitation of this method is that only a few substituted dipyrromethenes are able to withstand the severe reaction conditions. To overcome this limitation, in 1960 MacDonald and co-workers developed a new methodology, the so-called 2+2 method.<sup>3</sup> The key intermediate in the MacDonald 2+2 synthesis is dipyrromethane which can be symmetrical or unsymmetrical (Scheme 2, path *b*). This route is probably the most widely used pathway to syntheses  $\beta$ -substituted porphyrins. An interesting and useful variation of the MacDonald 2+2 method is the 3+1 route which was introduced by Momenteau's group in 1994.<sup>4</sup> The 3+1 strategy involves the acid-catalysed condensation of 2,5-diformylpyrrole with a tripyrrane followed by an oxidation process (Scheme 2, path *c*).



**Scheme 2.** Synthetic method to synthesis  $\beta$ -substituted porphyrins.

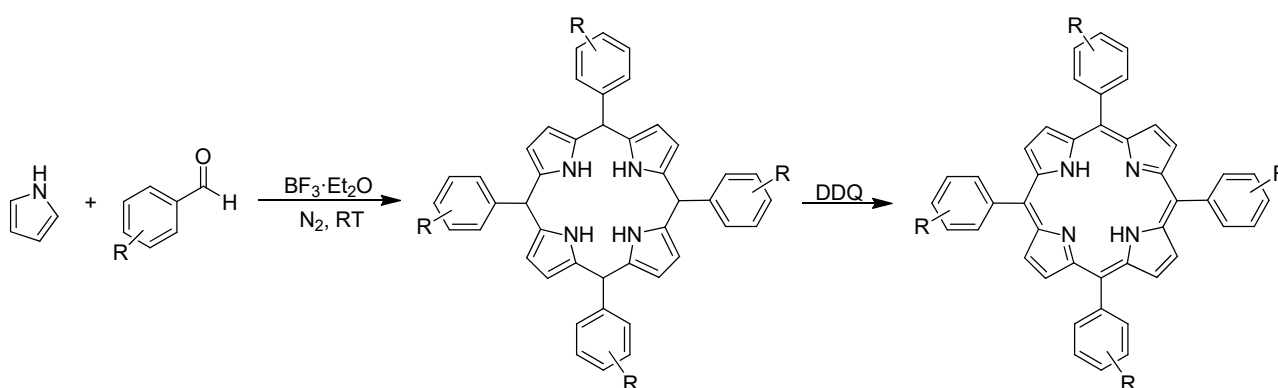
Even if the majority of natural porphyrins are  $\beta$ -substituted (e.g. chlorophyll, heme), *meso*-substituted porphyrins display a prominent role both in chemistry and biology due to their easy preparation. In 1935, Rothmund investigated the synthesis of *meso*-tetramethylporphyrin and *meso*-tetraphenylporphyrin (TPPH<sub>2</sub>) through the reaction between pyrrole and the corresponding aldehyde in methanol or pyridine in a sealed tube.<sup>5</sup> After this pioneering work, Rothmund's approach was improved by Adler and Longo who used refluxing propionic acid at atmospheric pressure (Scheme 3).<sup>6</sup> This reaction allows the conversion of a wide variety of substituted benzaldehyde to the corresponding *meso*-porphyrins in moderate yields (up to 20%) and it is still one of the most convenient methods to rapidly obtain a good amount of crystalline and relatively pure materials. The harsh reaction conditions do not allow the synthesis of derivatives carrying sensitive functional

groups and the purification may be difficult due to the large amount of reaction byproducts. To limit these problems minor modifications may be applied such as the use of a reaction solvent with a lower boiling point (e. g. acetic acid, nitrobenzene) or the use of microwave irradiations.<sup>7</sup>



**Scheme 3.** The classic Adler and Longo's synthesis of *meso*-tetraarylporphyrins.

The art of *meso*-tetraarylporphyrin synthesis has been significantly improved by the introduction of the Lindsey synthesis in 1987.<sup>8</sup> This method is a one-pot two-steps synthesis in which pyrrole and the desired benzaldehyde react at room temperature under anaerobic conditions in presence of an acid catalysis (e.g.  $\text{BF}_3 \cdot \text{Et}_2\text{O}$ ) to form the cyclic *meso*-tetraphenylporphyrinogen at thermodynamic equilibrium. Then, adding an oxidizing agent such as 2,3-dichloro-5,6-dicyano-1,4-benzoquinone (DDQ) to the reaction, the porphyrinogen undergoes oxidative aromatization to give the desired porphyrin (Scheme 4). The critical point of this methodology is the concentrations of benzaldehyde and pyrrole, in fact the reaction requires diluted solutions ( $10^{-2}$  M) to optimise the porphyrinogen formation in comparison to the polymerization of pyrrole; thus, making more difficult the reactions on large scale. However, using the Lindsey's method, sensitive aldehydes can be also employed for porphyrin synthesis to obtain the product in good yield (30-40%) without difficult purification problems and this is the main advantage of this synthesis.<sup>9</sup>



**Scheme 4.** General Lindsey's methodologies.

Thanks to the synthetic flexibility of Adler's and Lindsey's methodologies, and all their modifications and improvements, a large number of *meso* and/or  $\beta$ -substituted porphyrins are synthesised with a plethora of possible structural and electronic properties.



## 2. Porphyrin complexes

Porphyrins, thanks to the highly stable macrocycle ring and the rigid structure, are a unique class of ligands. They are able to coordinate the majority of elements in the periodic table. Porphyrins are called ‘free-bases’ in their neutral form, with two protonated pyrrolic units; when these two protons are removed, the porphyrin becomes a tetradentate dianionic ligand capable of coordinating a metal ion in the central cavity of the macrocycle ring.

Metal fragments bonded to the porphyrin ligand can exist in a large range of oxidation states, electronic configurations and spin states. On the basis of these properties, each metal porphyrin complex shows significantly different structures (e.g. coordination number (from 4 to 8), ‘out of plane’ geometry) and chemical reactivity.<sup>10</sup> Generally, the porphyrin core is large enough to accommodate the metal atom, therefore only two mutually trans sites become available; but if the metal atom is too large to fit in the porphyrin core, it is displaced outside of the plane and has additional ligands placed cis (Figure 1).

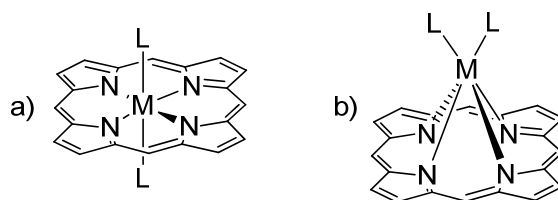
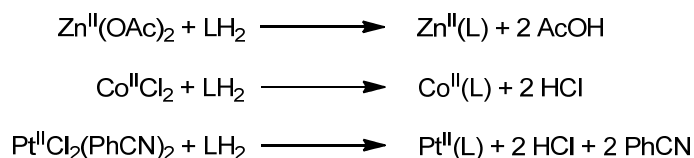


Figure 1. General coordination modes for porphyrin complexes.

### 2.1. Synthesis of metal porphyrin complexes

Different routes have been employed for the insertion of a metal or a M-L<sub>n</sub> fragment into a porphyrin ring, mostly depending on the nature of the metal source. Depending on the previous oxidation state of the metal, the reaction may involve coordination or oxidation of the metal center.

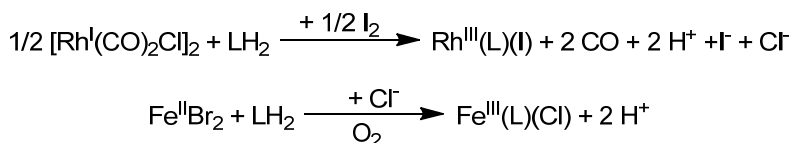
**A. Coordination of a metal from a M(II) salt:** the synthetic procedure simply consists in allowing the free-base and a divalent metal salt to react in the opportune solvent, in order to get the porphyrin ligand and the metallic reagent simultaneously in the solution under reactive conditions (Scheme 5). The main problem of this method is the solvent because a good solvent for porphyrins is generally a poor solvent for simple metallic ions and vice versa. Adler and co-workers proved that *N,N*-dimethylformamide (DMF) is a useful reaction medium and a large number of M(II)(porphyrin) complexes are obtained in good to excellent yields.<sup>11</sup> The addition of a weak Brønsted base promotes the reaction rate by removing the two pyrrolic protons from the free base.



Scheme 5. Synthesis of metal porphyrin complexes from metal(II) salts.

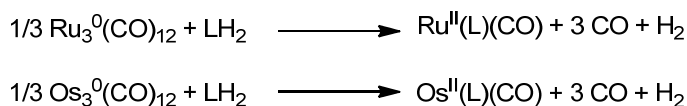
**B. Coordination and oxidation of a metal from a metal salt:** in some cases, the intermediate M(porphyrin), which is obtained by the coordination of a metal salt with porphyrin ligand, is oxidized by an external oxidant (e.g. air, iodine) to obtain an isolable and stable product. The oxidation can take place either *in situ* or during the work-up according to the metal atom. For example, using a Fe(II) metal source initially an iron(II) porphyrin intermediate is formed, it will then be oxidized to the more stable iron(III) complex during the work-

up in air and in presence of a donor ligand. On the other hand, in case of the insertion of rhodium as Rh(III), by starting from a carbonyl complex of Rh(I) ( $[\text{Rh}(\text{CO})_2\text{Cl}]_2$ ), the oxidant can be molecular iodine which can directly be added to the reaction mixture.



**Scheme 6.** Synthesis of metal porphyrin complexes by using an external oxidant.

**C. Spontaneous oxidation of the metal starting from M(0) cluster:** the more extensively reported way to prepare ruthenium(II)-carbonyl and osmium(II)-carbonyl porphyrin complexes involves the reaction between the free-base porphyrin with the neutral cluster  $\text{M}_3(\text{CO})_{12}$  in a high boiling point solvent (Scheme 7). In these cases, a spontaneous oxidation of the metal from 0 to +2 occurs, formally promoted by the two protons displaced from the free-base as molecular hydrogen.



**Scheme 7.** Synthesis of metal porphyrin complexes from metal(0) clusters.

## 2.2. Catalytic activity of metal porphyrin complexes in Nature

In Nature, the most important metal porphyrin complex is the iron complex of protoporphyrin IX, known as Heme (Figure 2). Heme and its derivatives play a vital role for many crucial biological processes because they are the prosthetic group in a wide range of active proteins. Among heme-containing enzymes, the cytochromes P450 occupy a prominent role and are present in many monooxygenase. This class of enzymes catalyses a series of oxidative reactions by the insertion of an activated oxygen atom; in particular, they promote the oxidation of nonactivated hydrocarbons at physiological temperature.

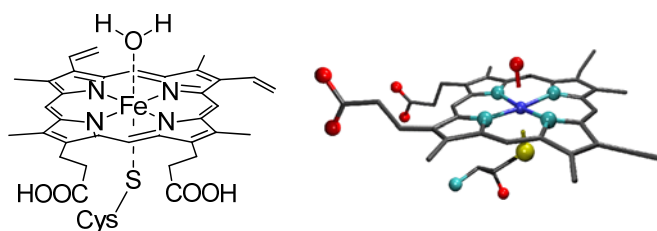
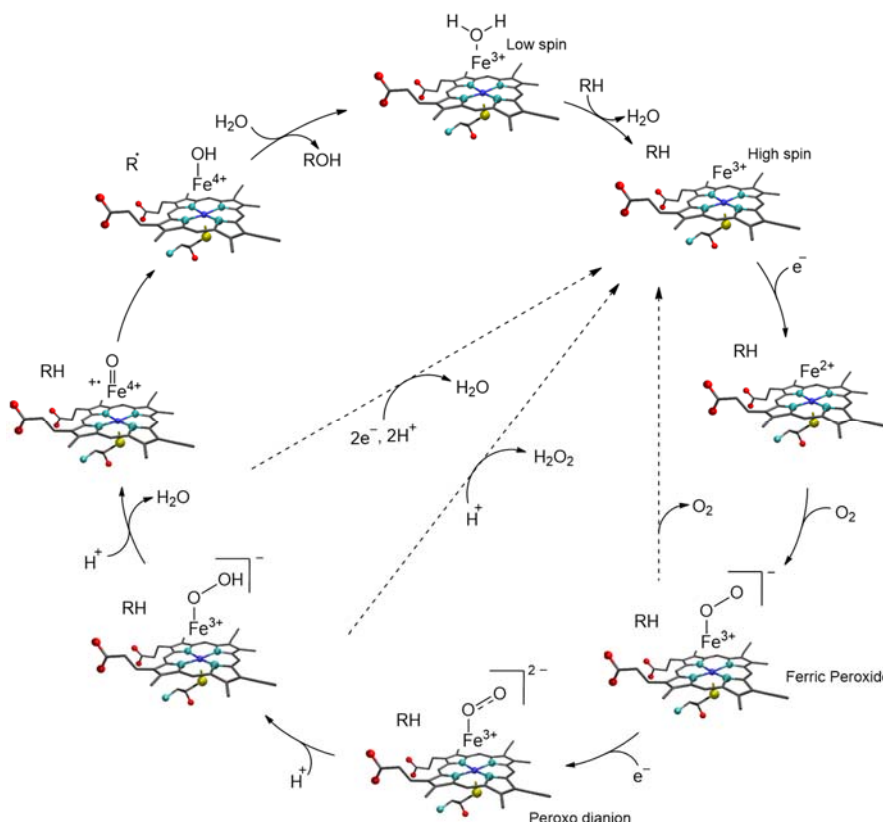


**Figure 2.** Iron(III) protoporphyrin IX complex (Heme).

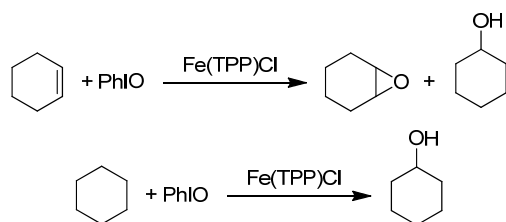
The X-ray crystal data of different cytochromes P450 revealed that the iron atom, which is placed in the porphyrin scaffold, is bound to a cysteine residue and, in turn, the heme-thiolate moiety is protected by the protein through non-covalent interactions with aminoacidic groups. The cytochromes contain also a water molecule which is the sixth ligand of the low spin iron atom. Moreover, the water molecule is part of a network which involves the so-called oxygen activation cycle. The catalytic cycle is described in Scheme 8. In the first step, the molecule of water is displaced from the hexacoordinated iron(III) complex forming a pentacoordinated iron(III) high spin state complex. The change in the iron electronic state shifts the reduction potential to more positive values promoting the reduction of iron(III) to iron(II), then the iron(II) complex binds a molecule of oxygen forming a ferric peroxide complex. In the next step, the ferric peroxide complex takes another electron becoming a ferric peroxo anion. The addition of two protons leads to the release of a water molecule and a very reactive oxoferryl intermediate which is stabilised by the donation of one electron

from the porphyrin ligand generating a radical Fe(IV) complex. The abstraction of a proton from the substrate generates a hydroxy ferric complex which hydroxylates the substrate according to a radical mechanism. At this point, the product is released regenerating the hexacoordinated iron(III) complex. The exact nature of the intermediate is a matter of debate but the formation of a radical iron(IV) complex is mostly accepted.



**Scheme 8.** Catalytic oxygen activation cycle of cytochrome P450.

Inspired by the outstanding catalytic activity of heme-containing enzymes, many efforts have been made to synthesise metal porphyrin complexes as artificial counterparts of these biological systems in oxo transfer reactions. In 1979, Groves *et al* reported the first biomimetic system for the catalytic hydrocarbon oxidation using Fe(TPP)Cl (TPP=dianion of tetraphenylporphyrin) and iodosylbenzene (PhIO) as the oxygen donor (Scheme 9).<sup>12</sup>



**Scheme 9.** First oxidation of alkenes and alkanes using synthetic iron porphyrin complex as catalyst.

The main problem of this methodology is the rapidly decrease in the catalytic activity due to the irreversible degradation of the iron centre. This data is in accordance with the studies of Collman and co-workers who discovered that the absence of the protein superstructure involves the formation of inert  $\mu$ -oxo iron(III) porphyrin dimers.<sup>13</sup> To overcome the dimerization and better mime the protein environment, many hindered iron-porphyrin systems were developed and the so-called iron ‘picket fence’ porphyrin complexes (Figure 3) are one of the most important class of catalysts which can bind the molecular oxygen.<sup>13-14</sup>

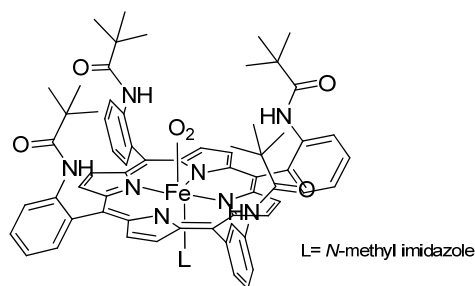


**Figure 3.** Example of iron(III) 'picket fence' porphyrin complex.

Although the iron-hemeproteins are the common natural oxygen activation systems, many other transition metal (ex. Cr, Mn, Co, Ru) porphyrin complexes are synthesised to use in both epoxidation of alkenes and hydroxylation of deactivated hydrocarbons. Thanks to the relationship to the iron atom (same periodic group and electronic structure in the outer shell), ruthenium porphyrins have shown high activity in the oxygen activation and they are able to oxidize many compounds such as amines, thioethers, phosphines etc.

Moreover, iron and ruthenium porphyrins have been studied in other atom/group transfer reactions, such as carbene and nitrene transfer reactions, in which they show a unique catalytic activity producing important compounds such as cyclopropanes, amines, aziridines and indoles in good yield and stereoselectivity.

### 3. Aim and outline of the thesis

Cyclopropanes and nitrogen-containing compounds, such as aziridines, indoles and amines, are interesting molecules from a synthetic point of view because they are often used as building blocks in organic synthesis. They also constitute the active part of many natural and synthetic products owing to their biological and pharmaceutical properties. Over the years, the scientific community focused its attention in the development of new eco-friendly catalytic process to obtain these compounds in good yields and selectivity respecting the basic principles of ‘green chemistry’.

Based on these concepts, carbene and nitrene transfer reactions are useful synthetic strategies to produce compounds stated above and they can be efficiently promoted by metal porphyrin complexes due to their high catalytic activity and chemical versatility.

The first part of this thesis describes the synthesis of cyclopropanes using chiral iron porphyrin complexes which show a ‘Totem’ tridimensional structure. In the second half part of the thesis we describe the ruthenium porphyrin-catalysed nitrene-transfer reactions to synthesis nitrogen-containing compounds.

In **Chapter II** we describe the synthesis of new ‘Totem porphyrin ligands’ and their iron(III) porphyrin complexes to promote cyclopropanation reactions. Since, high diastereo- and enantioselectivities are attributed to a synergic action of the active metal center with the ligand periphery, several structural modifications of the ligand skeleton were performed to give catalysts whose efficiency could be maximised by a metal/periphery synergy to promote stereoselective cyclopropanation reactions.

In **Chapter III** we describe the Ru(TPP)CO-catalysed aziridination of styrenes by aryl azides in mesoreactors under continuous flow conditions. We also report the reactivity of aziridines towards carbon dioxide. The coupling reaction between aziridines and carbon dioxide, the most abundant greenhouse gas, is one of the most important routes to obtain oxazolidinones. The mechanism of this reaction was also computationally investigated by using DFT methods.

In **Chapter IV** we report the synthesis of indoles by an intermolecular reaction between aryl azides and aryl alkynes using a ruthenium *bis*-imido complex as the catalyst. The generality of the reaction was proved by synthesising several indoles from differently substituted aryl azides and alkynes. We also performed kinetic and DFT studies to clarify the reaction mechanism.

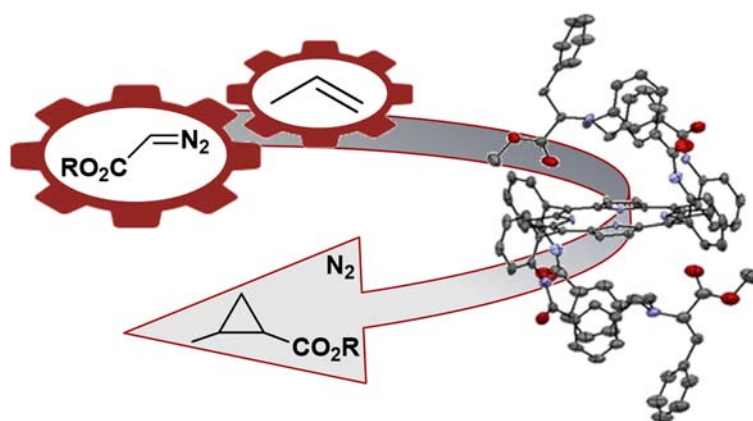
In **Chapter V** we describe the influence of the axial ligand electronic features on the catalytic activity of ruthenium porphyrin complexes in promoting amination reactions. The influence was studied both from an experimental and theoretical (DFT study) points of view, by comparing the catalytic performance of Ru(TPP)CO to that of Ru(TPP)(py)<sub>2</sub> (py=pyridine) complex.

## 4. References

1. K. Nicolaou. *Classics in total Synthesis*. **1996**, chap. 8, 99-136.
2. H. Fischer, K. Zeile. *Justus Liebigs Annalen der Chemie* **1929**, 468, 98-116.
3. G. P. Arsenault, E. Bullock, S. F. MacDonald. *J. Am. Chem. Soc.* **1960**, 82, 4384-4389.
4. (a) A. Boudif, M. Momenteau. *J. Chem. Soc., Chem. Commun.* **1994**, 2069-2070. (b) A. Boudif, M. Momenteau. *J. Chem. Soc. Perkin 1* **1996**, 1235-1242.
5. (a) P. Rothmund. *J. Am. Chem. Soc.* **1935**, 57, 2010-2011. (b) P. Rothmund, A. R. Menotti. *J. Am. Chem. Soc.* **1941**, 63, 267-270.
6. A. D. Adler, F. R. Longo, J. D. Finarelli, J. Goldmacher, J. Assour, L. Korsakoff. *J. Org. Chem.* **1967**, 32, 476-476.
7. M. O. Liu, C. H. Tai, W. Y. Wang, J. R. Chen, A. T. Hu, T. H. Wei. *J. Organomet. Chem.* **2004**, 689, 1078-1084.
8. J. S. Lindsey, I. C. Schreiman, H. C. Hsu, P. C. Kearney, A. M. Marguerettaz. *J. Org. Chem.* **1987**, 52, 827-836.
9. J. S. Lindsey, R. W. Wagner. *J. Org. Chem.* **1989**, 54, 828-836.
10. P. J. Brothers, J. P. Collman. *Acc. Chem. Res.* **1986**, 19, 209-215.
11. A. D. Adler, F. R. Longo, F. Kampas, J. Kim. *J. Inorg. Nuc. Chem.* **1970**, 32, 2443-2445.
12. J. T. Groves, T. E. Nemo, R. S. Myers. *J. Am. Chem. Soc.* **1979**, 101, 1032-1033.
13. J. P. Collman, R. R. Gagne, C. Reed, T. R. Halbert, G. Lang, W. T. Robinson. *J. Am. Chem. Soc.* **1975**, 97, 1427-1439.
14. E. Rose, A. Kossanyi, M. Quelquejeu, M. Soleilhavoup, F. Duwavran, N. Bernard, A. Lecas. *J. Am. Chem. Soc.* **1996**, 118, 1567-1568.

# Chapter II

## C-C bond formations: Cyclopropanes



*Parts of this chapter have been published and are reproduced here from:*

D. M. Carminati, D. Intrieri, S. Le Gac, T. Roisnel, B. Boitrel, L. Toma, L. Legnani and E. Gallo. *New J. Chem.* **2017**, 41, 5950-5959.

D. M. Carminati, D. Intrieri, A. Caselli, S. Le Gac, B. Boitrel, L. Toma, L. Legani and E. Gallo. *Chem. Eur. J.* **2016**, 22, 13599-13612.

D. Intrieri, D. M. Carminati and E. Gallo. *Dalton Transaction* **2016**, 45, 15746-15761. Cover.

# 1. Introduction

Cyclopropanes are one of the most important three-membered rings and are contained in many natural and synthetic products (ex. insecticides and pharmaceutical drugs) owing to their biological and pharmaceutical properties.<sup>1</sup> Moreover, the reactivity of the strained three-membered ring allows them to be used as versatile building blocks in organic chemistry for the synthesis of challenging complex molecules (Figure 4).<sup>2</sup>

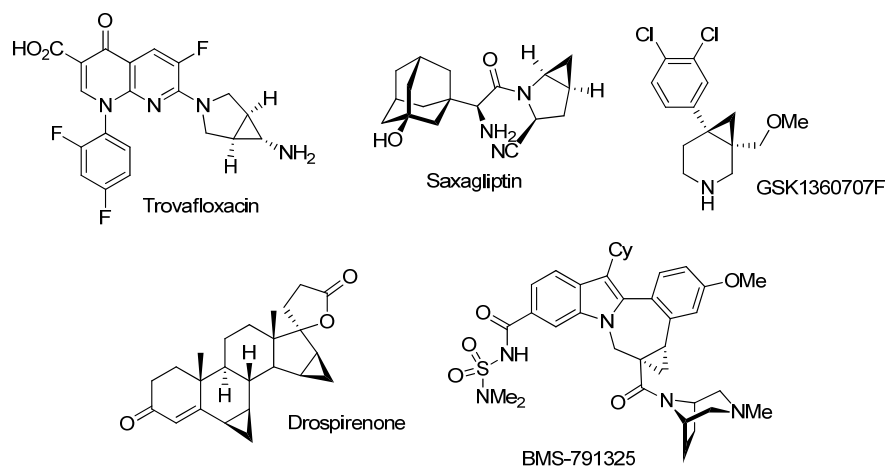
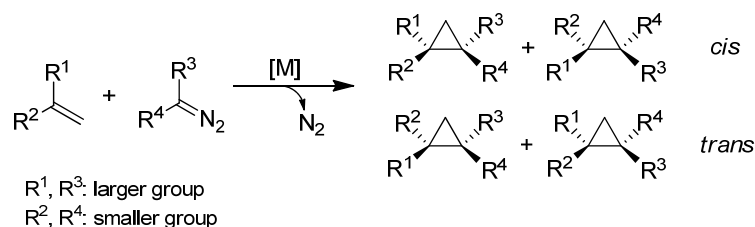


**Figure 4.** Marketed drugs and development candidates having a cyclopropyl ring system.

Over the years, the scientific community focused its attention in the development of new eco-friendly catalytic process to obtain cyclopropanes in good yields and selectivity (diastereo- and enantioselectivity), respecting the basic principles of ‘green chemistry’. Among all the available methods, the carbene transfer reaction from a diazo compound to an alkene is one of the most used strategies. Moreover, this one-pot reaction is a sustainable synthetic route due to the formation of eco-friendly molecular nitrogen as the only byproduct (Scheme 10).<sup>3</sup>



**Scheme 10.** Cyclopropanation of alkenes by diazocompounds.

Since the introduction of flow-chemistry process to obtain hazardous diazo compounds on an industrial scale, and the development of more active and selective metal catalysts, the cyclopropanation reaction has attracted more interest and investments. Among metal complexes which are used as catalysts in cyclopropanation reactions, metal porphyrins play a prominent role due to their high catalytic activity, stereoselectivity and chemical stability. Furthermore, porphyrins can be easily modified on their skeleton obtaining a plethora of unchiral or chiral ligands, and also metal porphyrin catalysts, with very different electronic and steric characteristics.<sup>4</sup>

Herein we discuss some important examples of chiral metal porphyrin complexes which are active in stereoselective carbene transfer reactions.



## 1.1. Chiral porphyrin ligands

The request for cyclopropane-containing compounds in a pure form by the chemical industry has brought to develop the synthesis of new chiral catalysts which efficiently promote enantioselective carbene transfer reactions. The high chemical versatility of porphyrin ligands makes them an important class of stereoselective catalysts, in fact metal porphyrin complexes can be easily modified introducing chiral moieties surrounding the active centre and, consequently, they can be obtained in a pure chiral form. Since the last decade, numerous chiral metal porphyrins have been synthesised to promote enantioselective reactions and the scientific interest in their catalytic use as developed in a continuously growing number of applications extending their utility.

Chiral porphyrins can be synthesised in many ways, but the most common approach involves the attachment of chiral moieties on *meso*-tetra(2-substituted)phenyl porphyrin or *meso*-tetra(2,2'-disubstituted)phenyl porphyrin. It is important to mention that, while the 2,2'-disubstituted porphyrins exist in only one conformation, the 2-monosubstituted porphyrin present four different isomers: the so-called atropoisomers.<sup>5</sup> In *meso*-tetraphenyl porphyrins, the four phenyl groups are perpendicular to the porphyrin plane projecting in this way the *ortho* substituents above or below the plane. The four atropoisomers ( $\alpha^4$ ,  $\alpha^3\beta$ ,  $\alpha^2\beta^2$ ,  $\alpha\beta\alpha\beta$ ) show different configurations according to the orientation of the *ortho*-substituents (Figure 5).

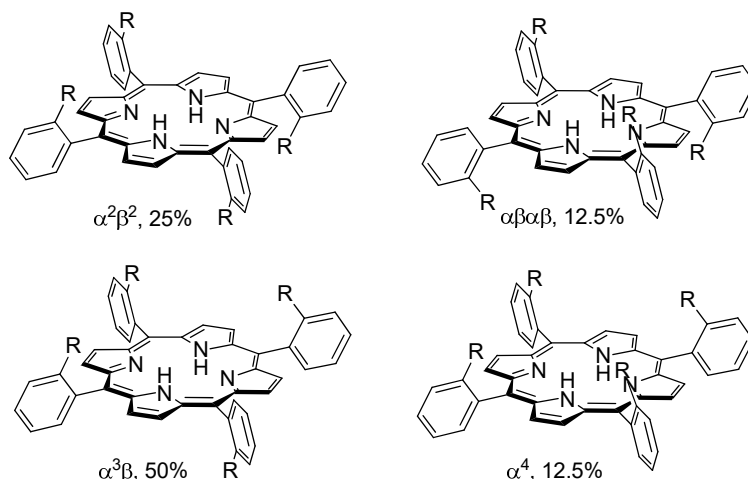


**Figure 5.** The four atropoisomers and the statistical percentage for *meso*-tetra(2-substituted)phenyl porphyrin.

The classic synthesis of *meso*-tetra(2-substituted)phenyl porphyrins starting from pyrrole and the related 2-substituted aldehyde brings the four atropoisomers in a statistical ratio of abundance. The atropoisomers can be interconverted and the interconversion conditions depend on the nature of the substituents: for example for *meso*-tetra(2-amino)phenyl porphyrin, the interconversion is possible even at room temperature, and becomes rapid over 70-80 °C.

The 'single-face' protected porphyrins are the first class of studied asymmetrical ligands thanks to their similarity with Heme. This type of porphyrins is synthesised starting from the atropoisomer  $\alpha^4$  of *meso*-tetra(2-monosubstituted)phenyl porphyrins with all the *ortho* substituents above the porphyrin's plane. The early single-face porphyrins were the so-called 'picket fence' porphyrins (Figure 6a) which were used as counterparts of the natural system in oxo transfer reactions due to their capacity to reduce the formation of the inactive  $\mu$ -oxo dimer (cap I, 2.2). Afterwards, Collman *et al* reported the synthesis of a new class of chiral single-face porphyrin called 'picnic basket' porphyrins which showed a linker to close the two 'arms' of the porphyrin ligands (Figure 6b).<sup>6</sup> The metal picnic basket porphyrin complexes were used as catalysts in

epoxidation of alkenes, but to prevent the approach of the substrate on the open achiral face, it was necessary to coordinate an anionic ligand to the metal center. The use of an anionic ligand, which is usually very expensive and difficult to prepare, made the picnic basket porphyrin complexes useless as industrial catalysts. However, they can discriminate O<sub>2</sub> with respect to CO so they have found a place in the field of cationic binding applications.<sup>7</sup>

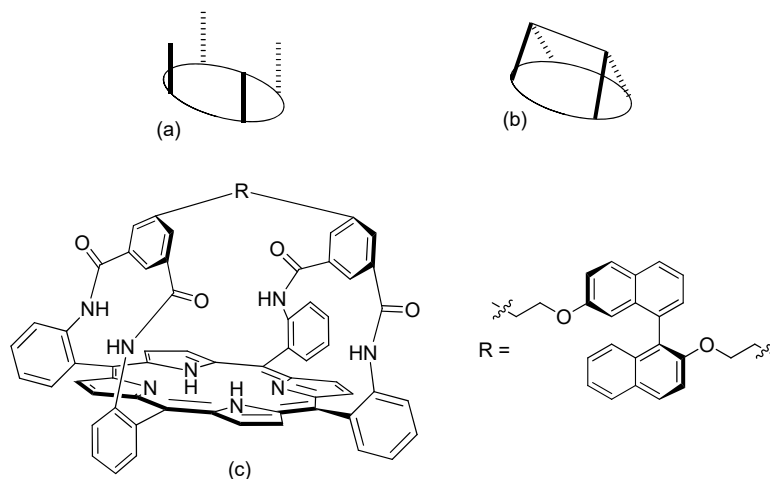


**Figure 6.** Schematic representation of ‘picket fence’ (a) and ‘picnic basket’ (b) porphyrins; example of ‘picnic basket’ porphyrin (c).

Another class of important chiral porphyrins is the double-faced picket porphyrins in which we can identify two main groups: the  $D_2$ -symmetric porphyrins and the  $D_4$ -symmetric porphyrins. As for the  $D_2$ -symmetric porphyrins, they are synthesised from *meso*-tetra(2,2'-disubstituted)phenyl porphyrin or  $\alpha\beta\alpha\beta$  atropoisomer of *meso*-tetra(2-monosubstitued)phenyl porphyrin (Figure 7, a). Numerous  $D_2$ -symmetric catalyst were tested in different reactions and in many cases good results have been obtained in terms of yield and enantioselectivity. Nevertheless, the catalytic activity of these kind of porphyrins strictly depends on the hindrance of the substitutes, as showed by the results obtained by Kodadek and co-workers.<sup>8</sup> Kodadek *et al* noted that the double face protected manganese  $\alpha\beta\alpha\beta$  *meso*-tetra[(*R*)-1,1'-binaphth-2-yl] porphyrin complex, called ‘Chiral Wall’, showed a good catalytic activity in the epoxidation of styrenes obtaining the products in good yield and selectivity. Indeed, when they increased the dimension of the chiral moiety, they observed worse results. These results confirmed that a certain degree of the surrounding bulk is necessary to achieve selectivity, but too hindered systems may easily result less efficient.

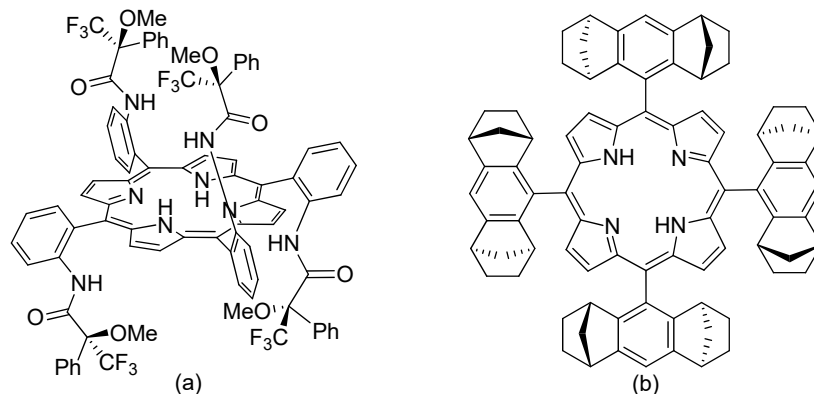
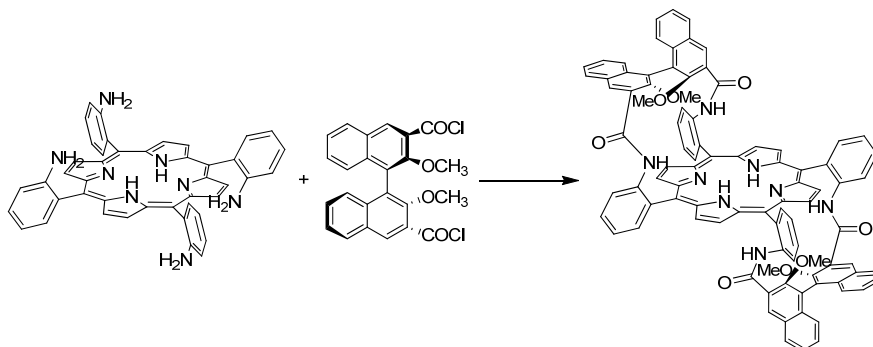


**Figure 7.** Example of  $D_2$ -symmetric (a) and  $D_4$ -symmetric (b) porphyrins.

Better results were obtained using the  $D_4$ -symmetric porphyrins which were synthesised for the first time by Halterman and co-workers (Figure 7, b).<sup>9</sup> Nowadays, these kinds of chiral ligands are extensively employed

with different metals and for various catalytic applications such as oxidation, cyclopropanation and amination reactions.

The last important class of chiral porphyrins is the  $C_2$ -symmetric porphyrins obtained by the functionalization of the atropoisomers  $\alpha_2\beta_2$  with chiral moieties (Scheme 11). The main feature of this family of ligands is that they show a free access to the active site for the substrate and at the same time they have a significant steric bulk surrounding the porphyrin core. As in the case of  $D_2$ -symmetric porphyrins, the catalytic activity of these kind of porphyrins depends on the hindrance of the chiral bulk and on its distance from the catalytic site.



**Scheme 11.** Typical methodology to synthesise  $C_2$ -symmetric porphyrin by the condensation of atropisomer  $\alpha_2\beta_2$  and a chiral binaphthyl moiety.

According to the idea that the efficiency of the catalyst would be improved by providing more access to the metal centre, some  $C_2$ -porphyrin ligands were synthesised increasing the distance from the chiral moieties to the active site. Unfortunately, their metal complexes showed a high catalytic activity in terms of yield but low values of enantioselectivity. This is due to the lower rigidity of the structure of the ligands and, as a consequence, a lower chirality induction. In other cases more hindrance chiral porphyrins were synthesised to increase the chirality induction, but the higher hindrance chiral moiety induced a lower enantioselectivity. Vice versa, better value of enantioselectivity were obtained using less bulky arrangements. These results suggest that it is very important to modify the porphyrin structure by balancing the size and the distance of the chiral bulk.

## 1.2. Group 8 chiral porphyrin-catalysed cyclopropanation reactions

### 1.2.1. $D_4$ -symmetric metal porphyrin complexes

The first enantioselective cyclopropanation reaction catalyzed by a  $D_4$ -symmetric porphyrin was separately reported in 1997 by Che and Berkessel using ruthenium (Haltermann) porphyrin complexes (Halt\*)Ru(CO) (**1**) and (Halt\*)Ru(CO)(EtOH) (**2**) (Figure 8).<sup>10</sup>

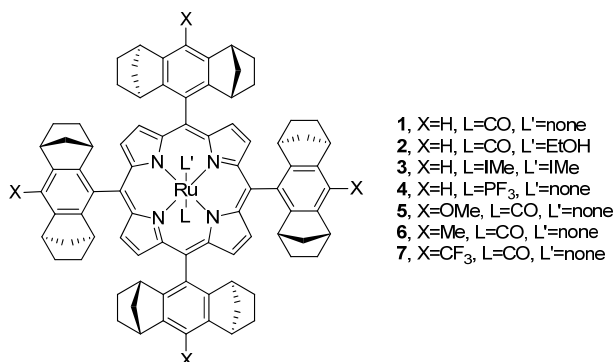
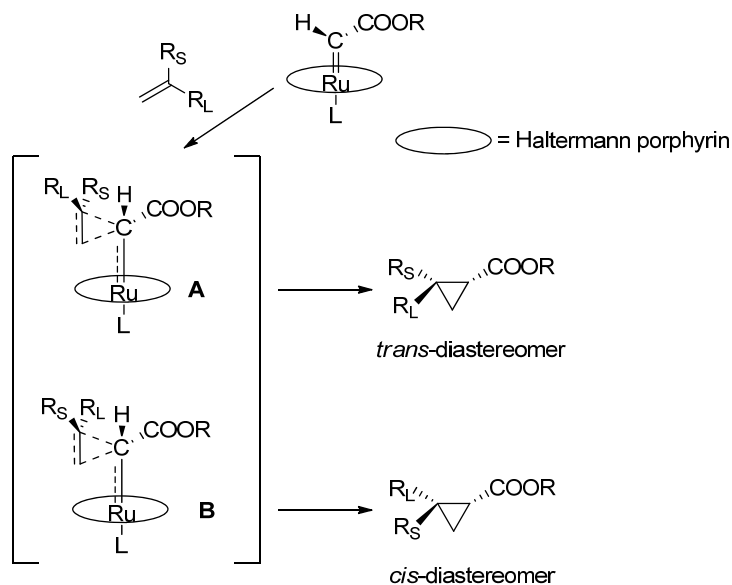


**Figure 8.** Ruthenium (Haltermann\*) porphyrin complexes.

The Authors reported the synthesis of several cyclopropanes with good yield, good *trans*-diastereoselectivity (up to 36:1) and enantioselectivities (up to 98%). The data revealed a good stereocontrol from the porphyrin ligand forming the more thermodynamically stable *trans*-diastereomer as the major product. Che *et al* explained these good results in terms of diastereoselectivity with the mechanism reported in Scheme 12, where the formation of the two transition states **A** and **B** is the consequence of the end-on approach of the alkene to the active site of the catalysts.<sup>11</sup> Thanks to the less extended steric interaction between the larger group  $R_L$  and the ester group on the carbene moiety, the transition state **A** results more stable than **B**, and the major product of the reaction is the *trans*-diastereoisomer. Moreover, this mechanism, with the parallel approach of the substrate, explains also why the nonterminal alkenes are less reactive than terminal ones.

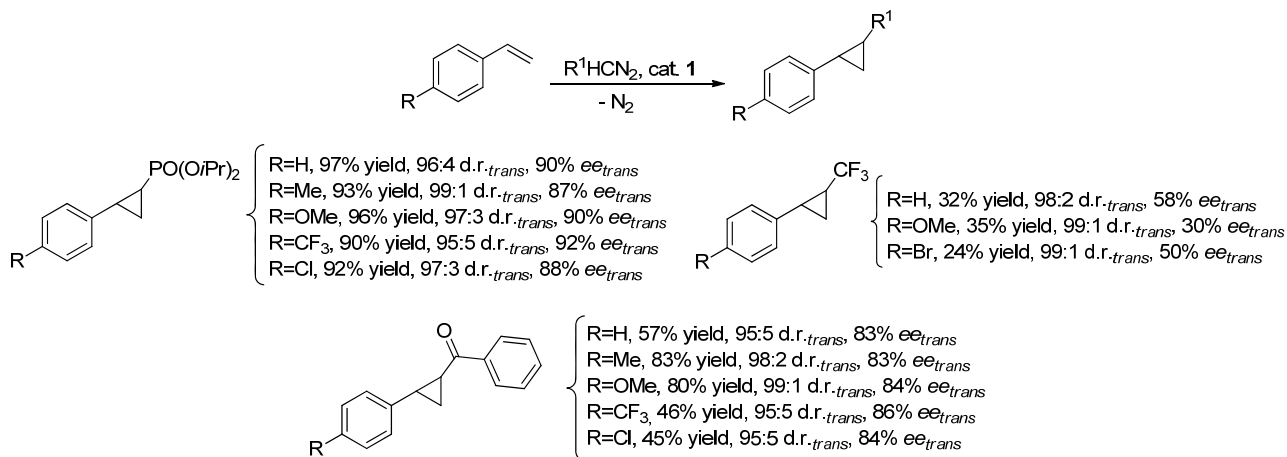


**Scheme 12.** Proposed transition states A and B of the **2**-catalysed cyclopropanation.

Che and co-authors also studied the influence of the axial ligands synthesising the complex **3** in which two *N*-heterocyclic carbenes (NHC) are the axial ligands on the ruthenium centre (Figure 8).<sup>12</sup> The presence of the two NHCs had a positive effect on the catalytic activity: in fact complex **3** was able to catalyse the cyclopropanation of styrene by ethyl diazoacetate (EDA) with a very low catalytic amount of 0.004 mol% and the cyclopropane was obtained with 95% yield, 95:5 *trans*-diastereoselectivity (d.r.*trans*) and 95% *trans*-enantioselectivity (*ee<sub>trans</sub>*). A DFT study revealed that the activation barrier for the decomposition of the diazo compound decreases thanks to the presence of the two NHC ligands which exhibit a strong  $\sigma$  donor, strength stabilizing the ruthenium-carbene on the *trans* position. Berkessel also studied the influence of axial ligands by comparing the catalytic activity of complex **1** with that of complex **4** in which the ligand CO was replaced by  $PF_3$  ligand (Figure 8).<sup>13</sup> Complex **4** resulted less active than complex **1** and this is probably due to the stronger bind between the ruthenium centre and the  $PF_3$  ligand. The authors suggested that the two complexes form different intermediates during the reaction: in the case of complex **1**, the CO ligand is lost to give a pentacoordinated carbene active species, whilst complex **4** does not lose the axial ligand obtaining a pseudo-octahedral carbene intermediate.

In order to improve the catalytic capacity of Haltermann porphyrins, Berkessel and co-authors studied the activity of new ruthenium (Halt\*)-substituted complexes (**5**, **6** and **7**) which exhibit diverse groups on the porphyrin scaffold (Figure 8).<sup>13</sup> All complexes showed a good catalytic activity, even if complex **7** is the most active and stable catalyst, probably due to electronic factors which can affect the catalyst stability more than the stereo-control of the reaction.

The reaction scope of enantioselective cyclopropanation reactions catalysed by **1** was expanded by Simonneaux who reported the use of diazo ketones, diisopropyl diazomethylphosphonate (DAMP) and 2,2,2-trifluorodiazoethane for the synthesis of optically active cyclopropanes (Scheme 13).<sup>14</sup> Simonneaux also reported the synthesis of the *para*-tetrasulfonated water soluble Haltermann-type porphyrin, complex **8**, to use in cyclopropanation reaction of alkenes in water.<sup>14c</sup>



**Scheme 13.** Cyclopropylketones, cyclopropylphosphonates and trifluoromethylphenyl cyclopropanes synthesised using complex **1** as catalyst.

To improve the recyclability and reuse of the ruthenium Haltermann catalysts, in 2002 Che and co-workers reported the first example of heterogeneous Ru(Halt\*)CO supported on the ordered mesoporous silica MCM-48.<sup>15</sup> This heterogeneous complex showed a high enantioselectivity and an excellent stability in the intramolecular cyclopropanation of *trans*-cinnamyl diazoacetate; the catalyst can be recycled for four consecutive times with the highest TON (turn over number) of 15000. Other heterogeneous complexes were synthesised by an anodic oxidation on a polymeric support, complexes poly-**9** and poly-**10** (Figure 9), and used as chiral polymer catalysts in the cyclopropanation of styrene by EDA.<sup>16</sup> Compared to their homogeneous analogues, complexes poly-**9** and poly-**10** showed a modest enantioselectivity and a lower catalytic activity, and these results are probably due to the cross-linked polymeric structure which can hinder the interaction between the substrate and the active sites. A more stereoselective catalyst was obtained by Simonneaux, who synthesised a ruthenium Haltermann porphyrin functionalised with four vinyl groups. This ruthenium complex was then polymerised with styrene and divinylbenzene forming a supported poly-ruthenium complex poly-**11** (Figure 9).<sup>17</sup> The poly-ruthenium catalyst was tested in the cyclopropanation reaction of styrenes with EDA, diazoacetone nitrile and 2,2,2-trifluorodiazoethane obtaining cyclopropanes with a good enantiomeric excess.

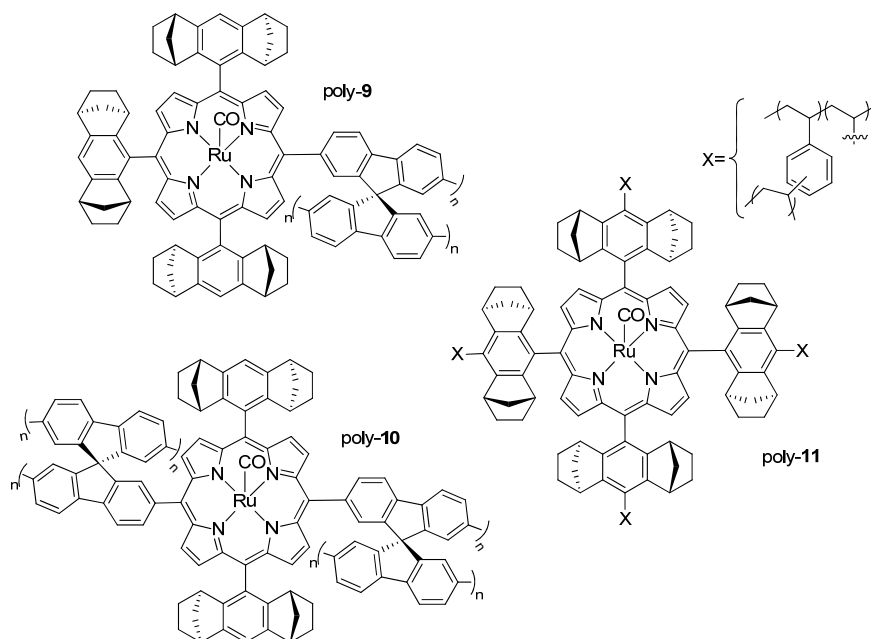
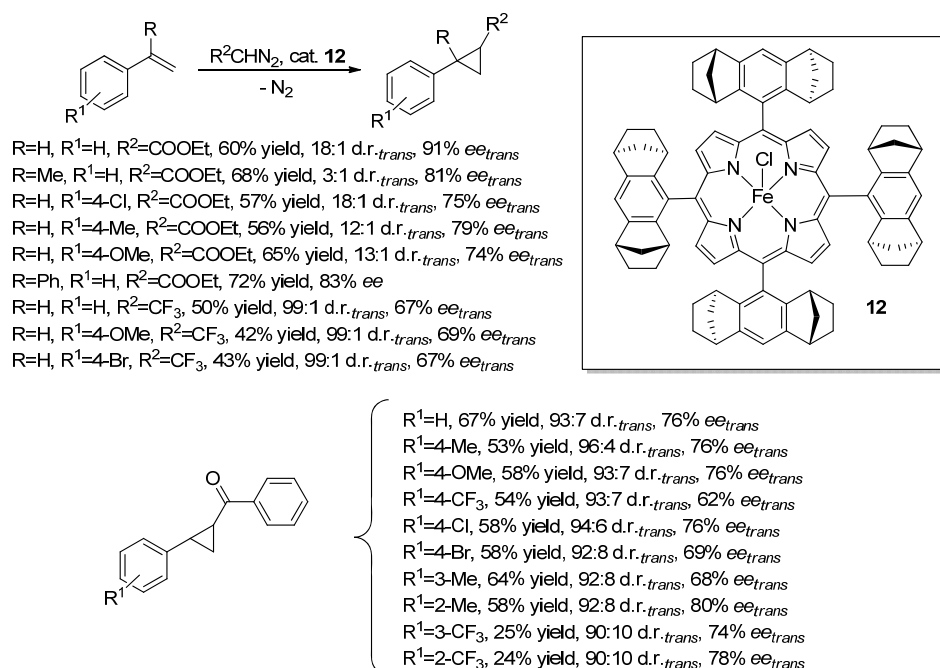


**Figure 9.** Heterogeneous ruthenium (Haltermann\*) porphyrin complexes.

Considering the importance to develop more sustainable catalytic protocols for the carbene transfer reactions, the interest of the scientific community is directed to the synthesis of low-toxicity cheap catalysts containing an iron centre: chiral  $D_4$ -symmetric porphyrins are ideal ligands to synthesise active iron derivatives.

The first use of an iron  $D_4$ -symmetric porphyrin complex was reported by Che and co-authors in 2006. They tested the catalytic activity of Fe(Halt\*)Cl (**12**) complex (Scheme 14) in the reaction between several substituted styrenes and EDA.<sup>18</sup> Cyclopropanes were obtained in good yields, good *trans*-diastereoselectivities, but lower values of enantioselectivities compared to its ruthenium counterpart. Complex **12** also catalysed the reaction of several styrenes with diazoacetophenone and 2,2,2-trifluorodiazomethane.<sup>14b, 19</sup>



**Scheme 14.** Iron Haltermann porphyrin-catalysed cyclopropanation of styrenes by EDA, diazoacetophenone and 2,2,2-trifluorodiazomethane.

Moreover, the reactions carried out without the addition of a reductive species, the authors supposed that complex **11** is electron poor enough to be reduced by EDA to an iron(II) complex, which can be transformed in an active carbene intermediate. The authors did not report direct experimental evidence of the formation of an iron carbene species, but the addition of an axial ligand such as pyridine or 1-methylimidazole gave a  $\text{Fe}(\text{Halt}^*)(\text{CHCOOEt})(\text{L})$  complex which was detected by the electrospray mass spectroscopy (ESMS). The presence of the additional axial ligand was also responsible for an improvement in the reaction's *trans*-diastereoselectivity.

G. Simonneaux also reported the synthesis of heterogeneous poly-**12** catalyst and a water soluble complex **13** in which four sulfonate groups were introduced in the porphyrin scaffold.<sup>14b, 20</sup> Both catalysts resulted active in cyclopropanation reactions, but also in these cases their catalytic activity was lower than poly-**11** and **8**.

### 1.2.2. $D_2$ -symmetric metal porphyrin complexes

During the last twenty years,  $D_2$ -symmetric porphyrin ligands were extensively used to form cobalt(II) complexes active in cyclopropanation reactions, where they result more active and stereo-selective than ruthenium and iron counterparts. In 1998, Simonneaux and co-workers studied the  $D_2$ -symmetrical ruthenium porphyrin complexes synthesising complex **14** and **15** (Figure 10). Each complex was used in cyclopropanation of styrenes with EDA but, unfortunately, the two complexes showed a very low enantioselectivity.<sup>21</sup> Bad results were also obtained using iron(III) porphyrin complex **16** reported in Figure 10. Even if high *trans*-diastereoselectivities were observed (up to 93:7), the reaction enantiocontrol was only modest (up to 28%).<sup>22</sup>

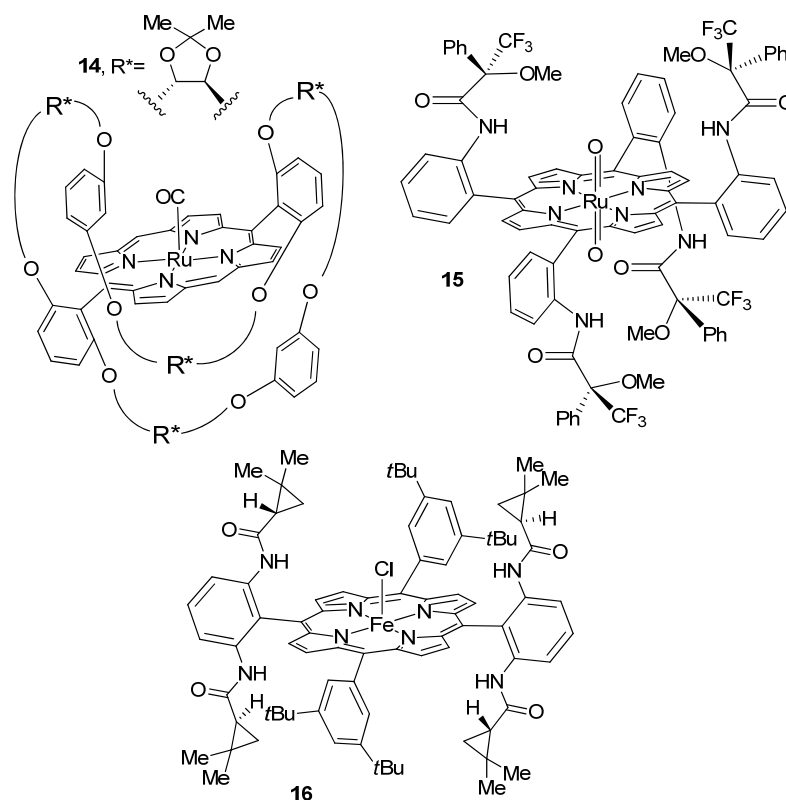


**Figure 10.**  $D_2$ -symmetrical iron and ruthenium chiral porphyrins **14**, **15** and **16**.

### 1.2.3. $C_2$ -symmetric metal porphyrin complexes

The functionalisation of the atropisomer  $\alpha_2\beta_2$  with chiral moieties produces  $C_2$ -symmetric porphyrin ligands which can be used for the synthesis of metal chiral catalyst. In 2002, Rose, Woo and co-workers reported the first synthesis of a  $C_2$ -symmetric chiral *bis*-binaphthyl porphyrin (Figure 11), the so called *bis*-strapped porphyrin.

This ligand is characterised by the presence of a significant steric bulk close to the active site thanks to the two chiral binaphthyl (BINAP) groups attached on the four picks of the  $\alpha_2\beta_2$  atropisomer of TAPPH<sub>2</sub>.  $C_2$ -symmetric chiral *bis*-binaphthyl porphyrin was employed to obtain an iron(II) complex which showed a modest catalytic activity in cyclopropanations.<sup>23</sup>

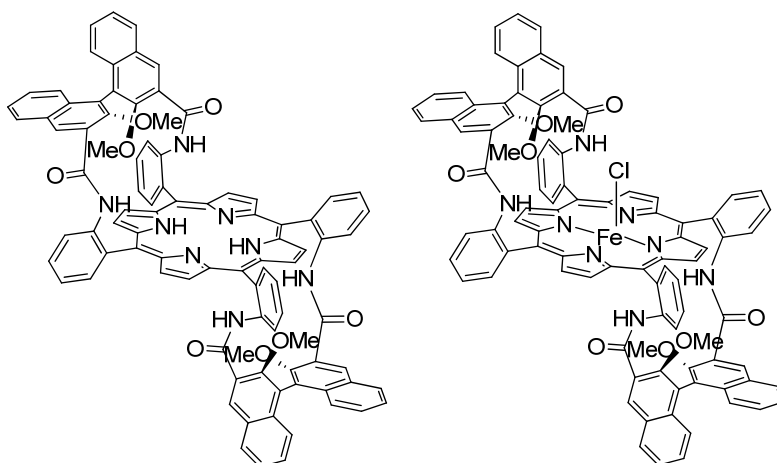


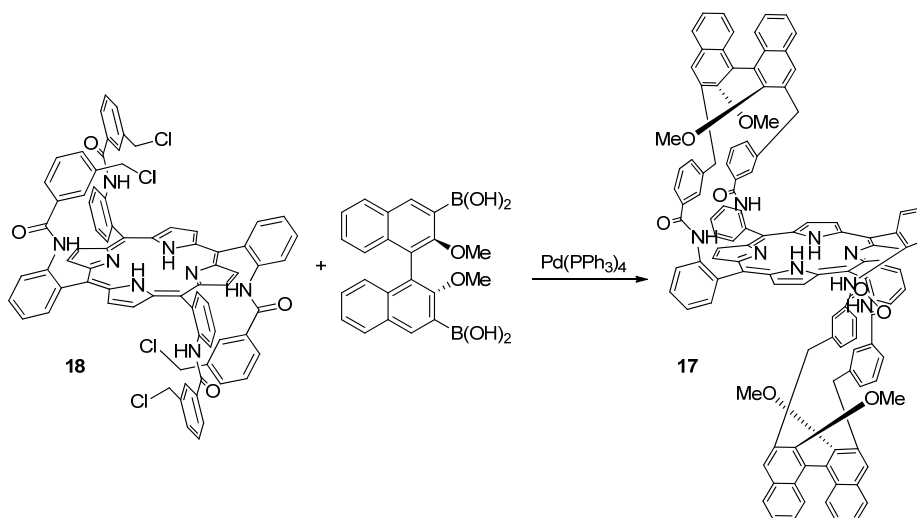
**Figure 11.**  $C_2$ -symmetric *bis*-binaphthyl porphyrin ligand and its iron(III) porphyrin complex used as chiral catalyst in alkene cyclopropanation reactions.



## 2. Discussion

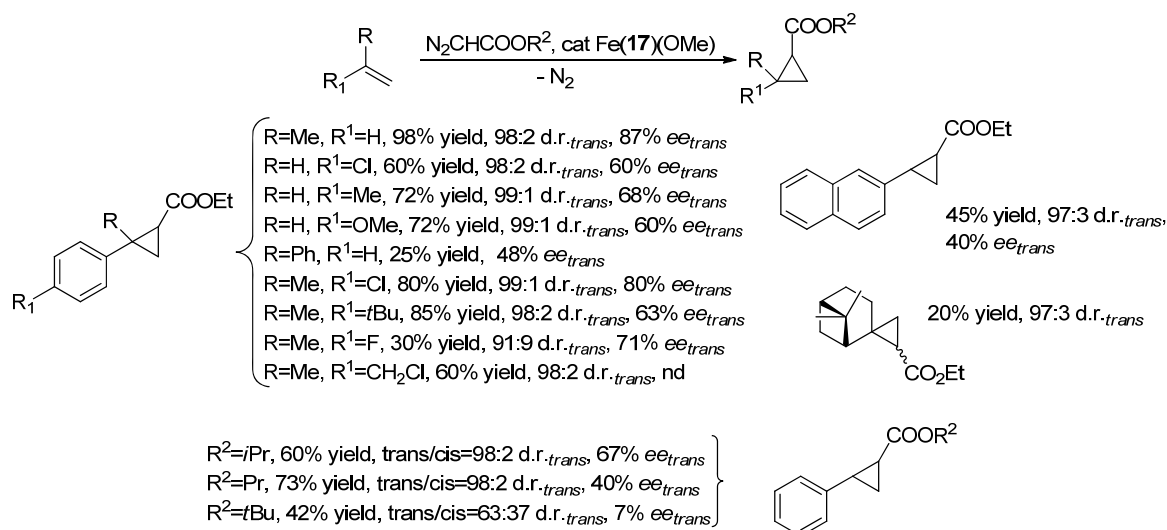
### 2.1. Cyclopropanation reactions catalysed by Fe(17)OMe

In 2014, Gallo and co-authors reported the synthesis and full characterization of a new  $C_2$ -symmetrical binaphthalene-strapped porphyrin (**17**) and its iron(III) complex (**Fe(17)OMe**). The  $C_2$ -porphyrin ligand **17** was obtained by the reaction between the atropisomer  $\alpha_2\beta_2$  of *meso*-tetra{2-[(3-chloromethyl) benzoylamido]phenyl} porphyrin (**18**) and (*R*)-(2,2'-dimethoxy-[1,1'-binaphthalene]-3,3'-diyl)diboronic acid in presence of  $(\text{Ph}_3\text{P})_4\text{Pd}$  (Scheme 15).<sup>24</sup> The porphyrin **17** shows one  $C_2$  axis within the porphyrin plane and exhibits an open space on each side for the substrate access. It also has a steric chiral bulk surrounding the *N*-core. Porphyrin **17** gives the iron(III) derivative **Fe(17)OMe** by reaction with  $\text{FeBr}_2$ .



Scheme 15. Synthesis of porphyrin ligand **17**.

During my thesis work, complex **Fe(17)OMe** was tested in the cyclopropanation reaction of several styrenes with diazo acetates obtaining good results in term of yields and diastereoselectivities. In each reaction excellent *trans*-diastereoselectivity was obtained (up to 99:1), even if a minor stereo-control was observed when high sterically hindered substrates were used (Scheme 16).<sup>25</sup> On the other hand, the reaction enantiocontrol was not always excellent, probably due to the too long distance between the chiral bulk and the active site. However, it should be noted that outstanding values of TON and TOF (20,000 and 120,000/h respectively) were obtained and the reactions were carried out without using an alkene excess, in accordance with the industrial request for sustainable processes, especially when expensive alkenes are involved.



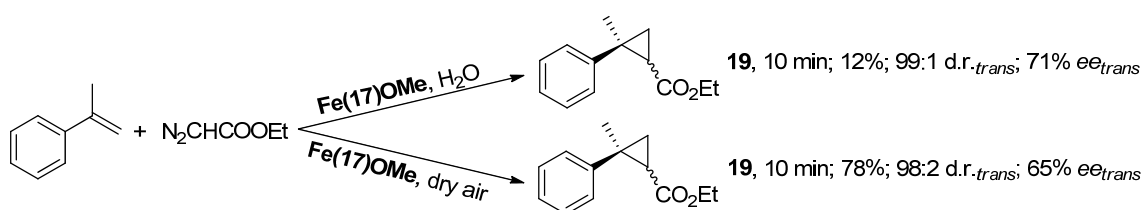
Scheme 16. Fe(17)OMe-catalysed cyclopropanation reactions.

Data reported up to now on the catalytic efficiency of metal symmetrical chiral porphyrin complexes indicate that the stereoselectivity of the catalyst depends on a synergic action of the active site with the porphyrin periphery. Consequently, porphyrin ligands could be considered a ‘*active ligands*’: their three-dimensional structure could be essential to opportunely drive the carbene moiety to the target substrate.

Unfortunately, the catalytic system was very sensitive to reaction conditions, therefore it was necessary to carefully check the experimental conditions by using purified substrates, dried solvents, and the catalyst had to be in solid state.

### 2.1.1. Recycling and recovery of Fe(17)OMe

To evaluate the robustness of the catalyst Fe(17)OMe, many tests on its recyclability were performed. In a previously published communication,<sup>24</sup> we reported that complex Fe(17)OMe can be recycled three consecutive times in the model cyclopropanation reaction of  $\alpha$ -methylstyrene by EDA under an inert atmosphere. Since the presence of an excess of EDA favoured the catalytic activity of Fe(17)OMe, we performed the catalyst recycle using an EDA excess. Each of the three runs gave the product **19** in good yield and similar stereoselectivities up to 98:2 *trans/cis* and 78% ee*trans*. This test was the last proof of the fundamental role played by EDA to preserve the catalyst from the deactivation. To also evaluate the catalyst recycle in a non-protected reaction medium, the experiment described above was repeated evaporating the reaction mixture to dryness, leaving it in the open air and then evaluating the yield and the stereoselectivity after each catalytic run. After the second run, the analysis revealed that product **19** was obtained in good stereoselectivity (*trans/cis*=98:2 and 75% ee*trans*) but in a very low yield (38%), indicating a decrease of the catalytic efficiency. Then, after the third run, the product was formed only in traces indicating that a catalyst deactivation had taken place.

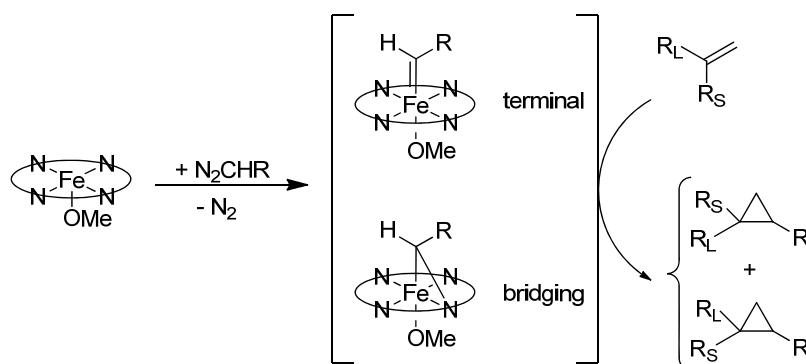


Scheme 17. Fe(17)OMe-catalysed cyclopropanation under no-protected conditions.

Since the catalyst deactivation is probably caused by the air, we separately investigated the influence of molecular oxygen and water on the catalytic activity of **Fe(17)OMe** by performing three different reactions between  $\alpha$ -methylstyrene and EDA. The first reaction was run in air by employing a flask equipped with a calcium chloride drying tube, the second one was performed in air by using activated molecular sieves and the last in presence of degassed water (Scheme 17). The first two reactions yielded the product with similar results: in the first case **19** was formed after 10 minutes in 78% yield with 98:2 d.r.*trans* and 65% *ee**trans* and in the second case the product was obtained in 64% yield, 97:3 d.r.*trans* and 75% *ee**trans*. It is important to note that the collected data were in accordance with those achieved when the reaction was run under nitrogen. On the contrary, when the reaction was carried out in presence of water, the product was obtained in lower yield (12%). These results suggested that the catalytic process inhibition, observed when the reaction mixture was exposed for a short period of time to air, was mainly due to the presence of humidity rather than to oxidative side reactions.

The inhibiting role of water on **Fe(17)OMe**-catalysed reaction was probably due to a replacement of the methoxy axial ligand with an hydroxy group and the resulting **Fe(17)OH** complex was poorly active as a catalyst. To confirm the catalytic importance of the methoxy group, we synthesised the complex **Fe(17)OH** by treating **Fe(17)OMe** with NaOH. **Fe(17)OH** was fully characterised and was tested in the model reaction observing a very poor catalytic activity, suggesting the important role of the methoxy ligand in mediating the carbene transfer reaction. In any case, **Fe(17)OH** can be easily turned back to **Fe(17)OMe** by a simple treatment with methanol for 10 hours.

Since the methoxy group results very important for the catalytic activity of **Fe(17)OMe** we tried to understand if it was lost during the reaction or not. Although we were not able to isolate the carbene species, at the end of the reaction we recovered the catalyst **Fe(17)OMe** to indicate that the methoxy ligand was not lost during the reaction. The experimental data were not sufficient to clarify the reaction mechanism, but thanks to other reported studies, we can suppose the mechanism reported in Scheme 18 in which the active species are either the *terminal* or the *bridging* carbene complexes.<sup>26</sup>

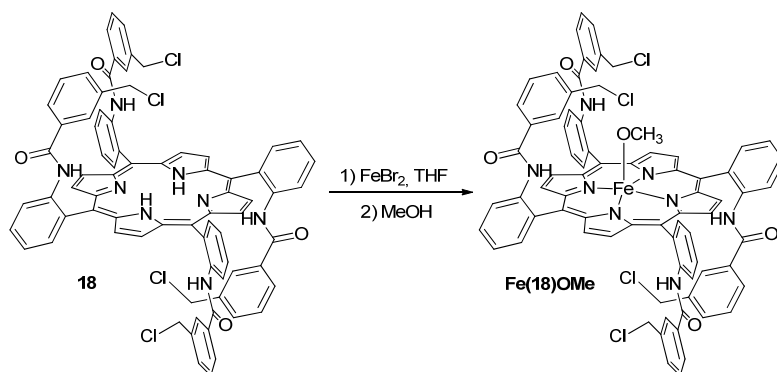


**Scheme 18.** Proposed mechanism for **Fe(17)OMe**-catalysed cyclopropanation.

### 2.1.2. Study of the steric effects of the **Fe(17)OMe** chiral bulk

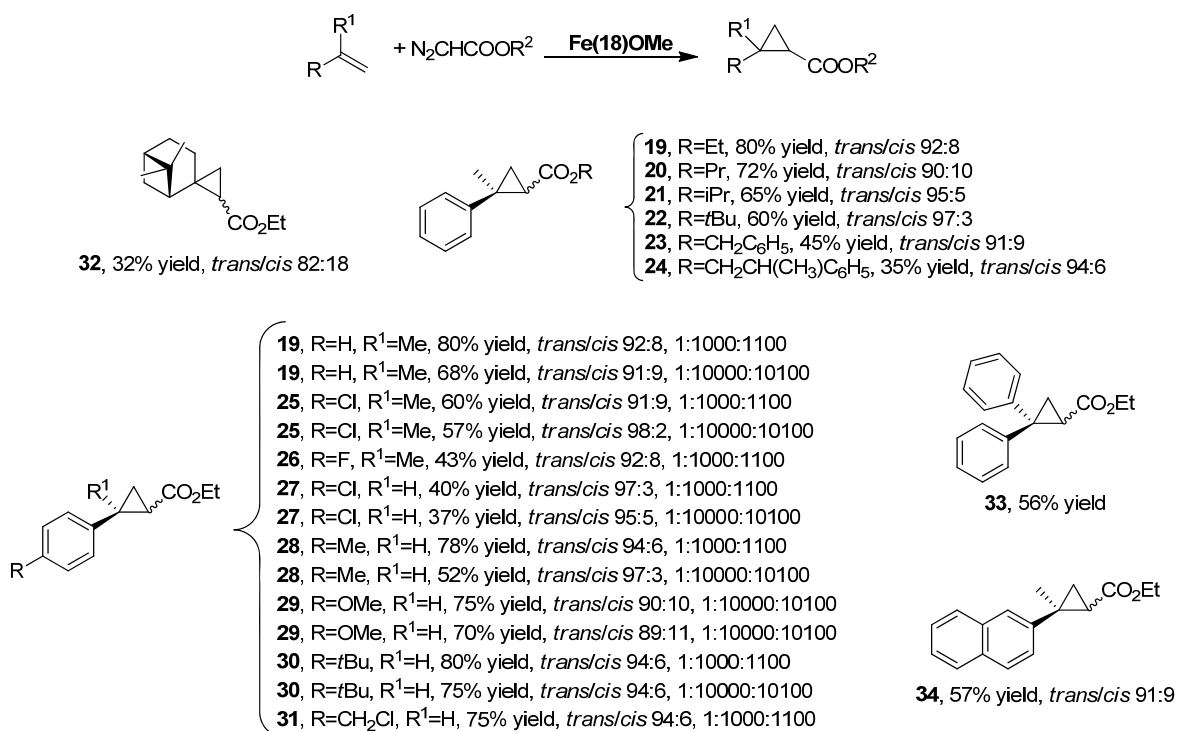
**Fe(17)OMe** complex catalysed the cyclopropanation of several aromatic alkenes by diazoacetates and products were obtained in good yields, excellent *trans*-diastereo- and enantioselectivities, except when very sterically hindered reagents were employed. When  $\alpha$ -methylstyrene was treated with benzyl 2-diazoacetate or 1-phenylpropan-2-yl-diazoacetate, products were not obtained. For this reason, we decided to study the steric effect of the chiral group on the catalytic activity of complex **Fe(17)OMe** by synthesising the iron(III) complex **Fe(18)OMe** in which ligand **17** was replaced by the less sterically encumbered ligand **18** (precursor of **17**).

The iron(III) complex was synthesised by reacting **18** with FeBr<sub>2</sub> and the consecutive treatment with MeOH (Scheme 19).



Scheme 19. Synthesis of Fe(18)OMe complex.

Complex Fe(18)OMe was tested in the reaction between several diazocompounds and alkenes, as reported in Scheme 20, and good results were obtained in terms of yield and *trans*-diastereoselectivity (**19-35**, Scheme 20). Whereas Fe(17)OMe resulted inactive when very hindered diazocompounds were employed, Fe(18)OMe was able to promote the reaction of  $\alpha$ -methylstyrene with benzyl diazoacetate, obtaining the product with an acceptable yield of 45% and good *trans* diastereoselection of 91:9. With 1-phenylpropan-2-yl-diazoacetate, the product **24** was obtained with 35% of yield and a *trans/cis* diastereoselection of 94:6. Complex Fe(18)OMe was also used at the lowest catalyst loading of 0.01% , obtaining cyclopropanes in reasonable yields and short reaction times with high values of TON and TOF.



Scheme 20. Screening of diazocompounds and alkenes using Fe(18)OMe complex.

These results confirmed that the absence of the chiral group surrounding the *N*-core allows an easier access of the substrate to the active metal without changing the reaction *trans*-diastereoselectivity. This indicates that precursor **18** is rigid enough to maintain a three-dimensional arrangement very similar to that of porphyrin **17**.

Data collected up to now on the catalytic activity of complexes **Fe(18)OMe** and **Fe(17)OMe**, have suggested that the high *trans*-diastereocontrol of the two catalysts was principally induced by the benzylic groups and that the chiral moiety did not influence the reaction diastereoselectivity. This result indicates that porphyrin **17** shows a ‘Totem’ structure which is formed by three different and independent elements. The first element is the tetrapyrrolic core where the metal centre is placed and it is responsible for the EDA activation, the second element is constituted by the benzoyl group which is responsible for the diastereoselectivity, and the last element is formed by the chiral ‘hat’ which is responsible for the enantioselectivity.

### 2.1.3. DFT theoretical studies

To better understand the influence of the three-dimensional structure on the reaction stereocontrol induced by catalysts **Fe(17)OMe** and **Fe(18)OMe**, DFT calculations were performed by Prof. Toma and Dr. Legnani of the University of Pavia in collaboration with our team at University of Milan. We started studying the geometrical conformation of porphyrin **18** and the simplified complex **Fe(35)OMe** in which the 3-(chloromethyl)benzoyl groups were replaced with benzoyl groups. In figure 12 we report the most stable conformers of the two compounds. Regarding the complex **Fe(35)OMe**, the high-spin sextet ( $S=5/2$ ) state was energetically favored in agreement with the experimental data and showed two conformers which differ for the position of the methyl of the methoxy group. In conformer **Fe(35)OMe-A** the methyl group points away from the phenyls of the pickets, whereas the methyl group of **Fe(35)OMe-B** is placed between them.

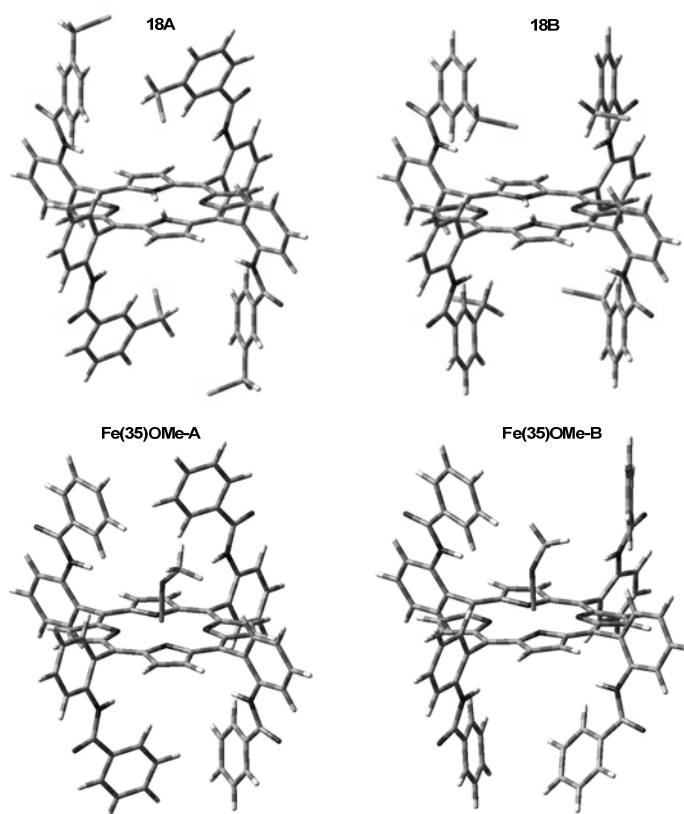


**Figure 12.** Preferred conformers of porphyrin **18** and model complex **Fe(35)OMe**.

Concerning ligand **17**, even if it shows a certain rigidity, it has several single bonds which show degrees of conformational freedom that can combine in a significant number of different geometries. To simplify the calculations, we started studying ligand **36**, which displays only a binaphthyl-handled. Four conformers resulted the most stable and the main differences among them are associated with the orientation of the naphthyl methoxy groups and with the distance between the phenyls of the pickets, that are closer in **36A** than

**36B-D** (Figure 13). The second handle was then added to obtain **17** but no noteworthy difference was observed, therefore all the other calculations were performed using ligand **36**. Also **Fe(36)OMe** was modelled and, as in the case of **Fe(35)OMe**, two preferred conformations were found.

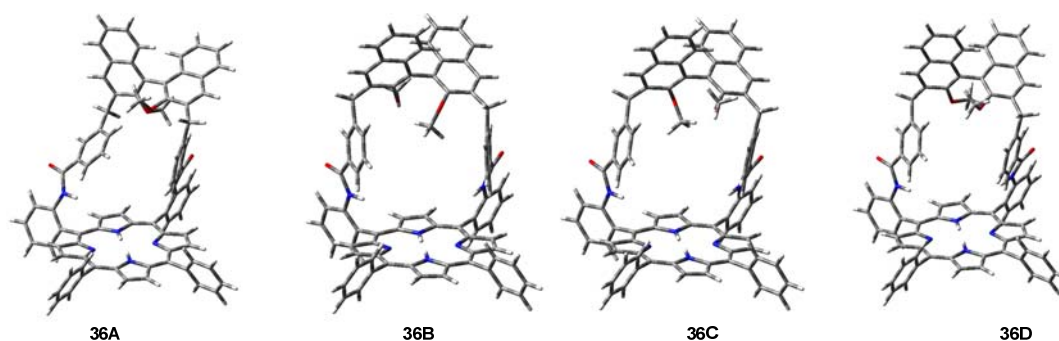


**Figure 13.** Preferred conformers of single-handed porphyrin **36**.

Our attention then focused on the cyclopropanation reaction and its intermediates. As reported in chap. 2.1.1., two active carbene species (*terminal* or *bridging*) are supposed to be the intermediates in the cyclopropanation reactions. The calculations were performed using the iron complex of the unsubstituted porphine, **Fe(porphine)OMe**. The data showed that the most stable carbene species is the *bridging-Fe(porphine)OMe*, in contrast with the other iron carbene porphyrin reported in literature.<sup>27</sup> Since the pickets and the binaphthyl moieties confer a rigidity to the structure, it was mandatory to study the carbene species of **Fe(35)OMe** and **Fe(36)OMe**. In both cases, we obtained the same results observed in the case of **Fe(porphine)OMe**.

At this point we moved to the *end-on* attack of  $\alpha$ -methylstyrene to the carbene species starting with the less hindered **Fe(PPP)OMe**-carbene intermediate. The *trans* and *cis* transition states (TS) showed a very asynchronous but concerted formation of the two new C-C bonds of cyclopropane without observation of any intermediate radical species. In addition, we studied the reverse reaction from the transition states to the reagents, obtaining  $\alpha$ -methylstyrene and *terminal* carbene. This result suggested that the *terminal* carbene should be the active catalytic species and thus the attack to the alkene must be preceded by the conversion of the carbene from the *bridging* to the *terminal* mode.

Finally, the structure of porphyrin **36** was built around the *trans*- and *cis*-TSs obtaining four transition states which produced four stereomeric cyclopropanes (two enantiomers for two diastereomers). The two *trans*-TSs resulted more stable than the *cis*-TSs, in agreement with the experimental data, but the energetic difference between the two *trans*-TSs was very low (Figure 14). This result can be explained with the wide distance of the chiral binaphthyl group from the catalytic site which makes the chiral moiety unable to produce a complete differentiation of the enantiomeric reaction paths and justifying the not excellent enantioselectivity of the catalyst.

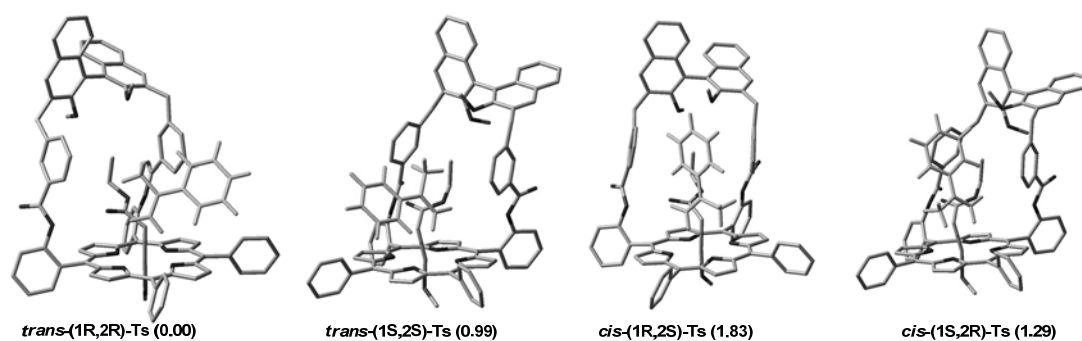


**Figure 14.** Transition states for the end-on attack of  $\alpha$ -methylstyrene at the terminal carbene deriving from **Fe(36)OMe** (relative energy values, kcal mol<sup>-1</sup>).

## 2.2. Synthesis of amino ester and glycoside conjugates porphyrin ligands

The iron(III) complex **Fe(17)OMe**, as reported above, exhibits a ‘Totem’ structure formed by three independent elements. These elements show different and complementary catalytic roles and each of them can be replaced to obtain a library of ‘Totem porphyrin ligands’ showing different chemical features (Figure 15). Furthermore, in collaboration with Dr. B. Boitrel (Université de Rennes 1, France), we synthesised new porphyrin ligands by modifying one element of porphyrin **17** making a small porphyrin library.

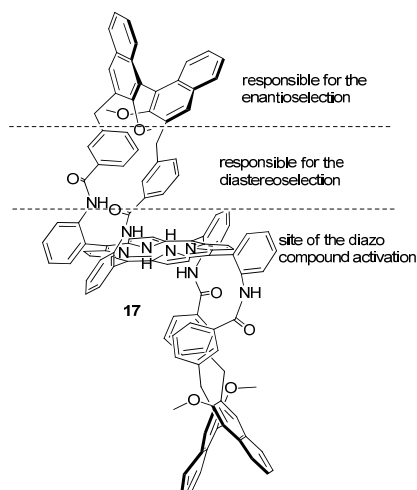
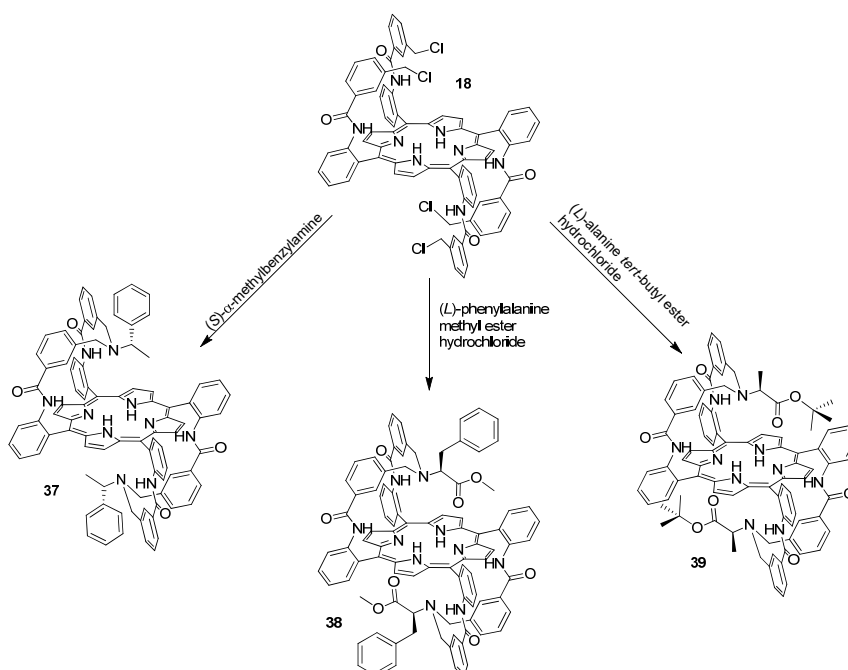


Figure 15. Totem structure of chiral porphyrin **17**.

### 2.2.1. Synthesis of glycoside and amino ester conjugates porphyrins

The first element that we decided to replace was the binaphthyl group, which is responsible for the catalytic enantioselectivity, with more biocompatible groups such as amino acids or glycoside groups.

First, the benzylic functionality of porphyrin **18** was reacted with the primary amino group of either chiral amines and natural amino ester compounds. The first porphyrin **37** was synthesised in good yield (67%) through the reaction between porphyrin **18** and (*S*)- $\alpha$ -methylbenzylamine in presence of potassium carbonate ( $K_2CO_3$ ) and sodium iodide (NaI) (Scheme 21).



Scheme 21. Synthesis of porphyrin **37**, **38** and **39**.

Using similar experimental conditions, we also synthesised porphyrin **38** and **39** where (*L*)-phenylalanine methyl ester and (*L*)-alanine tert-butyl ester replaced the binaphthyl group as the chiral group, thus improving the biocompatibility of our system introducing a natural amino acid in the structure (Scheme 21). All porphyrins were fully characterised and their three-dimensional pre-organisation was confirmed by NMR analysis. All characteristic protons placed in alpha positions with respect to the stereogenic centre are shifted toward lower ppm values due to the anisotropic effect of the porphyrin core. Furthermore, studying the NMR spectra of porphyrin **38** we can confirm the pinched conformation of the strap lying above the porphyrin thanks to the 2D NMR NOE correlations between the aromatic protons labelled 13 and the  $\beta$ -pyrrolic protons labelled a (Figure 16, red arrow).

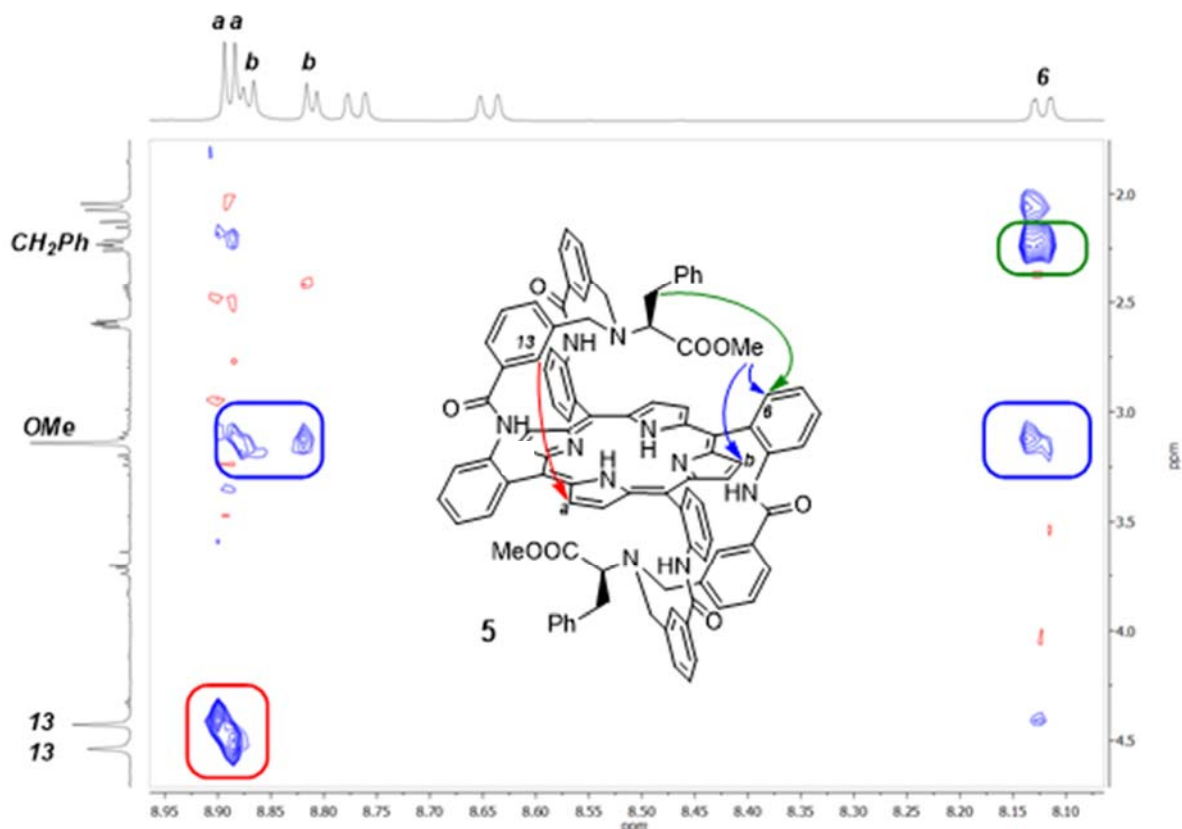


**Figure 16.** 2D ROESY NMR spectrum of porphyrin **38**.

NOE correlations were also observed between the OMe protons and (i) *meso*-aromatic protons labelled 6 and (ii)  $\beta$ -pyrrolic protons labelled b (Figure 16, blue arrows), as well as between the CH<sub>2</sub>Ph protons and the *meso*-aromatic protons labelled 6 (Figure 16, green arrow).

For porphyrin **38**, single crystals were obtained and the X-ray analysis showed the presence of two different conformations **A** and **B** in the solid state (Figure 17). The difference between the two conformations **A** and **B** regards the spatial location of the ester and lateral chain groups. In the case of **A**, the straps in the upper and lower sides have the same orientation, in fact both phenyl groups of the amino acid moieties point away from the porphyrin core. On the contrary, in conformation **B** the two straps have a different orientation in the upper strap: the ester group and the phenyl group are inverted and ester does not point anymore to the centre of the porphyrin, but to the outside. Although in solid state it is possible to observe the two conformations, in solution it is not possible (NMR analysis) and this means that **A** and **B** coexist in equilibrium.



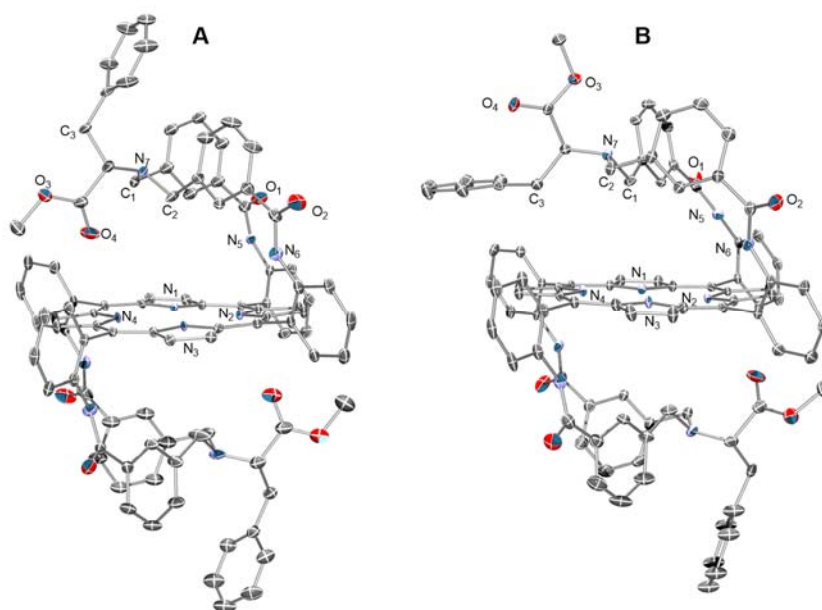
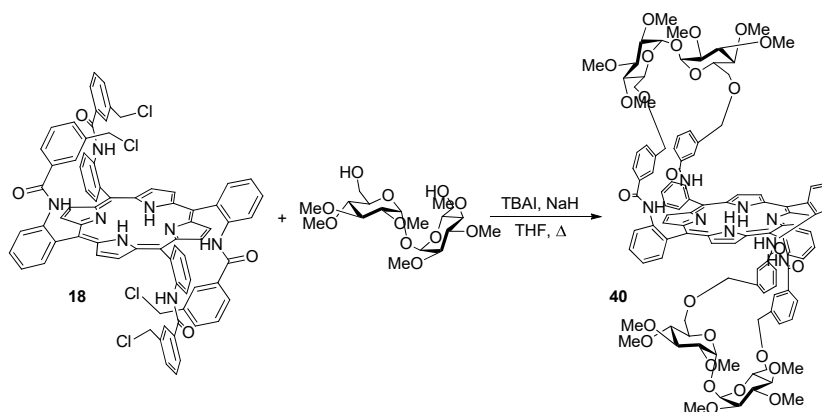


**Figure 17.** X-ray structure of porphyrin **38** (conformation A and B).

Then, we synthesised a glycoporphyrin ligand by using  $\alpha$ -trehalose, which was synthesised by prof. L. Lay's group (Università degli Studi di Milano, Italy), as the chiral glycoside 'hat' of the Totem structure. The reaction, carried in THF/DMF in presence of sodium hydride, formed the desired porphyrin **40** in 20% yield (Scheme 22).

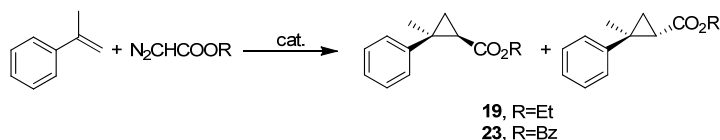


**Scheme 22.** Synthesis of porphyrin **40**.

The reaction of **37**, **38**, **39** and **40** with  $\text{FeBr}_2$  formed respectively **Fe(37)OMe**, **Fe(38)OMe**, **Fe(39)OMe** and **Fe(40)OMe** by the initial formation of an iron(II) porphyrin complex which was oxidised by air in presence of methanol yielding the desired complex in a quantitative yield. First of all, we tested the catalytic activity of complex **Fe(39)OMe** in the model cyclopropanation reaction between  $\alpha$ -methylstyrene and EDA (table 1, entry 1). Even if the reaction time was very short and the yield was good, the enantioselectivity was very low. The best result in term of *ee* was obtained when the reaction was run at  $0^\circ\text{C}$  (table 1, entry 3). It should be noted that in each case only the minor *cis*-isomer of **19** was formed with a moderate enantiocontrol in contrast with the results observed in the **Fe(17)OMe**-catalysed reactions. Regarding the diastereoselectivity, complex **Fe(39)OMe** showed a very high *trans*-diastereocontrol and this data confirmed that the diastereocontrol is independent from the nature of the chiral moiety and depends on the three-dimensional pre-organisation.

In order to improve the stereocontrol, the cyclopropanation reaction was performed using the more sterically hindered benzyl diazoacetate (BDA) as carbene source. Unfortunately, in this case the major *trans*-isomer of **23** was obtained in low *ee*, whereas the minor *cis*-isomer was formed with good enantioselectivity.

**Table 1.** Cyclopropanation reactions of  $\alpha$ -methylstyrene and diazocompounds.<sup>a</sup>



entry	Catalyst	diazo reagent	t (min) <sup>b</sup>	yield (%) <sup>c</sup>	<i>trans/cis</i> (%) <sup>c</sup>	<i>ee</i> <sub><i>trans</i></sub> (%) <sup>d</sup>	<i>ee</i> <sub><i>cis</i></sub> (%) <sup>d</sup>
1	<b>Fe(39)OMe</b>	EDA	5	<b>19</b> , 65	90:10	4.2	9
2 <sup>e</sup>	<b>Fe(39)OMe</b>	EDA	60	<b>19</b> , 90	89:11	4	12
3 <sup>f</sup>	<b>Fe(39)OMe</b>	EDA	5	<b>19</b> , 52	88:12	4	53
4	<b>Fe(39)OMe</b>	BDA	10	<b>23</b> , 50	93:7	1	69
5 <sup>e</sup>	<b>Fe(39)OMe</b>	BDA	60	<b>23</b> , 40	88:12	9	68
6 <sup>e,f</sup>	<b>Fe(39)OMe</b>	BDA	60	<b>23</b> , 45	90:10	4	72
7	<b>Fe(37)OMe</b>	EDA	5	<b>19</b> , 75	90:10	8	50
8	<b>Fe(38)OMe</b>	EDA	5	<b>19</b> , 78	95:5	9	54
9	<b>Fe(40)OMe</b>	EDA	4 hours	<b>19</b> , 65	98:2	2	60

<sup>a</sup>Reaction conditions: catalyst/ $\alpha$ -methylstyrene/diazo compound 1:1000:1100 in 2.5 mL of benzene at 25°C. <sup>b</sup>Time required for the EDA conversion monitored by IR spectroscopy. <sup>c</sup>Determined by <sup>1</sup>H NMR using 2,4-dinitrotoulene as internal standard. <sup>d</sup>Enantiomeric excess determined by HPLC analysis (DAI-CEL CHIRALCEL, IB, hexane/2-propanol=99.75:0.25). <sup>e</sup>The diazo compound was added by a syringe pump. <sup>f</sup>Reaction performed at 0°C.

We also tested the catalytic activity of the other complexes in the model reaction. Very good yields and excellent *trans*-diastereoselectivities were obtained, but even in these reactions the enantioselectivity resulted very low. Data obtained with **Fe(38)OMe** indicated that the more sterically hindered benzyl group of the (*L*)-phenylalanine's stereogenic centre did not confer a more rigidity to the chiral 'hat' and consequently a discrimination of the two enantiomers.

The lack of enantiocontrol, obtained with all complexes, was probably due to the long distance between the chiral bulk and the active metal centre, therefore, to better rationalise these data, a DFT study was carried out by Prof. L. Toma and Dr. L. Legnani of the University of Pavia.

### 2.2.2. DFT theoretical studies

The X-ray structure of porphyrin **38** reveals the presence of two different conformations, **A** and **B**, in which the chiral amino acid moiety shows a bent orientation. This orientation of the chiral 'hat' should have a heavy influence on the stereocontrol of the catalyst **Fe(38)OMe** during the cyclopropanation reaction and give better values of enantioselectivity. However, the low values of *ee* suggest that probably **A** and **B** are not the only ligand geometries which can be formed during the cyclopropanation reaction. Since our hypothesis foresees the formation of other geometrical arrangements of **38** different from **A** and **B**, we started studying all the conformations which can be assumed by **38**.

Initially, we used a simplified model porphyrin, porphyrin **41**, which showed only one strap and a methyl group instead of the chiral moiety. The optimization of the calculations gave five favourite geometries, **41A-E** (Figure 18).

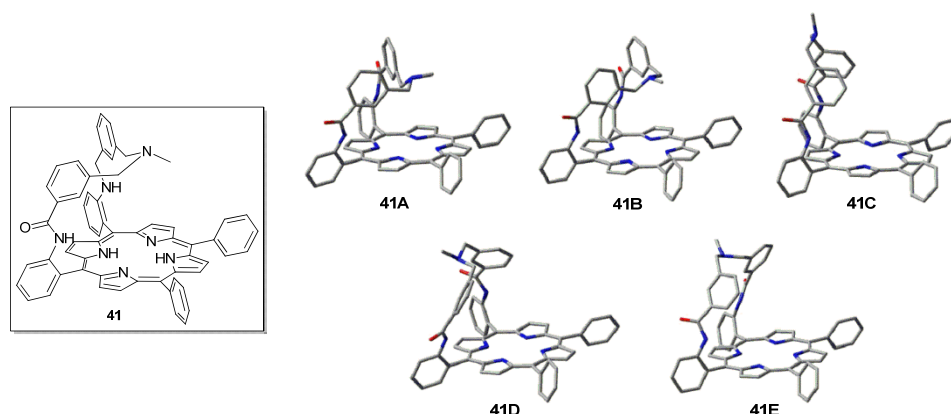


**Figure 18.** Model compound **41** and its preferred conformers.

The straps in conformers **41A** and **41B** show a bent orientation, such as **A** and **B**, and the methyl group points towards the porphyrin core. On the contrary, in conformers **41C-E** the methyl group points away from the molecular centre leaving an empty space above the porphyrin. The attention was then turned towards the transition states (TS) of the cyclopropanation reaction with EDA using the model structure previously described (chap. 2.1.3.). The ethyl group of the carbene moiety can show two different orientations, one pointing inside the handle and the other one pointing outside it. In all the cases we found a preference for the outside orientation, so we focused our attention on this arrangement.

The **41D-TS** and **41E-TS** resulted the most stable transition states due to the presence of the large pocket which favoured the accommodation of the carbene (Figure 19). Moreover, in all the cases the *trans*-TS are preferred over the *cis*-TS confirming the experimental data. Finally, the transition states of ligand **42** and **43**, containing a chiral moiety, were built in the *S* configuration like our porphyrins. The computational data, similar for both ligands, agreed with those obtained experimentally; the enantioselectivity was very poor for the *trans* product and better but not excellent for the *cis* one. This result is explained by a limited influence of the chiral moiety which pointed away from the reaction site.

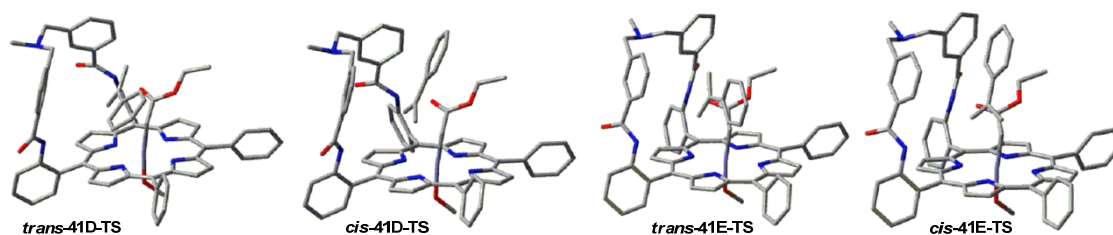


**Figure 19.** Lowest energy transition states for the attack of  $\alpha$ -methylstyrene to carbene species deriving from **41**.

### 2.2.3 Synthesis of new ‘Totem’ porphyrins

The data collected from the catalytic activity of ‘Totem’ porphyrins **37**, **38** and **39** revealed a poor influence of the chiral moieties on the reaction enantiocontrol, probably for the long distance of the chiral bulk from the active site where the reaction takes place. Therefore, we decided to synthesise a new class of ‘Totem’ porphyrins which show a three-dimensional conformation similar to those observed for other porphyrin ligands, but with a chiral moiety closer to the porphyrin core to better discriminate an enantio-pathway. First, we synthesised  $\alpha_2\beta_2$ -tetra[(2-methoxy-2-phenyl)acetamide] phenyl porphyrin, **44** by reaction of atropisomer

$\alpha_2\beta_2$  of *meso*-tetra(2-amino)phenyl porphyrin (o-TAPPH<sub>2</sub>) with (*R*)-2-methoxy-2-phenylacetic chloride. Porphyrin **44** (70% yield) was fully characterised and a single crystal was obtained and analysed by X-ray analysis (Figure 20).

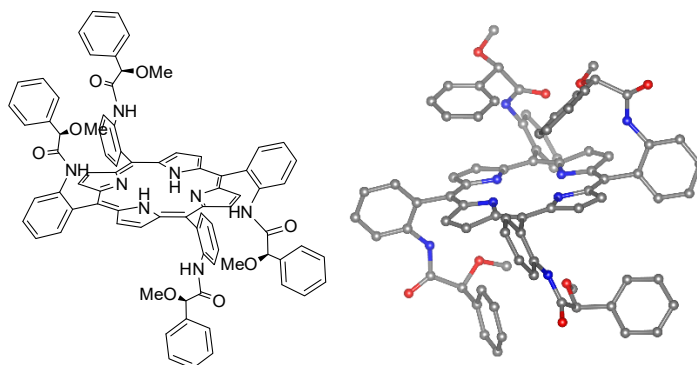
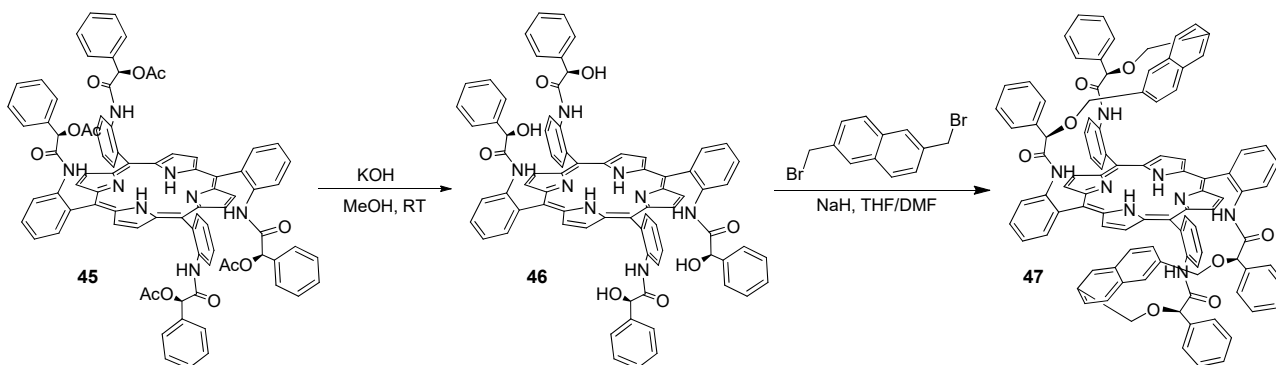


**Figure 20.** Porphyrin **44** and its crystal structure.

Then we synthesised the iron(III) porphyrin complex, **Fe(44)OMe**, which was tested in the model cyclopropanation reaction between  $\alpha$ -methylstyrene and EDA to form cyclopropane **19** in a very short time, good yield (70%) and *trans*-diastereoselectivity (*trans/cis*=77:23). Unfortunately, the enantioselectivity resulted very low (10% *ee*<sub>*trans*</sub> and 8% *ee*<sub>*cis*</sub>). This result is explained by the great mobility of the four pickets, which are not able to discriminate between the two enantiomeric pathways. Therefore, we decided to functionalise the pickets with a naphthyl group in order to decrease the mobility of the molecule. The new *bis*-strapped porphyrin **47** was synthesised by using  $\alpha_2\beta_2$ -tetra[(2-acetoxy-2-phenyl)acetamide] phenyl porphyrin as starting material. This was obtained by the reaction of o-TAPPH<sub>2</sub> with (*R*)-2-acetoxy-2-phenylacetic chloride. Porphyrin **45** was treated with KOH in methanol to transform acetoxy into hydroxy groups and then the reaction of the last ligand with 2,6-*bis*-(dibromomethyl)naphthalene gave porphyrin **47** (Scheme 23).



**Scheme 23.** Synthesis of *bis*-strapped porphyrin **47**.

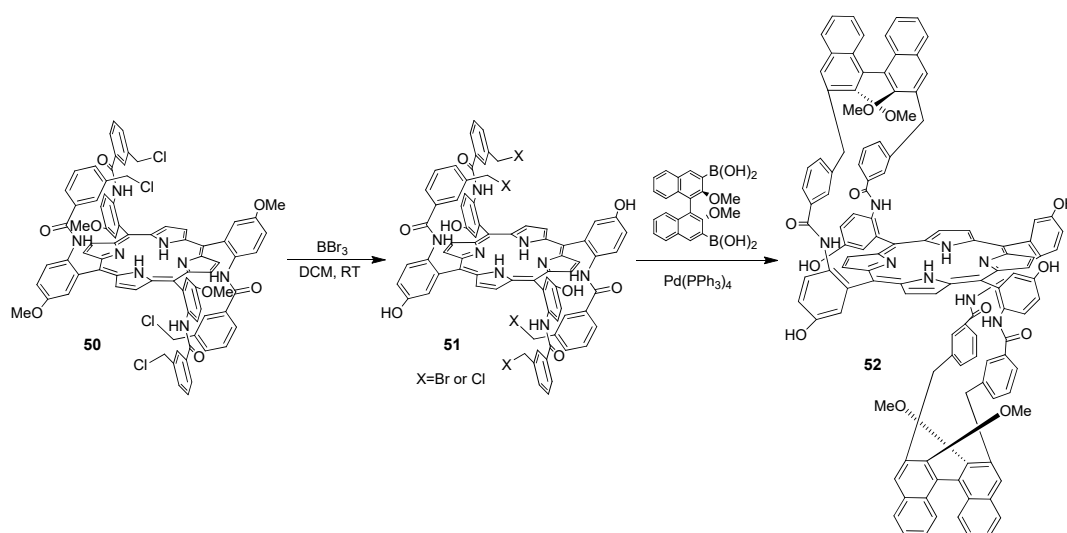
The synthesis, characterization and catalytic use of **Fe(47)OMe** complex is currently under investigation in our laboratory.

### 2.3. Synthesis of hydrophilic ‘Totem’ porphyrin

Based on the basic principles of Green Chemistry ‘*An ideal solvent facilitates the mass transfer but does not dissolve!*’ and should be nontoxic, cheap and readily available. Considering these characteristics, water results one of the best natural solvents also for the possibility to carry out the reaction ‘on-water’. In an ‘on-water’ reaction, the reagents react by floating on water to generate a hydrophobic layer containing the product, which is readily separable from the reaction mixture. Therefore, it is important to synthesise a hydrophilic catalyst to use for this type of reaction.

In order to enlarge the library of ‘Totem’ porphyrin ligands and increase the versatility of our catalytic system, we decided to synthesise a hydrophilic ‘Totem’ ligand by modifying the porphyrin scaffold of porphyrin **17**.

We started by synthesising the mixture of the four atropoisomers of *meso*-tetra(5-methoxy-2-amino)phenyl porphyrin **49** reducing the corresponding nitro porphyrin **48** by stannous chloride dihydrate ( $\text{SnCl}_2 \cdot \text{H}_2\text{O}$ ) in HCl. The four atropoisomers were separated by column chromatography on silica gel and the  $\alpha_2\beta_2$  atropoisomer was reacted with 3-(chloromethyl)benzoylchloride to synthesise the porphyrin **50**.



**Scheme 24.** Synthesis of porphyrin **52**.

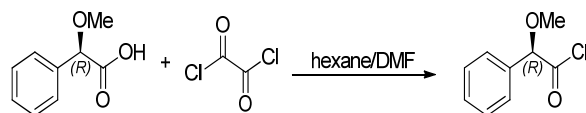
Porphyrin **50** was then treated with  $\text{BBr}_3$  to transform methoxy into hydroxy groups and then porphyrin **52** was obtained by a Suzuki coupling reaction with (*R*)-2,2'-dimethoxy-1,1'-binaphthyl-3,3'-diboronic acid in one step (Scheme 24). Unfortunately, the yield of this last step was very low due to the substitution of chlorine with bromine atoms in the previous step, which favoured the formation of porphyrin's polymers. The new porphyrin ligand so obtained is not soluble in water, but can be used as a precursor for the synthesis of other chiral porphyrin ligands by functionalisation of hydroxyl groups with hydrophilic groups such as PEG or others.

### 3. Experimental section

**General conditions:** Unless otherwise specified, all reactions were carried out under nitrogen or argon atmosphere employing standard Schlenk techniques and magnetic stirring. Dichloromethane, hexane, toluene, THF, DMF, pyrrole and alkenes were purified by using standard methods and stored under nitrogen atmosphere. All other starting materials were commercial products used as received. NMR spectra were recorded at room temperature on a Bruker Avance 300-DRX, operating at 300 MHz for  $^1\text{H}$ , at 75 MHz for  $^{13}\text{C}$  and 282 MHz for  $^{19}\text{F}$ , or on a Bruker Avance 400-DRX spectrometer, operating at 400 MHz for  $^1\text{H}$ , at 100 MHz for  $^{13}\text{C}$  and at 376 MHz for  $^{19}\text{F}$ , or on a Bruker Avance 500-DRX spectrometer operating at 500 MHz for  $^1\text{H}$  and at 125 MHz for  $^{13}\text{C}$ . Chemical shifts (ppm) are reported relative to TMS. The  $^1\text{H}$  NMR signals of the compounds described in the following were identified by 2 D NMR techniques. Assignments of the resonance in  $^{13}\text{C}$  NMR were made using the APT pulse sequence and HSQC and HMBC techniques. GC-MS analyses were performed on Shimadzu QP5050A instrument. Infrared spectra were recorded on a Varian Scimitar FTS 1000 spectrophotometer. UV/Vis spectra were recorded on an Agilent 8453E instrument.  $[\alpha]_{\text{D}}$  values were given in  $10^{-1} \text{ deg cm}^2 \text{ g}^{-1}$ . The ESR spectra were recorded from a sample powder at 77 K with Bruker EMX X-band spectrometer equipped with an Oxford cryostat. XRD were collected on a D8 VENTURE Bruker AXS diffractometer. Elemental analyses and mass spectra were recorded in the analytical laboratories of Milan and Rennes 1 Universities. XRD were collected on a D8 VENTURE Bruker AXS diffractometer.

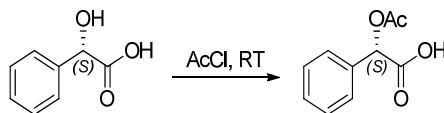
#### 3.1 Synthesis of organic precursors

##### 3.1.1. Synthesis of (*R*)-2-methoxy-2-phenylacetic chloride



(*R*)-2-Methoxy-2-phenylacetic acid (0.500 g,  $3.00 \cdot 10^{-3}$  mol) was dissolved in hexane (5.00 mL) and DMF (23.0  $\mu\text{L}$ ), then oxalyl chloride (2.58 mL,  $3.00 \cdot 10^{-2}$  mol) was added dropwise. The reaction was stirred overnight then the solvent was evaporated to dryness under reduced pressure and the crude was used without further purification.

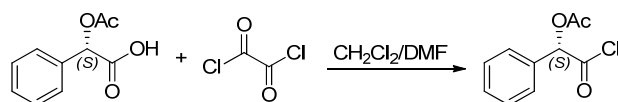
##### 3.1.2. Synthesis of (*S*)-2-acetoxy-2-phenylacetic acid



(*S*)-Mandelic acid (2.15 g,  $1.40 \cdot 10^{-2}$  mol) was dissolved in acetyl chloride (2.48 mL) and the reaction mixture was stirred at room temperature overnight. Then, acetyl chloride was evaporated to dryness to give the product as a yellow oil (0.788 g, 95.1%).

$^1\text{H}$  NMR (400 MHz,  $\text{CDCl}_3$ ):  $\delta$  11.45 (br, 1H,  $\text{HCOOH}$ ); 7.50-7.40 (m, 5H,  $\text{H}_{\text{Ar}}$ ), 5.95 (s, 1H,  $\text{H}_{\text{CH}}$ ), 2.20 ppm (s, 3H,  $\text{H}_{\text{CH}_3}$ ).

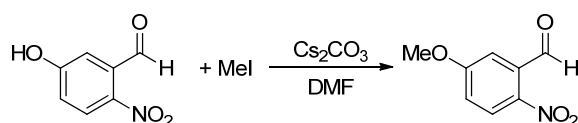
### 3.1.3. Synthesis of (*S*)-2-acetoxy-2-phenylacetic chloride



(*S*)-2-Acetoxy-2-phenylacetic acid (0.543 g,  $2.80 \cdot 10^{-3}$  mol) was dissolved in a solution of dichloromethane (12.0 mL) and DMF (70.0  $\mu$ L). Then, oxalyl chloride (2.40 mL,  $2.80 \cdot 10^{-3}$  mol) was added dropwise. The reaction was stirred overnight, then the solvent was evaporated to dryness under reduced pressure and the crude was used without furthermore purifications.

$^1\text{H NMR}$  (400 MHz,  $\text{CDCl}_3$ ):  $\delta$  7.50-7.45 (m, 5H,  $\text{H}_{\text{Ar}}$ ), 6.08 (s, 1H,  $\text{H}_{\text{CH}}$ ), 2.22 ppm (s, 3H,  $\text{H}_{\text{CH}_3}$ ).

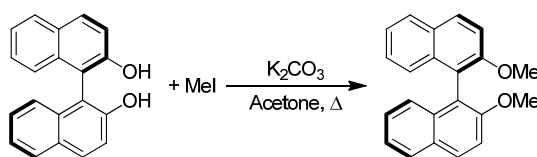
### 3.1.4. Synthesis of 5-methoxy-2-nitrobenzaldehyde



5-Hydroxy-2-nitrobenzaldehyde (25.0 g,  $0.150 \cdot 10^{-1}$  mol) and cesium carbonate (48.9 g,  $0.150 \cdot 10^{-1}$  mol) were dissolved in DMF. The orange solution was cooled at  $0^\circ\text{C}$  and methyl iodide (21.3 g,  $0.150 \cdot 10^{-1}$  mol) was added dropwise. The reaction mixture was stirred at room temperature for 3 days and then water (200 mL) and ethyl acetate (200 mL) were added. The organic phase was separated and extracted with AcOEt (100 mL for three times). The combined organic phase was then washed with water (200 mL), dried over  $\text{NaSO}_4$ , filtered and the solvent was evaporated to dryness under reduced pressure. The so-obtained yellowish solid was washed several times with diethyl ether to obtain a white solid (18.4 g, 67%).

$^1\text{H NMR}$  (400 MHz,  $\text{CDCl}_3$ ):  $\delta$  10.49 (s, 1H,  $\text{HCHO}$ ), 8.17 (d, 1H,  $J=9.05$  Hz,  $\text{H}_m$ ), 7.33 (d, 1H,  $^4J=2.87$  Hz,  $\text{H}_o$ ), 7.15 (dd, 1H,  $J=9.06$  and  $^4J=2.88$  Hz,  $\text{H}_p$ ), 3.96 ppm (s, 1H,  $\text{H}_{\text{OCH}_3}$ ).

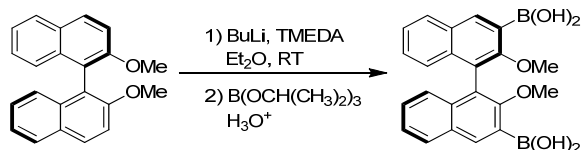
### 3.1.5. Synthesis of (*R*)-2,2'-dimethoxy-1,1'-binaphthalene



A suspension of (*R*)-(+)-1,1'-bi(2-naphthol) (3.01 g,  $1.05 \cdot 10^{-2}$  mol) in acetone (45.0 mL) was heated at  $50^\circ\text{C}$  to give a homogeneous solution. Then potassium carbonate (4.95 g,  $3.50 \cdot 10^{-2}$  mol) and methyl iodide (3.92 mL,  $6.30 \cdot 10^{-2}$  mol) were added and the mixture was refluxed for 12 hours. The mixture was concentrated to 10.0 mL and the residue was cooled to room temperature and treated with 50 mL of water. The mixture was stirred for 8 hours and a white solid was obtained. The resulting solid was collected in a filter, washed with water and dried to afford (*R*)-2,2'-dimethoxy-1,1'-dinaphthalene as a white powder (2.87 g, 87%).

$^1\text{H NMR}$  (300 MHz,  $\text{DMSO}-d_6$ ):  $\delta$  8.06 (d, 2H,  $J=9.0$  Hz,  $\text{H}_{\text{Ar}}$ ), 7.94 (d, 2H,  $J=8.0$  Hz,  $\text{H}_{\text{Ar}}$ ), 7.60 (d, 2H,  $J=9.0$  Hz,  $\text{H}_{\text{Ar}}$ ), 7.31 (t, 2H,  $J=7.3$  Hz,  $\text{H}_{\text{Ar}}$ ), 7.21 (t, 2H,  $J=7.6$  Hz,  $\text{H}_{\text{Ar}}$ ), 6.89 (d, 2H,  $J=8.4$  Hz,  $\text{H}_{\text{Ar}}$ ), 3.70 ppm (s, 6H,  $\text{H}_{\text{CH}_3}$ ).

### 3.1.6. Synthesis of (*R*)-2,2'-dimethoxy-1,1'-binaphthyl-3,3'-diboronic acid

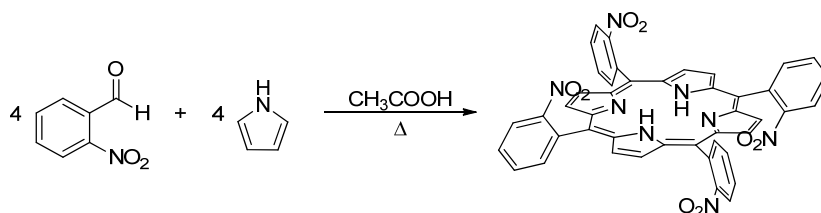


1.6 M BuLi in hexane (3.04 mL,  $4.87 \cdot 10^{-3}$  mol) was added at room temperature to a solution of tetramethylethylenediamine (0.973 mL,  $6.49 \cdot 10^{-3}$  mol) in diethyl ether (25.0 mL) and the reaction mixture was stirred at room temperature for 30 minutes. Then, (*R*)-2,2'-dimethoxy-1,1'-dinaphthalene (0.510 g,  $1.62 \cdot 10^{-3}$  mol) was added in one portion and the reaction mixture was stirred for 3 hours. The resulting light brown suspension was cooled to  $-78^{\circ}\text{C}$  and triisopropyl borate (2.24 mL,  $9.73 \cdot 10^{-3}$  mol) was added over a period of 10 minutes. The solution was allowed to warm to room temperature and stirred for 12 hours. The reaction mixture was then cooled to  $0^{\circ}\text{C}$  and 1M HCl solution (15.0 mL) was added. The resulting solution was stirred at room temperature for 2 hours. The organic layer was washed with 1M HCl solution and brine, dried over Na<sub>2</sub>SO<sub>4</sub> and the solvent was evaporated to dryness. The product was finally dried *in vacuo* (0.652, 99%).

<sup>1</sup>H NMR (300 MHz, CDCl<sub>3</sub>):  $\delta$  8.62 (s, 2H, H<sub>Ar</sub>), 7.99 (d, 2H,  $J=8.1\text{Hz}$ , H<sub>Ar</sub>), 7.44 (t, 2H,  $J=7.2\text{Hz}$ , H<sub>Ar</sub>), 7.32 (t, 2H,  $J=7.4\text{Hz}$ , H<sub>Ar</sub>), 7.16 (d, 2H,  $J=8.7\text{Hz}$ , H<sub>Ar</sub>), 6.03 (s, 2H, H<sub>Ar</sub>), 3.31 (s, 6H, H<sub>CH<sub>3</sub></sub>).

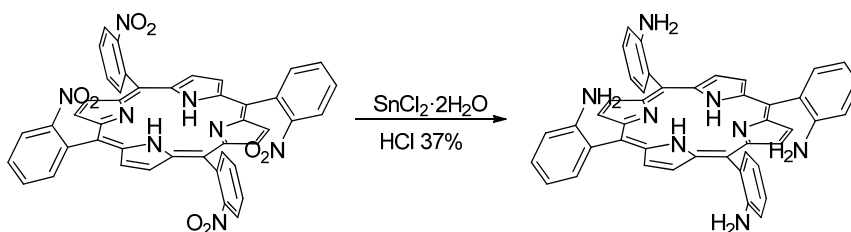
## 3.2. Synthesis of porphyrin ligands

### 3.2.1. Synthesis of *meso*-tetra(2-nitrophenyl) porphyrin (o-TNPPH<sub>2</sub>)



2-Nitrobenzaldehyde (101 g,  $6.72 \cdot 10^{-1}$  mol) was dissolved in acetic acid (2.00 L) in air. The solution was slowly brought to reflux and then distilled pyrrole (45.7 mL,  $6.59 \cdot 10^{-1}$  mol) was added dropwise in about 15 minutes. The mixture was refluxed for 45 minutes and during this period the mixture turned to red at first, then to deep black. The dark solution was allowed to cool at  $60^{\circ}\text{C}$  and then chloroform (500 mL) was gradually added obtaining a dark suspension. The obtained solid was filtered, washed with dichloromethane and dried *in vacuo* (10.7 g, 8.2%).

### 3.2.2. Synthesis of *meso*-tetra(2-aminophenyl) porphyrin (o-TAPPH<sub>2</sub>)



o-TNPPH<sub>2</sub> (36.0 g,  $4.53 \cdot 10^{-2}$  mol) was dissolved in HCl 37% (1.50 L) under vigorous magnetic stirring and then SnCl<sub>2</sub>·2H<sub>2</sub>O (153 g,  $6.79 \cdot 10^{-1}$  mol) was slowly added. The resulting green mixture was stirred at room temperature in air for 48 hours, then chloroform (1.00 L) was added. After 15 minutes the solution was cooled to  $0^{\circ}\text{C}$  and a saturated solution of KOH was added dropwise until a pH=10. The organic phase was separated

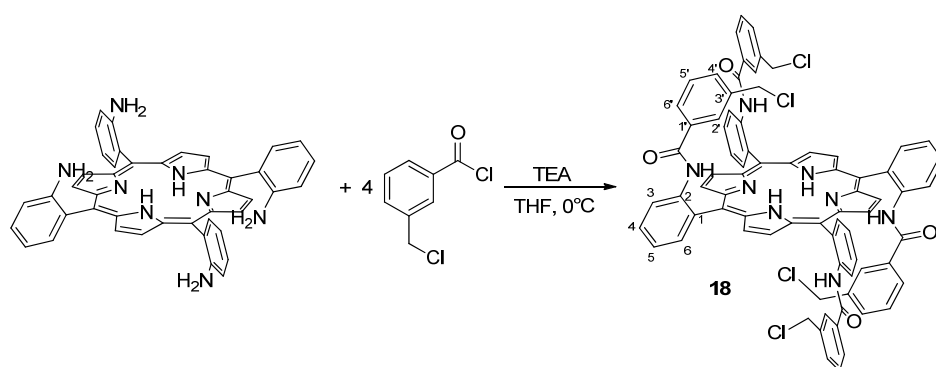


and filtered over septum to separate the solid. The aqueous phase was extracted several times with chloroform. The combined organic phase was evaporated under reduced pressure to obtain a dark purple solid containing the four atropoisomers.

The four atropoisomers were separated by flash chromatography (silica gel, 15  $\mu\text{m}$ ) with  $\text{CH}_2\text{Cl}_2$  for  $\alpha\beta$  (12.5%), 0.5% MeOH for  $\alpha_2\beta_2$  (25%), 3% MeOH for  $\alpha_3\beta$  (50%) and 5% MeOH for  $\alpha_4$  (12.5%).

**$\alpha_2\beta_2$  o-TAPPH<sub>2</sub>**: <sup>1</sup>H NMR (400 MHz,  $\text{CDCl}_3$ ):  $\delta$  8.92 (s, 8H,  $\text{H}_\beta$ ), 7.86 (d, 4H,  $J=7.4$  Hz,  $\text{H}_{\text{Ar}}$ ), 7.26 (t, 4H,  $J=7.8$  Hz,  $\text{H}_{\text{Ar}}$ ), 7.18 (t, 4H,  $J=7.4$  Hz,  $\text{H}_{\text{Ar}}$ ), 7.14 (d, 2H,  $J=8.1$  Hz,  $\text{H}_{\text{Ar}}$ ), 3.58 (s, 8H,  $\text{NH}_2$ ), -2.65 ppm (s, 2H,  $\text{NH}_{\text{pyr}}$ ).

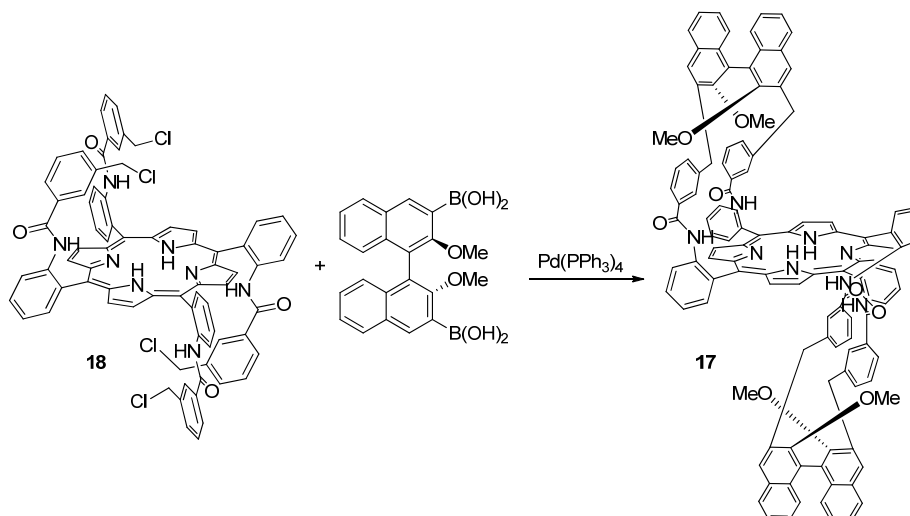
### 3.2.3. Synthesis of $\alpha_2\beta_2$ -tetra{2-[(3-chloromethyl)benzoylamido]phenyl} porphyrin (18)



The atropoisomer  $\alpha_2\beta_2$  of TAPPH<sub>2</sub> (2.90 g,  $4.29 \cdot 10^{-3}$  mol) was dissolved in THF (330 mL) at room temperature and TEA (4.78 mL,  $3.43 \cdot 10^{-3}$  mol) was added to the solution. The dark solution was cooled to 0°C and then 3-(chloromethyl)benzoyl chloride (3.65 mL,  $2.57 \cdot 10^{-2}$  mol) was added dropwise. The solution was stirred for 45 minutes at room temperature then MeOH was added to quench the reaction. The solvent was evaporated to dryness under reduced pressure and the crude was purified by flash chromatography (silica gel, 15  $\mu\text{m}$ , 0.5% MeOH in  $\text{CH}_2\text{Cl}_2$ ) to obtained dark purple solid (5.10 g, 92.5%).

<sup>1</sup>H NMR (400 MHz,  $\text{CDCl}_3$ ):  $\delta$  8.96 (s, 4H,  $\text{H}_\beta$ ), 8.95 (s, 4H,  $\text{H}_\beta$ ), 8.86 (d, 4H,  $J=8.4$  Hz,  $\text{H}^3$ ), 8.03 (d, 4H,  $J=6.5$  Hz,  $\text{H}^6$ ), 7.91 (t, 4H,  $J=8.5$  Hz,  $\text{H}^4$ ), 7.61 (s, 4H,  $-\text{HCONH}$ ), 7.57 (t, 4H,  $J=7.5$  Hz,  $\text{H}^5$ ), 6.71 (d, 4H,  $J=7.7$  Hz,  $\text{H}^{6'}$ ), 6.51 (s, 4H,  $\text{H}^{2'}$ ), 6.48 (d, 4H,  $J=6.7$  Hz,  $\text{H}^{4'}$ ), 6.35 (t, 4H,  $J=7.7$  Hz,  $\text{H}^{5'}$ ), 3.53 (d, 4H,  $J=12.1$  Hz,  $\text{H}_{\text{CH}_2}$ ), 3.48 (d, 4H,  $J=12.1$  Hz,  $\text{H}_{\text{CH}_2}$ ), -2.55 ppm (s, 2H,  $\text{NH}_{\text{pyr}}$ ).

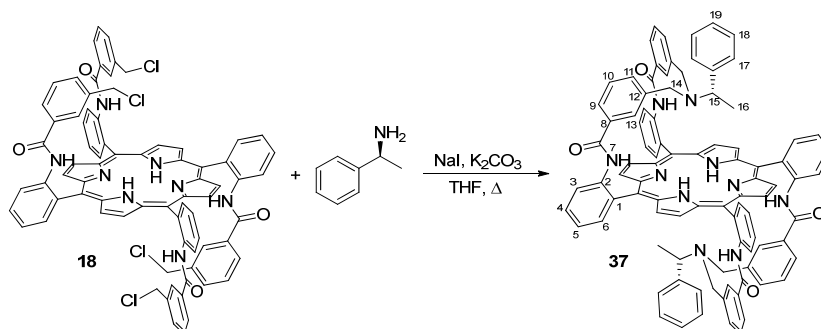
### 3.2.4. Synthesis of $\alpha_2\beta_2$ -bis{2,2'-[3,3'-(2,2'-dimethoxy-(1,1'-binaphthyl)benzoyl amido)}phenyl porphyrin (17)



Porphyrin **18** (0.300 g,  $2.33 \cdot 10^{-5}$  mol), (*R*)-2,2'-dimethoxy-1,1'-binaphthyl-3,3'-diboronic acid (0.226 g,  $5.60 \cdot 10^{-4}$  mol), tetrakis((triphenyl)phosphine) palladium(0) (0.108 g,  $9.34 \cdot 10^{-5}$  mol) and potassium carbonate (0.516 g,  $3.71 \cdot 10^{-3}$  mol) were dissolved in 16.0 mL of toluene, 5.0 mL of ethanol and 8.0 mL of water. The biphasic solution was refluxed for 4 hours until the complete consumption of **18** that was monitored by TLC (1% MeOH in  $\text{CH}_2\text{Cl}_2$ ). The resulting mixture was allowed to reach room temperature and the biphasic solution was diluted with 50.0 mL of saturated aqueous  $\text{NH}_4\text{Cl}$  and 50.0 mL of  $\text{CH}_2\text{Cl}_2$  and then it was separated. The aqueous phase was extracted with  $\text{CH}_2\text{Cl}_2$  (50.0 mL added two times), and the combined organic phases were washed with 50.0 mL of water and 50.0 mL of saturated aqueous  $\text{NaHCO}_3$ . The organic phase was dried over  $\text{Na}_2\text{SO}_4$  and filtered. The filtrate was evaporated to dryness *in vacuo* and then the residue was purified by flash chromatography (silica gel, 15  $\mu\text{m}$ , 0.5% MeOH in  $\text{CH}_2\text{Cl}_2$ ) to obtain the product (0.143 g, 35 %).

$^1\text{H NMR}$  (500 MHz,  $\text{CDCl}_3$ ):  $\delta$  9.07 (t, 2H,  $J=8$  Hz,  $\text{H}_{\text{Ar-meso}}$ ), 9.00 (s, 2H,  $\text{H}_\beta$ ), 8.95 (s, 2H,  $\text{H}_\beta$ ), 8.94 (d, 2H,  $J=4$  Hz,  $\text{H}_\beta$ ), 8.90 (t, 2H,  $J=8$  Hz,  $\text{H}_{\text{Ar-meso}}$ ), 8.88 (d, 2H,  $J=4$  Hz,  $\text{H}_\beta$ ), 7.98 (dd, 2H,  $^1J=1$  Hz,  $^2J=8$  Hz,  $\text{H}_{\text{Ar-meso}}$ ), 7.89 (dt, 2H,  $^1J=1$  Hz,  $^2J=8$  Hz,  $\text{H}_{\text{Ar-meso}}$ ), 7.86 (dt, 2H,  $^1J=1$  Hz,  $^2J=8$  Hz,  $\text{H}_{\text{Ar-meso}}$ ), 7.85 (s, 2H,  $\text{HNHCO}$ ), 7.83 (dd, 2H,  $^1J=1$  Hz,  $^2J=8$  Hz,  $\text{H}_{\text{Ar-meso}}$ ), 7.70 (d, 4H,  $J=8$  Hz,  $\text{H}_{\text{Ar-binap}}$ ), 7.64 (s, 2H,  $\text{H}_{\text{Ar-binap}}$ ), 7.63 (s, 2H,  $\text{H}_{\text{Ar-binap}}$ ), 7.62 (s, 2H,  $\text{HNHCO}$ ), 7.51 (dt, 2H,  $^1J=1$  Hz,  $^2J=8$  Hz,  $\text{H}_{\text{Ar-meso}}$ ), 7.49 (dt, 2H,  $^1J=1$  Hz,  $^2J=8$  Hz,  $\text{H}_{\text{Ar-meso}}$ ), 7.32 (s, 2H,  $\text{H}_{\text{Ar-strap}}$ ), 7.27 (m, 2H,  $\text{H}_{\text{Ar-binap}}$ ), 7.19 (s, 2H,  $\text{H}_{\text{Ar-strap}}$ ), 7.07 (m, 2H,  $\text{H}_{\text{Ar-binap}}$ ), 6.90 (d, 2H,  $J=8$  Hz,  $\text{H}_{\text{Ar-binap}}$ ), 6.83 (d, 2H,  $J=8$  Hz,  $\text{H}_{\text{Ar-binap}}$ ), 6.67 (d, 2H,  $J=8$  Hz,  $\text{H}_{\text{Ar-strap}}$ ), 6.39 (d, 2H,  $J=8$  Hz,  $\text{H}_{\text{Ar-strap}}$ ), 6.12 (t, 2H,  $J=8$  Hz,  $\text{H}_{\text{Ar-strap}}$ ), 5.98 (t, 2H,  $J=8$  Hz,  $\text{H}_{\text{Ar-strap}}$ ), 5.91 (d, 2H,  $J=8$  Hz,  $\text{H}_{\text{Ar-strap}}$ ), 5.78 (d, 2H,  $J=8$  Hz,  $\text{H}_{\text{Ar-strap}}$ ), 3.87 (d, 2H,  $J=8$  Hz,  $\text{H}_{\text{CH}_2}$ ), 3.72 (d, 2H,  $J=8$  Hz,  $\text{H}_{\text{CH}_2}$ ), 3.66 (d, 2H,  $J=8$  Hz,  $\text{H}_{\text{CH}_2}$ ), 3.55 (d, 2H,  $J=8$  Hz,  $\text{H}_{\text{CH}_2}$ ), 2.42 (s, 6H,  $\text{HOCH}_3$ ), 1.89 (s, 6H,  $\text{HOCH}_3$ ), -2.64 (s, 2H,  $\text{NH}_{\text{pyr}}$ ).

### 3.2.5. Synthesis of $\alpha_2\beta_2$ -bis(2,2'-{3,3'-[*N,N*-(1-phenylethane-1-amine)benzoyl amido]phenyl} porphyrin (37)

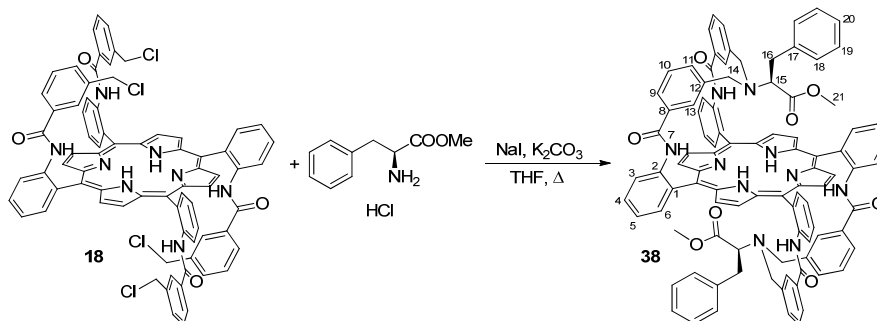


Porphyrin **18** (0.500 g,  $3.89 \cdot 10^{-4}$  mol), (*S*)- $\alpha$ -methylbenzylamine (0.235 g,  $1.94 \cdot 10^{-3}$  mol), NaI (0.583 g,  $3.89 \cdot 10^{-3}$  mol) and  $K_2CO_3$  (1.08 g,  $7.78 \cdot 10^{-3}$  mol) were dissolved in 450 mL of THF and 50.0 mL of DMF. The mixture was refluxed under stirring for 6 hours until the complete consumption of **18**, which was monitored by TLC (0.5% MeOH in  $CH_2Cl_2$ ). Then, the solvent was evaporated to dryness and 50.0 mL of  $CH_2Cl_2$  was added to the residue. The organic phase was extracted with 0.5 M HCl solution (50.0 mL added three times), water (50.0 mL added three times) and then dried over  $NaSO_4$  and filtered. The filtrate was evaporated to dryness under reduced pressure and the crude purified by flash chromatography (silica gel, 15  $\mu$ m, 0.2% MeOH in  $CH_2Cl_2$ ) to obtain a dark purple solid (0.359 g, 67%).

$^1H$  NMR (400 MHz,  $CDCl_3$ ):  $\delta$  9.19 (d, 2H,  $J=4.9$  Hz,  $H_\beta$ ), 9.15 (d, 2H,  $J=5.0$  Hz,  $H_\beta$ ), 8.99 (s, 2H,  $H_\beta$ ), 8.88 (d, 2H,  $J=8.2$  Hz,  $H^3$ ), 8.81 (s, 2H,  $H_\beta$ ), 8.60 (d, 2H,  $J=8.1$  Hz,  $H^3$ ), 8.23 (m, 4H,  $H^6$  and  $H^6$ ), 7.92 (m, 4H,  $H^4$  and  $H^4$ ), 7.60 (m, 4H,  $H^5$  and  $H^5$ ), 7.26 (m, 6H,  $H^7$  and  $H^{18}$ ), 7.19 (t, 2H,  $J=6.5$  Hz,  $H^9$ ), 7.17 (d, 2H,  $J=7.6$  Hz,  $H^{19}$ ), 7.06 (s, 2H,  $HCONH$ ), 7.0 (d, 4H,  $J=6.8$  Hz,  $H^{17}$ ), 6.79 (t, 2H,  $J=7.7$  Hz,  $H^{10}$ ), 6.70 (t, 2H,  $J=7.7$  Hz,  $H^{10}$ ), 6.69 (s, 2H,  $HCONH'$ ), 6.63 (d, 2H,  $J=7.7$  Hz,  $H^{11}$ ), 6.50 (d, 2H,  $J=7.6$  Hz,  $H^{11}$ ), 3.84 (s, 2H,  $H^{13}$ ), 2.89 (s, 2H,  $H^{13}$ ), 1.5 (d, 2H,  $^2J=13.0$  Hz,  $H^{14A}$ ), 1.16 (m, 2H,  $H^{15}$ ), -0.18 (d, 2H,  $^2J=13.0$  Hz,  $H^{14B}$ ), -0.35 (d, 2H,  $^2J=15.7$  Hz,  $H^{14A'}$ ), -0.54 (d, 6H,  $J=6.7$  Hz,  $H^{16}$ ), -0.73 (d, 2H,  $^2J=15.3$  Hz,  $H^{14B'}$ ), -2.04 ppm (s, 2H,  $NH_{pyr}$ ).

$^{13}C$  NMR (100 MHz,  $CDCl_3$ ):  $\delta$  207.0, 164.7, 164.6, 144.2, 140.4, 139.4, 138.4, 134.3, 133.9, 133.4, 132.6, 131.8, 131.3, 130.9, 130.8, 130.5, 130.0, 128.7, 128.6, 128.5, 127.3, 126.9, 125.9, 124.6, 124.0, 123.5, 122.0, 121.9, 120.7, 116.2, 115.7, 62.4, 55.6, 51.2, 31.7, 31.0, 29.2, 22.1, 18.1, 14.2, 11.6 ppm. **IR** ( $CH_2Cl_2$ ):  $\nu_{max}$ = 3683.1 (w), 3423.5 (w), 3312.4 (w), 1711.0 (w), 1683.8 (w), 1605.8 (w), 1581.5 (w), 1523.0 (w), 1448.1 (w), 1309.7 (w), 1259.3 (w), 1235.9  $cm^{-1}$  (w). **IR** (ATR):  $\nu_{max}$ = 3424.7 (w), 3309.2 (w), 1680.7 (w), 1605.1 (w), 1580.4 (w), 1514.5 (w), 1443.0 (w), 1304.4 (w), 1259.3 (w), 1235.9  $cm^{-1}$  (w). **UV-Vis** ( $CH_2Cl_2$ ):  $\lambda_{max}$  (log  $\epsilon$ ) 423 (5.37), 515 (4.16), 587 nm (2.67). **Elemental Analysis** calcd. for  $C_{92}H_{72}N_{10}O_4$ : C, 79.98; H, 5.25; N, 10.14. Found: C, 79.56; H, 5.07; N, 9.98. **MS** (ESI):  $m/z=1381.5$  [ $M^+$ ].

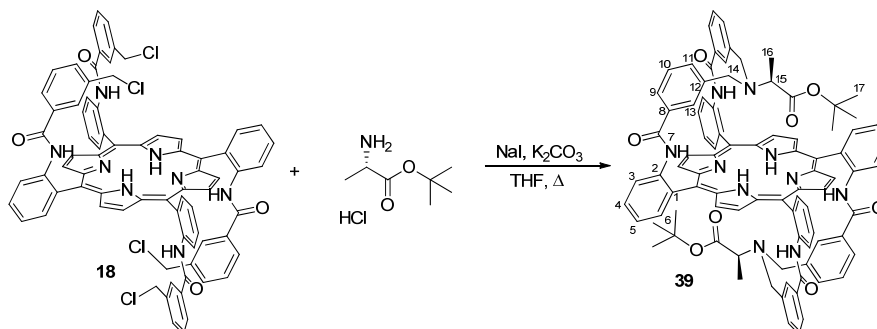
### 3.2.6. Synthesis of $\alpha_2\beta_2$ -bis(2,2'-{3,3'-[*N,N*-(methyl phenylalaninate)benzoyl amido]phenyl} porphyrin (**38**)



Porphyrin **18** (0.500 g,  $3.89 \cdot 10^{-4}$  mol), (*L*)-phenylalanine methyl ester hydrochloride (0.418 g,  $1.94 \cdot 10^{-3}$  mol), NaI (0.583 g,  $3.89 \cdot 10^{-3}$  mol) and  $K_2CO_3$  (1.08 g,  $7.78 \cdot 10^{-3}$  mol) were dissolved in 450 mL of THF and 50.0 mL of DMF. The mixture was refluxed under stirring for 6 hours until the complete consumption of **18**, which was monitored by TLC (0.5% MeOH in  $CH_2Cl_2$ ). Then, the solvent was evaporated to dryness and  $CH_2Cl_2$  was added to the residue. The organic phase was extracted with 0.5 M HCl solution (50.0 mL added three times), water (50.0 mL added three times) and then dried over  $NaSO_4$  and filtered. The filtrate was evaporated to dryness under reduced pressure and the crude purified by flash chromatography (silica gel, 15  $\mu$ m, 0.3% MeOH in  $CH_2Cl_2$ ) to obtain a dark purple solid (0.297 g, 55%).

**$^1H$  NMR** (500 MHz,  $CDCl_3$ ):  $\delta$  8.90 (s, 2H,  $H_\beta$ ), 8.89 (s, 2H,  $H_\beta$ ), 8.88 (d, 2H,  $J=5.14$  Hz,  $H_\beta$ ), 8.81 (d, 2H,  $J=4.8$  Hz,  $H_\beta$ ), 8.77 (d, 2H,  $J=8.28$  Hz,  $H^3$ ), 8.65 (d, 2H,  $J=8.11$  Hz,  $H^{3'}$ ), 8.13 (d, 2H,  $J=6.6$  Hz,  $H^6$ ), 7.96 (d, 2H,  $J=7.4$  Hz,  $H^6$ ), 7.91 (t, 2H,  $J=7.6$  Hz,  $H^4$ ), 7.87 (t, 2H,  $J=7.5$  Hz,  $H^{4'}$ ), 7.60 (t, 2H,  $J=7.5$  Hz,  $H^5$ ), 7.53 (t, 2H,  $J=7.5$  Hz,  $H^{5'}$ ), 7.21 (d, 2H,  $J=8.0$  Hz,  $H^9$ ), 7.18 (m, 6H,  $H^{19}$  and  $H^{20}$ ), 7.11 (d, 2H,  $J=7.7$  Hz,  $H^{9'}$ ), 7.08 (s, 2H,  $HCONH$ ), 7.01 (s, 2H,  $HCONH'$ ), 6.69 (t, 4H,  $J=7.5$  Hz,  $H^{10}$  e  $H^{10'}$ ), 6.68 (d, 2H,  $J=7.7$  Hz,  $H^{18}$ ), 6.57 (d, 2H,  $J=7.7$  Hz,  $H^{11'}$ ), 6.48 (d, 2H,  $J=7.6$  Hz,  $H^{11}$ ), 4.54 (s, 2H,  $H^{13'}$ ), 4.43 (s, 2H,  $H^{13}$ ), 3.15 (s, 6H,  $H^{21}$ ), 2.60 (dd, 2H,  $J=6.04, 8.95$  Hz,  $H^{15}$ ), 2.24 (dd, 2H,  $J=9.3$  Hz,  $^2J=13.6$  Hz,  $H^{16}$ ), 2.06 (d, 2H,  $J=14.2$  Hz,  $H^{14A}$ ), 1.68 (d, 2H,  $J=14.4$  Hz,  $H^{14A'}$ ), 1.40 (dd, 2H,  $J=5.7$  Hz,  $^2J=13.5$  Hz,  $H^{16'}$ ), 1.08 (d, 2H,  $J=14.7$  Hz,  $H^{14'B}$ ), 0.93 (d, 2H,  $J=15.4$  Hz,  $H^{14B}$ ), -2.31 ppm (s, 2H,  $NH_{pyr}$ ).  **$^{13}C$  NMR** (125 MHz,  $CDCl_3$ ):  $\delta$  171.4, 165.1, 165.1, 138.9, 138.8, 138.2, 137.3, 134.3, 134.1, 134.1, 133.8, 131.9, 131.6, 131.4, 131.1, 130.5, 130.4, 129.1, 128.6, 128.5, 126.8, 126.6, 126.1, 124.3, 123.9, 123.8, 122.1, 121.8, 115.5, 115.3, 64.0, 53.1, 52.7, 51.2, 32.5, 29.9, 14.3 ppm. **IR** ( $CH_2Cl_2$ ):  $\nu_{max}$ = 3678 (w), 3423 (w), 3315 (w), 1736 (w), 1680 (w), 1606 (w), 1581 (w), 1522 (w), 1447 (w), 1348 (w), 1308  $cm^{-1}$  (w). **IR** (ATR):  $\nu_{max}$ = 3419 (w), 1741 (w), 1680 (w), 1604 (w), 1580 (w), 1519 (w), 1446 (w), 1347 (w), 1312  $cm^{-1}$  (w). **UV-Vis** ( $CH_2Cl_2$ ):  $\lambda_{max}$  (log  $\epsilon$ ) 423 (5.68), 514 (5.02), 587 (4.15). **Elemental Analysis** calcd. for  $C_{96}H_{76}N_{10}O_8$ : C, 76.99; H, 5.11; N, 9.35. Found: C, 76.59; H, 5.50; N, 9.20. **MS** (ESI):  $m/z=1497.6$  [ $M^+$ ]. **X-ray** quality crystals were obtained by slow diffusion of a  $CH_2Cl_2$  solution of **38** into hexane.

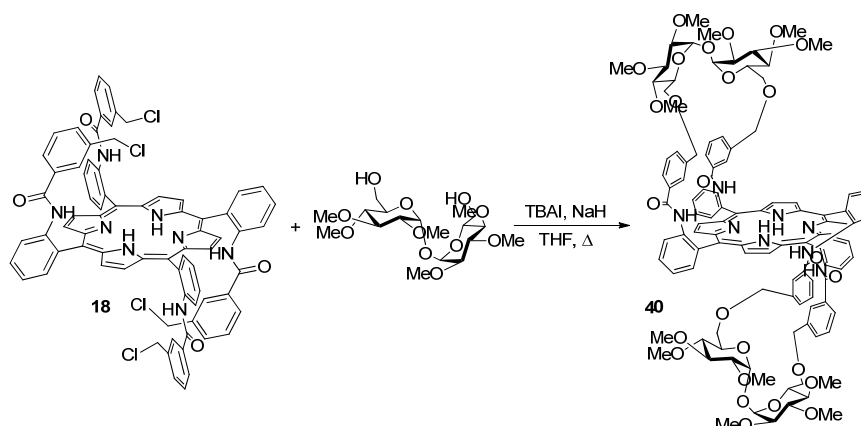
### 3.2.7. Synthesis of $\alpha_2\beta_2$ -bis(2,2'-{3,3'-[*N,N*-(*tert*-butyl alaninate)benzoylamido] phenyl} porphyrin (39)



Porphyrin **18** (80.0 mg,  $6.22 \cdot 10^{-5}$  mol), (*L*)-alanine *tert*-butyl ester hydrochloride (56.0 mg,  $3.11 \cdot 10^{-4}$  mol), NaI (93.0 mg,  $6.22 \cdot 10^{-4}$  mol) and K<sub>2</sub>CO<sub>3</sub> (0.172 g,  $1.24 \cdot 10^{-3}$  mol) were dissolved in 72.0 mL of THF and 8.00 mL of DMF. The mixture was refluxed under stirring for 8 hours until the complete consumption of **18**, which was monitored by TLC (0.5% MeOH in CH<sub>2</sub>Cl<sub>2</sub>). Then, the solvent was evaporated to dryness and 20.0 mL of CH<sub>2</sub>Cl<sub>2</sub> was added to the residue. The organic phase was extracted with 0.5 M HCl solution (three times with 20.0 mL each time), water (20.0 mL added three times) and then dried over NaSO<sub>4</sub> and filtered. The filtrate was evaporated to dryness under reduced pressure and the crude purified by flash chromatography (silica gel, 15 μm, 0.3% MeOH in CH<sub>2</sub>Cl<sub>2</sub>) to obtain a dark purple solid (49.0 mg, 55%).

**<sup>1</sup>H NMR** (500 MHz, CDCl<sub>3</sub>): δ 8.96 (m, 4H, H<sub>β</sub>), 8.93 (d, 2H, *J*=4.4 Hz, H<sub>β</sub>), 8.82 (s, 2H, H<sub>β</sub>), 8.83 (d, 2H, *J*=7.6 Hz, H<sup>3</sup>), 8.66 (d, 2H, *J*=7.6 Hz, H<sup>3</sup>), 8.12 (d, 4H, *J*=7.6 Hz, H<sup>6</sup> and H<sup>6'</sup>), 7.91 (m, 4H, H<sup>4</sup> and H<sup>4'</sup>), 7.60 (m, 4H, H<sup>5</sup> and H<sup>5'</sup>), 7.30 (d, 2H, *J*=7.6 Hz, H<sup>9</sup>), 7.20 (d, 2H, *J*=7.6 Hz, H<sup>9</sup>), 7.16 (s, 2H, HCONH), 7.04 (s, 2H, HCONH'), 6.81 (t, 2H, *J*=7.6 Hz, H<sup>10</sup>), 6.77 (d, 2H, *J*=7.6 Hz, H<sup>11</sup>), 6.74 (t, 2H, *J*=7.7 Hz, H<sup>10</sup>), 6.62 (d, 2H, *J*=7.6 Hz, H<sup>11</sup>), 4.41 (s, 2H, H<sup>13</sup>), 4.03 (s, 2H, H<sup>13</sup>), 2.08 (d, 2H, <sup>2</sup>*J*=13.1 Hz, H<sup>14A</sup>), 1.82 (q, 2H, *J*=6.8 Hz, H<sup>15</sup>), 1.26 (s, 18H, H<sup>17</sup>), 0.87 (d, 2H, <sup>2</sup>*J*=13.0 Hz, H<sup>14B</sup>), 0.63 (br, 4H, H<sup>14A'</sup> and H<sup>14B'</sup>), -0.80 (d, 6H, *J*=6.8 Hz, H<sup>16</sup>), -2.34 ppm (s, 2H, NH<sub>pyr</sub>). **<sup>13</sup>C NMR** (125 MHz, CDCl<sub>3</sub>): δ 171.7, 165.0, 164.7, 139.0, 138.9, 138.8, 138.3, 134.2, 134.0, 133.6, 132.2, 131.7, 131.2, 130.6, 130.5, 128.6, 128.5, 126.9, 126.3, 124.2, 123.8, 123.7, 123.4, 121.9, 121.6, 115.5, 115.4, 80.8, 57.5, 52.4, 31.7, 28.1, 10.1 ppm. **IR** (CH<sub>2</sub>Cl<sub>2</sub>): ν<sub>max</sub>= 3683 (w), 3423 (w), 3315 (w), 2978 (w), 2932 (w), 1727 (w), 1682 (w), 1606 (w), 1582 (w), 1522 (w), 1447 (w), 1308 (w), 1146 cm<sup>-1</sup> (w). **IR** (ATR): ν<sub>max</sub>= 3725 (w), 3005 (w), 1684 (w), 1507 (w), 1276 (w), 1261 (w), 758 (w), 751 cm<sup>-1</sup> (w). **UV-Vis** (CH<sub>2</sub>Cl<sub>2</sub>): λ<sub>max</sub> (log ε) 422 (5.60), 514 (4.11), 547 (3.46), 587 (3.60), 642 nm (3.08). **Elemental Analysis** calcd. for C<sub>90</sub>H<sub>80</sub>N<sub>10</sub>O<sub>8</sub>: C, 75.61; H, 5.64; N, 9.80. Found: C, 75.47; H, 5.73; N, 9.62. **MS** (ESI): *m/z*=1429.7 [M<sup>+</sup>].

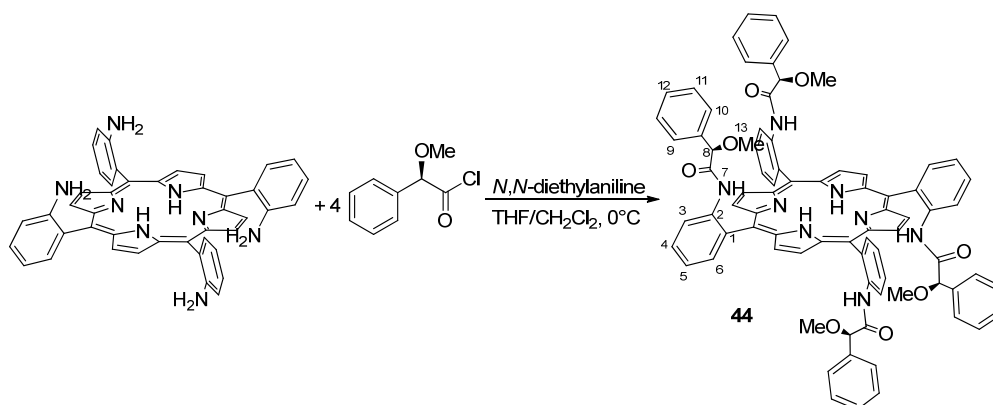
### 3.2.8. Synthesis of $\alpha_2\beta_2$ -bis(2,2'-{3,3'-[( $\alpha$ -trehalose)benzoylamido]phenyl} porphyrin (40)



Porphyrin **18** (0.300 g,  $2.33 \cdot 10^{-4}$  mol),  $\alpha$ -trehalose (0.495 g,  $1.17 \cdot 10^{-3}$  mol), tetrabutylammonium iodide (0.345 g,  $9.33 \cdot 10^{-4}$  mol) and sodium hydride (0.128 g,  $5.33 \cdot 10^{-3}$  mol) were dissolved in THF (75.0 mL) and DMF (15.0 mL). The green mixture was stirred for 24 hours at room temperature then  $\alpha$ -trehalose (0.199 g,  $4.68 \cdot 10^{-4}$  mol) and sodium hydride (11.2 mg,  $4.67 \cdot 10^{-4}$  mol) were added again. After 3 days at room temperature, MeOH was added to quench the reaction and the solvent was evaporated to dryness under reduced pressure. The crude was recovered with  $\text{CH}_2\text{Cl}_2$  and the organic phase was extracted with 0.5 M HCl solution (three times with 20.0 mL each time), water (20.0 mL added three times) and then dried over  $\text{NaSO}_4$  and filtered. The filtrate was evaporated to dryness under reduced pressure and the crude purified by flash chromatography (silica gel, 15  $\mu\text{m}$ , 3% MeOH in  $\text{CH}_2\text{Cl}_2$ ) to obtain a dark purple solid (65.0 mg, 14%).

**$^1\text{H NMR}$**  (400 MHz,  $\text{CDCl}_3$ ):  $\delta$  9.06 (s, 2H,  $\text{H}_\beta$ ), 9.04 (s, 2H,  $\text{H}_\beta$ ), 8.99 (m, 4H,  $\text{H}_\beta$ ), 8.94 (d, 2H,  $J=7.2$  Hz,  $\text{H}^3$ ), 8.93 (d, 2H,  $J=7.3$  Hz,  $\text{H}^3$ ), 8.03 (d, 2H,  $J=6.4$  Hz,  $\text{H}^6$ ), 7.93 (d, 2H,  $J=7.6$  Hz,  $\text{H}^6$ ), 7.89 (m, 4H,  $\text{H}^4$  and  $\text{H}^4$ ), 7.55 (m, 4H,  $\text{H}^5$  and  $\text{H}^5$ ), 7.83 (s, 2H,  $\text{HCONH}$ ), 7.33 (s, 2H,  $\text{HCONH}'$ ), 6.93 (d, 2H,  $J=8.0$  Hz,  $\text{H}^9$ ), 6.87 (d, 2H,  $J=7.6$  Hz,  $\text{H}^9$ ), 6.21 (t, 2H,  $J=7.7$  Hz,  $\text{H}^{10}$ ), 6.15 (t, 2H,  $J=7.8$  Hz,  $\text{H}^{10}$ ), 6.04 (d, 2H,  $J=7.5$  Hz,  $\text{H}^{11}$ ), 5.84 (d, 2H,  $J=7.8$  Hz,  $\text{H}^{11}$ ), 4.59 (d, 2H,  $J=3.5$  Hz,  $\text{HOCHO}$ ), 4.54 (d, 2H,  $J=3.6$  Hz,  $\text{HOCHO}$ ), 4.18 (d, 2H,  $^2J=11.8$  Hz,  $\text{H}^{14\text{A}}$ ), 4.17 (d, 2H,  $^2J=12.0$  Hz,  $\text{H}^{14\text{B}}$ ), 4.06 (d, 2H,  $^2J=17.7$  Hz,  $\text{H}^{14\text{A}'}$ ), 4.09 (d, 2H,  $^2J=18.0$  Hz,  $\text{H}^{14\text{B}'}$ ), .52 (s, 6H,  $\text{HOCH}_3$ ), 3.49 (s, 6H,  $\text{HOCH}_3$ ), 3.46 (s, 2H,  $\text{H}^{13}$  and  $\text{H}^{13'}$ ), 3.43 (s, 12H,  $\text{HOCH}_3$ ), 2.81-2.74 (m, 12H,  $\text{H}_{\text{trehalose}}$ , overlap of solvent signal), 3.17 (s, 6H,  $\text{HOCH}_3$ ), 3.13 (s, 6H,  $\text{HOCH}_3$ ), 2.81-2.74 (m, 6H,  $\text{H}_{\text{trehalose}}$ ), 2.66 (dd, 2H,  $J=9.6$  Hz,  $^2J=3.6$  Hz,  $\text{H}_{\text{trehalose}}$ ), -2.58 ppm (s, 2H,  $\text{NH}_{\text{pyr}}$ ). **IR** ( $\text{CH}_2\text{Cl}_2$ ):  $\nu_{\text{max}}$  = 3683 (w), 3423 (w), 3315 (w), 2978 (w), 2932 (w), 1727 (w), 1682 (w), 1606 (w), 1582 (w), 1522 (w), 1447 (w), 1308 (w), 1146  $\text{cm}^{-1}$  (w). **IR** (ATR):  $\nu_{\text{max}}$  = 3725 (w), 3005 (w), 1684 (w), 1507 (w), 1276 (w), 1261 (w), 758 (w), 751  $\text{cm}^{-1}$  (w). **UV-Vis** ( $\text{CH}_2\text{Cl}_2$ ):  $\lambda_{\text{max}}$  (log  $\epsilon$ ) 427 (5.25), 521 (4.03), 555 (3.57), 594 (3.52), 651 nm (3.19). **Elemental Analysis** calcd. for  $\text{C}_{112}\text{H}_{118}\text{N}_8\text{O}_{26}$ : C, 67.52; H, 5.97; N, 5.62. Found: C, 67.62; H, 6.00; N 5.60. **MS** (ESI):  $m/z=1990$  [ $\text{M}^+$ ].

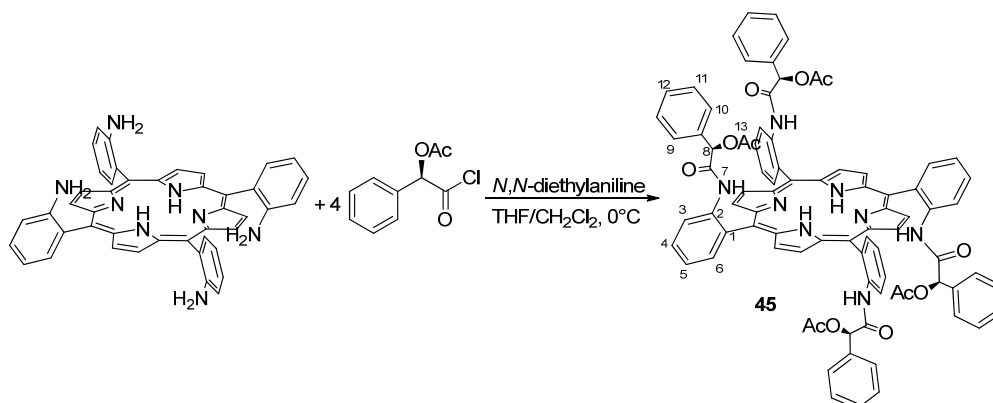
### 3.2.9. Synthesis of $\alpha_2\beta_2$ -tetra[(2-methoxy-2-phenyl)acetamide]phenyl porphyrin (**44**)



The atropoisomer  $\alpha_2\beta_2$  of TAPP<sub>H<sub>2</sub></sub> (0.100 g,  $1.48 \cdot 10^{-4}$  mol) was dissolved in THF (10.0 mL) and the solution was loaded in a syringe. Another syringe was charged with a solution of (*R*)-2-methoxy-2-phenylacetic chloride (0.110 g,  $5.93 \cdot 10^{-4}$  mol) in CH<sub>2</sub>Cl<sub>2</sub> (10.0 mL). A syringe pump was equipped with the two syringes and the reactants were simultaneously added over 1.5 hours at 0°C into a Schlenk flask containing a solution of *N,N*-diethylaniline (0.120 mL,  $5.93 \cdot 10^{-4}$  mol) in THF (60.0 mL). Then the red solution was stirred at room temperature overnight. The solvent was then evaporated to dryness under reduced pressure and the crude was purified by flash chromatography (silica gel, 15  $\mu$ m, starting from CH<sub>2</sub>Cl<sub>2</sub>/hexane 8:2 to 1% MeOH in CH<sub>2</sub>Cl<sub>2</sub>) to obtain dark purple solid (0.128 g, 70%).

**<sup>1</sup>H NMR** (300 MHz, CDCl<sub>3</sub>, 298 K):  $\delta$  8.89 (d, 4H,  $J=3.9$  Hz, H <sub>$\beta$</sub> ), 8.83 (d, 2H,  $J=4.6$  Hz, H <sub>$\beta$</sub> ), 8.77 (m, 6H, H <sub>$\beta$</sub>  and H<sup>3</sup> and H<sup>3'</sup>), 8.30 (s, 2H, HCONH), 8.26 (s, 2H, HCONH), 8.09 (d, 2H,  $J=7.2$  Hz, H<sup>6</sup>), 7.96 (d, 2H,  $J=6.9$  Hz, H<sup>6</sup>), 7.88 (t, 2H,  $J=7.8$  Hz, H<sup>4</sup>), 7.84 (t, 2H,  $J=7.8$  Hz, H<sup>4</sup>), 7.59 (t, 2H,  $J=7.44$  Hz, H<sup>5</sup>), 7.53 (t, 2H,  $J=7.46$  Hz, H<sup>5</sup>), 6.84, (m, 4H, H<sup>12</sup> and H<sup>12'</sup>), 6.73 (m, 8H, H<sup>11</sup> and H<sup>11'</sup>), 6.50 (d, 4H,  $J=7.5$  Hz, H<sup>10</sup>), 6.41 (d, 4H,  $J=7.3$  Hz, H<sup>10</sup>), 4.04 (s, 2H, H<sup>8</sup>), 3.87 (s, 2H, H<sup>8</sup>), 1.64 (s, 6H, H<sup>13</sup>), 1.39 (s, 6H, H<sup>13</sup>), -2.46 ppm (s, 2H, NH<sub>pyr</sub>). **<sup>13</sup>C NMR** (300 MHz, CDCl<sub>3</sub>):  $\delta$  168.7, 168.6, 138.2, 138.1, 136.1, 134.8, 131.4, 131.2, 130.3, 130.2, 128.3, 128.2, 128.1, 128.2, 123.4, 121.0, 120.8, 115.1, 114.9, 83.8, 83.5, 56.4, 56.0 ppm. **IR** (CH<sub>2</sub>Cl<sub>2</sub>):  $\nu_{\max}$  = 3361 (w), 3321 (w), 1734 (w), 1691 (w), 1582 (w), 1523 (w), 1466 (w), 1450 (w), 1098 (w) cm<sup>-1</sup>. **UV-Vis** (CH<sub>2</sub>Cl<sub>2</sub>):  $\lambda_{\max}$  (log  $\epsilon$ ) 420 (4.58), 513 (5.31), 548 (4.70) and 591 nm (4.78). **Elemental Analysis** calcd. for C<sub>80</sub>H<sub>66</sub>N<sub>8</sub>O<sub>8</sub>: C, 75.81; H, 5.25; N, 8.84. Found: C, 75.70; H, 5.23; N, 8.64. **MS** (ESI):  $m/z=1266.03$  [M<sup>+</sup>]. **X-ray** quality crystals were obtained by slow diffusion of a CH<sub>2</sub>Cl<sub>2</sub> solution of **49** into hexane.

### 3.2.10. Synthesis of $\alpha_2\beta_2$ -tetra[(2-acetoxy-2-phenyl)acetamide)phenyl] porphyrin (45)

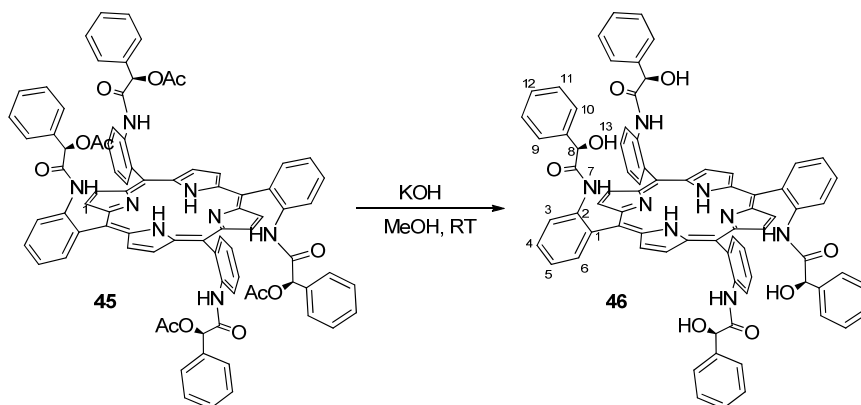


The atropoisomer  $\alpha_2\beta_2$  of TAPP $H_2$  (0.100 g,  $1.48 \cdot 10^{-4}$  mol) was dissolved in THF (10.0 mL) and the solution was loaded in a syringe. Another syringe was charged with a solution of (*R*)-2-acetoxy-2-phenylacetic chloride (0.126 g,  $5.93 \cdot 10^{-4}$  mol) in  $CH_2Cl_2$  (10.0 mL). A syringe pump was equipped with the two syringes and the reactants were simultaneously added over 1.5 hours at  $0^\circ C$  into a Schlenk flask containing a solution of *N,N*-diethylaniline (0.120 mL,  $5.93 \cdot 10^{-4}$  mol) in THF (60.0 mL). Then the red solution was stirred at room temperature overnight. The solvent was then evaporated to dryness under reduced pressure and the crude was purified by chromatography (silica gel, 15  $\mu m$ , starting from  $CH_2Cl_2$ /hexane=8:2 to 0.5% MeOH in  $CH_2Cl_2$ ) to obtain dark purple solid (0.120 g, 60%).

**$^1H$  NMR** (400 MHz,  $CDCl_3$ , 298 K):  $\delta$  8.91 (s, 2H,  $H_\beta$ ), 8.88 (d, 2H,  $J=4.6$  Hz,  $H_\beta$ ), 8.84 (d, 2H,  $J=4.9$  Hz,  $H_\beta$ ), 8.62 (s, 2H,  $H_\beta$ ), 8.79 (d, 2H,  $J=8.5$ ,  $H^3$ ), 8.50 (d, 2H,  $J=8.2$ ,  $H^3$ ), 8.20 (d, 2H,  $J=7.5$  Hz,  $H^6$ ), 7.98 (d, 2H,  $J=6.7$  Hz,  $H^6$ ), 7.90 (t, 4H,  $J=8.0$  Hz,  $H^4$  and  $H^4$ ), 7.82 (s, 2H,  $HCONH$ ), 7.67 (t, 2H,  $J=7.6$  Hz,  $H^5$ ), 7.60 (t, 2H,  $J=7.4$  Hz,  $H^5$ ), 7.37 (s, 2H,  $HCONH$ ), 6.62 (m, 4H,  $H_{Ar}$ ), 6.51 (t, 2H,  $J=7.7$  Hz,  $H_{Ar}$ ), 6.32 (d, 2H,  $J=7.7$  Hz,  $H_{Ar-ortho}$ ), 5.27 (d, 2H,  $J=6.0$  Hz,  $H_{Ar-ortho}$ ), 1.54 (s, 4H,  $H^8$  and  $H^8$ ), 1.25 (s, 3H,  $H_{CH_3}$ , overlap of solvent signal), 0.53 (s, 3H,  $H_{CH_3}$ ), -2.72 ppm (s, 2H,  $NH_{pyr}$ ).  **$^{13}C$  NMR** (300 MHz,  $CDCl_3$ ):  $\delta$  168.5, 167.0, 166.7, 166.3, 138.0, 135.0, 134.5, 132.5, 131.2, 130.7, 128.9, 128.5, 128.4, 127.2, 127.0, 124.6, 124.0, 122.9, 122.3, 115.6, 75.1, 74.8, 19.6, 17.9 ppm. **IR** ( $CH_2Cl_2$ ):  $\nu_{max}$ =3397.8 (w), 3321.4 (w), 2927.6 (w), 2854.9 (w), 1752.5 (w), 1700.0 (w), 1584.8 (w), 1372.9 (w), 1217.7  $cm^{-1}$  (w). **IR** (ATR):  $\nu_{max}$ = 3391.4 (w), 3315.9 (w), 2958.5 (w), 2922.6 (w), 2852.6 (w), 1743.5 (w), 1693.3 (w), 1581.0 (w), 1516.7 (w), 1444.9 (w), 1370.1 (w), 1346.8 (w), 1298.7 (w), 1212.2 (w), 1023.9 (w), 964.6 (w), 799.5  $cm^{-1}$  (w). **UV-Vis** ( $CH_2Cl_2$ ):  $\lambda_{max}$  (log  $\epsilon$ ) 421 (5.41), 514 (4.23), 548 (3.54), 588 (3.65), 644 nm (3.12). **Elemental Analysis** calcd. for  $C_{84}H_{66}N_8O_{12}$ : C, 73.14; H, 4.82; N, 8.12. Found: C, 73.0; H, 4.58; N, 8.20. **MS** (ESI):  $m/z$ =1377.79 [ $M^-$ ].



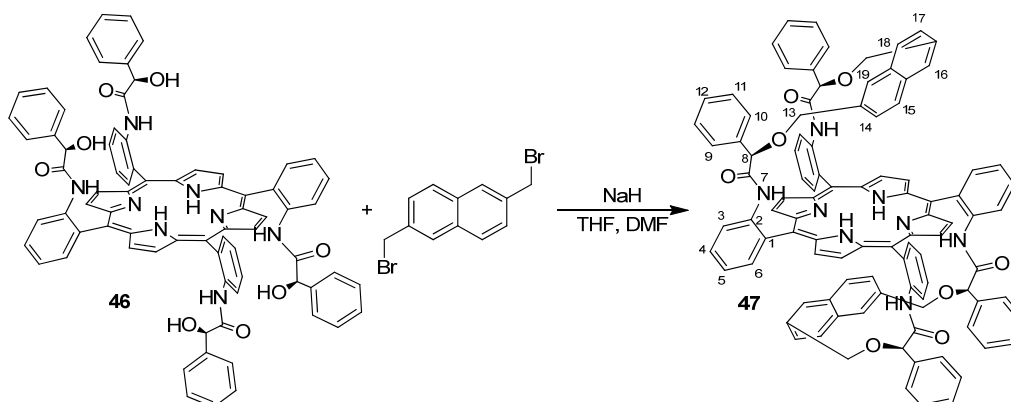
### 3.2.11. Synthesis of $\alpha_2\beta_2$ -tetra[(2-hydroxy-2-phenyl)acetamide]phenyl porphyrin (46)



Porphyrin **45** (0.100 g,  $2.75 \cdot 10^{-5}$  mol) was dissolved in a solution of KOH 5% in methanol (15.0 mL). The reaction stirred in air at room temperature for 3 days. Then water (20.0 mL) and  $\text{CH}_2\text{Cl}_2$  (20.0 mL) were added and the organic phase was extracted. The solvent was evaporated under reduced pressure and the crude was purified by flash chromatography (silica gel, 15 mm, 3% MeOH in  $\text{CH}_2\text{Cl}_2$ ) to obtain a dark solid (65.0 mg, 75%).

$^1\text{H NMR}$  (400 MHz,  $\text{CDCl}_3$ , 298 K):  $\delta$  8.90 (d, 2H,  $J=6.3$  Hz,  $\text{H}_\beta$ ), 8.78 (d, 2H,  $J=11.2$  Hz,  $\text{H}_\beta$ ), 8.75-8.68 (m, 4H,  $\text{H}_\beta$  and  $\text{H}^3$  and  $\text{H}^{3'}$ ), 8.22 (s, 1H,  $\text{H}_\beta$ ), 8.09 (m, 4H,  $\text{H}^6$  and  $\text{H}^{6'}$ ), 8.02 (s, 1H,  $\text{H}_\beta$ ), 7.85 (d, 2H,  $J=7.8$ ,  $\text{H}^4$ ), 7.80 (t, 2H,  $J=7.8$ ,  $\text{H}^4$ ), 7.59 (t, 2H,  $J=7.3$  Hz,  $\text{H}^5$ ), 7.54 (t, 2H,  $J=7.3$  Hz,  $\text{H}^5$ ), 6.49 (s, 2H,  $\text{HCONH}$ ), 6.47 (s, 2H,  $\text{HCONH}$ ), 6.43-6.38 (m, 4H,  $\text{H}_{\text{Ar}}$ ), 6.30 (t, 2H,  $J=7.3$  Hz,  $\text{H}_{\text{Ar}}$ ), 6.12 (m, 2H,  $J=7.5$  Hz,  $\text{H}_{\text{Ar-ortho}}$ ), 6.05 (d, 2H,  $J=7.4$  Hz,  $\text{H}_{\text{Ar-ortho}}$ ), 1.25 (s, 4H,  $\text{H}^8$  and  $\text{H}^{8'}$ , overlap of solvent signal), -2.70 ppm (s, 2H,  $\text{NH}_{\text{pyr}}$ ). **IR** ( $\text{CH}_2\text{Cl}_2$ ):  $\nu_{\text{max}}$  = 3686.4 (w), 3369.3 (w), 3369.3 (w), 3319.7 (w), 2928.4 (w), 2854.1 (w), 1735.0 (w), 11691.3 (w), 1604.2 (w), 1582.9 (w), 1523.8 (w), 1465.5 (w), 1448.3 (w), 1348.2  $\text{cm}^{-1}$  (w). **UV-Vis** ( $\text{CH}_2\text{Cl}_2$ ):  $\lambda_{\text{max}}$  (log  $\epsilon$ ) 421 (5.50), 514 (4.23), 548 (3.60), 588 (3.70) and 645 (3.07) nm. **MS** (ESI):  $m/z=1233.67$  [ $\text{M}+\text{Na}$ ].

### 3.2.12. Synthesis of $\alpha_2\beta_2$ -bis{2,2'-[(2-(1-naphthylmethoxy))-2-phenyl]acetamide} phenyl} porphyrin (47)

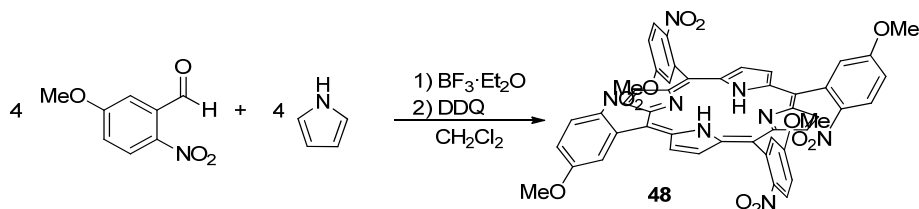


Porphyrin **46** (51.0 mg,  $4.21 \cdot 10^{-5}$  mol), 2,6-bis(dibromomethyl)naphthalene (39.7 mg,  $1.26 \cdot 10^{-4}$  mol) and sodium hydride (16.1 mg,  $6.73 \cdot 10^{-4}$  mol) were dissolved in THF (25.0 mL) and DMF (5.00 mL). The green solution was stirred at room temperature for 3 days then the solvent was evaporated to dryness under reduced pressure and the crude was recovered with  $\text{CH}_2\text{Cl}_2$ . The organic phase was extracted with 1.0 M HCl solution

(10.0 mL added four times), water (10.0 mL added two times) and then dried over NaSO<sub>4</sub> and filtered. The filtrate was evaporated to dryness under reduced pressure and the crude purified by flash chromatography (silica gel, 15 μm, 1% MeOH in CH<sub>2</sub>Cl<sub>2</sub>) to obtain a dark purple solid (7 mg, 11%).

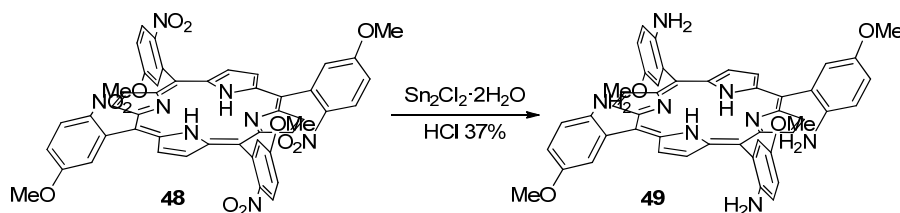
MS (ESI):  $m/z=1538.82$  [M+Na<sup>+</sup>].

### 3.2.13. Synthesis of *meso*-tetra(5-methoxy-2-nitrophenyl) porphyrin (**48**)



5-Methoxy-2-nitrobenzaldehyde (6.00 g,  $3.31 \cdot 10^{-2}$  mol) and pyrrole (2.29 mL,  $3.31 \cdot 10^{-2}$  mol) were dissolved in CH<sub>2</sub>Cl<sub>2</sub> (4.00 L) and BF<sub>3</sub>·Et<sub>2</sub>O (0.88 mL,  $3.31 \cdot 10^{-3}$  mol) was added dropwise. The reaction was stirred at room temperature. After 24 hours, 2,3-dichloro-5,6-dicyano-1,4-benzoquinone (DDQ) (7.50 g,  $3.31 \cdot 10^{-2}$  mol) was added twice time to the red solution and after 2 hours TEA (2.36 mL) was added to quench the reaction. The solvent was evaporated to dryness and the crude was washed three times with MeOH (100 mL) and then purified by flash chromatography (silica gel, 15 μm, 0.5% MeOH in CH<sub>2</sub>Cl<sub>2</sub>) to obtained dark purple solid (1.10 g, 15%). The mixture of four atropoisomers was used in the next step without furthermore purifications.

### 3.2.14. Synthesis of *meso*-tetra(5-methoxy-2-aminophenyl) porphyrin (**49**)

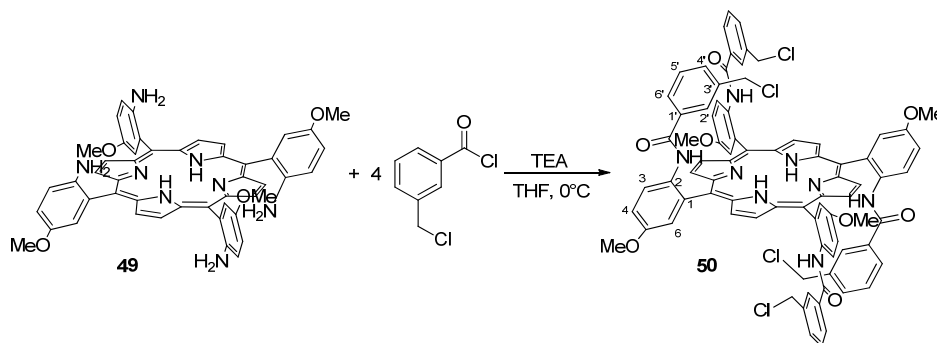


The mixture of four atropoisomers of *meso*-tetra(5-methoxy-2-nitrophenyl) porphyrin **48** (1.04 g,  $1.13 \cdot 10^{-3}$  mol) were dissolved in HCl 37% (78.0 mL) at room temperature followed by the addition of SnCl<sub>2</sub>·2H<sub>2</sub>O (3.84 g,  $1.70 \cdot 10^{-2}$  mol). The resulting green mixture was allowed to stir at RT in air for 48 hours then chloroform (50.0 mL) was added and the solution was stirred for 15 minutes. After 15 minutes, the reaction mixture was cooled to 0°C and a saturated solution of KOH was added dropwise until a pH=10. The organic phase was separated and filtered over septum to separate the solid. The aqueous phase was extracted several times with CHCl<sub>3</sub>. The solvent was evaporated under reduced pressure to obtain a dark purple solid.

The four atropoisomers were separated by flash chromatography (silica gel, 15 μm) with 0.6% of MeOH in CH<sub>2</sub>Cl<sub>2</sub> for αβ (12.5%), 0.7% MeOH for α<sub>2</sub>β<sub>2</sub> (25%), 1.5% MeOH for α<sub>3</sub>β (50%) and 3% MeOH for α<sub>4</sub> (12.5%).

**α<sub>2</sub>β<sub>2</sub> meso-tetra(5-methoxy-2-aminophenyl) porphyrin:** <sup>1</sup>H NMR (400 MHz, CDCl<sub>3</sub>): δ 8.92 (s, 8H, H<sub>β</sub>), 7.46 (d, 4H, <sup>4</sup>J=2.82 Hz, H<sub>o</sub>), 7.23 (dd, 4H, J=8.79, <sup>4</sup>J=2.85 Hz, H<sub>p</sub>), 7.07 (d, 4H, J=8.79 Hz, H<sub>m</sub>), 3.88 (s, 12H, H<sub>OCH<sub>3</sub></sub>), 3.30 (s, 8H, -NH<sub>2</sub>), -2.71 ppm (s, 2H, NH<sub>pyr</sub>).

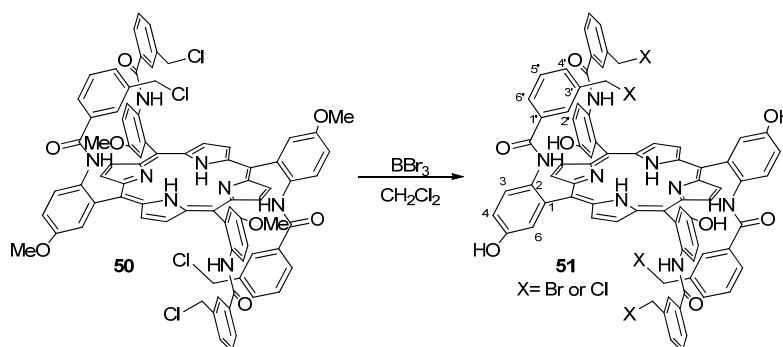
### 3.2.15. Synthesis of $\alpha_2\beta_2$ -tetra{5-methoxy-2-[(3-chloromethyl)benzoylamido] phenyl} porphyrin (**50**)



The atropisomer  $\alpha_2\beta_2$  of porphyrin **49** (0.554 g,  $6.96 \cdot 10^{-4}$  mol) was dissolved in THF (65.0 mL) at room temperature followed by the addition of TEA (0.774 mL,  $5.57 \cdot 10^{-3}$  mol). The dark solution was cooled to  $0^\circ\text{C}$  and 3-(chloromethyl)benzoyl chloride (0.595 mL,  $4.18 \cdot 10^{-3}$  mol) was added dropwise. The solution was stirred for 4 hours at room temperature then MeOH was added to quench the reaction. The solvent was evaporated to dryness under reduced pressure and the crude was purified by flash chromatography (silica gel, 15  $\mu\text{m}$ , 0.4% MeOH in  $\text{CH}_2\text{Cl}_2$ ) to obtain dark purple solid (0.619 g, 65%).

$^1\text{H NMR}$  (400 MHz,  $\text{CDCl}_3$ ):  $\delta$  9.00 (s, 4H,  $\text{H}_\beta$ ), 8.96 (s, 4H,  $\text{H}_\beta$ ), 8.65 (d, 4H,  $J=9.2$  Hz,  $\text{H}^3$ ), 7.58 (d, 4H,  $^4J=2.9$  Hz,  $\text{H}^6$ ), 7.44 (d, 4H,  $J=9.2$  Hz,  $^4J=2.9$  Hz,  $\text{H}^4$ ), 7.39 (s, 4H,  $\text{HCONH}$ ), 6.70 (d, 4H,  $J=7.8$  Hz,  $\text{H}^6$ ), 6.51 (s, 4H,  $\text{H}^{2'}$ ), 6.43 (d, 4H,  $J=7.8$  Hz,  $\text{H}^4$ ), 6.34 (pt(dd), 4H,  $J=7.6$  Hz,  $\text{H}^{5'}$ ), 3.96 (s, 12H,  $\text{HOCH}_3$ ), 3.52 (s, 8H,  $\text{H}_{\text{CH}_2}$ ), -2.63 ppm (s, 2H,  $\text{NH}_{\text{pyr}}$ ).

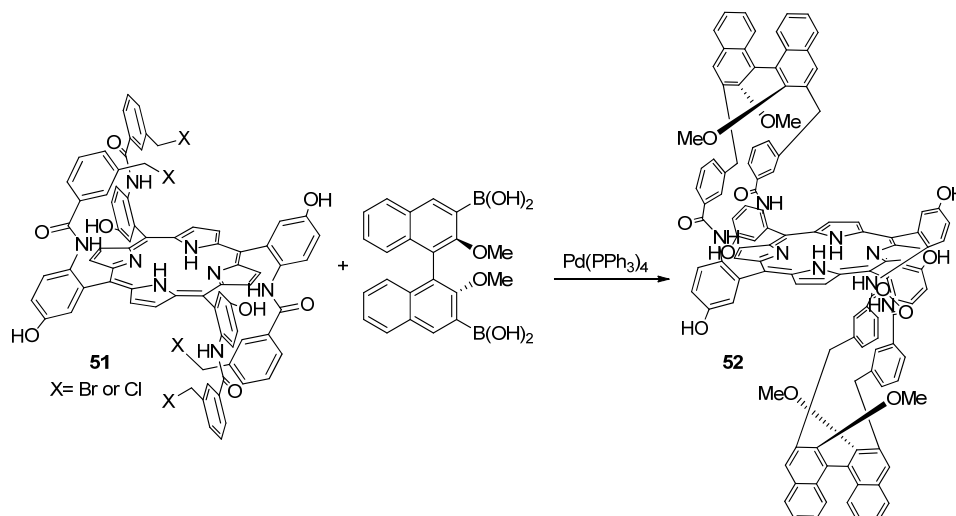
### 3.2.16 Synthesis of $\alpha_2\beta_2$ -tetra{5-hydroxy-2-[(3-chloromethyl)benzoylamido] phenyl} porphyrin (**51**)



Porphyrin **50** (0.251 g,  $1.78 \cdot 10^{-4}$  mol) was dissolved in  $\text{CH}_2\text{Cl}_2$  (100 mL) and the solution was cooled at  $0^\circ\text{C}$ , then  $\text{BBr}_3$  (1.00 mL,  $1.06 \cdot 10^{-2}$  mol) was added dropwise. The reaction mixture stirred at room temperature for 3 days then ethyl acetate (50.0 mL) and ice were added. After neutralization with  $\text{K}_2\text{CO}_3$ , the organic phase was separated and the aqueous phase was extracted with AcOEt (25.0 mL added three times). Then, the combined organic phase was dried over  $\text{NaSO}_4$  and filtered. The filtrate was evaporated to dryness under reduced pressure and the crude purified by flash chromatography (silica gel, 15  $\mu\text{m}$ , 2% MeOH in  $\text{CH}_2\text{Cl}_2$ ) to obtain the product. Unfortunately, we obtained a mixture of mono-, di-, tri- and tetra-bromo substituted porphyrin (0.200 g, 83.3%).

**MS** (MALDI):  $m/z=1393.55, 1438.00, 1482.46$  and  $1526.91$  [M].

### 3.2.17. Synthesis of $\alpha_2\beta_2$ -(5-hydroxy-bis{2,2'-[3,3'-(2,2'-dimethoxy-(1,1'-binaphthyl)benzoylamido)}phenyl) porphyrin (**52**)

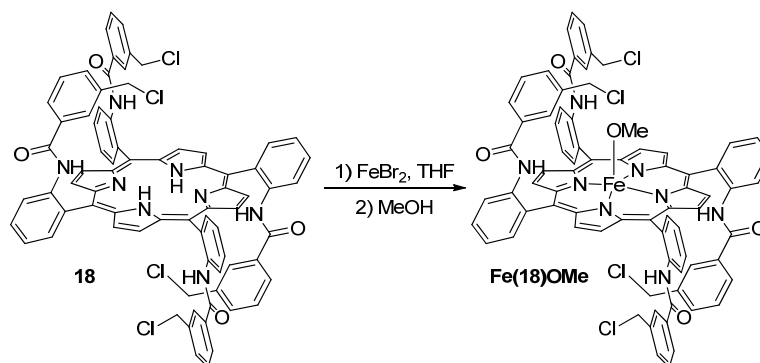


A mixture of mono-, di-, tri- and tetra-bromo porphyrin **51** (0.200 g), (*R*)-2,2'-dimethoxy-1,1'-binaphthyl-3,3'-diboronic acid (0.138 g,  $3.44 \cdot 10^{-4}$  mol), tetrakis(tri(phenyl)phosphine) palladium(0) (66.3 mg,  $5.74 \cdot 10^{-5}$  mol) and potassium carbonate (0.316 g,  $2.29 \cdot 10^{-3}$  mol) were dissolved in 16.0 mL of toluene, 5.00 mL of ethanol and 8.00 mL of water. The biphasic solution was refluxed for 4 hours until the complete consumption of **51** that was monitored by TLC (1% MeOH in  $\text{CH}_2\text{Cl}_2$ ). The resulting mixture was allowed to reach room temperature and the biphasic solution was diluted with 50.0 mL of saturated aqueous  $\text{NH}_4\text{Cl}$  and 50.0 mL of  $\text{CH}_2\text{Cl}_2$  and then it was separated. The aqueous phase was extracted with  $\text{CH}_2\text{Cl}_2$  (50.0 mL added two times) and the combined organic phases were washed with 50.0 mL of water and 50.0 mL of saturated aqueous  $\text{NaHCO}_3$ . The organic phase was dried over  $\text{Na}_2\text{SO}_4$  and filtered. The filtrate was evaporated to dryness *in vacuo* and the residue was purified by flash chromatography (silica gel, 15  $\mu\text{m}$ , 0.5% MeOH in  $\text{CH}_2\text{Cl}_2$ ) to obtain the product (4 mg, 1.5 %).

MS (MALDI):  $m/z=1830$  [M]

## 3.3. Synthesis of iron porphyrin complexes

### 3.3.1. Synthesis of Fe(18)OMe

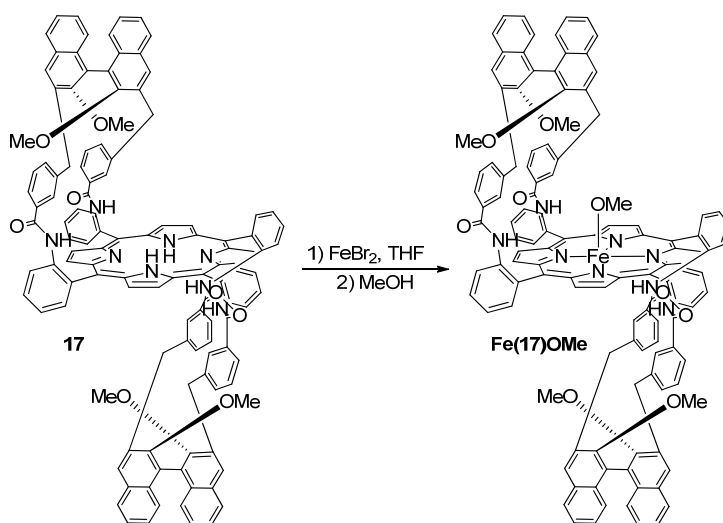


Porphyrin **18** (80.0 mg,  $6.22 \cdot 10^{-5}$  mol) and  $\text{FeBr}_2$  (0.134 g,  $6.22 \cdot 10^{-4}$  mol) were dissolved in THF (25.0 mL). The dark solution was refluxed for 7 hours until the complete consumption of **18** that was monitored by TLC

(1% MeOH in CH<sub>2</sub>Cl<sub>2</sub>). The mixture was evaporated to dryness and the residue purified by chromatography (alumina 0.063-0.200 μm, 0.5% MeOH in CH<sub>2</sub>Cl<sub>2</sub>) to obtain a dark solid. (83.0 mg, 97%).

**IR** (CH<sub>2</sub>Cl<sub>2</sub>):  $\nu_{\max}$ = 3421.3 (w), 2963.1 (w), 2927.5 (w), 2854.9 (w), 1740.1 (w), 1680.0 (w), 1582.2 (w), 1518.0 (w), 1448.3 (w), 1306.9 (w), 1259.9 cm<sup>-1</sup> (w). **IR** (ATR):  $\nu_{\max}$ = 3413.8 (w), 2961.7 (w), 2925.6 (w), 2853.4 (w), 1731.4 (w), 1672.0 (w), 1578.8 (w), 1510.7 (w), 1442.2 (w), 1300.2 (w), 1257.9 (w), 1081.6 (w), 1014.0 (w), 795.0 cm<sup>-1</sup> (w). **UV-Vis** (CH<sub>2</sub>Cl<sub>2</sub>):  $\lambda_{\max}$  (log ε) 420 (5.16), 620 nm (4.62). **ESR data** (experimental X-band (9.462 GHz) sample powder, 77 K): High spin S=5/2 was confirmed by the g tensor values ( $g_{\perp}$ =5.7 and  $g_{\parallel}$ =2.00). **Elemental analysis** calcd for C<sub>77</sub>H<sub>55</sub>Cl<sub>4</sub>FeN<sub>8</sub>O<sub>5</sub>: C, 67.51; H, 4.05; N, 8.18. Found: C, 67.26; H, 4.27; N, 8.20. **MS** (ESI):  $m/z$ =1392.2 [M+Na<sup>+</sup>].

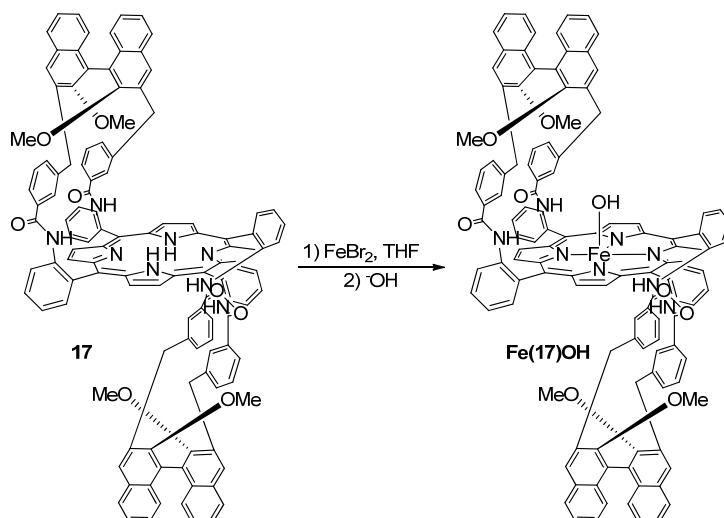
### 3.3.2. Synthesis of Fe(17)OMe



Porphyrin **17** (78.0 mg, 4.41·10<sup>-5</sup> mol) and FeBr<sub>2</sub> (0.095 g, 4.40·10<sup>-4</sup> mol) were dissolved in THF (25.0 mL). The dark solution was refluxed for 24 hours until the complete consumption of **17** that was monitored by TLC (1% MeOH in CH<sub>2</sub>Cl<sub>2</sub>). The mixture was evaporated to dryness and the residue purified by chromatography (alumina 0.063-0.200 μm, 0.5% MeOH in CH<sub>2</sub>Cl<sub>2</sub>) to obtain a dark solid (81.0 mg, 99 %).

$[\alpha]_D^{20}$  = -625.000 (c=8·10<sup>-4</sup> g/100mL; in CH<sub>2</sub>Cl<sub>2</sub>). **IR** (CH<sub>2</sub>Cl<sub>2</sub>):  $\nu_{\max}$ = 3685.7 (w), 3418.9 (w), 1723.7 (w), 1676.8 (w), 1605.3 (w), 1516.9 (w), 1278.4 (w), 1098.0 (w), 1009.5 cm<sup>-1</sup> (w). **IR** (ATR):  $\nu_{\max}$ = 3417.6 (w), 2962.0 (w), 2926.0 (w), 2854.1 (w), 1677.1 (w), 1513.6 (w), 1259.2 (w), 1087.3 (w), 1011.4 (w), 795.0 cm<sup>-1</sup> (w). **UV-Vis** (CH<sub>2</sub>Cl<sub>2</sub>):  $\lambda_{\max}$  (log ε) 420 (4.58), 576 nm (3.35). **ESR data** (experimental X-band (9.462 GHz) sample powder, 77 K): High spin S=5/2 was confirmed by the g tensor values ( $g_{\perp}$ =5.71 and  $g_{\parallel}$ =2.00). **Elemental analysis** calcd for C<sub>121</sub>H<sub>87</sub>FeN<sub>8</sub>O<sub>9</sub>: C, 78.43; H, 4.73; N, 6.05. Found: C, 78.83; H, 4.65; N, 6.15. **MS** (ESI):  $m/z$ =1875.6 [M+Na<sup>+</sup>].

### 3.3.3. Synthesis of Fe(17)OH



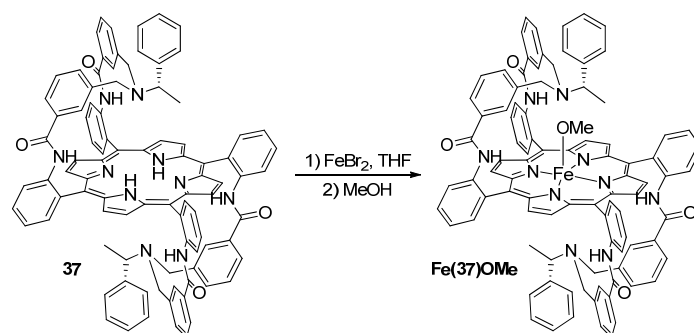
**Method a:** porphyrin **17** (78.0 mg,  $4.41 \cdot 10^{-5}$  mol) and  $\text{FeBr}_2$  (95.0 mg,  $4.40 \cdot 10^{-4}$  mol) were dissolved in THF (25.0 mL). The dark solution was refluxed for 24 hours until the complete consumption of **17** that was monitored by TLC (1% MeOH in  $\text{CH}_2\text{Cl}_2$ ). The mixture was evaporated to dryness and the residue purified by chromatography (alumina 0.063-0.200  $\mu\text{m}$ ,  $\text{CH}_2\text{Cl}_2$ ). The solid was treated with a water solution of NaOH (18.0 mg of NaOH in 10.0 ml of distilled water) and left for 48 hours at room temperature. The precipitated dark solid was then collected by filtration and dried *in vacuo* (81.0 mg, 99 %).

$[\alpha]_D^{20} = -625.000$  ( $c = 8 \cdot 10^{-4}$  g/100mL; in  $\text{CH}_2\text{Cl}_2$ ). **IR** ( $\text{CH}_2\text{Cl}_2$ ):  $\nu_{\text{max}} = 3416.6$  (w), 2961.7 (w), 2929.2 (w), 2855.9 (w), 1730.7 (w), 1677.4 (w), 1603.1 (w), 1516.1 (w), 1241.9 (w), 1099.7 (w), 1010.4  $\text{cm}^{-1}$  (w). **IR** (ATR):  $\nu_{\text{max}} = 3419.3$  (w), 2960.0 (w), 2922.9 (w), 2854.2 (w), 1679.3 (w), 1511.9 (w), 1258.2 (w), 1079.0 (w), 1011.5 (w), 792.0  $\text{cm}^{-1}$  (w). **UV-Vis** ( $\text{CH}_2\text{Cl}_2$ ):  $\lambda_{\text{max}}$  (log  $\epsilon$ ) 420 (4.68), 577 nm (3.50). **ESR data** (experimental X-band (9.462 GHz) sample powder, 77 K): High spin  $S=5/2$  was confirmed by the g tensor values ( $g_{\perp} = 5.71$  and  $g_{\parallel} = 2.00$ ). **Elemental analysis** calcd for  $\text{C}_{120}\text{H}_{85}\text{FeN}_8\text{O}_9$ : C, 78.38; H, 4.66; N, 6.09. Found: C, 78.83; H, 4.65; N, 6.12. **MS** (ESI):  $m/z = 1861.6$  [ $\text{M} + \text{Na}^+$ ].

**Method b:** Complex **Fe(17)OMe** (10.0 mg) were dissolved in toluene (5.00 mL) containing 0.03% of water and the resulting solution was stirred at room temperature for 24 hours. Then the solvent was evaporated to dryness and the solid dried *in vacuo*.

**IR** ( $\text{CH}_2\text{Cl}_2$ ):  $\nu_{\text{max}} = 3416.6$  (w), 2961.7 (w), 2929.2 (w), 2855.9 (w), 1730.7 (w), 1677.4 (w), 1603.1 (w), 1516.1 (w), 1241.9 (w), 1099.7 (w), 1010.4  $\text{cm}^{-1}$  (w). **IR** (ATR):  $\nu_{\text{max}} = 3419.3$  (w), 2960.0 (w), 2922.9 (w), 2854.2 (w), 1679.3 (w), 1511.9 (w), 1258.2 (w), 1079.0 (w), 1011.5 (w), 792.0  $\text{cm}^{-1}$  (w). **UV-Vis** ( $\text{CH}_2\text{Cl}_2$ ):  $\lambda_{\text{max}}$  (log  $\epsilon$ ) 420 (4.68), 577 nm (3.50). **Elemental analysis** calcd for  $\text{C}_{120}\text{H}_{85}\text{FeN}_8\text{O}_9$ : C, 78.38; H, 4.66; N, 6.09. Found: C, 78.75; H, 4.57; N, 6.22. **MS** (ESI):  $m/z = 1861.6$  [ $\text{M} + \text{Na}^+$ ].

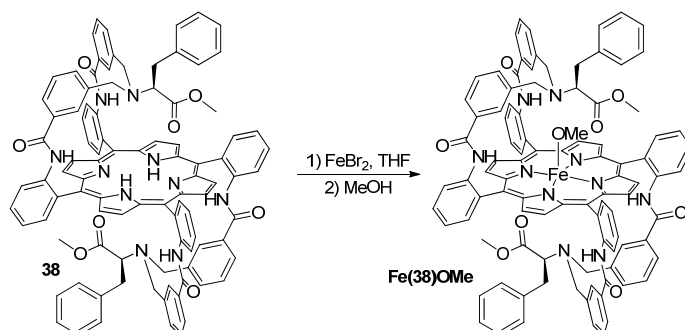
### 3.3.4. Synthesis of Fe(37)OMe



Porphyrin **37** (30.0 mg,  $2.17 \cdot 10^{-5}$  mol) and  $\text{FeBr}_2$  (47.0 mg,  $2.17 \cdot 10^{-4}$  mol) were dissolved in THF (12.0 mL). The resulting dark solution was refluxed under stirring for 4 hours until the complete consumption of **37**, that was monitored by TLC (1% MeOH in  $\text{CH}_2\text{Cl}_2$ ). The solvent was evaporated to dryness under reduced pressure and the crude purified by chromatography (alumina 0.063-0.200  $\mu\text{m}$ , 0.3% MeOH in  $\text{CH}_2\text{Cl}_2$ ) to obtain a dark brown solid (28.0 mg, 90%).

**IR** ( $\text{CH}_2\text{Cl}_2$ ):  $\nu_{\text{max}}$  = 3684 (w), 3425 (w), 3313 (w), 1711 (w), 1685 (w), 1606 (w), 1581 (w), 1523 (w), 1448 (w), 1308 (w), 1258 (w), 1237  $\text{cm}^{-1}$  (w). **IR** (ATR):  $\nu_{\text{max}}$  = 3424 (w), 3310 (w), 1681 (w), 1606 (w), 1580 (w), 1516 (w), 1443 (w), 1305 (w), 1260 (w), 1237  $\text{cm}^{-1}$  (w). **UV-Vis** ( $\text{CH}_2\text{Cl}_2$ ):  $\lambda_{\text{max}}$  (log  $\epsilon$ ) 420 (5.40), 578 nm (2.75). **Elemental Analysis** calcd. for  $\text{C}_{93}\text{H}_{73}\text{FeN}_{10}\text{O}_5$ : C, 76.17; H, 5.02; N, 9.55. Found: C, 76.30; H, 5.10; N, 9.40. **MS** (ESI):  $m/z$  = 1466 [ $\text{M}^+$ ].

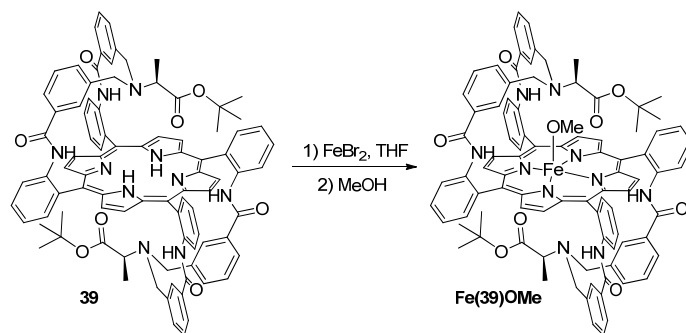
### 3.3.5. Synthesis of Fe(38)OMe



Porphyrin **38** (30.0 mg,  $2.0 \cdot 10^{-5}$  mol) and  $\text{FeBr}_2$  (43.0 mg,  $2.0 \cdot 10^{-4}$  mol) were dissolved in THF (12.0 mL) and the resulting dark solution was refluxed for 4 hours under stirring until the complete consumption of **38**, that was monitored by TLC (1% MeOH in  $\text{CH}_2\text{Cl}_2$ ). The solvent was evaporated to dryness under reduced pressure and the crude purified by chromatography (alumina 0.063-0.200  $\mu\text{m}$ , 0.5% MeOH in  $\text{CH}_2\text{Cl}_2$ ) to obtain a dark brown solid (29.0 mg, 92%).

**IR** ( $\text{CH}_2\text{Cl}_2$ ):  $\nu_{\text{max}}$  = 3680 (w), 3421 (w), 3314 (w), 1732 (w), 1683 (w), 1608 (w), 1583 (w), 1448 (w), 1350 (w), 1308  $\text{cm}^{-1}$  (w). **IR** (ATR):  $\nu_{\text{max}}$  = 3420 (w), 1735 (w), 1680 (w), 1579 (w), 1445 (w), 1310  $\text{cm}^{-1}$  (w). **UV-Vis** ( $\text{CH}_2\text{Cl}_2$ ):  $\lambda_{\text{max}}$  (log  $\epsilon$ ) 423 (5.50), 584 nm (3.97). **MS** (ESI):  $m/z$  = 1581 [ $\text{M}^+$ ].

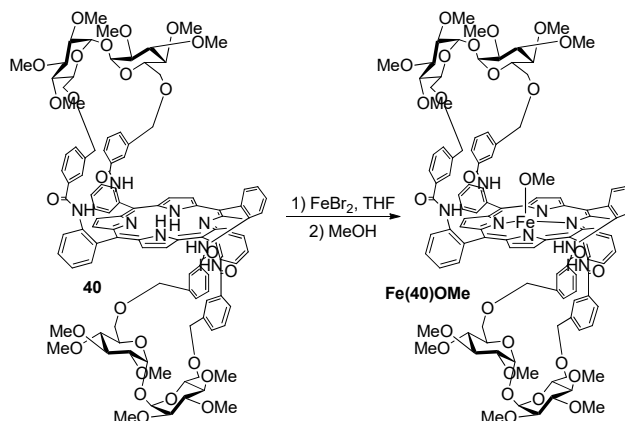
### 3.3.6. Synthesis of Fe(39)OMe



Porphyrin **39** (30.0 mg,  $2.10 \cdot 10^{-5}$  mol) and  $\text{FeBr}_2$  (45.0 mg,  $2.10 \cdot 10^{-4}$  mol) were dissolved in THF (12.0 mL) and the resulting dark solution was refluxed for 12 hours under stirring until the complete consumption of **39**, that was monitored by TLC (1% MeOH in  $\text{CH}_2\text{Cl}_2$ ). The solvent was evaporated to dryness under reduced pressure and the crude purified by chromatography (alumina 0.063-0.200  $\mu\text{m}$ , 0.5% MeOH in  $\text{CH}_2\text{Cl}_2$ ) to obtain a dark brown solid (29.0 g, 94%).

**IR** ( $\text{CH}_2\text{Cl}_2$ ):  $\nu_{\text{max}}$  = 3688 (w), 3421 (w), 2962 (w), 2929 (w), 2855 (w), 1726 (w), 1683 (w), 1581 (w), 1516 (w), 1448 (w), 1096 (w), 1012  $\text{cm}^{-1}$  (w). **IR** (ATR):  $\nu_{\text{max}}$  = 2962 (w), 1260 (w), 1101 (w), 1017 (w), 800  $\text{cm}^{-1}$  (w). **UV-Vis** ( $\text{CH}_2\text{Cl}_2$ ):  $\lambda_{\text{max}}$  (log  $\epsilon$ ) 420 (5.36), 569 nm (3.87). **MS** (ESI):  $m/z$  = 1552.6 [ $\text{M}+\text{K}^+$ ].

### 3.3.7. Synthesis of Fe(40)OMe

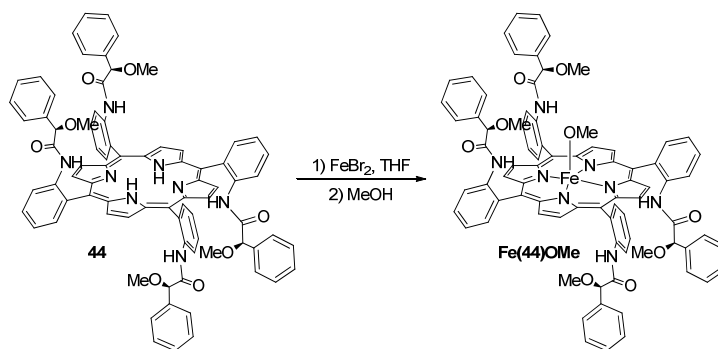


Porphyrin **40** (30.0 mg,  $1.50 \cdot 10^{-5}$  mol) and  $\text{FeBr}_2$  (32.0 mg,  $1.50 \cdot 10^{-4}$  mol) were dissolved in THF (12.0 mL) and the resulting dark solution was refluxed for 4 hours under stirring until the complete consumption of **40**, that was monitored by TLC (1% MeOH in  $\text{CH}_2\text{Cl}_2$ ). The solvent was evaporated to dryness under reduced pressure and the crude purified by chromatography (alumina 0.063-0.200  $\mu\text{m}$ , 0.5% MeOH in  $\text{CH}_2\text{Cl}_2$ ) to obtain a dark brown solid (28.0 mg, 90%).

**IR** ( $\text{CH}_2\text{Cl}_2$ ):  $\nu_{\text{max}}$  = 3686 (w), 3421 (w), 2962 (w), 2930 (w), 2853 (w), 1733 (w), 1679 (w), 1581 (w), 1517 (w), 1446 (w), 1098 (w), 1046 (w), 1011  $\text{cm}^{-1}$  (w). **IR** (ATR):  $\nu_{\text{max}}$  = 2962 (w), 2926 (w), 2854 (w), 1738 (w), 1656 (w), 1579 (w), 1516 (w), 1444 (w), 1397 (w), 1258 (w), 1010 (w), 864 (w), 789  $\text{cm}^{-1}$  (w). **UV-Vis** ( $\text{CH}_2\text{Cl}_2$ ):  $\lambda_{\text{max}}$  (log  $\epsilon$ ) 425 (4.94), 581 (3.80), 656 nm (3.36). **MS** (ESI):  $m/z$  = 2045 [ $\text{M}-\text{OMe}$ ].



### 3.3.8. Synthesis of Fe(44)OMe

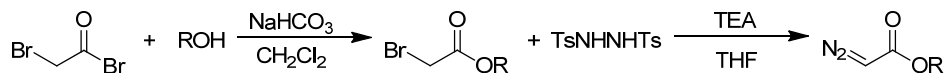


Porphyrin **44** (30.0 mg,  $2.37 \cdot 10^{-5}$  mol) and  $\text{FeBr}_2$  (51.1 mg,  $2.37 \cdot 10^{-4}$  mol) were dissolved in THF (12.0 mL) and the resulting dark solution was refluxed for 4 hours under stirring until the complete consumption of **44**, that was monitored by TLC (1% MeOH in  $\text{CH}_2\text{Cl}_2$ ). The solvent was evaporated to dryness under reduced pressure and the crude purified by chromatography (alumina 0.063-0.200  $\mu\text{m}$ , 0.5% MeOH in  $\text{CH}_2\text{Cl}_2$ ) to obtain a dark brown solid (31.0 mg, 96%).

**IR** ( $\text{CH}_2\text{Cl}_2$ ):  $\nu_{\text{max}}$  = 3688 (w), 3361 (w), 2931 (w), 1733 (w), 1692 (w), 1602(w), 1582 (w), 1520 (w), 1468 (w), 1452 (w), 1099 (w), 998  $\text{cm}^{-1}$  (w). **IR** (ATR):  $\nu_{\text{max}}$  = 2917 (w), 2852 (w), 1733 (w), 1695 (w), 1581 (w), 1557 (w), 1507 (w), 1444 (w), 1099 (w), 1066 (w), 996  $\text{cm}^{-1}$ (w). **UV-Vis** ( $\text{CH}_2\text{Cl}_2$ ):  $\lambda_{\text{max}}$  (log  $\epsilon$ ) 419 (4.88), 508 (3.88), 579 (3.54), 642 nm (3.30). **MS** (ESI):  $m/z$ =1320.4 [M-OMe].

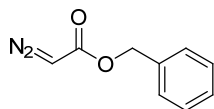
## 3.4. Synthesis of cyclopropanes catalysed by chiral iron(III) porphyrin complexes

### 3.4.1. Synthesis of diazo compounds



**General procedure:** The diazo compounds were synthesised by modifying the procedure reported by Fukuyama.<sup>28</sup> The desired alcohol ( $5.52 \cdot 10^{-3}$  mol) and sodium bicarbonate (1.16 g,  $1.38 \cdot 10^{-2}$  mol) were dissolved in 15.0 mL of  $\text{CH}_2\text{Cl}_2$  and the reaction mixture was stirred at  $0^\circ\text{C}$  in an ice bath for 5 min. Bromoacetyl bromide (1.67 g,  $8.28 \cdot 10^{-3}$  mol) was added under vigorous magnetic stirring by a syringe over a period of 30 minutes and then the mixture was stirred for additional 3 hours. The reaction was quenched with 10.0 mL of 0.5 M HCl solution, stirred for 5 minutes at RT and 10.0 mL of water and 10.0 mL of brine were added to the mixture. The aqueous phase was extracted with  $\text{CH}_2\text{Cl}_2$  (10.0 mL added two times), the combined organic phases were washed with aqueous  $\text{NaHCO}_3$  (10% wt) and brine, dried over  $\text{Na}_2\text{SO}_4$  and filtered. The filtrate was evaporated to dryness to give the bromoacetate ( $1.47 \cdot 10^{-3}$  mol) which was dissolved in 10.0 mL of THF with *N,N*-ditosylhydrazine (0.752 g,  $2.21 \cdot 10^{-3}$  mol). DBU (1.34 g,  $8.86 \cdot 10^{-3}$  mol) was added dropwise at  $-10^\circ\text{C}$  by a syringe to the resulting mixture which was stirred at room temperature for 1 h, after 5 min a white precipitate was formed and the solution turned to red/orange. The reaction was quenched with saturated aqueous  $\text{NaHCO}_3$  and extracted with diethyl ether (20.0 mL added three times), the combined organic phase was washed with 20.0 mL brine and dried over  $\text{Na}_2\text{SO}_4$ . The solvent was evaporated under reduced pressure to give the crude product which was purified by flash chromatography (silica gel, 60  $\mu\text{m}$ , AcOEt/hexane 1:20).

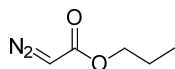
### 3.4.1.1. Benzyl 2-diazoacetate



The general procedure for the synthesis of diazo compounds was followed starting from benzyl alcohol as the starting material to obtain a yellowish oil (81%). The collected data are in accord with those reported in literature.<sup>28</sup>

<sup>1</sup>H NMR (300 MHz, CDCl<sub>3</sub>): δ 7.37 (m, 5H, H<sub>Ar</sub>), 5.21 (s, 2H, H<sub>CH2</sub>), 4.80 ppm (br, 1H, H<sub>CHN2</sub>). IR (neat): ν<sub>max</sub> = 2112 cm<sup>-1</sup> (C=N<sub>2</sub>).

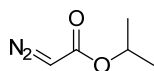
### 3.4.1.2. Propyl 2-diazoacetate



The general procedure for the synthesis of diazo compounds was followed starting from propyl alcohol as the starting material to obtain a yellowish oil (41%). The data are in accord with those reported in literature.<sup>29</sup>

<sup>1</sup>H NMR (400 MHz, CDCl<sub>3</sub>): δ 4.75 (br, 1H, H<sub>CHN2</sub>), 4.12 (t, 2H, J=6.7 Hz, H<sub>OCH2</sub>), 1.71-1.63 (m, 2H, H<sub>CH2</sub>), 0.95 ppm (t, 3H, J=7.4 Hz, H<sub>CH3</sub>). IR (neat): ν<sub>max</sub> = 2113 cm<sup>-1</sup> (C=N<sub>2</sub>).

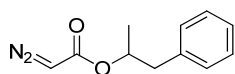
### 3.4.1.3. Isopropyl 2-diazoacetate



The general procedure for the synthesis of diazo compounds was followed starting from isopropyl alcohol as the starting material to obtain a yellowish oil (30%). The data are in accord with those reported in literature.<sup>29</sup>

<sup>1</sup>H NMR (300 MHz, CDCl<sub>3</sub>): δ 5.05 (heptet, 1H, J=6.3 Hz, H<sub>OCH</sub>), 4.67 (br, 1H, H<sub>CHN2</sub>), 1.22 ppm (d, 6H, J=6.3 Hz, 6H, H<sub>CH3</sub>). IR (neat): ν<sub>max</sub> = 2110 cm<sup>-1</sup> (C=N<sub>2</sub>).

### 3.4.1.4. 1-Phenylpropan-2-yl 2-diazoacetate



The general procedure for the synthesis of diazo compounds was followed starting from 1-phenylpropan-2-ol as the starting material to obtain a yellowish oil (43%). The collected data are in accord with those reported in literature.<sup>28</sup>

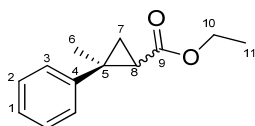
<sup>1</sup>H NMR (300 MHz, CDCl<sub>3</sub>): δ 7.34-7.20 (m, 5H, H<sub>Ar</sub>), 5.28-5.17 (m, 1H, H<sub>OCH</sub>), 4.69 (br, 1H, H<sub>CHN2</sub>), 2.97 (dd, 1H, <sup>2</sup>J=13.6 Hz, J=6.6 Hz, H<sub>CH2</sub>), 2.81 (dd, 1H, <sup>2</sup>J=13.6 Hz, J=6.4 Hz, H<sub>CH2</sub>), 1.27 ppm (d, 3H, J=6.2 Hz, H<sub>CH3</sub>). IR (neat): ν<sub>max</sub> = 2110 cm<sup>-1</sup> (C=N<sub>2</sub>).

## 3.4.2. Synthesis of cyclopropanes

**General catalytic procedures:** The stock solution 6.80·10<sup>-4</sup> mol/L of the catalyst was prepared by dissolving 6.80·10<sup>-6</sup> mol of the opportune catalyst in 10.0 mL of anhydrous toluene. The obtained solution was used for the following catalytic reactions. **Method a.** In a typical run, 1.00 mL of the stock solution was dissolved in

2.00 mL of anhydrous toluene. Then alkene and diazo compound were added in a molar ratio catalyst/ $\alpha$ -methylstyrene/diazo compound=1:1000:1100 at the selected temperature. The consumption of the diazo compound was monitored by IR spectroscopy by measuring the decrease of the characteristic N<sub>2</sub> absorbance at  $\approx$ 2110 cm<sup>-1</sup>. The reaction was considered completed when the absorbance went below 0.03 (by using a 0.5 mm-thickness cell). The solvent was evaporated to dryness and the residue was purified and analysed by <sup>1</sup>H NMR and by HPLC by using a chiral column. **Method b.** The procedure illustrated for *method a* was repeated by using an alkene/diazo compound molar ratio of 10000:10100 at 0°C. **Method c: Fe(17)OMe** (1.00 mL of the stock solution) was dissolved in 2.00 mL of dry toluene in a flask equipped with a calcium chloride drying tube, then  $\alpha$ -methylstyrene and EDA were added with a molar ratio of **Fe(17)OMe**/ $\alpha$ -methylstyrene/EDA of 1:1000:1000. **Method d: Fe(17)OMe** (1.00 mL of the stock solution) was dissolved in 2.00 mL of toluene in air and in presence of activated 4Å molecular sieves. Then  $\alpha$ -methylstyrene and EDA were added with a molar ratio of **Fe(17)OMe**/ $\alpha$ -methylstyrene/EDA of 1:1000:1000. **Method e: Fe(17)OMe** (1.00 mL of the stock solution) was dissolved in 2.00 mL of dry toluene containing 0.03% of degassed water. Then  $\alpha$ -methylstyrene and EDA were added with a molar ratio of **Fe(17)OMe**/ $\alpha$ -methylstyrene/EDA of 1:1000:1000. **Method f.** The procedure illustrated for *method a* was repeated using a syringe pump to add the diazo compound.

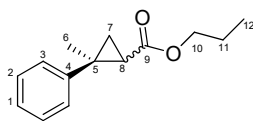
#### 3.4.2.1. Synthesis of *trans* ethyl-2-methyl-2-phenylcyclopropanecarboxylate (19)



Compound **19** was synthesised from  $\alpha$ -methylstyrene and EDA. The crude was purified by flash chromatography (silica gel, 60 $\mu$ m, AcOEt/hexane 0.5:9.5) to give a yellow oil which was analysed by NMR and by HPLC by using a chiral column (DAI-CEL CHIRALCEL, IB, hexane/2-propanol 99.75:0.25). The collected analytical data are in accord with those reported in the literature.<sup>30</sup>

<sup>1</sup>H NMR (300 Hz, CDCl<sub>3</sub>):  $\delta$  7.31 (d, 4H,  $J$ =4.4 Hz, H<sup>2</sup> and H<sup>3</sup>), 7.22 (m, 1H, H<sup>1</sup>), 4.20 (q, 2H,  $J$ =7.1 Hz, H<sup>10</sup>), 1.97 (dd, 1H,  $J$ =8.2, 6.1 Hz, H<sup>8</sup>), 1.54 (s, 3H, H<sup>6</sup>), 1.49-1.39 (m, 2H, H<sup>7</sup>), 1.31 ppm (t, 3H,  $J$ =7.1 Hz, H<sup>11</sup>).

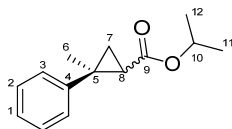
#### 3.4.2.2. Synthesis of *trans* propyl-2-methyl-2-phenylcyclopropanecarboxylate (20)



Compound **20** was synthesised from  $\alpha$ -methylstyrene and propyl diazoacetate. The crude was purified by flash chromatography (silica gel, 60 $\mu$ m, AcOEt/hexane 0.5:9.5) to give a yellow oil which was analysed by NMR and HPLC by using a chiral column (DAI-CEL CHIRALCEL, IB, hexane/2-propanol 99.75:0.25).

<sup>1</sup>H NMR (300 Hz, CDCl<sub>3</sub>):  $\delta$  7.28 (dd, 4H,  $J$ =4.4 Hz, H<sup>2</sup> and H<sup>3</sup>), 7.21 (m, 1H, H<sup>1</sup>), 4.10 (t, 2H,  $J$ =6.7 Hz, H<sup>10</sup>), 1.97 (dd, 1H,  $J$ =8.3, 6.1 Hz, H<sup>8</sup>), 1.79-1.58 (m, 2H, H<sup>11</sup>), 1.52 (s, 3H, H<sup>6</sup>), 1.48-1.38 (m, 2H, H<sup>7</sup>), 0.97 ppm (t, 3H,  $J$ =7.1 Hz, H<sup>12</sup>). <sup>13</sup>C NMR (75 Hz, CDCl<sub>3</sub>):  $\delta$  172.2 (C9), 145.9 (C4), 128.4 (C2), 127.3 (C3), 126.4 (C1), 66.1 (C10), 30.5 (C5), 27.9 (C8), 22.1 (C11), 20.7 (C7), 19.9 (C6), 10.4 (C12). MS (EI):  $m/z$ =218 [M].

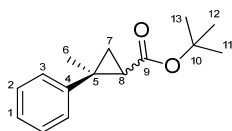
### 3.4.2.3. Synthesis of *trans* isopropyl-2-methyl-2-phenylcyclopropanecarboxylate (21)



Compound **21** was obtained from  $\alpha$ -methylstyrene and isopropyl diazoacetate. The crude was purified by flash chromatography (silica gel, 60 $\mu$ m, AcOEt/hexane 0.5:9.5) to give a yellow oil which was analysed by NMR and HPLC by using a chiral column (DAI-CEL CHIRALCEL, IB, hexane/2-propanol 99.75:0.25).

$^1\text{H NMR}$  (300 MHz,  $\text{CDCl}_3$ ):  $\delta$  7.34-7.27 (m, 4H,  $\text{H}^2$  e  $\text{H}^3$ ), 7.23-7.14 (m, 1H,  $\text{H}^1$ ), 5.06 (heptet, 1H,  $J=6.2$  Hz,  $\text{H}^{10}$ ), 1.93 (dd, 1H,  $J=8.3, 6.0$  Hz,  $\text{H}^8$ ), 1.51 (s, 3H,  $\text{H}^6$ ), 1.42-1.36 (m, 2H,  $\text{H}^7$ ), 1.26 ppm (d, 6H,  $J=6.2$  Hz,  $\text{H}^{11}$  and  $\text{H}^{12}$ ).  $^{13}\text{C NMR}$  (75 MHz,  $\text{CDCl}_3$ ):  $\delta$  171.7 (C9), 146.1 (C4), 128.5 (C2), 127.3 (C3), 126.5 (C1), 67.9 (C10), 30.4 (C5), 28.4 (C8), 22.2 (C11), 22.0 (C12), 20.7 (C7), 19.9 ppm (C6). **MS** (EI):  $m/z=218$  [M].

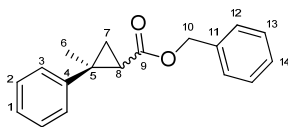
### 3.4.2.4. Synthesis of *trans tert*-butyl-2-methyl-2-phenylcyclopropanecarboxylate (22)



Compound **22** was synthesised from  $\alpha$ -methylstyrene and *tert*-butyl diazoacetate. The crude was purified by flash chromatography (silica gel, 60 $\mu$ m, AcOEt/hexane 0.5:9.5) to give a yellow oil which was analysed by NMR and by HPLC by using a chiral column (DAI-CEL CHIRALCEL, IB, hexane/2-propanol 99.75:0.25). The collected analytical data are in accord with those reported in the literature.<sup>31</sup>

$^1\text{H NMR}$  (400 MHz,  $\text{CDCl}_3$ ):  $\delta$  7.29 (m, 4H,  $\text{H}^2$  and  $\text{H}^3$ ), 7.18 (m, 1H,  $\text{H}^1$ ), 1.89 (dd, 1H,  $J=8.2, 6.0$  Hz,  $\text{H}^1$  and  $\text{H}^8$ ), 1.56 (s, 3H,  $\text{H}^6$ ), 1.53 (s, 9H,  $\text{H}^{11}$  and  $\text{H}^{12}$  and  $\text{H}^{13}$ ), 1.40 (dd, 1H,  $J=6.0$  Hz,  $^2J=4.8$  Hz,  $\text{H}^7$ ), 1.37 ppm (dd, 1H,  $J=8.3$  Hz,  $^2J=4.8$  Hz,  $\text{H}^7$ ).

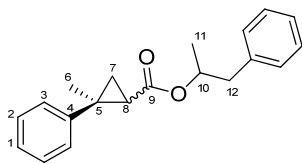
### 3.4.2.5. Synthesis of *trans* benzyl-2-methyl-2-phenylcyclopropanecarboxylate (23)



Compound **23** was synthesised from  $\alpha$ -methylstyrene and benzyl diazoacetate. The crude was purified by flash chromatography (silica gel, 60 $\mu$ m, AcOEt/hexane 0.5:9.5) to give a yellow oil which was analysed by NMR and by HPLC by using a chiral column (DAI-CEL CHIRALCEL, IB, hexane/2-propanol 99.75:0.25). The collected analytical data are in accord with those reported in the literature.<sup>32</sup>

$^1\text{H NMR}$  (300 MHz,  $\text{CDCl}_3$ ):  $\delta$  7.33 (m, 9H,  $\text{H}_{\text{Ar}}$ ), 7.21 (m, 1H,  $\text{H}^1$ ), 5.25-5.16 (m, 2H,  $\text{H}^{10}$ ), 2.05 (dd, 1H,  $J=8.3, 6.0$  Hz,  $\text{H}^8$ ), 1.54 (s, 3H,  $\text{H}^6$ ), 1.47 ppm (m, 2H,  $\text{H}^7$ ).

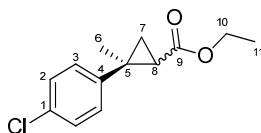
### 3.4.2.6. Synthesis of *trans* 1-phenylpropyl-2-methyl-2-phenylcyclopropane carboxylate (24)



Compound **24** was obtained from  $\alpha$ -methylstyrene and 1-phenylpropan-2-yl 2-diazoacetate. The crude was purified by flash chromatography (silica gel, 60 $\mu$ m, AcOEt/hexane 0.5:9.5). Two *trans* diastereomers were obtained in mixture and they were analysed by NMR.

$^1\text{H NMR}$  (400 MHz,  $\text{CDCl}_3$ ):  $\delta$  7.49-7.12 (m, 20H,  $\text{H}_{\text{Ar}}$ ), 5.31-5.01 (m, 2H,  $\text{H}^{10}$ ), 3.05-2.88 (m, 2H,  $\text{H}^{12}$ ), 2.86-2.68 (m, 2H,  $\text{H}^{12'}$ ), 2.08-1.72 (m, 2H,  $\text{H}^8$ ), 1.47 (s, 3H,  $\text{H}^{6\text{A}}$ ), 1.41-1.33 (m, 4H,  $\text{H}^7$ ), 1.28 (s, 3H,  $\text{H}^{6\text{B}}$ ), 1.27 (m, 6H,  $\text{H}^{11}$ ).  $^{13}\text{C NMR}$  (400 MHz,  $\text{CDCl}_3$ ):  $\delta$  171.7, 171.6, 146.2, 146.1, 138, 137.9, 129.6, 128.6, 128.5, 127.6, 127.4, 126.6, 71.9, 71.5, 42.7, 42.5, 30.7, 30.4, 28.4, 28.1, 20.7, 20.4, 20.0, 19.9 ppm. **MS** (EI):  $m/z=294$  [M].

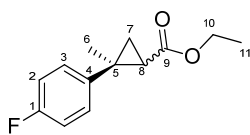
### 3.4.2.7. Synthesis of *trans* ethyl-2-(4-chlorophenyl)-2-methylcyclopropane carboxylate (25)



Compound **25** was synthesised from  $\alpha$ -methyl-4-chlorostyrene and EDA. The crude was purified by flash chromatography (silica gel, 60 $\mu$ m, AcOEt/hexane 0.5:9.5) to give a yellow oil which was analysed by NMR and HPLC by using a chiral column (DAI-CEL CHIRALCEL, IB, hexane/2-propanol 99.75:0.25). The collected analytical data are in accord with those reported in the literature.<sup>33</sup>

$^1\text{H NMR}$  (400 MHz,  $\text{CDCl}_3$ ):  $\delta$  7.26 (q, 4H,  $J=8.5$  Hz,  $\text{H}^2$  and  $\text{H}^3$ ), 4.26-4.18 (m, 2H,  $\text{H}^{10}$ ), 1.94 (dd, 1H,  $J=8.3, 6.1$  Hz,  $\text{H}^8$ ), 1.52 (s, 3H,  $\text{H}^6$ ), 1.47 (m, 1H,  $\text{H}^7$ ), 1.39 (dd, 1H,  $J=8.4, 4.8$  Hz,  $\text{H}^7$ ), 1.32 ppm (t, 3H,  $J=7.1$  Hz,  $\text{H}^{11}$ ).

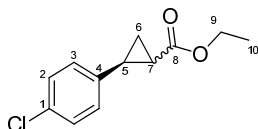
### 3.4.2.8. Synthesis of *trans* ethyl-2-methyl-2-(4-fluorophenyl)cyclopropane carboxylate (26)



Compound **26** was synthesised from  $\alpha$ -methyl-4-fluorostyrene and EDA. The crude was purified by flash chromatography (silica gel, 60 $\mu$ m, AcOEt/hexane 0.5:9.5) to give a yellow oil which was analysed by NMR and HPLC by using a chiral column (DAI-CEL CHIRALCEL, IB, hexane/2-propanol 99.75:0.25).

$^1\text{H NMR}$  (300 MHz,  $\text{CDCl}_3$ ):  $\delta$  7.36-7.21 (m, 2H,  $\text{H}^3$ ), 7.01-6.95 (m, 2H,  $\text{H}^2$ ), 4.29-4.14 (m, 2H,  $\text{H}^{10}$ ), 1.93 (m, 1H,  $\text{H}^8$ ), 1.52 (s, 3H,  $\text{H}^6$ ), 1.45 (m, 1H,  $\text{H}^7$ ), 1.42-1.35 (m, 1H,  $\text{H}^7$ ), 1.33 ppm (t, 3H,  $J=7.1$  Hz,  $\text{H}^{11}$ ).  $^{13}\text{C NMR}$  (75 MHz,  $\text{CDCl}_3$ ):  $\delta$  172.4 (C9), 161.8 (d,  $^1J_{\text{CF}}=244.9$  Hz, C1), 142.1 (d,  $^4J_{\text{CF}}=3.1$  Hz, C4), 129.4 (d,  $^3J_{\text{CF}}=8.1$  Hz, C3), 115.6 (d,  $^2J_{\text{CF}}=21.3$  Hz, C2), 60.9 (C10), 30.4 (C5), 28.1 (C8), 21.1 (C7), 20.5 (C6), 14.8 ppm (C11).  $^{19}\text{F NMR}$  (282 MHz,  $\text{CDCl}_3$ ):  $\delta$  -116.65 ppm (s). **MS** (EI):  $m/z=222$  [M].

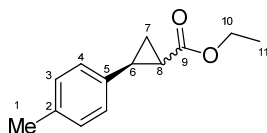
### 3.4.2.9. Synthesis of *trans* ethyl-2-(4-chlorophenyl)cyclopropanecarboxylate (27)



Compound **27** was synthesised from 4-chlorostyrene and EDA. The crude was purified by flash chromatography (silica gel, 60 $\mu$ m, AcOEt/hexane 1:9) to give a yellow oil which was analysed by NMR and by HPLC by using a chiral column (DAI-CEL CHIRALCEL, OJ, hexane/2-propanol 99:1). The collected analytical data are in accord with those reported in the literature.<sup>34</sup>

<sup>1</sup>H NMR (300 MHz, CDCl<sub>3</sub>):  $\delta$  7.22 (d, 2H,  $J=8.5$  Hz, H<sup>3</sup>), 7.01 (d, 2H,  $J=8.4$  Hz, H<sup>2</sup>), 4.16 (q, 2H,  $J=7.1$  Hz, H<sup>9</sup>), 2.51-2.44 (m, 1H, H<sup>7</sup>), 1.90-1.80 (m, 1H, H<sup>5</sup>), 1.60-1.57 (m, 1H, H<sup>6</sup>), 1.27 (t, 3H,  $J=7.1$  Hz, H<sup>10</sup>), 1.25 ppm (m, 1H, H<sup>6</sup>).

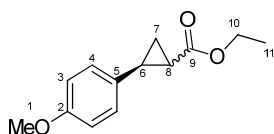
### 3.4.2.10. Synthesis of *trans* ethyl 2-(4-methylphenyl)cyclopropanecarboxylate (28)



Compound **28** was synthesised from 4-methylstyrene and EDA. The crude was purified by flash chromatography (silica gel, 60 $\mu$ m, AcOEt/hexane 0.5:9.5) to give a yellow oil which was analysed by NMR and by HPLC by using a chiral column (DAI-CEL CHIRALCEL, OJ, hexane/2-propanol 99:1). The collected analytical data are in accord with those reported in the literature.<sup>30</sup>

<sup>1</sup>H NMR (400 MHz, CDCl<sub>3</sub>):  $\delta$  7.10 (d, 2H,  $J=7.9$  Hz, H<sup>4</sup>), 7.01 (d, 2H,  $J=8.1$  Hz, H<sup>3</sup>), 4.18 (q, 2H,  $J=7.1$  Hz, H<sup>10</sup>), 2.53-2.48 (m, 1H, H<sup>8</sup>), 2.32 (s, 3H, H<sup>1</sup>), 1.86 (ddd, 1H,  $J=8.4, 5.2, 4.2$  Hz, H<sup>6</sup>), 1.58 (ddd, 1H,  $J=9.6, 5.1$  Hz,  $^2J=4.6$ , H<sup>7</sup>), 1.28 (t, 3H,  $J=7.1$  Hz, H<sup>11</sup>), 1.27 ppm (m, 1H, H<sup>7</sup>).

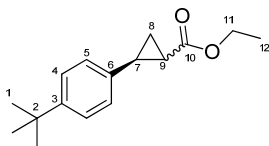
### 3.4.2.11. Synthesis of *trans* ethyl 2-(4-methoxyphenyl)cyclopropanecarboxylate (29)



Compound **29** was synthesised from 4-methoxystyrene and EDA. The crude was purified by flash chromatography (silica gel, 60 $\mu$ m, AcOEt/hexane 0.5:9.5) to give a yellow oil which was analysed by NMR and by HPLC by using a chiral column (DAI-CEL CHIRALCEL, OJ, hexane/2-propanol 99:1). The collected analytical data are in accord with those reported in the literature.<sup>30</sup>

<sup>1</sup>H NMR (300 MHz, CDCl<sub>3</sub>):  $\delta$  7.03 (d, 2H,  $J=8.7$  Hz, H<sup>4</sup>), 6.82 (d, 2H,  $J=8.7$  Hz, H<sup>3</sup>), 4.16 (q, 2H,  $J=7.1$  Hz, H<sup>10</sup>), 3.78 (s, 3H, H<sup>1</sup>), 2.51-2.45 (m, 1H, H<sup>8</sup>), 1.83-1.81 (m, 1H, H<sup>6</sup>), 1.65-1.53 (m, 1H, H<sup>7</sup>), 1.28 (t, 3H,  $J=7.1$  Hz, H<sup>11</sup>), 1.28-1.25 ppm (m, 1H, H<sup>7</sup>).

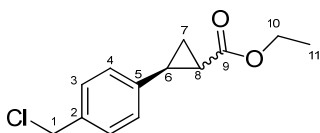
### 3.4.2.12. Synthesis of *trans* ethyl 2-(4-*tert*-butylphenyl)cyclopropanecarboxylate (30)



Compound **30** was synthesised from 4-*tert*-butylstyrene and EDA. The crude was purified by flash chromatography (silica gel, 60 $\mu$ m, AcOEt/hexane 0.5:9.5) to give a yellow oil which was analysed by NMR and by HPLC by using a chiral column (DAI-CEL CHIRALCEL, OJ, hexane/2-propanol 99:1). The collected analytical data are in accord with those reported in the literature.<sup>30</sup>

<sup>1</sup>H NMR (300 MHz, CDCl<sub>3</sub>):  $\delta$  7.34 (d, 2H,  $J=8.3$  Hz, H<sup>5</sup>), 7.07 (d, 2H,  $J=8.3$  Hz, H<sup>4</sup>), 4.20 (q, 2H,  $J=7.1$  Hz, H<sup>11</sup>), 2.56-2.50 (m, 1H, H<sup>9</sup>), 1.93-1.90 (m, 1H, H<sup>7</sup>), 1.63-1.60 (m, 1H, H<sup>8</sup>), 1.33 (s, 9H, H<sup>1</sup>), 1.29 (t, 3H,  $J=7.1$  Hz, H<sup>12</sup>), 1.33-1.28 ppm (m, 1H, H<sup>8</sup>).

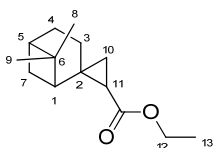
### 3.4.2.13. Synthesis of *trans* ethyl 2-(4-chloromethylphenyl)cyclopropanecarboxylate (31)



Compound **31** was synthesised from 4-chloromethylstyrene and EDA. The crude was purified by flash chromatography (silica gel, 60 $\mu$ m, AcOEt/hexane 1:9) to give a yellow oil which was analysed by NMR.

<sup>1</sup>H NMR (300 MHz, CDCl<sub>3</sub>):  $\delta$  7.30 (d, 2H,  $J=8.1$  Hz, H<sup>3</sup>), 7.09 (d, 2H,  $J=8.1$  Hz, H<sup>4</sup>), 4.56 (s, 2H, H<sup>1</sup>), 4.17 (q, 2H,  $J=7.1$  Hz, H<sup>10</sup>), 2.61-2.46 (m, 1H, H<sup>8</sup>), 1.89 (ddd, 1H,  $J=8.5, 5.3, 4.2$  Hz, H<sup>6</sup>), 1.61 (ddd, 1H,  $J=9.2, 5.2, ^2J=4.6$  Hz, H<sup>7</sup>), 1.33 (m, 1H, H<sup>7</sup>), 1.28 ppm (t, 3H,  $J=7.1$  Hz, H<sup>11</sup>). <sup>13</sup>C NMR (75 MHz, CDCl<sub>3</sub>):  $\delta$  173.4 (C<sup>9</sup>), 140.7 (C<sup>5</sup>), 135.9 (C<sup>2</sup>), 128.9 (C<sup>3</sup>), 126.7 (C<sup>4</sup>), 60.9 (C<sup>10</sup>), 46.1 (C<sup>1</sup>), 26.0 (C<sup>6</sup>), 24.4 (C<sup>8</sup>), 17.2 (C<sup>7</sup>), 14.4 ppm (C<sup>11</sup>). MS (EI):  $m/z=238$  [M].

### 3.4.2.14. Synthesis of (1*R*,2*R*,2'*R*) and (1*R*,2*R*,2'*S*) Ethyl-6,6-dimethyl-spiro[bicycle [3.1.1]heptanes-2,1'-cyclopropane]-2'-carboxylate (32)

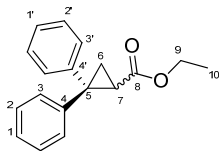


The two isomers of compound **32** were synthesised from  $\beta$ -pinene and EDA. The crude was purified by flash chromatography (silica gel, 60 $\mu$ m, AcOEt/hexane 1:9) to give a yellow oil. The two diastereoisomers were obtained in mixture and they were analysed by NMR. The collected analytical data are in accord with those reported in the literature.<sup>35</sup>

**(1*R*,2*R*,2'*R*) Ethyl-6,6-dimethyl-spiro[bicycle[3.1.1]heptanes-2,1'-cyclopropane]-2'-carboxylate:** <sup>1</sup>H NMR (400 MHz, CDCl<sub>3</sub>):  $\delta$  4.10 (q, 2H,  $J=7.1$  Hz, H<sup>12</sup>), 2.24-2.13 (m, 2H, H<sup>7</sup> and H<sup>4</sup>), 1.98-1.77 (m, 4H, H<sup>1</sup> and H<sup>3</sup> and H<sup>5</sup>), 1.43 (d, 1H,  $J=10.1$  Hz, H<sup>7</sup>), 1.38 (dd, 1H,  $J=7.9, 6.0$  Hz, H<sup>2'</sup>), 1.30 (m, 1H, H<sup>4</sup>), 1.25 (m, 3H, H<sup>13</sup>), 1.21 (s, 3H, H<sup>9</sup>), 1.16 (m, 1H, H<sup>3'</sup>), 1.04 (dd, 1H,  $J=8.0, 4.6$  Hz, H<sup>3'</sup>), 0.95 ppm (s, 3H, H<sup>8</sup>).

**(1R,2R,2'S) Ethyl-6,6-dimethyl-spiro[bicyclo[3.1.1]heptanes-2,1'-cyclopropane]-2'-carboxylate:** <sup>1</sup>H NMR (400 MHz, CDCl<sub>3</sub>): δ 4.16 (q, 2H, *J*=7.1 Hz, H<sup>12</sup>), 2.35-2.33 (m, 2H, H<sup>7</sup> and H<sup>4</sup>), 1.9.97-1.85 (m, 4H, H<sup>5</sup> and H<sup>3</sup> and H<sup>4</sup>), 1.63-1.57 (m, 1H, H<sup>3</sup>), 1.53 (m, 1H, H<sup>7</sup>), 1.35 (m, 1H, H<sup>2</sup>), 1.30-1.24 (m, 4H, H<sup>3'</sup> and H<sup>13</sup>), 1.23-1.16 (m, 4H, H<sup>1</sup> and H<sup>9</sup>), 0.96 (s, 3H, H<sup>8</sup>), 0.93-0.90 ppm (m, 1H, H<sup>3'</sup>).

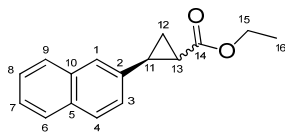
### 3.4.2.15. Synthesis of *trans* ethyl-2,2'-diphenylcyclopropanecarboxylate (33)



Compound **33** was synthesised from 1,1'-diphenylethylene and EDA. The crude was purified by flash chromatography (silica gel, 60μm, AcOEt/hexane 1:9) to give a yellow oil which was analysed by NMR and by HPLC by using a chiral column (DAI-CEL CHIRALCEL, IB, hexane/2-propanol 98:2). The collected analytical data are in accord with those reported in the literature.<sup>30</sup>

<sup>1</sup>H NMR (400 MHz, CDCl<sub>3</sub>): δ 7.38-7.32 (m, 2H, H<sup>2</sup> and H<sup>2'</sup>), 7.26-7.12 (m, 8H, H<sub>Ar</sub> and H<sub>Ar'</sub>), 3.92 (m, 2H, H<sup>9</sup>), 2.54 (dd, 1H, *J*=8.1, 5.9 Hz, H<sup>7</sup>), 2.18 (dd, 1H, *J*=5.9 Hz, <sup>2</sup>*J*=4.9 Hz, H<sup>6</sup>), 1.59 (dd, 1H, *J*=8.1 Hz, <sup>2</sup>*J*=4.9 Hz, H<sup>6</sup>), 1.01 (t, 3H, *J*=7.1 Hz, H<sup>10</sup>).

### 3.4.2.16. Synthesis of *trans* ethyl 2-(2-naphthalenyl)cyclopropanecarboxylate (34)



Compound **34** was synthesised from 2-vinylnaphthalene and EDA. The crude was purified by flash chromatography (silica gel, 60μm, AcOEt/hexane 0.5:9.5) to give a yellow oil which was analysed by NMR and by HPLC by using a chiral column (DAI-CEL CHIRALCEL, OJ, hexane/2-propanol 99:1). The collected analytical data are in accord with those reported in the literature.<sup>30</sup>

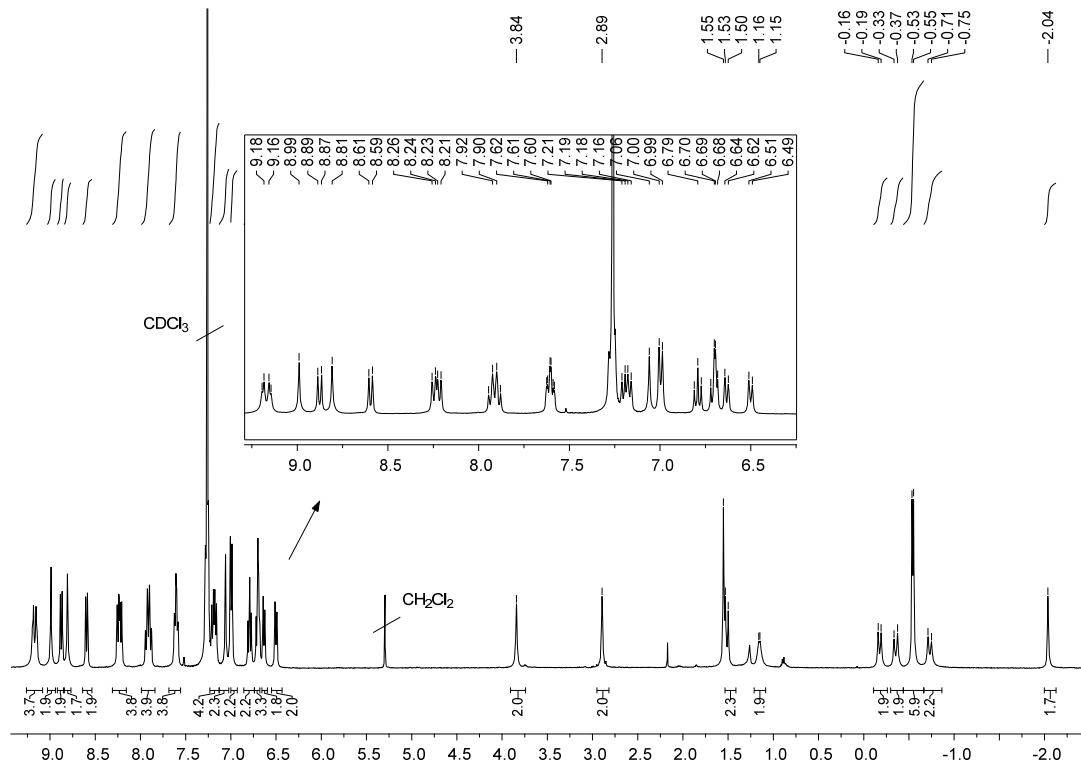
<sup>1</sup>H NMR (300 MHz, CDCl<sub>3</sub>): δ 7.76 (m, 3H, H<sup>4</sup> and H<sup>6</sup> and H<sup>9</sup>), 7.56 (s, 1H, H<sup>1</sup>), 7.44 (m, 2, H<sup>8</sup> and H<sup>7</sup>), 7.19 (d, 1H, *J*=8.1 Hz, H<sup>3</sup>), 4.19 (q, 2H, *J*=7.1 Hz, H<sup>15</sup>), 2.72-2.65 (m, 1H, H<sup>13</sup>), 2.01-1.97 (m, 1H, H<sup>11</sup>), 1.66 (m, 1H, H<sup>12</sup>), 1.41 (m, 1H, H<sup>12'</sup>), 1.28 ppm (t, 1H, *J*=7.1 Hz, H<sup>16</sup>).



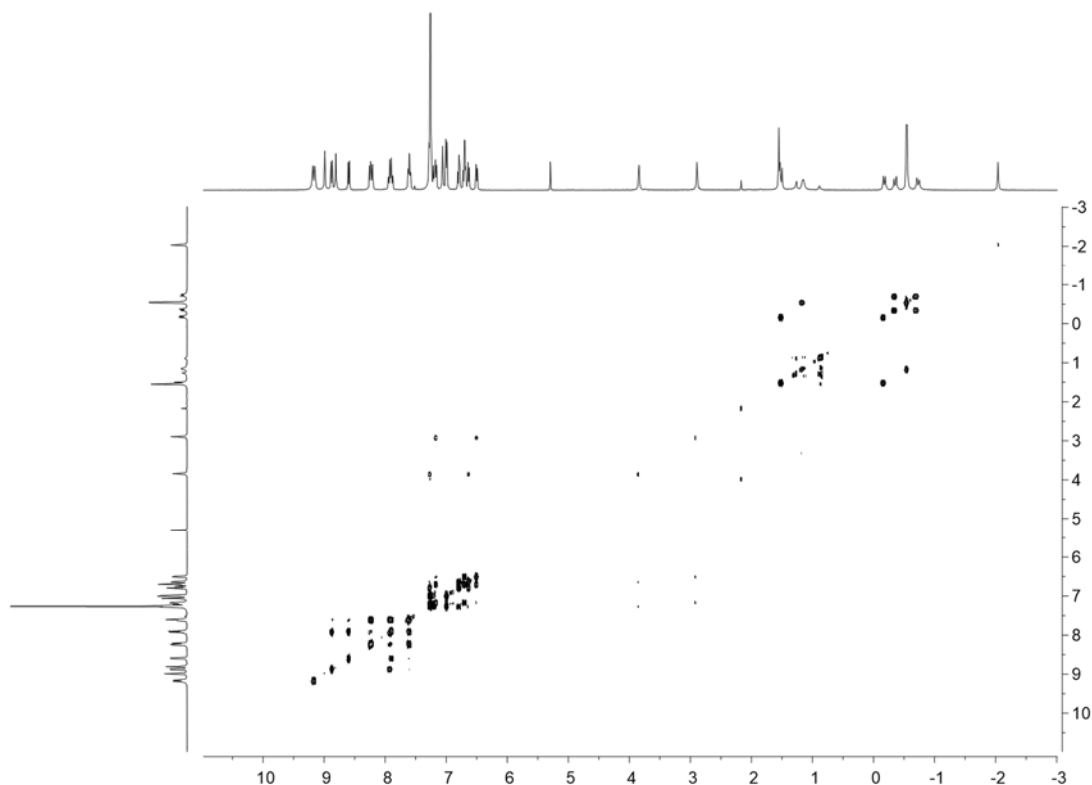
### 3.5. NMR spectra

#### 3.5.1. $\alpha_2\beta_2$ -bis(2,2'-{3,3'-[*N,N*-(1-phenylethane-1-amine)benzoyl amido]phenyl} porphyrin (37)

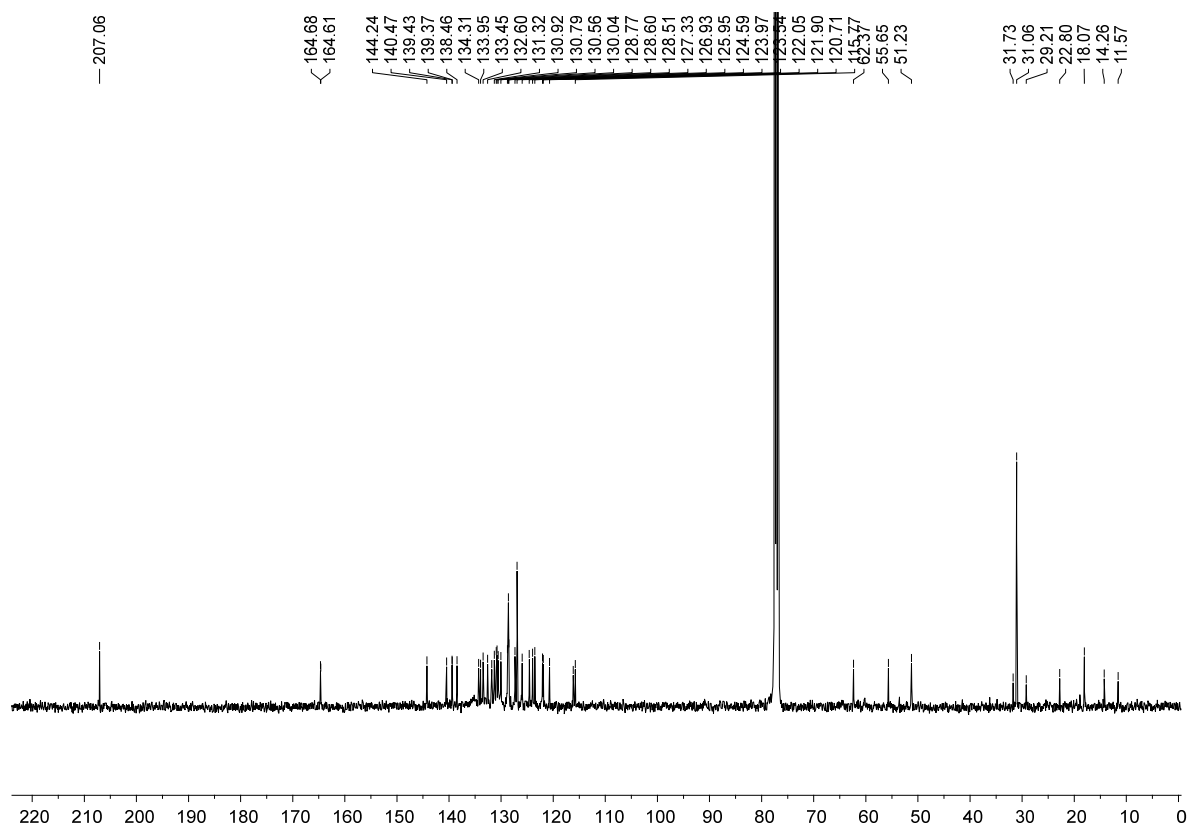
##### 3.5.1.1. $^1\text{H}$ NMR spectrum (400 MHz, $\text{CDCl}_3$ , 298 K)



##### 3.5.1.2. COSY 2D NMR spectrum (400 MHz, $\text{CDCl}_3$ , 298 K)

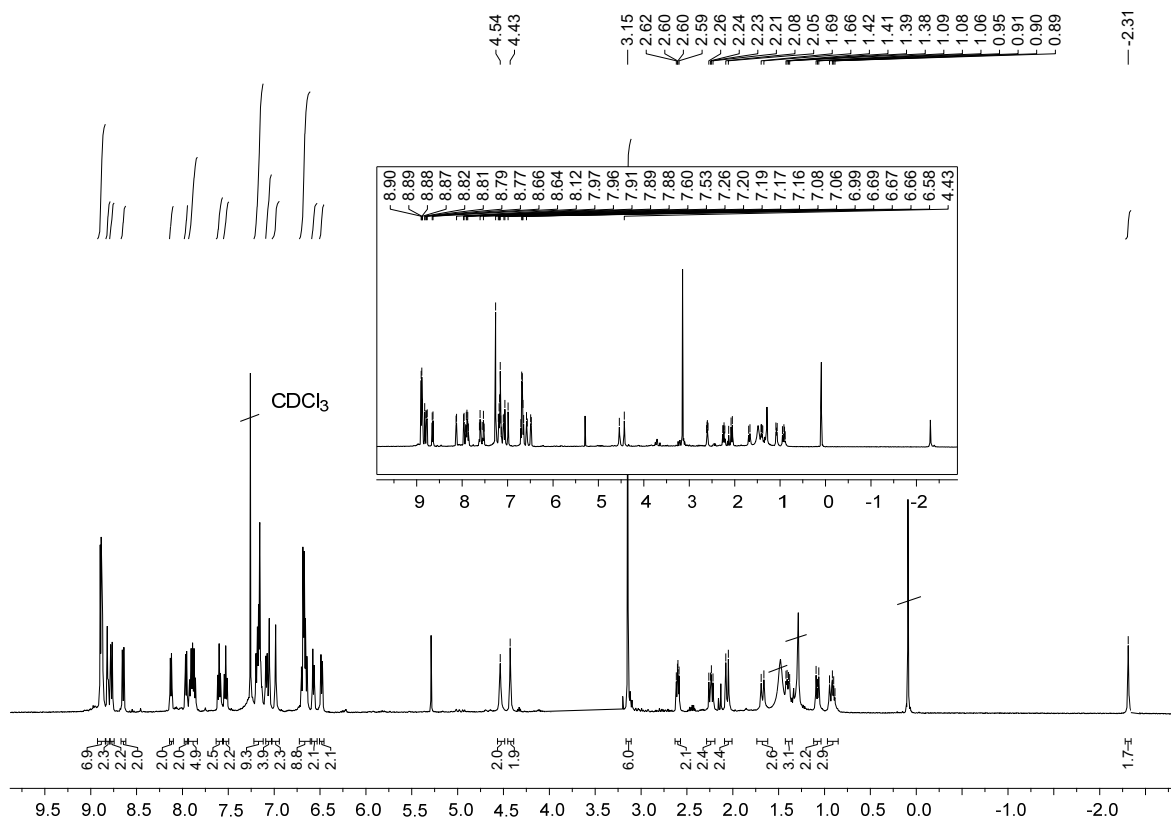


### 3.5.1.3. $^{13}\text{C}$ NMR spectrum (100 MHz, $\text{CDCl}_3$ , 298 K)

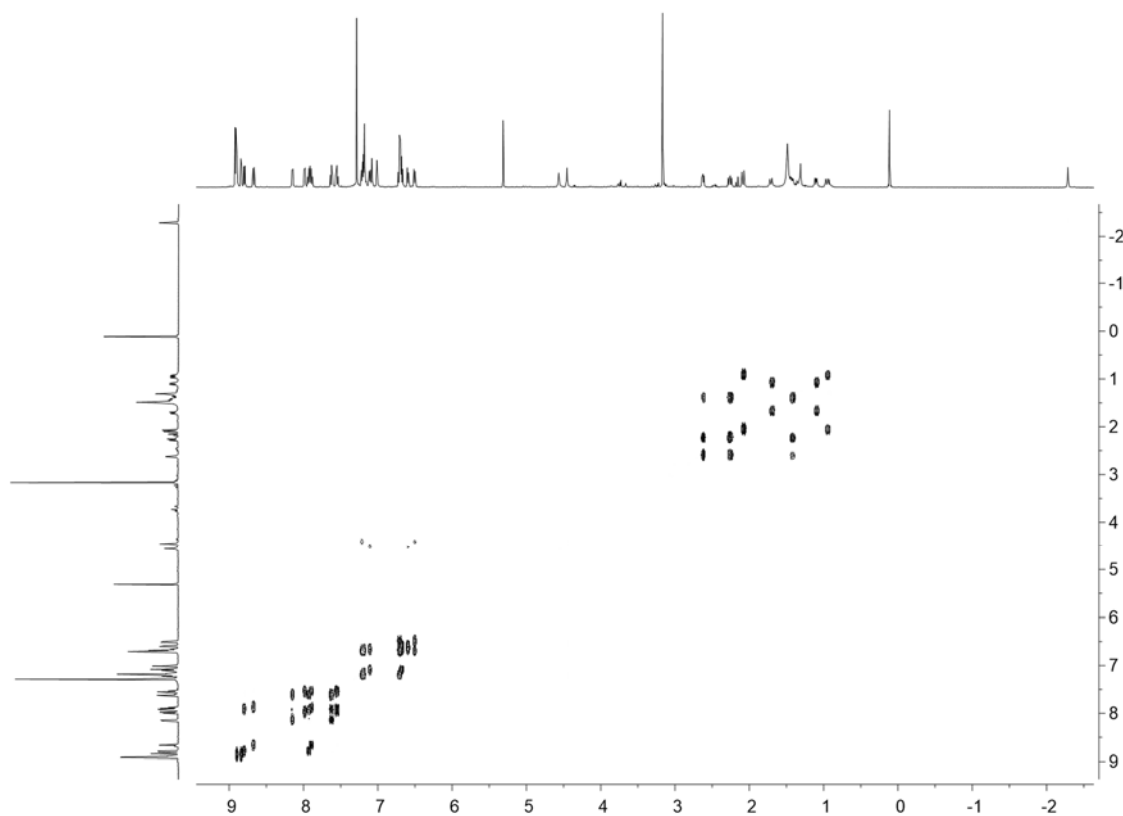


### 3.5.2. $\alpha_2\beta_2$ -bis(2,2'-{3,3'-[*N,N*-(methyl phenylalaninate)benzoyl amido]phenyl} porphyrin (38)

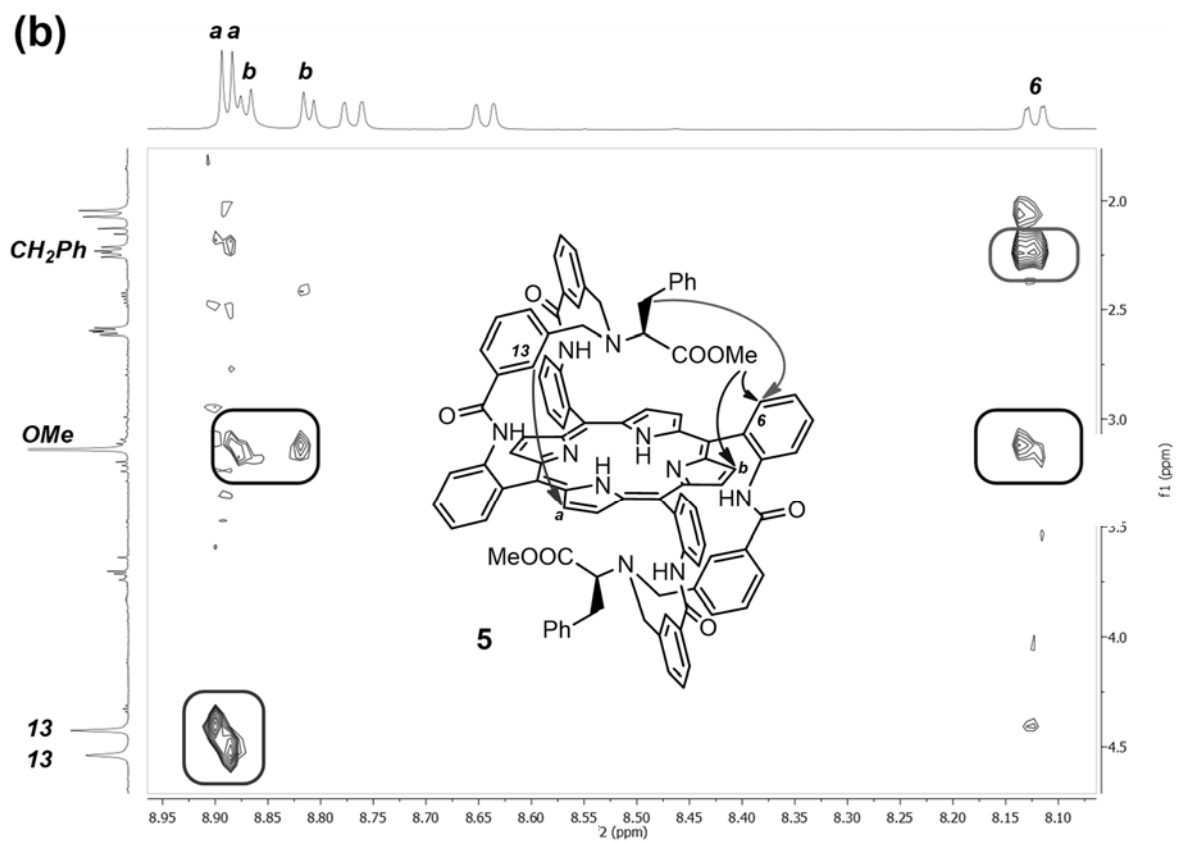
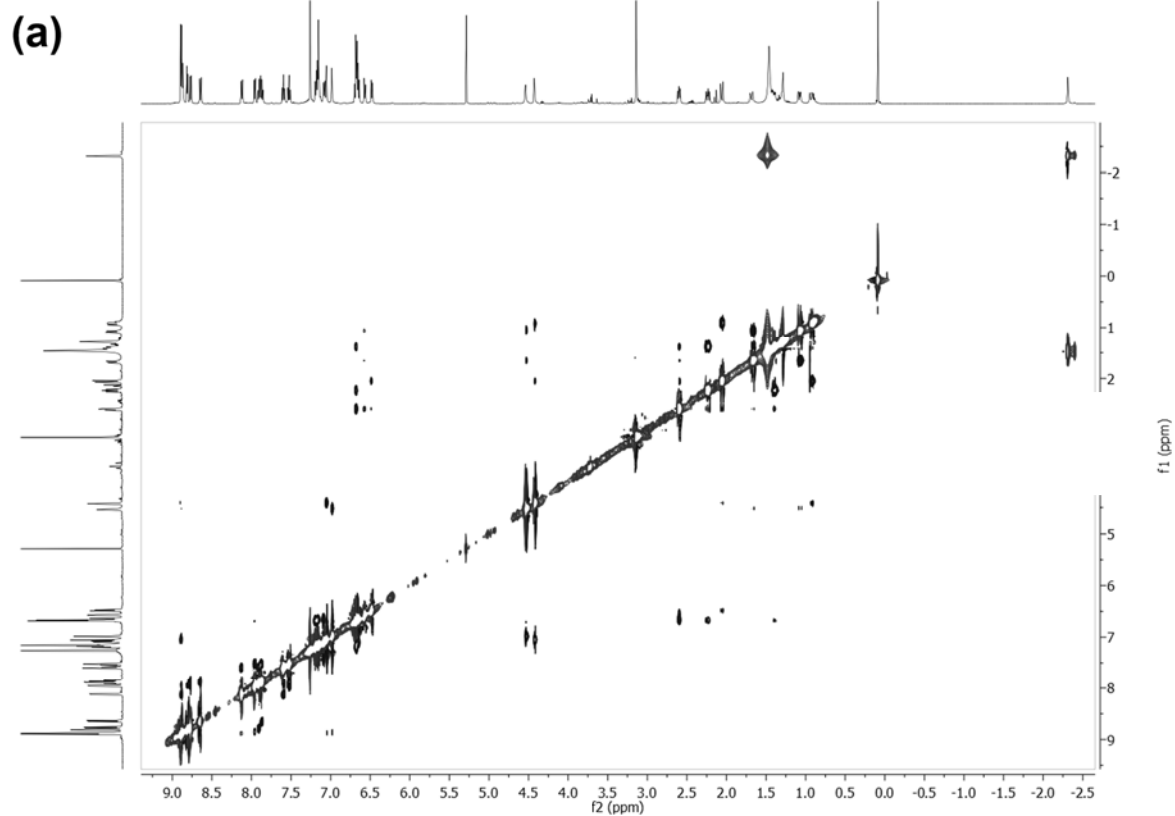
#### 3.5.2.1. $^1\text{H}$ NMR spectrum (500 MHz, $\text{CDCl}_3$ , 298 K)



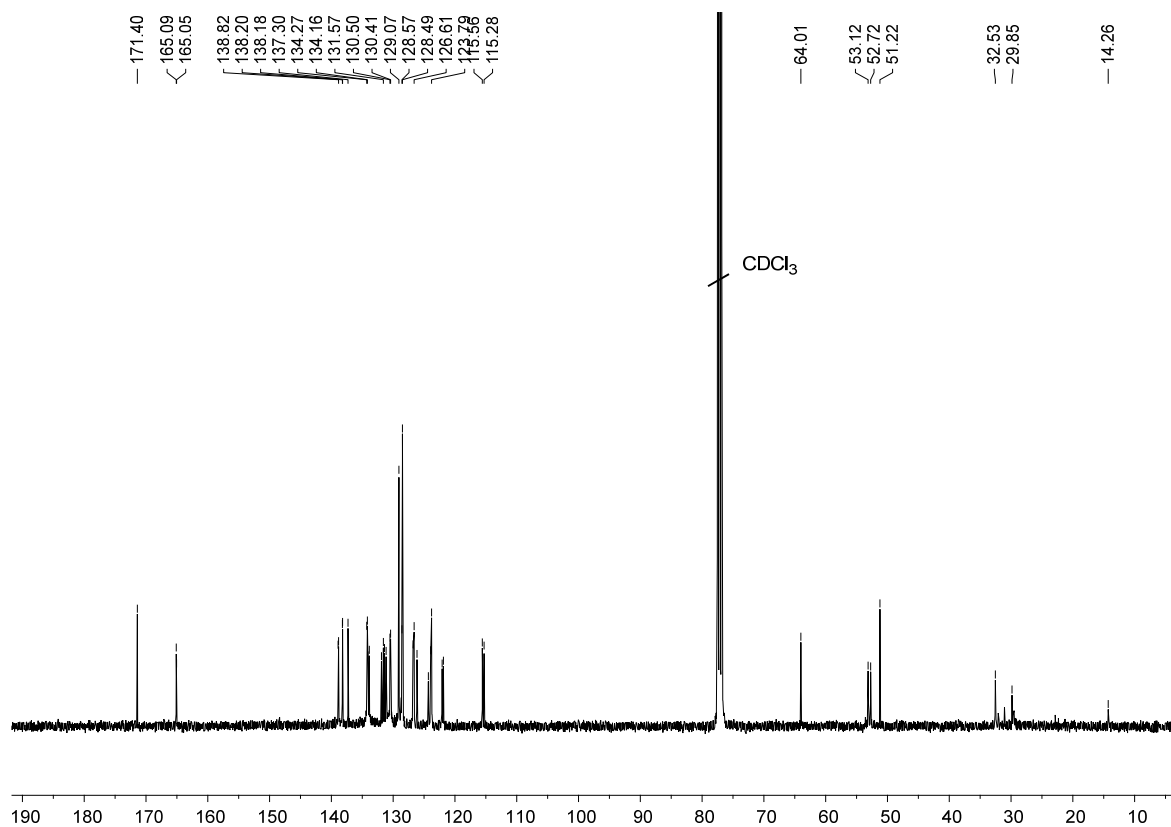
#### 3.5.2.2. COSY 2D NMR spectrum (500 MHz, $\text{CDCl}_3$ , 298 K)



### 3.5.2.3. 2D ROESY NMR spectrum (500 MHz, CDCl<sub>3</sub>, 298 K)

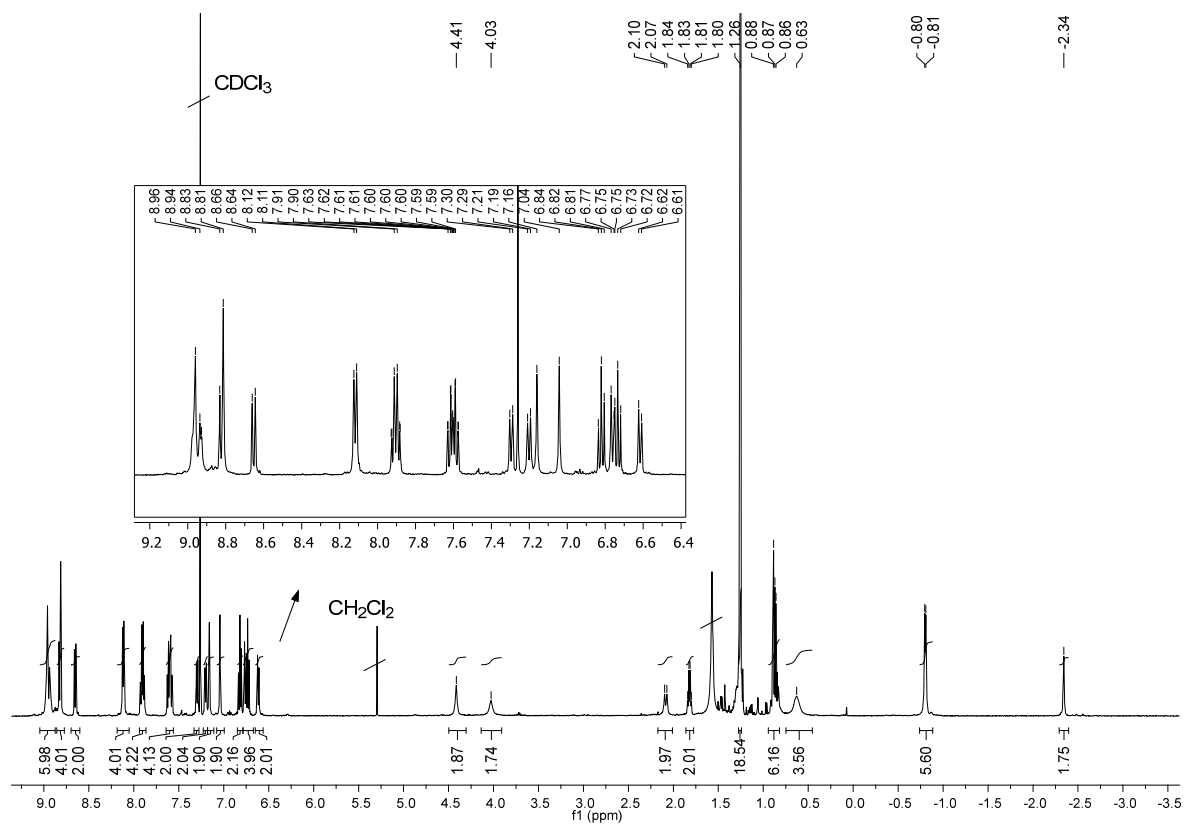


### 3.5.2.4. $^{13}\text{C}$ NMR spectrum (125 MHz, $\text{CDCl}_3$ , 298 K)

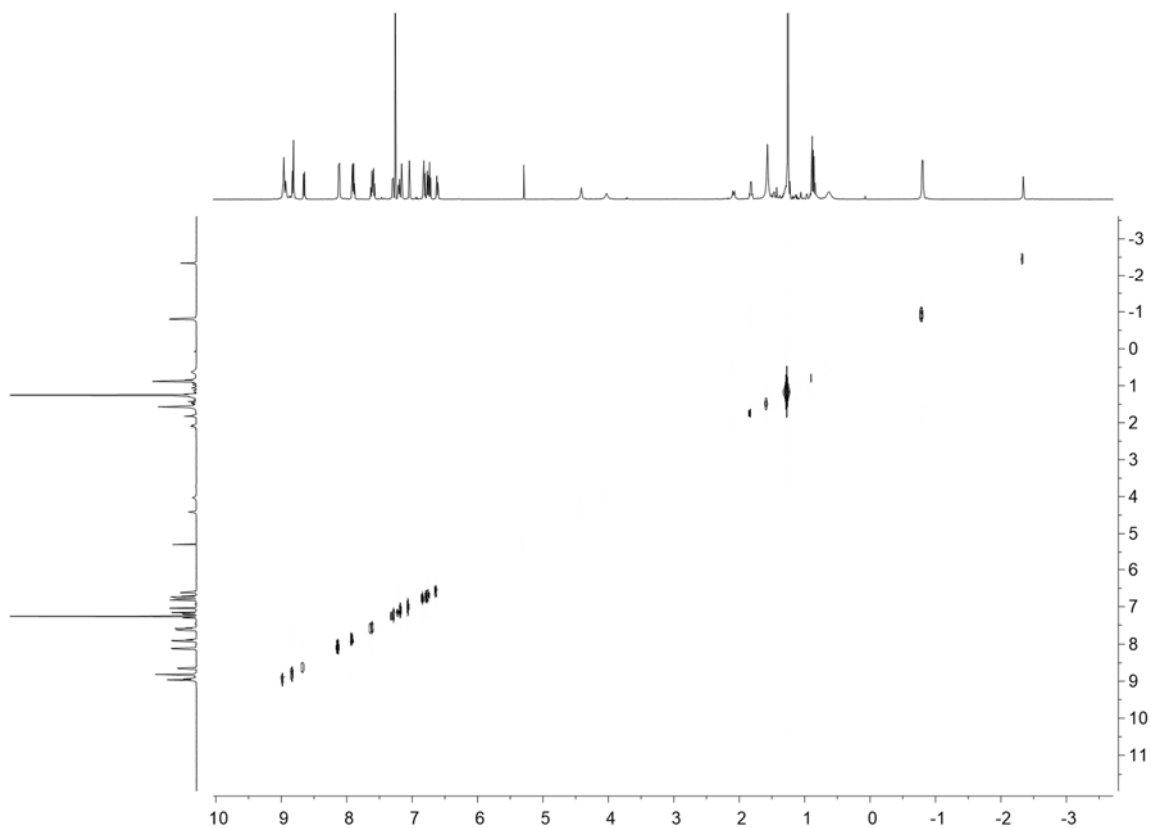


### 3.5.3. $\alpha_2\beta_2$ -bis(2,2'-{3,3'-[*N,N*-(tert-butylalaninate)benzoylamido]phenyl} porphyrin (39)

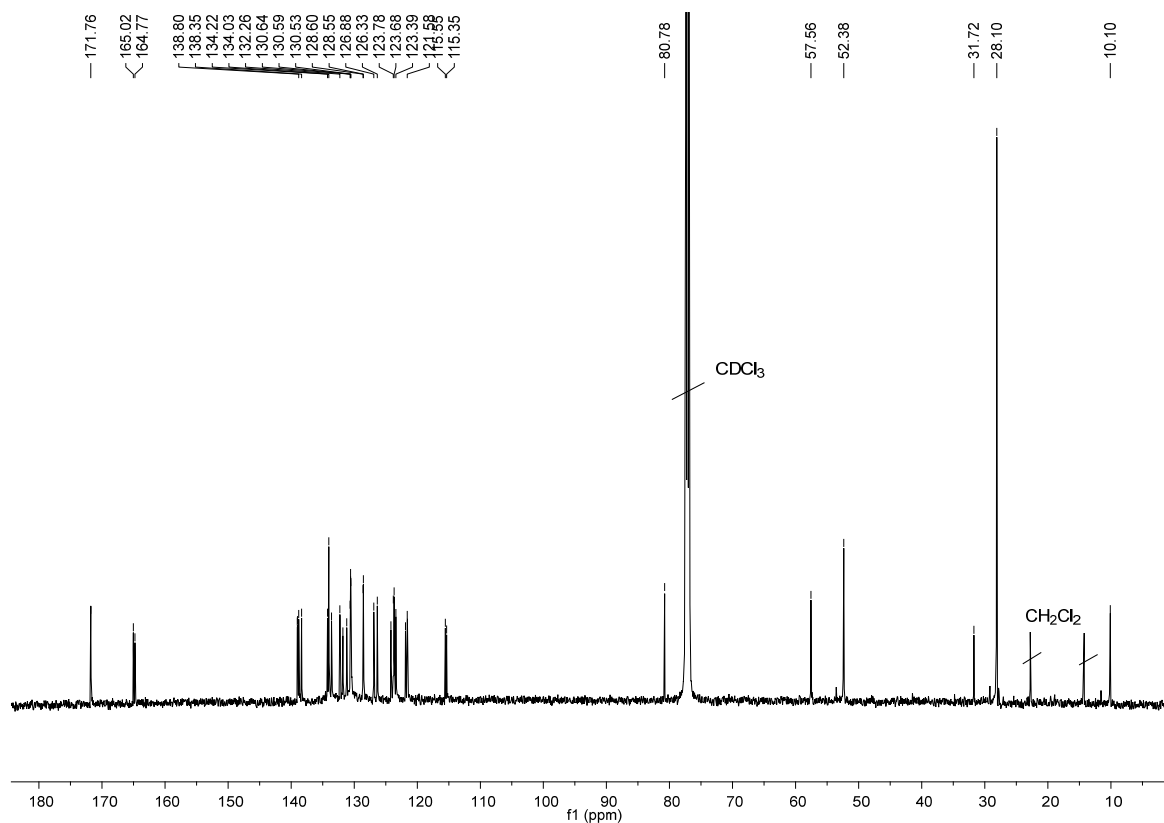
#### 3.5.3.1. $^1\text{H}$ NMR spectrum (500 MHz, $\text{CDCl}_3$ , 298 K)



#### 3.5.3.2. COSY 2D NMR spectrum (500 MHz, $\text{CDCl}_3$ , 298 K)

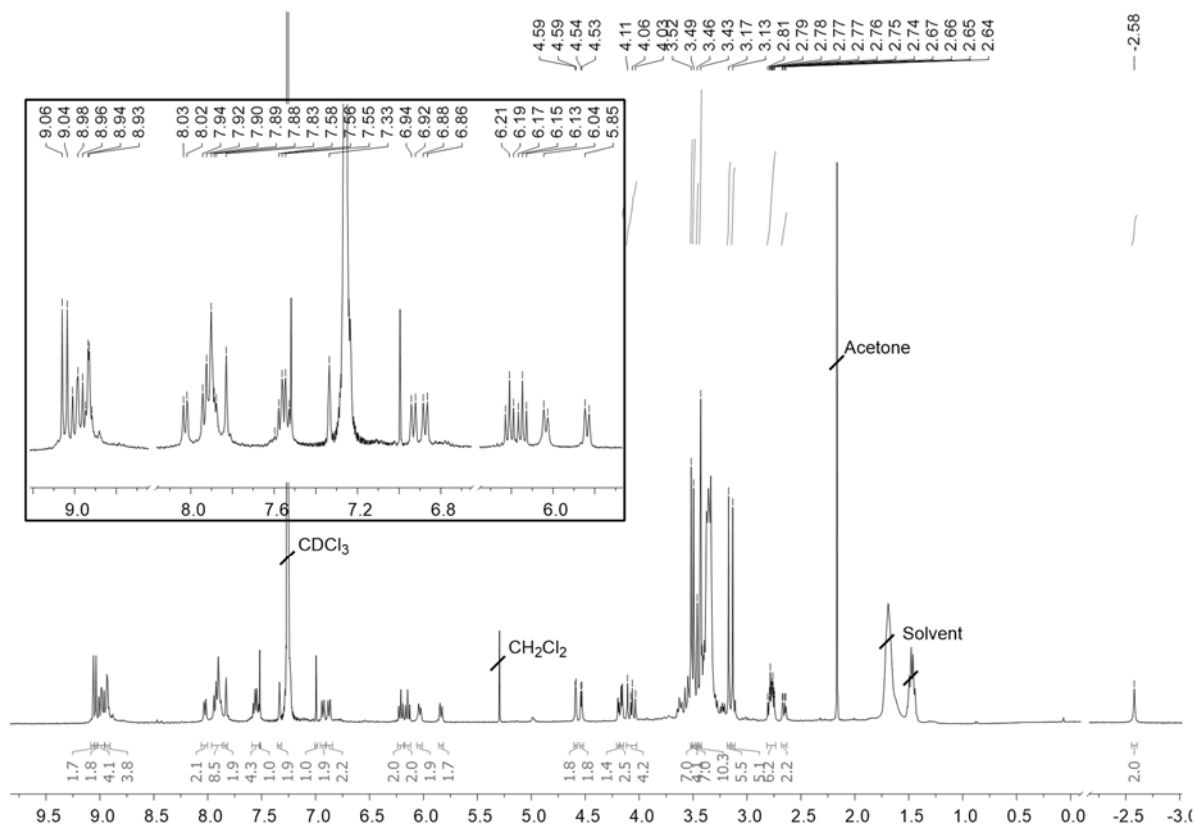


### 3.5.3.3. $^{13}\text{C}$ NMR spectrum (125 MHz, $\text{CDCl}_3$ , 298 K)



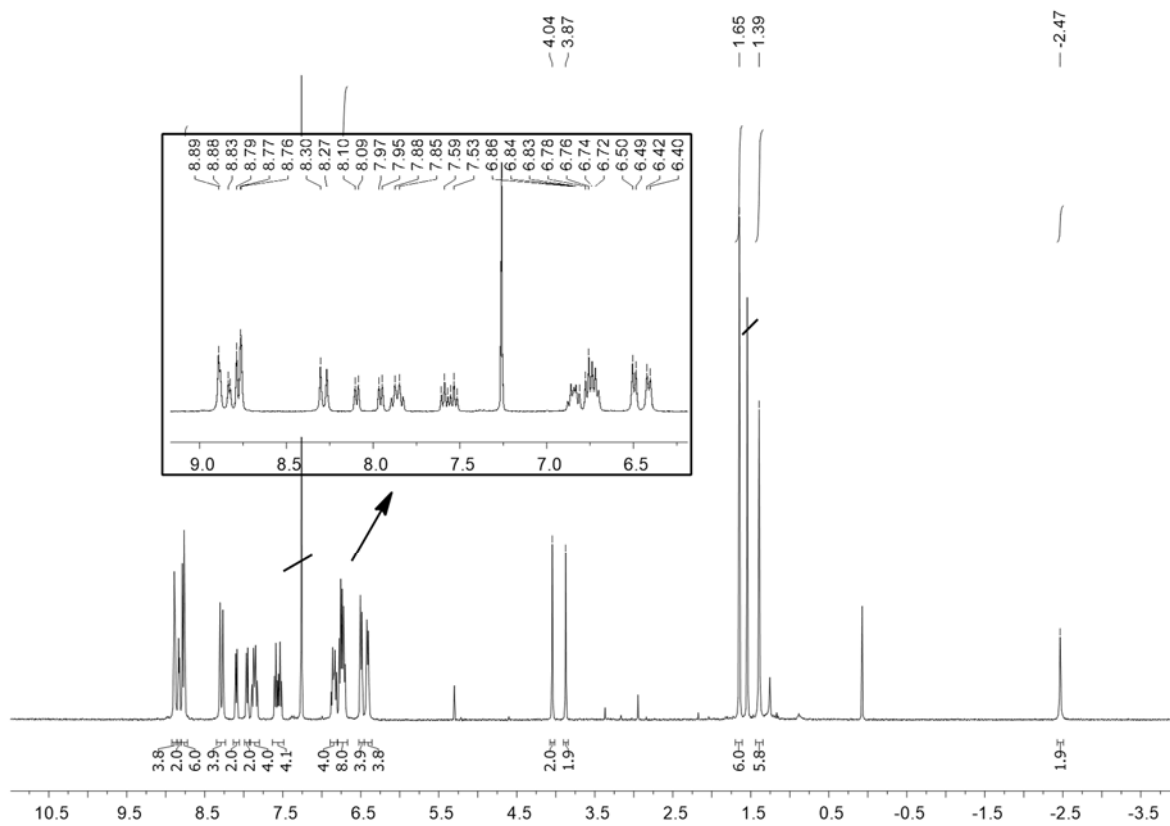
### 3.5.4. $\alpha_2\beta_2$ -bis(2,2'-{3,3'-[( $\alpha$ -trehalose)benzoylamido]phenyl} porphyrin (40)

#### 3.5.4.1. $^1\text{H}$ NMR (400 MHz, $\text{CDCl}_3$ , 298 K)

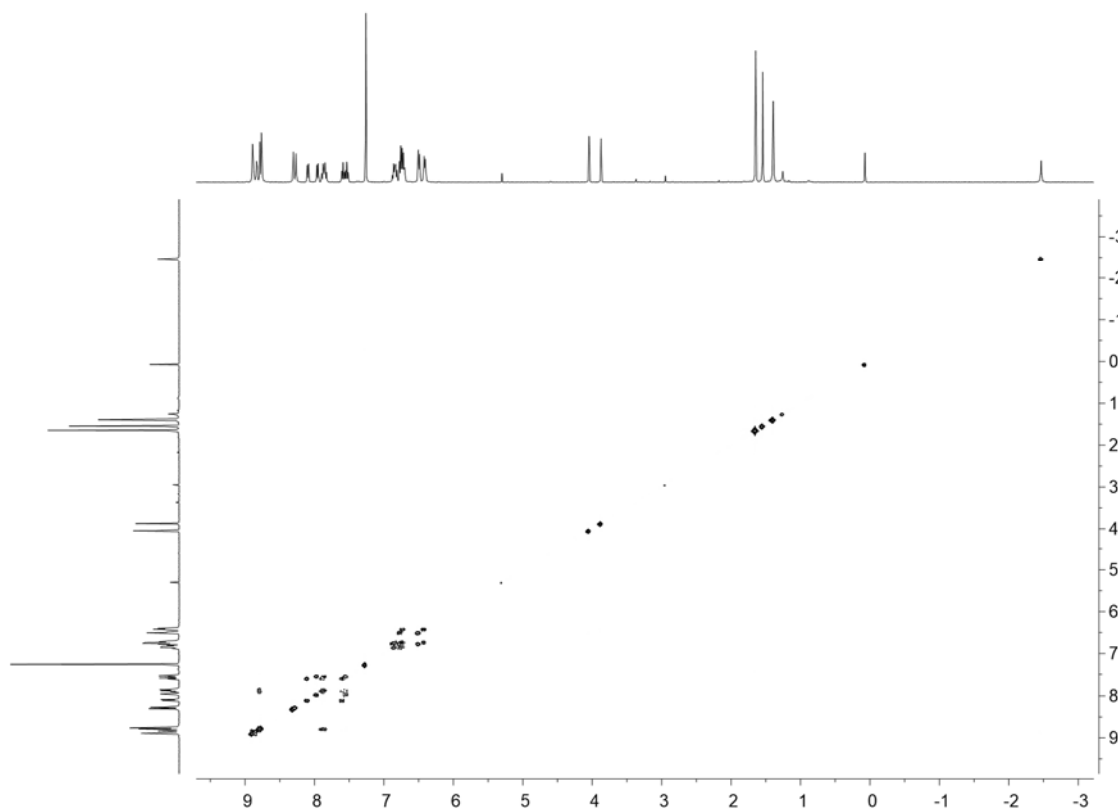


### 3.5.5. $\alpha_2\beta_2$ -tetra[(2-methoxy-2-phenyl)acetamide)phenyl] porphyrin (44)

#### 3.5.5.1. $^1\text{H}$ NMR spectrum (400 MHz, $\text{CDCl}_3$ , 298 K)

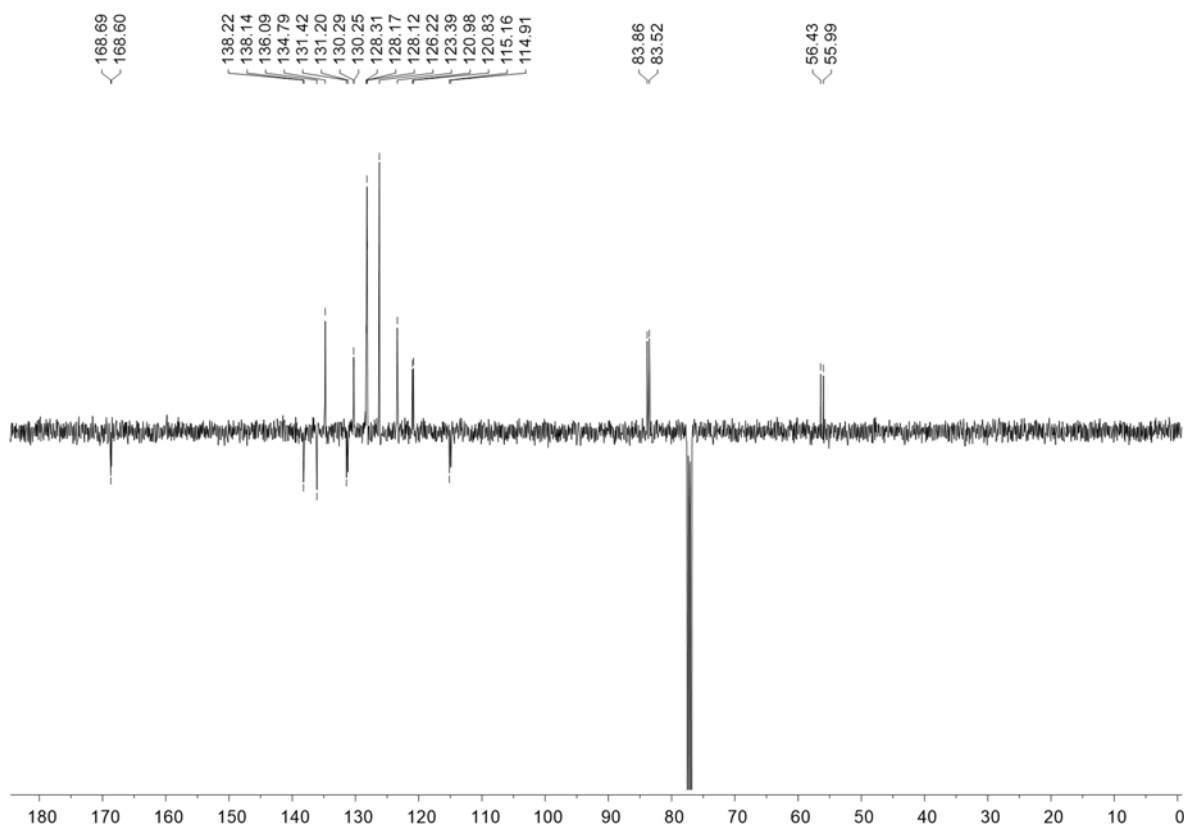


#### 3.5.5.2. COSY 2D NMR spectrum (400 MHz, $\text{CDCl}_3$ , 298 K)



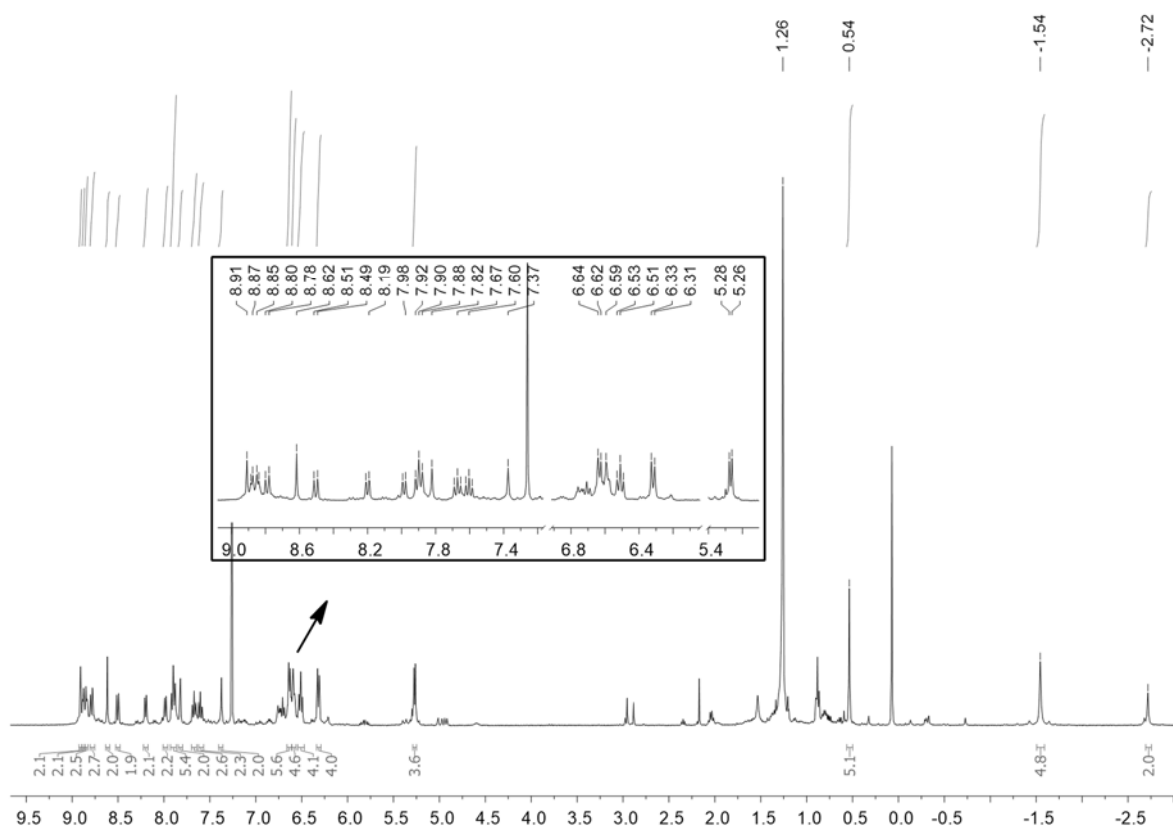


### 3.5.5.3. $^{13}\text{C}$ NMR spectrum (100 MHz, $\text{CDCl}_3$ , 298 K)

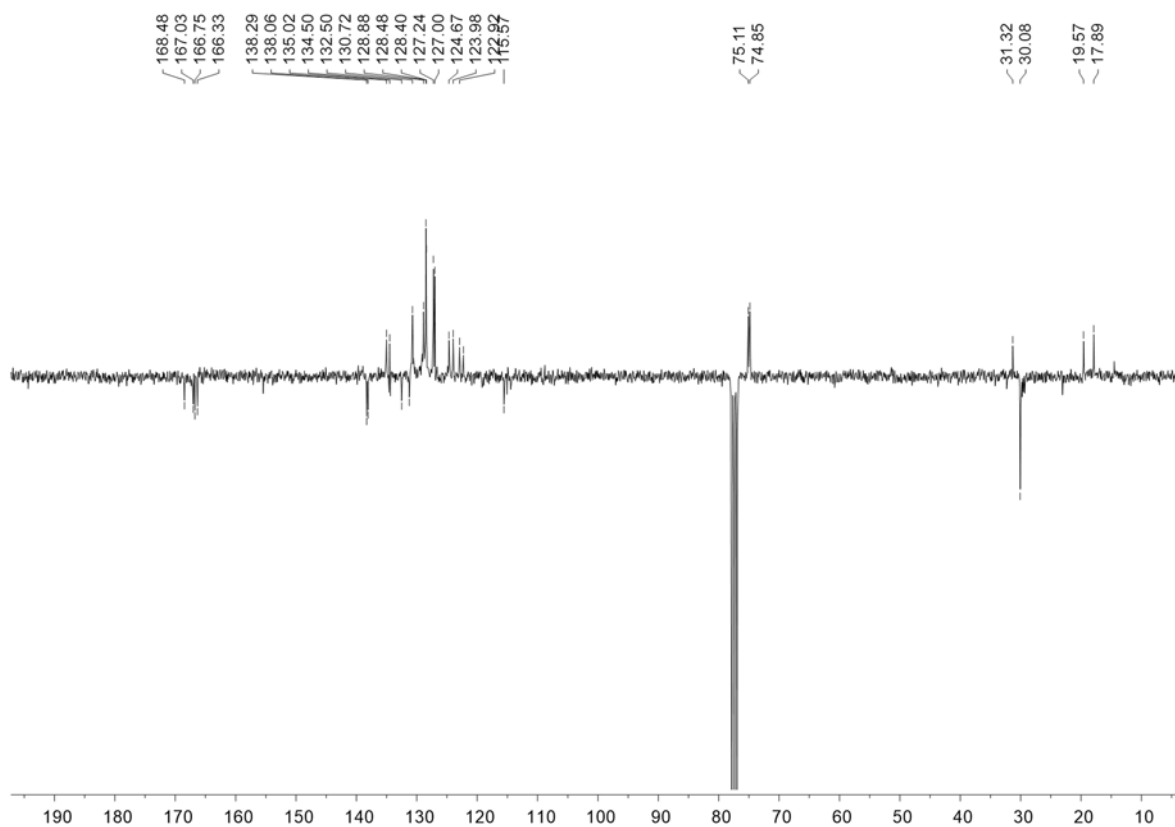


### 3.5.6. $\alpha_2\beta_2$ -tetra[(2-acetoxy-2-phenyl)acetamide)phenyl] porphyrin (45)

#### 3.5.6.1. $^1\text{H}$ NMR spectrum (400 MHz, $\text{CDCl}_3$ , 298 K)

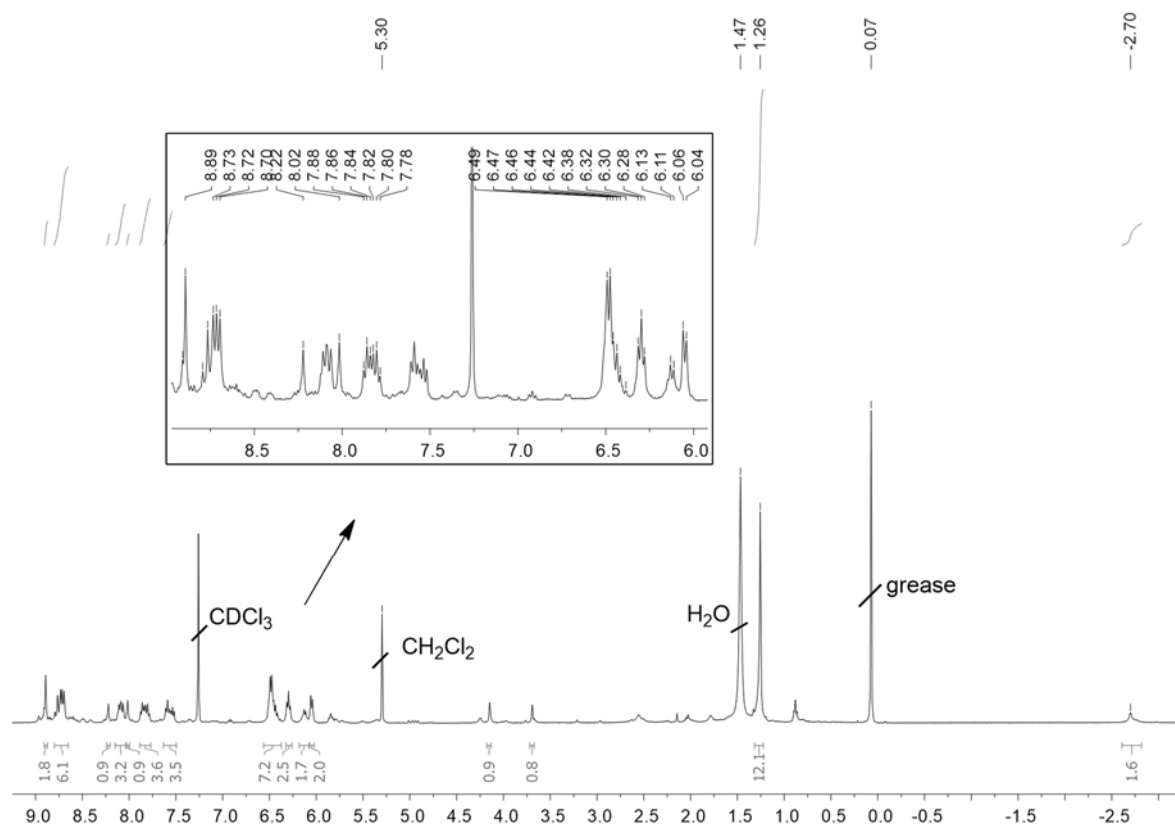


### 3.5.6.2. $^{13}\text{C}$ NMR spectrum (75 MHz, $\text{CDCl}_3$ , 298 K)



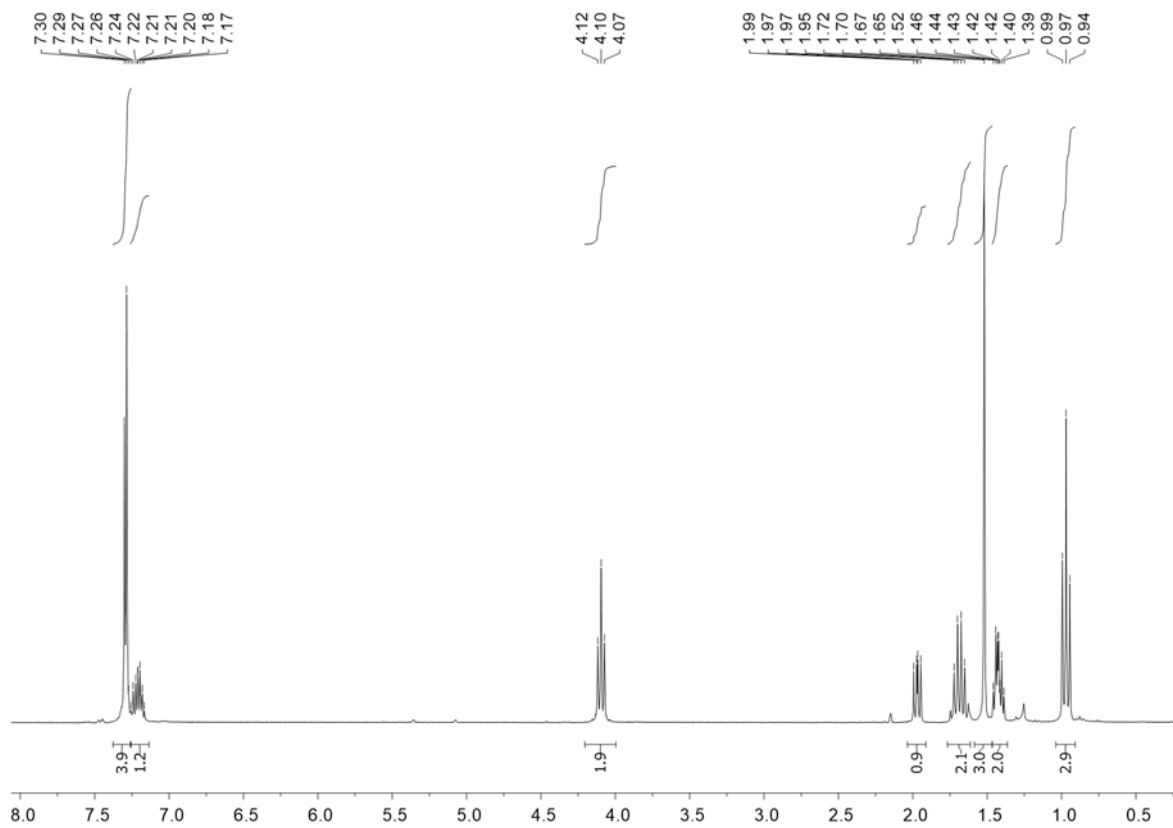
### 3.5.7. $\alpha_2\beta_2$ -tetra[(2-hydroxy-2-phenyl)acetamide)phenyl] porphyrin (46)

#### 3.5.7.1. $^1\text{H}$ NMR spectrum (400 MHz, $\text{CDCl}_3$ , 298 K)

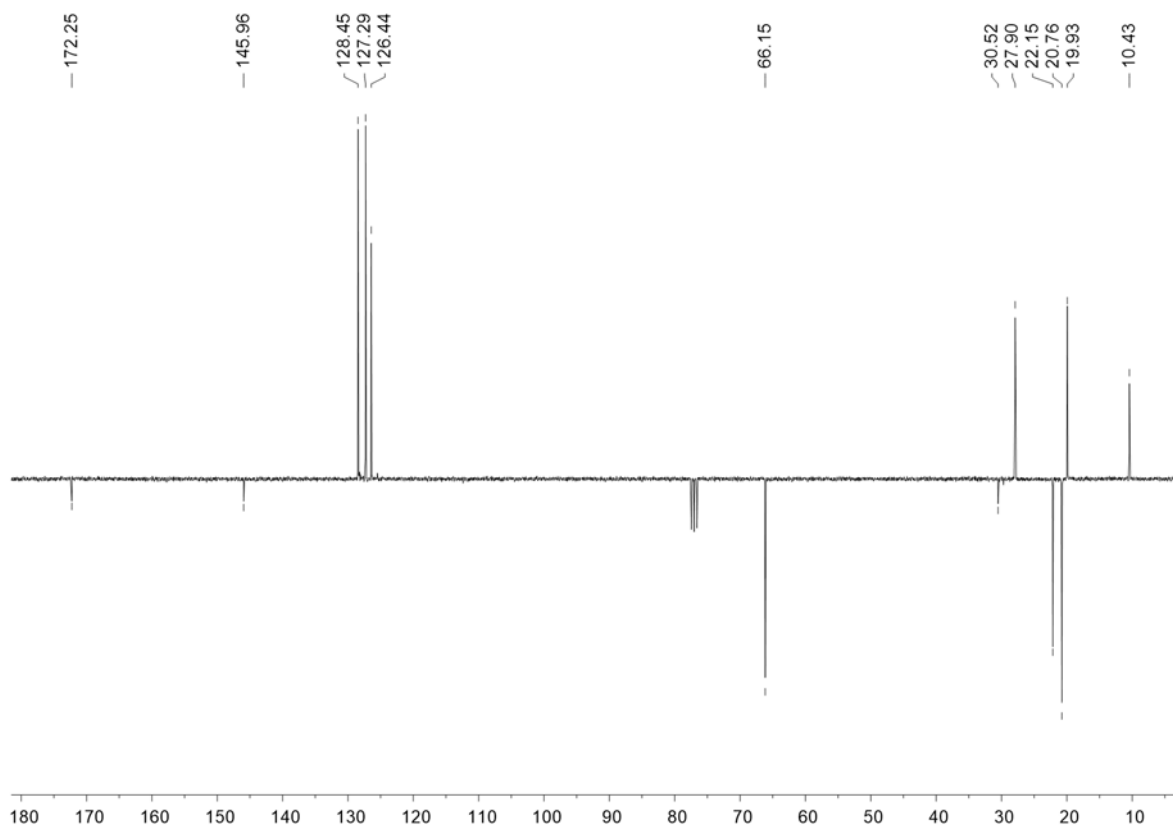


### 3.5.8. *trans* Propyl-2-methyl-2-phenylcyclopropanecarboxylate (20)

#### 3.5.8.1. $^1\text{H}$ NMR (400 MHz, $\text{CDCl}_3$ , 300 K)

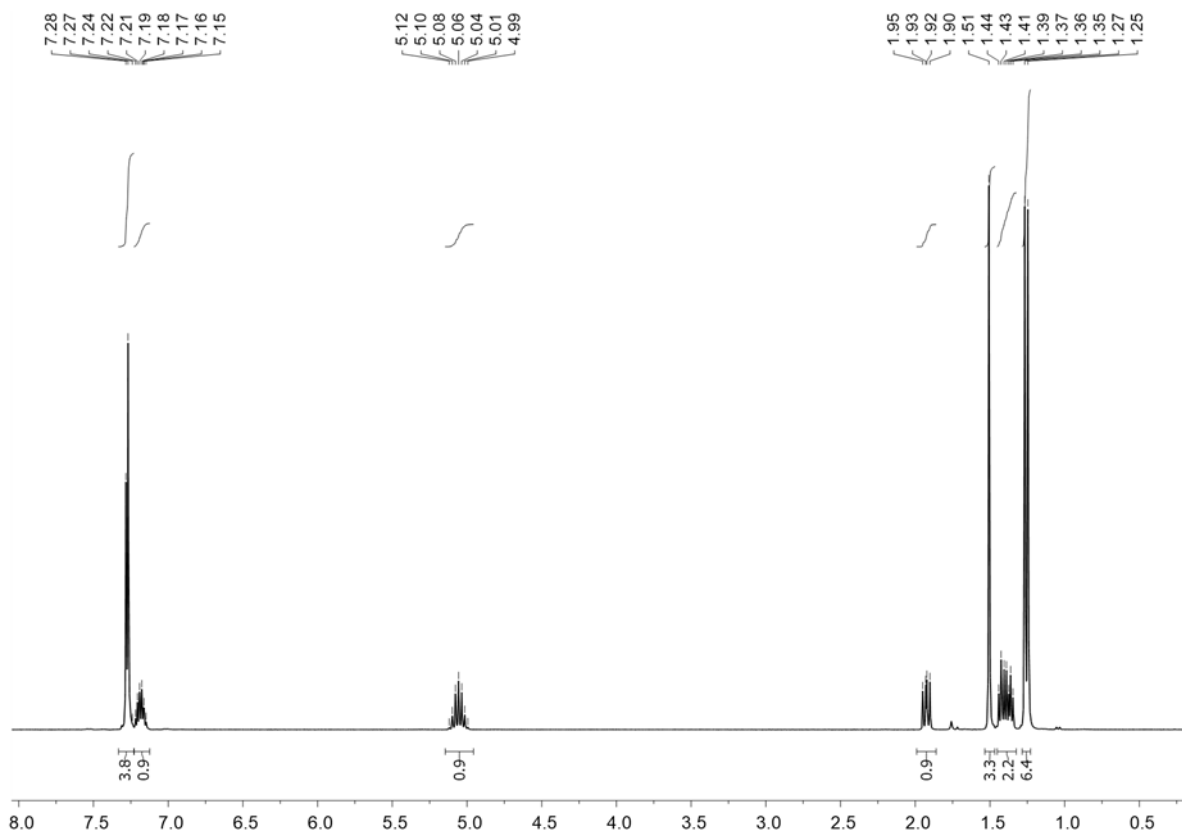


#### 3.5.8.2. $^{13}\text{C}$ NMR (75 MHz, $\text{CDCl}_3$ , 300 K)

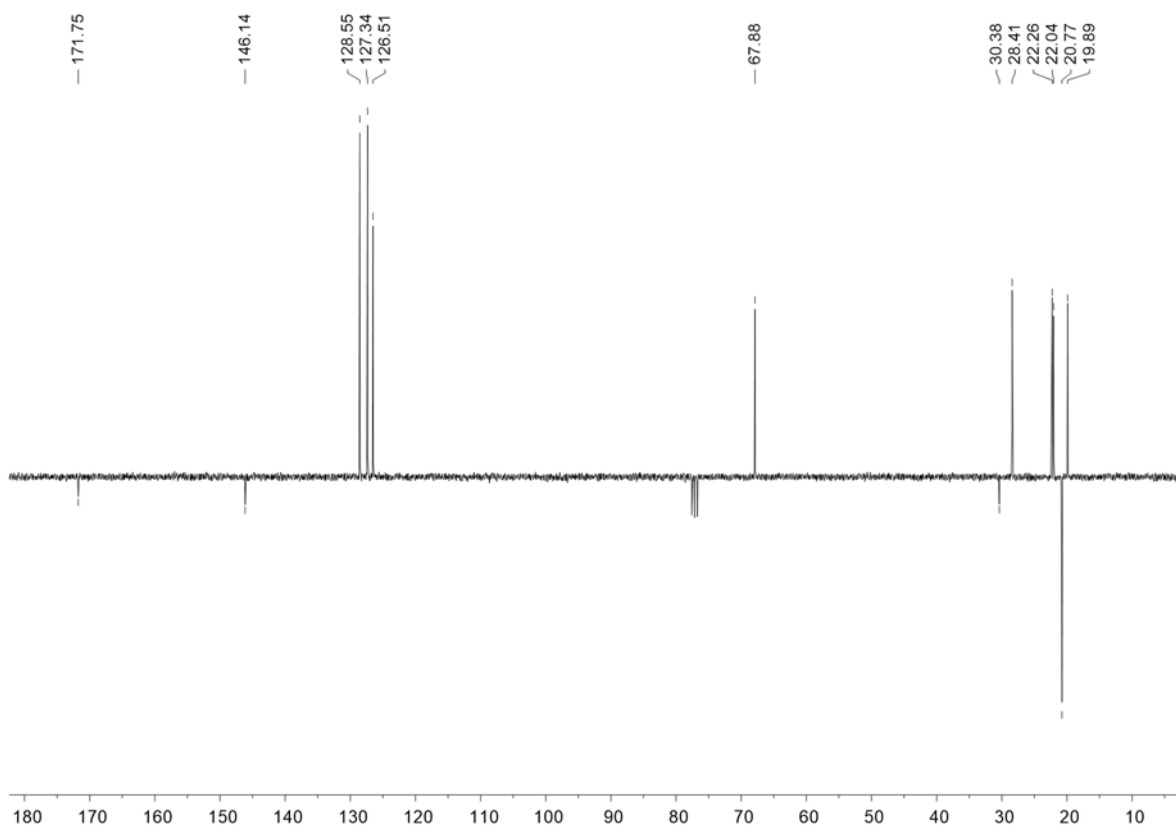


### 3.5.9. *trans* Isopropyl-2-methyl-2-phenylcyclopropanecarboxylate (21)

#### 3.5.9.1. $^1\text{H}$ NMR (300 MHz, $\text{CDCl}_3$ , 300 K)

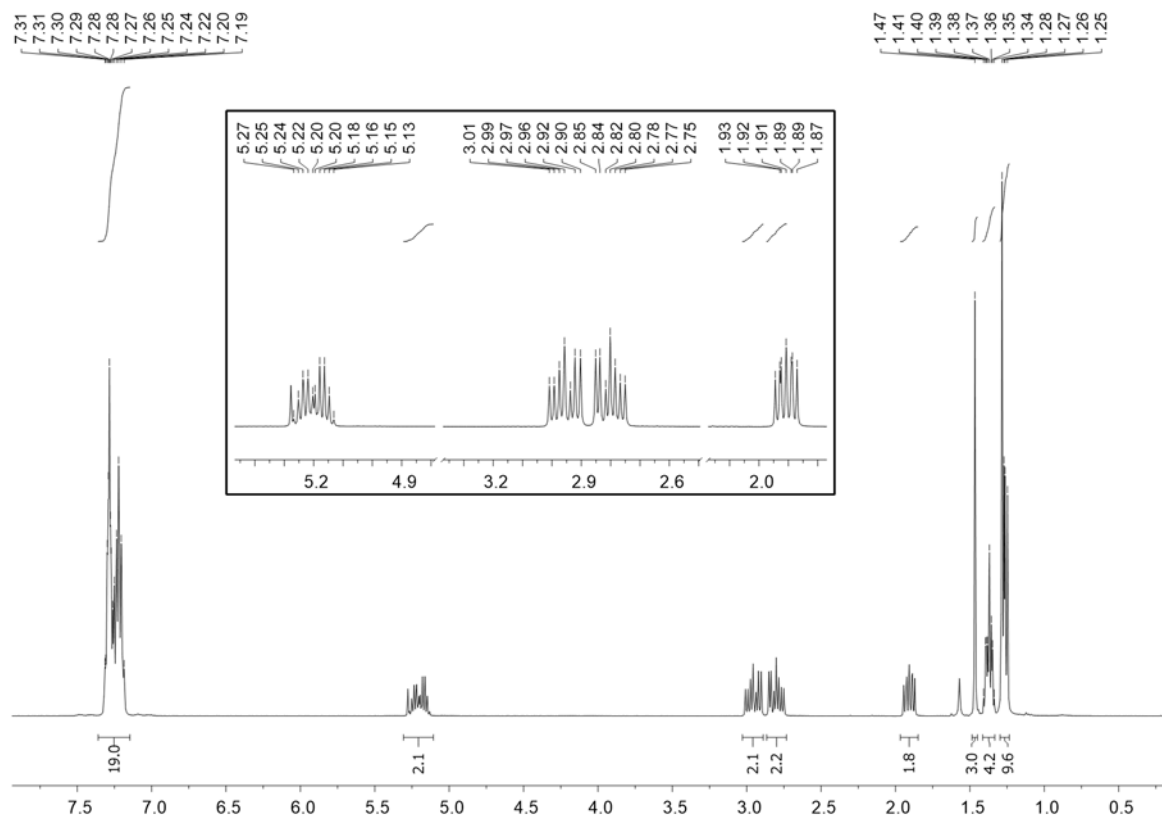


#### 3.5.9.2. $^{13}\text{C}$ NMR (75 MHz, $\text{CDCl}_3$ , 300 K)

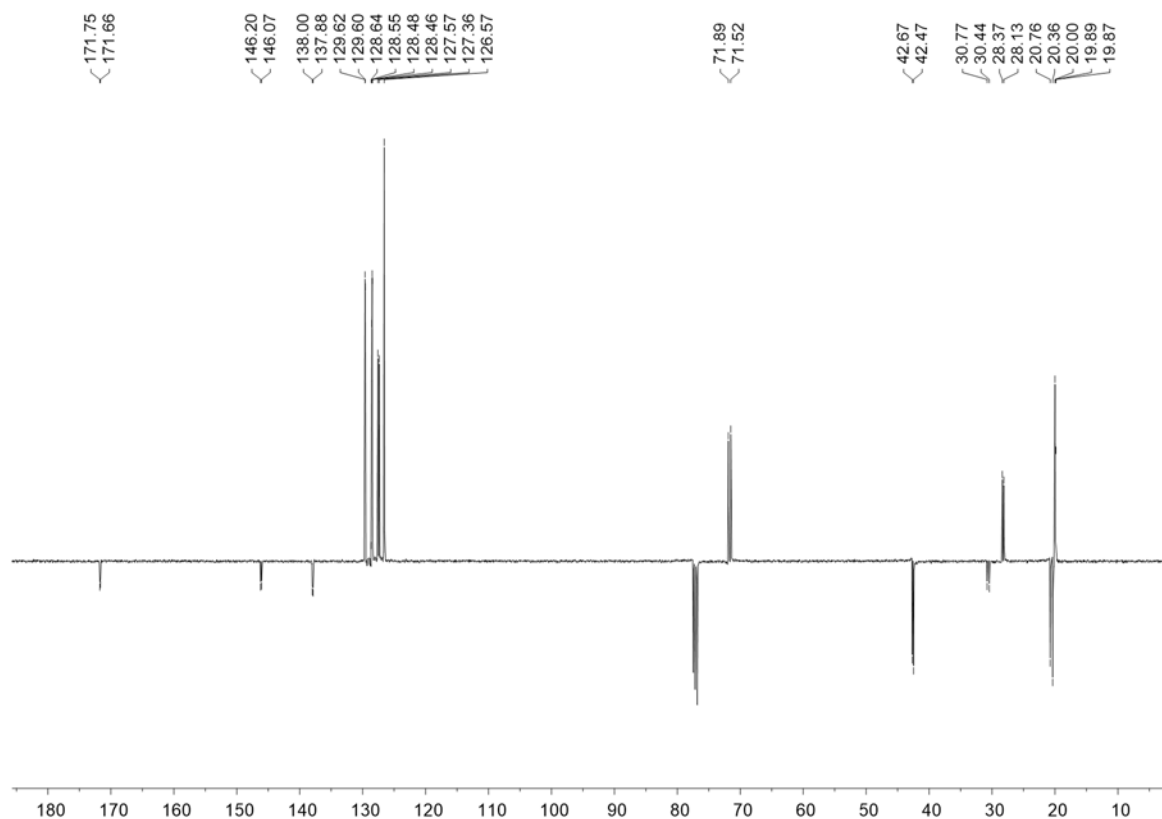


### 3.5.10. *trans* 1-Phenylpropyl-2-methyl-2-phenylcyclopropanecarboxylate (24)

#### 3.5.10.1. $^1\text{H}$ NMR (400 MHz, $\text{CDCl}_3$ , 300 K)

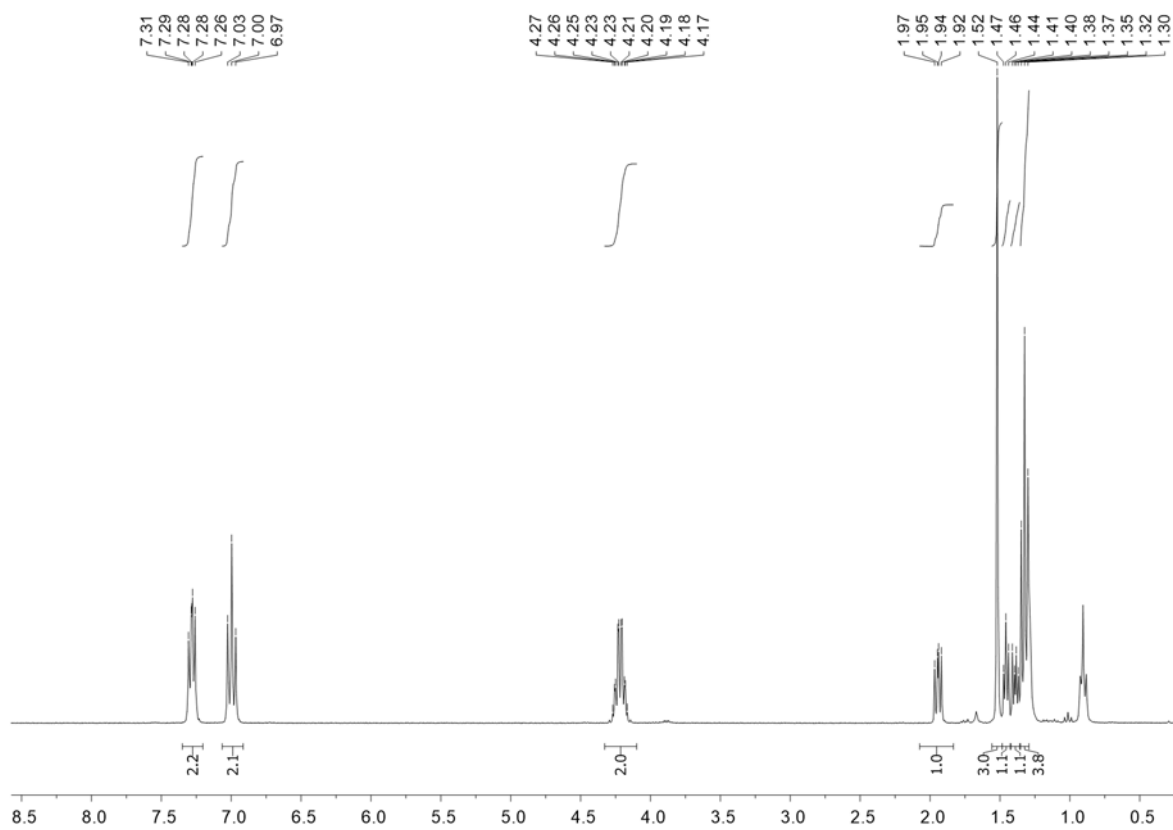


#### 3.5.10.2. $^{13}\text{C}$ NMR (100 MHz, $\text{CDCl}_3$ , 300K)

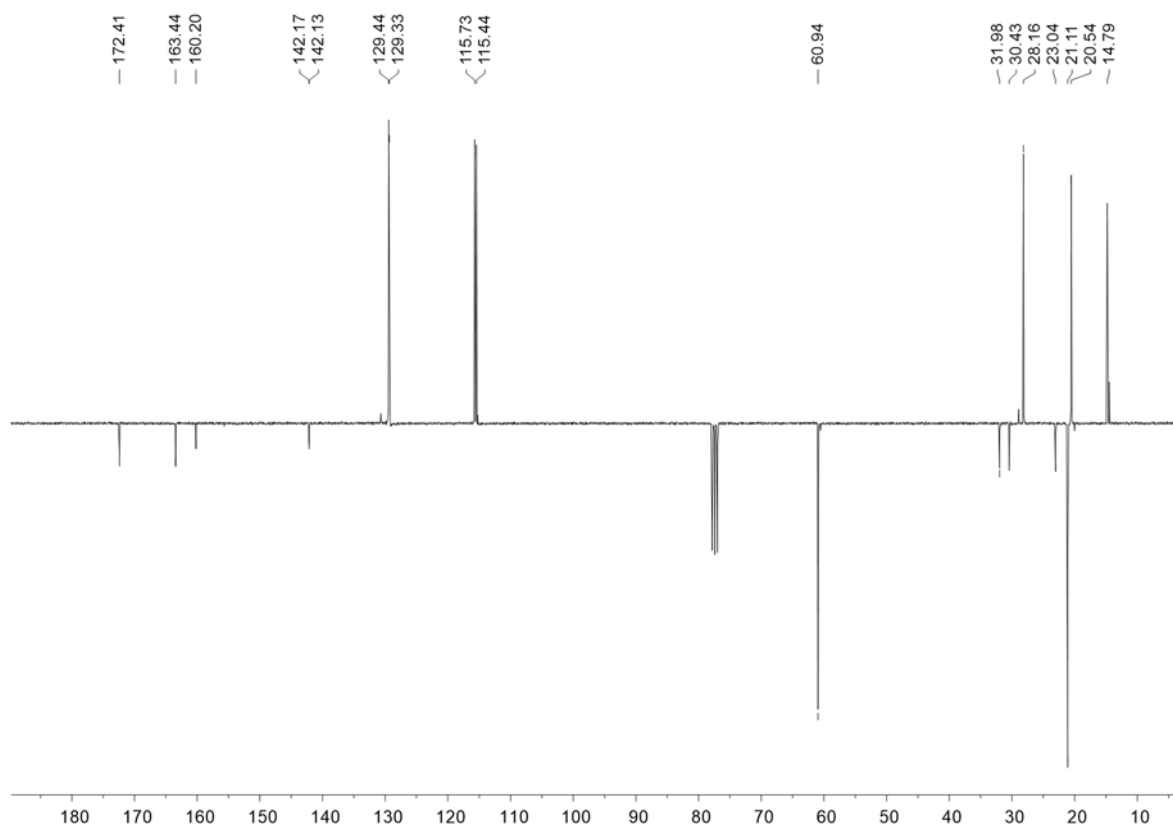


### 3.5.11. *trans* Ethyl 2-methyl-2-(4-fluorophenyl)cyclopropanecarboxylate (26)

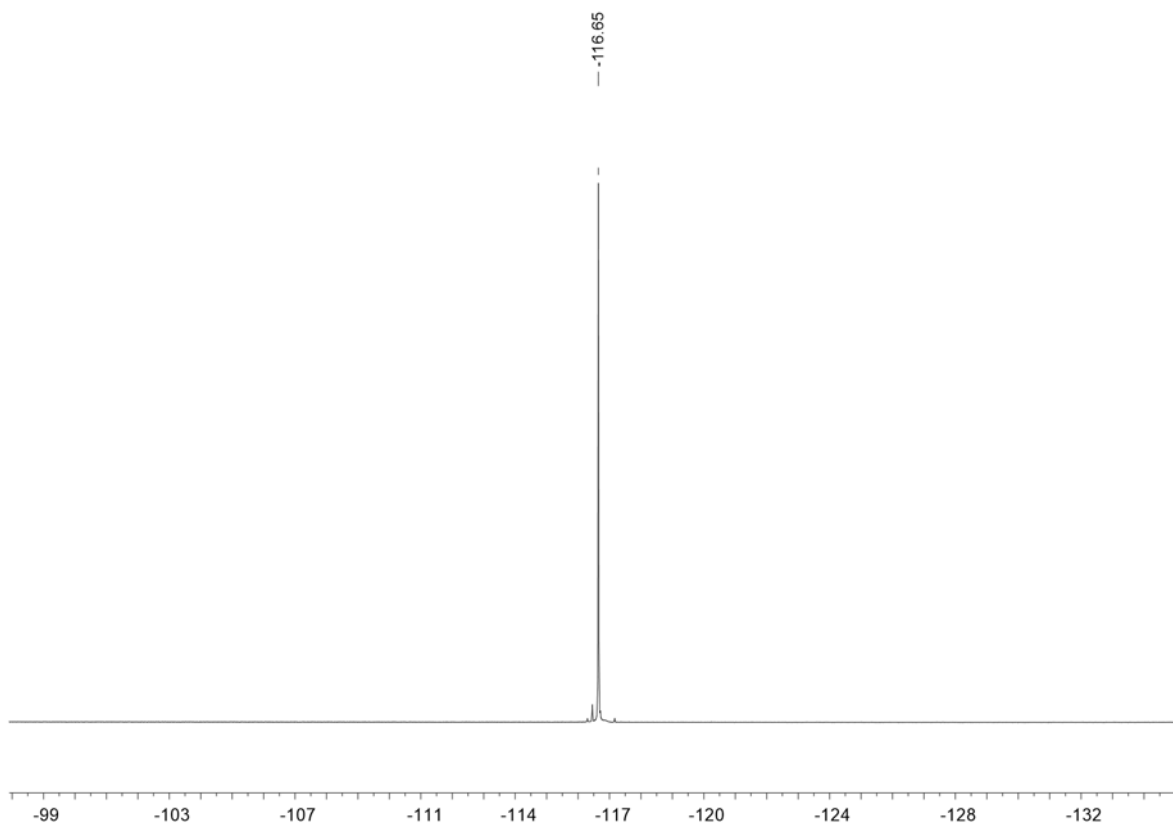
#### 3.5.11.1. $^1\text{H}$ NMR (400 MHz, $\text{CDCl}_3$ , 300 K)



#### 3.5.11.2. $^{13}\text{C}$ NMR (75 MHz, $\text{CDCl}_3$ , 300 K)

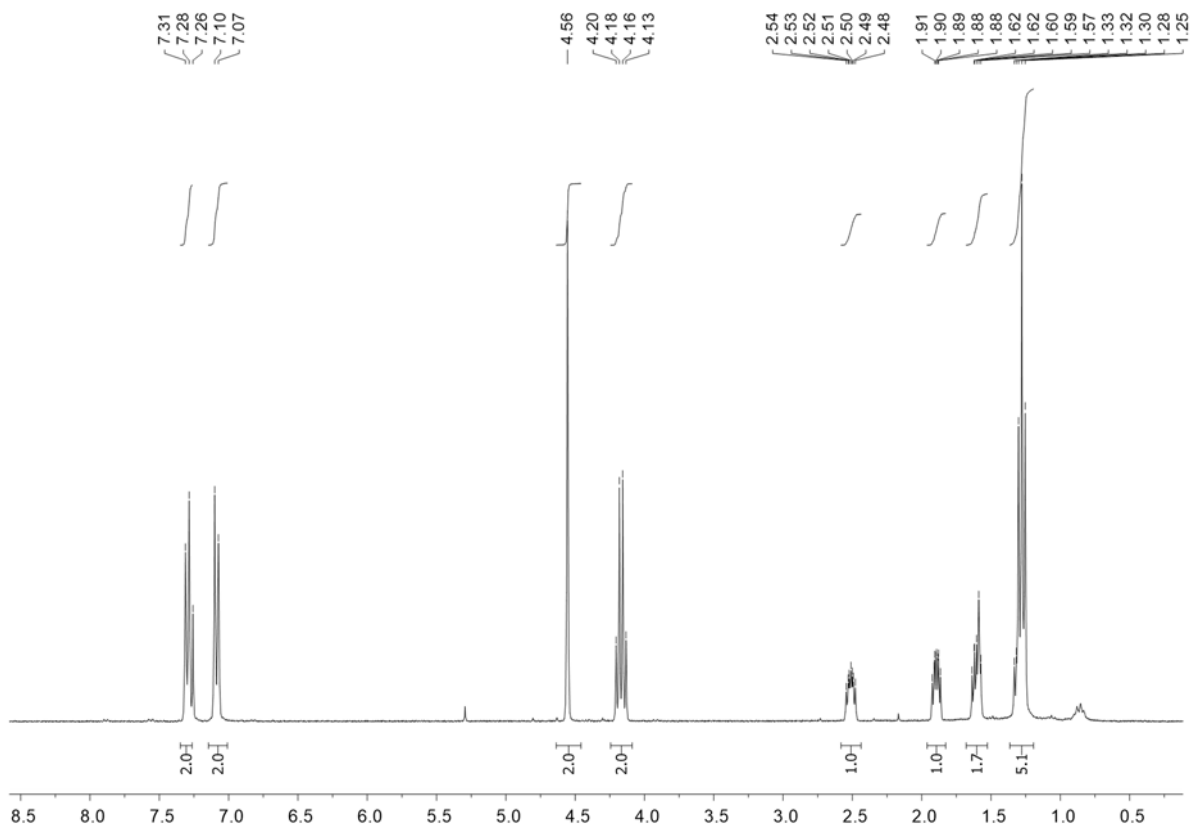


### 3.5.11.3. $^{19}\text{F}$ NMR (282 MHz, $\text{CDCl}_3$ , 300 K)

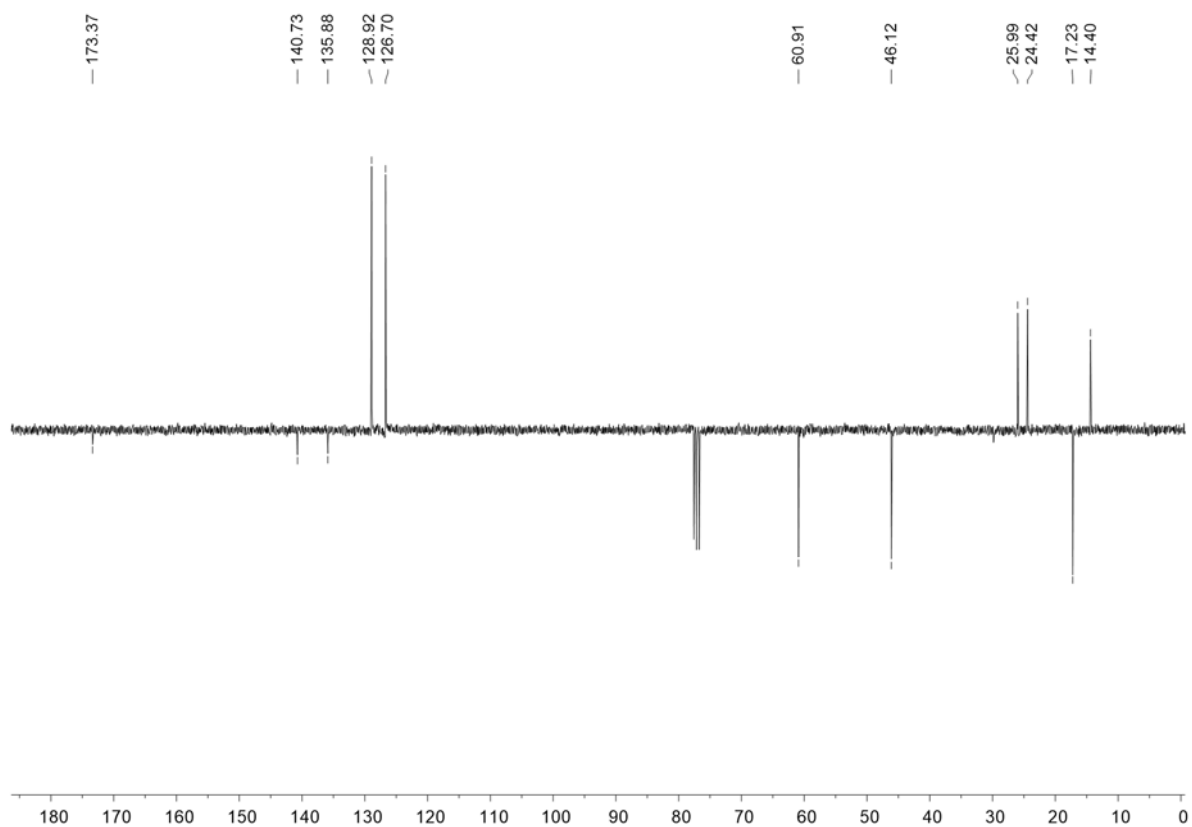


### 3.5.12. *trans* Ethyl 2-(4-chloromethylphenyl)cyclopropanecarboxylate (31)

#### 3.5.12.1. $^1\text{H}$ NMR (300 MHz, $\text{CDCl}_3$ , 300 K)



### 3.5.12.2. $^{13}\text{C}$ NMR (75 MHz, $\text{CDCl}_3$ , 300 K)





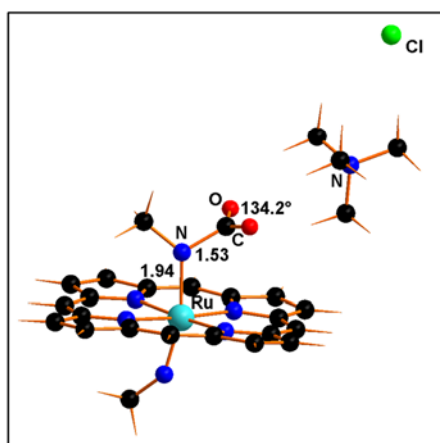
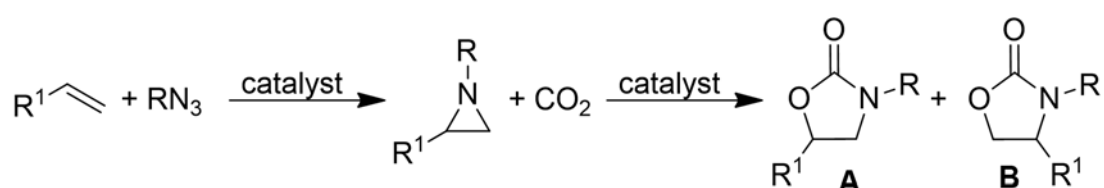
## 4. References

1. T. T. Talele. *J. Med. Chem.* **2016**, 59, 8712-8756.
2. (a) D. Y. K. Chen, R. H. Pouwer, J. A. Richard. *Chem. Soc. Rev.* **2012**, 41, 4631-4642. (b) P. Tang, Y. Qin. *Synthesis* **2012**, 44, 2969-2984. (c) V. Ganesh, S. Chandrasekaran. *Synthesis* **2016**, 48, 4347-4380. (d) C. Ebner, E. M. Carreira. *Chem. Rev.* **2017**, 117, 11651-11679. (e) S. J. Gharpure, L. N. Nanda. *Tetrahedron Lett.* **2017**, 58, 711-720.
3. (a) A. Ford, H. Miel, A. Ring, C. N. Slattery, A. R. Maguire, M. A. McKerverey. *Chem. Rev.* **2015**, 115, 9981-10080. (b) M. Meazza, H. Guo, R. Rios. *Org. Biomol. Chem.* **2017**, 15, 2479-2490.
4. (a) D. Intriери, D. M. Carminati, E. Gallo. *Dalton Transactions* **2016**, 45, 15746-15761. (b) D. Intriери, D. M. Carminati, E. Gallo. in *Handbook of Porphyrin Science; eds.* **2016**, vol. 38, set. 8; (c) K. Rybicka-Jasińska, L. W. Ciszewski, D. T. Gryko, D. Gryko. *J. Porphyrins Phthalocyanines* **2016**, 20, 76-95.
5. L. K. Gottwald, E. F. Ullman. *Tetrahedron Lett.* **1969**, 10, 3071-3074.
6. J. P. Collman, V. J. Lee, C. J. Kellen-Yuen, X. Zhang. *J. Am. Chem. Soc.* **1995**, 117, 692-703.
7. (a) E. Rose, B. Boitrel, M. Quelquejeu, A. Kossanyi. *Tetrahedron Lett.* **1993**, 34, 7267-7270. (b) L. Michaudet, P. Richard, B. Boitrel. *Chem. Commun.* **2000**, 1589-1590. (c) L. Michaudet, P. Richard, B. Boitrel. *Tetrahedron Lett.* **2000**, 41, 8289-8292.
8. (a) S. O'Malley, T. Kodadek. *J. Am. Chem. Soc.* **1989**, 111, 9116-9117. (b) S. O'Malley, T. Kodadek. *Organometallics* **1992**, 11, 2299-2302.
9. R. L. Halterman, S. T. Jan. *J. Org. Chem.* **1991**, 56, 5253-5254.
10. (a) M. Frauenkron, A. Berkessel. *Tetrahedron Lett.* **1997**, 38, 7175-7176. (b) W. C. Lo, C. M. Che, K. F. Cheng, T. C. W. Mak. *Chem. Commun.* **1997**, 1205-1206.
11. C. M. Che, J. S. Huang, F. W. Lee, Y. Li, T. S. Lai, H. L. Kwong, P. F. Teng, W. S. Lee, W. C. Lo, S. M. Peng, Z. Y. Zhou. *J. Am. Chem. Soc.* **2001**, 123, 4119-4129.
12. K. H. Chan, X. Guan, V. K. Y. Lo, C. M. Che. *Angew. Chem. Int. Ed.* **2014**, 53, 2982-2987.
13. A. Berkessel, P. Kaiser, J. Lex. *Chem. Eur. J.* **2003**, 9, 4746-4756.
14. (a) Y. Ferrand, P. Le Maux, G. Simonneaux. *Organic Lett.* **2004**, 6, 3211-3214. (b) P. Le Maux, S. Juillard, G. Simonneaux. *Synthesis* **2006**, 2006, 1701-1704. (c) I. Nicolas, P. Le Maux, G. Simonneaux. *Tetrahedron Lett.* **2008**, 49, 2111-2113.
15. J. L. Zhang, Y. L. Liu, C. M. Che. *Chem. Commun.* **2002**, 2906-2907.
16. Y. Ferrand, C. Poriel, P. Le Maux, J. Rault-Berthelot, G. Simonneaux. *Tetrahedron: Asymmetry* **2005**, 16, 1463-1472.
17. Y. Ferrand, P. Le Maux, G. Simonneaux. *Tetrahedron: Asymmetry* **2005**, 16, 3829-3836.
18. T. S. Lai, F. Y. Chan, P. K. So, D. L. Ma, K. Y. Wong, C. M. Che. *Dalton Transactions* **2006**, 4845-4851.
19. I. Nicolas, T. Roisnel, P. Le Maux, G. Simonneaux. *Tetrahedron Letters* **2009**, 50, 5149-5151.
20. I. Nicolas, P. Le Maux, G. Simonneaux. *Tetrahedron Lett.* **2008**, 49, 5793-5795.
21. (a) E. Galardon, P. Le Maux, G. Simonneaux. *Chem. Commun.* **1997**, 927-928. (b) E. Galardon, S. Roué, P. Le Maux, G. Simonneaux. *Tetrahedron Lett.* **1998**, 39, 2333-2334.
22. Y. Chen, X. P. Zhang. *J. Org. Chem.* **2007**, 72, 5931-5934.
23. G. Du, B. Andrioletti, E. Rose, L. K. Woo. *Organometallics* **2002**, 21, 4490-4495.
24. D. Intriери, S. Le Gac, A. Caselli, E. Rose, B. Boitrel, E. Gallo. *Chem. Commun.* **2014**, 50, 1811-1813.
25. D. M. Carminati, D. Intriери, A. Caselli, S. Le Gac, B. Boitrel, L. Toma, L. Legnani, E. Gallo. *Chem. Eur. J.* **2016**, 22, 13599-13612.
26. (a) H. M. Mbuvi, L. K. *Organometallics* **2008**, 27, 637-645. (b) P. Vinš, A. de Cózar, I. Rivilla, K. Nováková, R. Zangi, J. Cvačka, I. Arrastia, A. Arrieta, P. Drašar, J. I. Miranda, F. P. Cossío. *Tetrahedron* **2016**, 72, 1120-1131.
27. R. L. Khade, Y. Zhang. *J. Am. Chem. Soc.* **2015**, 137, 7560-7563.
28. T. Toma, J. Shimokawa, T. Fukuyama. *Organic Letters* **2007**, 9, 3195-3197.

29. D. M. Hodgson, D. Angrish. *Chem. Eur. J.* **2007**, 13, 3470-3479.
30. Y. Chen, X. P. Zhang. *J. Org. Chem.* **2004**, 69, 2431-2435.
31. J. I. Ito, S. Ujiie, H. Nishiyama. *Chem. Eur. J.* **2010**, 16, 4986-4990.
32. S. Ishikawa, R. Hudson, M. Masnadi, M. Bateman, A. Castonguay, N. Braidy, A. Moores, C. J. Li. *Tetrahedron* **2014**, 70, 6162-6168.
33. S. Fantauzzi, E. Gallo, E. Rose, N. Raoul, A. Caselli, S. Issa, F. Ragaini, S. Cenini. *Organometallics* **2008**, 27, 6143-6151.
34. B. Castano, E. Gallo, D. J. Cole-Hamilton, V. Dal Santo, R. Psaro, A. Caselli. *Green Chem.* **2014**, 16, 3202-3209.
35. M. Hagar, F. Ragaini, E. Monticelli, A. Caselli, P. Macchi, N. Casati. *Chem. Commun.* **2010**, 46, 6153-6155.

# Chapter III

## C-N bond formations: Aziridines



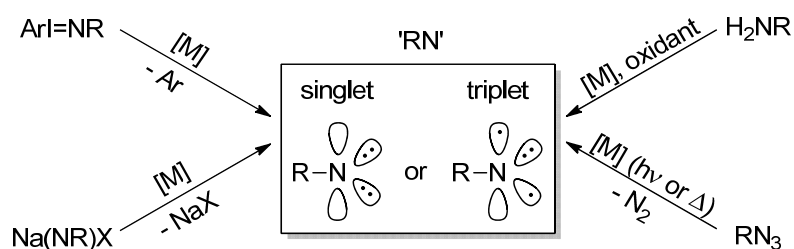
*Parts of this chapter have been published and are reproduced here from:*

S. Rossi, A. Puglisi, M. Benaglia, D. M. Carminati, D. Intriari and E. Gallo. *Catal. Sci. Technol.* **2016**, 6, 4700-4704.

# 1. Introduction

Nitrogen-containing compounds have a prominent role in the pharmaceutical industry due to their biological properties. The scientific community is interested in developing new 'green' methods for the direct and selective C-N bond formation. The transfer reaction of a nitrene 'NR' moiety into an organic molecule represents an important methodology to synthesise organonitrogen compounds.

Nitrenes are the nitrogen analogues of carbenes and they show four non-bonding electrons which are responsible for their high chemical reactivity. Nitrenes can exist in two different spin states: a singlet state, in which the electrons are arranged as two lone pairs, and a triplet state, where the electrons are placed in three orbitals showing a diradical behaviour (Scheme 25).

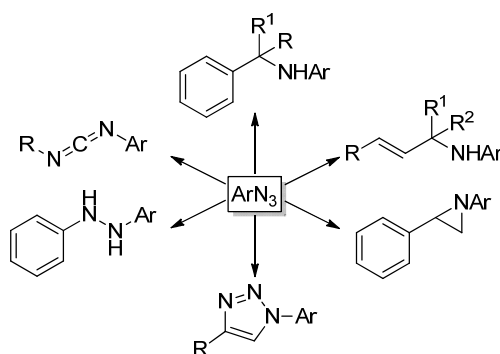


**Scheme 25.** General scheme of the nitrene formation.

Over the years, numerous nitrene sources have been studied to generate the 'RN' moiety and the most important nitrene sources are: aryl iminodiodanenes, amides in presence of a hypervalent iodine reagents, Chloramine-T, Bromamine-T and organic azides ( $RN_3$ ) (Scheme 25).

In the past two decades an increasing interest in the use of organic azides could be observed due to their high reactivity and synthetic versatility. Organic azides are used as nitrene reagents in many productions of important compounds such as isocyanates, aziridines, triazoles, triazenes and azirines, but their potential hazardous properties must be carefully considered. Organic azides often exhibit explosive properties due to the presence of the azido group, which is an energy-rich functional group, and they can undergo a strong exothermic dissociation reaction. Therefore, the explosive character of azides depends on the azido content and, usually, they result sufficiently stable for a safety manipulation if the rule concerning the number of carbon and nitrogen is respected ( $(N_C+N_O)/N_N > 3$ ).<sup>1</sup>

Among all organic azides, aryl azides show a good reactivity/stability relationship and they can be easily synthesised and manipulated in laboratory. Moreover, in 2011 an efficient and safe procedure to obtain aryl azides in bulk amounts has been developed making them commercially available.<sup>2</sup> This, coupled with the production of molecular nitrogen as the only by product during the formation of nitrene unit 'RN', makes aryl azides one of the best nitrene class sources (Scheme 26).



**Scheme 26.** Example of intermolecular aryl azide reactions

## 1.1. Aziridination reactions

Several antitumor compounds, antibiotics and enzyme inhibitors contain the smallest *N*-heterocycle ring: the aziridine. Aziridines show biological and pharmaceutical properties and, thanks to the energy associated to the strained three-membered ring, they have a prominent role in industry as building blocks in the synthesis of more complex molecules (Figure 21).

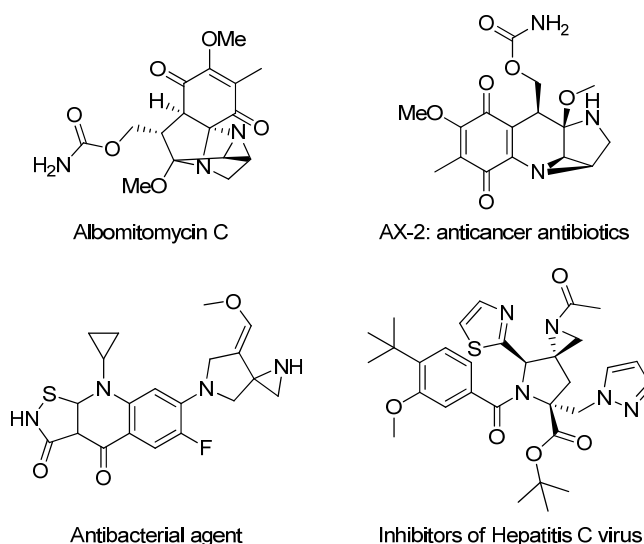
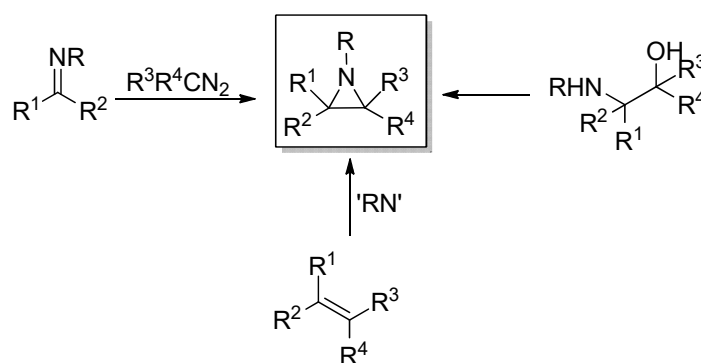


**Figure 21.** Example of aziridine-containing compounds.

Often, the traditional aziridine syntheses, such as the cyclization of amino alcohols (scheme 27), result in low efficiencies and the scientific community is constantly interested in the development of new useful and green synthetic approaches for the synthesis of this important class of compounds.

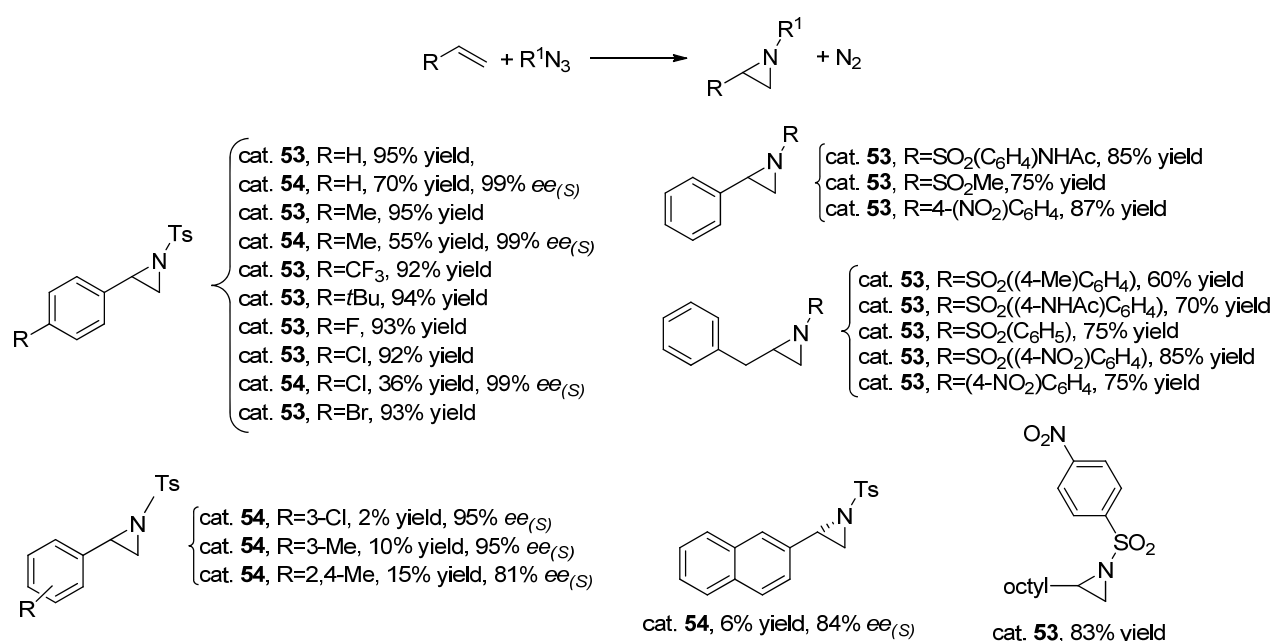


**Scheme 27.** General synthetic pathways affording aziridines.

Among available synthetic strategies, one of the most suitable methodology is the direct transfer reaction of the 'nitrene' moiety into alkenes (aziridination reaction) and among all the catalysts, metal porphyrin complexes show a high catalytic activity. In particular, we will focus our attention on the catalytic activity of iron and ruthenium porphyrin complexes as catalysts in the aziridination reactions using organic azides as nitrene sources.

### 1.1.1. Group 8 porphyrin-catalysed aziridination reactions

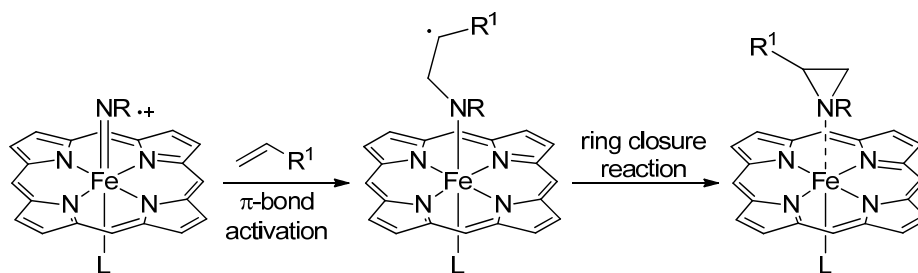
The first aziridination of alkenes catalysed by an iron porphyrin complex was reported by Mansuy and co-authors who used *N*-tosylimino aryliodinane, PhI=NTs, as the nitrene source.<sup>3</sup> After this work, several papers were published confirming the good catalytic activity of iron porphyrins to promote the reaction of alkenes and iminoiodinanes. Despite the extensive use of ArI=NR, they result bad ‘green’ nitrene sources due to the formation of iodo aryl compound as the stoichiometric byproduct of the nitrene reaction. For this reason, the scientific community attention is focused towards the use of more eco-friendly nitrene sources such as organic azides, which produce only molecular nitrogen as byproduct. Concerning that, in 2010, Che and co-workers reported the aziridination of electron-poor and electron-rich substituted styrenes with tosyl azide (TsN<sub>3</sub>), using Fe(F<sub>20</sub>TPP)Cl (**53**) as catalyst (Scheme 28). Substituted styrenes formed aziridines in excellent yields, up to 95%, and also aliphatic alkenes, under microwave irradiations, reacted with tosyl azide giving the corresponding aziridines in good yields.



**Scheme 28.** Iron porphyrin-catalysed aziridination of alkenes by organic azides.

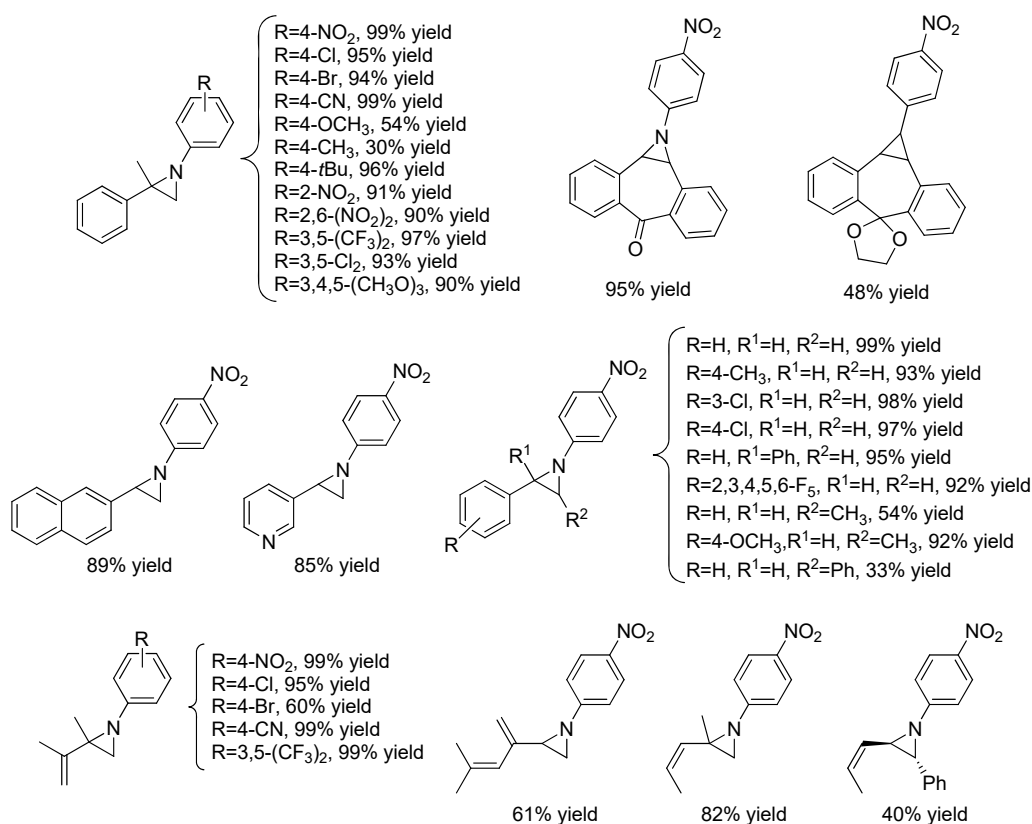
Tosyl azide was also used by Arnold for the enantioselective synthesis of aziridines using mutated enzymes in which an iron porphyrin was the active site.<sup>4</sup> Biocatalysts P-I263F (P=P411BM3-CIS-T438S) and P-I263F-A328V-L437V (**54**) showed a very good catalytic activity forming aziridines in good yields and excellent enantioselectivities (99%  $ee_{(S)}$ ).

Up to now, the mechanism of the iron porphyrin-catalysed aziridination remains unclear, but probably, the reaction proceeds by the formation of an iron(IV) imido intermediate, (porphyrin)<sup>+</sup>Fe=NR(L). DFT calculation, which was performed by Shaik, revealed that the reaction involves three steps in which there is an activation of the alkene  $\pi$ -bond and a subsequent ring closure.<sup>5</sup> All intermediates can possess degenerate doublet and quartet spin states which depend on the nature of the imido group and on the axial ligand of the iron atom (Scheme 29).



**Scheme 29.** Mechanism proposed for iron-catalysed aziridination.

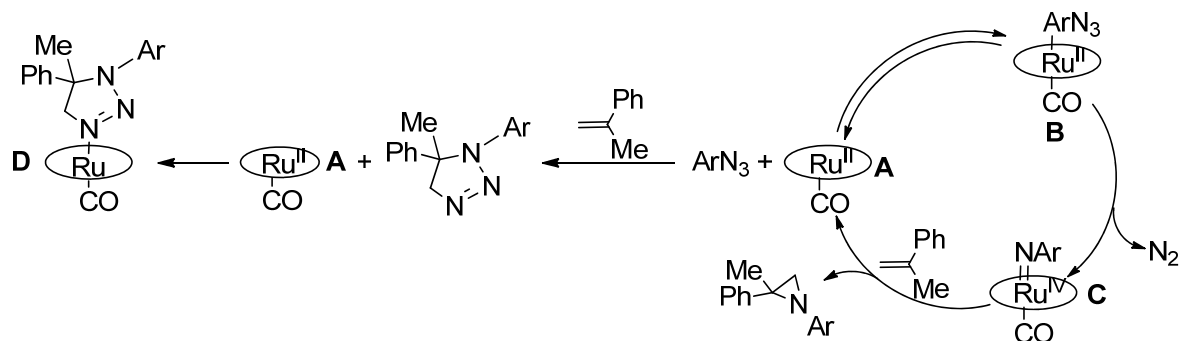
Concerning ruthenium porphyrin complexes, they are very active promoters of aziridination reaction, using organic azides as nitrene source. In 2007, Cenini and co-workers reported the use of ruthenium porphyrin complexes as catalyst in the aziridination reaction of several aryl alkenes with aryl azides.<sup>6</sup> Among all the tested ruthenium porphyrin catalysts, the commercially available Ru(TPP)CO resulted the best catalyst both with electron-poor and electron-rich aryl azides (Scheme 30).



**Scheme 30.** Ru(TPP)CO-catalysed aziridination reaction.

The aziridination reaction between aryl alkenes and aryl azides was also studied by using kinetic and theoretical approaches by Gallo, Manca *et al.*<sup>7</sup> They demonstrated that the kinetics of the reaction depends on two factors: the electronic nature of the catalyst and the concentration of the alkene. As for the first factor, they reported that the presence of an electron-withdrawing group on the porphyrin scaffold favours the coordination of the azide to the ruthenium atom and then the formation of the *mono*-imido complex, which is probably the active species. As stated above, the second factor is the concentration of the alkene. They found that, at high substrate concentration, azide reacts with alkene forming triazoline, which is responsible for the catalyst deactivation due to the formation of the inactive triazoline-complex (Scheme 31, **D**). Thanks to the kinetic data and previous mechanistic studies, the authors proposed a *mono*-imido-based catalytic cycle, because the

isolation of Ru(porphyrin)CO complex at the end of the catalytic excludes the formation of *bis*-imido complex as the key-intermediate species (Scheme 31).



**Scheme 31.** Suggested mechanism of the Ru(porp)CO-catalysed aziridination of styrenes.

The mechanism was also confirmed by the DFT calculation which was performed by using a ruthenium porphine complex as catalyst,  $\alpha$ -methylstyrene as substrate and phenyl azide as nitrene source.<sup>7</sup>

The starting point of the DFT study is the formation of the *mono*-imido complex in the triplet state which can radically activate alkene to obtain the desired aziridine compound by a radical re-combination step (Figure 22).

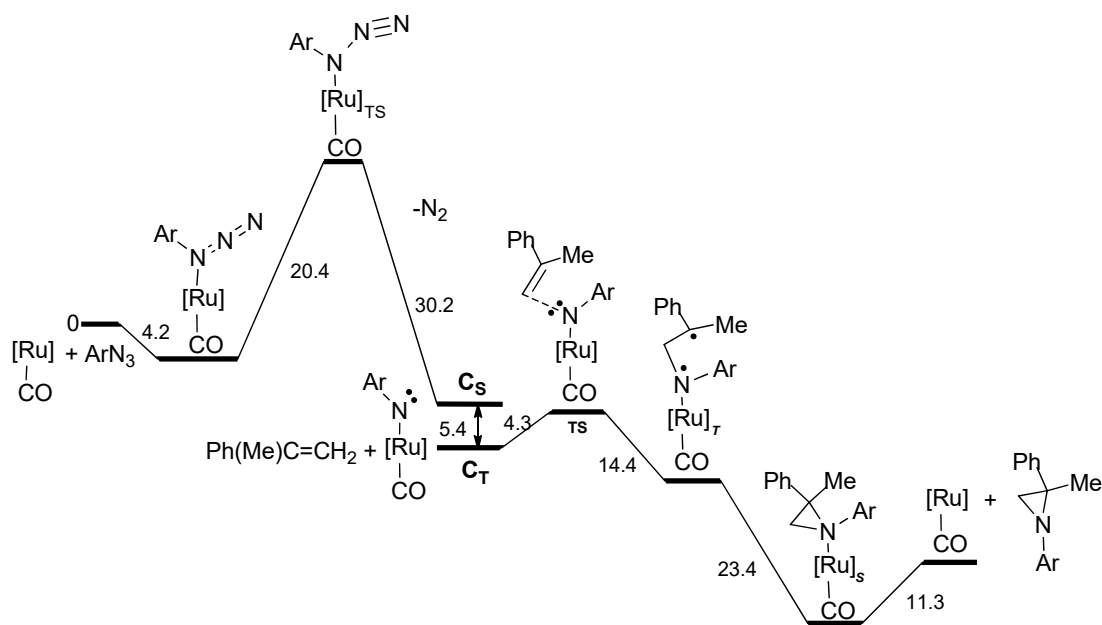
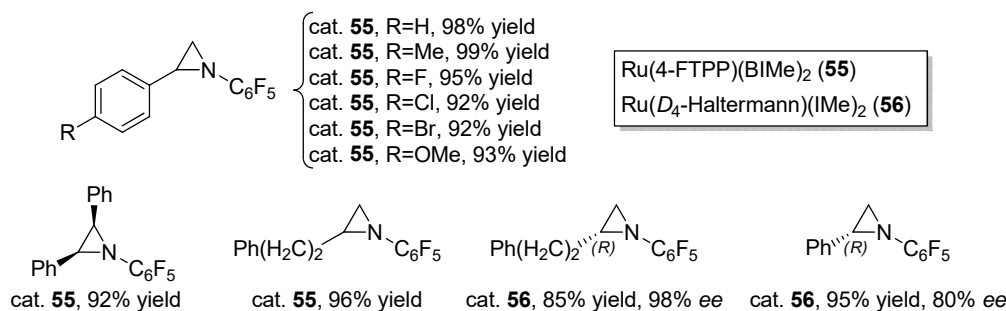


**Figure 22.** Energy profile of the aziridination of  $\alpha$ -methylstyrene using Ru(porphine)CO as catalyst.

The scope of the ruthenium porphyrin-catalysed aziridination was improved by using conjugated dienes which were employed to synthesise *N*-aryl-2-vinylaziridines. This class of compounds is very reactive and can evolve by a ring-opening or ring-expansion reaction forming benzoazepines, 2,3-dihydropyrroles and 2,5-dihydropyrroles (Scheme 30).<sup>6c</sup> The catalytic activity of ruthenium porphyrins was also improved by Che and co-authors, who synthesised two *bis*(*N*-heterocyclic carbene)ruthenium porphyrin complexes: **55** (Ru(4-F TPP)(Ime)<sub>2</sub>) and **56** (Ru(*D*<sub>4</sub>-Haltermann)(BIme)<sub>2</sub>) in which the two  $\sigma$ -electron donor NHCs increased the reactivity of the *trans*-metal-nitrene unit.<sup>8</sup> Complex **55** resulted a good catalyst in the aziridination of several alkenes by pentafluorophenyl azides. Aziridines were obtained in good yields and in excellent enantioselectivities when catalyst **56** was employed as catalyst (Scheme 32).





**Scheme 32.** Aziridination by pentafluorophenyl azides using complexes **55** and **56**.

To improve the recyclability and reuse of the ruthenium porphyrin catalysts, Gallo and co-workers reported the synthesis of a catalytic membrane in which Ru(4-(CF<sub>3</sub>)TPP)CO **57** was embedded into a perfluorinated polymer Hyflon AD60X (HF).<sup>9</sup> Heterogeneous catalyst HF-**57** was efficient for the synthesis of *N*-aryl aziridines which were obtained with selectivity larger than 98%.<sup>10</sup>

## 1.2. Reactivity of aziridines with carbon dioxide

Over the last decades, aziridine's chemistry, in terms of synthesis and applications, has been extensively studied because aziridines are analogous to epoxides and cyclopropanes. Thanks to the high energy of the ring-strained, aziridines result very active reagents and they can react with several molecules to form more challenging compounds such as obtain oxazolidinones which are obtained by reacting aziridines with CO<sub>2</sub>.

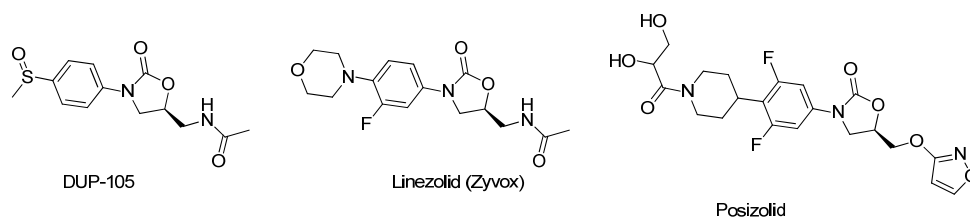
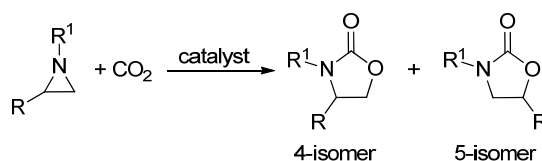


**Figure 23.** Structures of some oxazolidinone-based biologically relevant compounds.

The five-membered cyclic carbamates, known as oxazolidinones, occupy a special place among heterocyclic compounds and they are used in many industrial fields. Oxazolidinones are widely used in medicine for the synthesis of several commercially available drugs due to their antibacterial and antimicrobial properties (Figure 23).<sup>11</sup> Furthermore, the enantiomerically pure 4-substituted oxazolidinones are one of the most used classes of chiral auxiliaries in asymmetric synthesis since Evans reported their use in 1981.<sup>12</sup> All these applications made oxazolidinones commercially attractive molecules and fostered the development of new synthetic routes, especially of those that are based on the use of CO<sub>2</sub> as the starting reagent.

The conventional preparation of oxazolidinones includes the use of environmentally harmful and toxic reagents such as phosgene, isocyanates and carbon monoxide; for this reason the coupling reaction between CO<sub>2</sub> and aziridines represents an attractive route due to the 100% atom efficiency and the use of the most abundant greenhouse gas (Scheme 33).

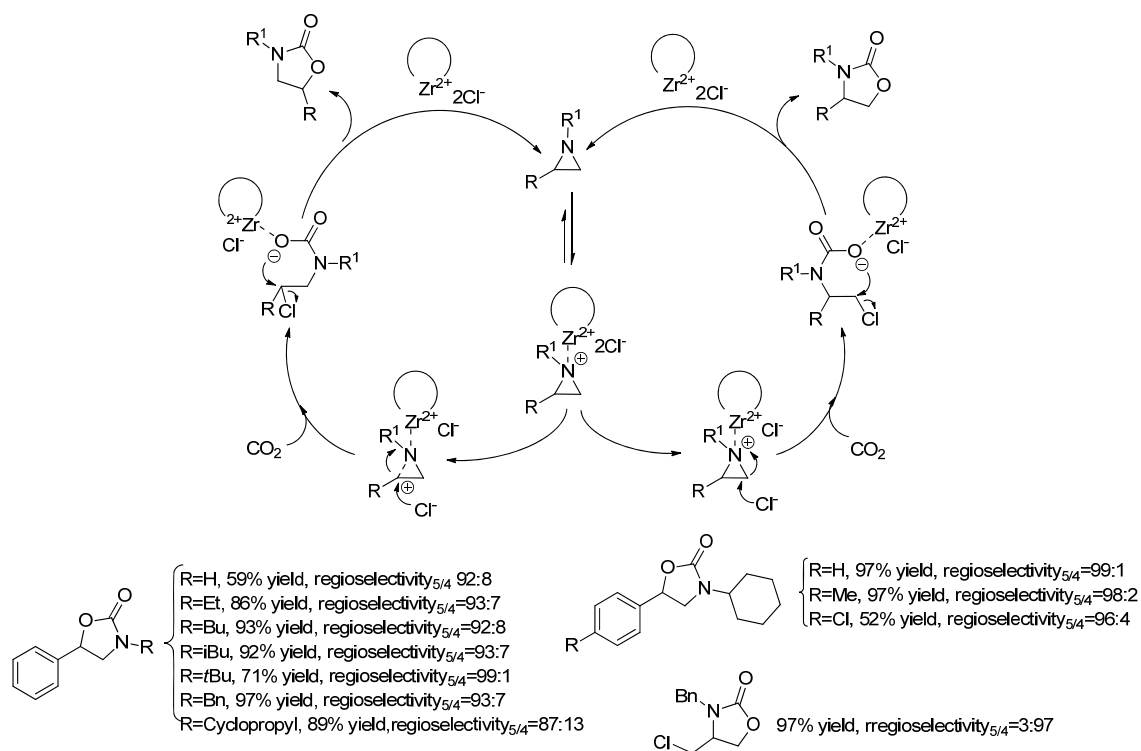


**Scheme 33.** Scheme of the coupling reaction between carbon dioxide and aziridine.

The first synthesis of oxazolidinones from aziridines and CO<sub>2</sub>, was reported in 1976 by Soga *et al* using I<sub>2</sub>. After this work, many papers were published, but the use of high pressure, temperature and toxic solvent/reagents limited the industrial application of this process. Good results were obtained by Davies and Manning who synthesised oxazolidinones in good yields (50-99%) and moderate regioselectivity (50-84%) under mild reaction conditions using stable nickel cyclam and bipyridine complexes.<sup>13</sup>

Alkali metal halides were also employed as catalysts, in particular Endo and co-workers demonstrated that the simple and cheap lithium bromide, which is used in epoxide/CO<sub>2</sub> coupling reaction, efficiently catalysed the reaction of 2-methyl and 2-phenylaziridine giving their corresponding oxazolidinones with an excellent regioselectivity.<sup>14</sup> Lithium and ammonium halides were also studied by Pinhas *et al* for the conversion of *N*-substituted aziridines under similar conditions as those reported by Endo.<sup>15</sup> In each case the authors supposed that the role of the anion X<sup>-</sup> is to promote the ring opening reaction of the aziridines followed by the insertion of the carbon dioxide and the formation of the five-membered ring.

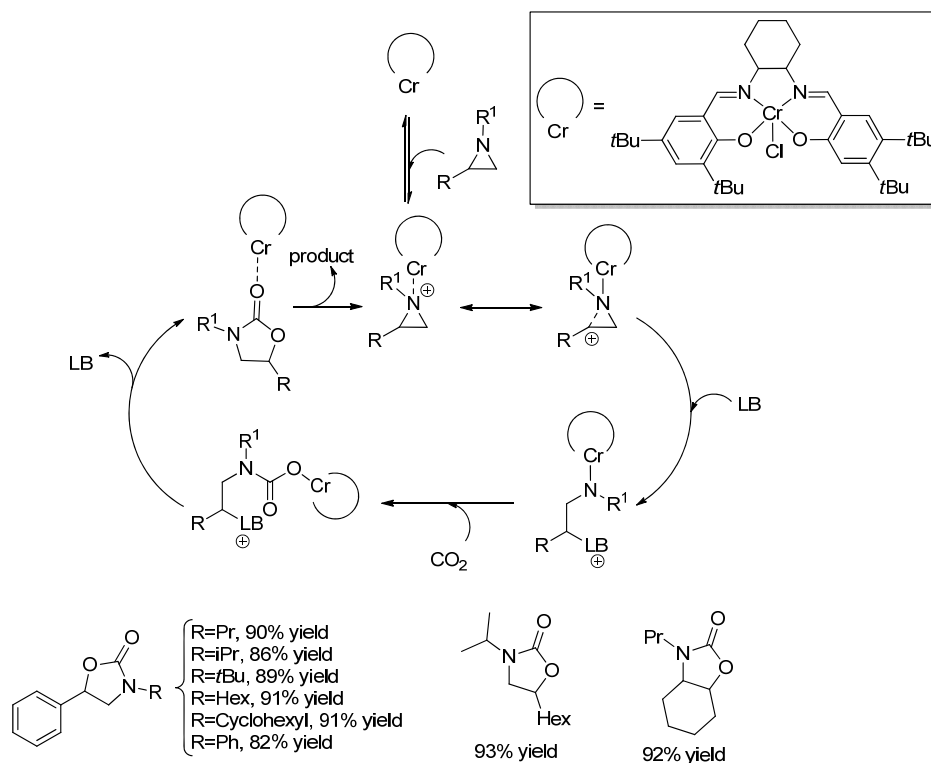
A different method to obtain 5-substituted oxazolidinones in excellent yield and regioselectivity under solvent-free conditions was reported by Wu and co-authors using solid zirconyl chloride (ZrOCl<sub>2</sub>·8H<sub>2</sub>O). This methodology was successfully applied to the synthesis of a large variety of *N*-alkyl-2-phenylaziridines to obtain *N*-alkyl-5-phenyl-based oxazolidinones as the major products (Scheme 34).<sup>16</sup> The catalytic activity of ZrOCl<sub>2</sub>·8H<sub>2</sub>O can be explained by the formation of a cationic cluster which is able to coordinate the aziridine ring forming intermediate A (Scheme 34). Intermediate A can undergo the ring-opening reaction thanks to the chloride atom: this can happen in two different ways depending on the nature of the group on the *N*-position. After the ring-opening reaction, the authors proposed a CO<sub>2</sub> insertion and a subsequent cyclization via an intramolecular nucleophilic attack.



**Scheme 34.** Proposed mechanism and scope of zirconyl chloride-catalysed reaction.

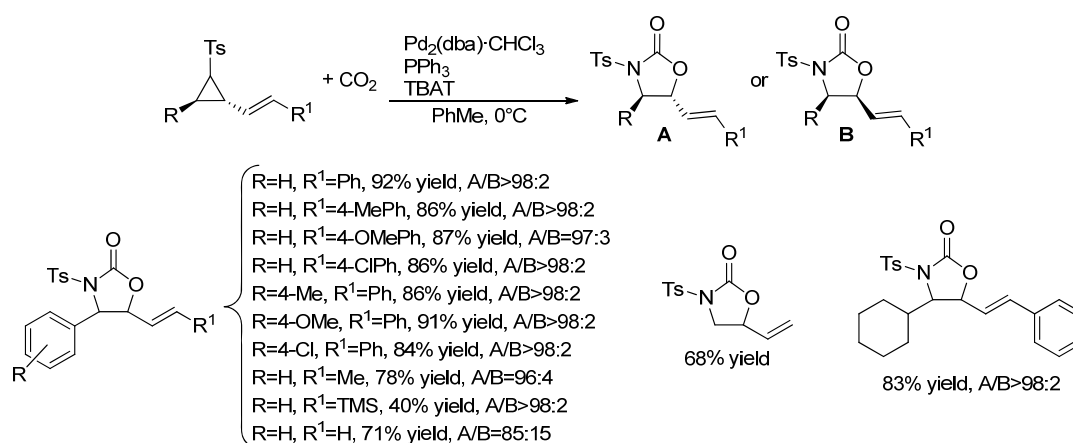
Even if all these methods gave the *N*-alkyl oxazolidinones in good yield using a relative cheap catalyst, the biological relevant *N*-aryl oxazolidinones were never synthesised.<sup>11a, 11b</sup> To the best of our knowledge, only the simple *N*-phenyl oxazolidinone was obtained by Nguyen using a chromium salen complex in presence of

4-dimethylaminopyridine (DMAP) as co-catalyst (Scheme 35).<sup>17</sup> As in the  $\text{ZrOCl}_2 \cdot 8\text{H}_2\text{O}$ -catalysed mechanism, the authors proposed a first step where the Lewis acidic chromium salen complex coordinates the aziridine giving partial cationic nitrogen. The aziridine can be attacked by the co-catalyst to the more substituted carbon giving intermediate **B**. Then, a molecule of carbon dioxide inserts forming intermediate **C** which undergoes a cyclization to give the 5-oxazolidinone as product.



**Scheme 35.** Proposed mechanism and scope of chromium salen-catalysed reaction

The scope of the coupling reaction between aziridines and  $\text{CO}_2$  was expanded by Aggarwal *et al* who reported the efficient conversion of 2-allyl-3-substituted aziridines to the corresponding oxazolidinones in mild conditions (Scheme 36).<sup>18</sup>



**Scheme 36.** Synthesis of vinyloxazolidinones.

To improve the eco-sustainability of this methodology, the recyclability and easy recover of the catalyst are important issues. Concerning that, He and Bhanage reported the use of functionalised PEG respectively with quaternary ammonium salts ( $\text{NR}_3\text{Br}$ ) and phosphonium salts ( $\text{PR}_3\text{Br}$ ).<sup>19</sup> Both catalytic systems resulted highly efficient and recyclable: in fact, they could be recovered by a simple centrifugation and reused with retention

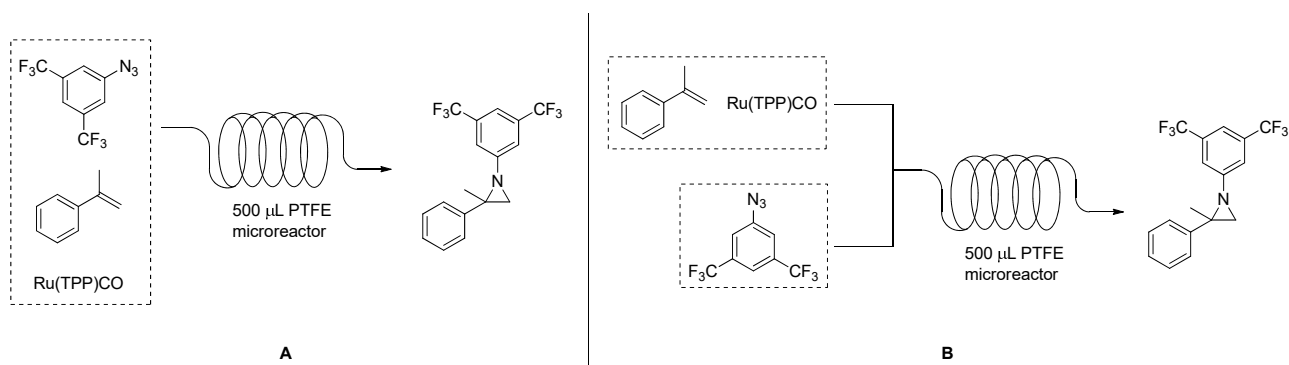
of high catalytic activity and regioselectivities (up to 99:1). Moreover, several oxazolidinones were obtained in good yields and high 5-regioselectivities under mild conditions and without any added organic solvent and co-catalyst.

## 2. Discussion

### 2.1. Aziridination reaction under continuous flow conditions

As reported in the previous chapter, the aziridination by using organic azides shows a very high efficiency in terms of eco-sustainability and atom efficiency thanks to the formation of eco-friendly molecular nitrogen as the only byproduct. However, the manipulation of azides is a delicate process, due to their inherent propensity for decomposition, and the use of a continuous flow methodology can be a positive solution to overcome this problem. The intrinsically small volumes, short reaction times and highly controlled reaction conditions render continuous flow microreactors ideal systems for the manipulation of hazardous reagents or very reactive intermediates. Considering that the ruthenium porphyrin-catalysed aziridination of alkenes by aryl azide was largely studied in our research group from both the experimental and theoretical points of view, in order to increase the efficiency and safety of the reaction, we investigated the Ru(TPP)CO-catalysed aziridination in mesoreactors under continuous flow conditions.

In preliminary studies, the experimental conditions were tested in the model reaction between 3,5-bis(trifluoromethyl)phenyl azide and  $\alpha$ -methylstyrene. The model reaction was conducted in a mesoreactor made of commercially available PTFE tubing that was coiled in a bundle and immersed in a preheated oil bath. All reagents, the catalyst and the solvent were mixed in one Hamilton gastight 10 mL syringe and pumped by a New Era NE 300 syringe pump (Scheme 37, A).



**Scheme 37.** Reaction between 3,5-bis(trifluoromethyl)phenyl azide and  $\alpha$ -methylstyrene promoted by Ru(TPP)CO: in a one-syringe continuous flow system (A) and in a two-syringe continuous flow system (B).

As reported in table 2, low conversions of azide were obtained when the reactions were performed at 90°C, both in benzene and  $\alpha$ -methylstyrene, in short residence times (table 2, entry 1 and 3), while a higher conversion was detected by increasing the temperature at 120°C using  $\alpha$ -methylstyrene as solvent (table 2, entry 4). Note that the replacement of benzene with  $\alpha$ -methylstyrene has a beneficial effect in terms of reaction eco-compatibility. In fact, solvent-free reactions are cleaner especially when the substrate, used as the reaction solvent, can be recycled in a continuous flow process. More beneficial effects were achieved splitting the addition of the reactants into two different Hamilton gastight 2.5 mL syringe (Scheme 37, B). Running the reactions in a two-syringe continuous-flow system we increased the efficiency of the catalytic system and the best result, in terms of conversion and selectivity, was obtained working in  $\alpha$ -methylstyrene at 120°C after 30 minutes residence time (table 2, entry 8).

**Table 2.** Ru(TPP)CO-catalysed aziridination reactions of  $\alpha$ -methylstyrene and 3,5-bis(trifluoromethyl)phenyl azide.<sup>a</sup>

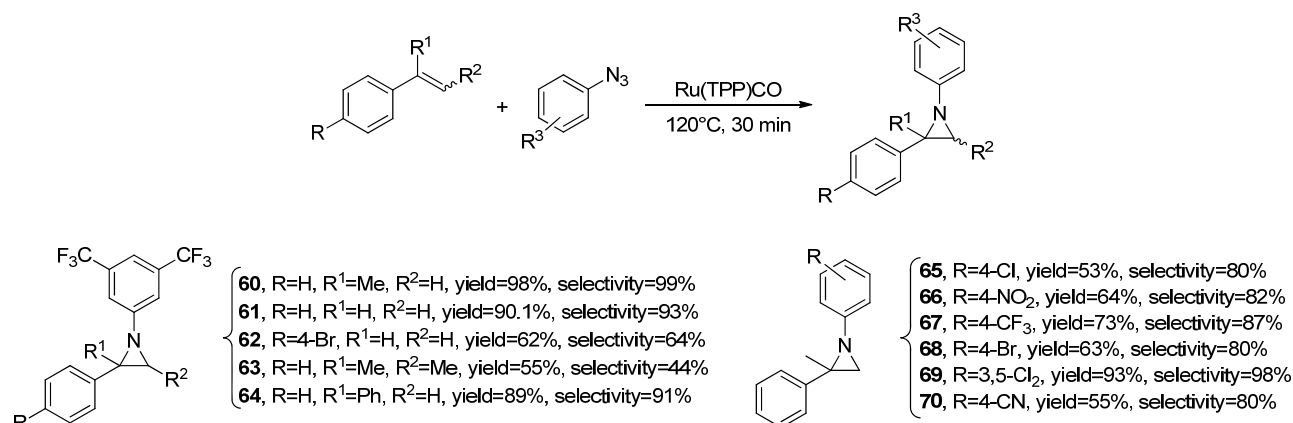
Entry	Solvent	residence time (min)	temperature (°C)	conversion (%) <sup>b</sup>	selectivity (%) <sup>b</sup>	yield (%) <sup>b</sup>
1 <sup>d</sup>	Benzene	10	90	49.4	80.3	39.7
2 <sup>d</sup>	Benzene	30	90	62.8	74.2	46.6
3 <sup>d</sup>	$\alpha$ -methylstyrene	5	90	44.1	95.0	41.9
4 <sup>d</sup>	$\alpha$ -methylstyrene	5	120	54.8	75.9	41.6
5 <sup>e</sup>	Benzene	5	90	12.4	77.4	9.6
6 <sup>e</sup>	$\alpha$ -methylstyrene	5	120	90.6	96.7	87.6
7 <sup>e</sup>	$\alpha$ -methylstyrene	10	120	97.7	97.4	95.1
8 <sup>e</sup>	$\alpha$ -methylstyrene	30	120	98.9	99.1	98.0

<sup>a</sup>Reaction conditions: catalyst/azide/ $\alpha$ -methylstyrene 1:50:250 with a azide concentration inside the microreactor of 0.02 M.

<sup>b</sup>Determined by GC using biphenyl as internal standard. <sup>d</sup>The reaction was carried out in a one-syringe flow system. <sup>e</sup>The reaction was carried out in a two-syringe flow system.

We also tested the influence of the azide concentration using a 0.2 M solution of azide. No substantial difference in terms of conversion and yield was observed, so for convenience we decided to perform the future reactions using a 0.2 M solution of azide.

Since the reaction conditions and parameters were optimised ( $\alpha$ -methylstyrene as the solvent, [azide]=0.2 M, 120°C and 30 minutes), a screening of azides and alkenes was performed. Aziridines were obtained in good yields and high selectivities and the achieved results were comparable with those reported for the batch reactions. Aryl azide with strongly electron-withdrawing groups in meta positions resulted more active forming the corresponding aziridines in almost quantitative yields (compare products **60** and **69**, Scheme 38). On the contrary, the presence of a EWG on styrene ring reduces the reactivity: in fact 4-bromo styrene resulted less reactive than styrene producing the aziridine in 62% yield (compare products **62** and **61**, Scheme 38). Also internal alkenes resulted less active:  $\beta$ -methylstyrene gave the corresponding product as a mixture of 9:1 *cis:trans* isomers in a quantitative conversion but only 55% yield (product **63**, Scheme 38).

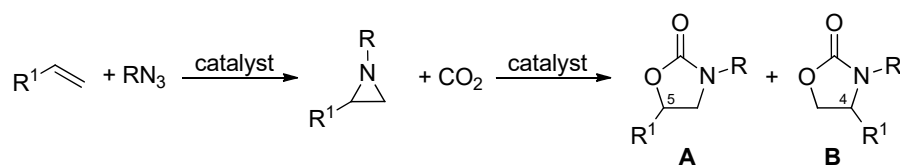
**Scheme 38.** Scope of the reaction.

The Ru(TPP)CO-catalysed aziridination was successfully accomplished in a PTFE mesoreactor under continuous-flow conditions with advantages of operating with smaller reaction volumes and free-solvent condition. The methodology opens new opportunities for a very convenient synthesis of functionalized aziridines with a safe, fast and experimentally simple procedure.

## 2.2. Aziridines reactivity: synthesis of oxazolidinones

Thanks to the high energy of the ring-strained, aziridines result very active reagents and can react with several molecules forming more challenging compounds such as oxazolidinones. Oxazolidinone moieties are of great chemical interest due to the applications of these molecules as starting materials in organic synthesis to produce pharmaceutical and/or biological compounds. Among all the methodologies to synthesise oxazolidinones, the direct coupling reaction between aziridines and carbon dioxide is one of the most important routes.

Moreover, given that aziridines can be obtained *via* a nitrene transfer reaction from aryl azides to alkenes catalysed by metal porphyrin complexes, we decided to study the synthesis of oxazolidinones in two-steps one-batch by using only one porphyrin catalyst (Scheme 39).



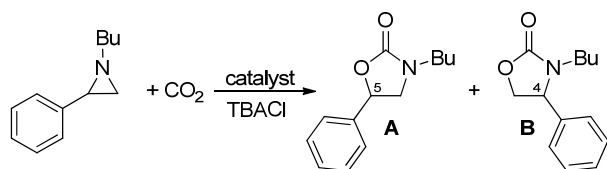
**Scheme 39.** Synthesis of oxazolidinones in two-steps and one batch.

We started our work by studying the second step of the two-step one-batch process, in particular we studied the model coupling reaction between 1-butyl-2-phenyl aziridine and carbon dioxide. First of all, we performed the catalyst-free reaction of 1-butyl-2-phenyl aziridine with CO<sub>2</sub> and we observed that the reaction did not occur (table 3, entry 1). After that, we performed the model reaction in presence of several metal porphyrin complexes as catalysts. The reactions occurred with an excellent chemo- and regioselectivity, the two regioisomers **A** and **B** were formed with the less hindered oxazolidinone **A** as the major compound, but with very low yields (see experimental section, table 1, entry 2-7). Considering that tetralkyl ammonium salts are generally used as co-catalysts in the metal porphyrin-catalysed coupling reaction of CO<sub>2</sub> and epoxides, we decided to employ tetrabutyl ammonium chloride (TBACl) as co-catalyst in our system. The combination of metal porphyrin catalyst and TBACl increased the catalytic efficiency of our system both in terms of yields and regioselectivities (see experimental section, table 1, entry 8-12).

Since the main aim of this project is the synthesis of oxazolidinones in two steps and one batch by using only one porphyrin catalyst, we focused our attention on the use of ruthenium porphyrin complexes because they efficiently catalyse aziridination reactions. Thus, we investigated the catalytic activity of ruthenium(II) complexes, Ru(TPP)CO and Ru(TPP)(py)<sub>2</sub>, but they showed a low catalytic activity and the desired oxazolidinones were obtained in very low yields (table 3, entries 2 and 3). When the ruthenium(IV) [Ru(TPP)OCH<sub>3</sub>]<sub>2</sub>O complex was employed as the catalyst (table 3, entry 4), a slight improvement of the reaction yield was observed and the isomer **A** was formed with an excellent regioselectivity. Better results were achieved by using ruthenium(VI) *bis*-imido porphyrin complexes Ru(TPP)(NAr)<sub>2</sub> which formed the 5-regioisomer **A** as the major product. The catalytic activity of Ru(TPP)(NAr)<sub>2</sub> complexes is independent from the electronic nature of the substituents on the imido aryl moiety: similar results, in terms of yield and regioselectivity, were obtained by using both Ru(TPP)(NAr)<sub>2</sub> (Ar=3,5-(CF<sub>3</sub>)<sub>2</sub>C<sub>6</sub>H<sub>3</sub>) (**71**) and Ru(TPP)(NAr)<sub>2</sub> (Ar=4(*t*Bu)C<sub>6</sub>H<sub>4</sub>) as catalysts (table 3, entries 5 and 6). We also investigated the effect of the electronic nature of the porphyrin ring and moderate yields were observed both with electronic withdrawing or electronic donating groups present on the porphyrin skeleton (table 3, entries 7 and 8). This result indicated that the catalytic efficiency was more dependent on the steric hindrance of the porphyrin ring than on its electronic nature. Therefore, we tested the catalytic activity of the less sterically hindered ruthenium (VI) *bis*-imido octaethylporphyrin complex, Ru(OEP)(NAr)<sub>2</sub> (Ar=3,5-(CF<sub>3</sub>)<sub>2</sub>C<sub>6</sub>H<sub>3</sub>), in which the ethyl groups are placed in β

position of the porphyrin scaffold. The isomer **A** was formed in good yield and high regioselectivity and the catalytic efficiency Ru(OEP)(NAr)<sub>2</sub> was comparable to that of complex **71**. This result confirmed the previous hypothesis about the high dependence of the catalytic efficiency on the steric hindrance of the porphyrin scaffold.

**Table 3.** Model reaction of 1-butyl-2-phenylaziridine and CO<sub>2</sub>.<sup>a</sup>



Entry	Catalyst	Co-catalyst	yield (%) <sup>b</sup>	A/B <sup>b</sup>
1	-	-	-	-
2	Ru(TPP)CO	TBACl	-	-
3	Ru(TPP)(py) <sub>2</sub>	TBACl	12	95:5
4	[Ru(TPP)OCH <sub>3</sub> ] <sub>2</sub> O	TBACl	35	91:9
5	Ru(TPP)(NAr) <sub>2</sub> Ar=3,5(CF <sub>3</sub> ) <sub>2</sub> C <sub>6</sub> H <sub>3</sub>	TBACl	71	88:12
6	Ru(TPP)(NAr) <sub>2</sub> Ar=4( <i>t</i> Bu)C <sub>6</sub> H <sub>4</sub>	TBACl	62	90:10
7	Ru(F <sub>20</sub> TPP)(NAr) <sub>2</sub> Ar=3,5(CF <sub>3</sub> ) <sub>2</sub> C <sub>6</sub> H <sub>3</sub>	TBACl	34	85:15
8	Ru(TMP)(NAr) <sub>2</sub> Ar=3,5(CF <sub>3</sub> ) <sub>2</sub> C <sub>6</sub> H <sub>3</sub>	TBACl	41	88:12
9	Ru(OEP)(NAr) <sub>2</sub> Ar=3,5(CF <sub>3</sub> ) <sub>2</sub> C <sub>6</sub> H <sub>3</sub>	TBACl	65	90:10

<sup>a</sup>Reaction conditions: cat./co-cat./aziridine 1:10:100 in benzene. In a steel autoclave at 100°C and 30 bar CO<sub>2</sub> for 6 h.

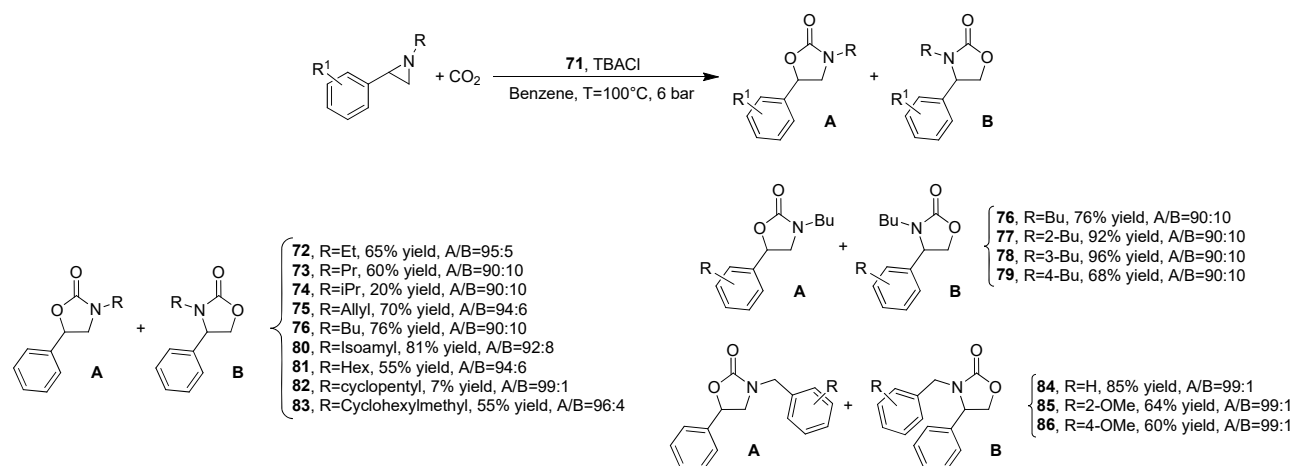
<sup>b</sup>Determined by <sup>1</sup>H NMR using 2,4-dinitrotoluene as the internal standard.

Considering that ruthenium *bis*-imido porphyrin complex **71**/TBACl was the best catalytic system, we optimised the experimental conditions by studying the effect of the tetrabutyl ammonium salt's anion, temperature, solvent polarity and CO<sub>2</sub> pressure (see experimental section). First, we checked the catalytic influence of the anion of the tetrabutyl ammonium salt by employing TBACl, TBABr and TBAI as co-catalyst. We observed that same results were obtained by using TBACl and TBABr, whereas, when the reaction was performed in presence of TBAI, the product was not formed (see experimental section, table 2, entry 1-3). For convenience, we decided to use TBACl as co-catalyst to perform the screening of the other reaction conditions. Then, we decreased the reaction temperature, but unfortunately, when the reaction was performed at 50°C, the product was not obtained. Therefore we maintained the temperature at 100°C and we changed the solvent polarity, which did not produce a positive catalytic effect in terms of reaction yield. In fact, the addition of 10% of DMF to the benzene solution or the use of dichloroethane were responsible for a decrease of the reaction yield (from 70 to 45%) but it is worth noting that the **A** isomer was formed as the only reaction product (A/B ratio=1:99) (see experimental section, table 2, entry 5 and 6). Finally, we performed an optimisation of the CO<sub>2</sub> pressure. No great differences were observed by using either 30 or 6 atm of carbon dioxide (see experimental section, table 2, entry 7). On the other hand, the decrease of CO<sub>2</sub> pressure to 1 atmosphere was



responsible for a large decrease of the catalytic performance and oxazolidinones were obtained with 35% yield and the A/B ratio of 94:6. A similar result was achieved by performing the reaction in a pressure tube: even if a good A/B ratio of 93:7 was obtained, the desired oxazolidinones formed in a low yield (13%) (see experimental section, table 2, entry 8 and 9).

Then, we performed a screening of aziridines and a series of *N*-substituted-5-phenyl oxazolidinones was obtained from moderate to good yields and very high regioselectivities (up to 99:1) (Scheme 40).



**Scheme 40.** Synthesis of oxazolidinones by the coupling reaction between aziridines and carbon dioxide.

Collected data indicated that the catalytic efficiency depends on the steric hindrance of the R substituent on the aziridine nitrogen atom. Aziridines in which the R substituent was a linear alkyl gave the products in good yields, whereas, when 1-branched-chain alkyl-2-phenyl aziridines were employed as the reagent, the products were obtained in low yields. This trend was confirmed by employing 1-cyclohexyl phenyl aziridine and 1-phenyl-2-phenyl aziridine as starting reagents, where no products were obtained. On the other hand, when 1-cyclohexylmethyl- and 1-benzyl-2-phenyl aziridines were employed, the corresponding oxazolidinones were formed in good yields (**83** (55% yield and A/B=96:4) and **84** (85% yield and A/B=99:1), Scheme 40).

These results and those obtained by the catalysts screening (table 3, entry 5, 7 and 8) suggest a sterically interaction between the R group on the aziridine's nitrogen atom and the porphyrin scaffold during the reaction. When the hindrance of one of them was increased, worse results were obtained in term of yields. On the contrary, the presence of an electron-donor substituent on the aryl moiety of the aziridine improved the reaction yield: in fact when 1-butyl-2-(2-methyl)phenyl aziridine and 1-butyl-2-(3-methyl)phenyl aziridine were employed as reagents, the corresponding oxazolidinones were obtained in excellent yields and regioselectivities (**77** (92% yield and A/B=90:10) and **78** (96% yield and A/B=90:10), Scheme 40).

Considering that the presence of tetrabutylammonium chloride as co-catalyst is necessary to obtain oxazolidinones in good yields, we synthesised ligand porphyrins showing an ammonium salt within the structure in order to have both the catalytically active functionalities (the central metal atom and ammonium salt) in the same molecule. Porphyrins **87**, **88**, **89** and **90** were synthesised by the reaction between 5-(2-(3-bromopropoxy)phenyl)-10,15,20-tris(pentafluorophenyl) porphyrin (**A<sub>3</sub>B-Br**) and the desired amines. All porphyrins were fully characterised and the molecular structure of compound **87** was also solved by X-ray analysis on a single crystal (Figure 24).

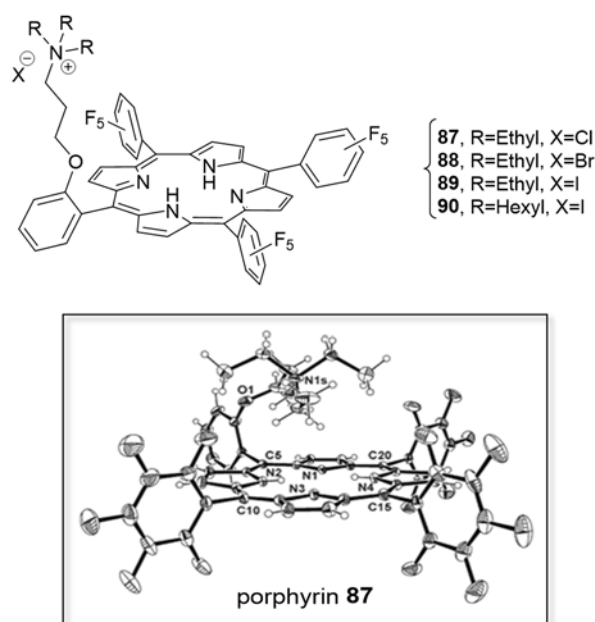
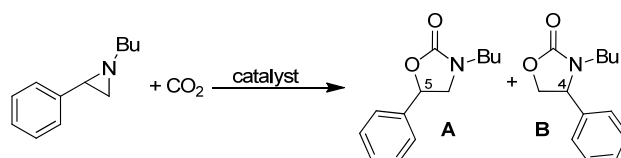


**Figure 24.** Structure of bifunctional porphyrin ligands, ruthenium complexes and crystal structure of porphyrin **87**.

All free porphyrins were tested in the model reaction and, as reported in table 4, we noted that the best anion was the iodide atom, in fact, only porphyrin **89** formed the product among porphyrins **87**, **88** and **89** (table 4, entry 1, 2 and 3). This result is opposite to that obtained using tetrabutyl ammonium salts as external co-catalysts and suggests that the mechanism is different for the two catalytic systems. Moreover, we observed an increase of the catalytic activity by enlarging the alkyl chain length (table 4, entry 3 and 4). Free porphyrins **87-90** are actually under investigation to synthesise corresponding ruthenium derivatives.

**Table 4.** Model reaction of 1-butyl-2-phenylaziridine and CO<sub>2</sub>.<sup>a</sup>

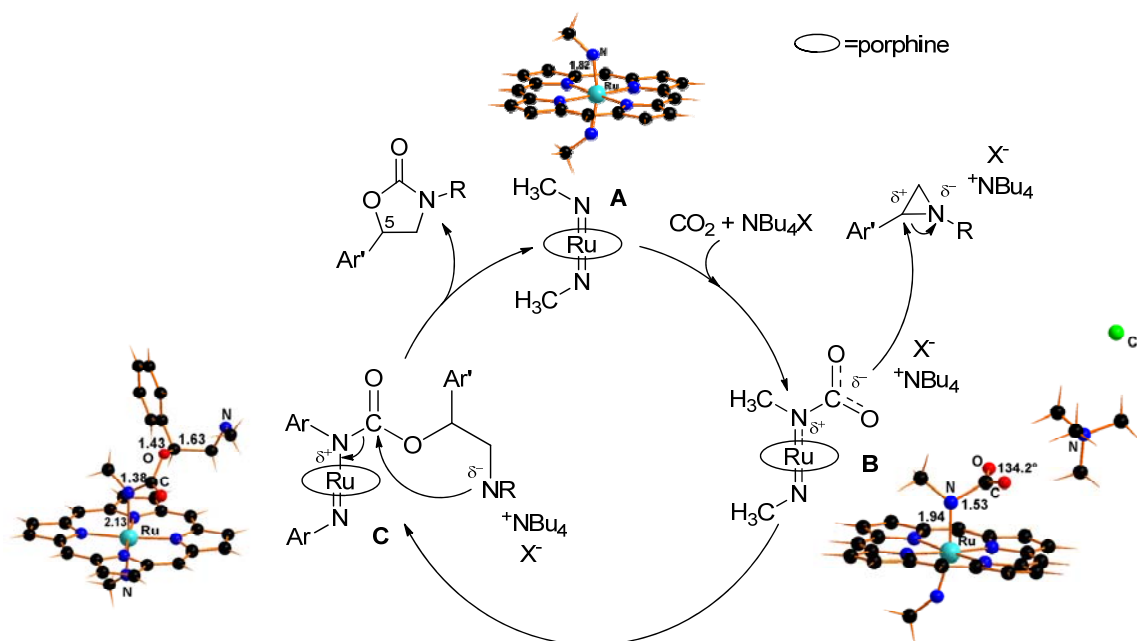


Entry	Catalyst	X <sup>-</sup>	yield (%) <sup>b</sup>	A/B <sup>b</sup>
1	<b>87</b>	Cl	Trace	-
2	<b>88</b>	Br	Trace	-
3	<b>89</b>	I	14	93:7
4	<b>90</b>	I	20	99:1

<sup>a</sup>Reaction conditions: cat./aziridine 1:100 in benzene. In a steel autoclave at 100°C and 6 bar CO<sub>2</sub> for 6 h. <sup>b</sup>Determined by <sup>1</sup>H NMR using 2,4-dinitrotoluene as the internal standard.

In collaboration with Dr. G. Manca and Dr. C. Mealli, who performed DFT studies by using a simplified model of our catalyst, we proposed the reaction mechanism which is reported in Scheme 41. The first step is the polarization of a molecule of carbon dioxide and the formation of intermediate **B** where carbon dioxide is bonded to the imido moiety of the catalyst. Then the intermediate **B** attacks the aziridine three-membered ring, in which bonds are polarized by the interaction with tetrabutyl ammonium salt, forming intermediate **C**.

Intermediate **C** undergoes a cyclization to give the 5-oxazolidinone as a product and regenerates the catalytic species **A**.



**Scheme 41.** Proposed mechanism for ruthenium porphyrin-catalysed aziridines/CO<sub>2</sub> coupling.

It is important to note that this is the first case where the first step of the catalytic cycle is the activation of CO<sub>2</sub> instead of the coordination of aziridine to the active metal centre. The formation of CO<sub>2</sub>/bis-imido complex, intermediate **B**, is supported by the isolation of the inactive species **94** which was analysed by MS spectroscopy (Figure 25). DFT studies indicate that the electron density of the N-imido atom is responsible for the CO<sub>2</sub> polarization which in turn can perform a nucleophilic attack to aziridine. It is important to underline the crucial role of the co-catalyst in activating aziridine towards the reaction with carbon dioxide.

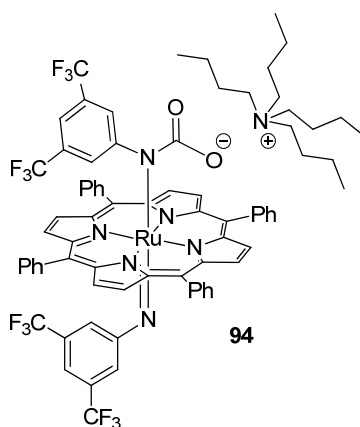


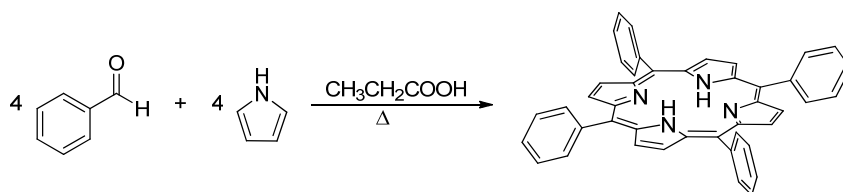
**Figure 25.** Structure of the inactive species **94**.

## 3. Experimental Section

**General conditions:** Unless otherwise specified, all reactions were carried out under nitrogen atmosphere employing standard Schlenk techniques and magnetic stirring. Dichloromethane, hexane, toluene, benzene, chloroform, acetone, trichlorobenzene, THF, DMF and alkenes were purified by using standard methods and stored under nitrogen atmosphere. Octaethylporphyrin and all other starting materials were commercial products used as received. NMR spectra were recorded at room temperature on a Bruker Avance 300-DRX, operating at 300 MHz for  $^1\text{H}$ , at 75 MHz for  $^{13}\text{C}$  and 282 MHz for  $^{19}\text{F}$ , or on a Bruker Avance 400-DRX spectrometer, operating at 400 MHz for  $^1\text{H}$ , at 100 MHz for  $^{13}\text{C}$  and at 376 MHz for  $^{19}\text{F}$ . Chemical shifts (ppm) are reported relative to TMS. The  $^1\text{H}$  NMR signals of the compounds described in the following were identified by 2 D NMR techniques. Assignments of the resonance in  $^{13}\text{C}$  NMR were made using the APT pulse sequence and HSQC and HMBC techniques. GC-MS analyses were performed on Shimadzu QP5050A instrument. Infrared spectra were recorded on a Varian Scimitar FTS 1000 spectrophotometer. UV/Vis spectra were recorded on an Agilent 8453E instrument. Elemental analyses and mass spectra were recorded in the analytical laboratories of Milan.

### 3.1. Synthesis of porphyrin ligands

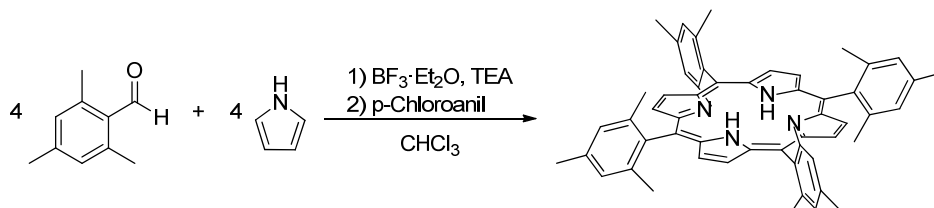
#### 3.1.1. Synthesis of *meso*-tetraphenyl porphyrin (TPPH<sub>2</sub>)



Reagent grade benzaldehyde (36.5 mL,  $3.60 \cdot 10^{-1}$  mol) was dissolved in propionic acid (500 mL) under air. The colourless mixture was heated to  $50^\circ\text{C}$ , then a solution of distilled pyrrole (25.0 mL,  $3.60 \cdot 10^{-1}$  mol) in propionic acid (30.0 mL) was added dropwise in about 10 minutes. The resulting mixture was refluxed for 30 minutes. During this period, the mixture turned to red at first, then to deep black. The reaction mixture was allowed to cool at RT and the formation of crystalline violet precipitate was observed. The dark suspension was filtered, washed with methanol (50.0 mL), water (50.0 mL) and again with methanol until the filtrate was clear. The crystalline purple solid was dried *in vacuo* (10.6 g, 19.2%).

$^1\text{H}$  NMR (300 MHz,  $\text{CDCl}_3$ ):  $\delta$  8.86 (s, 8H,  $\text{H}_\beta$ ), 8.22 (m, 8H,  $\text{H}_\alpha$ ), 7.78 (m, 12H,  $\text{H}_m$  and  $\text{H}_p$ ), -2.74 ppm (s, 2H,  $\text{NH}_{\text{pyr}}$ ). UV-Vis ( $\text{CH}_2\text{Cl}_2$ ):  $\lambda_{\text{max}}$  (log  $\epsilon$ ) 417 (5.66), 514 (4.30), 549 (3.91), 590 (3.73), 647 nm (3.74).

#### 3.1.2. Synthesis of *meso*-tetramesityl porphyrin (TMPH<sub>2</sub>)

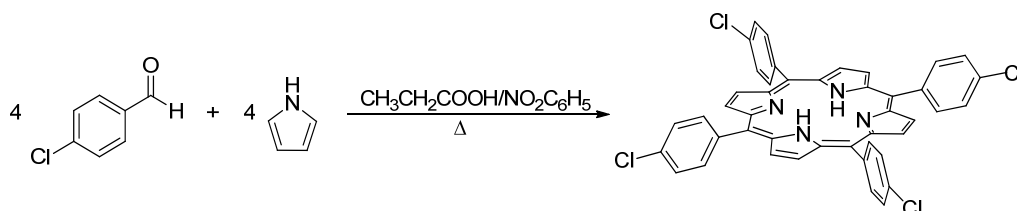


Mesityl benzaldehyde (0.110 mL,  $5.00 \cdot 10^{-3}$  mol) and distilled pyrrole (0.350 mL,  $5.00 \cdot 10^{-3}$  mol) were dissolved in dry chloroform (500 mL). The reaction mixture was shielded from light and  $\text{BF}_3 \cdot \text{O} \cdot \text{Et}_2$  (0.200 mL,  $2.26 \cdot 10^{-4}$  mol) was added by syringe. The pale orange solution was stirred at room temperature, under inert

atmosphere, for 3 hours then TEA (0.229 mL,  $1.65 \cdot 10^{-3}$  mol) was added to quench the reaction. Tetrachloro-1,4-benzoquinone (*p*-chloranil) (0.615 g,  $2.50 \cdot 10^{-3}$  mol) was added and the reaction was refluxed in air for 6 hours. The solvent was evaporated under reduced pressure and the resulting black solid was purified by flash chromatography giving the product (0.263 g, 26.9%) as a dark purple solid.

$^1\text{H NMR}$  (300 MHz,  $\text{CDCl}_3$ ):  $\delta$  8.61 (s, 8H,  $\text{H}_\beta$ ), 7.72 (m, 8H,  $\text{H}_m$ ), 2.26 (s, 12H,  $\text{H}_{\text{CH}_3\text{-para}}$ ), 1.85 (s, 12H,  $\text{H}_{\text{CH}_3\text{-ortho}}$ ), -2.51 ppm (s, 2H,  $\text{NH}_{\text{pyr}}$ ).

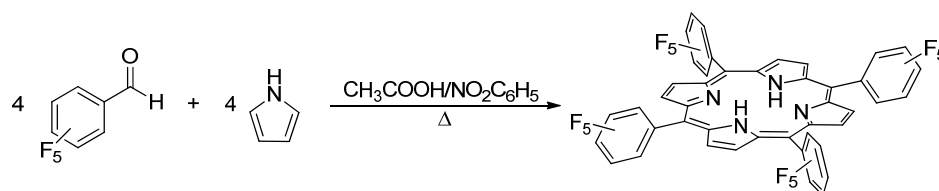
### 3.1.3. Synthesis of *meso*-tetra(4-chlorophenyl) porphyrin (4-CITPPH<sub>2</sub>)



In a pre-heated (140°C) solution of propionic acid (45.0 mL) and nitrobenzene (42.0 mL), a solution of 4-chlorobenzaldehyde (1.43 g,  $1.02 \cdot 10^{-2}$  mol) and distilled pyrrole (0.707 mL,  $1.02 \cdot 10^{-2}$  mol) in propionic acid (7.00 mL) was added dropwise. The reaction was refluxed in air for 1 hour. During this period, the mixture turned to yellow at first, then to deep black. The reaction mixture was allowed to cool at RT and the formation of crystalline violet precipitate was observed. The dark suspension was filtered, washed with water (30.0 mL) and with methanol (15.0 mL) until the filtrate was clear. The crystalline purple solid was dried *in vacuo* (0.375 g, 19.5%).

$^1\text{H NMR}$  (300 MHz,  $\text{CDCl}_3$ ):  $\delta$  8.85 (s, 8H,  $\text{H}_\beta$ ), 8.14 (m, 8H,  $\text{H}_m$ ), 7.75 (m, 8H,  $\text{H}_o$ ), -2.95 ppm (s, 2H,  $\text{NH}_{\text{pyr}}$ ).

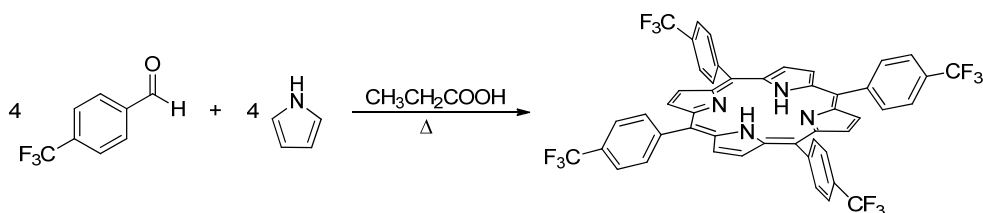
### 3.1.4. Synthesis of *meso*-tetra(pentafluorophenyl) porphyrin (F<sub>20</sub>TPPH<sub>2</sub>)



Pentafluorobenzaldehyde (1.81 g,  $9.20 \cdot 10^{-3}$  mol) was dissolved in a mixture of glacial acetic acid (60.0 mL) and nitrobenzene (50.0 mL). The solution was heated to 50°C then a solution of pyrrole (0.638 mL,  $9.20 \cdot 10^{-2}$  mol) in acetic acid was added dropwise and the obtained mixture was refluxed for 2 hours. The solvent was evaporated under reduced pressure giving a black tar which was purified by chromatography (alumina 0.063-0.200  $\mu\text{m}$ , hexane/ $\text{CH}_2\text{Cl}_2$  100:2). The porphyrin fraction was evaporated to dryness and dried *in vacuo* (0.249 g, 11.1%).

$^1\text{H NMR}$  (300 MHz,  $\text{CDCl}_3$ ):  $\delta$  8.92 (s, 8H,  $\text{H}_\beta$ ), -2.90 ppm (s, 2H,  $\text{NH}_{\text{pyr}}$ ).  $^{19}\text{F NMR}$  (282 MHz,  $\text{CDCl}_3$ ):  $\delta$  -136.8 (dd, 8F,  $J_{\text{FF}}=23.6$  Hz,  $^4J_{\text{FF}}=6.6$  Hz,  $\text{F}_o$ ), -151.53 (t, 4F,  $J_{\text{FF}}=21.0$  Hz,  $\text{F}_p$ ), -161.71 ppm (td, 8F,  $J_{\text{FF}}=23.6$  Hz,  $^4J_{\text{FF}}=8.3$  Hz,  $\text{F}_m$ ). **UV-Vis** ( $\text{CH}_2\text{Cl}_2$ ):  $\lambda_{\text{max}}$  (log  $\epsilon$ ) 411 (7.43), 506 (6.32), 582 (5.83), 637, 658 nm.

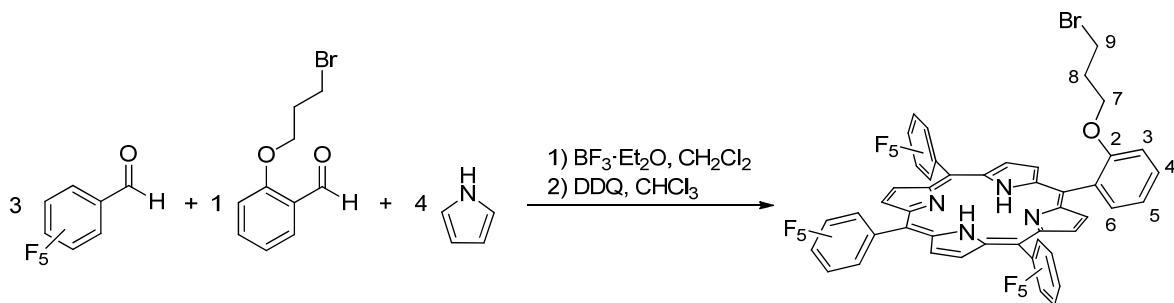
### 3.1.5. Synthesis of *meso*-tetra(4-(trifluoromethyl)phenyl) porphyrin (4-CF<sub>3</sub>TPPH<sub>2</sub>)



4-(Trifluoromethyl)benzaldehyde (4.50 mL,  $3.30 \cdot 10^{-2}$  mol) was dissolved in propionic acid (100 mL) and the colourless solution was heated to 50°C. Then a solution of distilled pyrrole (2.50 mL,  $3.60 \cdot 10^{-3}$  mol) in 30.0 mL of propionic acid was added dropwise in about 10 minutes. The resulting mixture was refluxed in air for 30 minutes during which the mixture turned to deep black. The reaction was allowed to cool at room temperature and the formation of a crystalline violet precipitate was observed. The dark suspension was filtered, washed with water (10.0 mL) and methanol until the filtrate was clear. The crystalline purple was dried *in vacuo* (1.56 g, 21.4%).

<sup>1</sup>H NMR (300 MHz, CDCl<sub>3</sub>):  $\delta$  8.82 (s, 8H, H <sub>$\beta$</sub> ), 8.34 (d, 8H,  $J=8.1$  Hz, H <sub>$\alpha$</sub> ), 8.05 (d, 8H,  $J=8.1$  Hz, H <sub>$m$</sub> ), -2.95 ppm (s, 2H, NH<sub>pyr</sub>).

### 3.1.6. Synthesis of 5-(2-(3-bromopropoxy)phenyl)-10,15,20-tri(pentafluorophenyl) porphyrin (A<sub>3</sub>B-Br)

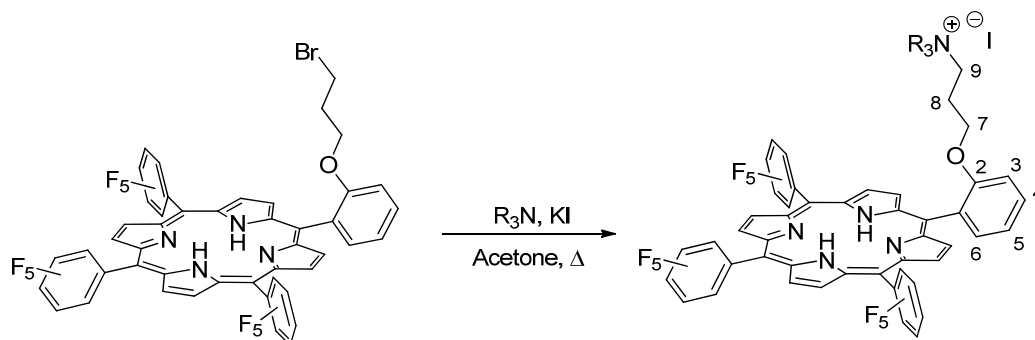


Pentafluorobenzaldehyde (0.467 mL,  $3.78 \cdot 10^{-3}$  mol), 2-(3-bromopropoxy)benzaldehyde (0.220 mL,  $1.29 \cdot 10^{-3}$  mol) and distilled pyrrole (0.350 mL,  $5.05 \cdot 10^{-3}$  mol) were dissolved in dichloromethane (500 mL) under inert atmosphere. The reaction mixture was shielded from ambient light and BF<sub>3</sub>O·Et<sub>2</sub> (64.0  $\mu$ L,  $5.09 \cdot 10^{-4}$  mol) was added by syringe. The pale orange solution was stirred at room temperature overnight, then TEA (6.90  $\mu$ L,  $4.96 \cdot 10^{-4}$  mol) was added to quench the reaction and dichloromethane was removed under reduced pressure. The crude was recovered with chloroform (100 mL) and 2,3-dichloro-5,6-dicyano-1,4-benzoquinone (DDQ) (0.576 g,  $4.96 \cdot 10^{-4}$  mol) was added. The reaction mixture was refluxed in air for 2 hours. After that the solvent was evaporated under reduced pressure to obtain a dark solid which was purified by flash chromatography (silica gel, 60  $\mu$ m, hexane/CH<sub>2</sub>Cl<sub>2</sub> 90:10) giving porphyrin A<sub>3</sub>B-Br (0.389 g, 15%) as a purple solid.

<sup>1</sup>H NMR (300 MHz, CDCl<sub>3</sub>):  $\delta$  8.97 (d, 2H,  $J=4.8$  Hz, H <sub>$\beta$</sub> ), 8.91 (s, 4H, H <sub>$\beta$</sub> ), 8.82 (d, 2H,  $J=4.7$  Hz, H <sub>$\beta$</sub> ), 8.08 (dd, 1H,  $J=7.4, 1.5$  Hz, H<sup>3</sup>), 7.83 (td, 1H,  $J=8.3, 1.6$  Hz, H<sup>5</sup>), 7.44 (t, 1H,  $J=7.5$  Hz, H<sup>4</sup>), 7.38 (d, 1H,  $J=8.3$  Hz, H<sup>6</sup>), 4.10 (t, 2H,  $J=5.4$  Hz, H<sup>7</sup>), 2.26 (t, 2H,  $J=6.0$  Hz, H<sup>8</sup>), 1.51-1.41 (m, 2H, H<sup>9</sup>), -2.81 (s, 2H, NH<sub>pyr</sub>). <sup>13</sup>C NMR (75 MHz, CDCl<sub>3</sub>):  $\delta$  158.3, 147.8, 145.4, 143.4, 140.9, 138.8, 136.3, 135.6, 130.6, 129.7, 119.9, 119.4, 116.0, 117.7, 102.7, 101.9, 65.1, 31.3, 29.7 ppm. Six quaternary carbon atoms were not detected. <sup>19</sup>F NMR (282 MHz, CDCl<sub>3</sub>):  $\delta$  -136.9 (m, 6F, F <sub>$\alpha$</sub> ), -152.1 (m, 3F, F <sub>$\beta$</sub> ), -162.0 ppm (m, 6F, F <sub>$m$</sub> ). IR (CH<sub>2</sub>Cl<sub>2</sub>):  $\nu_{\max}$  = 1499

(w), 1518 (w), 1604 (w), 2928 (w), 3322 (w), 3684  $\text{cm}^{-1}$  (w). **UV-Vis** (MeOH):  $\lambda_{\text{max}}$  (log  $\epsilon$ ) 410 (5.39), 506 (4.47), 536 (3.61), 582 (3.98), 643 nm (3.15). **Elemental Analysis** calcd. for  $\text{C}_{47}\text{H}_{20}\text{BrF}_{15}\text{N}_4\text{O}$ : C, 55.26; H, 1.97; N, 5.48. Found: C, 55.66; H, 2.11; N, 5.31. **MS** (ESI):  $m/z=1021.06$  [ $\text{M}+\text{H}^+$ ].

### 3.1.7. Synthesis of 5-(2-(3-(R)<sub>3</sub>ammoniopropoxy)phenyl)-10,15,20-tris(pentafluorophenyl) porphyrin iodide (**A<sub>3</sub>B-NR<sub>3</sub>**)<sup>+</sup>X<sup>-</sup>:



Porphyrin **A<sub>3</sub>B-Br** (0.260 g,  $2.55 \cdot 10^{-4}$  mol) was dissolved in dry acetone (30.0 mL) and the desired amine ( $2.55 \cdot 10^{-3}$  mol) and potassium iodide (0.422 g,  $2.55 \cdot 10^{-3}$  mol) were added. The dark brown mixture was refluxed for 6 hours. The solvent was removed under reduced pressure and the resulting solid was purified by flash chromatography (silica gel, 60  $\mu\text{m}$ , 3% MeOH in  $\text{CH}_2\text{Cl}_2$ ) giving porphyrin as a dark red solid.

**5-(2-(3-triethylammoniopropoxy)phenyl)-10,15,20-tris(pentafluorophenyl)porphyrin chloride (**A<sub>3</sub>B-NEt<sub>3</sub>**)<sup>+</sup>Cl<sup>-</sup> (**87**)** (53% yield). **<sup>1</sup>H NMR** (300 MHz,  $\text{CDCl}_3$ ):  $\delta$  8.95 (d, 2H,  $J=5.0$  Hz,  $\text{H}_\beta$ ), 8.93 (s, 4H,  $\text{H}_\beta$ ), 8.87 (d, 2H,  $J=4.5$  Hz,  $\text{H}_\beta$ ), 8.20 (dd, 1H,  $J=7.4, 1.5$  Hz,  $\text{H}^3$ ), 7.84 (td, 1H,  $J=8.2, 1.5$  Hz,  $\text{H}^5$ ), 7.52 (t, 1H,  $J=7.3$  Hz,  $\text{H}^4$ ), 7.35 (d, 1H,  $J=8.2$  Hz,  $\text{H}^6$ ), 3.94 (t, 2H,  $J=4.9$  Hz,  $\text{H}^7$ ), 1.24-1.20 (m, 2H,  $\text{H}^8$ ), 0.95 (m, 6H,  $\text{H}_{\text{CH}_2}$ ), 0.63-0.57 (m, 2H,  $\text{H}^9$ ), -1.28 (t, 9H,  $J=7.0$  Hz,  $\text{H}_{\text{CH}_3}$ ), -2.96 ppm (s, 2H,  $\text{NH}_{\text{pyr}}$ ). **<sup>13</sup>C NMR** (75 MHz,  $\text{CDCl}_3$ ):  $\delta$  158.3, 148.3, 144.9, 133.9, 131.4, 130.4, 121.4, 119.6, 114.2, 103.2, 102.6, 65.6, 52.5, 51.2, 22.0, 5.0 ppm. **<sup>19</sup>F NMR** (282 MHz,  $\text{CDCl}_3$ ):  $\delta$  -136.7 (m, 3F,  $\text{F}_o$ ), -137.7 (m, 1F,  $\text{F}_o$ ), -138.6 (m, 2F,  $\text{F}_o$ ), -150.8 (t, 2F,  $J_{\text{FF}}=21.0$ ,  $\text{F}_p$ ), -151.0 (t, 1F,  $J_{\text{FF}}=20.9$  Hz,  $\text{F}_p$ ), -160.9 (m, 2F,  $\text{F}_m$ ), -161.1 (m, 3F,  $\text{F}_m$ ), -161.3 ppm (m, 1F,  $\text{F}_m$ ). **IR** ( $\text{CH}_2\text{Cl}_2$ ):  $\nu_{\text{max}}$  = 1498 (w), 1519 (w), 1603 (w), 1711 (w), 2959 (w), 3040 (w), 3320 (w), 3683  $\text{cm}^{-1}$  (w). **UV-Vis** (MeOH):  $\lambda_{\text{max}}$  (log  $\epsilon$ ) 409 (5.49), 505 (4.27), 535 (3.39), 580 (3.76), 635 nm (2.96). **UV-Vis** ( $\text{CH}_2\text{Cl}_2$ ):  $\lambda_{\text{max}}$  (log  $\epsilon$ ) 413 (5.49), 507 (4.28), 536 (3.47), 583 (3.80), 636 nm (3.14). **Elemental Analysis** calcd. for  $\text{C}_{53}\text{H}_{35}\text{F}_{15}\text{N}_5\text{O}$ : C, 54.42; H, 3.02; N, 5.99. Found: C, 54.23; H, 3.11; N, 6.06. **MS** (ESI):  $m/z=1042.4$  [ $\text{M}$ ]<sup>+</sup>, 34.97 [ $\text{X}$ ].

**5-(2-(3-triethylammoniopropoxy)phenyl)-10,15,20-tris(pentafluorophenyl)porphyrin bromide (**A<sub>3</sub>B-NEt<sub>3</sub>**)<sup>+</sup>Br<sup>-</sup> (**88**)** (51% yield). **<sup>1</sup>H NMR** (300 MHz,  $\text{CDCl}_3$ ):  $\delta$  8.95 (d, 2H,  $J=5.0$  Hz,  $\text{H}_\beta$ ), 8.93 (s, 4H,  $\text{H}_\beta$ ), 8.87 (d, 2H,  $J=4.5$  Hz,  $\text{H}_\beta$ ), 8.20 (dd, 1H,  $J=7.4, 1.5$  Hz,  $\text{H}^3$ ), 7.84 (td, 1H,  $J=8.2, 1.5$  Hz,  $\text{H}^5$ ), 7.52 (t, 1H,  $J=7.3$  Hz,  $\text{H}^4$ ), 7.35 (d, 1H,  $J=8.2$  Hz,  $\text{H}^6$ ), 3.94 (t, 2H,  $J=4.9$  Hz,  $\text{H}^7$ ), 1.24-1.20 (m, 2H,  $\text{H}^8$ ), 0.95 (m, 6H,  $\text{H}_{\text{CH}_2}$ ), 0.63-0.57 (m, 2H,  $\text{H}^9$ ), -1.28 (t, 9H,  $J=7.0$  Hz,  $\text{H}_{\text{CH}_3}$ ), -2.96 ppm (s, 2H,  $\text{NH}_{\text{pyr}}$ ). **<sup>13</sup>C NMR** (75 MHz,  $\text{CDCl}_3$ ):  $\delta$  158.3, 148.3, 144.9, 133.9, 131.4, 130.4, 121.4, 119.6, 114.2, 103.2, 102.6, 65.6, 52.5, 51.2, 22.0, 5.0 ppm. **<sup>19</sup>F NMR** (282 MHz,  $\text{CDCl}_3$ ):  $\delta$  -136.7 (m, 3F,  $\text{F}_o$ ), -137.7 (m, 1F,  $\text{F}_o$ ), -138.6 (m, 2F,  $\text{F}_o$ ), -150.8 (t, 2F,  $J_{\text{FF}}=21.0$ ,  $\text{F}_p$ ), -151.0 (t, 1F,  $J_{\text{FF}}=20.9$  Hz,  $\text{F}_p$ ), -160.9 (m, 2F,  $\text{F}_m$ ), -161.1 (m, 3F,  $\text{F}_m$ ), -161.3 ppm (m, 1F,  $\text{F}_m$ ). **IR** ( $\text{CH}_2\text{Cl}_2$ ):  $\nu_{\text{max}}$  = 1498 (w), 1519 (w), 1603 (w), 1711 (w), 2959 (w), 3040 (w), 3320 (w), 3683  $\text{cm}^{-1}$  (w).

**UV-Vis** (MeOH):  $\lambda_{\max}$  (log  $\epsilon$ ) 409 (5.49), 505 (4.27), 535 (3.39), 580 (3.76), 635 nm (2.96). **UV-Vis** (CH<sub>2</sub>Cl<sub>2</sub>):  $\lambda_{\max}$  (log  $\epsilon$ ) 413 (5.49), 507 (4.28), 536 (3.47), 583 (3.80), 636 nm (3.14). **Elemental Analysis** calcd. for C<sub>53</sub>H<sub>35</sub>F<sub>15</sub>IN<sub>5</sub>O: C, 54.42; H, 3.02; N, 5.99. Found: C, 54.23; H, 3.11; N, 6.06. **MS** (ESI):  $m/z=1042.4$  [M]<sup>+</sup>, 78.92 [X<sup>-</sup>].

**5-(2-(3-triethylammoniopropoxy)phenyl)-10,15,20-tris(pentafluorophenyl)porphyrin iodide (A<sub>3</sub>B-NEt<sub>3</sub>)<sup>+</sup>I<sup>-</sup> (89)** (53% yield). **<sup>1</sup>H NMR** (300 MHz, CDCl<sub>3</sub>):  $\delta$  8.95 (d, 2H,  $J=5.0$  Hz, H <sub>$\beta$</sub> ), 8.93 (s, 4H, H <sub>$\beta$</sub> ), 8.87 (d, 2H,  $J=4.5$  Hz, H <sub>$\beta$</sub> ), 8.20 (dd, 1H,  $J=7.4, 1.5$  Hz, H<sup>3</sup>), 7.84 (td, 1H,  $J=8.2, 1.5$  Hz, H<sup>5</sup>), 7.52 (t, 1H,  $J=7.3$  Hz, H<sup>4</sup>), 7.35 (d, 1H,  $J=8.2$  Hz, H<sup>6</sup>), 3.94 (t, 2H,  $J=4.9$  Hz, H<sup>7</sup>), 1.24-1.20 (m, 2H, H<sup>8</sup>), 0.95 (m, 6H, H<sub>CH<sub>2</sub></sub>), 0.63-0.57 (m, 2H, H<sup>9</sup>), -1.28 (t, 9H,  $J=7.0$  Hz, H<sub>CH<sub>3</sub></sub>), -2.96 ppm (s, 2H, NH<sub>pyr</sub>). **<sup>13</sup>C NMR** (75 MHz, CDCl<sub>3</sub>):  $\delta$  158.3, 148.3, 144.9, 133.9, 131.4, 130.4, 121.4, 119.6, 114.2, 103.2, 102.6, 65.6, 52.5, 51.2, 22.0, 5.0 ppm. **<sup>19</sup>F NMR** (282 MHz, CDCl<sub>3</sub>):  $\delta$  -136.7 (m, 3F, F<sub>o</sub>), -137.7 (m, 1F, F<sub>o</sub>), -138.6 (m, 2F, F<sub>o</sub>), -150.8 (t, 2F,  $J_{\text{FF}}=21.0$ , F<sub>p</sub>), -151.0 (t, 1F,  $J_{\text{FF}}=20.9$  Hz, F<sub>p</sub>), -160.9 (m, 2F, F<sub>m</sub>), -161.1 (m, 3F, F<sub>m</sub>), -161.3 ppm (m, 1F, F<sub>m</sub>). **IR** (CH<sub>2</sub>Cl<sub>2</sub>):  $\nu_{\max}$  = 1498 (w), 1519 (w), 1603 (w), 1711 (w), 2959 (w), 3040 (w), 3320 (w), 3683 cm<sup>-1</sup> (w). **UV-Vis** (MeOH):  $\lambda_{\max}$  (log  $\epsilon$ ) 409 (5.49), 505 (4.27), 535 (3.39), 580 (3.76), 635 nm (2.96). **UV-Vis** (CH<sub>2</sub>Cl<sub>2</sub>):  $\lambda_{\max}$  (log  $\epsilon$ ) 413 (5.49), 507 (4.28), 536 (3.47), 583 (3.80), 636 nm (3.14). **Elemental Analysis** calcd. for C<sub>53</sub>H<sub>35</sub>F<sub>15</sub>IN<sub>5</sub>O: C, 54.42; H, 3.02; N, 5.99. Found: C, 54.23; H, 3.11; N, 6.06. **MS** (ESI):  $m/z=1042.4$  [M]<sup>+</sup>, 126.90 [X<sup>-</sup>].

**5-(2-(3-trihexylammoniopropoxy)phenyl)-10,15,20-tris(pentafluorophenyl)porphyrin iodide (A<sub>3</sub>B-NHex<sub>3</sub>)<sup>+</sup>I<sup>-</sup> (90)** (63% yield): **<sup>1</sup>H NMR** (400 MHz, CDCl<sub>3</sub>):  $\delta$  8.98 (d, 2H,  $J=4.4$  Hz, H <sub>$\beta$</sub> ), 8.90 (s, 4H, H <sub>$\beta$</sub> ), 8.84 (d, 2H,  $J=4.2$  Hz, H <sub>$\beta$</sub> ), 7.94 (dd, 1H,  $J=7.2, 1.1$  Hz, H<sup>3</sup>), 7.84 (t, 1H,  $J=7.4$  Hz, H<sup>5</sup>), 7.45 (d, 1H,  $J=8.4$  Hz, H<sup>6</sup>), 7.43 (td, 1H,  $J=7.4, 1.3$  Hz, H<sup>5</sup>), 4.29-4.23 (m, 2H, H<sup>7</sup>), 2.20-2.16 (m, 2H, H<sup>9</sup>), 1.85-1.80 (m, 6H, H<sub>NCH<sub>2</sub></sub>), 1.56 (2H, H<sup>8</sup>, overlap of solvent signal), 0.33 (d, 9H,  $J=2.6$  Hz, H<sub>CH<sub>3</sub></sub>), 0.33-0.28 (m, 6H, H<sub>CH<sub>2</sub></sub>), 0.045-0.015 (m, 6H, H<sub>CH<sub>2</sub></sub>), -0.20 (m, 6H, H<sub>CH<sub>2</sub></sub>), -0.32 (m, 6H, H<sub>CH<sub>2</sub></sub>), -2.88 ppm (s, 2H, NH<sub>pyr</sub>). **<sup>13</sup>C NMR** (100 MHz, CDCl<sub>3</sub>):  $\delta$  157.8, 135.4, 131.7, 129.1, 120.8, 112.9, 64.8, 57.9, 55.2, 30.1, 24.5, 22.7, 21.6, 20.3, 13.3 ppm. **<sup>19</sup>F NMR** (376 MHz, CDCl<sub>3</sub>):  $\delta$  -136.6 (m, 3F, F<sub>o</sub>), -137.8 (m, 1F, F<sub>o</sub>), 138.3 (m, 2F, F<sub>o</sub>), -151.1 (t, 2F,  $J_{\text{FF}}=20.9$  Hz, F<sub>p</sub>), -151.4 (t, 1F,  $J_{\text{FF}}=20.9$  Hz, F<sub>p</sub>), -160.9 (m, 2F, F<sub>m</sub>), -161.3 (m, 1F, F<sub>m</sub>), -161.5 (m, 2F, F<sub>m</sub>), -161.8 ppm (m, 1F, F<sub>m</sub>). **IR** (CH<sub>2</sub>Cl<sub>2</sub>):  $\nu_{\max}$  = 3322 (w), 3058 (w), 2986 (w), 2961 (w), 2931 (w), 2874 (w), 2860 (w), 1650 (w), 1518 (w), 1499 (w), 1482 (w), 1266 (w), 989 (w) cm<sup>-1</sup>. **IR** (ATR):  $\nu_{\max}$  = 3321 (w), 2958 (w), 2923 (w), 2855 (w), 1727 (w), 1652 (w), 1516 (w), 1495 (w), 1398 (w), 1342 (w), 1259 (w), 1039 (w), 1023 (w), 984 (w), 916 (w), 800 (w), 753 (w), 724 (w) cm<sup>-1</sup>. **UV-Vis** (CH<sub>2</sub>Cl<sub>2</sub>):  $\lambda_{\max}$  (log  $\epsilon$ ) 414 (6.27), 507 (5.10), 583 (4.63), 638 (3.49) nm. **Elemental Analysis** calcd. for C<sub>65</sub>H<sub>59</sub>F<sub>15</sub>IN<sub>5</sub>O: C, 58.34; H, 4.44; N, 5.23. Found: C, 58.40; H, 4.48; N, 5.20. **MS** (ESI):  $m/z=1210.5$  [M]<sup>+</sup>, 126.90 [X<sup>-</sup>].

## 3.2. Synthesis of ruthenium porphyrin complexes

### 3.2.1. Synthesis of Ru<sub>3</sub>(CO)<sub>12</sub>



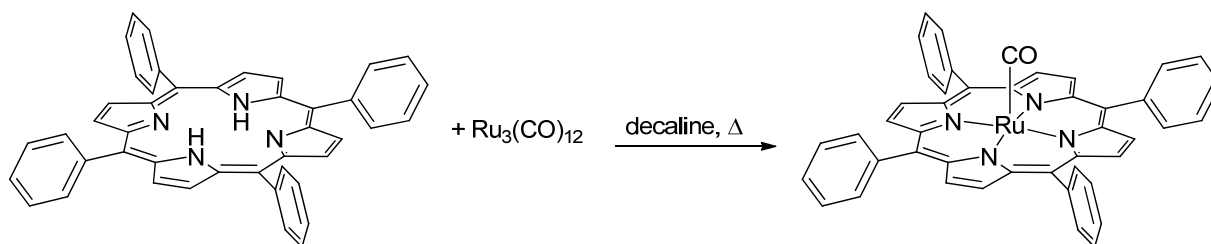
Trihydrate ruthenium trichloride (1.24 g, 4.80·10<sup>-3</sup> mol) was dissolved in methanol (30.0 mL), inside a 100 mL glass liner equipped with a screw cap and a glass wool. The dark mixture was cooled with liquid nitrogen and the flask was transferred into a stainless-steel autoclave, three vacuum-nitrogen cycles were performed



and CO (60 bar) was charged at room temperature. The autoclave was placed in a preheated oil bath at 120 °C and stirred for 8 hours, then it was cooled at room temperature and slowly vented. The obtained orange suspension was filtered, the solid was dissolved in THF and purified by filtration in continuous on a celite pad. The solvent was evaporated to dryness and an orange crystalline solid was obtained (0.736 g, 73%) The mother liquors of the filtration were collected and stored at 4°C to be used as solvent for the subsequent Ru<sub>3</sub>(CO)<sub>12</sub> synthesis (the same methanol solution was re-used maximum twice).

**IR** (nujol):  $\nu = 2059.7, 2015.4, 1996.6 \text{ cm}^{-1}$ . **Elemental Analysis** calcd. for C<sub>12</sub>O<sub>12</sub>Ru<sub>3</sub>: C, 22.54. Found: C, 23.01.

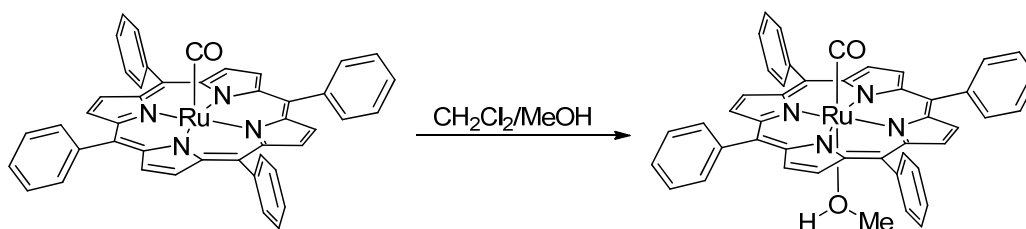
### 3.2.2. Synthesis of Ru(TPP)(CO)



Ru<sub>3</sub>(CO)<sub>12</sub> (0.626 g, 9.80·10<sup>-1</sup> mol) and TPPH<sub>2</sub> (1.23 g, 2.00·10<sup>-3</sup> mol) were suspended in dry decalin (60.0 mL). The reaction mixture was refluxed for 7 hours, cooled at room temperature and the precipitate was collected and washed three times with hexane (10.0 mL). The violet solid was then purified by flash chromatography (silica gel, 60 μm, starting from hexane/CH<sub>2</sub>Cl<sub>2</sub> 8:2 to CH<sub>2</sub>Cl<sub>2</sub>). The Ru(TPP)CO fraction was evaporated to dryness and dried *in vacuo* at 120°C. The product was obtained as a purple crystalline solid (1.09 g, 73%).

<sup>1</sup>H NMR (300 MHz, CDCl<sub>3</sub>):  $\delta$  8.68 (s, 8H, H<sub>β</sub>), 8.22 (m, 4H, H<sub>o</sub>), 8.11 (m, 4H, H<sub>o</sub>), 7.73 ppm (m, 12H, H<sub>m</sub> and H<sub>p</sub>). **IR** (ATR):  $\nu_{\text{CO}} = 1956 \text{ cm}^{-1}$ .

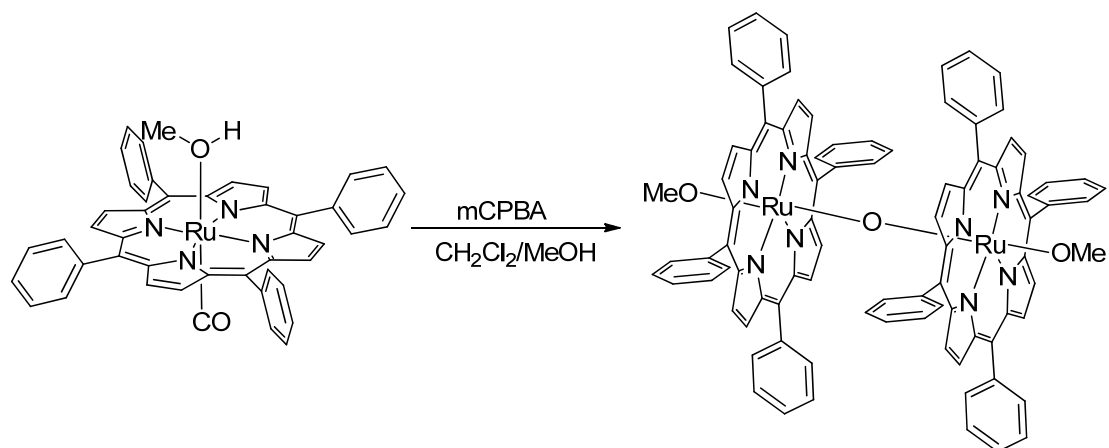
### 3.2.3. Synthesis of Ru(TPP)(CO)(MeOH)



Ru(TPP)CO (0.767 g, 1.00·10<sup>-3</sup> mol) was suspended in 33.0 mL of mixture CH<sub>2</sub>Cl<sub>2</sub>/MeOH 1:2 and refluxed for 3 hours. The reaction was followed by IR spectroscopy. The orange precipitate was filtered and dried *in vacuo* at room temperature (0.751 g, 94%).

<sup>1</sup>H NMR (300 MHz, CDCl<sub>3</sub>):  $\delta$  8.71 (s, 8H, H<sub>β</sub>), 8.21 (m, 8H, H<sub>o</sub>), 7.74 ppm (m, 12H, H<sub>m</sub> and H<sub>p</sub>). **IR** (nujol):  $\nu_{\text{CO}} = 1939 \text{ cm}^{-1}$ .

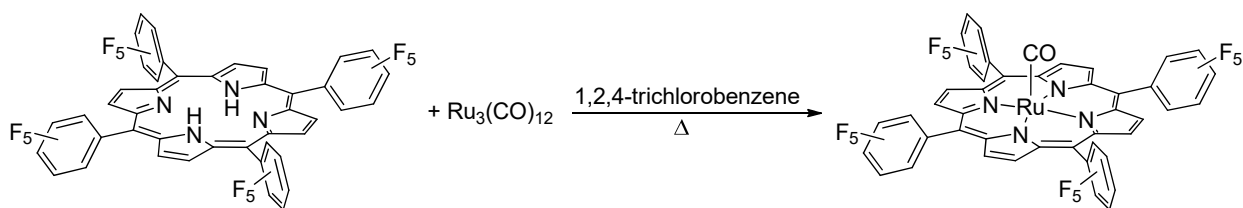
### 3.2.4. Synthesis of [Ru(TPP)(OMe)]<sub>2</sub>O



The synthesis was performed under air. Ru(TPP)(CO)(MeOH) (0.103 g,  $1.30 \cdot 10^{-4}$  mol) was suspended in CH<sub>2</sub>Cl<sub>2</sub> (20.0 mL) and a solution of 3-Chloroperbenzoic acid (*m*CPBA) (0.137 g,  $8.00 \cdot 10^{-4}$  mol) in CH<sub>2</sub>Cl<sub>2</sub> (30.0 mL) and MeOH (3.00 mL) was added dropwise in 40 minutes. The initial red suspension turned into a dark red solution. The reaction was monitored by TLC (5% MeOH in CH<sub>2</sub>Cl<sub>2</sub>). After 5 hours, an additional amount of *m*CPBA (45.0 mg,  $2.60 \cdot 10^{-4}$  mol) was added and the solution was stirred overnight. Then the solution was washed with a saturated solution of NaHCO<sub>3</sub> (four times with 50.0 mL), dried over Na<sub>2</sub>SO<sub>4</sub> and the solvent was evaporated under reduced pressure. The solid was purified by chromatography (alumina 0.063-0.200 μm, 4% MeOH in CH<sub>2</sub>Cl<sub>2</sub>) giving the product as a dark violet crystalline solid (80.0 mg, 81%).

<sup>1</sup>H NMR (400 MHz, CDCl<sub>3</sub>): δ 9.18 (d, 8H, *J*=7.5 Hz, H<sub>o</sub>), 8.70 (s, 16H, H<sub>β</sub>), 7.86 (t, 8H, *J*=7.5 Hz, H<sub>m</sub>), 7.60 (t, 8H, *J*=6.9 Hz, H<sub>p</sub>), 7.26 (m, 16H, H<sub>m</sub> and H<sub>o</sub>), -3.22 ppm (s, 6H, H<sub>CH3</sub>). IR (nujol): ν<sub>(oxidation marker band)</sub> = 1012 cm<sup>-1</sup>.

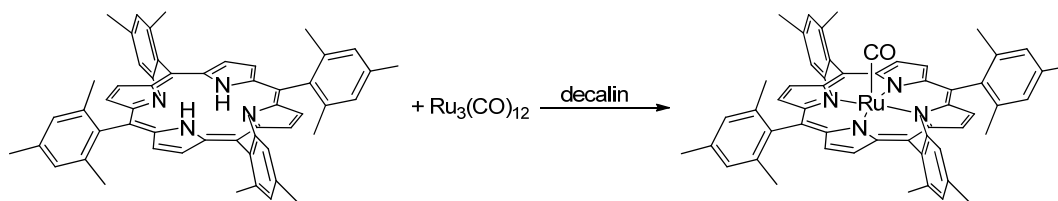
### 3.2.5. Synthesis of Ru(F<sub>20</sub>TPP)(CO)



F<sub>20</sub>TPPH<sub>2</sub> (0.130 g,  $1.30 \cdot 10^{-4}$  mol) and Ru<sub>3</sub>(CO)<sub>12</sub> (85.0 mg,  $1.30 \cdot 10^{-4}$  mol) were dissolved in trichlorobenzene (20.0 mL). The mixture was refluxed for 6 hours, then the solvent was evaporated to dryness. The crude was purified by chromatography (alumina 0.063-0.200 μm, starting from hexane/CH<sub>2</sub>Cl<sub>2</sub> 1:1 to CH<sub>2</sub>Cl<sub>2</sub>/acetone 1:1). The product was dried *in vacuo* to give a red solid (0.115 g, 78%).

<sup>1</sup>H NMR (300 MHz, CDCl<sub>3</sub>): δ 8.71 ppm (s, 8H, H<sub>β</sub>). <sup>19</sup>F NMR (282 MHz, CDCl<sub>3</sub>): δ -136.0 (d, 2F, *J*<sub>FF</sub>=23.4 Hz), -137.6 (d, 2F, *J*<sub>FF</sub>=20.3 Hz), -152.0 (t, 1F, *J*<sub>FF</sub>=20.0 Hz), -161.4 (m, 2F), -162.0 ppm (m, 2F).

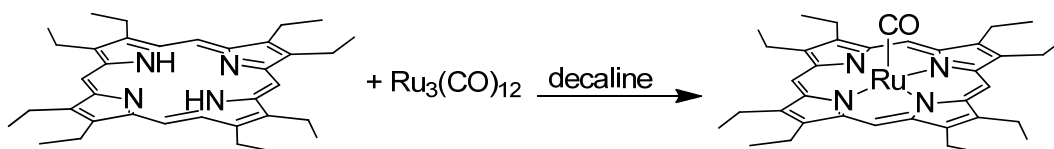
### 3.2.6. Synthesis of Ru(TMP)(CO)



$\text{Ru}_3(\text{CO})_{12}$  (50.0 mg,  $6.38 \cdot 10^{-5}$  mol) and  $\text{TMPH}_2$  (59.0 g,  $9.22 \cdot 10^{-5}$  mol) were suspended in dry decalin and the reaction mixture was refluxed for 4 hours. During the reaction, a purple solid precipitated and it was collected and washed three times with hexane (10.0 mL). The violet solid was then purified by flash chromatography (silica gel, 60  $\mu\text{m}$ , starting from hexane/ $\text{CH}_2\text{Cl}_2$  8:2 + 2% of ethyl acetate). The product was obtained as a purple crystalline solid (27.0 mg, 47%).

$^1\text{H NMR}$  (300 MHz,  $\text{CDCl}_3$ ):  $\delta$  8.50 (s, 8H,  $\text{H}_\beta$ ), 7.27 (s, 8H,  $\text{H}_m$ ), 2.63 (s, 12H,  $\text{H}_{\text{CH}_3\text{-para}}$ ), 1.90 ppm (s, 24H,  $\text{H}_{\text{CH}_3\text{-ortho}}$ ). **IR** (nujol):  $\nu_{\text{CO}} = 1932 \text{ cm}^{-1}$ .

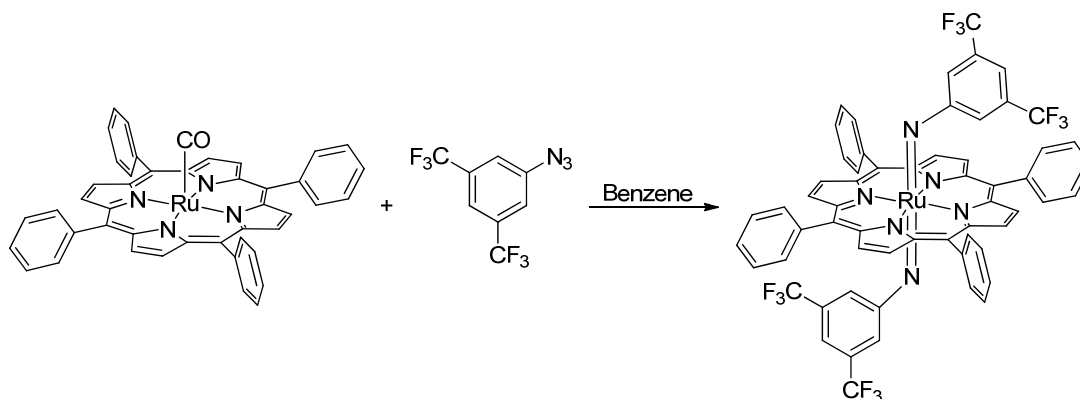
### 3.2.7. Synthesis of Ru(OEP)(CO)



$\text{Ru}_3(\text{CO})_{12}$  (0.298 g,  $4.67 \cdot 10^{-4}$  mol) and  $\text{OEPH}_2$  (0.500 g,  $9.35 \cdot 10^{-4}$  mol) were suspended in dry decalin (60.0 mL). The reaction mixture was refluxed for 7 hours, cooled at room temperature and the precipitate was collected and washed three times with hexane (10.0 mL). The violet solid was then purified by flash chromatography (silica gel, 60  $\mu\text{m}$ , starting from hexane/ $\text{CH}_2\text{Cl}_2$  8:2 to  $\text{CH}_2\text{Cl}_2$ ). The  $\text{Ru}(\text{OEP})\text{CO}$  fraction was evaporated to dryness and dried *in vacuo* at  $120^\circ\text{C}$ . The product was obtained as a purple crystalline solid (0.310 g, 50%).

$^1\text{H NMR}$  (300 MHz,  $\text{CDCl}_3$ ):  $\delta$  10.23 (s, 8H,  $\text{H}_{\text{meso}}$ ), 4.09 (q, 16H,  $J=7.6$  Hz,  $\text{H}_{\text{CH}_2}$ ), 1.93 ppm (t, 24H,  $J=7.6$  Hz,  $\text{H}_{\text{CH}_3}$ ). **IR** (ATR):  $\nu_{\text{CO}} = 1956 \text{ cm}^{-1}$ .

### 3.2.8. Synthesis of Ru(TPP)(NAr)<sub>2</sub> (Ar=3,5-(CF<sub>3</sub>)<sub>2</sub>C<sub>6</sub>H<sub>3</sub>)

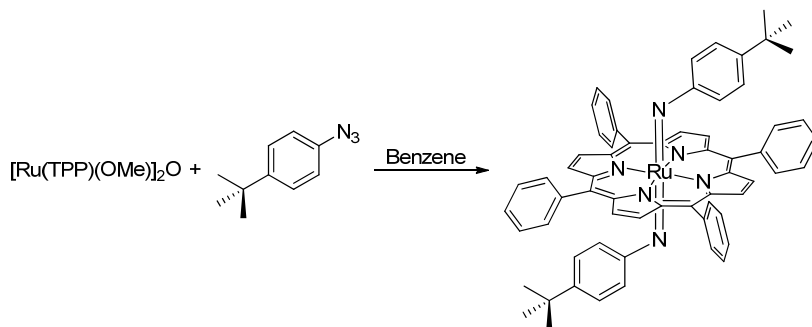


3,5-Bis(trifluoromethyl)phenyl azide (0.154 g,  $6.06 \cdot 10^{-3}$  mol) was added to a benzene (30.0 mL) suspension of  $\text{Ru}(\text{TPP})\text{CO}$  (0.150 g,  $2.02 \cdot 10^{-4}$  mol). The resulting dark mixture was refluxed for 2.5 hours observing the

complete consumption of Ru(TPP)CO by TLC (hexane/CH<sub>2</sub>Cl<sub>2</sub> 1:1). The solution was concentrated to about 5 mL and hexane (20.0 mL) was added. A crystalline violet solid was collected by filtration and dried *in vacuo* (0.165 g, 70%).

<sup>1</sup>H NMR (300 MHz, CDCl<sub>3</sub>): δ 8.87 (s, 8H, H<sub>β</sub>), 8.08 (d, 8H, *J*=6.9 Hz, H<sub>o</sub>), 7.83-7.76 (m, 12H, H<sub>m</sub> and H<sub>p</sub>), 6.60 (s, 2H, H<sub>Ar-meta</sub>), 2.66 ppm (s, 4H, H<sub>Ar-ortho</sub>). IR (ATR): ν= 877 cm<sup>-1</sup>.

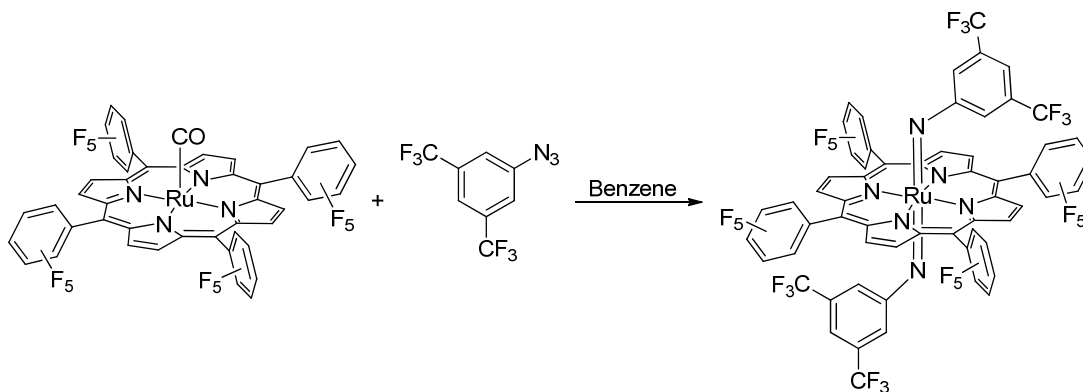
### 3.2.9. Synthesis of Ru(TPP)(NAr)<sub>2</sub> (Ar=4-*t*BuC<sub>6</sub>H<sub>4</sub>)



4-*t*Butylphenyl azide (32.0 mg, 1.82·10<sup>-4</sup> mol) was added to a benzene (35.0 mL) suspension of [Ru(TPP)(OMe)<sub>2</sub>]<sub>2</sub>O (42.0 mg, 2.80·10<sup>-4</sup> mol). The resulting dark mixture was refluxed for 8 hours observing the complete consumption of [Ru(TPP)(OMe)<sub>2</sub>]<sub>2</sub>O by TLC (hexane/CH<sub>2</sub>Cl<sub>2</sub> 1:1). The solution was concentrated to about 5 mL and hexane (15.0 mL) was added. A crystalline violet solid was collected by filtration and dried *in vacuo* (91.0 mg, 60%).

<sup>1</sup>H NMR (300 MHz, C<sub>6</sub>D<sub>6</sub>): δ 8.93 (s, 8H, H<sub>β</sub>), 8.12 (d, 8H, *J*=6.9 Hz, H<sub>o</sub>), 7.47 (m, 12H, H<sub>m</sub> and H<sub>p</sub>), 5.78 (d, 4H, *J*=8.7 Hz, H<sub>Ar-meta</sub>), 2.77 (d, 4H, *J*=8.7 Hz, H<sub>Ar-ortho</sub>), 0.64 ppm (s, 9H, H<sub>CH<sub>3</sub></sub>). IR (ATR): ν= 2954, 1012 cm<sup>-1</sup>.

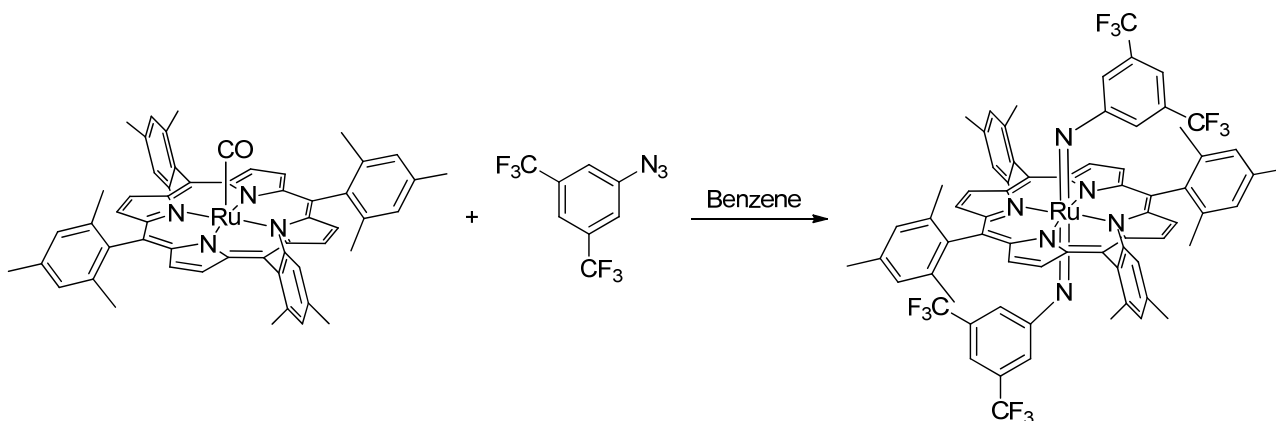
### 3.2.10. Synthesis of Ru(F<sub>20</sub>TPP)(NAr)<sub>2</sub> (Ar=3,5-(CF<sub>3</sub>)<sub>2</sub>C<sub>6</sub>H<sub>3</sub>)



3,5-Bis(trifluoromethyl)phenyl azide (64.7 mg, 2.54·10<sup>-4</sup> mol) was added to a benzene (20.0 mL) suspension of Ru(F<sub>20</sub>TPP)CO (0.100 g, 8.46·10<sup>-5</sup> mol). The resulting dark mixture was refluxed for 4 hours observing the complete consumption of Ru(F<sub>20</sub>TPP)CO by TLC (hexane/CH<sub>2</sub>Cl<sub>2</sub> 1:1). The solution was concentrated to about 5 mL and hexane (20.0 mL) was added. A crystalline violet solid was collected by filtration and dried *in vacuo* (74.8 mg, 55%).

<sup>1</sup>H NMR (300 MHz, CDCl<sub>3</sub>): δ 8.87 (s, 8H, H<sub>β</sub>), 8.08 (d, 8H, *J*=6.9 Hz, H<sub>o</sub>), 7.83-7.76 (m, 12H, H<sub>m</sub> and H<sub>p</sub>), 6.60 (s, 2H, H<sub>Ar-para</sub>), 2.66 ppm (s, 4H, H<sub>Ar-ortho</sub>). IR (ATR): ν= 877 cm<sup>-1</sup>.

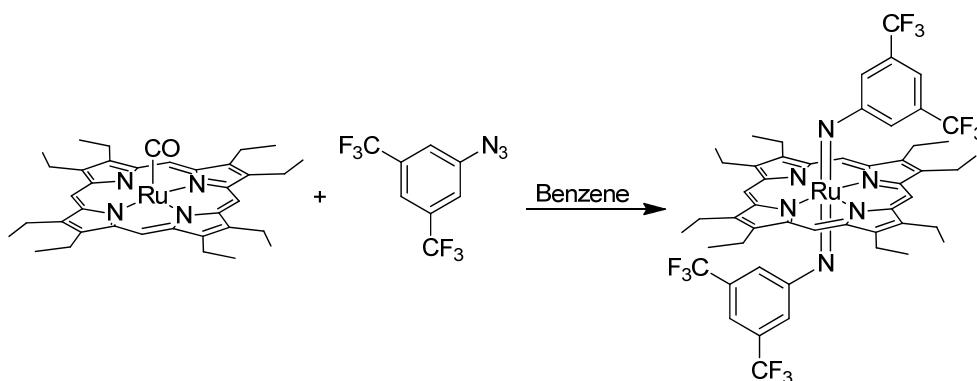
### 3.2.11. Synthesis of Ru(TMP)(NAr)<sub>2</sub> (Ar=3,5(CF<sub>3</sub>)<sub>2</sub>C<sub>6</sub>H<sub>3</sub>)



3,5-Bis(trifluoromethyl)phenyl azide (31.8 mg,  $1.25 \cdot 10^{-4}$  mol) was added to a benzene (6 mL) suspension of Ru(TMP)CO (28.4 mg,  $3.12 \cdot 10^{-5}$  mol). The resulting dark mixture was refluxed for 4 hours observing the complete consumption of Ru(TMP)CO by TLC (hexane/CH<sub>2</sub>Cl<sub>2</sub> 1:1). The solvent was evaporated under reduced pressure and the crude was purified by chromatography (alumina 0.063-0.200  $\mu$ m, hexane/CH<sub>2</sub>Cl<sub>2</sub> 7:3) giving the product as a purple solid (0. g, 60%).

<sup>1</sup>H NMR (300 MHz, CDCl<sub>3</sub>):  $\delta$  8.64 (s, 8H, H <sub>$\beta$</sub> ), 7.27 (d, 8H,  $J=6.9$  Hz, H<sub>o</sub>), 6.38 (m, 12H, H<sub>m</sub> and H<sub>o</sub>), 3.06 (s, 2H, H<sub>Ar</sub>), 2.62 (s, 4H, H<sub>Ar</sub>), 1.71 ppm (s, 24H, H<sub>CH<sub>3</sub></sub>). IR (ATR):  $\nu=879$  cm<sup>-1</sup>.

### 3.2.12. Synthesis of Ru(OEP)(NAr)<sub>2</sub> (Ar=3,5(CF<sub>3</sub>)<sub>2</sub>C<sub>6</sub>H<sub>3</sub>)

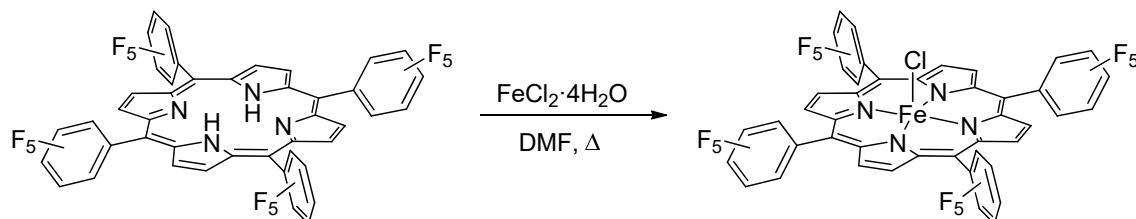


3,5-Bis(trifluoromethyl)phenyl azide (0.177 g,  $6.95 \cdot 10^{-3}$  mol) was added to a benzene (30.0 mL) suspension of Ru(OEP)CO (0.115 g,  $1.74 \cdot 10^{-4}$  mol). The resulting dark mixture was refluxed for 4 hours observing the complete consumption of Ru(OEP)CO by TLC (hexane/CH<sub>2</sub>Cl<sub>2</sub> 1:1). The solution was concentrated to about 5 mL and hexane (20.0 mL) was added. A crystalline violet solid was collected by filtration and dried *in vacuo* (0.113 g, 60%).

<sup>1</sup>H NMR (300 MHz, CDCl<sub>3</sub>):  $\delta$  10.23 (s, 4H, H<sub>meso</sub>), 6.36 (s, 2H, H<sub>Ar-para</sub>), 4.09 (q, 16H,  $J=7.6$  Hz, H<sub>CH<sub>2</sub></sub>), 2.22 (s, 4H, H<sub>Ar-ortho</sub>), 1.93 ppm (t, 24H,  $J=7.6$  Hz, H<sub>CH<sub>3</sub></sub>). <sup>13</sup>C NMR (75 MHz, CDCl<sub>3</sub>):  $\delta$  151.9, 142.3, 139.7, 117.4, 117.0, 99.6, 19.8, 18.5 ppm. <sup>19</sup>F NMR (282 MHz, CDCl<sub>3</sub>):  $\delta$  -64.0 ppm (s, 12F, CF<sub>3</sub>). MS (ESI):  $m/z=1088.2$  [M<sup>+</sup>].

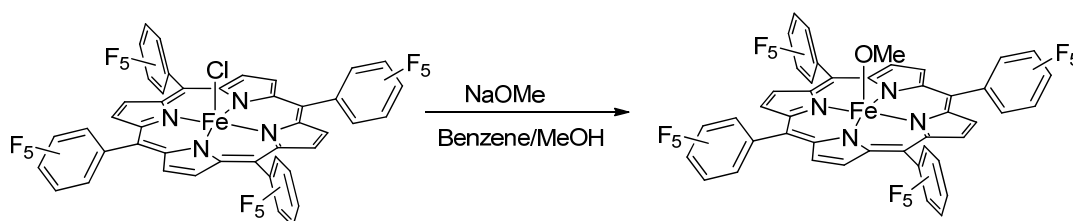
### 3.3. Synthesis of metal porphyrin complexes

#### 3.3.1. Synthesis of Fe(F<sub>20</sub>TPP)Cl



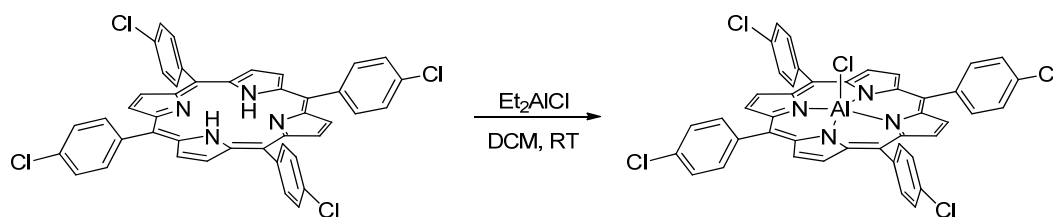
Iron chloride tetrahydrate (0.942 g,  $4.74 \cdot 10^{-3}$  mol) and F<sub>20</sub>TPPH<sub>2</sub> (0.200 g,  $1.89 \cdot 10^{-4}$  mol) were dissolved in 50.0 mL of DMF and the resulting mixture was stirred at reflux until the complete consumption of F<sub>20</sub>TPPH<sub>2</sub> which was monitored by TLC (hexane/AcOEt 7:3). Then the solution was cooled to room temperature and 25.0 mL of HCl 6N was added dropwise. The so-formed precipitate was collected by filtration. After being washed three times with 20.0 mL of HCl 3N and one time with 20.0 mL of water. The product was obtained as a dark brown solid and dried *in vacuo* (0.194 g, 90%).

#### 3.3.2. Synthesis of Fe(F<sub>20</sub>TPP)(OMe)



Fe(F<sub>20</sub>TPP)Cl (0.100 g,  $8.74 \cdot 10^{-5}$  mol) was dissolved in benzene (35.0 mL) and methanol (15.0 mL), then a solution of sodium methoxide in methanol (0.670 mL of a 30% w/w solution) was added dropwise. During the addition, the reaction colour changed from dark green to dark red. The solution was stirred at room temperature for 1 hour and then it was concentrated to about 5 mL. A crystalline dark solid was collected by filtration and dried *in vacuo* (98.0 mg, 98%).

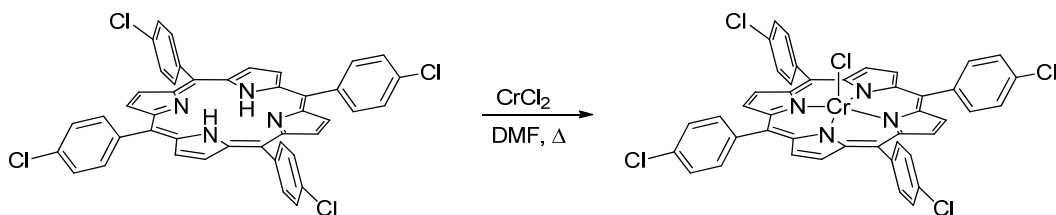
#### 3.3.3. Synthesis of Al(4-CITPP)Cl



*meso*-Tetra(4-chlorophenyl) porphyrin (4-CITPPH<sub>2</sub>) (0.150 g,  $1.99 \cdot 10^{-4}$  mol) was dissolved in 4.00 mL of dry dichloromethane and then diethyl aluminium chloride (31.0 mg,  $2.59 \cdot 10^{-4}$  mol) was added at 0°C. The resulting green mixture was stirred at room temperature until the complete consumption of 4-CITPPH<sub>2</sub> which was monitored by TLC (1% MeOH in CH<sub>2</sub>Cl<sub>2</sub>). Then the solvent was evaporated and the crude was purified by chromatography (alumina 0.063-0.200  $\mu$ m, 0.5% MeOH in CH<sub>2</sub>Cl<sub>2</sub>). The product was obtained as a purple crystalline solid (0.144 g, 89%).

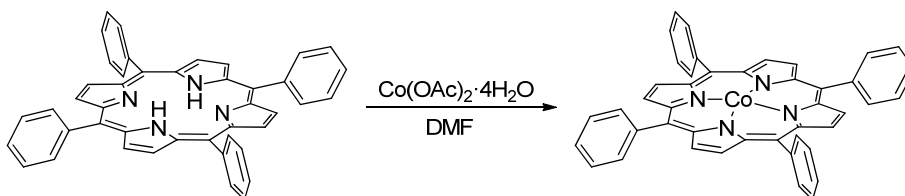
<sup>1</sup>H NMR (300 MHz, DMSO-*d*<sub>6</sub>):  $\delta$  9.01 (s, 8H, H <sub>$\beta$</sub> ), 8.25 (m, 8H, H <sub>$m$</sub> ), 7.98 ppm (m, 8H, H <sub>$o$</sub> ).

### 3.3.4. Synthesis of Cr(4-CITPP)Cl



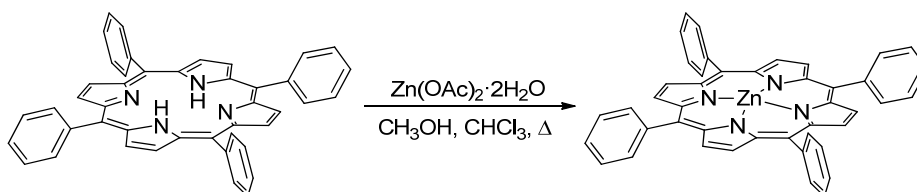
*meso*-Tetra(4-chlorophenyl) porphyrin (4-CITPPH<sub>2</sub>) (0.100 g, 1.33 · 10<sup>-4</sup> mol) was dissolved in 15.0 mL of dry DMF and then chromium dichloride (24.0 mg, 1.99 · 10<sup>-4</sup> mol) was added. The mixture was refluxed for 3 hours until the complete consumption of 4-TCIPPH<sub>2</sub> which was monitored by TLC (1% MeOH in CH<sub>2</sub>Cl<sub>2</sub>). Then the solution was cooled to room temperature and 50.0 mL of HCl 0.1N was added dropwise. The so-formed precipitate was collected by filtration. After being washed three times with 20.0 mL of HCl 0.1N the product was obtained as a dark brown solid and purified by chromatography (alumina 0.063-0.200 μm, 0.5% MeOH in CH<sub>2</sub>Cl<sub>2</sub>). The product was obtained as a dark solid (0.105 g, 95%).

### 3.3.5. Synthesis of Co(TPP)



*meso*-Tetraphenyl porphyrin (TPPH<sub>2</sub>) (0.100 g, 1.63 · 10<sup>-4</sup> mol) was dissolved in 30.0 mL of dry DMF and then the solution was heated to 50°C. Cobalt acetate tetrahydrate (0.121 g, 4.88 · 10<sup>-4</sup> mol) was added and the reaction was refluxed for 4 hours until the complete consumption of TPPH<sub>2</sub> which was monitored by TLC (hexane/CH<sub>2</sub>Cl<sub>2</sub> 1:1). Then the solvent was evaporated to dryness and the dark solid was washed several times with water (0.098 g, 90%).

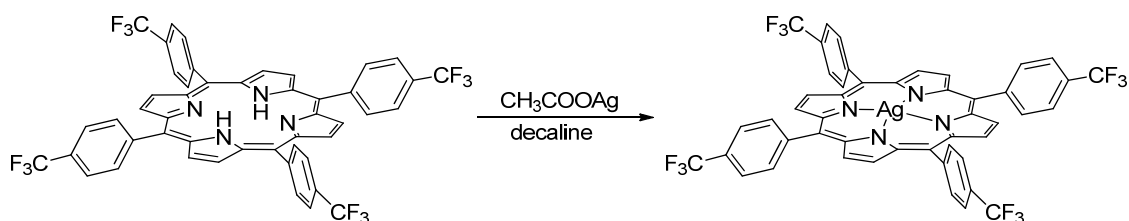
### 3.3.6. Synthesis of Zn(TPP)



TPPH<sub>2</sub> (60.0 mg, 9.76 · 10<sup>-5</sup> mol) was dissolved in 7.00 mL of chloroform and then a solution of zinc acetate dihydrate (0.215 g, 9.76 · 10<sup>-4</sup> mol) in 18.0 mL of methanol was added. The resulting mixture was refluxed for 2 hours until the complete consumption of TPPH<sub>2</sub> which was monitored by TLC (hexane/CH<sub>2</sub>Cl<sub>2</sub> 1:1). Then the solvent was evaporated and the crude was recovered with CH<sub>2</sub>Cl<sub>2</sub> (15.0 mL). The organic phase was extracted with a solution of NaHCO<sub>3</sub> 5%wt (15.0 mL added three times), water (15.0 mL added three times) and then dried over NaSO<sub>4</sub> and filtered. The filtrate was evaporated to dryness under reduced pressure giving the product as a purple solid (66.0 mg, 100%).

<sup>1</sup>H NMR (400 MHz, CDCl<sub>3</sub>): δ 8.99 (s, 8H, H<sub>β</sub>), 8.26 (d, 8H, *J*=5.6 Hz, H<sub>o</sub>), 7.81-7.79 ppm (m, 12H, H<sub>m</sub> and H<sub>p</sub>).

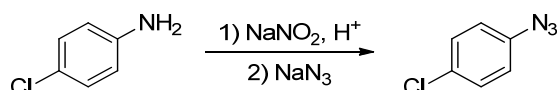
### 3.3.7. Synthesis of Ag(4-CF<sub>3</sub>TPP)



Under dark *meso*-tetra(4-(trifluoromethyl) phenyl) porphyrin (4-CF<sub>3</sub>TPPH<sub>2</sub>) (0.295 g, 3.39 · 10<sup>-4</sup> mol) and silver acetate (0.274 g, 1.60 · 10<sup>-3</sup> mol) were dissolved in 120 mL of dry decaline and the mixture was refluxed for 5 hours until the complete consumption of 4-CF<sub>3</sub>TPPH<sub>2</sub> which was monitored by TLC (hexane/CH<sub>2</sub>Cl<sub>2</sub> 1:1). Then the reaction was filtered and the solvent was evaporated. The crude was purified by flash chromatography (silica gel, 60 μm, starting from CH<sub>2</sub>Cl<sub>2</sub>/hexane 1:9 to CH<sub>2</sub>Cl<sub>2</sub>/hexane 3:7). The product was obtained as a purple/red crystalline solid (0.241 g, 73%).

## 3.4. Synthesis of azides

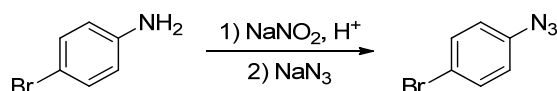
### 3.4.1. Synthesis of 4-chlorophenyl azide



4-Chloroaniline (3.59 g, 2.81 · 10<sup>-2</sup> mol) was dissolved in a solution of 50.0 mL of HCl at 37% and 50.0 mL of water under air. The mixture was heating up to the completely dissolution of aniline then the colourless solution was cooled at 0° C in an ice bath and a solution of NaNO<sub>2</sub> (2.30 g, 3.33 · 10<sup>-2</sup> mol) in 30.0 mL of water was added. The reaction was stirred for 1 hour and then urea (0.320 g, 5.32 · 10<sup>-3</sup> mol) was added in one portion. Under vigorous magnetic stirring a solution of sodium azide (2.20 g, 3.38 · 10<sup>-2</sup> mol) in 50.0 mL of water was added to the cold mixture in about 15 minutes. The resulting mixture was then allowed to reach room temperature and further stirred for 1 hour. Diethyl ether (100 mL) was added and the phases were separated. The aqueous phase was washed twice with 50.0 mL of diethyl ether and the combined organic phases were dried over Na<sub>2</sub>SO<sub>4</sub>. The solvent was evaporated under reduced pressure and the product was obtained as a yellow oil (3.25 g, 75%).

<sup>1</sup>H NMR (300 MHz, C<sub>6</sub>D<sub>6</sub>): δ 6.95 (d, 2H, *J*=8.8 Hz, H<sub>m</sub>), 6.46 ppm (d, 2H, *J*=8.8 Hz, H<sub>o</sub>). IR (CH<sub>2</sub>Cl<sub>2</sub>): ν<sub>max</sub>= 2111 cm<sup>-1</sup>.

### 3.4.2. Synthesis of 4-bromophenyl azide



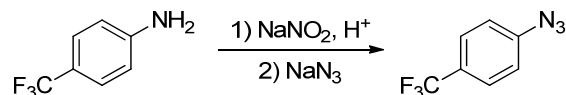
4-Bromoaniline (3.60 g, 2.10 · 10<sup>-2</sup> mol) was dissolved in a solution of 15.0 mL of H<sub>2</sub>SO<sub>4</sub> conc. and 60.0 mL of water under air. The mixture was cooled at 0° C in an ice bath and a solution of NaNO<sub>2</sub> (1.83 g, 2.60 · 10<sup>-2</sup> mol) in 25.0 mL of water was added. The reaction was stirred for 30 minutes and then urea (0.220 g, 3.66 · 10<sup>-3</sup> mol) was added in one portion. Under vigorous magnetic stirring a solution of sodium azide (1.77 g, 2.70 · 10<sup>-2</sup> mol) in 20.0 mL of water was added to the cold mixture in about 15 minutes. The resulting mixture was then allowed to reach room temperature and further stirred for 30 minutes. Diisopropyl ether (50.0 mL) was added and the phases were separated. The aqueous phase was washed three times with 50.0 mL of diisopropyl ether and the



combined organic phases were dried over  $\text{Na}_2\text{SO}_4$ . The solvent was evaporated under reduced pressure to give a yellow oil (3.44 g, 82%).

$^1\text{H NMR}$  (300 MHz,  $\text{C}_6\text{D}_6$ ):  $\delta$  7.70 (d, 2H,  $J=8.4$  Hz,  $\text{H}_m$ ), 6.40 ppm (d, 2H,  $J=8.4$  Hz,  $\text{H}_o$ ). **IR** ( $\text{CH}_2\text{Cl}_2$ ):  $\nu_{\text{max}}=2128$   $\text{cm}^{-1}$ .

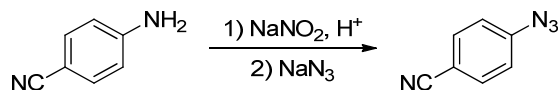
### 3.4.3. Synthesis of 4-(trifluoromethyl)phenyl azide



4-(Trifluoromethyl)aniline (3.00 mL,  $2.5 \cdot 10^{-2}$  mol) was dissolved in a solution of 30.0 mL of HCl 37% and 42.0 mL of water under air. The mixture was cooled at 0° C in an ice bath and a solution of  $\text{NaNO}_2$  (2.28 g,  $3.3 \cdot 10^{-2}$  mol) in 30.0 mL of water was added to the white suspension. The reaction was stirred for 30 minutes and then urea (0.660 g,  $1.1 \cdot 10^{-2}$  mol) was added in one portion. Under vigorous magnetic stirring a solution of sodium azide (3.18 g,  $4.9 \cdot 10^{-2}$  mol) in 45.0 mL of water was added to the cold mixture in about 15 minutes. The resulting mixture was then allowed to reach room temperature and further stirred for 30 minutes. Diisopropyl ether (50.0 mL) was added and the phases were separated. The aqueous phase was washed three times with 50.0 mL of diisopropyl ether and the combined organic phases were dried over  $\text{Na}_2\text{SO}_4$ . The solvent was evaporated under reduced pressure to give a yellow oil (3.18 g, 68%).

$^1\text{H NMR}$  (300 MHz,  $\text{C}_6\text{D}_6$ ):  $\delta$  7.63 (d, 2H,  $J=8.4$  Hz,  $\text{H}_m$ ), 7.14 ppm (d, 2H,  $J=8.4$  Hz,  $\text{H}_o$ ). **IR** ( $\text{CH}_2\text{Cl}_2$ ):  $\nu_{\text{max}}=2129$   $\text{cm}^{-1}$ .

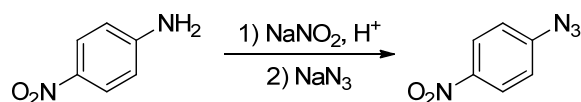
### 3.4.4. Synthesis of 4-cyanophenyl azide



4-Cyanoaniline (5.02 g,  $4.25 \cdot 10^{-2}$  mol) was dissolved in a solution of 50.0 mL of  $\text{H}_2\text{SO}_4$  conc. and 50.0 mL of water under air. The mixture was cooled at 0° C in an ice bath and a solution of  $\text{NaNO}_2$  (3.75 g,  $5.43 \cdot 10^{-2}$  mol) in 25.0 mL of water was added. The reaction was stirred for 30 minutes and then urea (1.38 g,  $2.29 \cdot 10^{-2}$  mol) was added in one portion. Under vigorous magnetic stirring a solution of sodium azide (7.02 g,  $1.08 \cdot 10^{-1}$  mol) in 50.0 mL of water was added to the cold mixture in about 15 minutes. The resulting mixture was then allowed to reach room temperature and further stirred for 30 minutes. Dichloromethane (100 mL) was added and the phases were separated. The aqueous phase was washed twice with 50.0 mL of dichloromethane and the combined organic phases were dried over  $\text{Na}_2\text{SO}_4$ . The solvent was evaporated under reduced pressure up to about 5 mL and heptane (50.0 mL) was added. The yellow precipitate was collected by filtration and dried *in vacuo* (4.90 g, 80%).

$^1\text{H NMR}$  (300 MHz,  $\text{CDCl}_3$ ):  $\delta$  7.70 (d, 2H,  $J=8.4$  Hz,  $\text{H}_m$ ), 6.40 ppm (d, 2H,  $J=8.4$  Hz,  $\text{H}_o$ ). **IR** ( $\text{CH}_2\text{Cl}_2$ ):  $\nu_{\text{max}}=2111$   $\text{cm}^{-1}$ .

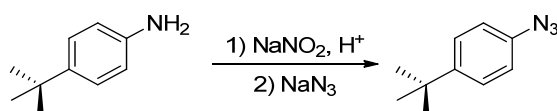
### 3.4.5. Synthesis of 4-nitrophenyl azide



4-Nitroaniline (5.20 g,  $3.80 \cdot 10^{-2}$  mol) was dissolved in a solution of H<sub>2</sub>SO<sub>4</sub> 30% (75.0 mL) under air. The yellow mixture was cooled at 0° C in an ice bath and a solution of NaNO<sub>2</sub> (2.75 g,  $3.98 \cdot 10^{-2}$  mol) in 25.0 mL of water was added. The reaction was stirred for 30 minutes and then urea (1.30 g,  $2.16 \cdot 10^{-2}$  mol) was added in one portion. Under vigorous magnetic stirring a solution of sodium azide (3.50 g,  $5.38 \cdot 10^{-2}$  mol) in 20.0 mL of water was added to the cold mixture in about 15 minutes. The resulting mixture was then allowed to reach room temperature and further stirred for 30 minutes. Dichloromethane (100 mL) was added and the phases were separated. The aqueous phase was washed twice with 50.0 mL of dichloromethane and the combined organic phases were dried over Na<sub>2</sub>SO<sub>4</sub>. The solvent was evaporated under reduced pressure up to 10 mL and hexane (15.0 mL) was added. The yellow precipitate was collected by filtration and dried *in vacuo* (4.30 g, 70%).

<sup>1</sup>H NMR (300 MHz, C<sub>6</sub>D<sub>6</sub>): δ 7.62 (d, 2H, *J*=9.1 Hz, H<sub>m</sub>), 6.15 ppm (d, 2H, *J*=9.1 Hz, H<sub>o</sub>). IR (CH<sub>2</sub>Cl<sub>2</sub>): ν<sub>max</sub>= 2125 cm<sup>-1</sup>.

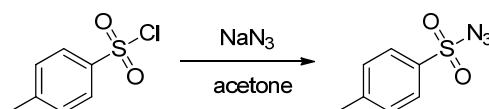
### 3.4.6. Synthesis of 4-*tert*-butylphenyl azide



4-*Tert*-butylaniline (15.9 mL,  $9.98 \cdot 10^{-2}$  mol) was dissolved in a solution of HCl 37% (50.0 mL) and water (50.0 mL) under air. The yellowish mixture was cooled at 0° C in an ice bath and a solution of NaNO<sub>2</sub> (7.20 g,  $1.04 \cdot 10^{-1}$  mol) in 25.0 mL of water was added. The reaction was stirred for 10 minutes and then, under vigorous magnetic stirring, a solution of sodium azide (6.70 g,  $1.03 \cdot 10^{-1}$  mol) in 30.0 mL of water was added to the cold mixture in about 15 minutes. The resulting mixture was stirred for 30 minutes, then it was allowed to reach room temperature and further stirred for 3 hours. Hexane (100 mL) was added and the phases were separated. The aqueous phase was washed twice with 100 mL of hexane and the combined organic phases were dried over Na<sub>2</sub>SO<sub>4</sub>. The solvent was evaporated under reduced pressure and the crude was purified by flash chromatography (SiO<sub>2</sub>, 60 μm, hexane/AcOEt 9:1) to obtain an orange oil (16.2 g, 92%).

<sup>1</sup>H NMR (300 MHz, CDCl<sub>3</sub>): δ 7.37 (d, 2H, *J*=7.2 Hz, H<sub>m</sub>), 6.98 (d, 2H, *J*=7.2 Hz, H<sub>o</sub>), 1.32 ppm (s, 3H, H<sub>CH<sub>3</sub></sub>). IR (CH<sub>2</sub>Cl<sub>2</sub>): ν<sub>max</sub>= 2124 cm<sup>-1</sup>.

### 3.4.7. Synthesis of 4-toluenesulfonyl azide

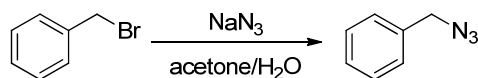


Tosyl chloride (18.0 g,  $9.44 \cdot 10^{-2}$  mol) was dissolved in acetone (40.0 mL) and the solution was cooled at 0°C in an ice bath. Then, a solution of sodium azide (6.50 g,  $1.00 \cdot 10^{-1}$  mol) in water (10.0 mL) was added dropwise under a vigorous stirring. The mixture was allowed to reach room temperature and further stirred for 2 hours. Diethyl ether (20.0 mL) was added to the reaction mixture and the phases were separated. The aqueous phase

was washed twice time with 20.0 mL of diethyl ether and the combined organic phases were dried over NaSO<sub>4</sub>. The solvent was evaporated under reduced pressure to give the product as a white oil (16.0 g, 86%).

<sup>1</sup>H NMR (300 MHz, C<sub>6</sub>D<sub>6</sub>): δ 7.72 (d, 2H, *J*=8.0 Hz, H<sub>o</sub>), 6.67 (d, 2H, *J*=8.0 Hz, H<sub>m</sub>), 2.32 ppm (s, 3H, H<sub>CH3</sub>).  
IR (CH<sub>2</sub>Cl<sub>2</sub>): ν<sub>max</sub>= 2123 cm<sup>-1</sup>.

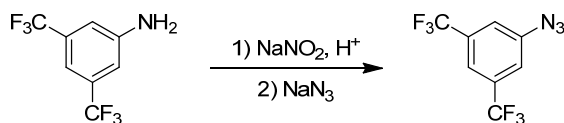
### 3.4.8. Synthesis of benzyl azide



Benzyl bromide (0.690 mL, 5.84·10<sup>-3</sup> mol) and sodium azide (0.570 g, 8.76·10<sup>-3</sup> mol) were dissolved in a solution of acetone (12.0 mL) and water (8.00 mL). The reaction was refluxed for 14 hours and then acetone was evaporated under reduced pressure and diethyl ether (20.0 mL) was added to the aqueous mixture. The two phases were separated and the aqueous phase was washed twice with 20.0 mL of diethyl ether. The combined organic phases were dried over NaSO<sub>4</sub> and the solvent was evaporated under reduced pressure to give the product as a yellow oil (0.626 g, 81%).

<sup>1</sup>H NMR (300 MHz, CDCl<sub>3</sub>): δ 7.40-7.29 (m, 5H, H<sub>Ar</sub>), 4.33 ppm (s, 2H, H<sub>CH2</sub>). IR (CH<sub>2</sub>Cl<sub>2</sub>): ν<sub>max</sub>= 2096 cm<sup>-1</sup>.

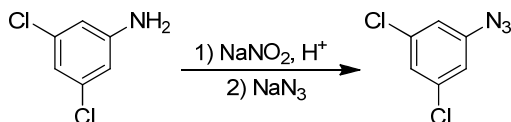
### 3.4.9. Synthesis of 3,5-bis(trifluoromethyl)phenyl azide



3,5-Bis(trifluoromethyl)aniline (3.75 mL, 2.40·10<sup>-2</sup> mol) was dissolved in a solution of 30.0 mL of HCl 37% and 42.0 mL of water under air. The mixture was cooled at 0° C in an ice bath and a solution of NaNO<sub>2</sub> (2.28 g, 3.30·10<sup>-2</sup> mol) in 30.0 mL of water was added to the white suspension. The reaction was stirred for 30 minutes and then urea (0.660 g, 1.10·10<sup>-2</sup> mol) was added in one portion. Under vigorous magnetic stirring a solution of sodium azide (3.18 g, 4.90·10<sup>-2</sup> mol) in 45.0 mL of water was added to the cold mixture in about 15 minutes. The resulting mixture was then allowed to reach room temperature and further stirred for 30 minutes. Diisopropyl ether (50.0 mL) was added and the phases were separated. The aqueous phase was washed three times with 50.0 mL of diisopropyl ether and the combined organic phases were dried over Na<sub>2</sub>SO<sub>4</sub>. The solvent was evaporated under reduced pressure to give a yellow oil (3.86 g, 70%).

<sup>1</sup>H NMR (300 MHz, C<sub>6</sub>D<sub>6</sub>): δ 7.65 (s, 1H, H<sub>p</sub>), 7.14 ppm (s, 2H, H<sub>o</sub>). IR (nujol): ν<sub>max</sub>= 2116 cm<sup>-1</sup>.

### 3.4.10. Synthesis of 3,5-dichlorophenyl azide



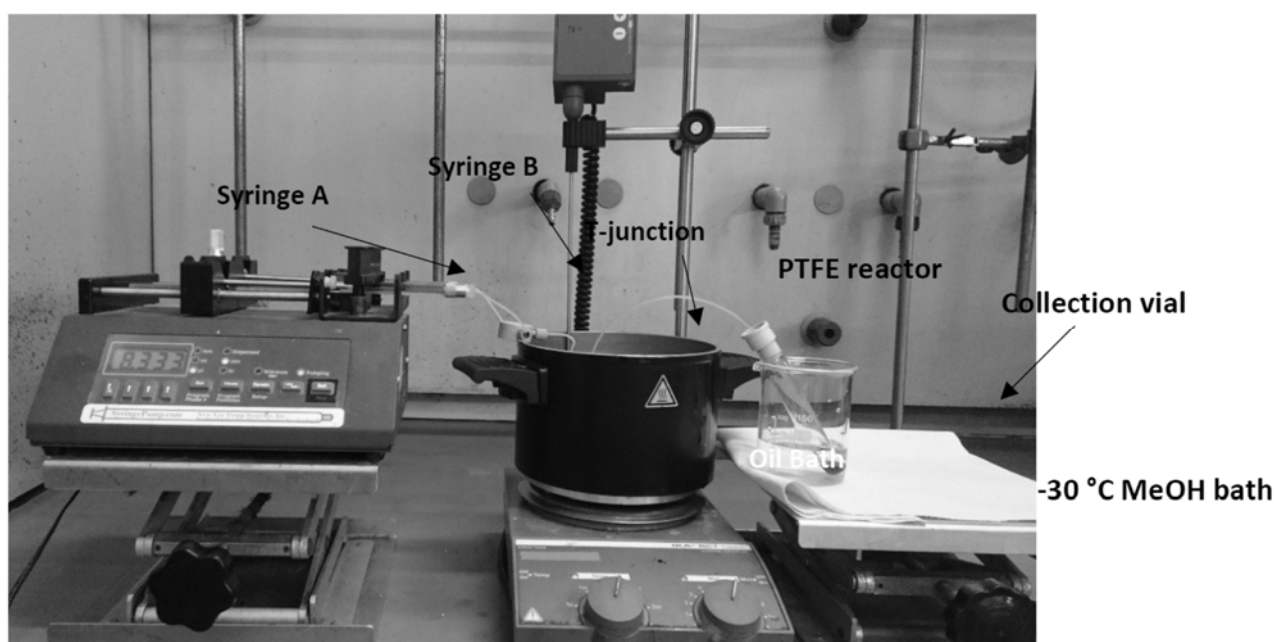
3,5-Dichloroaniline (3.88 g, 2.40·10<sup>-2</sup> mol) was dissolved in a solution of 30.0 mL of HCl 37% and 42.0 mL of water under air. The mixture was cooled at 0° C in an ice bath and a solution of NaNO<sub>2</sub> (2.28 g, 3.30·10<sup>-2</sup> mol) in 30.0 mL of water was added to the white suspension. The reaction was stirred for 30 minutes and then urea (0.660 g, 1.10·10<sup>-2</sup> mol) was added in one portion. Under vigorous magnetic stirring a solution of sodium azide (3.18 g, 4.90·10<sup>-2</sup> mol) in 45.0 mL of water was added to the cold mixture in about 15 minutes. The

resulting mixture was then allowed to reach room temperature and further stirred for 30 minutes. Diisopropyl ether (50.0 mL) was added and the phases were separated. The aqueous phase was washed three times with 50.0 mL of diisopropyl ether and the combined organic phases were dried over Na<sub>2</sub>SO<sub>4</sub>. The solvent was evaporated under reduced pressure to give a yellow oil (3.60 g, 80%).

<sup>1</sup>H NMR (300 MHz, C<sub>6</sub>D<sub>6</sub>): δ 7.50 (s, 1H, H<sub>p</sub>), 7.33 ppm (s, 2H, H<sub>o</sub>). IR (nujol): ν<sub>max</sub> = 2116 cm<sup>-1</sup>.

### 3.5. Aziridination reactions catalysed by Ru(TPP)(CO)

**500 μL fluidic module:** This module was constructed using a PTFE tubing (1.58 mm outer diameter, 0.58 mm inner diameter, 1.89 m length, 500 μL effective volume), coiled in a bundle and immersed in an oil bath. A new Era NE 300 syringe pumps, equipped with one or two Hamilton gastight syringes, fed the reactant solutions through a T-junction into the above-mentioned PTFE tubing.



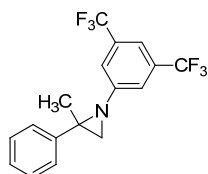
#### 3.5.1. Synthesis of aziridines

**General catalytic procedure (Method A):** In a typical reaction, a syringe was filled with a solution of Ru(TPP)(CO) (3.03 mg, 4.10·10<sup>-6</sup> mol) in 10.0 mL of the appropriate solvent, the mixture was sonicated for 10 min prior the addition of 3,5-*bis*(trifluoromethyl)phenyl azide (51.0 mg, 2.00·10<sup>-4</sup> mol), α-methylstyrene (0.130 mL, 1.00·10<sup>-3</sup> mol) and byphenyl (2.30 mg, 1.50·10<sup>-5</sup> mol) as internal standard. The syringe was then connected to a syringe pump and the reagents were fed into the PTFE mesoreactor at the desired flow rate (mL/min) and temperature. One reactor volume was discarded before starting sample collection in order to achieve steady-state conditions. Reaction outcome was collected into a vial cooled at -30°C and directly analysed through GC.

**General catalytic procedure (Method B):** in a typical experiment, syringe A was filled with a mixture obtained dissolving Ru(TPP)(CO) (12.1 mg, 1.6·10<sup>-5</sup> mol) in 2.00 ml of the desired alkene in order to have 0.008 M concentration of catalyst. The mixture was sonicated for 10 min and heated until a complete dissolution of the catalyst. Syringe B was filled with a mixture obtained dissolving azide (8.00·10<sup>-4</sup> mol) and byphenyl (9.20 mg, 6.00·10<sup>-5</sup> mol) as internal standard in 2.00 ml of the desired alkene in order to have 0.4 M concentration of azide. Syringes A and B were connected to a syringe pump and the reagents were pumped

into PTFE mesoreactor through a T-junction at the desired flow rate ( $\mu\text{L}/\text{min}$ ) at the desired temperature. One reactor volume was discarded before starting sample collection in order to achieve steady-state conditions. Reaction outcome was collected into a vial cooled at  $-30\text{ }^\circ\text{C}$  and directly analysed through GC or  $^1\text{H}$  NMR.

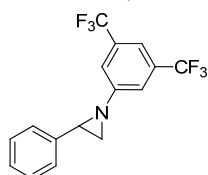
#### 3.5.1.1. *N*-(3,5-bis(trifluoromethyl)phenyl)-2-methyl-2-phenyl aziridine (60)



Compound **60** was obtained from  $\alpha$ -methylstyrene and 3,5-bis(trifluoromethyl)phenyl azide. The crude was purified by flash chromatography (silica gel,  $60\ \mu\text{m}$ , AcOEt/hexane 1:9 + 5% of TEA). The collected data are in accord with those reported in literature.<sup>6b</sup>

$^1\text{H}$  NMR (300 MHz,  $\text{CDCl}_3$ ):  $\delta$  7.55-7.51 (m, 3H,  $\text{H}_{\text{Ar}}$ ), 7.44 (m, 5H,  $\text{H}_{\text{Ar}}$ ), 2.70 (s, 1H,  $\text{H}_{\text{CH}_2}$ ), 2.42 (s, 1H,  $\text{H}_{\text{CH}_2}$ ), 1.50 ppm (s, 3H,  $\text{H}_{\text{CH}_3}$ ).

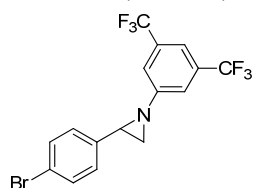
#### 3.5.1.2. *N*-(3,5-bis(trifluoromethyl)phenyl)-2-phenyl aziridine (61)



Compound **61** was obtained from styrene and 3,5-bis(trifluoromethyl)phenyl azide. The crude was purified by flash chromatography (silica gel,  $60\ \mu\text{m}$ , AcOEt/hexane 1:9 + 5% of TEA). The collected data are in accord with those reported in literature.<sup>6b</sup>

$^1\text{H}$  NMR (300 MHz,  $\text{CDCl}_3$ ):  $\delta$  7.53-7.37 (m, 8H,  $\text{H}_{\text{Ar}}$ ), 3.28 (dd, 1H,  $J=6.4, 3.3\ \text{Hz}$ ,  $\text{H}_{\text{CH}}$ ), 2.60 (d, 1H,  $J=6.4\ \text{Hz}$ ,  $\text{H}_{\text{CH}_2}$ ), 2.58 ppm (d, 1H,  $J=3.3\ \text{Hz}$ ,  $\text{H}_{\text{CH}_2}$ ).

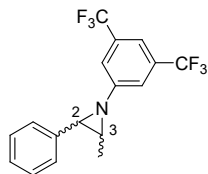
#### 3.5.1.3. *N*-(3,5-bis(trifluoromethyl)phenyl)-2-(4-bromophenyl) aziridine (62)



Compound **62** was obtained from 4-bromostyrene and 3,5-bis(trifluoromethyl)phenyl azide. The crude was purified by flash chromatography (silica gel,  $60\ \mu\text{m}$ , AcOEt/hexane 1:9 + 5% of TEA).

$^1\text{H}$  NMR (300 MHz,  $\text{C}_6\text{D}_6$ ):  $\delta$  7.54 (s, 1H,  $\text{H}_{\text{Ar}}$ ), 7.25 (d, 2H,  $J=8.4\ \text{Hz}$ ,  $\text{H}_{\text{Ar}}$ ), 7.10 (s, 2H,  $\text{H}_{\text{Ar}}$ ), 6.83 (d, 2H,  $J=8.4\ \text{Hz}$ ,  $\text{H}_{\text{Ar}}$ ), 6.72 (d, 2H,  $J=8.4\ \text{Hz}$ ,  $\text{H}_{\text{Ar}}$ ), 2.28 (dd, 1H,  $J=6.4, 3.3\ \text{Hz}$ ,  $\text{H}_{\text{CH}}$ ), 1.66 (d, 1H,  $J=3.2\ \text{Hz}$ ,  $\text{H}_{\text{CH}_2}$ ), 1.54 ppm (d, 1H,  $J=6.4\ \text{Hz}$ ,  $\text{H}_{\text{CH}_2}$ ).  $^{13}\text{C}$  NMR (75 MHz,  $\text{C}_6\text{D}_6$ ):  $\delta$  155.6, 137.0, 132.3, 131.5, 131.2, 130.0, 129.4, 120.5 (q,  $J_{\text{CF}}=279.0\ \text{Hz}$ , CF), 120.3, 115.7, 116.5, 40.7, 37.3 ppm.  $^{19}\text{F}$  NMR (282 MHz,  $\text{CDCl}_3$ ):  $\delta$  -63.4 ppm (s, 6F,  $\text{CF}_3$ ). MS (ESI):  $m/z=410.1\ [\text{M}^+]$ .

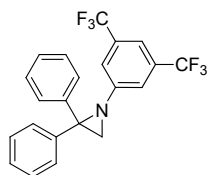
#### 3.5.1.4. *N*-(3,5-bis(trifluoromethyl)phenyl)-2-phenyl-3-methyl aziridine (**63**)



Compound **63** was obtained from  $\beta$ -methylstyrene and 3,5-bis(trifluoromethyl)phenyl azide. The crude was purified by flash chromatography (silica gel, 60  $\mu$ m, AcOEt/hexane 1:9 + 5% of TEA) and the product was isolated as a 9:1 mixture of *cis:trans* isomers.

$^1\text{H NMR}$  (300 MHz,  $\text{CDCl}_3$ ):  $\delta$  7.48 (s, 1H,  $\text{H}_{\text{Ar}}$ ), 7.44-7.28 (m, 7H,  $\text{H}_{\text{Ar}}$ ), 3.44 (d, 1H,  $J=6.5$  Hz,  $\text{H}^2, \text{trans}$ ), 3.08 (d, 1H,  $J=2.6$  Hz,  $\text{H}^2, \text{cis}$ ), 2.80-2.71 (m, 1H,  $\text{H}^3, \text{trans}$ ), 2.70-2.62 (m, 1H,  $\text{H}^3, \text{cis}$ ), 1.32 (d, 3H,  $J=5.7$  Hz,  $\text{H}_{\text{CH}_3, \text{cis}}$ ), 1.21 ppm (d, 3H,  $J=5.7$  Hz,  $\text{H}_{\text{CH}_3, \text{trans}}$ ).  $^{13}\text{C NMR}$  (75 MHz,  $\text{CDCl}_3$ ):  $\delta$  151.3, 137.2, 132.2 (q,  $^2J_{\text{CF}}=33.2$  Hz,  $\text{CCF}_3$ ), 128.6, 127.8, 126.4, 123.3 (q,  $^1J_{\text{CF}}=272.8$  Hz,  $\text{CF}_3$ ), 120.7, 116.4 (heptet,  $^3J_{\text{CF}}=3.8$  Hz,  $\text{CHCF}_3$ ), 48.5, 44.2, 15.0 ppm.  $^{19}\text{F NMR}$  (282 MHz,  $\text{CDCl}_3$ ):  $\delta$  -63.5 ppm (s, 6F,  $\text{CF}_3$ ). **MS** (ESI):  $m/z=346.1$  [ $\text{M}^+$ ].

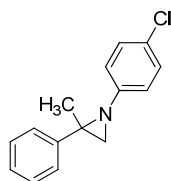
#### 3.5.1.5. *N*-(3,5-bis(trifluoromethyl)phenyl)-2-diphenyl aziridine (**64**)



Compound **64** was obtained from diphenylethylene and 3,5-bis(trifluoromethyl)phenyl azide. The crude was purified by flash chromatography (silica gel, 60  $\mu$ m, AcOEt/hexane 1:9 + 5% of TEA).

$^1\text{H NMR}$  (300 MHz,  $\text{CDCl}_3$ ):  $\delta$  7.84 (d, 1H,  $J=7.3$  Hz,  $\text{H}_{\text{Ar}}$ ), 7.65-7.58 (m, 1H,  $\text{H}_{\text{Ar}}$ ), 7.54-7.46 (m, 1H,  $\text{H}_{\text{Ar}}$ ), 7.30 (s, 8H,  $\text{H}_{\text{Ar}}$ ), 3.09 ppm (s, 2H,  $\text{H}_{\text{CH}_2}$ ).  $^{13}\text{C NMR}$  (75 MHz,  $\text{CDCl}_3$ ):  $\delta$  151.2, 138.3, 137.6, 132.4, 131.5 (q,  $^2J_{\text{CF}}=33.1$  Hz,  $\text{CCF}_3$ ), 130.1, 128.7, 128.4, 128.3, 127.9, 115.1 (heptet,  $^3J_{\text{CF}}=4.5$  Hz,  $\text{CHCF}_3$ ), 53.0, 40.5 ppm.  $^{19}\text{F NMR}$  (282 MHz,  $\text{CDCl}_3$ ):  $\delta$  -63.6 ppm (s, 6F,  $\text{CF}_3$ ). **MS** (ESI):  $m/z=408.1$  [ $\text{M}^+$ ].

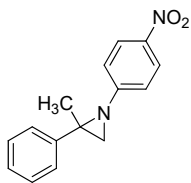
#### 3.5.1.6. *N*-(4-chlorophenyl)-2-methyl-2-phenyl aziridine (**65**)



Compound **65** was obtained from  $\alpha$ -methylstyrene and 4-chlorophenyl azide. The crude was purified by flash chromatography (silica gel, 60  $\mu$ m, AcOEt/hexane 1:9 + 5% of TEA). The collected data are in accord with those reported in literature.<sup>6b</sup>

$^1\text{H NMR}$  (300 MHz,  $\text{CDCl}_3$ ):  $\delta$  8.19 (d, 2H,  $J=9.0$  Hz,  $\text{H}_{\text{Ar}}$ ), 7.51 (d, 2H,  $J=7.2$  Hz,  $\text{H}_{\text{Ar}}$ ), 7.40 (pst, 2H,  $J=7.2$  Hz,  $\text{H}_{\text{Ar}}$ ), 7.34 (t, 1H,  $J=7.2$  Hz,  $\text{H}_{\text{Ar}}$ ), 7.02 (d, 2H,  $J=9.0$  Hz,  $\text{H}_{\text{Ar}}$ ), 2.69 (s, 1H,  $\text{H}_{\text{CH}_2}$ ), 2.42 (s, 1H,  $\text{H}_{\text{CH}_2}$ ), 1.50 ppm (s, 3H,  $\text{H}_{\text{CH}_3}$ ).

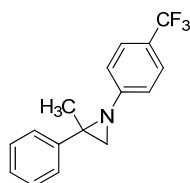
### 3.5.1.7. *N*-(4-nitrophenyl)-2-methyl-2-phenyl aziridine (**66**)



Compound **66** was obtained from  $\alpha$ -methylstyrene and 4-nitrophenyl azide. The crude was purified by flash chromatography (silica gel, 60  $\mu$ m, AcOEt/hexane 1:9 + 5% of TEA). The collected data are in accord with those reported in literature.<sup>6b</sup>

<sup>1</sup>H NMR (300 MHz, CDCl<sub>3</sub>):  $\delta$  8.19 (d, 2H,  $J$ =9.0 Hz, H<sub>Ar</sub>), 7.51 (d, 2H,  $J$ =7.2 Hz, H<sub>Ar</sub>), 7.40 (pst, 2H,  $J$ =7.2 Hz, H<sub>Ar</sub>), 7.34 (t, 1H,  $J$ =7.2 Hz, H<sub>Ar</sub>), 7.02 (d, 2H,  $J$ =9.0 Hz, H<sub>Ar</sub>), 2.69 (s, 1H, H<sub>CH2</sub>), 2.42 (s, 1H, H<sub>CH2</sub>), 1.50 ppm (s, 3H, H<sub>CH3</sub>).

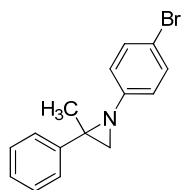
### 3.5.1.8. *N*-(4-(trifluoromethyl)phenyl)-2-methyl-2-phenyl aziridine (**67**)



Compound **67** was obtained from  $\alpha$ -methylstyrene and 4-(trifluoromethyl)phenyl azide. The crude was purified by flash chromatography (silica gel, 60  $\mu$ m, AcOEt/hexane 1:9 + 5% of TEA).

<sup>1</sup>H NMR (300 MHz, CDCl<sub>3</sub>):  $\delta$  7.55 (d, 2H,  $J$ =4.4 Hz, H<sub>Ar</sub>), 7.52 (d, 2H,  $J$ =4.8 Hz, H<sub>Ar</sub>), 7.40 (t, 2H,  $J$ =6.9 Hz, H<sub>Ar</sub>), 7.34-7.28 (m, 1H, H<sub>Ar</sub>), 7.04 (d, 2H,  $J$ =4.4 Hz, H<sub>Ar</sub>), 2.60 (s, 1H, H<sub>CH2</sub>), 2.34 (s, 1H, H<sub>CH2</sub>), 1.44 ppm (s, 3H, H<sub>CH3</sub>). <sup>13</sup>C NMR (75 MHz, CDCl<sub>3</sub>):  $\delta$  153.6, 142.7, 128.4, 127.2, 126.2, 126.1, 126.0, 123.5, (q,  $J_{CF}$ =39 Hz, CF<sub>3</sub>), 120.6, 43.9, 42.1, 20.0 ppm. <sup>19</sup>F NMR (282 MHz, CDCl<sub>3</sub>):  $\delta$  -62.03 ppm (s, 3F, CF<sub>3</sub>). MS (ESI):  $m/z$ =278.1 [M<sup>+</sup>].

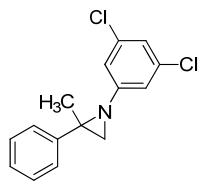
### 3.5.1.9. *N*-(4-bromophenyl)-2-methyl-2-phenyl aziridine (**68**)



Compound **68** was obtained from  $\alpha$ -methylstyrene and 4-bromophenyl azide. The crude was purified by flash chromatography (silica gel, 60  $\mu$ m, AcOEt/hexane 1:9 + 5% of TEA). The collected data are in accord with those reported in literature.<sup>6b</sup>

<sup>1</sup>H NMR (400 MHz, CDCl<sub>3</sub>):  $\delta$  7.53-7.50 (m, 2H, H<sub>Ar</sub>), 7.40 (d, 2H,  $J$ =8.4 Hz, H<sub>Ar</sub>), 7.39-7.36 (m, 2H, H<sub>Ar</sub>), 7.33-7.31 (m, 1H, H<sub>Ar</sub>), 6.86 (d, 2H,  $J$ =8.4 Hz, H<sub>Ar</sub>), 2.55 (s, 1H, H<sub>CH2</sub>), 2.28 (s, 1H, H<sub>CH2</sub>), 1.41 ppm (s, 3H, H<sub>CH3</sub>).

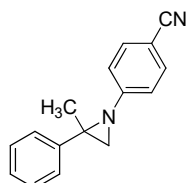
### 3.5.1.10. *N*-(3,5-dichlorophenyl)-2-methyl-2-phenyl aziridine (69)



Compound **69** was obtained from  $\alpha$ -methylstyrene and 3,5-dichlorophenyl azide. The crude was purified by flash chromatography (silica gel, 60  $\mu$ m, AcOEt/hexane 1:9 + 5% of TEA). The collected data are in accord with those reported in literature.<sup>6b</sup>

<sup>1</sup>H NMR (300 MHz, CDCl<sub>3</sub>):  $\delta$  7.50 (d, 2H,  $J=7.2$  Hz, H<sub>Ar</sub>), 7.40 (pst, 2H,  $J=7.2$  Hz, H<sub>Ar</sub>), 7.33 (t, 1H,  $J=7.2$  Hz, H<sub>Ar</sub>), 7.27-7.23 (m, 2H, H<sub>Ar</sub>), 7.01 (d, 2H,  $J=8.5$  Hz, H<sub>Ar</sub>), 2.63 (s, 1H, H<sub>CH2</sub>), 2.35 (s, 1H, H<sub>CH2</sub>), 1.46 ppm (s, 3H, H<sub>CH3</sub>).

### 3.5.1.11. *N*-(4-cyanophenyl)-2-methyl-2-phenyl aziridine (70)

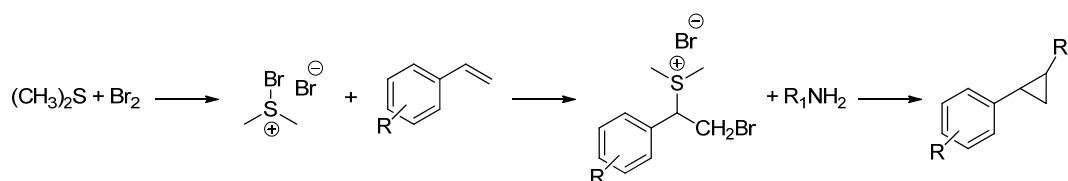


Compound **70** was obtained from  $\alpha$ -methylstyrene and 4-cyanophenyl azide. The crude was purified by flash chromatography (silica gel, 60  $\mu$ m, AcOEt/hexane 1:9 + 5% of TEA). The collected data are in accord with those reported in literature.<sup>6b</sup>

<sup>1</sup>H NMR (300 MHz, CDCl<sub>3</sub>):  $\delta$  7.56 (d, 2H,  $J=8.5$  Hz, H<sub>Ar</sub>), 7.50 (d, 2H,  $J=7.2$  Hz, H<sub>Ar</sub>), 7.40 (pst, 2H,  $J=7.2$  Hz, H<sub>Ar</sub>), 7.33 (t, 1H,  $J=7.2$  Hz, H<sub>Ar</sub>), 7.01 (d, 2H,  $J=8.5$  Hz, H<sub>Ar</sub>), 2.63 (s, 1H, H<sub>CH2</sub>), 2.35 (s, 1H, H<sub>CH2</sub>), 1.46 ppm (s, 3H, H<sub>CH3</sub>).

## 3.6. Synthesis of oxazolidinones

### 3.6.1 Synthesis of *N*-alkyl-phenylaziridines

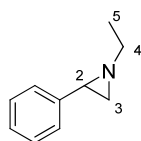


**General procedure:** dimethyl sulphide (14.7 mL,  $2.00 \cdot 10^{-1}$  mol) was dissolved in 90.0 mL of acetonitrile under air. The solution was placed in an ice bath and a solution of bromine (10.2 mL,  $2.00 \cdot 10^{-1}$  mol) in 10.0 mL of acetonitrile was added dropwise over 30 minutes. During the addition, the formation of light orange crystals of bromodimethyl sulfonium bromide was observed. At the end of the addition, the reaction was stirred for 10 minutes then the desired styrene ( $2.00 \cdot 10^{-1}$  mol) was added to the solution. The reaction mixture was stirred for 30 minutes and 70.0 mL of diethyl ether was added. A white solid precipitated and it was collected by filtration, washed several times with diethyl ether and dried *in vacuo*. The white crystals of styrene sulphonium bromide ( $8.62 \cdot 10^{-3}$  mol) were suspended in 20.0 mL of water and a solution of amine ( $4.30 \cdot 10^{-2}$  mol) in 5.00 mL of water was added dropwise and the resulting mixture was stirred overnight. Then, 20.0 mL



of brine and 20.0 mL of diethyl ether were added and the phases were separated. Aqueous phase was washed twice with 20.0 mL of diethyl ether and the combined organic phases were dried over Na<sub>2</sub>SO<sub>4</sub>. The solvent was evaporated under reduced pressure and the crude was purified by flash chromatography.

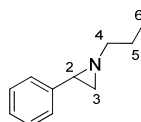
### 3.6.1.1. Synthesis of 1-ethyl-2-phenylaziridine



The general procedure for the synthesis of aziridines was followed using styrene and ethylamine as reagents to obtain a yellowish oil (0.221, 20%). The collected data are in accord with those reported in literature.<sup>20</sup>

<sup>1</sup>H NMR (400 MHz, CDCl<sub>3</sub>): δ 7.32-7.12 (m, 5H, H<sub>Ar</sub>), 2.42 (q, 2H, *J*=7.1 Hz, H<sup>4</sup>), 2.27 (dd, 1H, *J*=6.4, 3.3 Hz, H<sup>2</sup>), 1.87 (d, 1H, *J*=3.2, H<sup>3A</sup>), 1.62 (d, 1H, *J*=6.5 Hz, H<sup>3B</sup>), 1.19 ppm (t, 3H, *J*=7.1 Hz, H<sup>5</sup>).

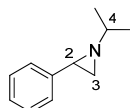
### 3.6.1.2. Synthesis of 1-propyl-2-phenylaziridine



The general procedure for the synthesis of aziridines was followed using styrene and propylamine as reagents to obtain a yellowish oil (0.303 g, 21%). The collected data are in accord with those reported in literature.<sup>20</sup>

<sup>1</sup>H NMR (400 MHz, CDCl<sub>3</sub>): δ 7.34-7.19 (m, 5H, H<sub>Ar</sub>), 2.48 (dt, 1H, <sup>2</sup>*J*=11.5 Hz, *J*=7.5 Hz, H<sup>4A</sup>), 2.30 (m, 2H, H<sup>4B</sup> and H<sup>2</sup>), 1.90 (d, 1H, *J*=3.2 Hz, H<sup>3B</sup>), 1.65 (m, 3H, H<sup>3A</sup> and H<sup>5</sup>), 0.97 ppm (t, 3H, *J*=7.4 Hz, H<sup>6</sup>).

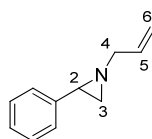
### 3.6.1.3. Synthesis of 1-isopropyl-2-phenylaziridine



The general procedure for the synthesis of aziridines was followed using styrene and isopropylamine as reagents to obtain a yellowish oil (0.511 g, 37%). The collected data are in accord with those reported in literature.<sup>20</sup>

<sup>1</sup>H NMR (400 MHz, CDCl<sub>3</sub>): δ 7.30-7.18 (m, 5H, H<sub>Ar</sub>), 2.34 (dd, 1H, *J*=6.4, 3.3 Hz, H<sup>2</sup>), 1.89 (d, 1H, *J*=3.3 Hz, H<sup>3B</sup>), 1.66 (d, 1H, *J*=6.6 Hz, H<sup>3A</sup>), 1.61 (m, 1H, H<sup>4</sup>), 1.19 (d, 3H, *J*=1.4 Hz, H<sub>CH<sub>3</sub></sub>), 1.17 ppm (d, 3H, *J*=1.3 Hz, H<sub>CH<sub>3</sub></sub>).

### 3.6.1.4. Synthesis of 1-allyl-2-phenylaziridine

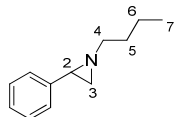


The general procedure for the synthesis of aziridines was followed using styrene and allylamine as reagents to obtain a yellowish oil (0.848 g, 60%). The collected data are in accord with those reported in literature.<sup>21</sup>

<sup>1</sup>H NMR (300 MHz, CDCl<sub>3</sub>): δ 7.31-7.18 (m, 5H, H<sub>Ar</sub>), 5.96 (ddd, 1H, *J*=22.4, 10.7, 5.5 Hz, H<sup>5</sup>), 5.22 (d, 1H,

$J=17.2$  Hz,  $H^{6, trans}$ ), 5.10 (d, 1H,  $J=10.4$  Hz,  $H^{6, cis}$ ), 3.14 (dd, 1H,  $^2J=14.3$  Hz,  $J=5.4$  Hz,  $H^{4B}$ ), 2.98 (dd, 1H,  $^2J=14.2$  Hz,  $J=5.4$  Hz,  $H^{4A}$ ), 2.35 (dd, 1H,  $J=6.4, 3.4$  Hz,  $H^2$ ), 1.93 (d, 1H,  $J=3.3$  Hz,  $H^{3A}$ ), 1.71 ppm (d, 1H,  $J=6.5$  Hz,  $H^{3B}$ ).

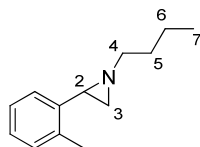
### 3.6.1.5. Synthesis of 1-butyl-2-phenylaziridine



The general procedure for the synthesis of aziridines was followed using styrene and butylamine as reagents to obtain a yellowish oil (2.02 g, 60%). The collected data are in accord with those reported in literature.<sup>20</sup>

$^1H$  NMR (400 MHz,  $CDCl_3$ ):  $\delta$  7.29-7.12 (5H, m,  $H_{Ar}$ ), 2.45 (dt, 1H,  $^2J=11.5$  Hz,  $J=7.3$  Hz,  $H^{4A}$ ), 2.28 (dt, 1H,  $^2J=11.5$  Hz,  $J=7.3$  Hz,  $H^{4B}$ ), 2.23 (dd, 1H,  $J=6.4, 3.2$  Hz,  $H^2$ ), 1.83 (d, 1H,  $J=3.2$  Hz,  $H^{3A}$ ), 1.59 (d, 1H,  $J=6.5$  Hz,  $H^{3B}$ ), 1.55 (m, 2H,  $H^5$ ), 1.35 (m, 2H,  $H^6$ ), 0.88 ppm (t, 3H,  $J=7.3$  Hz,  $H^7$ ).

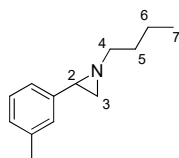
### 3.6.1.6. Synthesis of 1-butyl-2-(2-methyl)phenylaziridine



The general procedure for the synthesis of aziridines was followed using 2-methylstyrene and butylamine as reagents to obtain a yellowish oil (0.359 g, 55%).

$^1H$  NMR (400 MHz,  $CDCl_3$ ):  $\delta$  7.32-7.27 (1H, m,  $H_{Ar}$ ), 7.20-7.09 (3H, m,  $H_{Ar}$ ), 2.51 (dt, 1H,  $^2J=11.0$  Hz,  $J=7.5$  Hz,  $H^{4A}$ ), 2.45-2.35 (m, 2H,  $H^{4B}$  and  $H^2$ ), 2.41 (s, 3H,  $H_{CH_3}$ ), 1.80 (d, 1H,  $J=3.1$  Hz,  $H^{3A}$ ), 1.66 (d, 1H,  $J=6.5$  Hz,  $H^{3B}$ ), 1.65-1.58 (m, 2H,  $H^5$ ), 1.50-1.37 (m, 2H,  $H^6$ ), 0.95 ppm (t, 3H,  $J=7.3$  Hz,  $H^7$ ).  $^{13}C$  NMR (100 MHz,  $CDCl_3$ ):  $\delta$  138.5, 136.3, 129.6, 126.6, 126.2, 126.1, 61.7, 39.5, 36.7, 32.2, 20.7, 19.2, 14.2 ppm. MS (ESI):  $m/z=190.18$  [M+H].

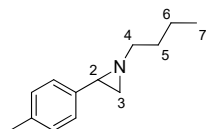
### 3.6.1.7. Synthesis of 1-butyl-2-(3-methyl)phenylaziridine



The general procedure for the synthesis of aziridines was followed using 3-methylstyrene and butylamine as reagents to obtain a yellowish oil (0.254 g, 46%).

$^1H$  NMR (300 MHz,  $CDCl_3$ ):  $\delta$  7.22-7.17 (1H, m,  $H_{Ar}$ ), 7.08-7.03 (3H, m,  $H_{Ar}$ ), 2.51 (dt, 1H,  $^2J=11.5$  Hz,  $J=7.3$  Hz,  $H^{4A}$ ), 2.35 (m, 1H,  $H^{4B}$ ), 2.35 (s, 3H,  $H_{CH_3}$ ), 2.27 (dd, 1H,  $J=6.4, 3.2$  Hz,  $H^2$ ), 1.89 (d, 1H,  $J=3.3$  Hz,  $H^{3A}$ ), 1.65 (d, 1H,  $J=6.5$  Hz,  $H^{3B}$ ), 1.63 (m, 2H,  $H^5$ ), 1.41 (dq, 2H,  $J=14.5, 7.2$  Hz,  $H^6$ ), 0.94 ppm (t, 3H,  $J=7.3$  Hz,  $H^7$ ).  $^{13}C$  NMR (75 MHz,  $CDCl_3$ ):  $\delta$  158.8, 140.3, 131.3, 129.2, 128.4, 126.9, 126.4, 113.9, 64.3, 55.3, 41.5, 37.9 ppm. MS (ESI):  $m/z=190.18$  [M+H].

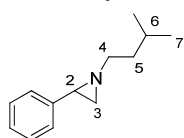
### 3.6.1.8. Synthesis of 1-butyl-2-(4-methyl)phenylaziridine



The general procedure for the synthesis of aziridines was followed using 4-methylstyrene and butylamine as reagents to obtain a yellowish oil (0.416 g, 54%). The collected data are in accord with those reported in literature.<sup>22</sup>

**<sup>1</sup>H NMR** (400 MHz, CDCl<sub>3</sub>): δ 7.13 (q, 4H, *J*=8.1 Hz, H<sub>Ar</sub>), 2.52 (dt, 1H, <sup>2</sup>*J*=11.5 Hz, *J*=7.3 Hz, H<sup>4A</sup>), 2.32-2.25 (m, 2H, H<sup>4B</sup> and H<sup>2</sup>), 2.33 (s, 3H, H<sub>CH3</sub>), 1.87 (d, 1H, *J*=3.2 Hz, H<sup>3A</sup>), 1.63 (d, 1H, *J*=6.3 Hz, H<sup>3B</sup>), 1.65-1.58 (m, 2H, H<sup>5</sup>), 1.49-1.33 (m, 2H, H<sup>6</sup>), 0.93 ppm (t, 3H, *J*=7.3 Hz, H<sup>7</sup>). **<sup>13</sup>C NMR** (100 MHz, CDCl<sub>3</sub>): δ 137.6, 136.4, 129.1, 126.2, 61.7, 41.2, 37.2, 32.1, 21.2, 20.7, 14.2 ppm.

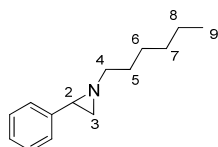
### 3.6.1.9. Synthesis of 1-isoamyl-2-phenylaziridine



The general procedure for the synthesis of aziridines was followed using styrene and isoamylamine as reagents to obtain a yellowish oil (1.24 g, 68%). The data are in accord with those reported in literature.<sup>19a</sup>

**<sup>1</sup>H NMR** (400 MHz, CDCl<sub>3</sub>): δ 7.37-7.31 (m, 4H, H<sub>Ar</sub>), 7.29-7.24 (m, 1H, H<sub>Ar</sub>), 2.61-2.50 (m, 1H, H<sup>4A</sup>), 2.48-2.37 (m, 1H, H<sup>4B</sup>), 2.35 (dd, 1H, *J*=6.5, 3.3 Hz, H<sup>2</sup>), 1.94 (d, 1H, *J*=3.1 Hz, H<sup>3A</sup>), 1.77 (heptet, 1H, *J*=6.6 Hz, H<sup>6</sup>), 1.70 (d, 1H, *J*=6.5 Hz, H<sup>3B</sup>), 1.65-1.55 (m, 2H, H<sup>5</sup>), 0.99 ppm (dd, 6H, *J*=6.9 Hz, <sup>4</sup>*J*=1.6 Hz, H<sup>7</sup>). **<sup>13</sup>C NMR** (100 MHz, CDCl<sub>3</sub>): δ 140.6, 128.2, 126.7, 126.1, 60.0, 41.2, 38.7, 37.8, 26.2, 22.7 ppm.

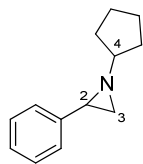
### 3.6.1.10. Synthesis of 1-hexyl-2-phenylaziridine



The general procedure for the synthesis of aziridines was followed using styrene and hexylamine as reagents to obtain a yellowish oil (2.31 g, 72%). The data are in accord with those reported in literature.<sup>19b</sup>

**<sup>1</sup>H NMR** (400 MHz, CDCl<sub>3</sub>): δ 7.40-7.05 (m, 5H, H<sub>Ar</sub>), 2.46 (dt, 1H, <sup>2</sup>*J*=11.5 Hz, *J*=7.3 Hz, H<sup>4A</sup>), 2.28 (dt, 1H, <sup>2</sup>*J*=11.5 Hz, *J*=7.3 Hz, H<sup>4B</sup>), 2.26 (dd, 1H, *J*=6.4, 3.2 Hz, H<sup>2</sup>), 1.85 (d, 1H, *J*=3.2 Hz, H<sup>3A</sup>), 1.62 (d, 1H, *J*=6.3 Hz, H<sup>3B</sup>), 1.60 (m, 2H, H<sup>5</sup>), 1.35 (m, 2H, H<sup>6</sup>), 1.31 (m, 4H, H<sup>7</sup> and H<sup>8</sup>), 0.86 ppm (t, 3H, *J*=6.9 Hz, H<sup>9</sup>). **<sup>13</sup>C NMR** (100 MHz, CDCl<sub>3</sub>): δ 140.6, 128.3, 126.8, 126.2, 61.9, 41.3, 37.8, 31.9, 29.8, 27.2, 22.6, 14.1 ppm.

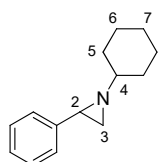
### 3.6.1.11. Synthesis of 1-cyclopentyl-2-phenylaziridine



The general procedure for the synthesis of aziridines was followed using styrene and cyclopentylamine as reagents to obtain a yellowish oil (1.43 g, 81%). The collected data are in accord with those reported in literature.<sup>22</sup>

**<sup>1</sup>H NMR** (300 MHz, CDCl<sub>3</sub>): δ 7.26-7.24 (m, 4H, H<sub>Ar</sub>), 7.18-7.15 (m, 1H, H<sub>Ar</sub>), 2.34 (dd, 1H, *J*=6.5, 3.3 Hz, H<sup>2</sup>), 2.09-2.00 (m, 1H, H<sup>4</sup>), 1.81 (d, 1H, *J*=3.1 Hz, H<sup>3A</sup>), 1.79-1.74 (m, 1H, H<sub>cyclopentyl</sub>), 1.72-1.66 (m, 4H, H<sub>cyclopentyl</sub>), 1.64 (d, 1H, *J*=6.5 Hz, H<sup>3B</sup>), 1.53-1.49 ppm (m, 2H, H<sub>cyclopentyl</sub>). **<sup>13</sup>C NMR** (75 MHz, CDCl<sub>3</sub>): δ 140.8, 128.2, 126.7, 126.5, 72.49, 40.9, 37.0, 33.0, 32.3, 24.5, 24.4 ppm.

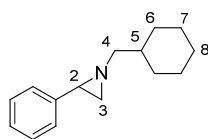
### 3.6.1.12. Synthesis of 1-cyclohexyl-2-phenylaziridine



The general procedure for the synthesis of aziridines was followed using styrene and cyclohexylamine as reagents to obtain a yellowish oil (1.17 g, 77%). The collected data are in accord with those reported in literature.<sup>20</sup>

**<sup>1</sup>H NMR** (400 MHz, CDCl<sub>3</sub>): δ 7.24-7.20 (m, 4H, H<sub>Ar</sub>), 7.19-7.12 (m, 1H, H<sub>Ar</sub>), 2.30 (dd, 1H, *J*=6.5, 3.3 Hz, H<sup>2</sup>), 1.85-1.80 (m, 1H, H<sup>4</sup>), 1.83 (d, 1H, *J*=3.1 Hz, H<sup>3A</sup>), 1.82-1.70 (m, 2H, H<sub>cyclohexyl</sub>), 1.61 (d, 1H, *J*=6.5 Hz, H<sup>3B</sup>), 1.47-1.37 (m, 2H, H<sub>cyclohexyl</sub>), 1.28-1.15 ppm (m, 6H, H<sub>cyclohexyl</sub>).

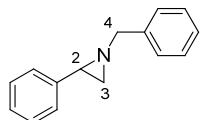
### 3.6.1.13. Synthesis of 1-cyclohexylmethyl-2-phenylaziridine



The general procedure for the synthesis of aziridines was followed using styrene and cyclohexylmethylamine as reagents to obtain a yellowish oil (1.57 g, 82%). The collected data are in accord with those reported in literature.<sup>23</sup>

**<sup>1</sup>H NMR** (300 MHz, CDCl<sub>3</sub>): δ 7.30-7.17 (m, 5H, H<sub>Ar</sub>), 2.42 (dd, 1H, <sup>2</sup>*J*=11.7 Hz, *J*=7.0 Hz, H<sup>4A</sup>), 2.25 (dd, 1H, *J*=6.4, 3.2 Hz, H<sup>2</sup>), 2.09 (dd, 1H, <sup>2</sup>*J*=11.7 Hz, *J*=6.4 Hz, H<sup>4B</sup>), 1.85 (d, 1H, *J*=6.5 Hz, H<sup>3A</sup>), 1.79-1.58 (m, 5H, H<sub>cyclohexyl</sub>), 1.62 (d, 1H, *J*=6.5 Hz, H<sup>3B</sup>), 1.20-1.10 (m, 3H, H<sub>cyclohexyl</sub>), 0.98-0.90 ppm (m, 2H, H<sub>cyclohexyl</sub>).

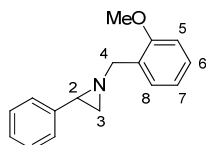
### 3.6.1.14. Synthesis of 1-benzyl-2-phenylaziridine



The general procedure for the synthesis of aziridines was followed using styrene and benzylamine as reagents to obtain a yellowish oil (1.46 g, 80%). The collected data are in accord with those reported in literature.<sup>20</sup>

**<sup>1</sup>H NMR** (400 MHz, CDCl<sub>3</sub>): δ 7.47-7.28 (m, 10H, H<sub>Ar</sub>), 3.74 (ABq, 2H, *J*=13.7 Hz, Δ*v*<sub>AB</sub>=30.57 Hz, H<sup>4</sup>), 2.59 (dd, 1H, *J*=6.4, 3.3 Hz, H<sup>2</sup>), 2.07 (d, 1H, *J*=3.3 Hz, H<sup>3A</sup>), 1.93 ppm (d, 1H, *J*=6.5 Hz, H<sup>3B</sup>).

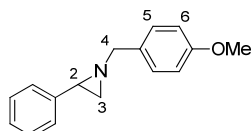
### 3.6.1.15. Synthesis of 1-(2-methoxy)benzyl-2-phenylaziridine



The general procedure for the synthesis of aziridines was followed using styrene and (2-methoxy)benzylamine as reagents to obtain a yellowish oil (1.52 g, 84%).

**<sup>1</sup>H NMR** (400 MHz, CDCl<sub>3</sub>): δ 7.47 (d, 1H, *J*=7.5 Hz, H<sup>8</sup>), 7.30-7.25 (m, 4H, H<sub>Ar</sub>), 7.18-7.22 (m, 1H, H<sup>6</sup>), 6.90 (dd, 1H, *J*=7.8, 7.1 Hz, H<sup>7</sup>), 6.83 (d, 1H, *J*=8.1 Hz, H<sup>5</sup>), 3.80 (s, 3H, H<sub>OCH<sub>3</sub></sub>), 3.79 (d, 1H, *J*=13.4 Hz, H<sup>4B</sup>), 3.53 (d, 1H, *J*=14.9 Hz, H<sup>4A</sup>), 2.48 (dd, 1H, *J*=6.5, 3.4 Hz, H<sup>2</sup>), 2.00 (d, 1H, *J*=3.4 Hz, H<sup>3B</sup>), 1.86 ppm (d, 1H, *J*=6.5 Hz, H<sup>3A</sup>). **<sup>13</sup>C NMR** (100 MHz, CDCl<sub>3</sub>): δ 156.9, 140.6, 128.9, 128.4, 127.9, 127.8, 126.9, 126.4, 120.7, 109.9, 59.1, 55.3, 41.7, 38.2 ppm. **MS** (ESI): *m/z*=240.39 [M+H].

### 3.6.1.16. Synthesis of 1-(4-methoxy)benzyl-2-phenylaziridine



The general procedure for the synthesis of aziridines was followed using styrene and 4-(methoxy)benzylamine as reagents to obtain a yellowish oil (1.46 g, 80%).

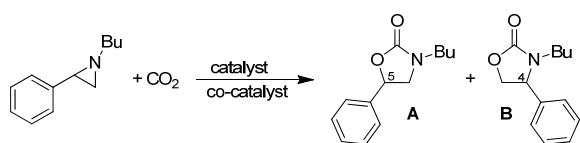
**<sup>1</sup>H NMR** (300 MHz, CDCl<sub>3</sub>): δ 7.29-7.18 (m, 7H, H<sub>Ar</sub>), 6.84 (d, 2H, *J*=8.6 Hz, H<sup>6</sup>), 3.77 (s, 3H, H<sub>OCH<sub>3</sub></sub>), 3.57 (ABq, 2H, *J*=13.4 Hz, Δ*v*<sub>AB</sub>=22.8 Hz, H<sup>4</sup>), 2.48 (dd, 1H, *J*=6.5, 3.3 Hz, H<sup>2</sup>), 1.95 (d, 1H, *J*=3.3 Hz, H<sup>3A</sup>), 1.82 ppm (d, 1H, *J*=6.5 Hz, H<sup>3B</sup>). **<sup>13</sup>C NMR** (75 MHz, CDCl<sub>3</sub>): δ 158.8, 140.3, 131.3, 129.2, 128.4, 126.9, 126.4, 113.9, 64.3, 55.3, 41.5, 37.9 ppm. **MS** (ESI): *m/z*=240.14 [M+H].

## 3.6.2 Synthesis of oxazolidinones

**General catalytic procedure:** In a 100 mL glass liner equipped with a screw cap and a glass wool, tetrabutyl ammonium chloride (14.2 mg, 5.13·10<sup>-5</sup> mol) and aziridine (5.13·10<sup>-4</sup> mol) were added to a solution of catalyst (5.13·10<sup>-6</sup> mol) in benzene (2.50 mL). The dark mixture was cooled with liquid nitrogen and the flask was transferred into a stainless-steel autoclave, three vacuum-nitrogen cycles were performed and CO<sub>2</sub> was charged at room temperature. The autoclave was placed in a preheated oil bath and stirred for the desired time, then it

was cooled at room temperature and slowly vented. The solvent was evaporated to dryness and the crude was purified by flash chromatography.

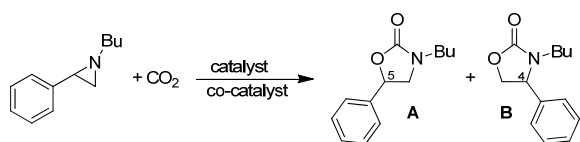
**Table 1.** Screening of catalysts.<sup>a</sup>



Entry	Catalyst	co-catalyst	yield (%) <sup>b</sup>	A/B <sup>b</sup>
1	-	-	-	-
2	Zn(TPP)	-	-	-
3	Co(TPP)	-	-	-
4	Ag(4-CF <sub>3</sub> TPP)	-	-	-
5	Fe(F <sub>20</sub> TPP)Cl	-	6	80:20
6	Ru(TPP)CO	-	-	-
7	Ru(TPP)(NAr) <sub>2</sub> Ar=3,5(CF <sub>3</sub> ) <sub>2</sub> C <sub>6</sub> H <sub>3</sub>	-	10	99:1
8	Fe(F <sub>20</sub> TPP)Cl	TBACl	30	95:5
9	Fe(F <sub>20</sub> TPP)OMe	TBACl	34	92:8
10	Cr(4-CITPP)Cl	TBACl	-	-
12	Ru(TPP)(NAr) <sub>2</sub> Ar=3,5(CF <sub>3</sub> ) <sub>2</sub> C <sub>6</sub> H <sub>3</sub>	TBACl	71	88:12

<sup>a</sup>Reaction conditions: cat./co-cat./aziridine 1:10:100 in benzene. In a steel autoclave at 100°C and 30 bar CO<sub>2</sub> for 6 h. <sup>b</sup>Determined by <sup>1</sup>H NMR using 2,4-dinitrotoluene as the internal standard.

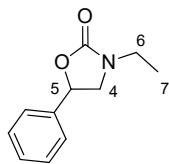
**Table 2.** Screenign of the reaction conditions.<sup>a</sup>



Entry	Temperature (°C)	CO <sub>2</sub> Pressure (bar)	Solvent	Co-catalyst	yield (%) <sup>b</sup>	A/B <sup>b</sup>
1	100	30	Benzene	TBACl	71	88:12
2	100	30	Benzene	TBABr	68	85:15
3	100	30	Benzene	TBAI	-	-
4	50	30	Benzene	TBACl	-	-
5	100	30	Benzene/DMF (10%)	TBACl	45	99:1
6	100	30	Dichloroethane	TBACl	22	90:10
7	100	6	Benzene	TBACl	70	90:10
8	100	1	Benzene	TBACl	35	94:6
9	100	Pressure tube	Benzene	TBACl	13	93:7

<sup>a</sup>Reaction conditions: cat./co-cat./aziridine 1:10:100 in the desired solvent. In a steel autoclave for 6 h. <sup>b</sup>Determined by <sup>1</sup>H NMR using 2,4-dinitrotoluene as the internal standard.

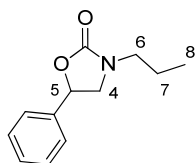
### 3.6.2.1. 3-Ethyl-5-phenyloxazolidin-2-one (72)



Compound **72** was synthesised from *N*-ethyl-phenyl aziridine. The crude was purified by flash chromatography (silica gel, 60  $\mu$ m, AcOEt/hexane 2:8) to obtain a yellowish oil. The collected data are in accord with those reported in literature.<sup>19a</sup>

<sup>1</sup>H NMR (300 MHz, CDCl<sub>3</sub>):  $\delta$  7.34-7.65 (m, 5H, H<sub>Ar</sub>), 5.46 (m, 1H, H<sup>5</sup>), 3.93 (t, 1H,  $J=8.8$  Hz, H<sup>4A</sup>), 3.40-3.39 (m, 3H, H<sup>4B</sup> and H<sup>6</sup>), 1.14 ppm (t, 3H,  $J=7.1$  Hz, H<sup>7</sup>).

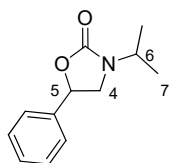
### 3.6.2.2. 3-Propyl-5-phenyloxazolidin-2-one (73)



Compound **73** was synthesised from *N*-propyl-phenyl aziridine. The crude was purified by flash chromatography (silica gel, 60  $\mu$ m, AcOEt/hexane 2:8) to obtain a yellowish oil. The collected data are in accord with those reported in literature.<sup>19a</sup>

<sup>1</sup>H NMR (300 MHz, CDCl<sub>3</sub>):  $\delta$  7.42-7.34 (m, 5H, H<sub>Ar</sub>), 5.49 (t, 1H,  $J=8.1$  Hz, H<sup>5</sup>), 3.91 (t, 1H,  $J=8.7$  Hz, H<sup>4B</sup>), 3.43 (dd, 1H,  $J=8.5$ ,  $J=7.5$  Hz, H<sup>4A</sup>), 3.35-3.17 (m, 2H, H<sup>6</sup>), 1.67-1.51 (m, 2H, H<sup>7</sup>), 0.94 ppm (t, 3H,  $J=7.4$  Hz, H<sup>8</sup>).

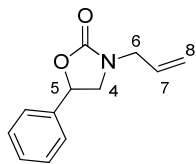
### 3.6.2.3. 3-Isopropyl-5-phenyloxazolidin-2-one (74)



Compound **74** was synthesised from *N*-isopropyl-phenyl aziridine. The crude was purified by flash chromatography (silica gel, 60  $\mu$ m, AcOEt/hexane 2:8) to obtain a yellowish oil. The collected data are in accord with those reported in literature.<sup>19a</sup>

<sup>1</sup>H NMR (400 MHz, CDCl<sub>3</sub>):  $\delta$  7.42-7.31 (m, 5H, H<sub>Ar</sub>), 5.47 (t, 1H,  $J=8.1$  Hz, H<sup>5</sup>), 4.18 (dt, 1H,  $J=13.5$ , 6.7 Hz, H<sup>6</sup>), 3.86 (t, 1H,  $J=8.7$  Hz, H<sup>4B</sup>), 3.37 (t, 1H,  $J=8.0$ , H<sup>4A</sup>), 1.22 (d, 3H,  $J=6.8$  Hz, H<sup>7A</sup>), 1.16 ppm (d, 3H,  $J=6.7$  Hz, H<sup>7B</sup>).

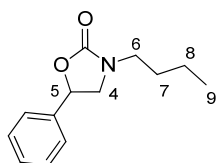
#### 3.6.2.4. 3-Allyl-5-phenyloxazolidin-2-one (75)



Compound **75** was synthesised from *N*-allyl-phenyl aziridine. The crude was purified by flash chromatography (silica gel, 60  $\mu$ m, AcOEt/hexane 2:8) to obtain a yellowish oil. The collected data are in accord with those reported in literature.<sup>24</sup>

<sup>1</sup>H NMR (400 MHz, CDCl<sub>3</sub>):  $\delta$  7.43-7.35 (m, 5H, H<sub>Ar</sub>), 5.804-5.73 (m, 1H, H<sup>7</sup>), 5.50 (t, 1H,  $J$ =8.0 Hz, H<sup>8A</sup>), 5.28-5.22 (m, 2H, H<sup>8B</sup> and H<sup>5</sup>), 3.98-3.84 (m, 3H, H<sup>4A</sup>, H<sup>4B</sup> and H<sup>6A</sup>), 3.44-3.38 ppm (m, 1H, H<sup>6B</sup>).

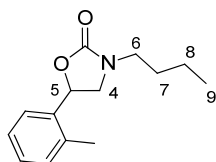
#### 3.6.2.5. 3-Butyl-5-phenyloxazolidin-2-one (76)



Compound **76** was synthesised from *N*-butyl-phenyl aziridine. The crude was purified by flash chromatography (silica gel, 60  $\mu$ m, AcOEt/hexane 2:8) to obtain a yellowish oil. The collected data are in accord with those reported in literature.<sup>19a</sup>

<sup>1</sup>H NMR (400 MHz, CDCl<sub>3</sub>):  $\delta$  7.37 (m, 5H, H<sub>Ar</sub>), 5.48 (t, 1H,  $J$ =8.0 Hz, H<sup>5</sup>), 3.91 (t, 1H,  $J$ =8.6 Hz, H<sup>4B</sup>), 3.43 (t, 1H,  $J$ =8.0, H<sup>4A</sup>), 3.38-3.20 (m, 2H, H<sup>6</sup>), 1.63-1.47 (m, 1H, H<sub>CH2</sub>), 1.42-1.30 (m, 1H, H<sub>CH2</sub>), 0.94 ppm (t, 3H,  $J$ =7.3 Hz, H<sup>9</sup>).

#### 3.6.2.6. 3-Butyl-5-(2-methyl)phenyloxazolidin-2-one (77)

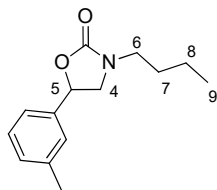


Compound **77** was synthesised from *N*-butyl-2-(2-methyl)phenyl aziridine. The crude was purified by flash chromatography (silica gel, 60  $\mu$ m, AcOEt/hexane 2:8) to obtain a yellowish oil.

<sup>1</sup>H NMR (400 MHz, CDCl<sub>3</sub>):  $\delta$  7.27 (dd, 1H,  $J$ =8.8, 6.4 Hz, H<sub>Ar</sub>), 7.16-7.12 (m, 4H, H<sub>Ar</sub>), 5.43 (t, 1H,  $J$ =8.1 Hz, H<sup>5</sup>), 3.89 (d, 1H,  $J$ =13.4 Hz, H<sup>4B</sup>), 3.40 (dd, 1H,  $J$ =8.6, 6.4 Hz, H<sup>4A</sup>), 3.37-3.20 (m, 2H, H<sup>6</sup>), 2.35 (s, 3H, H<sub>CH3</sub>), 1.58-1.48 (m, 1H, H<sub>CH2</sub>), 1.38-1.30 (m, 1H, H<sub>CH2</sub>), 0.93 ppm (t, 3H,  $J$ =7.3 Hz, H<sup>9</sup>). <sup>13</sup>C NMR (100 MHz, CDCl<sub>3</sub>):  $\delta$  158.0, 138.7, 129.5, 128.8, 126.1, 122.6, 74.39, 52.2, 43.9, 29.4, 21.4, 19.9, 13.7 ppm. MS (ESI):  $m/z$ =256.24 [M+Na].



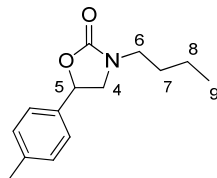
### 3.6.2.7. 3-Butyl-5-(3-methyl)phenyloxazolidin-2-one (78)



Compound **78** was synthesised from *N*-butyl-2-(3-methyl)phenyl aziridine. The crude was purified by flash chromatography (silica gel, 60  $\mu$ m, AcOEt/hexane 2:8) to obtain a yellowish oil.

$^1\text{H NMR}$  (400 MHz,  $\text{CDCl}_3$ ):  $\delta$  7.48-7.40 ppm (m, 1H,  $\text{H}_{\text{Ar-ortho}}$ ), 7.30-7.25 (m, 4H,  $\text{H}_{\text{Ar-meta}}$  and  $\text{H}_{\text{Ar-para}}$ ), 7.21-7.16 (m, 1H,  $\text{H}_{\text{Ar-ortho}}$ ), 5.67 (t, 1H,  $J=8.1$  Hz,  $\text{H}^5$ ), 3.95 (t, 1H,  $J=8.7$  Hz,  $\text{H}^{4\text{A}}$ ), 3.40-3.20 (m, 3H,  $\text{H}^{4\text{B}}$  and  $\text{H}^6$ ), 2.31 (s, 3H,  $\text{H}_{\text{CH}_3}$ ), 1.60-1.47 (m, 2H,  $\text{H}^7$ ), 1.41-1.29 (m, 2H,  $\text{H}^8$ ), 0.94 ppm (t, 3H,  $J=7.3$  Hz,  $\text{H}^9$ ).  $^{13}\text{C NMR}$  (100 MHz,  $\text{CDCl}_3$ ):  $\delta$  157.9, 137.2, 134.1, 130.7, 128.4, 126.5, 124.6, 72.0, 51.3, 43.9, 29.4, 19.8, 18.9, 13.6 ppm. **MS** (ESI):  $m/z=256.27$  [ $\text{M}+\text{Na}$ ].

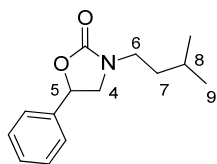
### 3.6.2.8. 3-Butyl-5-(4-methyl)phenyloxazolidin-2-one (79)



Compound **79** was synthesised from *N*-butyl-2-(4-methyl)phenyl. The crude was purified by flash chromatography (silica gel, 60  $\mu$ m, AcOEt/hexane 2:8) to obtain a yellowish oil. The collected data are in accord with those reported in literature.<sup>22</sup>

$^1\text{H NMR}$  (400 MHz,  $\text{CDCl}_3$ ):  $\delta$  7.23 (dd, 4H,  $J=17.4$ , 9.1 Hz,  $\text{H}_{\text{Ar}}$ ), 5.44 (t, 1H,  $J=8.0$  Hz,  $\text{H}^5$ ), 3.88 (t, 1H,  $J=8.7$  Hz,  $\text{H}^{4\text{B}}$ ), 3.41 (t, 1H,  $J=8.1$  Hz,  $\text{H}^{4\text{A}}$ ), 3.38-3.22 (m, 2H,  $\text{H}^6$ ), 2.36 (s, 3H,  $\text{H}_{\text{CH}_3}$ ), 1.57-1.50 (m, 2H,  $\text{H}_{\text{CH}_2}$ ), 1.39-1.33 (m, 2H,  $\text{H}_{\text{CH}_2}$ ), 0.94 ppm (t, 3H,  $J=7.3$  Hz,  $\text{H}^9$ ).

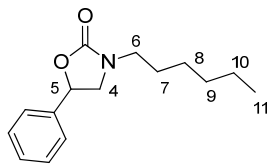
### 3.6.2.9. 3-Isoamyl-5-phenyloxazolidin-2-one-2 (80)



Compound **80** was synthesised from *N*-isoamyl-phenyl aziridine. The crude was purified by flash chromatography (silica gel, 60  $\mu$ m, AcOEt/hexane 2:8) to obtain a yellowish oil. The collected data are in accord with those reported in literature.<sup>19a</sup>

$^1\text{H NMR}$  (400 MHz,  $\text{CDCl}_3$ ):  $\delta$  7.43-7.32 (m, 5H,  $\text{H}_{\text{Ar}}$ ), 5.47 (t, 1H,  $J=8.1$  Hz,  $\text{H}^5$ ), 3.90 (t, 1H,  $J=8.7$  Hz,  $\text{H}^{4\text{B}}$ ), 3.41 (t, 1H,  $J=8.0$ ,  $J=7.5$  Hz,  $\text{H}^{4\text{A}}$ ), 3.37-3.20 (m, 2H,  $\text{H}^6$ ), 1.66-1.54 (m, 1H,  $\text{H}^8$ ), 1.49-1.39 (m, 2H,  $\text{H}^7$ ), 0.94 (d, 3H,  $J=3.3$  Hz,  $\text{H}_{\text{CH}_3}$ ), 0.92 ppm (t, 3H,  $J=7.4$  Hz,  $\text{H}_{\text{CH}_3}$ ).

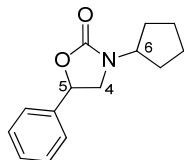
### 3.6.2.10. 3-Hexyl-5-phenyloxazolidin-2-one (81)



Compound **81** was synthesised from *N*-hexyl-phenyl aziridine. The crude was purified by flash chromatography (silica gel, 60  $\mu$ m, AcOEt/hexane 2:8) to obtain a yellowish oil. The collected data are in accord with those reported in literature.<sup>25</sup>

<sup>1</sup>H NMR (400 MHz, CDCl<sub>3</sub>):  $\delta$  7.31-7.25 (m, 5H, H<sub>Ar</sub>), 5.37 (t, 1H,  $J=8.0$  Hz, H<sup>5</sup>), 3.82 (t, 1H,  $J=8.8$  Hz, H<sup>4A</sup>), 3.31 (t, 1H,  $J=8.0$  Hz, H<sup>4B</sup>), 3.23-3.13 (m, 2H, H<sup>6</sup>), 1.47-1.43 (m, 2H, H<sub>CH2</sub>), 1.24-1.20 (m, 6H, H<sub>CH2</sub>), 0.79 ppm (t, 3H,  $J=6.6$  Hz, H<sup>11</sup>).

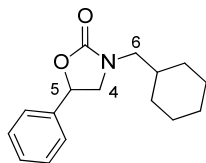
### 3.6.2.11. 3-Cyclopentyl-5-phenyloxazolidin-2-one (82)



Compound **82** was synthesised from *N*-cyclopentyl-phenyl aziridine. The crude was purified by flash chromatography (silica gel, 60  $\mu$ m, AcOEt/hexane 2:8) to obtain a yellowish oil. The collected data are in accord with those reported in literature.<sup>26</sup>

<sup>1</sup>H NMR (400 MHz, CDCl<sub>3</sub>):  $\delta$  7.31-7.25 (m, 5H, H<sub>Ar</sub>), 5.47 (t, 1H,  $J=8.0$  Hz, H<sup>5</sup>), 4.29 (t, 1H,  $J=8.8$  Hz, H<sup>4A</sup>), 3.88 (t, 1H,  $J=8.0$  Hz, H<sup>4B</sup>), 3.23-3.13 (m, 1H, H<sup>6</sup>), 1.90-1.87 (m, 2H, H<sub>cyclopentyl</sub>), 1.49-1.67 ppm (m, 6H, H<sub>cyclopentyl</sub>).

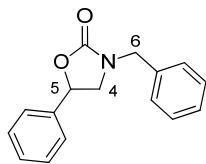
### 3.6.2.12. 3-Cyclohexanemethyl-5-phenyloxazolidin-2-one (83)



Compound **83** was synthesised from *N*-cyclohexylmethyl-phenyl aziridine. The crude was purified by flash chromatography (silica gel, 60  $\mu$ m, AcOEt/hexane 2:8) to obtain a yellowish oil. The collected data are in accord with those reported in literature.<sup>22</sup>

<sup>1</sup>H NMR (400 MHz, CDCl<sub>3</sub>):  $\delta$  7.34-7.24 (m, 5H, H<sub>Ar</sub>), 5.44 (t, 1H,  $J=8.0$  Hz, H<sup>5</sup>), 3.89 (t, 1H,  $J=8.7$  Hz, H<sup>4A</sup>), 3.39 (t, 1H,  $J=8.0$  Hz, H<sup>4B</sup>), 3.13 (dd, 1H,  $^2J=13.7$  Hz,  $J=7.4$  Hz, H<sup>6A</sup>), 3.03 (dd, 1H,  $^2J=13.7$  Hz,  $J=7.2$  Hz, H<sup>6B</sup>), 1.67-1.58 (m, 5H, H<sub>cyclohexyl</sub>), 1.19-1.09 (m, 3H, H<sub>cyclohexyl</sub>), 0.98-0.92 ppm (m, 2H, H<sub>cyclohexyl</sub>).

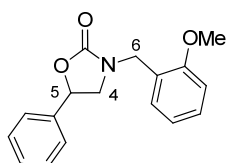
### 3.6.2.13. 3-Benzyl-5-phenyloxazolidin-2-one (84)



Compound **84** was synthesised from *N*-benzyl-phenyl aziridine. The crude was purified by flash chromatography (silica gel, 60  $\mu$ m, AcOEt/hexane 2:8) to obtain a yellowish oil. The collected data are in accord with those reported in literature.<sup>19a</sup>

**<sup>1</sup>H NMR** (300 MHz, CDCl<sub>3</sub>):  $\delta$  7.35-7.27 (m, 10H, H<sub>Ar</sub>), 5.43 (t, 1H,  $J$ =8.1 Hz, H<sup>5</sup>), 4.45 (ABq, 2H,  $J_{AB}$ =15.0 Hz,  $\Delta v_{AB}$ =36.0 Hz, H<sup>6</sup>), 3.75 (t, 1H,  $J$ =8.7 Hz, H<sup>4A</sup>), 3.28 ppm (t, 1H,  $J$ =8.4 Hz, H<sup>4B</sup>).

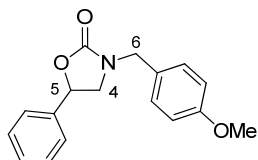
### 3.6.2.14. 3-(2-Methoxy)benzyl-5-phenyloxazolidin-2-one (85)



Compound **85** was synthesised from *N*-(2-methoxy)benzyl-phenyl aziridine. The crude was purified by flash chromatography (silica gel, 60  $\mu$ m, AcOEt/hexane 2:8) to obtain a yellowish oil.

**<sup>1</sup>H NMR** (300 MHz, CDCl<sub>3</sub>):  $\delta$  7.40-7.26 (m, 7H, H<sub>Ar</sub>), 6.94 (t, 1H,  $J$ =7.5 Hz, H<sub>Ar</sub>), 6.87 (d, 1H,  $J$ =8.1 Hz, H<sub>Ar</sub>), 5.43 (t, 1H,  $J$ =8.1 Hz, H<sup>5</sup>), 4.51 (ABq, 2H,  $J_{AB}$ =14.0 Hz,  $\Delta v_{AB}$ =36.0 Hz, H<sub>CH2</sub>), 3.78 (s, 3H, H<sub>OCH3</sub>), 3.77-3.76 (m, 1H, H<sup>4A</sup>), 3.35-3.29 ppm (m, 1H, H<sup>4B</sup>). **<sup>13</sup>C NMR** (75 MHz, CDCl<sub>3</sub>):  $\delta$  130.3, 129.5, 128.9, 125.7, 120.9, 110.5, 74.6, 55.5, 52.1, 43.2 ppm. **MS** (ESI):  $m/z$ =306.40 [M+Na].

### 3.6.2.15. 3-(4-Methoxy)benzyl-5-phenyloxazolidin-2-one (86)



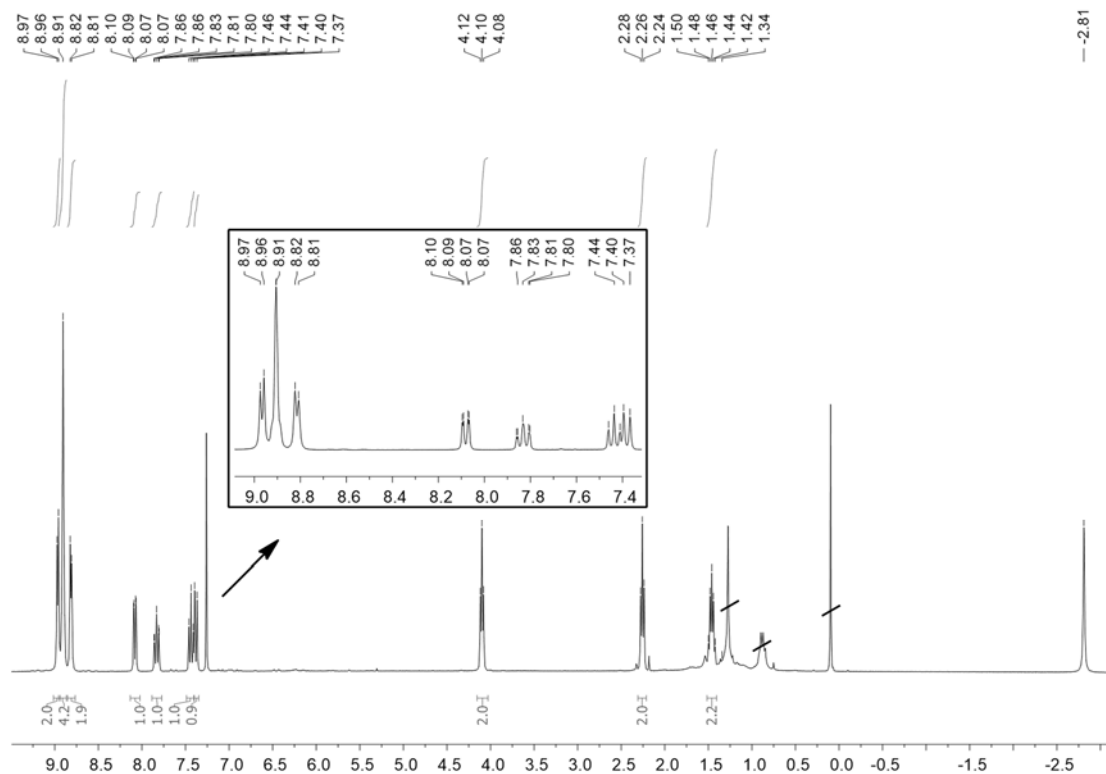
Compound **84** was synthesised from *N*-(4-methoxy)benzyl-phenyl aziridine. The crude was purified by flash chromatography (silica gel, 60  $\mu$ m, AcOEt/hexane 2:8) to obtain a yellowish oil.

**<sup>1</sup>H NMR** (400 MHz, CDCl<sub>3</sub>):  $\delta$  7.38-7.32 (m, 3H, H<sub>Ar</sub>), 7.31-7.28 (m, 2H, H<sub>Ar</sub>), 7.21 (d, 2H,  $J$ =8.8 Hz, H<sub>benzyl-ortho</sub>), 6.87 (d, 2H,  $J$ =8.6 Hz, H<sub>benzyl-meta</sub>), 5.45 (t, 1H,  $J$ =8.2 Hz, H<sup>5</sup>), 4.41 (ABq, 2H,  $J_{AB}$ =14.7 Hz,  $\Delta v_{AB}$ =36.0 Hz, H<sub>CH2</sub>), 3.74 (t, 1H,  $J$ =8.8 Hz, H<sup>4A</sup>), 3.28 ppm (dd, 1H,  $J$ =8.7, 7.6 Hz, H<sup>4B</sup>). **<sup>13</sup>C NMR** (100 MHz, CDCl<sub>3</sub>):  $\delta$  7. **MS** (ESI):  $m/z$ =306.31 [M+Na].

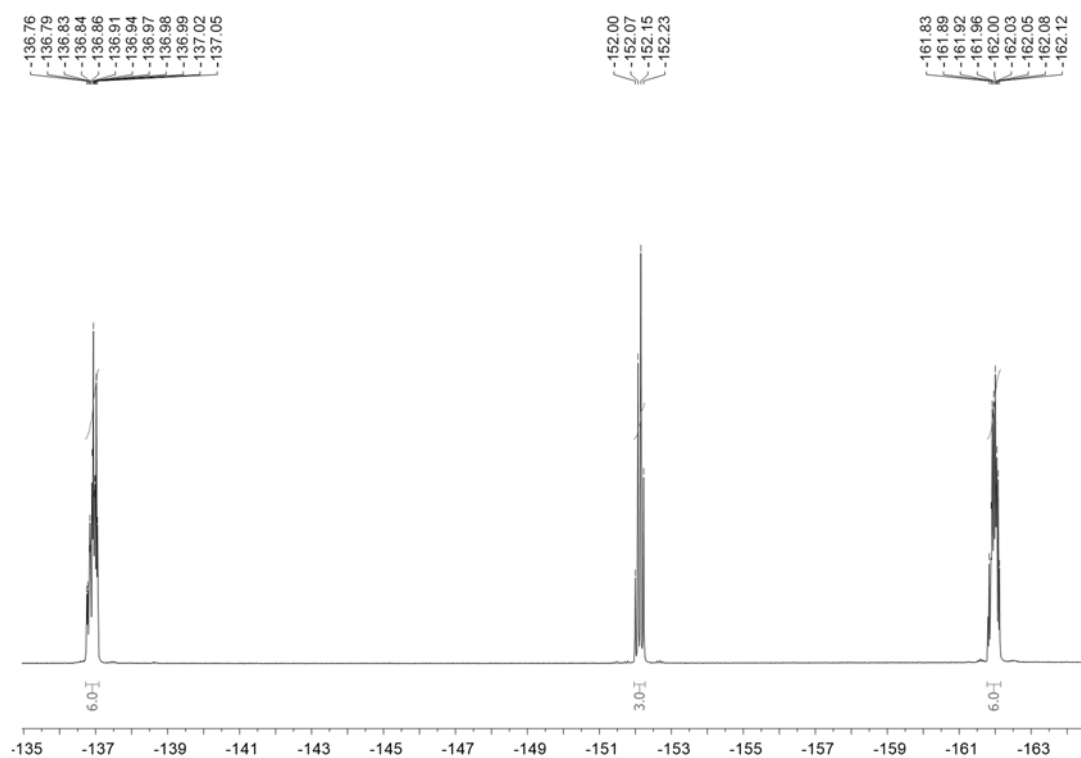
## 3.7. NMR spectra

### 3.7.1 Synthesis of 5-(2-(3-bromopropoxy)phenyl)-10,15,20-tris(pentafluorophenyl)porphyrin (A<sub>3</sub>B-Br)

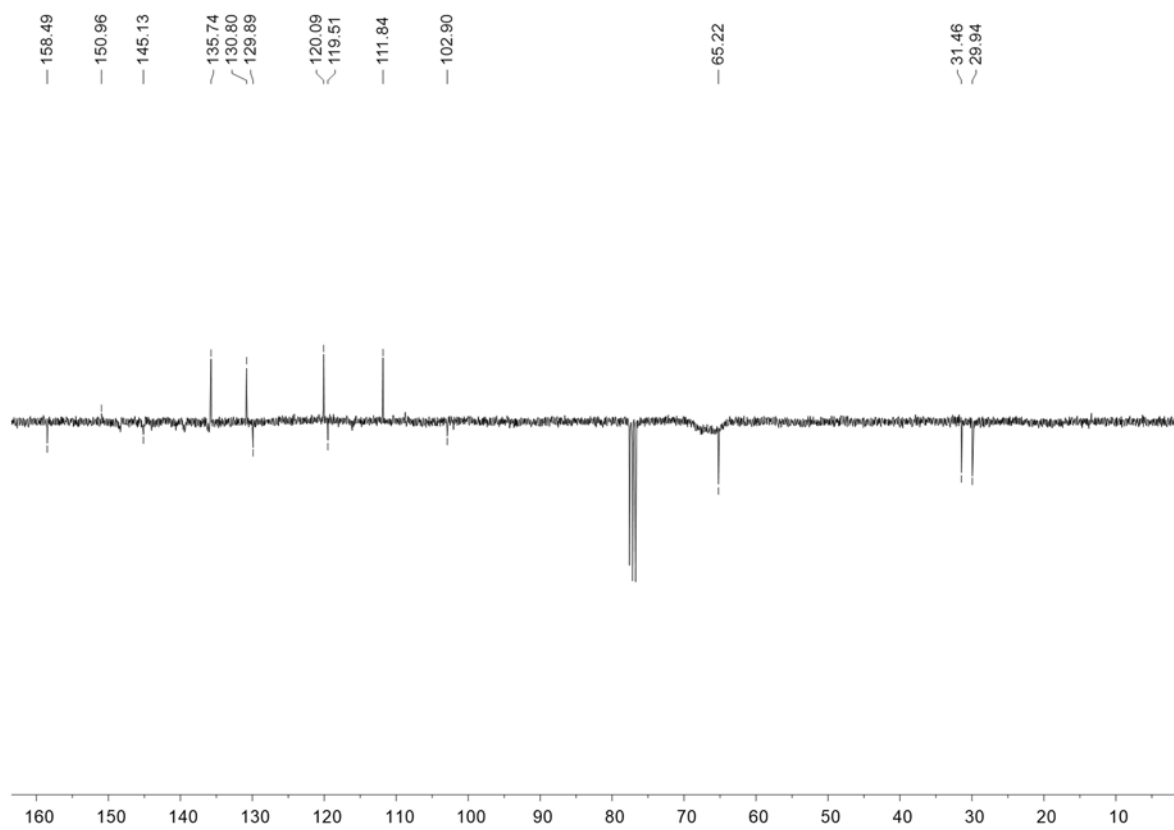
#### 3.7.1.1. <sup>1</sup>H NMR spectrum (300 MHz, CDCl<sub>3</sub>, 298 K)



#### 3.7.1.2. <sup>19</sup>F NMR spectrum (282 MHz, CDCl<sub>3</sub>, 298 K)

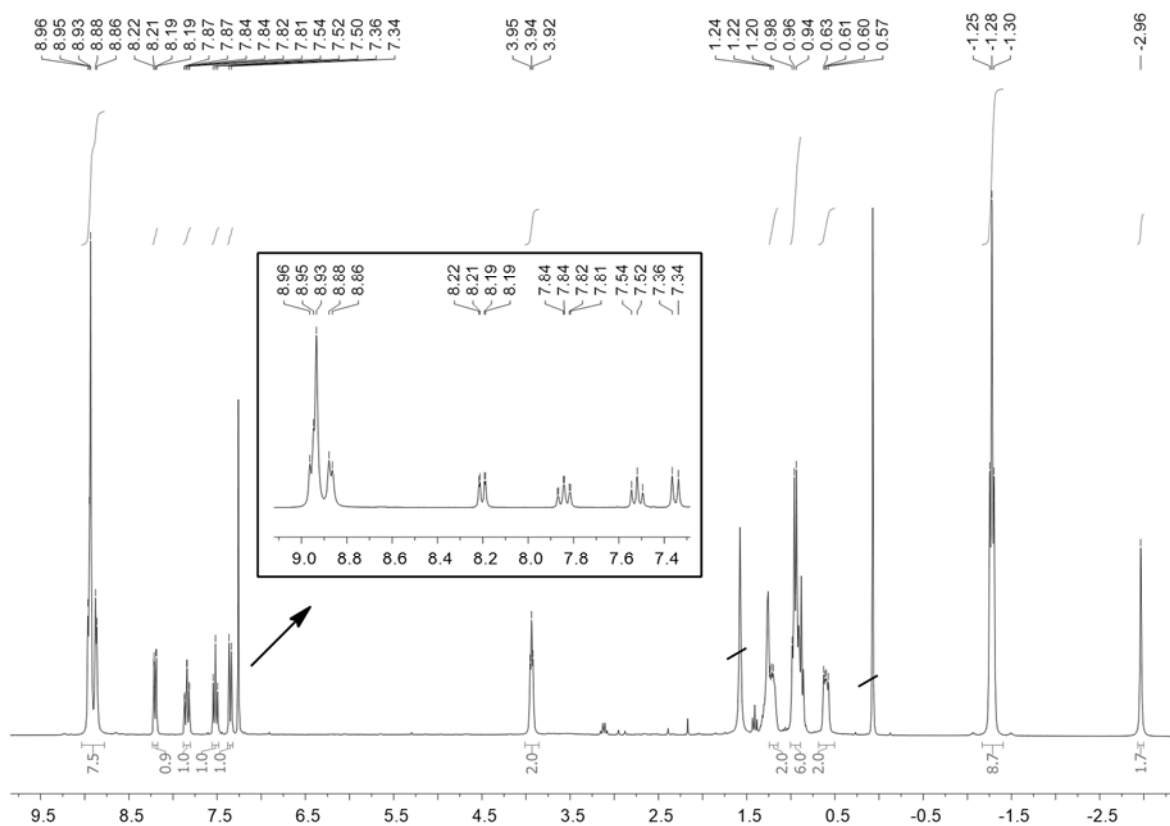


### 3.7.1.3. $^{13}\text{C}$ NMR spectrum (75 MHz, $\text{CDCl}_3$ , 298 K)

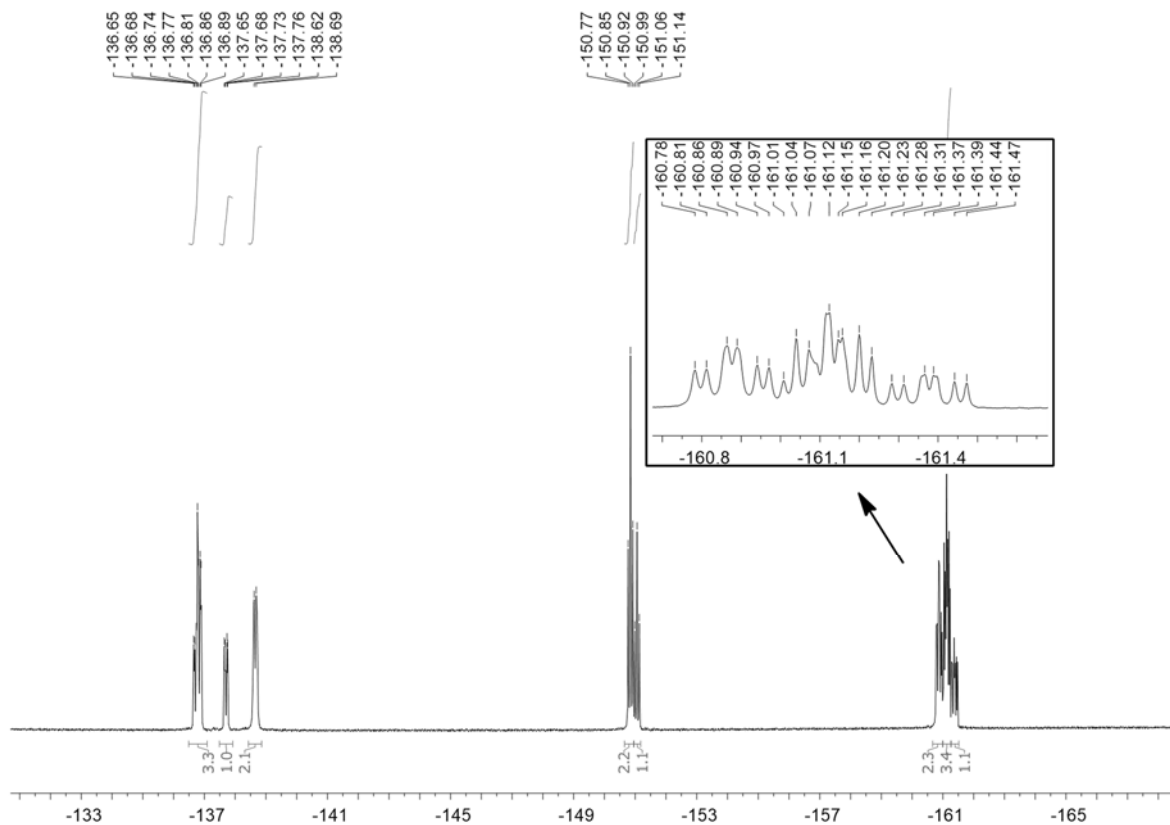


### 3.7.2. 5-(2-(3-triethylammoniopropoxy)phenyl)-10,15,20-tris(pentafluorophenyl) porphyrin iodide ( $A_3B-NEt_3^+I^-$ ) (89)

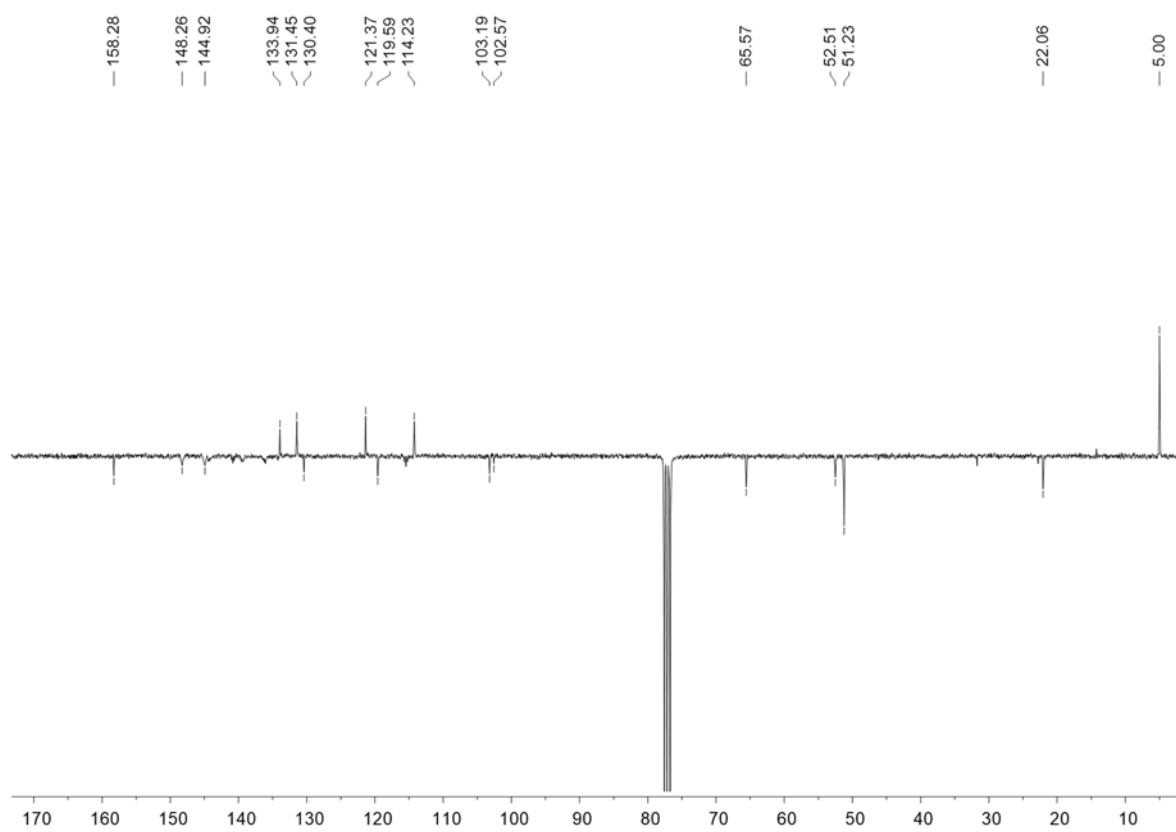
#### 3.7.2.1. $^1H$ NMR spectrum (300 MHz, $CDCl_3$ , 298 K)



#### 3.7.2.2. $^{19}F$ NMR spectrum (282 MHz, $CDCl_3$ , 298 K)

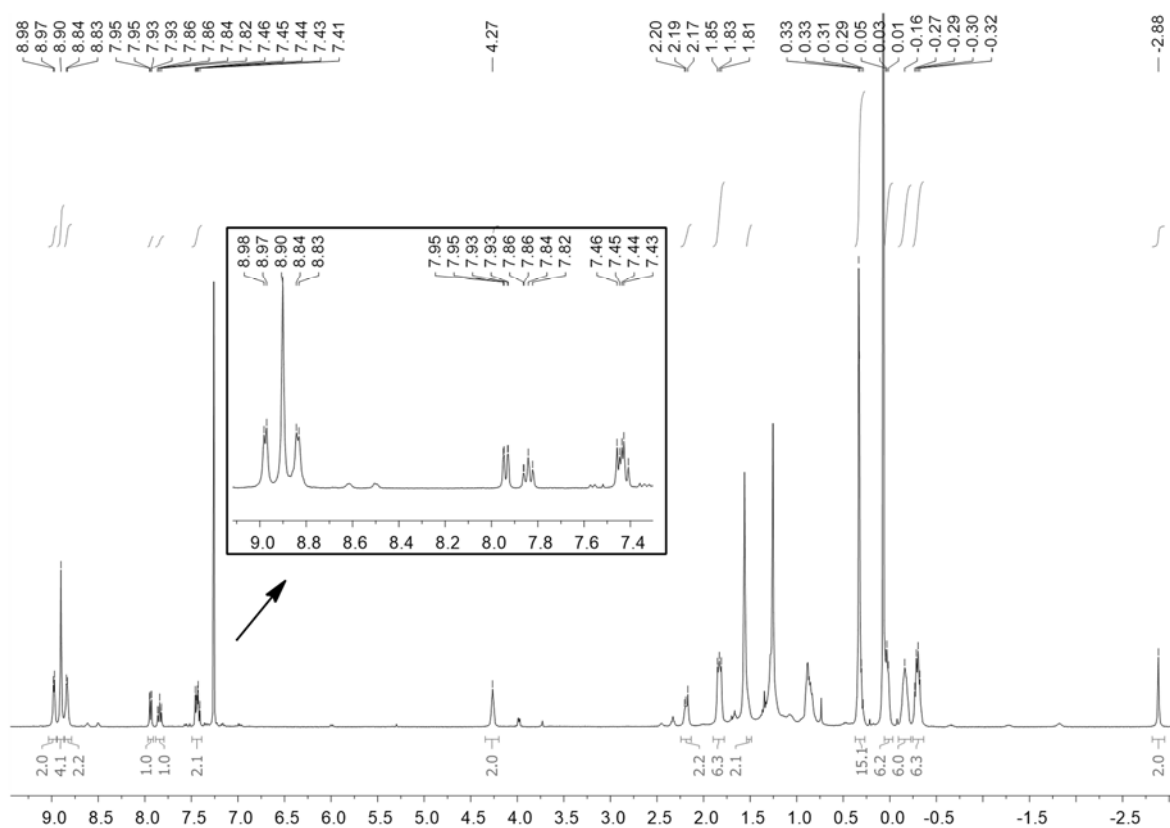


### 3.7.2.3. $^{13}\text{C}$ NMR spectrum (75 MHz, $\text{CDCl}_3$ , 298 K)

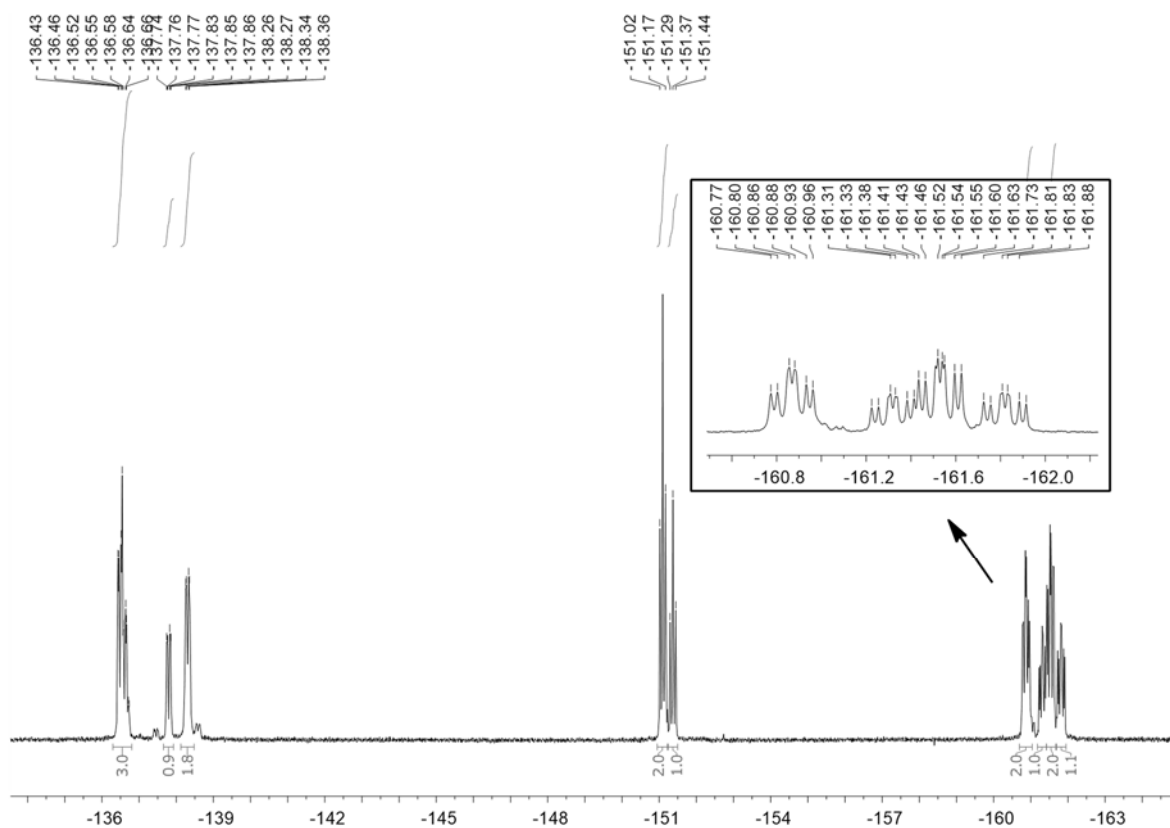


### 3.7.3. 5-(2-(3-trihexylammoniopropoxy)phenyl)-10,15,20-tris(pentafluorophenyl) porphyrin iodide ( $A_3B-NHex_3$ )<sup>+</sup>I<sup>-</sup> (90)

#### 3.7.3.1. <sup>1</sup>H NMR spectrum (400 MHz, CDCl<sub>3</sub>, 298 K)

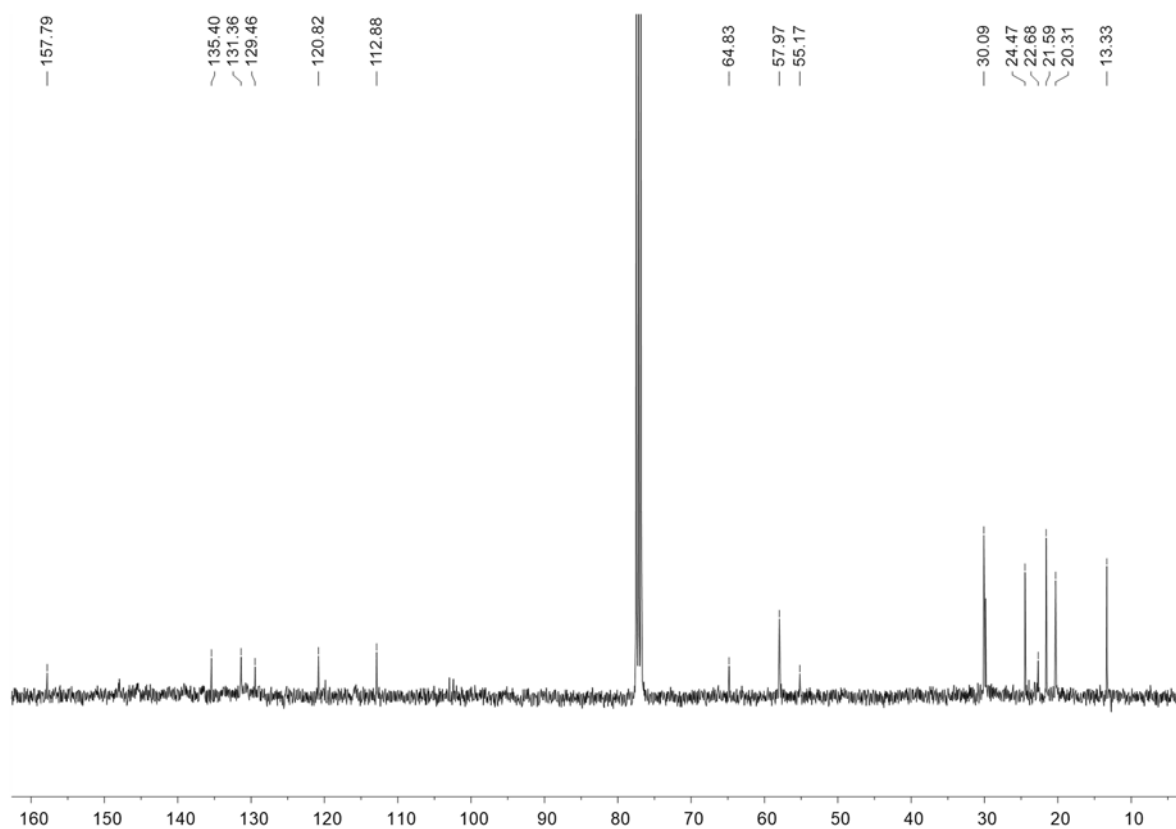


#### 3.7.3.2. <sup>19</sup>F NMR spectrum (376 MHz, CDCl<sub>3</sub>, 298 K)



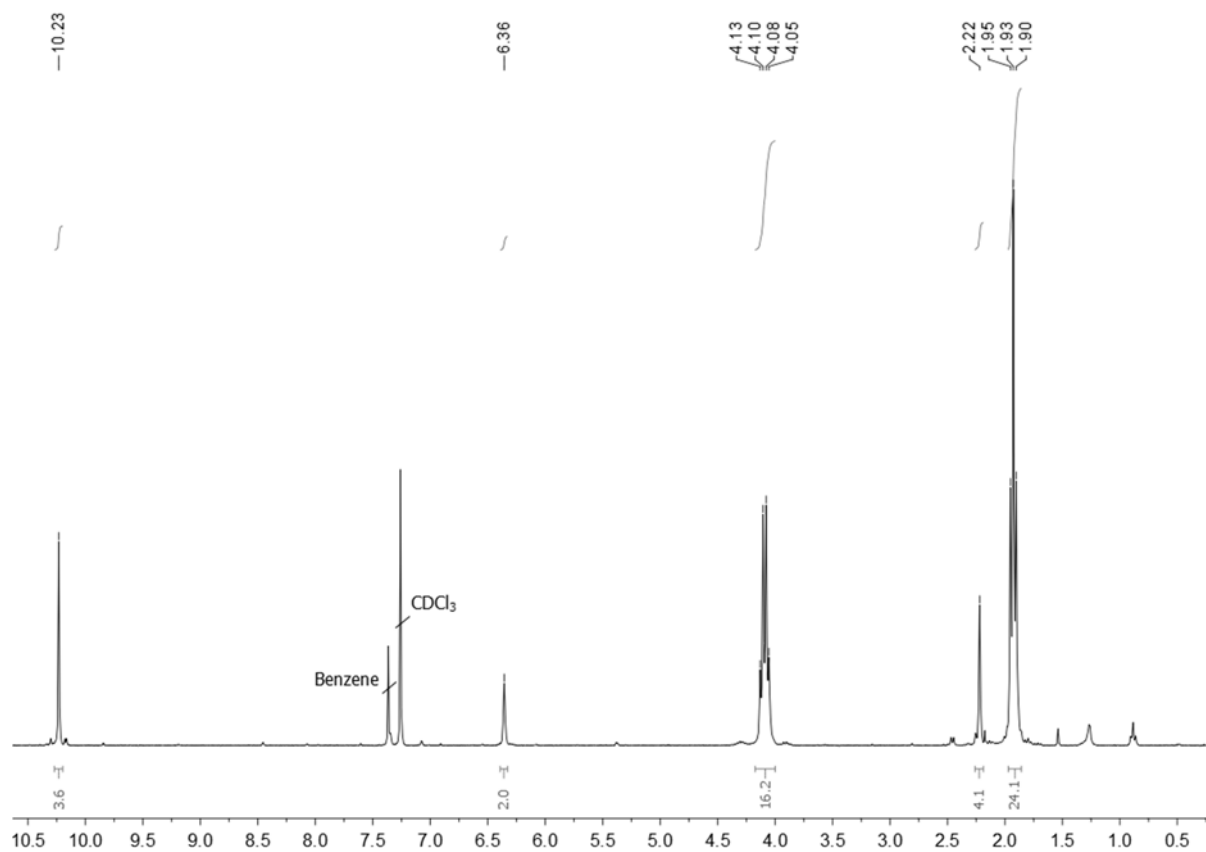


### 3.7.3.3. $^{13}\text{C}$ NMR spectrum (100 MHz, $\text{CDCl}_3$ , 298 K)

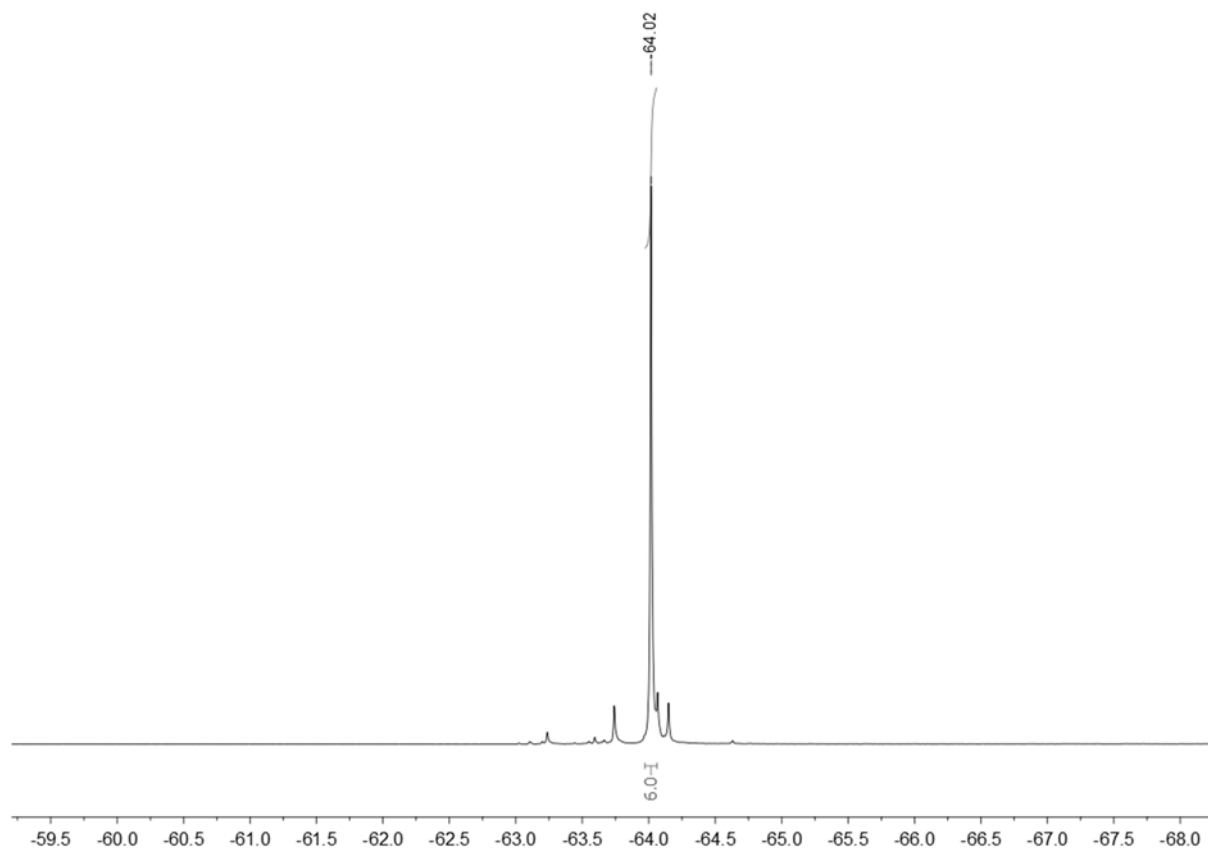


### 3.7.4. $\text{Ru}(\text{OEP})(\text{NAr})_2$ ( $\text{Ar}=\text{3,5}-(\text{CF}_3)_2\text{C}_6\text{H}_3$ )

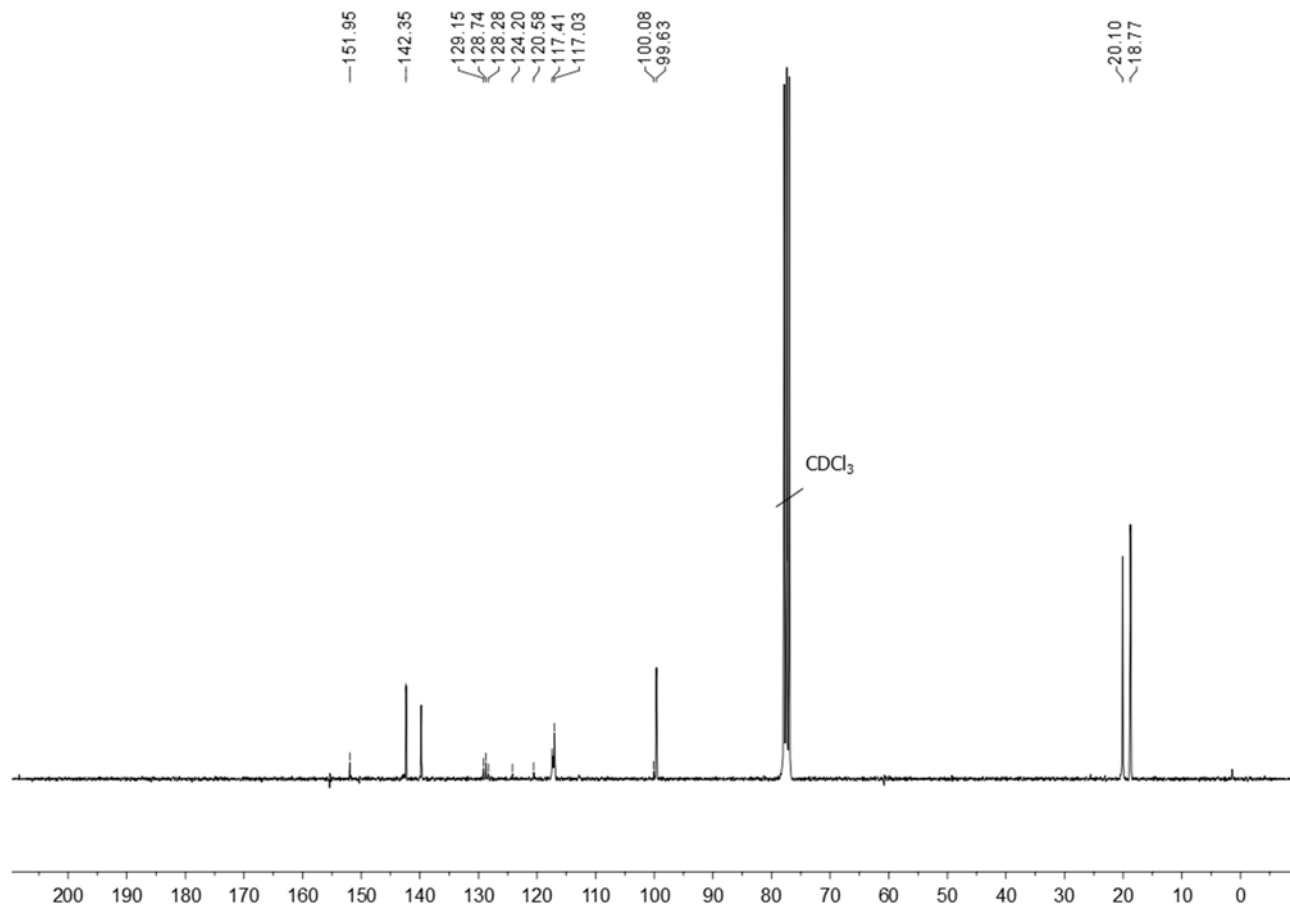
#### 3.7.4.1. $^1\text{H}$ NMR spectrum (300 MHz, $\text{CDCl}_3$ , 298 K)



3.7.4.1.  $^{19}\text{F}$  NMR spectrum (282 MHz,  $\text{CDCl}_3$ , 298 K)

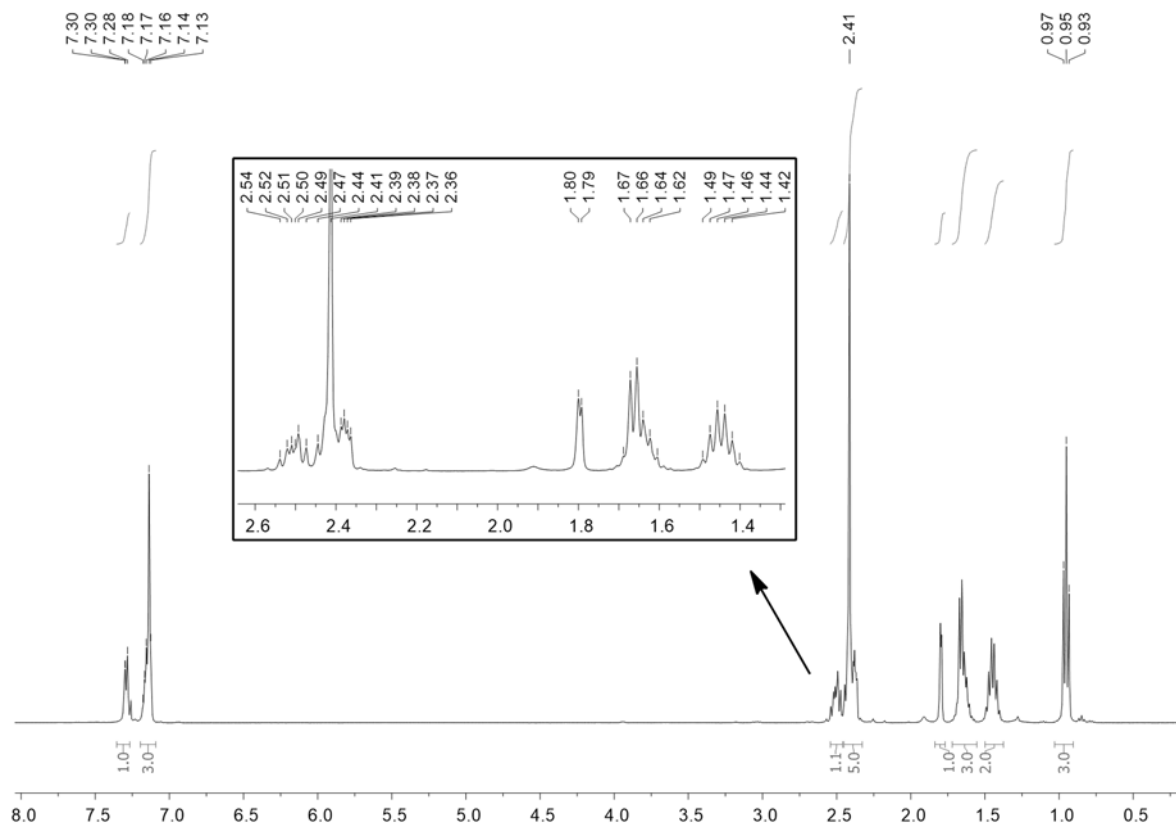


3.7.4.1.  $^{13}\text{C}$  NMR spectrum (75 MHz,  $\text{CDCl}_3$ , 298 K)

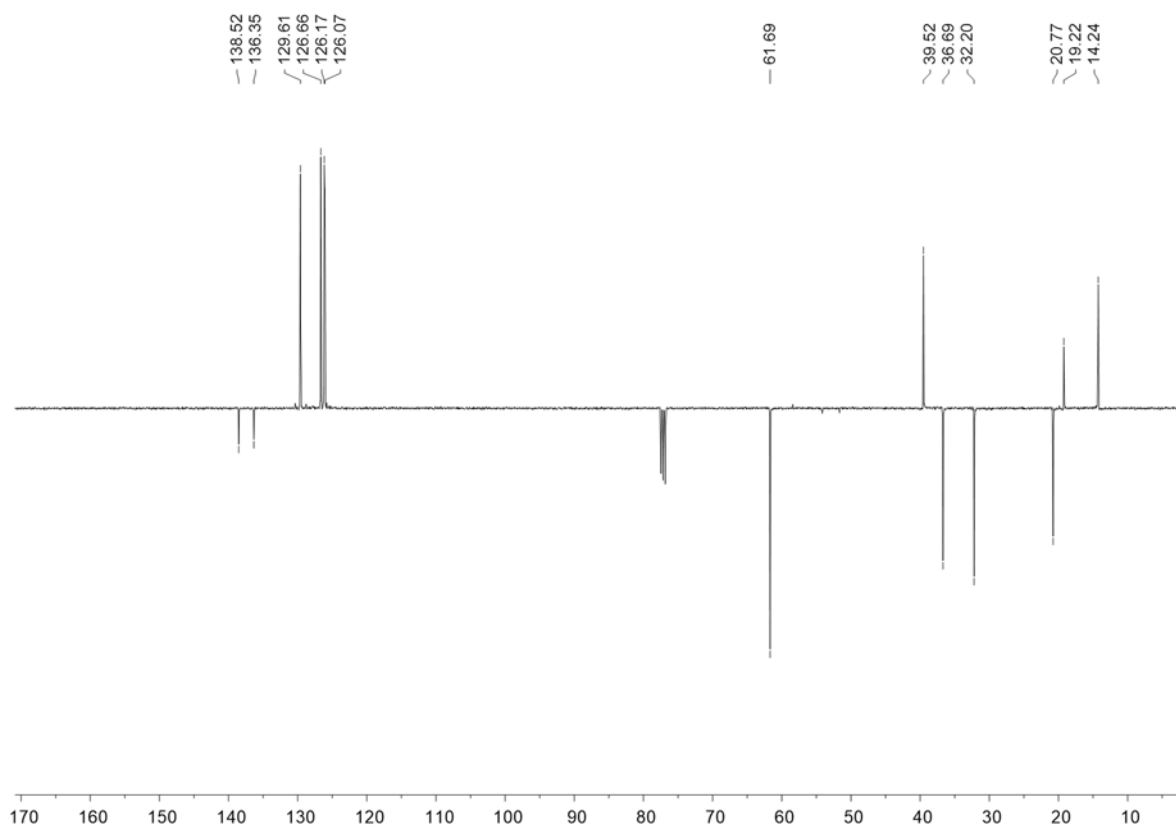


### 3.7.5 *N*-butyl-2-(2-methyl)phenyl aziridine

#### 3.7.5.1. $^1\text{H}$ NMR (400 MHz, $\text{CDCl}_3$ , 298 K)

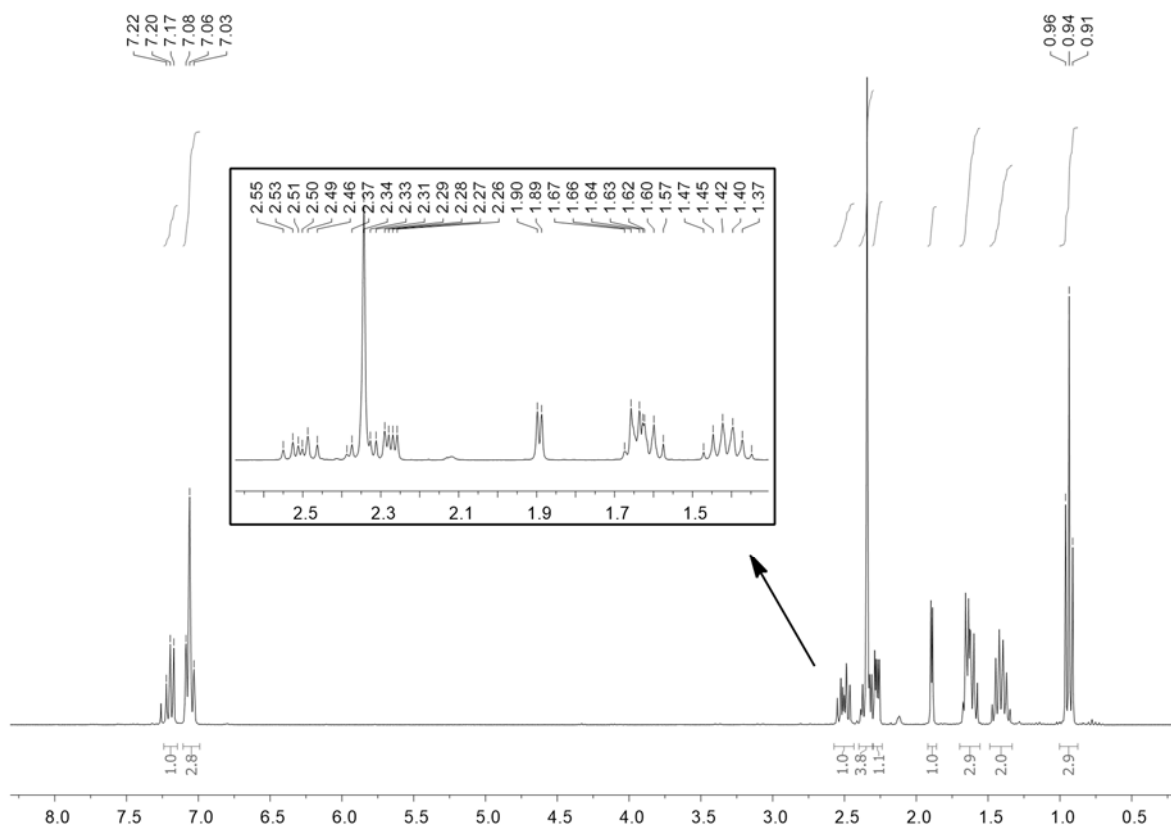


#### 3.7.5.2. $^{13}\text{C}$ NMR (100 MHz, $\text{CDCl}_3$ , 298 K)

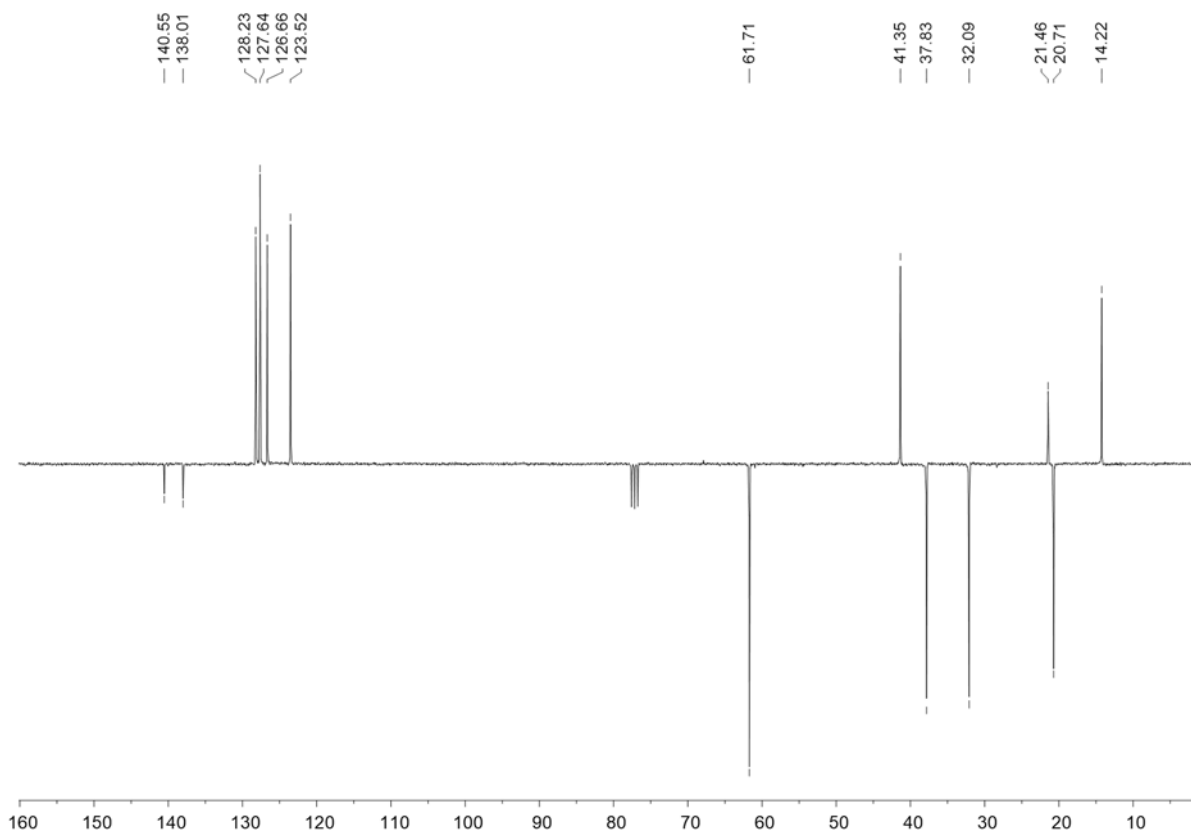


### 3.7.6. *N*-butyl-2-(3-methyl)phenyl aziridine

#### 3.7.6.1. $^1\text{H}$ NMR (300 MHz, $\text{CDCl}_3$ , 298 K)

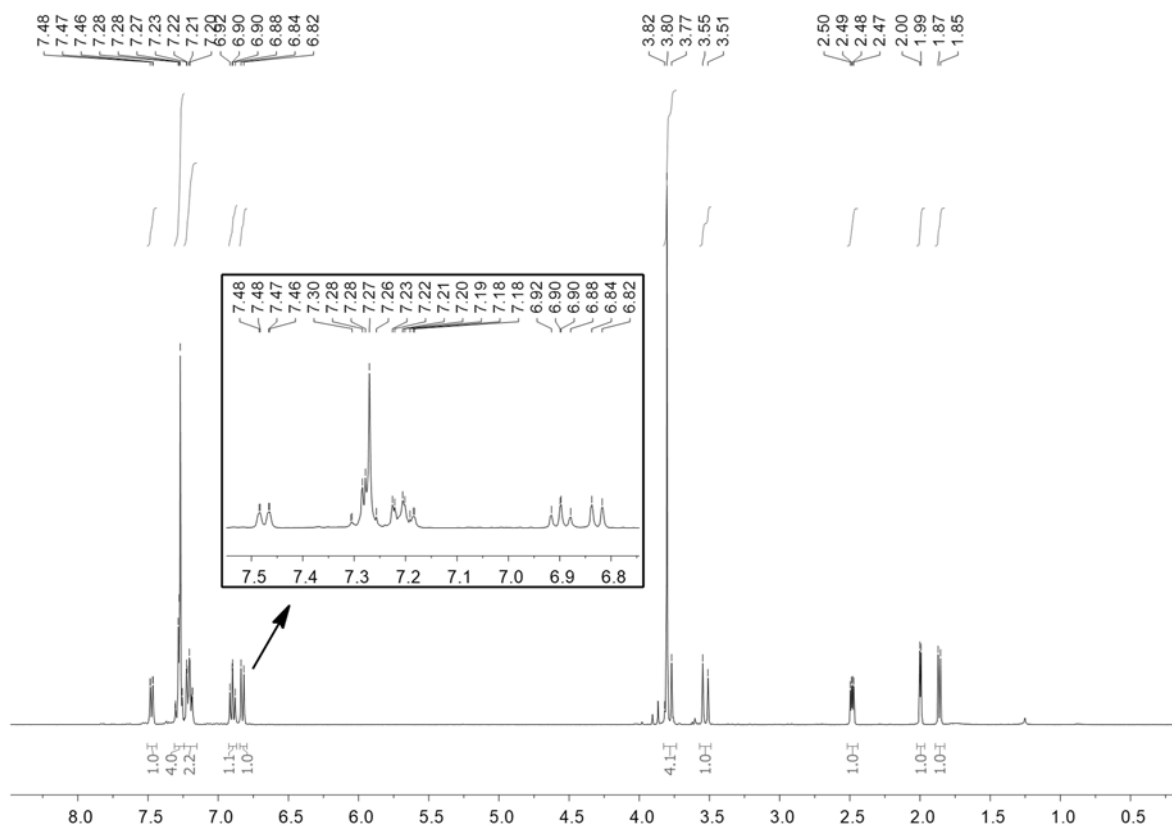


#### 3.7.6.2. $^{13}\text{C}$ NMR (100 MHz, $\text{CDCl}_3$ , 298 K)

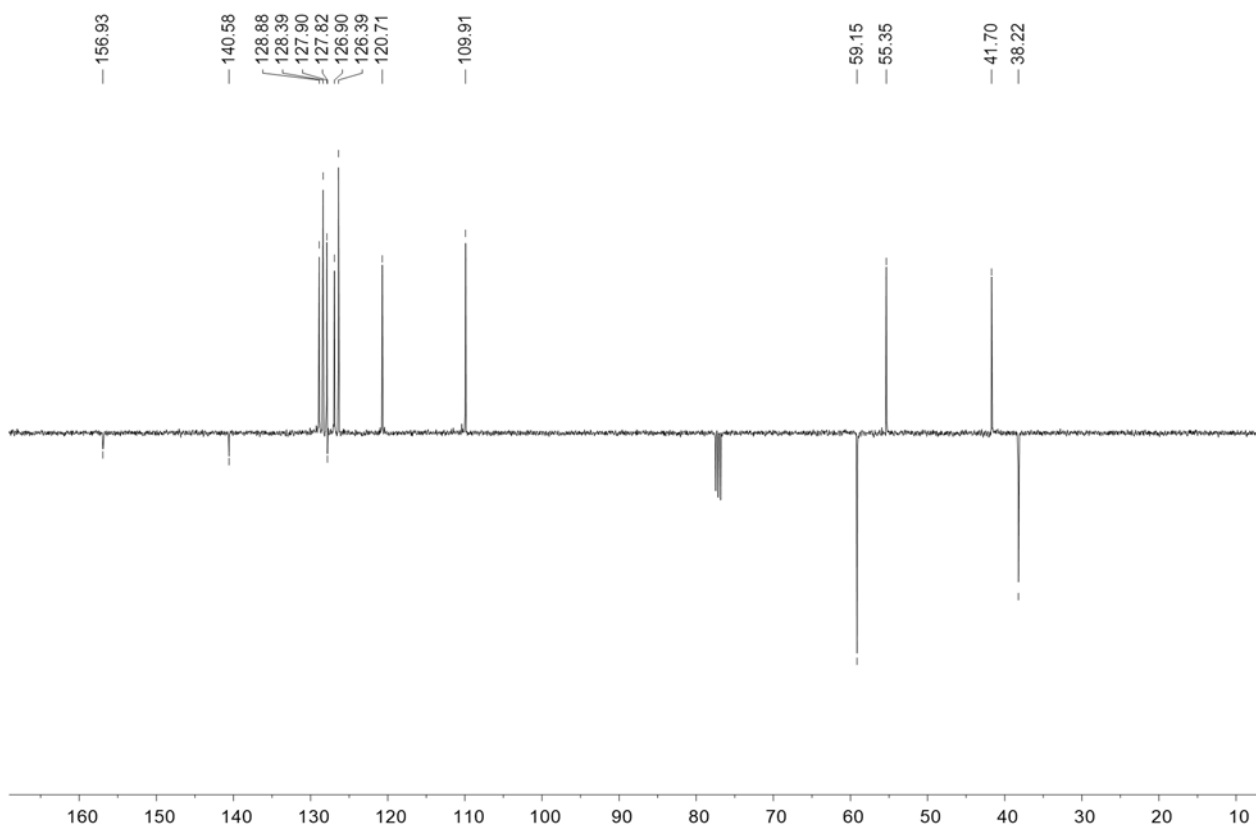


### 3.7.7. *N*-(2-methoxy)benzyl-2-phenyl aziridine

#### 3.7.7.1. $^1\text{H}$ NMR (400 MHz, $\text{CDCl}_3$ , 298 K)

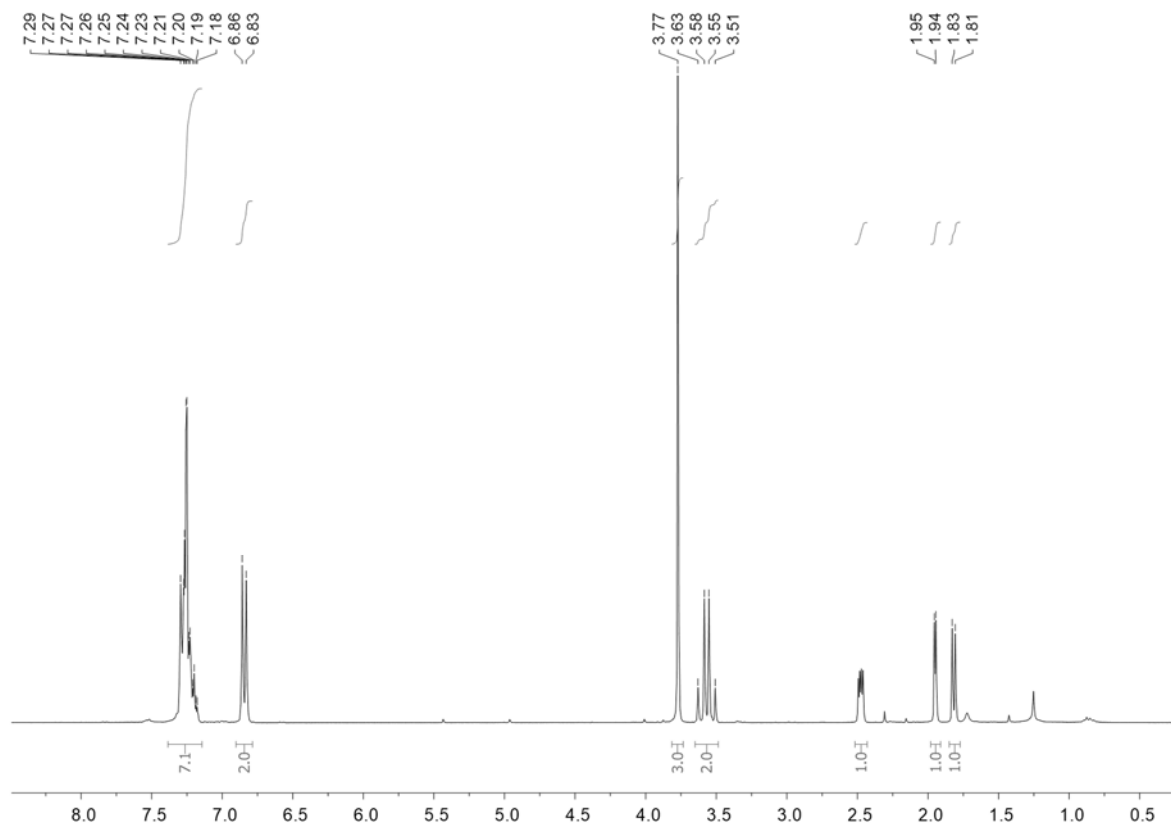


#### 3.7.7.2. $^{13}\text{C}$ NMR (100 MHz, $\text{CDCl}_3$ , 298 K)

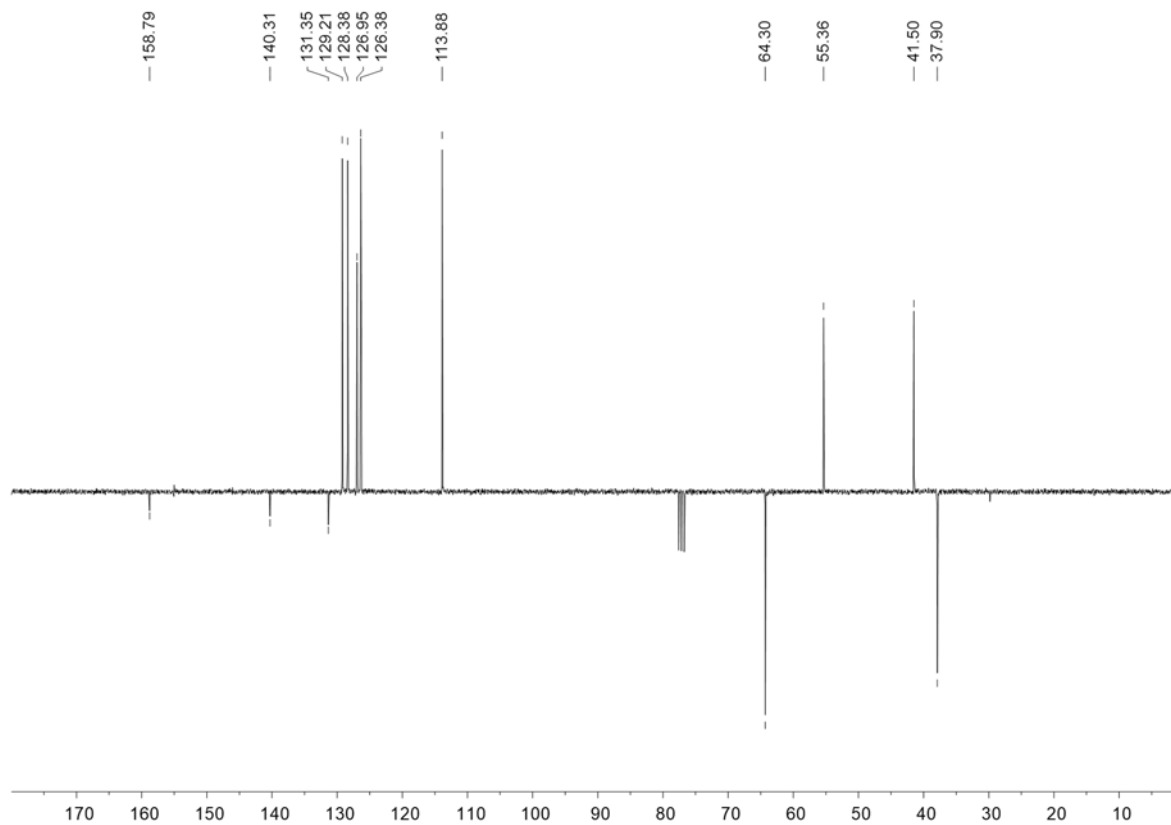


### 3.7.8. *N*-(4-methoxy)benzyl-2-phenyl aziridine

#### 3.7.8.1. $^1\text{H}$ NMR (300 MHz, $\text{CDCl}_3$ , 298 K)

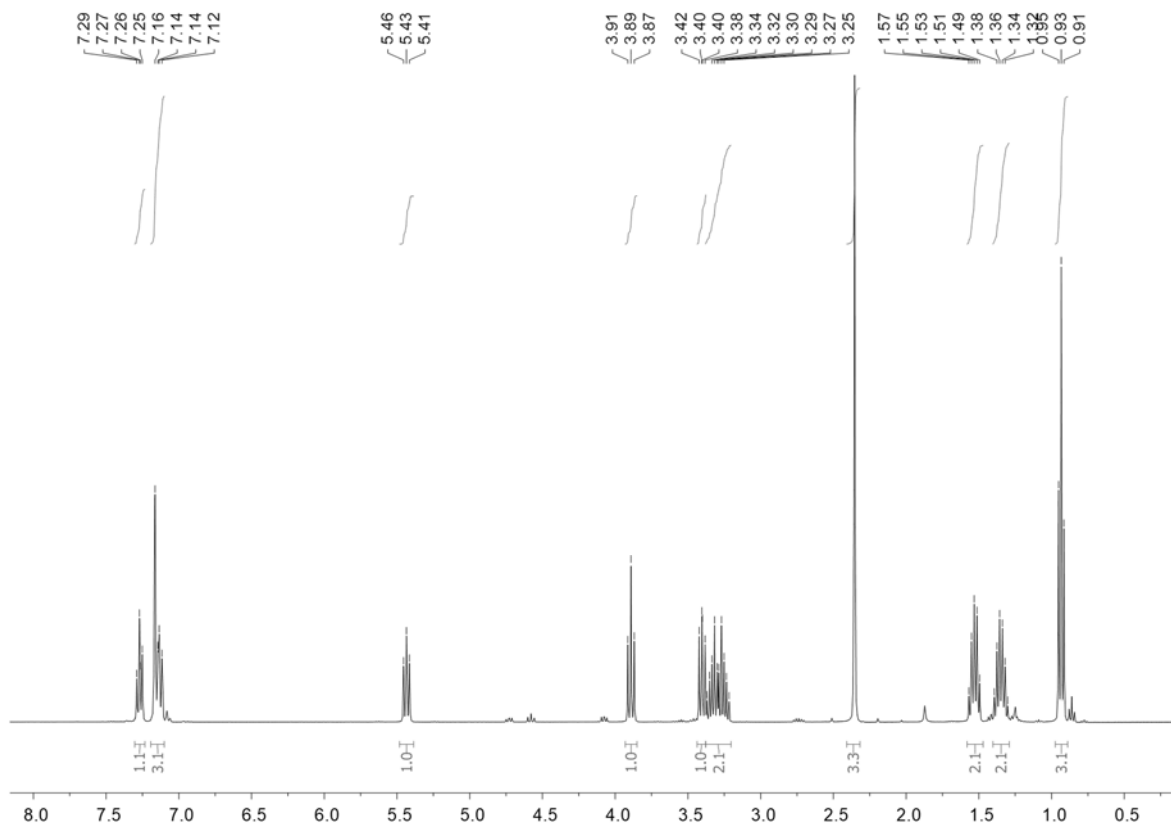


#### 3.7.8.2. $^{13}\text{C}$ NMR (75 MHz, $\text{CDCl}_3$ , 298 K)

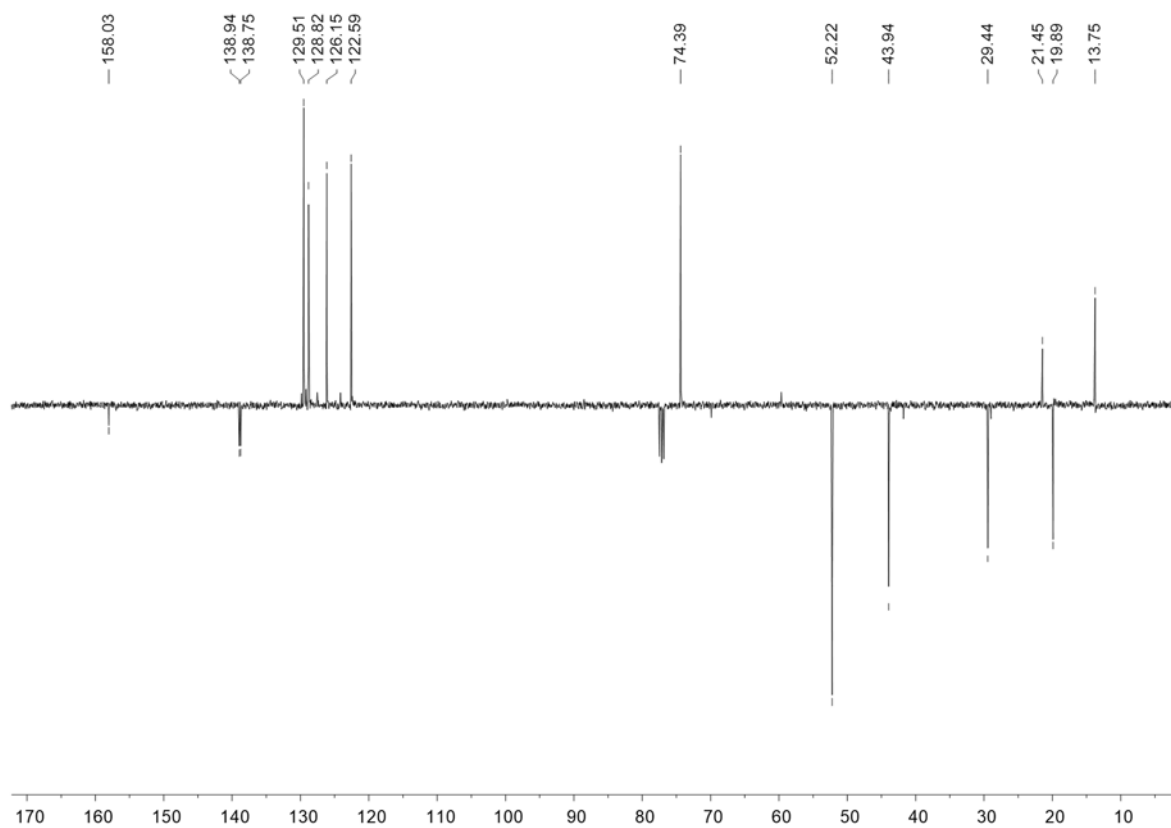


### 3.7.9. 3-Butyl-5-(2-methyl)phenyloxazolidin-2-one (77)

#### 3.7.9.1. $^1\text{H}$ NMR (400 MHz, $\text{CDCl}_3$ , 298 K)

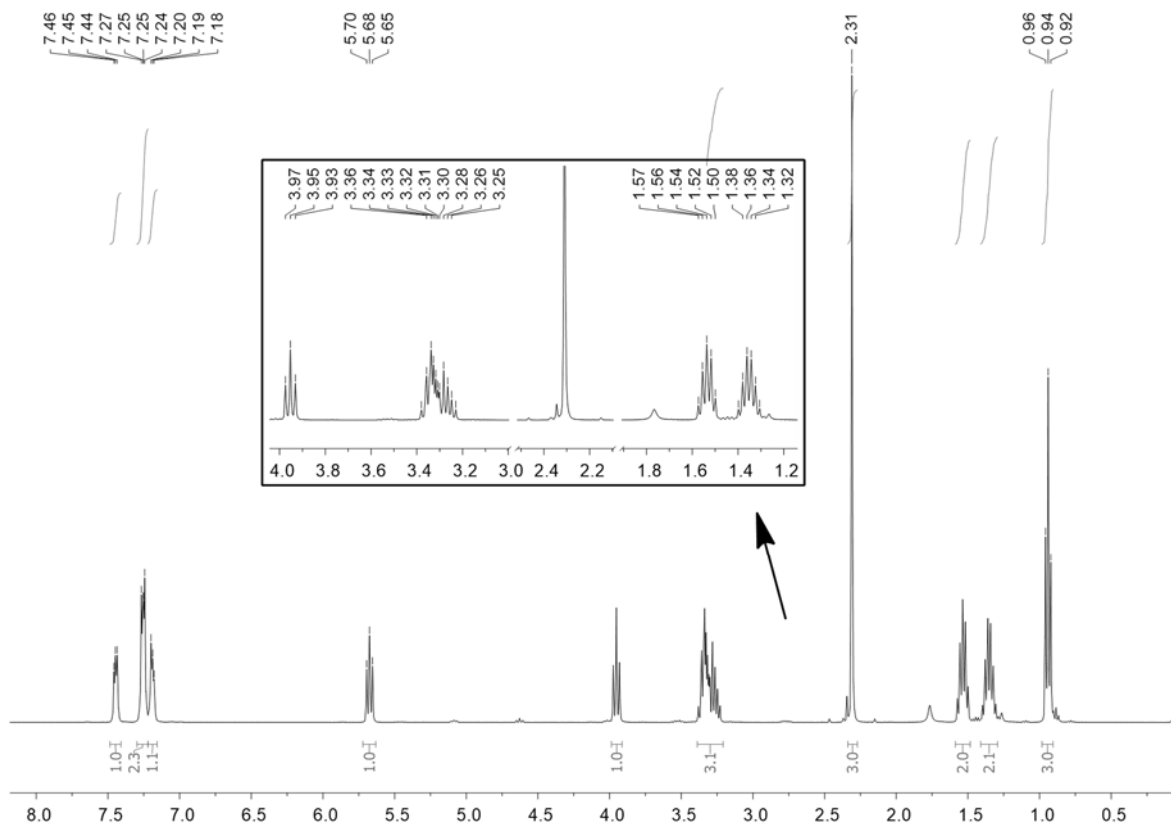


#### 3.7.9.2. $^{13}\text{C}$ NMR spectrum (100 MHz, $\text{CDCl}_3$ , 298 K)

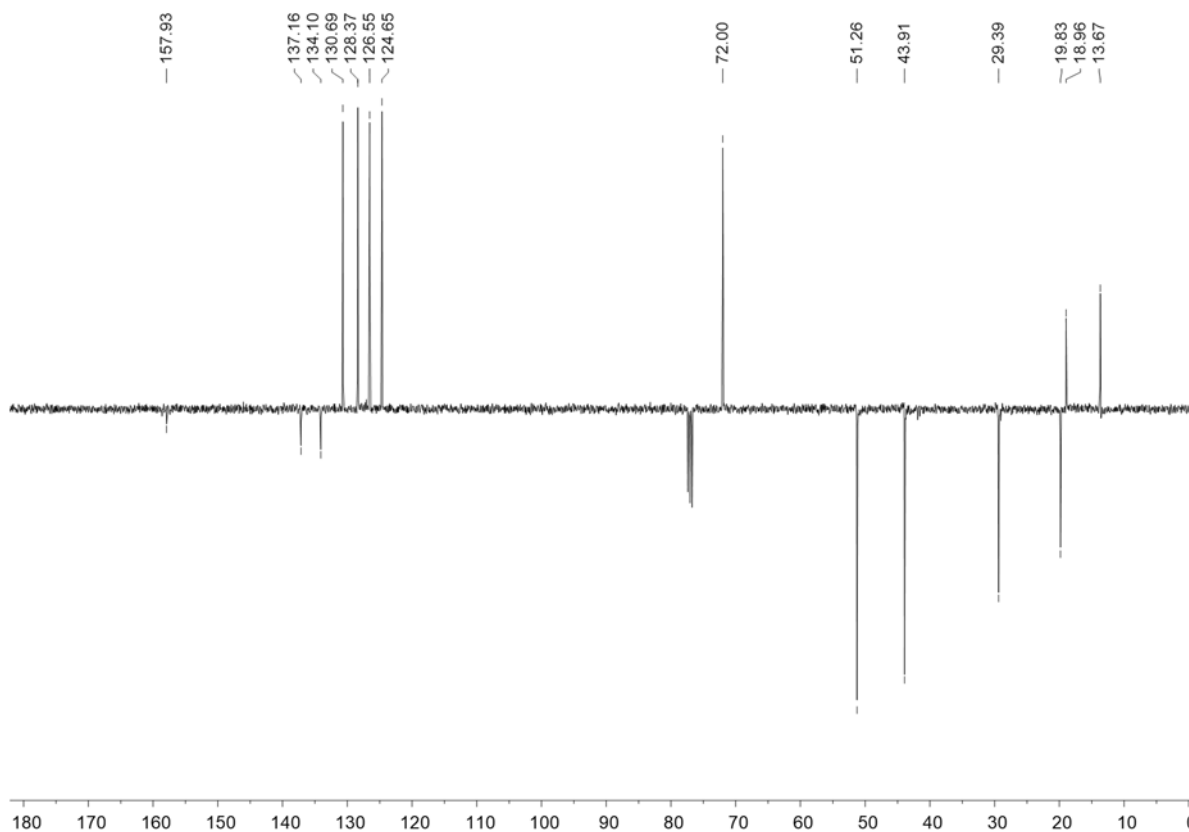


### 3.7.10. 3-Butyl-5-(3-methyl)phenyloxazolidin-2-one (78)

#### 3.7.10.1. $^1\text{H}$ NMR (400 MHz, $\text{CDCl}_3$ , 298 K)



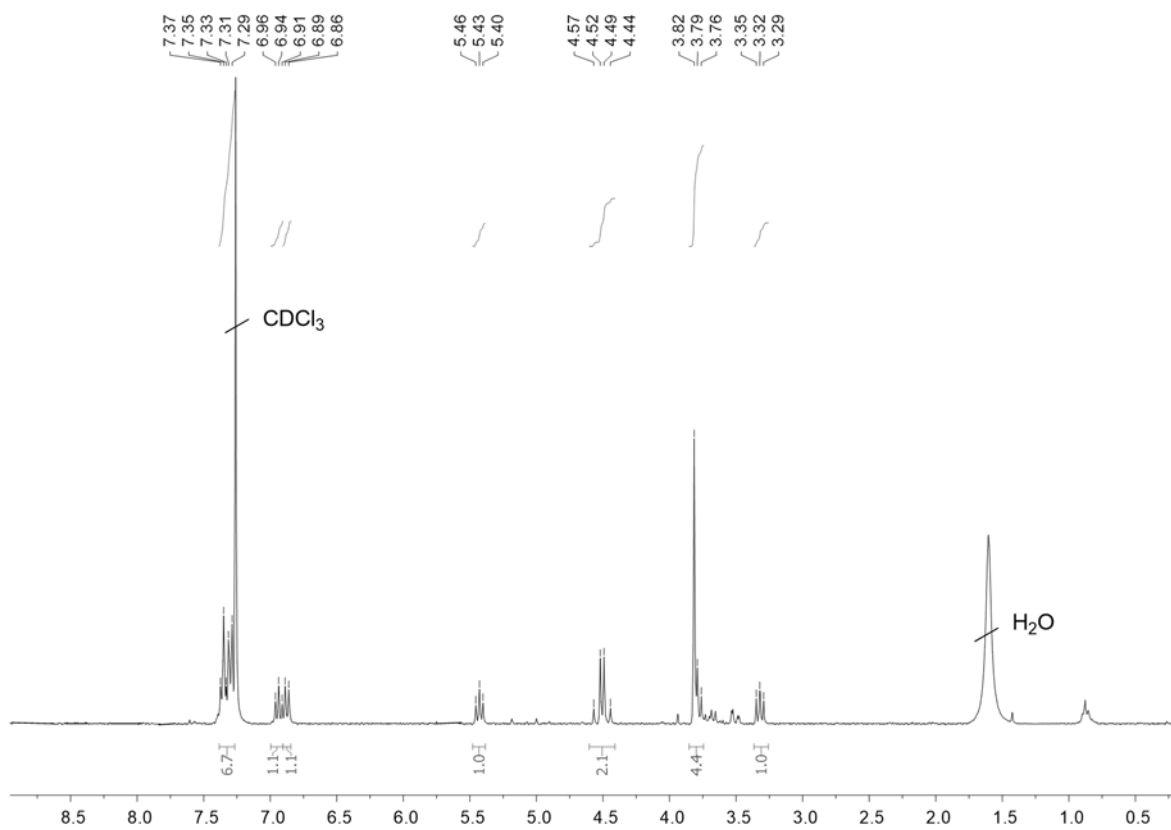
#### 3.7.10.2. $^{13}\text{C}$ NMR spectrum (100 MHz, $\text{CDCl}_3$ , 298 K)



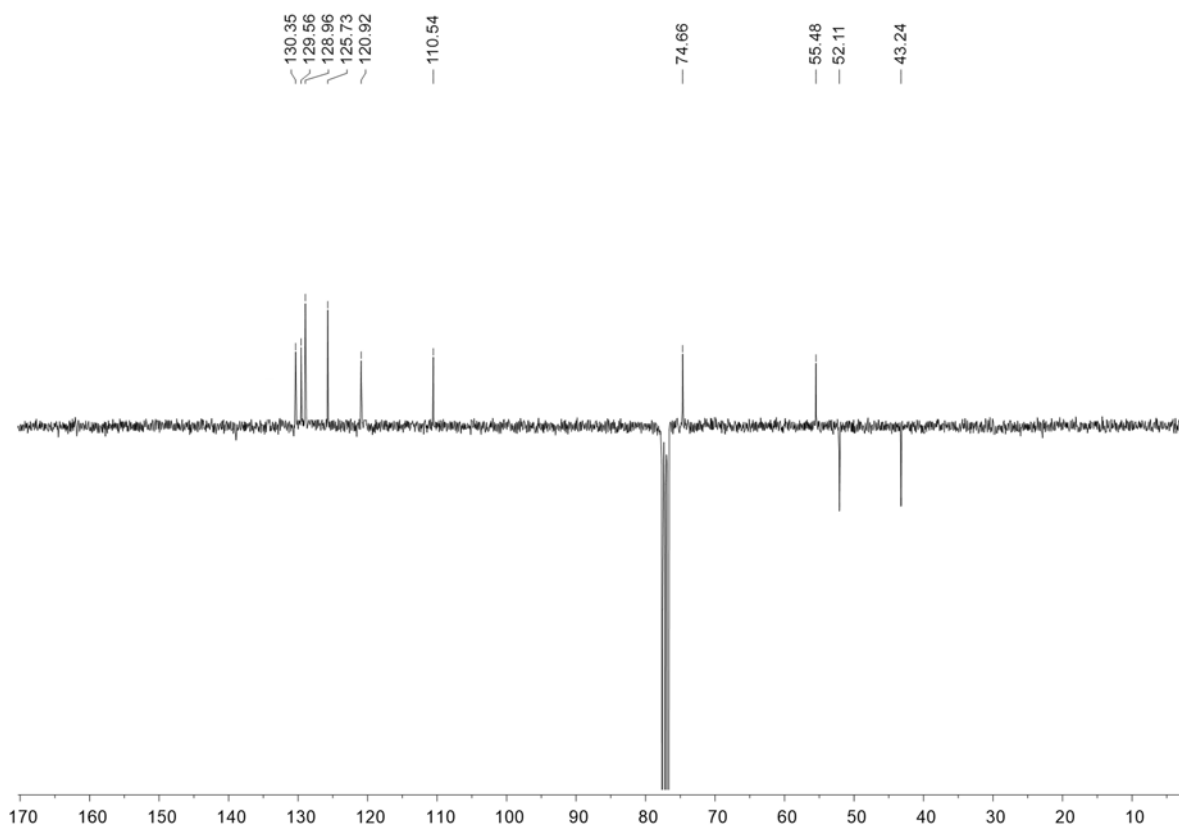


### 3.7.11. 3-(2-Methoxy)benzyl-5-phenyloxazolidin-2-one (85)

#### 3.7.11.1. $^1\text{H}$ NMR (300 MHz, $\text{CDCl}_3$ , 298 K)

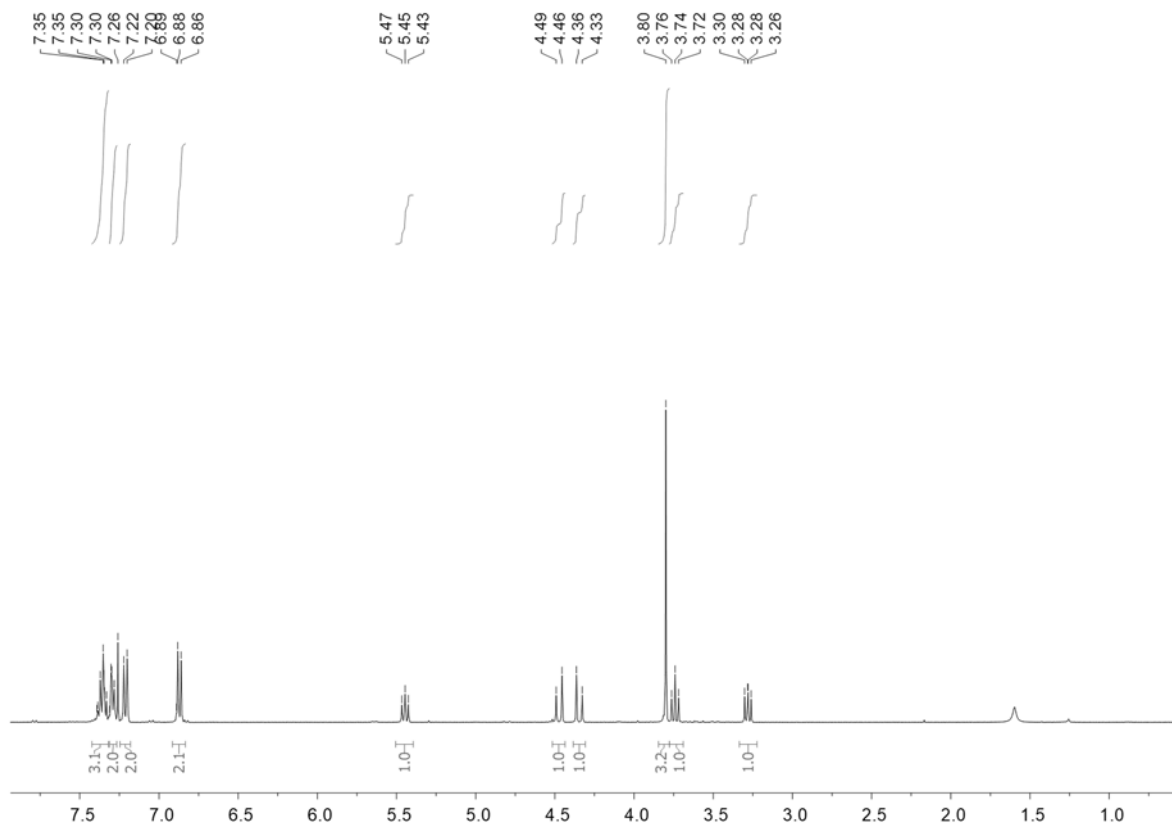


#### 3.7.11.2. $^{13}\text{C}$ NMR spectrum (75 MHz, $\text{CDCl}_3$ , 298 K)

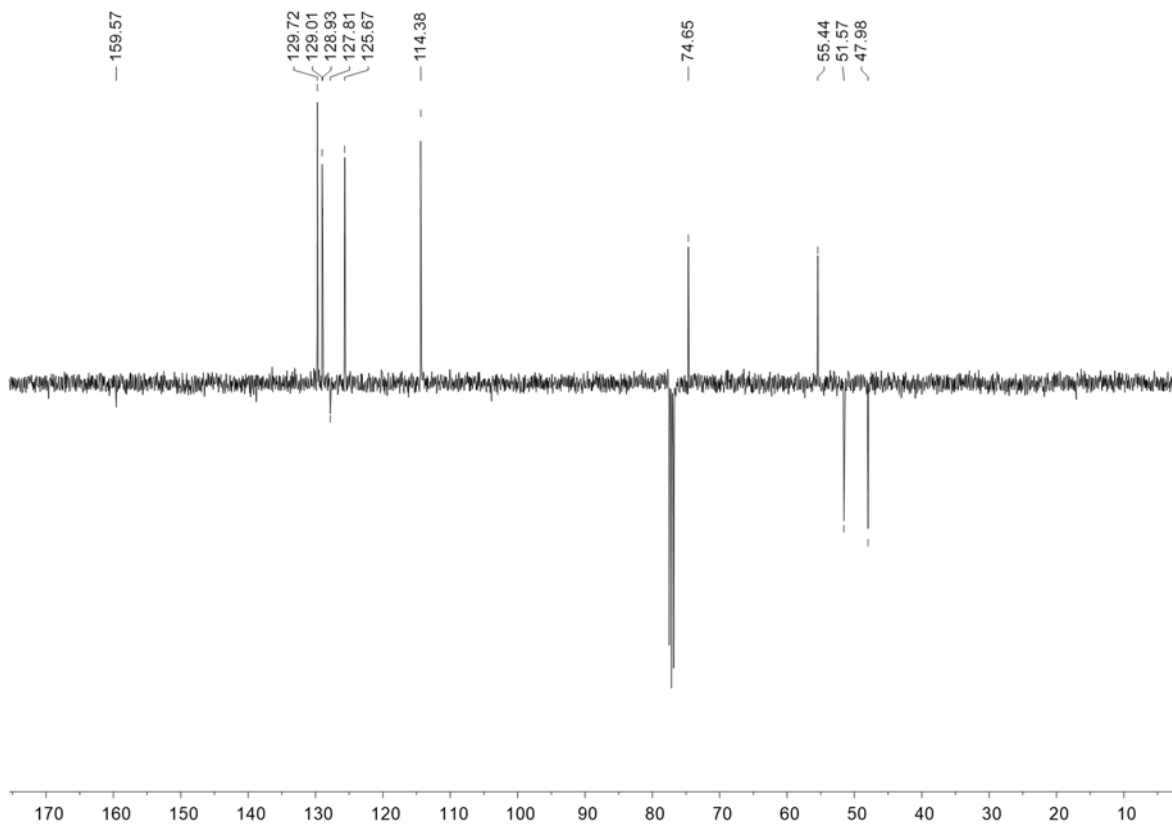


### 3.7.12. 3-(4-Methoxy)benzyl-5-phenyloxazolidin-2-one (86)

#### 3.7.12.1. $^1\text{H}$ NMR (400 MHz, $\text{CDCl}_3$ , 298 K)



#### 3.7.12.2. $^{13}\text{C}$ NMR spectrum (100 MHz, $\text{CDCl}_3$ , 298 K)



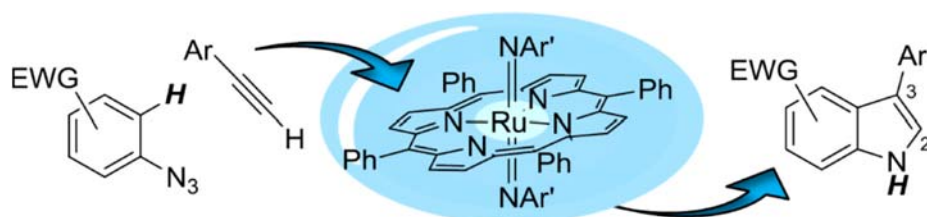
## 4. References

1. S. Braese, K. Banert, Editors, *Organic Azides Syntheses And Applications*. John Wiley & Sons Ltd. **2010**.
2. R. K. K. Becker, P. J. Nieuwland, F. P. J. T. Rutjes. *Chim. Oggi-Chem. Today* **2011**, 29, 47-49.
3. D. Mansuy, J. P. Mahy, A. Dureault, G. Bedi, P. Battioni. *J. Chem. Soc., Chem. Commun.* **1984**, 1161-1163.
4. C. C. Farwell, R. K. Zhang, J. A. McIntosh, T. K. Hyster, F. H. Arnold. *ACS Cent. Sci.* **2015**, 1, 89-93.
5. Y. Moreau, H. Chen, E. Derat, H. Hirao, C. Bolm, S. Shaik. *J. Phys. Chem. B* **2007**, 111, 10288-10299.
6. (a) S. Cenini, S. Tollari, A. Penoni, C. Cereda. *J. Mol. Catal. A: Chemical* **1999**, 137, 135-146. (b) S. Fantauzzi, E. Gallo, A. Caselli, C. Piangiolino, F. Ragaini, S. Cenini. *Eur. J. Org. Chem.* **2007**, 2007, 6053-6059. (c) C. Piangiolino, E. Gallo, A. Caselli, S. Fantauzzi, F. Ragaini, S. Cenini. *Eur. J. Org. Chem.* **2007**, 2007, 743-750.
7. P. Zardi, A. Pozzoli, F. Ferretti, G. Manca, C. Mealli, E. Gallo. *Dalton Transactions* **2015**, 44, 10479-10489.
8. K. H. Chan, X. Guan, V. K. Y. Lo, C. M. Che. *Angew. Chem. Int. Ed.* **2014**, 53, 2982-2987.
9. (a) M. G. Buonomenna, E. Gallo, F. Ragaini, S. Cenini, E. Drioli. *Desalination* **2006**, 199, 167-169. (b) M. G. Buonomenna, E. Gallo, F. Ragaini, A. Caselli, S. Cenini, E. Drioli. *Appl. Catal. A: General* **2008**, 335, 37-45.
10. E. Gallo, M. G. Buonomenna, L. Viganò, F. Ragaini, A. Caselli, S. Fantauzzi, S. Cenini, E. Drioli. *J. Mol. Catal. A: Chemical* **2008**, 282, 85-91.
11. (a) F. H. Malik Nasibullah, A. R. K. Naseem Ahmad, R. Masihur. *Adv. Sci. Eng. Med.* **2015**, 7, 91-111. (b) S. J. Pradeep, D. V. Maulikkumar, M. D. Tejas, K. C. Asit. *Curr. Med. Chem.* **2015**, 22, 4379-4397. (c) A. Bhushan, N. J. Martucci, O. B. Usta, M. L. Yarmush. *Expert Opin. Drug Metab. Toxicol.* **2016**, 12, 475-477. (d) Clemens Lamberth (Editor), J. D. E., *Bioactive Carboxylic Compound Classes: Pharmaceuticals and Agrochemicals* **2016**.
12. (a) D. A. Evans, J. Bartroli, T. L. Shih. *J. Am. Chem. Soc.* **1981**, 103, 2127-2129. (b) M. Shamszad, M. T. Crimmins. In *Comprehensive Chirality*, Elsevier **2012**. (c) M. M. Heravi, V. Zadsirjan, B. Farajpour. *RSC Advances* **2016**, 6, 30498-30551.
13. H. M. L. Davies, J. R. Manning. *Nature* **2008**, 451, 417.
14. A. Sudo, Y. Morioka, E. Koizumi, F. Sanda, T. Endo. *Tetrahedron Lett.* **2003**, 44, 7889-7891.
15. C. Phung, A. R. Pinhas. *Tetrahedron Lett.* **2010**, 51, 4552-4554.
16. Y. Wu, L. N. He, Y. Du, J. Q. Wang, C. X. Miao, W. Li. *Tetrahedron* **2009**, 65, 6204-6210.
17. A. W. Miller, S. T. Nguyen. *Organic Letters* **2004**, 6, 2301-2304.
18. F. Fontana, C. C. Chen, V. K. Aggarwal. *Organic Letters* **2011**, 13, 3454-3457.
19. (a) Y. Du, Y. Wu, A. H. Liu, L. N. He. *J. Org. Chem.* **2008**, 73, 4709-4712. (b) R. A. Watile, D. B. Bagal, Y. P. Patil, B. M. Bhanage. *Tetrahedron Lett.* **2011**, 52, 6383-6387.
20. Z. Z. Yang, Y. N. Li, Y. Y. Wei, L. N. He. *Green Chem.* **2011**, 13, 2351-2353.
21. D. Stephens, Y. Zhang, M. Cormier, G. Chavez, H. Arman, O. V. Larionov. *Chem. Commun.* **2013**, 49, 6558-6560.
22. V. B. Saptal, B. M. Bhanage. *ChemSusChem* **2016**, 9, 1980-1985.
23. D. B. Nale, S. Rana, K. Parida, B. M. Bhanage. *Appl. Catal. A: General* **2014**, 469, 340-349.
24. A. Baba, K. Seki, H. Matsuda. *J. Org. Chem.* **1991**, 58, 2684-2688.
25. C. Qi, J. Ye, W. Zeng, H. Jiang. *Adv. Synt. Catal.* **2010**, 352, 1925-1933.
26. Y. Zhang, Y. Zhang, Y. Ren, O. Ramström. *J. Mol. Catal. B: Enzymatic* **2015**, 122, 29-34.



# Chapter IV

## C-N bond formations: Indoles



*Parts of this chapter have been published and are reproduced here from:*

P. Zardi, A. Savoldelli, D. M. Carminati, A. Caselli, F. Ragaini and E. Gallo. *ACS catal.* **2014**, 4, 3820-3823.

# 1. Introduction

Indoles are electron rich aromatic heterocycles which play a prominent role in Nature thanks to their biological properties. Their structural motif is contained in several natural and synthetic drugs and this has pushed the academical and industrial researchers to develop new, versatile, cheap and ‘green’ methodologies for their synthesis (Figure 26).

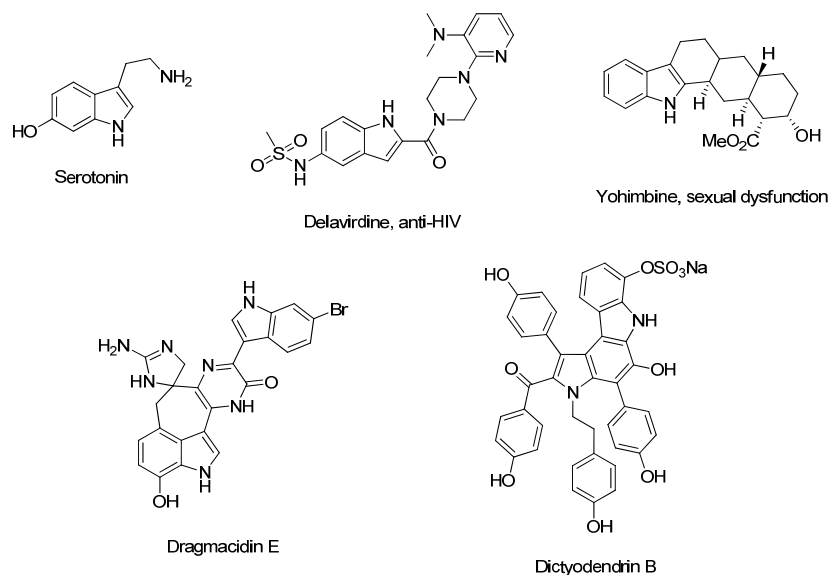


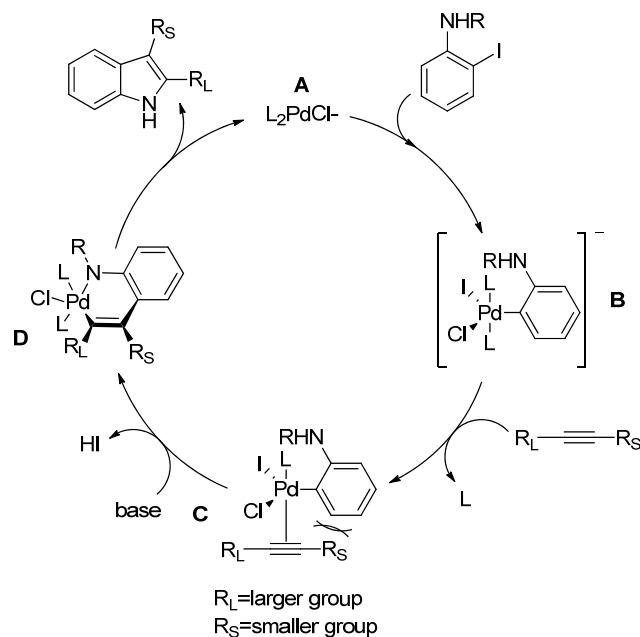
**Figure 26.** Example of indole-containing compounds with important biological activities.

A great number of procedures were developed besides the classical Fisher’s synthesis due to the high diversity of indoles, and here we report an overview of metal-catalysed indole synthesis.<sup>1</sup>

## 1.1. Synthesis of indoles

### 1.1.1. Larock indole synthesis

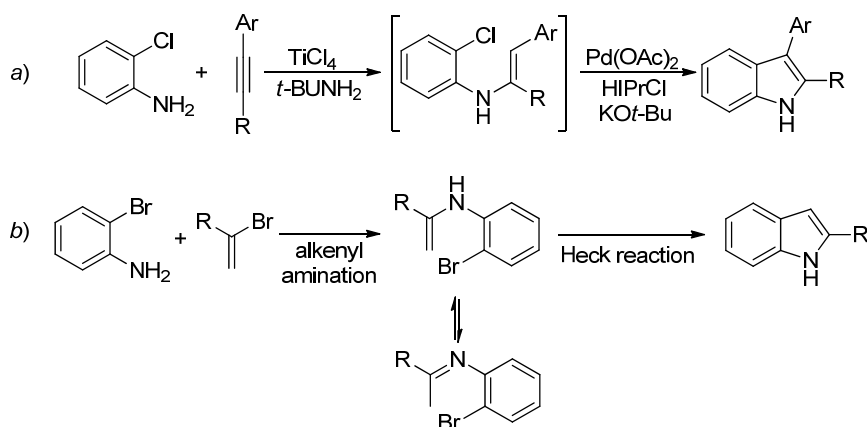
In 1991, Larock *et al* reported for the first time a new practical strategy for the synthesis of 2,3-substituted indoles: the so-called Larock synthesis.<sup>2</sup> It consists of a palladium-catalysed heteroannulation of internal alkynes with *N*-protected 2-haloanilines, usually iodoanilines, giving the final product (Scheme 42). When unsymmetrical alkynes are used, a high regioselectivity was observed due to the sterical effect between the aryl moiety and the more hindered group of the alkyne in the intermediate C. Instead a mixture of regioisomers are obtained using similarly substituted alkynes.



**Scheme 42.** Mechanism for the Larock synthesis.

After this pioneering work, two more regioselective procedures were studied by Ackermann and Barluenga using *o*-haloanilines and alkynes in the first case, and alkenes in the second one.<sup>3</sup> In 2004, Ackermann reported the one-pot titanium-catalysed hydroamination of asymmetrical aromatics alkynes followed by a 5-*endo* Heck coupling reaction (Scheme 43, *a*). During the reaction, a sterically hindered imidazole-2ylidene palladium complex was generated *in-situ* and this complex allowed the formation of products with a regioselectivity C2/C3 up to 99:1.

The Barluenga strategy involved a Pd-catalysed cascade process in which an enamine was formed by alkenyl amination and then underwent an intramolecular Heck reaction (Scheme 43, *b*). This strategy is the first example of a palladium-catalysed sequential process to synthesise important compounds such as indoles. The reactions were performed using both 1,1- and trans-1,2-disubstituted bromoalkenes and showed a good compatibility with several groups.

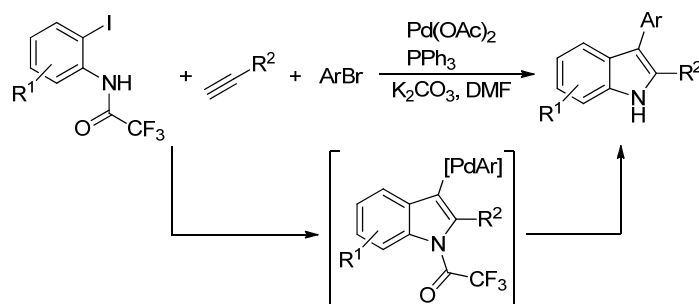


**Scheme 43.** General Ackermann (*a*) and Barluenga (*b*) reaction.

### 1.1.2. Cyclization of 2-alkynylanilines

Based on Larock's protocol, the hydroamination of 2-alkylanilines has become an established approach for the preparation of 2-substituted indoles involving the formation of 2-alkylaniline by a Sonogashira coupling and then a cyclisation to form the product. This methodology presents many advantages, but the most important are the high regioselectivity and the mild reaction conditions, which are fundamental when thermal labile molecules are employed. Unfortunately, the use of costly palladium catalyst for the first step and a wide variety of other metal catalysts for the cyclization make this strategy less interesting.

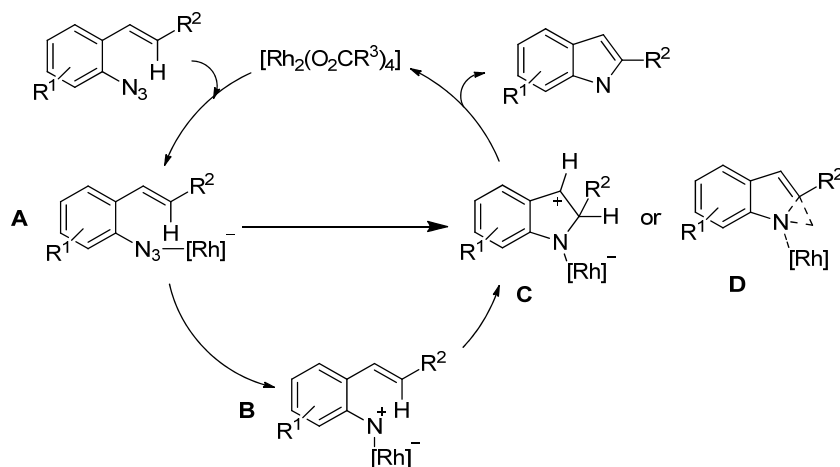
To overcome the high cost of the process, Lu *et al* reported a helpful and practical one-pot domino process starting from 2-iodoanilines and obtaining the 2,3-disubstituted indoles in excellent yields (Scheme 44).<sup>4</sup>



Scheme 44. One-pot domino reaction by Lu.

### 1.1.3. Synthesis of indole *via* metal-catalysed nitrene insertions

In the previous chapters, we reported some examples of nitrene transfer reactions for the synthesis of nitrogen-containing compounds such as amines and aziridines. Moreover, this class of reaction is also used to synthesise indole starting from azides and 2*H*-azirine. Concerning azides, Driver reported a series of studies in which  $\beta$ -styrylazides and 2-vinylarylazides underwent a regioselective intramolecular amination giving C2-substituted indoles in good yields.<sup>5</sup> The exact mechanism is unclear, but the authors proposed that the first step is the coordination of the azide by the rhodium catalyst and then the formation of complex B releasing molecular nitrogen. The second step can occur by two pathways: a concerted insertion of the nitrogen into an *ortho* C-H bond (intermediate C) or a stepwise electrophilic aromatic substitution forming intermediate D. After the formation of C (or D), the catalyst is regenerated releasing the 1*H*-indole (Scheme 45).



Scheme 45. Proposed mechanism for Driver's synthesis.

Another example using azides is the gold-catalysed reaction reported by Zhang between a 2-azidophenylalkyn and a nucleophile.<sup>6</sup> The azidophenylalkyn delivered a nitrene species which formed a gold carbene intermediate



containing the indole scaffold. The C3-position of this indole-gold complex is very electrophilic and reacts with several nucleophiles giving a large variety of functional indoles in good yields.

Nitrene species can be also generated thermally or catalytically *in situ* from 2*H*-azirines. Zheng described the synthesis of indoles via ring opening of 2-aryl-2*H*-azirines using cheap and nontoxic iron(II) chloride as catalyst. The reaction took place through the coordination of the iron centre to the nitrogen of the azirine forming a complex which provided an iron vinyl nitrene complex, after that the formation of indole occurred by intramolecular amination. Many functional groups, such as amides, aryl, halides, trifluoromethyl group, OTBS and OPiv, were tolerated and indoles were obtained in good yields and modest regioselectivities (Figure 27).<sup>7</sup>

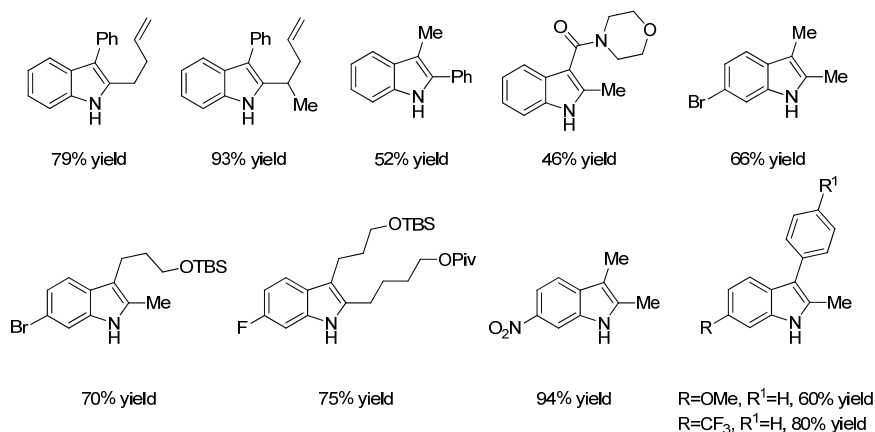
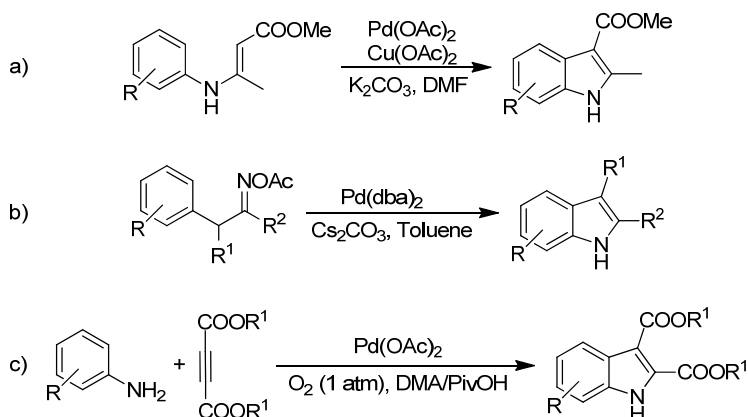


Figure 27. Indoles synthesised by Zheng *et al.*

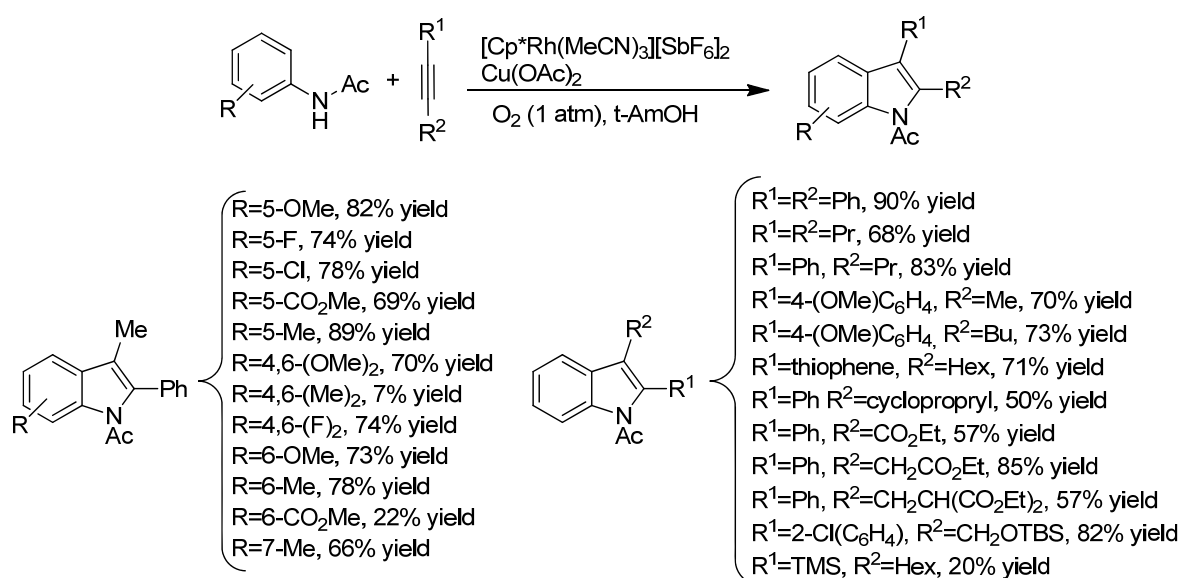
#### 1.1.4. C-H functionalisation by oxidative coupling

The catalytic methods, reported in the previous chapter, require the use of *ortho* disubstituted arenes which usually need to be synthesised lengthening the overall process. An approach starting from mono-functionalised arenes, which should involve a C-H bond activation, would be highly desirable. The first indoles synthesis through oxidative C-H bond functionalizations is the cyclization of *N*-aryl enamines published by Glorius.<sup>8</sup> The authors reported an efficient synthesis of functionalized indoles from easy-to-prepare enamines by palladium-catalysed intramolecular oxidative coupling. However, a large excess of copper salt was required as the terminal oxidant (Scheme 46a). After this work, Hartwig and co-workers reported a new approach to the direct amination of aromatic C-H bonds using oxime esters under redox neutral conditions.<sup>9</sup> These reactions occurred with relatively low catalyst loadings through a Pd(II) complex generated from N-O bond oxidative addition (Scheme 46b).



Scheme 46. Indole synthesis developed by a) Glorius, b) Hartwig and c) Jiao.

In terms of accessibility of the starting materials, intermolecular oxidative couplings would be more convenient approaches to the indoles: in fact, this strategy was successfully devised by Fagnou and Jiao, who reported the synthesis of indoles using anilines and alkynes as starting reagents. In particular, Jiao's methodology involved a palladium-catalysed reaction between simple anilines and electron-deficient alkynes (Scheme 46c), while Fagnou *et al* developed a rhodium-catalysed oxidative coupling of *N*-acetyl anilines and alkynes.<sup>10</sup> Both methods proceeded under mild conditions and by using molecular oxygen as the terminal oxidant. Using Fagnou's procedure, a range of new and functionally diverse alkynes resulted compatible, and both aryl/aryl and alkyl/alkyl symmetrically substituted internal alkynes produced 2,3-disubstituted indoles in moderate to excellent yields. However, when an unsymmetrical alkyl/alkyl substituted internal alkyne was employed in the reaction, a mixture of C2/C3 indole regioisomers was obtained in low yield and low regioselectivity. Conversely, alkyl/aryl internal alkynes reacted with near exclusive regioselectivity (>40:1), placing the aryl substituent proximal to the indole nitrogen (Scheme 47).



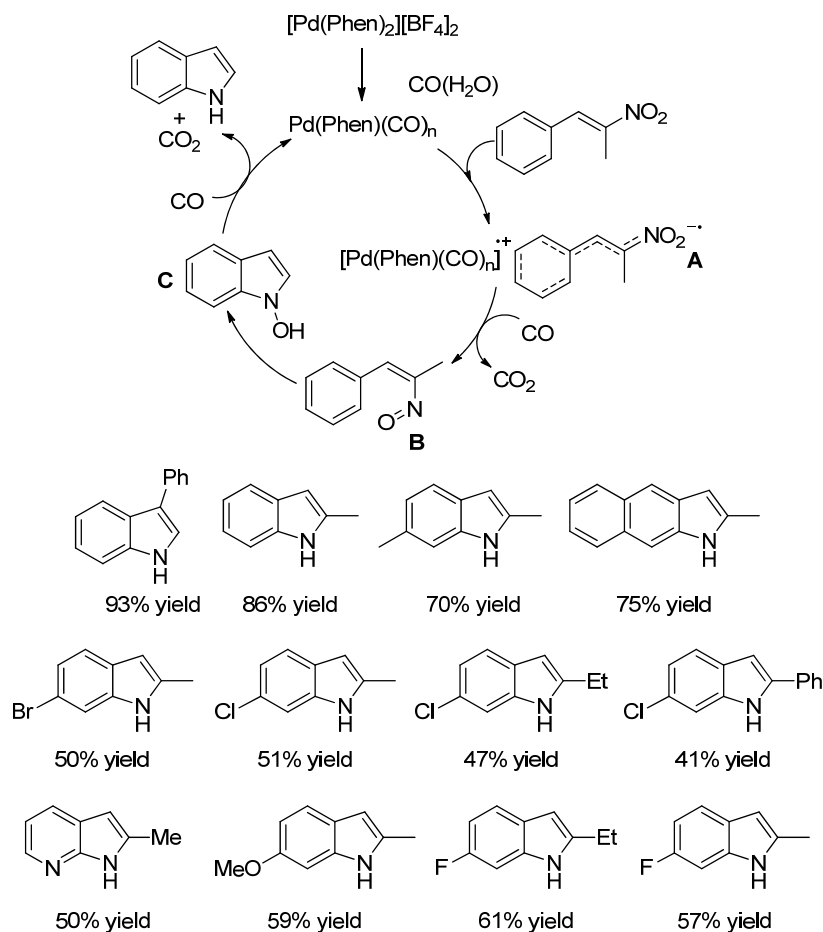
Scheme 47. Fagnou's catalytic system.

### 1.1.5. Reductive cyclization of nitroarenes

In the early 60s, Cadogan and co-workers reported the first reductive cyclization of nitroarenes for the synthesis of heterocycles using a phosphite/phosphate reductant system. After this pioneering work, many other papers have been published and the use of ruthenium, rhodium and palladium complexes have made this strategy highly selective and efficient. Among all catalytic systems, the palladium-phenanthroline complexes resulted the most active catalysts. In 2006, Ragaini and co-authors reported the reductive carbonylation of nitroarenes to nitrosoarene, followed by the intermolecular reaction with substituted phenylacetylenes. Then the cyclization reaction using [Pd(phen)<sub>2</sub>][BF<sub>4</sub>]<sub>2</sub> and carbon monoxide was carried out.<sup>11</sup> The presence of the aryl group on the alkyne is required, since it is believed to stabilize charges or radicals at the  $\alpha$  position of the intermediate.

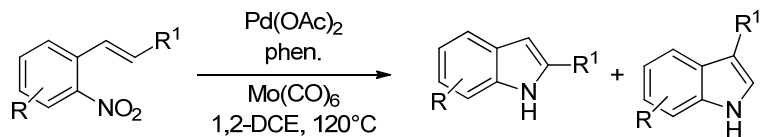
Complex [Pd(phen)<sub>2</sub>][BF<sub>4</sub>]<sub>2</sub> also catalyzed the intramolecular reductive cyclization of  $\beta$ -nitrostyrenes in presence of CO, giving indoles in moderate yields due to the difficulty in finding a good solvent.<sup>12</sup> Ragaini *et al* proposed a mechanism in which the nitro group is involved in a single-electron transfer forming a radical anion, complex A (Scheme 48), which, thanks to the delocalization of the radical, reacts with carbon monoxide.

Then, a cyclization of the nitroso complex occurs giving complex C which is reduced by another molecule of CO.



**Scheme 48.** Reductive cyclization of  $\beta$ -nitrostyrenes catalyzed by  $[\text{Pd}(\text{phen})_2][\text{BF}_4]_2$ .

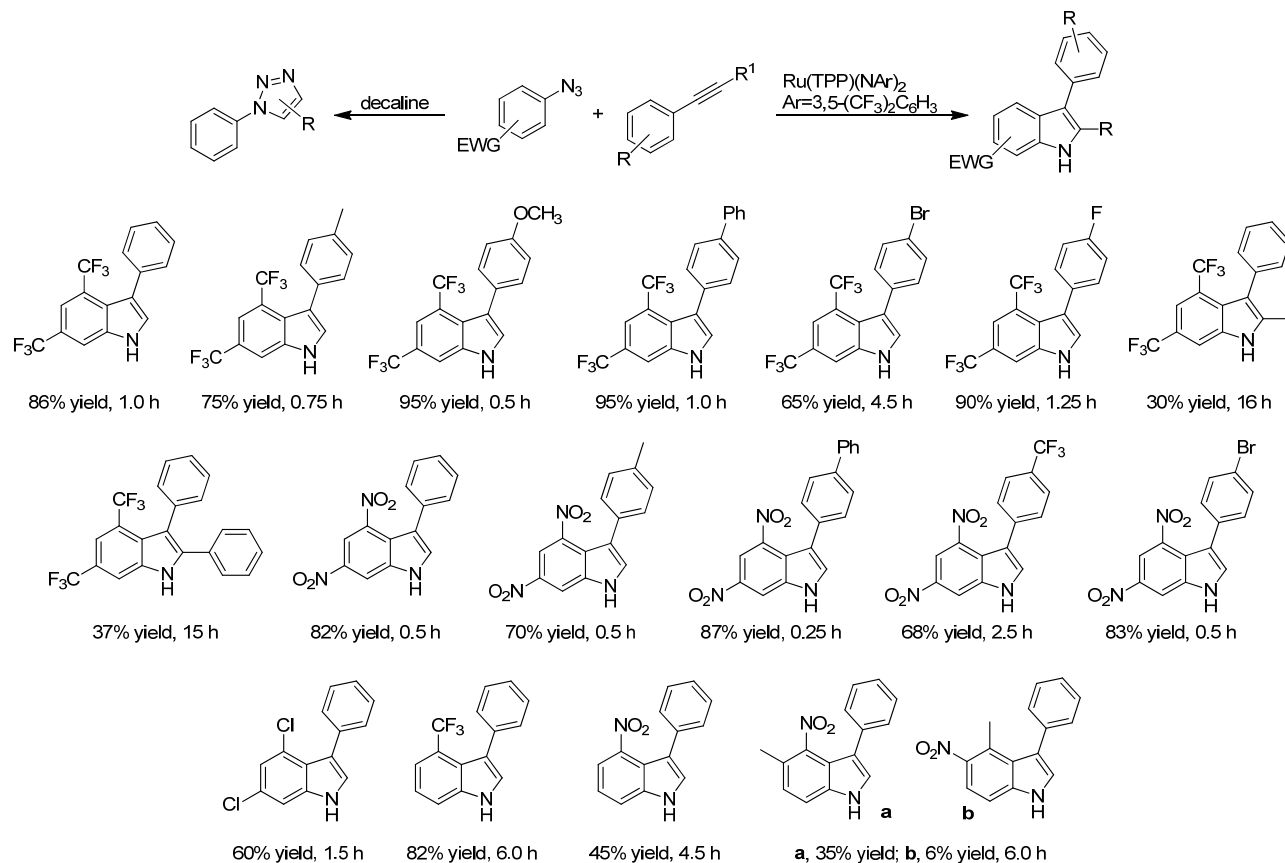
Since carbon monoxide is a very toxic gas, Driver and co-workers developed a new strategy in which  $\text{Mo}(\text{CO})_6$  was employed as a source of carbon monoxide. The reaction involved the transformation of trisubstituted nitrostyrenes in functionalized 3H-indoles using a combination of palladium acetate and  $\text{Mo}(\text{CO})_6$  (Scheme 49).<sup>13</sup> A large variety of indoles were obtained in good yields and several withdrawing and donor groups were tolerated both on the arene skeleton and in  $\beta$  position of the alkene.



**Scheme 49.** Palladium/ $\text{Mo}(\text{CO})_6$ -catalysed reaction of nitrostyrenes.

## 2. Discussion

In 2014 our research group reported the first synthetic strategy to obtain indoles by an intermolecular reaction between aryl azides and aryl alkynes using ruthenium *bis*-imido complex Ru(TPP)(NAr)<sub>2</sub> (Ar=3,5-(CF<sub>3</sub>)<sub>2</sub>C<sub>6</sub>H<sub>3</sub>) **71** as catalyst (Scheme 50).<sup>14</sup> This methodology assumes a particular importance considering that transition metal-catalysed intermolecular reactions of ArN<sub>3</sub> with alkynes usually give triazoles.



**Scheme 50.** Synthesis of indoles by intermolecular reaction between aryl azides and aryl alkynes.

The catalytic reaction, occurred in presence of 2% of Ru(TPP)(NAr)<sub>2</sub>, produced C3-functionalised indoles which bear EWG on the azide-deriving fragment, with yields up to 95% and with complete regioselectivity (Scheme 50). In order to improve the generality of the reaction, a screening of aryl azides and alkynes was performed (Figure 28). Since the catalytic efficiency of the reaction depends on the electronic characteristic of the substituent on the aryl azides, several electron-withdrawing and electron-donor aryl azides were tested. Unfortunately, no products were obtained when electron rich aryl azides were employed, and these results confirmed the importance of the presence of EWGs on the aryl azides. Also, using the 3,5-dicarboxyphenyl azide as starting material the product was not formed, and this is probably due to the low solubility of the starting reagent in the reaction medium. Moreover, the presence of the EWGs also influences the regioselectivity of the reaction: in fact when 3-chloro-5-(trifluoromethyl)phenyl azide was used as starting reagent, 6-chloro-3-phenyl-4-(trifluoromethyl)-1*H*-indole (**101a**) and 4-chloro-3-phenyl-6-(trifluoromethyl)-1*H*-indole (**101b**) were obtained with a regioselectivity of *a/b*=40:10. Therefore, a more electron-withdrawing group, such as the trifluoromethyl group, activates the cleavage of the C-H bond placed in an ortho position better than a less electron-withdrawing group such as the chlorine atom.

Considering the importance of the electron-withdrawing groups on the aryl moiety of the aryl azide, the alkynes screening was performed using 3,5-dinitrophenyl azide as starting reagent. The use of 3,5-dinitrophenyl azide allowed the simple recovery of 3-aryl-4,6-dinitroindoles through a simple filtration, given their insolubility in the reaction medium. Collected data showed a very good catalytic activity of complex **71**; C3-functionalised indoles were obtained in good yields and complete regioselectivity by using both electron poor and electron rich alkynes. Complete regioselectivity was also obtained by using a very sterically hindered aryl alkyne such as 2,4,5-trimethylphenyl acetylene, but the product was formed in low yield.

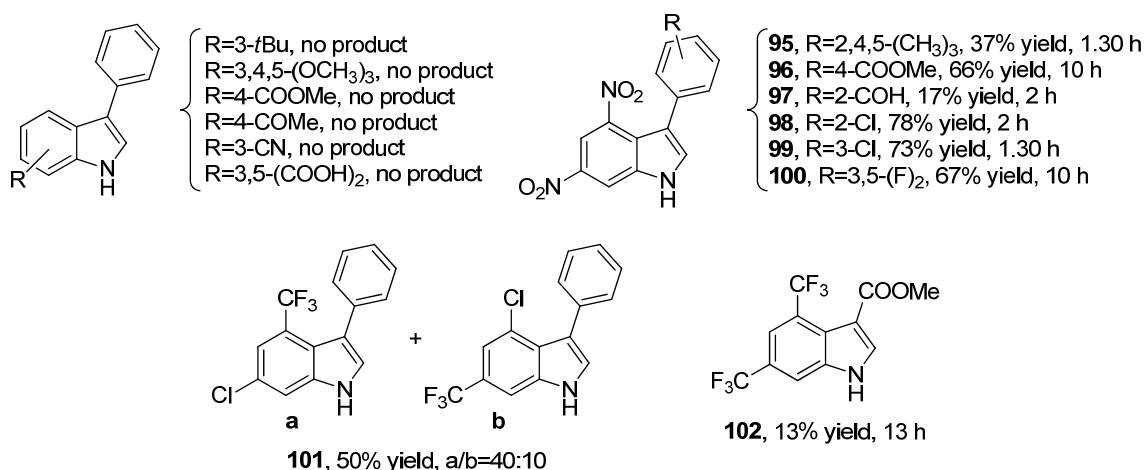
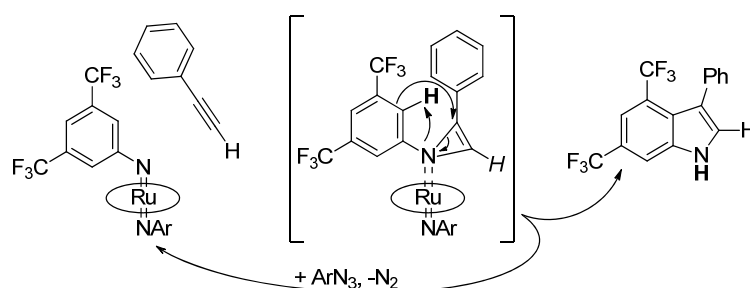


**Figure 28.** Scope of the intermolecular reaction between aryl azides and aryl alkynes.

In the previous work we suggested the reaction mechanism reported in Scheme 51, in which the first step of the cycle could be the formation of the ‘elusive’ *N*-substituted-*IH*-azirine, which cannot rearrange itself to become a more stable *2H*-azirine and can easily be involved in a ring opening reaction.<sup>14</sup> The polarization of a sp<sup>2</sup> C-H aromatic bond, placed in ortho positions with respect to a EWG, favours a hydrogen-transfer reaction (HAT) which is responsible for the indole formation. DFT study, which was performed by G. Manca and C. Mealli, revealed that the *N*-substituted-*IH*-azirine is not the reaction intermediate and its formation is not probable. Therefore, we proposed a new mechanism based on DFT calculations which were performed by using an asymmetric *bis*-imido complex as catalyst instead of complex **71** to speed up the calculations.



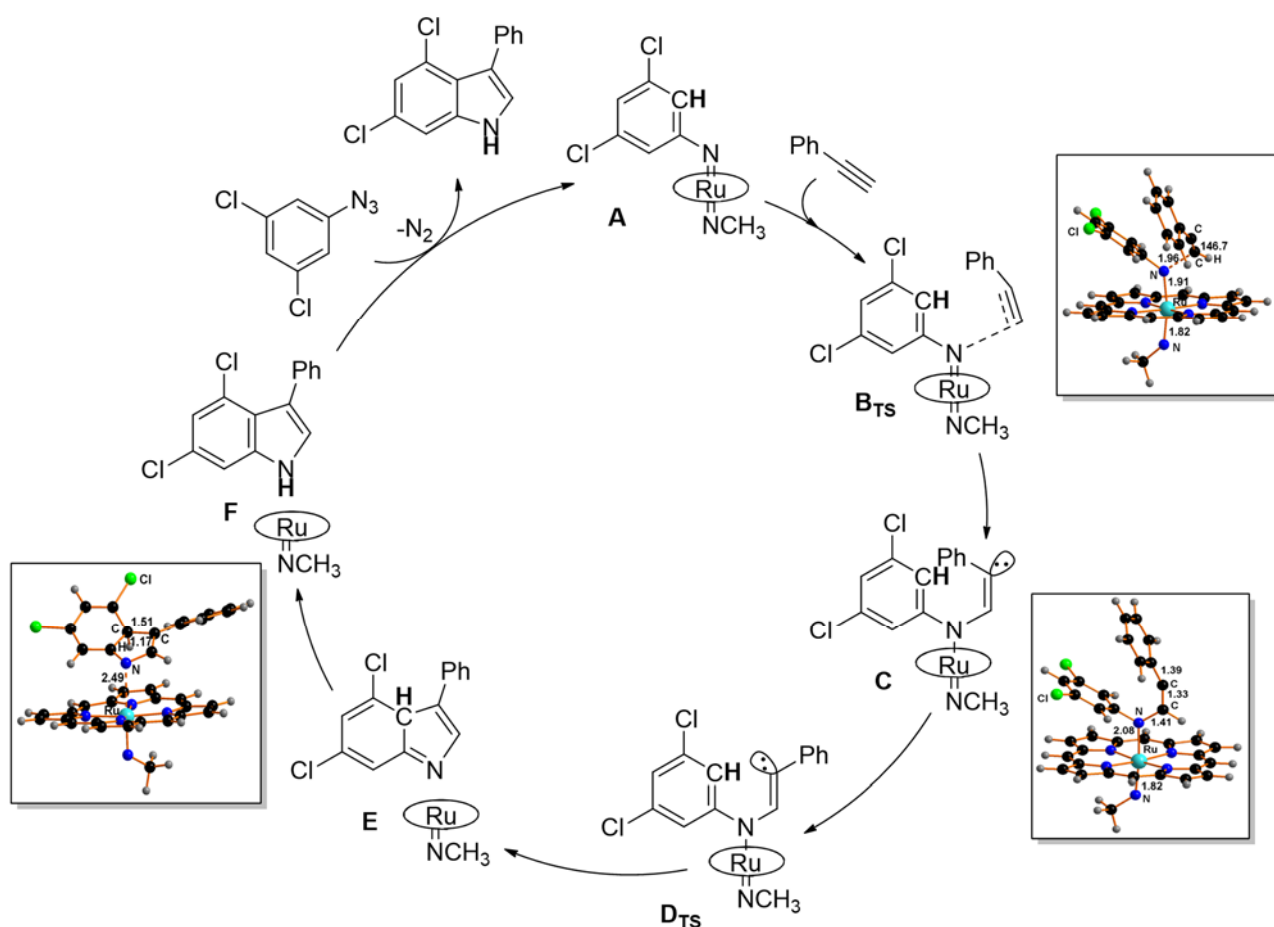
**Scheme 51.** Proposed mechanism via *N*-substituted-*IH*-azirine.

In particular, we used a Ru(porphine)(NC<sub>6</sub>H<sub>3</sub>Cl<sub>2</sub>)(NCH<sub>3</sub>) complex, **A** (Scheme 52), in which the tetraphenyl porphyrin ligand was replaced by the unsubstituted porphine, and one of the two axial imido ligands was replaced by a simpler NCH<sub>3</sub> group. The first step of the catalytic cycle is the approach of the phenylacetylene to the imido moiety of complex **A** forming the transition state **B<sub>TS</sub>** with an associated free energy cost of +13.9 kcal·mol<sup>-1</sup>. The DFT structure of **B<sub>TS</sub>** shows a N(imido)-C(alkyl) distance of 1.96 Å and the triple bond of the alkyl displays a more pronounced double bond character with a H-C-C angle of the alkyl moiety of 146.7°. Then, the transition state **B<sub>TS</sub>** forms the amido-imido species Ru(porphine)(N(C<sub>6</sub>H<sub>3</sub>Cl<sub>2</sub>)(CH=CC<sub>6</sub>H<sub>5</sub>))(NCH<sub>3</sub>),

**C**, with the formation of the N-C bond (1.41 Å). The formation of an amido apical ligand causes the elongation of the involved Ru-N distance up to 2.08 Å, while the other bond distance remains unaltered.

Since intermediate **C** shows the lone pair on the distal carbon oriented far away from the imido-ligand aryl moiety, a rotation around the C=C bond is fundamental to orient the lone pair towards the aryl moiety, allowing the close-ring reaction and the formation of the indole. The energy cost associated to the rotation is very low and, as soon as the rotation happens, the formation of the C-C bond occurs between the distal carbon atom of the alkyne moiety and the one in *ortho* to the aryl's chloride atom (intermediate **D<sub>Ts</sub>**, Scheme 52).

At this point, thanks to the ring closure reaction, the distance between the ruthenium atom and the nitrogen atom increases by promoting the rearrangement toward the indole and the dismissal of the product from the ruthenium complex.



**Scheme 52.** New proposed mechanism for the synthesis of indoles.

To shed more light on this proposed mechanism, we also performed a kinetic study. The **71**-catalysed reaction between 3,5-*bis*(trifluoromethyl)phenyl azide and phenylacetylene was taken as model reaction for all kinetic experiments. The reactions were followed by IR spectroscopy, which monitored the intensity of the aryl azide absorption at  $2116\text{ cm}^{-1}$ . All the kinetic experiments were run at  $75^\circ\text{C}$  to avoid boiling benzene. The rate of the model reaction showed a first-order dependence with respect to 3,5-*bis*(trifluoromethyl)phenyl azide, phenylacetylene and catalyst concentrations (Figure 29).

These data suggest that both the azide coordination on the ruthenium atom and the formation of the C-N bond of intermediate **C** occur with similar rates and both can be rate determining step of the catalytic cycle.

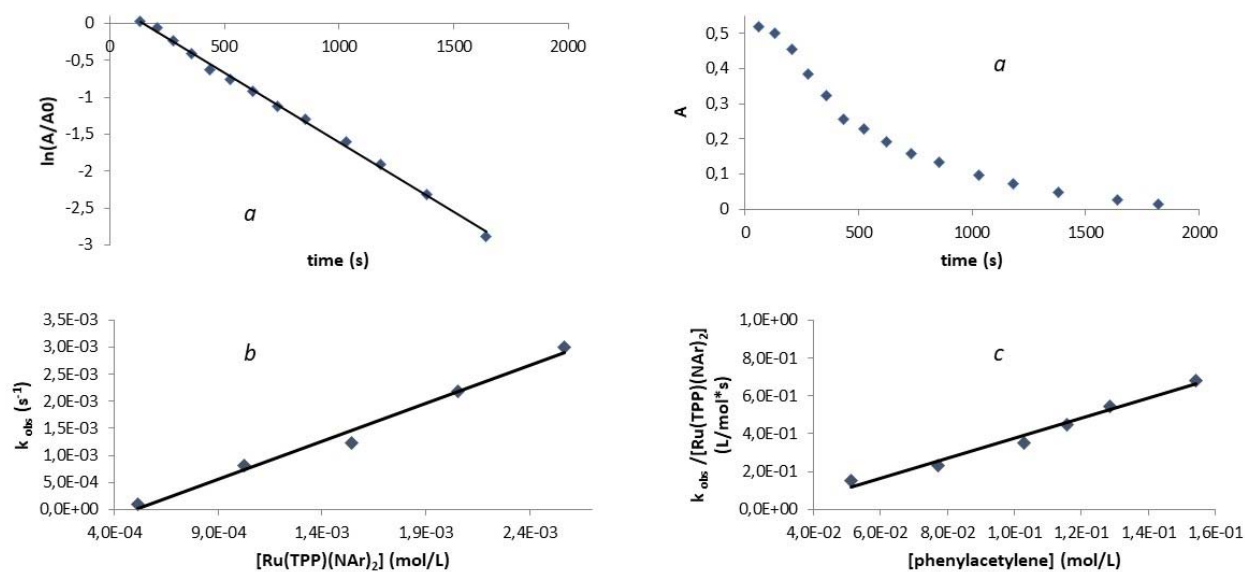


**Figure 29.** Kinetic dependence of the reaction rate with respect to the concentration of 3,5-bis(trifluoromethyl)phenyl azide (a), catalyst **71** (b) and phenylacetylene (c).

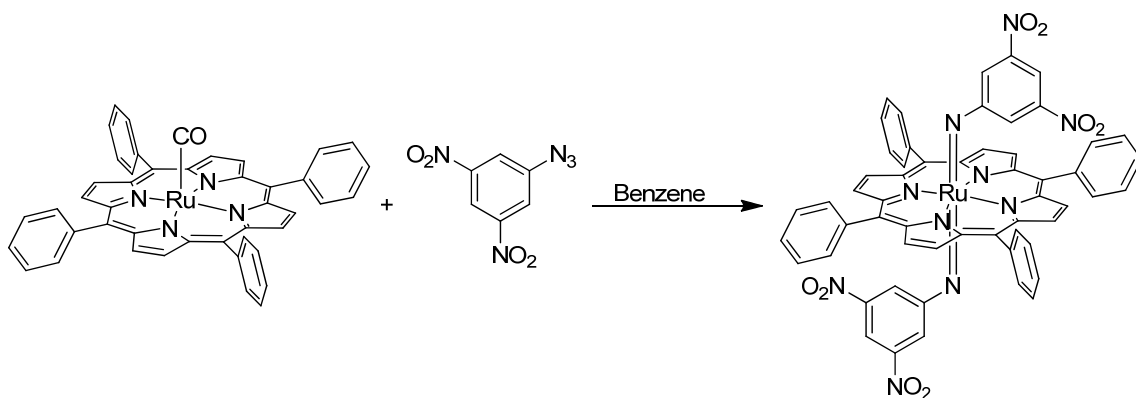
Kinetic data are in agreement to DFT calculations which suggest that the ring-closure reaction forming **E** is the most favorable step of the cycle.

### 3. Experimental Section

**General conditions:** Unless otherwise specified, all reactions were carried out under nitrogen or argon atmosphere employing standard Schlenk techniques and magnetic stirring. Dichloromethane, hexane, toluene, benzene were purified by using standard methods and stored under nitrogen atmosphere. All other starting materials were commercial products used as received. NMR spectra were recorded at room temperature on a Bruker Avance 300-DRX, operating at 300 MHz for  $^1\text{H}$ , at 75 MHz for  $^{13}\text{C}$  and 282 MHz for  $^{19}\text{F}$ , or on a Bruker Avance 400-DRX spectrometer, operating at 400 MHz for  $^1\text{H}$ , at 100 MHz for  $^{13}\text{C}$  and at 376 MHz for  $^{19}\text{F}$ . Chemical shifts (ppm) are reported relative to TMS. The  $^1\text{H}$  NMR signals of the compounds described in the following were identified by 2 D NMR techniques. Assignments of the resonance in  $^{13}\text{C}$  NMR were made using the APT pulse sequence and HSQC and HMBC techniques. GC-MS analyses were performed on Shimadzu QP5050A instrument. Infrared spectra were recorded on a Varian Scimitar FTS 1000 spectrophotometer. UV/Vis spectra were recorded on an Agilent 8453E instrument. Elemental analyses and mass spectra were recorded in the analytical laboratories of Milan.

#### 3.1. Synthesis of ruthenium porphyrin complexes

##### 3.1.1. Synthesis of $\text{Ru}(\text{TPP})(\text{NAr})_2$ ( $\text{Ar}=3,5(\text{NO}_2)_2\text{C}_6\text{H}_3$ )



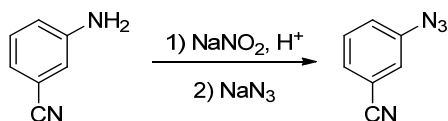
3,5-Dinitrophenyl azide (70.0 mg,  $3.35 \cdot 10^{-3}$  mol) was added to a benzene (25.0 mL) suspension of  $\text{Ru}(\text{TPP})\text{CO}$  (0.100 g,  $1.35 \cdot 10^{-4}$  mol). The resulting dark mixture was refluxed for 20 minutes observing the complete consumption of  $\text{Ru}(\text{TPP})\text{CO}$  by TLC (hexane/AcOEt 7:3). The solution was concentrated to about 5 mL and hexane (10.0 mL) was added. A crystalline violet solid was collected by filtration and dried *in vacuo* (97.0 mg, 69%).

$^1\text{H}$  NMR (300 MHz,  $\text{C}_6\text{D}_6$ ):  $\delta$  8.90 (s, 8H,  $\text{H}_\beta$ ), 8.16 (d, 8H,  $J=6.9$  Hz,  $\text{H}_\alpha$ ), 7.48 (m, 12H,  $\text{H}_m$  and  $\text{H}_p$ ), 7.16 (s, 2H,  $\text{H}_{\text{Ar-para}}$ , overlapped with the solvent signal), 3.36 ppm (s, 4H,  $\text{H}_{\text{Ar-ortho}}$ ). IR (ATR):  $\nu=889$   $\text{cm}^{-1}$ .



## 3.2. Synthesis of aryl azides

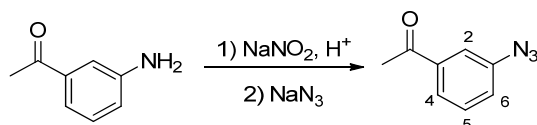
### 3.2.1. Synthesis of 3-cyanophenyl azide



3-Cyanoaniline (0.498 g,  $4.21 \cdot 10^{-3}$  mol) was dissolved in a solution of 5.00 mL of HCl at 37% and 7.00 mL of water under air. The mixture was cooled at  $0^\circ$  C in an ice bath and a solution of  $\text{NaNO}_2$  (0.290 g,  $4.21 \cdot 10^{-3}$  mol) in 5.00 mL of water was added. The reaction was stirred for 30 minutes and then urea (23.0 mg,  $3.82 \cdot 10^{-4}$  mol) was added in one portion. Under vigorous magnetic stirring a solution of sodium azide (0.273 g,  $4.21 \cdot 10^{-3}$  mol) in 7.00 mL of water was added to the cold mixture in about 15 minutes. The resulting mixture was then allowed to reach room temperature and further stirred for 1 hour. Diethyl ether (10.0 mL) was added and the phases were separated. The aqueous phase was washed twice with 10.0 mL of diethyl ether and the combined organic phases were dried over  $\text{Na}_2\text{SO}_4$ . The solvent was evaporated under reduced pressure to obtain the product as a yellowish solid (0.530 g, 83%).

$^1\text{H NMR}$  (400 MHz,  $\text{CDCl}_3$ ):  $\delta$  7.49-7.42 (m, 2H,  $\text{H}_{\text{Ar}}$ ), 7.29-7.27 ppm (m, 2H,  $\text{H}_{\text{Ar}}$ ). **IR** ( $\text{CH}_2\text{Cl}_2$ ):  $\nu_{\text{max}} = 2117 \text{ cm}^{-1}$ .

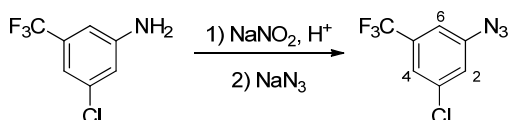
### 3.2.2. Synthesis of 3-azido acetophenone



3-Amino-acetophenone (0.494 g,  $3.65 \cdot 10^{-3}$  mol) was suspended in a solution of 7.00 mL of water and 5.00 mL of HCl 37%. The suspension was placed in an ice bath and a solution of  $\text{NaNO}_2$  (0.251 g,  $3.65 \cdot 10^{-3}$  mol) in 5.00 mL of water was added dropwise. After 30 minutes urea (20.4 mg,  $3.39 \cdot 10^{-3}$  mol) was added in one portion. Under vigorous magnetic stirring a solution of sodium azide (0.237 g,  $3.65 \cdot 10^{-3}$  mol) in 7.00 mL of water was added dropwise to the cold mixture. The resulting mixture was then allowed to reach room temperature and further stirred for 1 hour. Diethyl ether (10.0 mL) was then added and the phases were separated. Aqueous phase was washed three times with 5.00 mL of diethyl ether and the combined organic phases were dried over  $\text{Na}_2\text{SO}_4$ . The solvent was evaporated under reduced pressure to obtain the product as a yellow oil (0.510 g, 87%).

$^1\text{H NMR}$  (400 MHz,  $\text{CDCl}_3$ ):  $\delta$  7.71 (d, 1H,  $J=7.7 \text{ Hz}$ ,  $\text{H}^4$ ), 7.61 (m, 1H,  $\text{H}^2$ ), 7.46 (t, 1H,  $J=7.8 \text{ Hz}$ ,  $\text{H}^5$ ), 7.22-7.20 (m, 1H,  $\text{H}^6$ ), 2.60 ppm (s, 3H,  $\text{H}_{\text{CH}_3}$ ). **IR** ( $\text{CH}_2\text{Cl}_2$ ):  $\nu_{\text{max}} = 2110 \text{ cm}^{-1}$ .

### 3.2.3. Synthesis of 3-chloro-5-(trifluoromethyl)phenyl azide

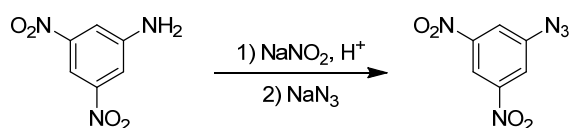


3-Chloro-5-(trifluoromethyl)aniline (0.221 g,  $1.12 \cdot 10^{-3}$  mol) was dissolved in a solution of 2.60 mL of HCl 37% and 7.10 mL of water under air. The orange suspension was cooled at  $0^\circ$  C in an ice bath and a solution of  $\text{NaNO}_2$  (0.110 g,  $1.60 \cdot 10^{-3}$  mol) in 1.40 mL of water was added to the white suspension. The reaction was

stirred for 30 minutes and then urea (27.6 mg,  $4.59 \cdot 10^{-4}$  mol) was added in one portion. Under vigorous magnetic stirring a solution of sodium azide (0.143 g,  $2.20 \cdot 10^{-3}$  mol) in 2.00 mL of water was added to the cold mixture in about 15 minutes. The resulting mixture was then allowed to reach room temperature and further stirred for 1 hour and 30 minutes. Diethyl ether (7.00 mL) was added and the phases were separated. The aqueous phase was washed three times with 5.00 mL of diethyl ether and the combined organic phases were dried over  $\text{Na}_2\text{SO}_4$ . The solvent was evaporated under reduced pressure to give a yellow oil (0.234 g, 94%).

$^1\text{H NMR}$  (300 MHz,  $\text{CDCl}_3$ ):  $\delta$  7.38 (s, 1H,  $\text{H}^4$ ), 7.20 (s, 1H,  $\text{H}^6$ ), 7.15 ppm (s, 1H,  $\text{H}^2$ ).  $^{19}\text{F}$  (282 MHz,  $\text{CDCl}_3$ ):  $\delta$  -63.74 ppm (s, 3F,  $\text{CF}_3$ ). **IR** (nujol):  $\nu_{\text{max}} = 2114 \text{ cm}^{-1}$ .

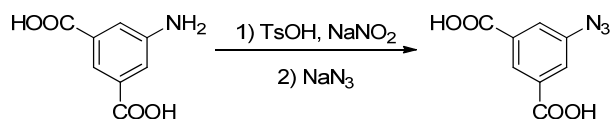
### 3.2.4. Synthesis of 3,5-dinitrophenyl azide



3,5-Dinitroaniline (1.58 g,  $8.62 \cdot 10^{-3}$  mol) was suspended in a solution of 20.0 mL of water and 5.00 mL of  $\text{H}_2\text{SO}_4$  conc. under air. The suspension was placed in an ice bath and a solution of  $\text{NaNO}_2$  (0.640 g,  $9.27 \cdot 10^{-3}$  mol) in 8.00 mL of water was added dropwise. After 30 minutes urea (0.150 g,  $2.49 \cdot 10^{-3}$  mol) was added in one portion. Under vigorous magnetic stirring a solution of sodium azide (0.688 g,  $1.06 \cdot 10^{-2}$  mol) in 8.00 mL of water was added dropwise to the cold mixture. The resulting mixture was then allowed to reach room temperature and further stirred for 45 minutes. Dichloromethane (55.0 mL) was then added and the phases were separated. Aqueous phase was washed twice with 30.0 mL of dichloromethane and the combined organic phases were dried over  $\text{Na}_2\text{SO}_4$ . The solvent was evaporated under reduced pressure and the crude was purified by flash chromatographic ( $\text{SiO}_2$ , 60  $\mu\text{m}$ , hexane/ $\text{AcOEt}$  8:2). The product was obtained as a yellow solid (1.55 g, 86%).

$^1\text{H NMR}$  (300 MHz,  $\text{CDCl}_3$ ):  $\delta$  8.80 (t, 1H,  $J=1.9$  Hz,  $\text{H}_p$ ), 8.19 (d, 2H,  $J=1.9$  Hz,  $\text{H}_o$ ). **IR** ( $\text{CH}_2\text{Cl}_2$ ):  $\nu_{\text{max}} = 2130 \text{ cm}^{-1}$ .

### 3.2.5. Synthesis of 5-azido isophthalic acid



5-Amino isophthalic acid (1.02 g,  $5.65 \cdot 10^{-3}$  mol) was added to a solution of 50.0 mL of water and tosyl acid (9.56 g,  $4.95 \cdot 10^{-2}$  mol) under air. Then  $\text{NaNO}_2$  (3.33 g,  $4.95 \cdot 10^{-2}$  mol) was added in three portions and the reaction was stirred at room temperature overnight. Under vigorous magnetic stirring, sodium azide (0.574 g,  $8.80 \cdot 10^{-3}$  mol) was added and the mixture was stirred for 30 minutes giving a white solid. The solid was recovered by filtration and dried *in vacuo* (1.03 g, 86%).

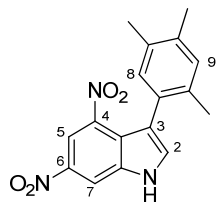
$^1\text{H NMR}$  (300 MHz,  $\text{DMSO}-d_6$ ):  $\delta$  13.54 (s, 2H,  $\text{HCOOH}$ ), 8.24 (s, 1H,  $\text{H}_p$ ), 7.77 ppm (s, 2H,  $\text{H}_o$ ). **IR** (nujol):  $\nu_{\text{max}} = 2114 \text{ cm}^{-1}$ .

### 3.3. Synthesis of indoles catalysed by ruthenium porphyrin complexes

#### 3.3.1. Synthesis of indoles

**General catalytic procedure:** alkyne (2.50 mmol) and aryl azide (0.50 mmol) were added to a solution of Ru(TPP)(NAr)<sub>2</sub> (Ar=3,5-(CF<sub>3</sub>)<sub>2</sub>C<sub>6</sub>H<sub>3</sub>) (**71**) (11.7 mg, 0.010 mmol) in benzene (10.0 mL) and then the resulting mixture was refluxed until the complete consumption of aryl azide. The consumption of aryl azide was monitored by IR spectroscopy by measuring the decrease of the characteristic N<sub>3</sub> absorbance at ≈2100 cm<sup>-1</sup>. The solvent was evaporated to dryness and the residue was purified.

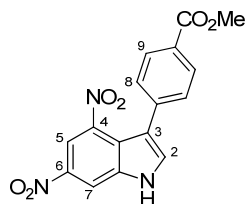
##### 3.3.1.1. Synthesis of 4,6-dinitro-3-(2,4,5-trimethyl)-phenyl-1H-indole (**95**)



Compound **95** was obtained from 1-ethynyl-2,4,5-trimethylbenzene and 3,5-dinitrophenyl azide. At the end of the reaction, benzene was evaporated to dryness and CH<sub>2</sub>Cl<sub>2</sub> (10.0 mL) was added to the crude. Compound **95** was recovered by filtration as a yellow solid.

<sup>1</sup>H NMR (300 MHz, DMSO-*d*<sub>6</sub>): δ 12.81 (br, 1H, *H*NH), 8.72 (d, 1H, <sup>4</sup>*J*=1.35 Hz, H<sup>7</sup>), 8.54 (d, 1H, <sup>4</sup>*J*=1.32 Hz, H<sup>5</sup>), 8.05 (s, 1H, H<sup>2</sup>), 7.01 (s, 1H, H<sup>9</sup>), 6.89 (s, 1H, H<sup>8</sup>), 2.23 (s, 3H, H<sub>CH<sub>3</sub>-para</sub>), 2.18 (s, 3H, H<sub>CH<sub>3</sub>-meta</sub>), 1.91 ppm (s, 3H, H<sub>CH<sub>3</sub>-ortho</sub>). <sup>13</sup>C NMR (75 MHz, DMSO-*d*<sub>6</sub>): δ 140.6 (C4), 139.8 (C6), 137.1 (C7-C-NH), 136.2 (C2-H), 134.8 (C-CH<sub>3</sub> para), 133.6 (C-CH<sub>3</sub> ortho), 132.5 (C-CH<sub>3</sub> meta), 131.0 (C3-C-C8), 130.9 (C8-H), 130.6 (C9-H), 121.2 (C4-C-C3), 116.1 (C3), 113.4 (C7-H), 111.6 (C5-H), 19.2 (CH<sub>3</sub> ortho), 18.9 (CH<sub>3</sub> meta), 18.8 ppm (CH<sub>3</sub> para). **Elemental analysis** calcd for C<sub>17</sub>H<sub>15</sub>N<sub>3</sub>O<sub>4</sub>: C, 62.76; H, 4.65; N, 12.92. Found: C, 62.62; H, 4.38; N, 11.40. **MS** (EI): *m/z*=324 [M-1].

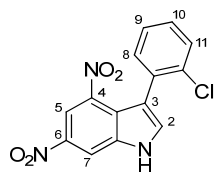
##### 3.3.1.2. Synthesis of methyl 4-(4,6-dinitro-1H-indol-3-yl)benzoate (**96**)



Compound **96** was obtained from methyl 4-ethynylbenzoate and 3,5-dinitrophenyl azide. At the end of the reaction, benzene was evaporated to dryness and CH<sub>2</sub>Cl<sub>2</sub> (10.0 mL) was added to the crude. Compound **96** was recovered by filtration as a yellow solid.

<sup>1</sup>H NMR (300 MHz, DMSO-*d*<sub>6</sub>): δ 13.04 (s, 1H, NH), 8.75 (d, 1H, <sup>4</sup>*J*=1.89 Hz, H<sup>7</sup>), 8.60 (d, 1H, <sup>4</sup>*J*=1.86 Hz, H<sup>5</sup>), 8.36 (s, 1H, H<sup>2</sup>), 7.97 (d, 2H, *J*=8.2 Hz, H<sup>9</sup>), 7.39 (d, 2H, *J*=8.2 Hz, H<sup>8</sup>), 3.88 ppm (s, 3H, H<sub>CH<sub>3</sub></sub>). <sup>13</sup>C NMR (75 MHz, DMSO-*d*<sub>6</sub>): δ 166.1 (CO<sub>2</sub>Me), 140.7 (C4), 140.3 (C6), 139.2 (C9-C-CO<sub>2</sub>Me), 137.6 (C7-C-NH), 136.7 (C2-H), 128.7 (C8-H), 128.5 (C9-H), 127.6 (C8-C-C3), 119.6 (C3-C-C4), 116.1 (C3), 113.7 (C7-H), 112.2 (C5-H), 52.1 ppm (CH<sub>3</sub>). **Elemental analysis** calcd for C<sub>16</sub>H<sub>11</sub>N<sub>3</sub>O<sub>6</sub>: C, 56.31; H, 3.25; N, 12.31. Found: C, 55.68; H, 3.20; N, 12.36. **MS** (EI): *m/z*=340 [M-1].

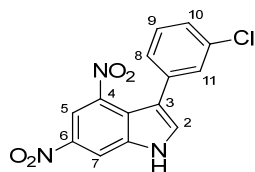
### 3.3.1.3. Synthesis of 4,6-dinitro-3-(2-chloro)-phenyl-1H-indole (98)



Compound **98** was obtained from methyl 1-ethynyl-2-chlorobenzene and 3,5-dinitrophenyl azide. At the end of the reaction, benzene was evaporated to dryness and  $\text{CH}_2\text{Cl}_2$  (10.0 mL) was added to the crude. Compound **98** was recovered by filtration as a yellow solid.

$^1\text{H NMR}$  (300 MHz,  $\text{DMSO}-d_6$ ):  $\delta$  12.98 (br, 1H, NH), 8.77 (d, 1H,  $^4J=2.0$  Hz,  $\text{H}^7$ ), 8.63 (d, 1H,  $^4J=2.0$  Hz,  $\text{H}^5$ ), 8.23 (s, 1H,  $\text{H}^2$ ), 7.51-7.48 (m, 2H,  $\text{H}^8$  and  $\text{H}^{11}$ ), 7.42-7.36 ppm (m, 2H,  $\text{H}^9$  and  $\text{H}^{10}$ ).  $^{13}\text{C NMR}$  (75 MHz,  $\text{DMSO}-d_6$ ):  $\delta$  141.56 (C4), 141.0 (C6), 138.2 (C7-C-NH), 138.1 (C2-H), 135.1 (C3-C-C8), 134.6 (C-Cl), 132.1 (C11-H), 129.6 (C10-H), 129.4 (C8-H), 127.7 (C9-H), 121.9 (C4-C-C3), 115.33 (C3), 114.9 (C7-H), 113.1 ppm (C5-H). **Elemental Analysis** calcd for  $\text{C}_{14}\text{H}_8\text{N}_3\text{ClO}_4$ : C, 52.93; H, 2.54; N, 13.23. Found: C, 52.66; H, 2.55; N, 12.70. **MS** (EI):  $m/z=316$  [M-1].

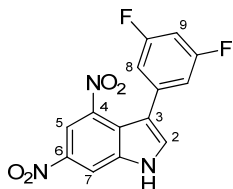
### 3.3.1.4. Synthesis of 4,6-dinitro-3-(3-chloro)-phenyl-1H-indole (99)



Compound **99** was obtained from methyl 1-ethynyl-3-chlorobenzene and 3,5-dinitrophenyl azide. At the end of the reaction, benzene was evaporated to dryness and  $\text{CH}_2\text{Cl}_2$  (10.0 mL) was added to the crude. Compound **99** was recovered by filtration as a yellow solid.

$^1\text{H NMR}$  (300 MHz,  $\text{DMSO}-d_6$ ):  $\delta$  12.98 (br, 1H, NH), 8.74 (d, 1H,  $^4J=2.0$  Hz,  $\text{H}^7$ ), 8.59 (d, 1H,  $^4J=2.0$  Hz,  $\text{H}^5$ ), 8.32 (s, 1H,  $\text{H}^2$ ), 7.42-7.36 (m, 3H,  $\text{H}^8$  and  $\text{H}^9$  and  $\text{H}^{10}$ ), 7.19-7.16 ppm (m, 1H,  $\text{H}^{11}$ ).  $^{13}\text{C NMR}$  (75 MHz,  $\text{DMSO}-d_6$ ):  $\delta$  140.6 (C4), 140.2 (C6), 137.4 (C7-C-NH), 136.6 (C2-H), 136.3 (C3-C-C8), 132.5 (C-Cl), 129.5 (C9-H), 127.9 (C8-H), 127.2 (C11-H), 126.5 (C10-H), 119.7 (C4-C-C3), 115.7 (C3), 113.6 (C7-H), 112.0 ppm (C5-H). **Elemental Analysis** calcd for  $\text{C}_{14}\text{H}_8\text{N}_3\text{ClO}_4$ : C, 52.93; H, 2.54; N, 13.23. Found: C, 52.85; H, 2.57; N, 12.09. **MS** (EI):  $m/z=316$  [M-1].

### 3.3.1.5. Synthesis of 4,6-dinitro-3-(3,5-difluoro)phenyl-1H-indole (100)

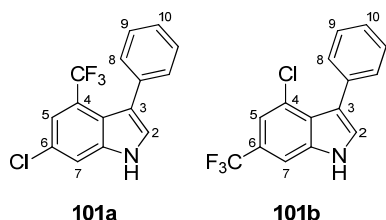


Compound **100** was obtained from methyl 1-ethynyl-3,5-difluorobenzene and 3,5-dinitrophenyl azide. At the end of the reaction, benzene was evaporated to dryness and  $\text{CH}_2\text{Cl}_2$  (10.0 mL) was added to the crude. Compound **100** was recovered by filtration as a yellow solid.

$^1\text{H NMR}$  (300 MHz,  $\text{DMSO}-d_6$ ):  $\delta$  13.02 (br, 1H, NH), 8.75 (d, 1H,  $^4J=1.8$  Hz,  $\text{H}^7$ ), 8.61 (d, 1H,  $^4J=1.8$  Hz,  $\text{H}^5$ ), 8.34 (s, 1H,  $\text{H}^2$ ), 7.20 (tt, 1H,  $J_{\text{HF}}=9.4$  Hz,  $^4J=2.3$  Hz,  $\text{H}^9$ ), 7.02 ppm (dd, 2H,  $^3J_{\text{HF}}=8.7$  Hz,  $^4J=2.2$  Hz,  $\text{H}^8$ ).

**<sup>13</sup>C NMR** (75 MHz, DMSO-*d*<sub>6</sub>): δ 163.4 (dd, <sup>1</sup>*J*<sub>CF</sub>=243.7 Hz, *J*<sub>CF</sub>=13.7 Hz, C-F), 140.6 (C6), 140.3 (C4), 138.0 (C3-C-C8), 137.5 (C7-C-NH), 136.9 (C2-H), 119.7 (C4-C-C3), 115.0 (C3), 113.7 (C7-H), 112.2 (C5-H), 111.9 (dd, <sup>2</sup>*J*<sub>CF</sub>=24.7 Hz, <sup>4</sup>*J*<sub>CF</sub>=8 Hz, C8), 101.9 ppm (t, <sup>2</sup>*J*<sub>CF</sub>=25.5 Hz, C9). **<sup>19</sup>F NMR** (282 MHz, DMSO): δ -111.7 ppm (F). **Elemental Analysis** calcd for C<sub>14</sub>H<sub>7</sub>N<sub>3</sub>F<sub>2</sub>O<sub>4</sub>: C, 52.68; H, 2.21; N, 13.16. Found: C, 52.70; H, 2.17; N, 12.56. **MS** (EI): *m/z*=318 [M-1].

### 3.3.1.6. Synthesis of 4-chloro-3-phenyl-6-(trifluoromethyl)-1*H*-indole (101a) and 4-(trifluoromethyl)-3-phenyl-6-chloro -1*H*-indole (101b)

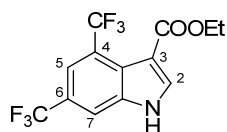


The two isomers **101a** and **101b** were obtained from methyl phenylacetylene and 3-chloro-5-(trifluoromethyl)phenyl azide. At the end of the reaction, benzene was evaporated and the crude was purified by flash chromatography (silica gel, 60 μm, AcOEt/hexane 1:9) to obtain a mixture of **101a/101b** in a 4:1 ratio (evaluated by <sup>19</sup>F NMR).

**Compound 101a:** **<sup>1</sup>H NMR** (300 MHz, CDCl<sub>3</sub>): δ 8.49 (br, 1H, NH), 7.61 (s, 1H, H<sup>7</sup>), 7.47 (s, 1H, H<sup>5</sup>), 7.37 (m, 5H, H<sub>Ar</sub>), 7.23 ppm (d, 1H, *J*=2.5 Hz, H<sup>2</sup>). **<sup>13</sup>C NMR** (75 MHz, CDCl<sub>3</sub>): δ 130.9 (C<sub>Ar</sub>), 127.6 (C<sub>Ar</sub>), 127.2 (C<sub>Ar</sub>), 126.5 (C2-H), 119.6 (q, *J*<sub>CF</sub>=6 Hz, C5-H), 115.0 ppm (C7-H). Quaternary carbon atom were not detected. **<sup>19</sup>F NMR** (282 MHz, CDCl<sub>3</sub>): -58.11 ppm (CF<sub>3</sub>).

**Compound 101b:** **<sup>1</sup>H NMR** (300 MHz, CDCl<sub>3</sub>): δ 8.59 (br, 1H, NH), 7.64 (s, 1H, H<sup>5</sup>), 7.49 (d, 1H, *J*=1.5 Hz, H<sup>2</sup>), 7.37 ppm (m, 6H, H<sup>7</sup> and H<sub>Ar</sub>). **<sup>13</sup>C NMR** (75 MHz, CDCl<sub>3</sub>): δ 131.37 (C2-H), 130.88 (C<sub>Ar</sub>), 127.05 (C<sub>Ar</sub>), 126.91 (C<sub>Ar</sub>), 118.1 (q, *J*<sub>CF</sub>=7.5 Hz, C7-H), 107.88 ppm (q, *J*<sub>CF</sub>=7.5 Hz, C5-H). Quaternary carbon atom were not detected. **<sup>19</sup>F NMR** (282 MHz, CDCl<sub>3</sub>): -60.93 ppm (CF<sub>3</sub>). **Elemental Analysis** calcd for C<sub>15</sub>H<sub>9</sub>ClF<sub>3</sub>N: C, 60.93; H, 3.07; N, 4.74. Found: C, 60.75; H, 3.25; N, 4.69. **MS** (EI): *m/z*=295 [M]<sup>+</sup>.

### 3.3.1.7. Synthesis of ethyl 4,6-bis(trifluoromethyl)-1*H*-indole-3-carboxylate (102)



Compound **102** was obtained from ethyl propiolate and 3,5-*bis*(trifluoromethyl)phenyl azide. The crude was purified by flash chromatography (silica gel, 60 μm, AcOEt/hexane 2:8) to obtain a yellow solid.

**<sup>1</sup>H NMR** (400 MHz, CDCl<sub>3</sub>): δ 9.26 (s, 1H, H<sub>NH</sub>), 8.10 (s, 1H, H<sup>7</sup>), 7.91 (s, 1H, H<sup>5</sup>), 7.87 (s, 1H, H<sup>2</sup>), 4.38 (q, 2H, *J*=7.1 Hz, H<sub>CH2</sub>), 1.39 ppm (t, 3H, *J*=7.1 Hz, H<sub>CH3</sub>).

### 3.3.2. Kinetic studies

**General kinetic procedure:** to a Schlenk flask, phenylacetylene and 3,5-*bis*(trifluoromethyl)phenyl azide were added to a benzene (5.00 mL) solution of Ru(TPP)(NAr)<sub>2</sub> (Ar=3,5-(CF<sub>3</sub>)<sub>2</sub>C<sub>6</sub>H<sub>3</sub>) (**71**). The flask was capped with a rubber septum and immediately placed in an oil bath preheated to 75°C. Consumption of the aryl azide was followed by IR spectroscopy ( $\nu \approx 2114 \text{ cm}^{-1}$ ) by withdrawing samples of the solution (0.1 mL) at regular times. The rate constants were fitted to the equation  $-d[\text{azide}]/dt = k_{\text{app}}[\text{azide}][\text{alkyne}][\text{catalyst}]$ . The concentration of catalyst was calculated by exact amount of catalyst weighed in each run and was considered to remain constant during the reaction.

#### 3.3.2.1. Kinetic order with respect to aryl azide concentration

The general kinetic procedure was followed using a catalyst/azide/phenylacetylene ratio of 2:50:250 (Ru(TPP)(NAr)<sub>2</sub> (Ar=3,5-(CF<sub>3</sub>)<sub>2</sub>C<sub>6</sub>H<sub>3</sub>) (12.0 mg,  $1.02 \cdot 10^{-5}$  mol), 3,5-*bis*(trifluoromethyl)phenyl azide (91.0  $\mu\text{L}$ ,  $5.14 \cdot 10^{-4}$  mol), phenylacetylene (0.280 mL,  $2.55 \cdot 10^{-3}$  mol).

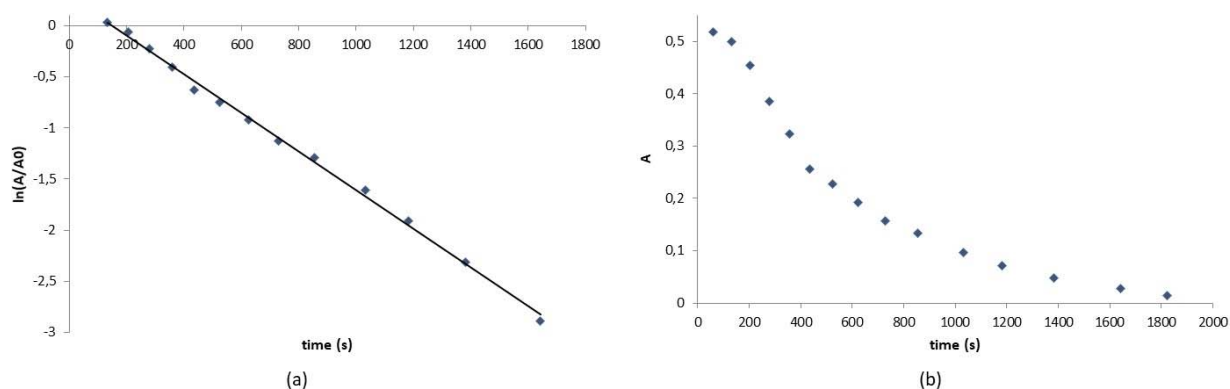


**Figure 1.** First-order kinetic with respect to the aryl azide.

#### 3.3.2.2. Kinetic order with respect to Ru(TPP)(NAr)<sub>2</sub> (Ar=3,5-(CF<sub>3</sub>)<sub>2</sub>C<sub>6</sub>H<sub>3</sub>) concentration (**71**)

The general kinetic procedure was followed using 3,5-*bis*(trifluoromethyl)phenyl azide (91.0  $\mu\text{L}$ ,  $5.14 \cdot 10^{-4}$  mol) and phenylacetylene (0.280 mL,  $2.55 \cdot 10^{-3}$  mol).

Ru(TPP)(NAr) <sub>2</sub> (mol)	[Ru(TPP)(NAr) <sub>2</sub> ] (mol/L)	<b>K</b> <sub>obs</sub> (s <sup>-1</sup> )
$2.57 \cdot 10^{-3}$	$5.13 \cdot 10^{-4}$	$9.50 \cdot 10^{-5}$
$5.13 \cdot 10^{-3}$	$1.02 \cdot 10^{-3}$	$8.05 \cdot 10^{-4}$
$7.70 \cdot 10^{-3}$	$1.54 \cdot 10^{-3}$	$1.22 \cdot 10^{-3}$
$1.02 \cdot 10^{-2}$	$2.05 \cdot 10^{-3}$	$2.18 \cdot 10^{-3}$
$1.28 \cdot 10^{-2}$	$2.57 \cdot 10^{-3}$	$3.01 \cdot 10^{-3}$

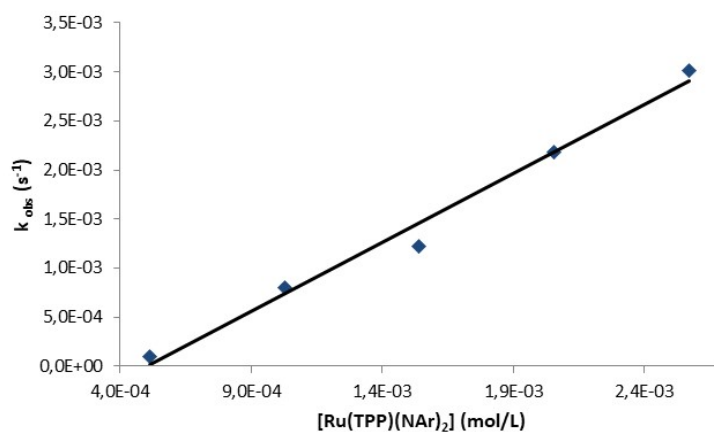


Figure 2. First-order kinetic with respect to the catalyst concentration.

### 3.3.2.3. Kinetic order with respect to phenylacetylene concentration

The general kinetic procedure was followed using Ru(TPP)(NAr)<sub>2</sub> (Ar=3,5(CF<sub>3</sub>)<sub>2</sub>C<sub>6</sub>H<sub>3</sub>) (6.00 mg, 5.10·10<sup>-6</sup> mol) and 3,5-bis(trifluoromethyl)phenyl azide (91.0 μL, 5.14·10<sup>-4</sup> mol).

[phenylacetylene] (mol/L)	$K_{obs}$ (s <sup>-1</sup> )	$K_{obs}/[Ru(TPP)(NAr)_2]$ (M <sup>-1</sup> s <sup>-1</sup> )
5.14·10 <sup>-2</sup>	8.10·10 <sup>-5</sup>	1.58·10 <sup>-1</sup>
1.03·10 <sup>-1</sup>	1.81·10 <sup>-4</sup>	3.52·10 <sup>-1</sup>
1.15·10 <sup>-1</sup>	2.30·10 <sup>-4</sup>	4.48·10 <sup>-1</sup>
2.54·10 <sup>-1</sup>	3.49·10 <sup>-4</sup>	6.79·10 <sup>-1</sup>
1.80·10 <sup>-1</sup>	2.89·10 <sup>-4</sup>	5.63·10 <sup>-1</sup>

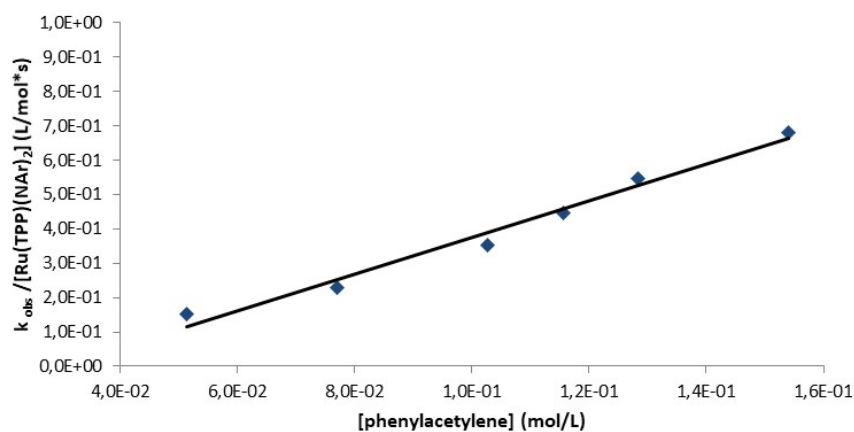
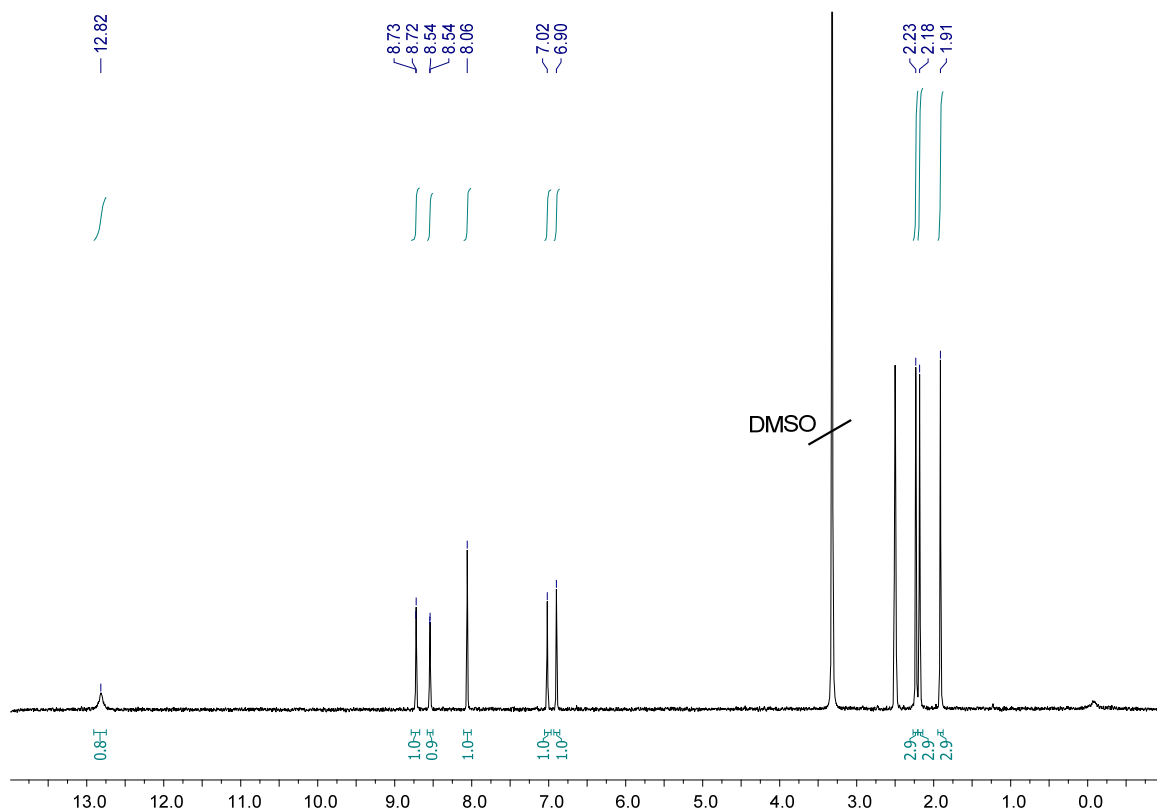


Figure 3. First-order kinetic with respect to the phenylacetylene concentration.

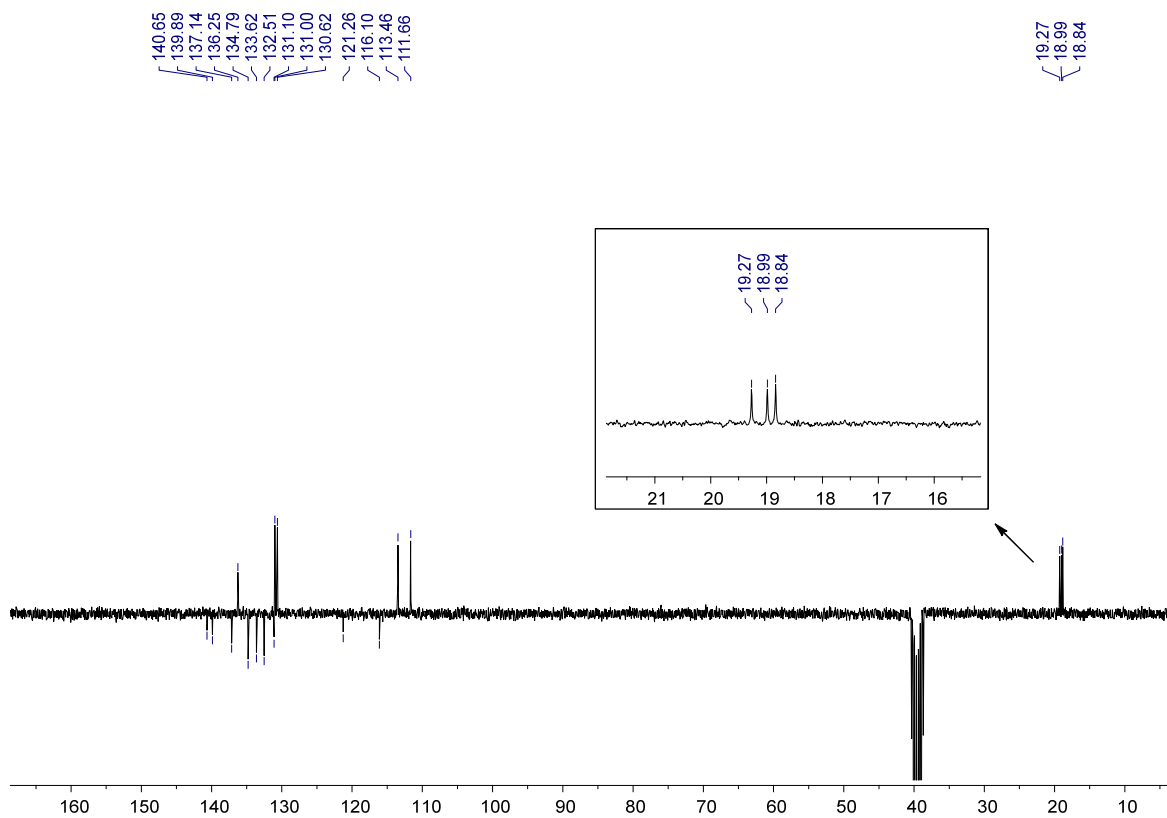
### 3.4. NMR spectra

#### 3.4.1. 4,6-Dinitro-3-(2,4,5-trimethyl)-phenyl-1*H*-indole (95)

##### 3.4.1.1. <sup>1</sup>H NMR (300 MHz, DMSO, 298 K)



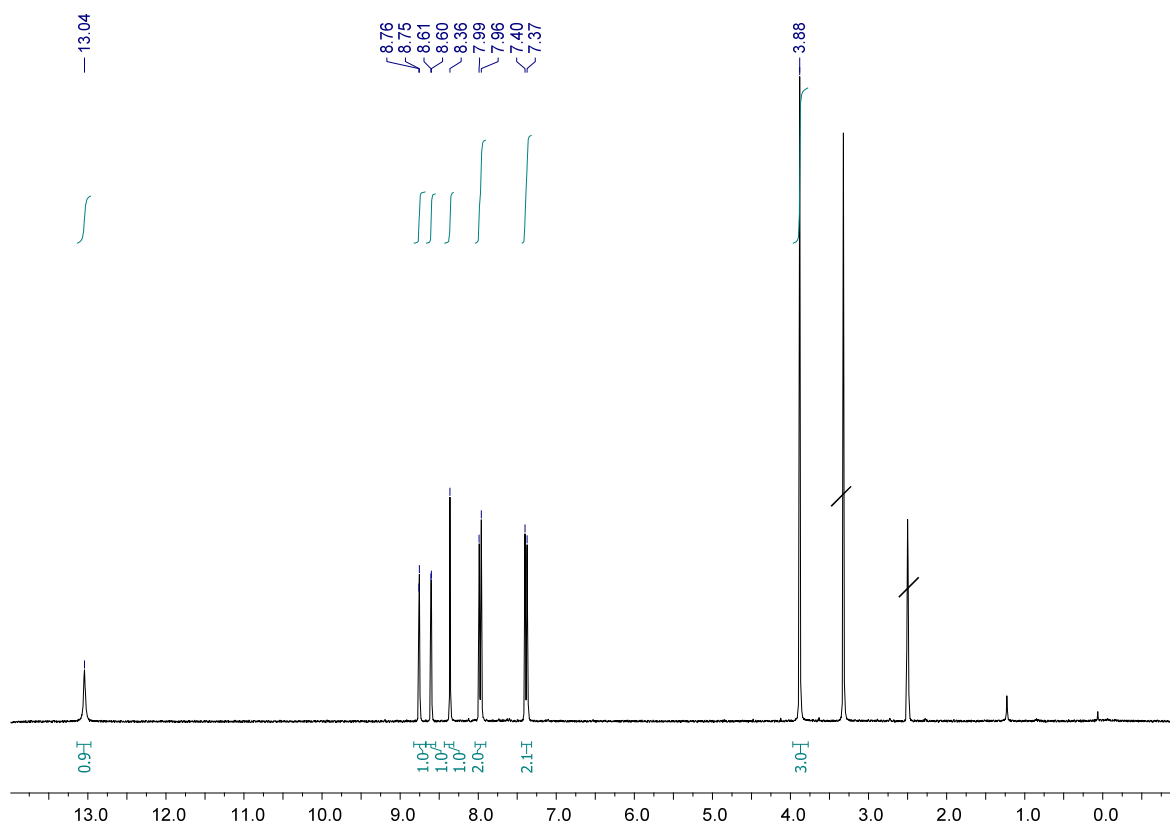
##### 3.4.1.2. <sup>13</sup>C NMR (75 MHz, DMSO, 298 K)



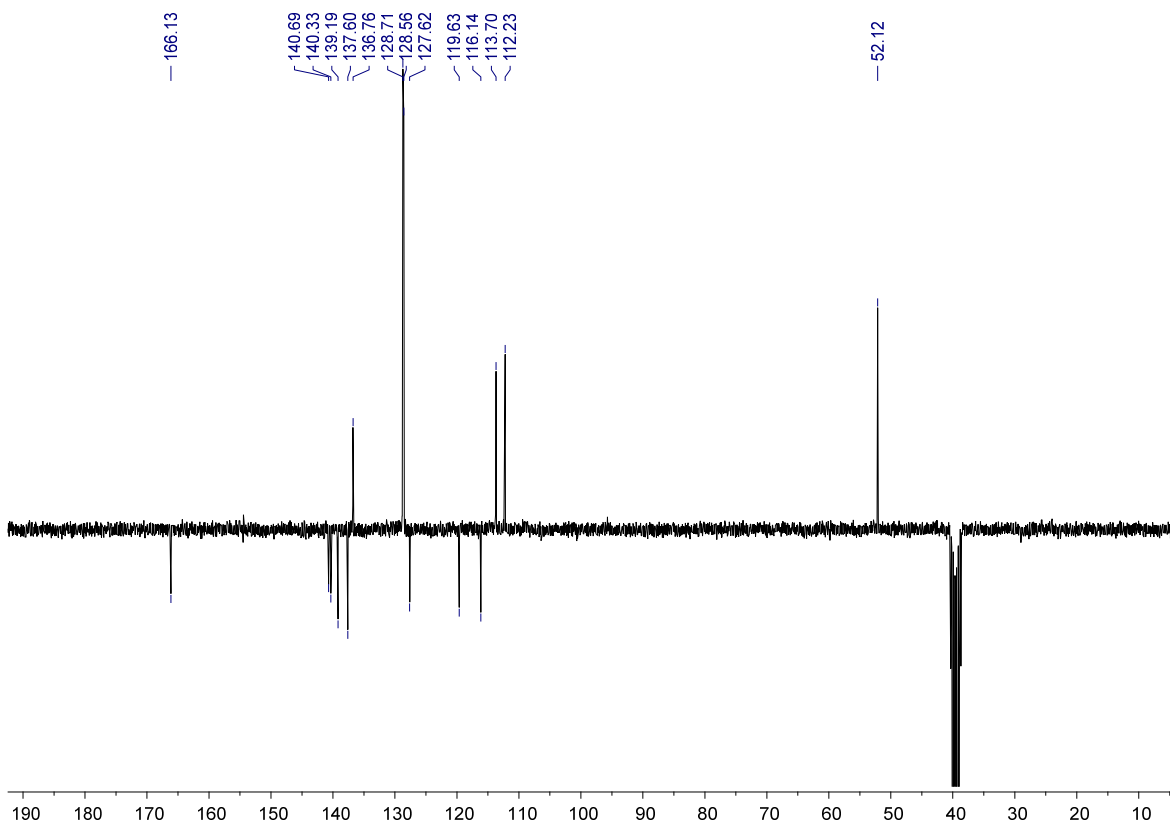


### 3.4.2. Methyl 4-(4,6-dinitro-1H-indol-3-yl)benzoate (96)

#### 3.4.2.1. <sup>1</sup>H NMR (300 MHz, DMSO, 298 K)

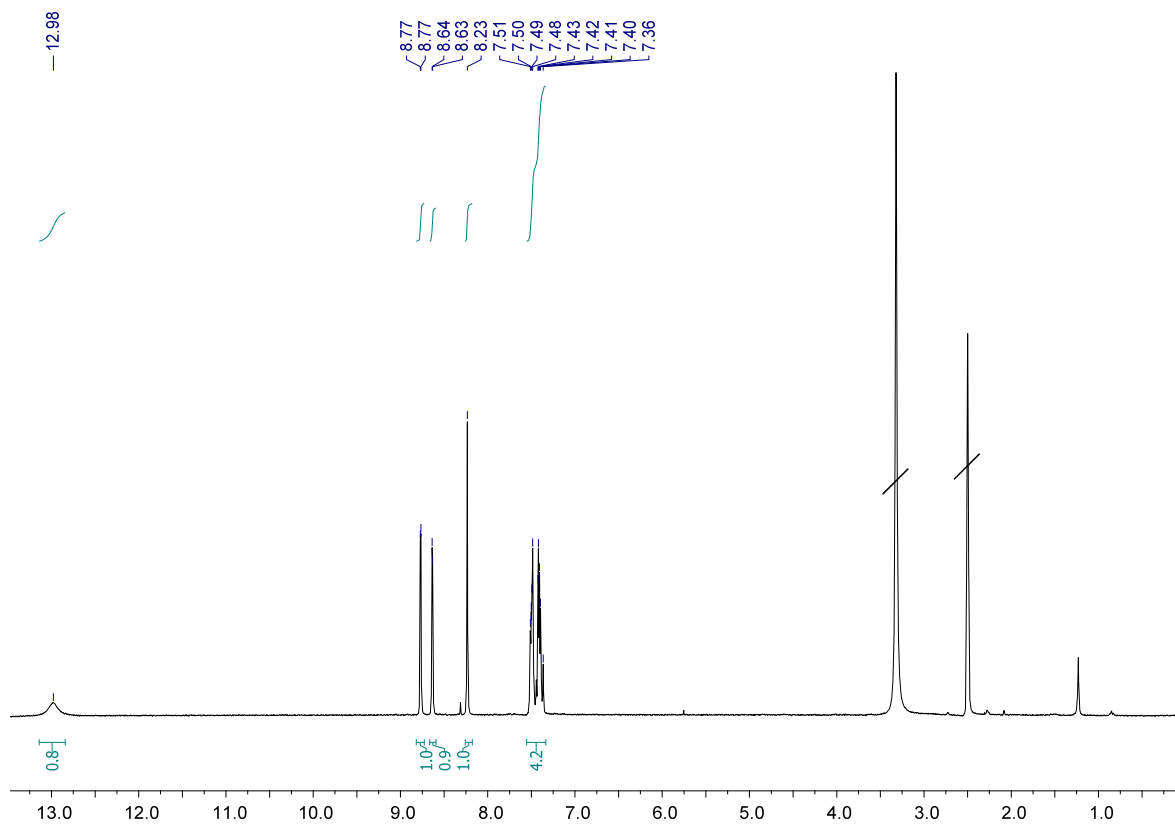


#### 3.4.2.2. <sup>13</sup>C NMR (75 MHz, DMSO, 298 K)

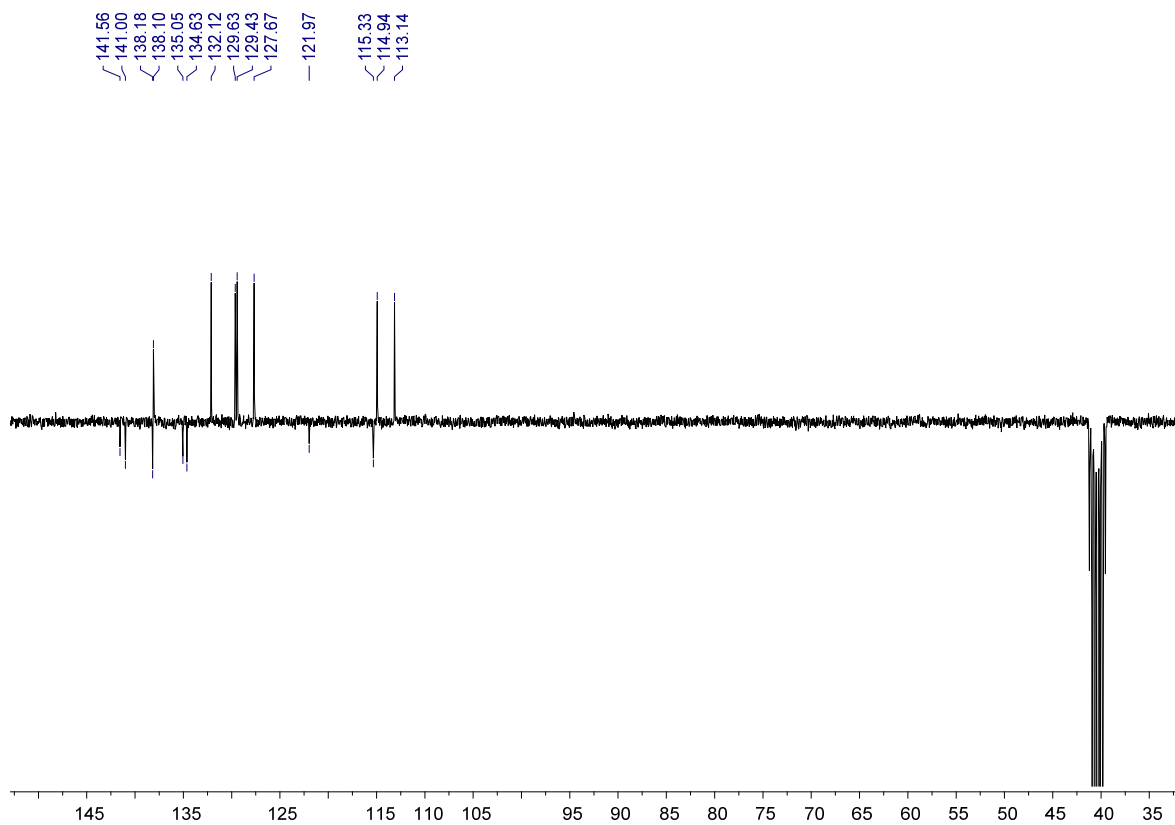


### 3.4.3. 4,6-Dinitro-3-(2-chloro)-phenyl-1H-indole (98)

#### 3.4.3.1. $^1\text{H}$ NMR (300 MHz, DMSO, 298 K)

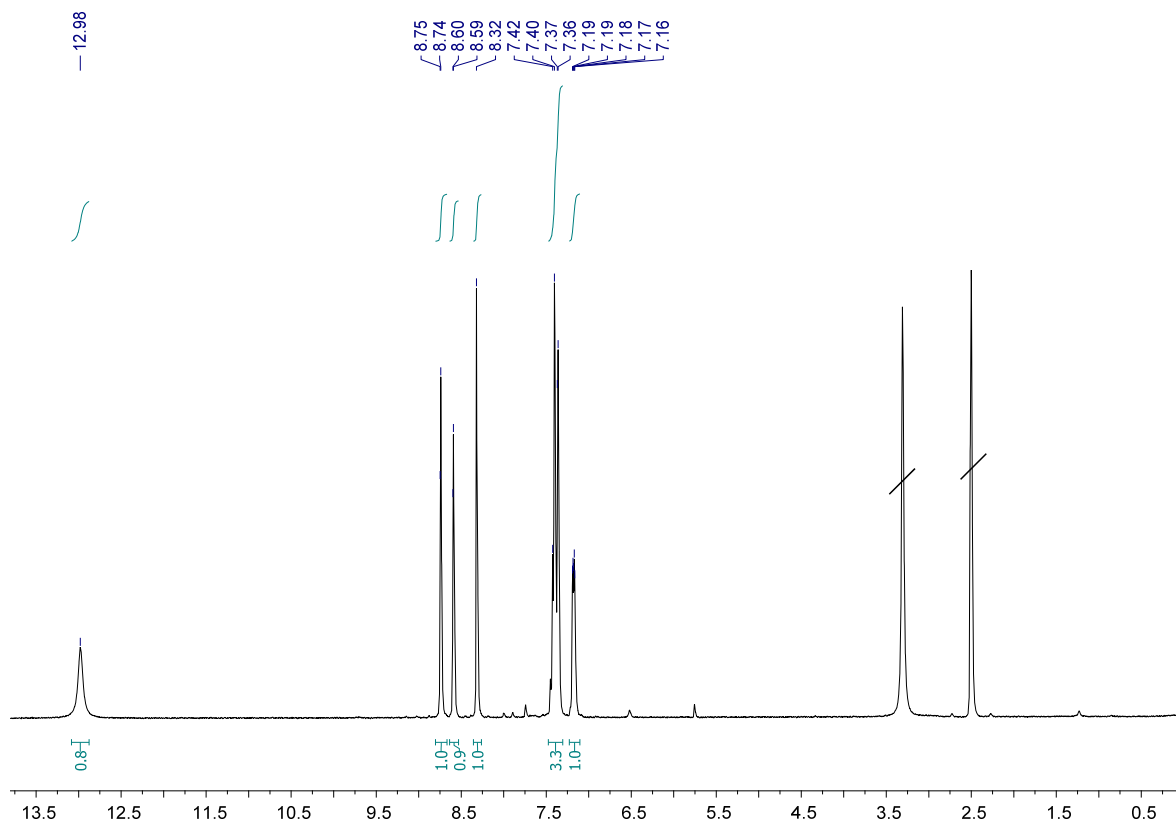


#### 3.4.3.2. $^{13}\text{C}$ NMR (75 MHz, DMSO, 298 K)

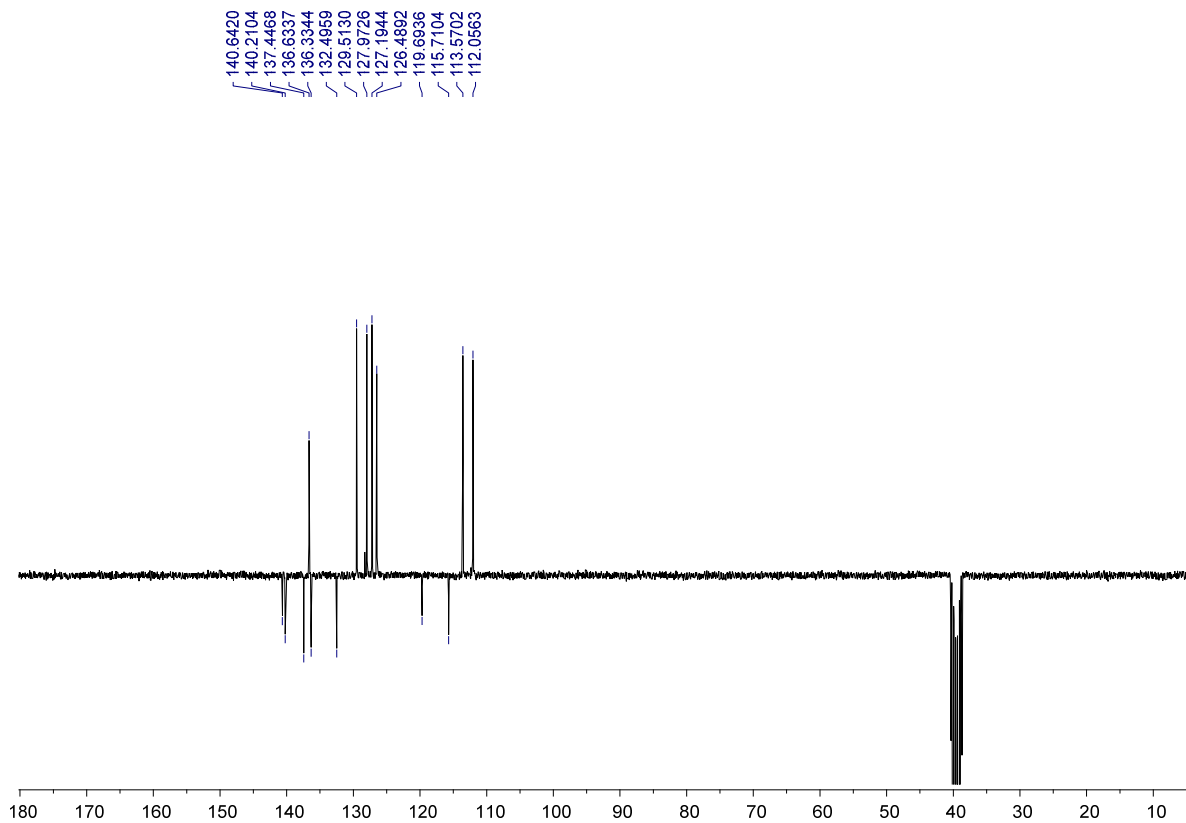


### 3.4.4. 4,6-Dinitro-3-(3-chloro)-phenyl-1H-indole (99)

#### 3.4.4.1. $^1\text{H}$ NMR (300 MHz, DMSO, 298 K)

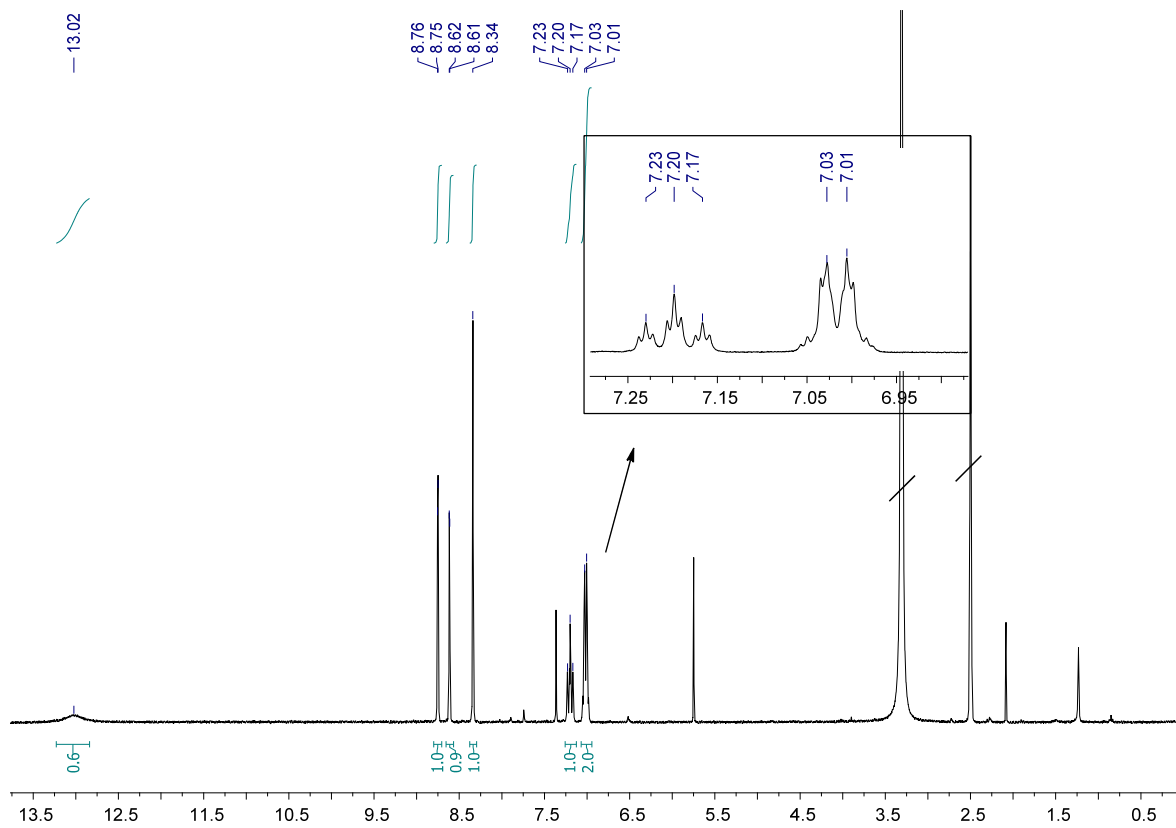


#### 3.4.4.2. $^{13}\text{C}$ NMR (75 MHz, DMSO, 298 K)

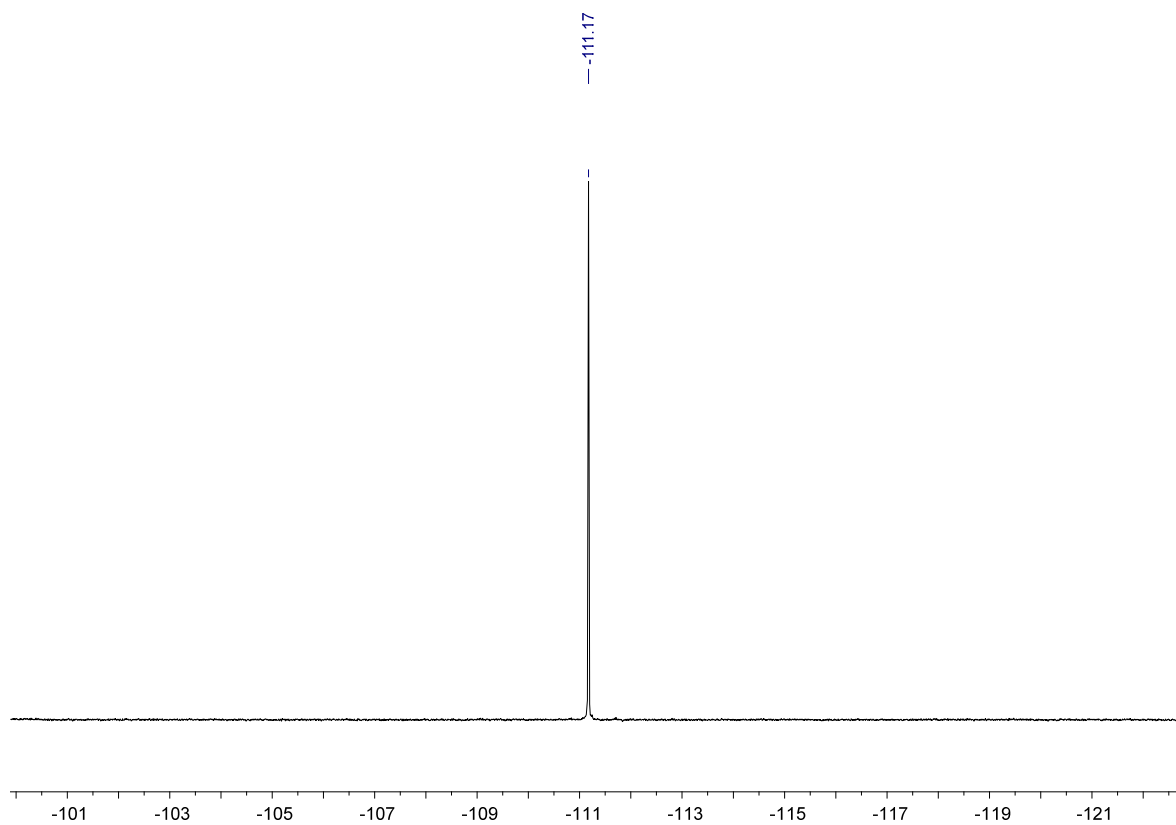


### 3.4.5. 4,6-Dinitro-3-(3,5-difluoro)-phenyl-1H-indole (100)

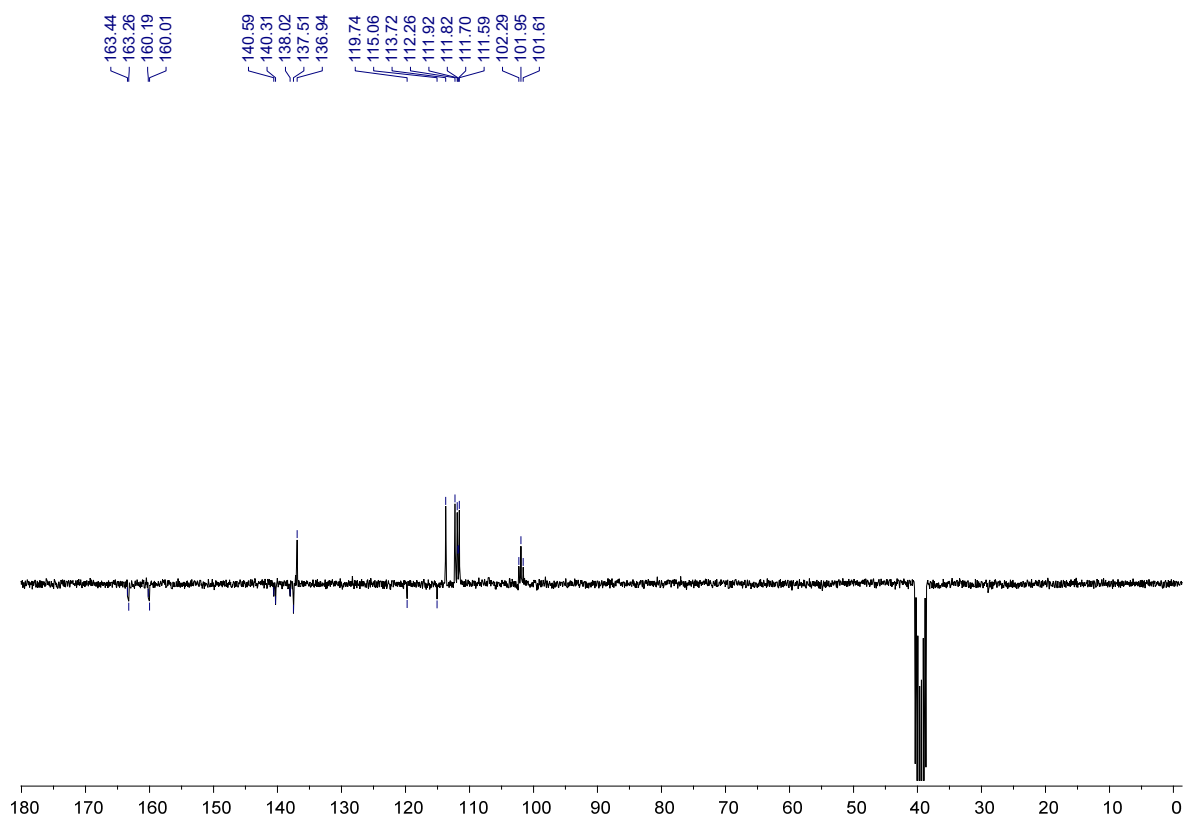
#### 3.4.5.1. $^1\text{H}$ NMR (300 MHz, DMSO, 298 K)



#### 3.4.5.2. $^{19}\text{F}$ NMR (282 MHz, DMSO, 298 K)

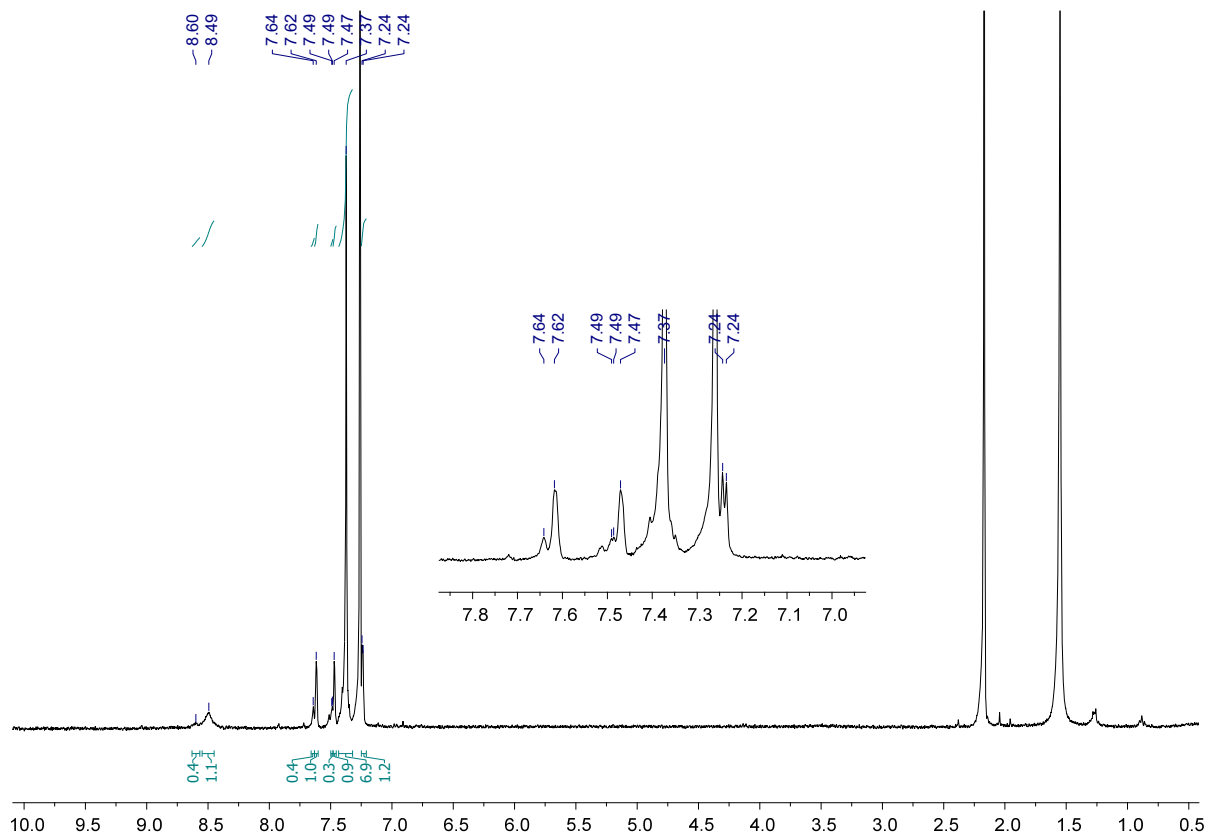


### 3.4.5.3. $^{13}\text{C}$ NMR (75 MHz, DMSO, 298 K)

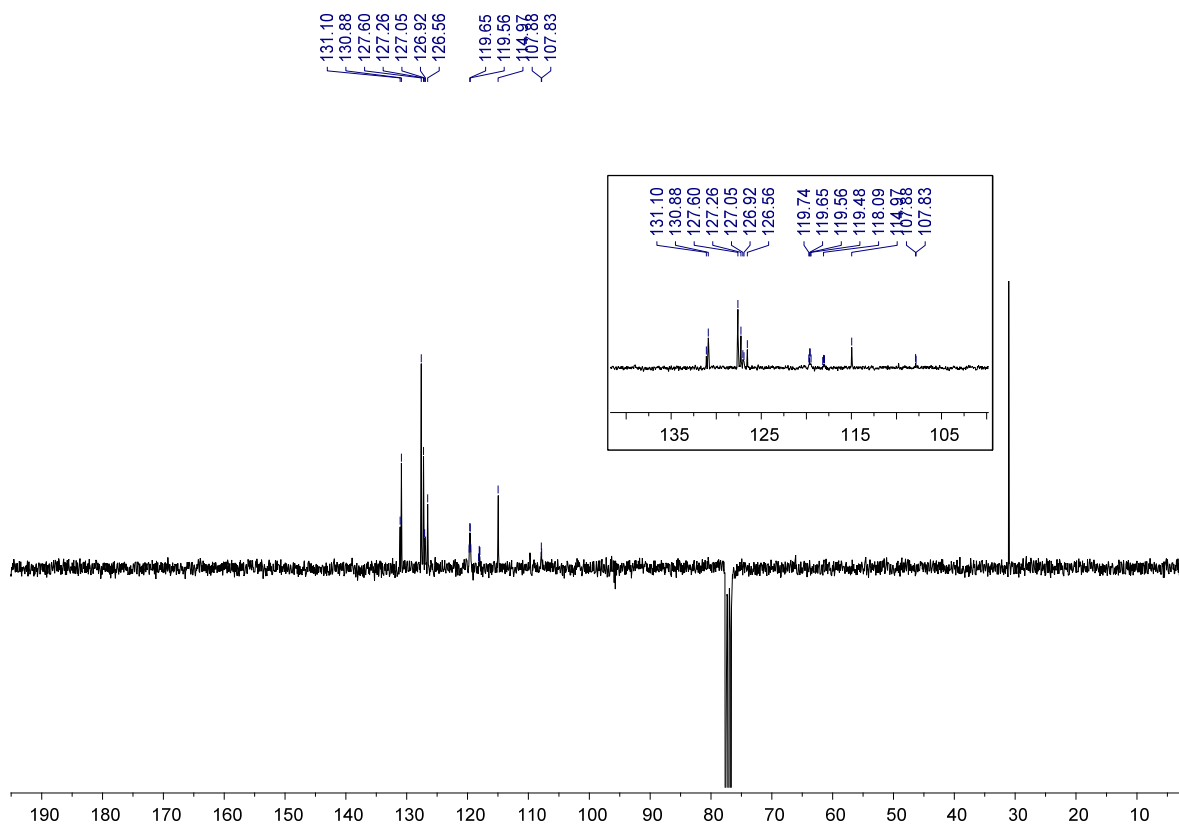


### 3.4.6. 4-Chloro-3-phenyl-6-(trifluoromethyl)-1H-indole (101b) and 4-(trifluoromethyl)-3-phenyl-6-chloro-1H-indole (101a)

#### 3.4.6.1. $^1\text{H}$ NMR (300 MHz, $\text{CDCl}_3$ , 298 K)

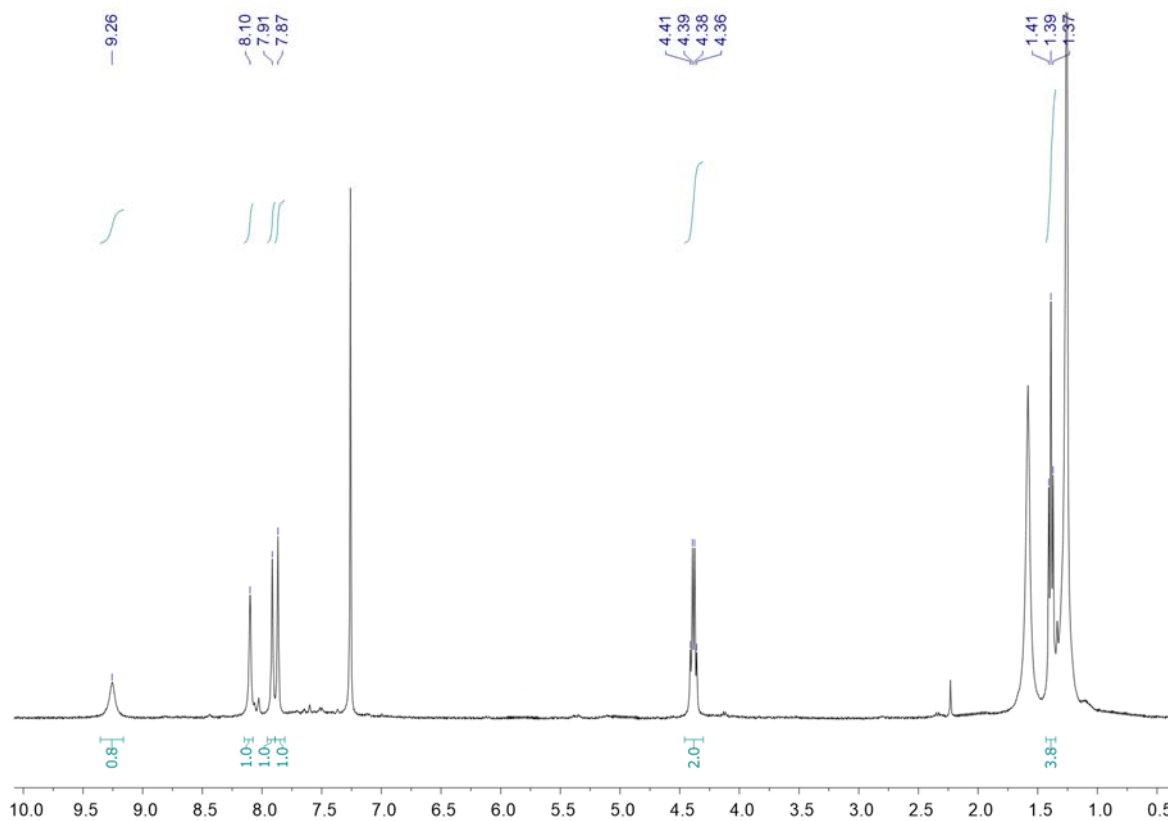


### 3.4.6.2. $^{13}\text{C}$ NMR (75 MHz, $\text{CDCl}_3$ , 298 K)



### 3.4.7. 4,6-Bis(trifluoromethyl)-2-methyl-3-phenyl-1H-indole (102)

#### 3.4.7.1. $^1\text{H}$ NMR spectrum (400 MHz, $\text{CDCl}_3$ , 298 K)



## 4. References

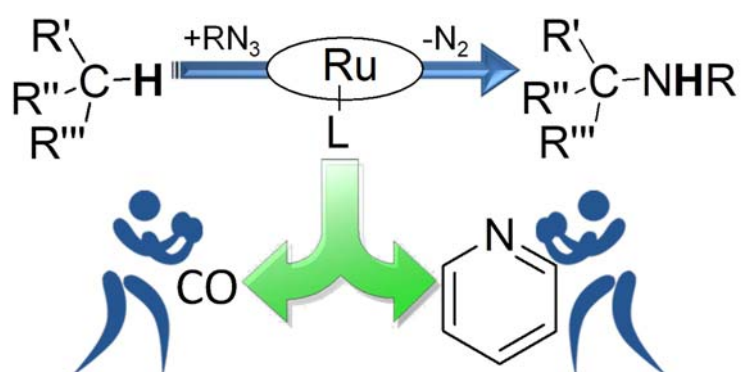
1. G: R. Humphrey, J. T. Kuethe. *Chem. Rev.* **2006**, 106, 2875-2911.
2. R. C. Larock, E. K. Yum. *J. Am. Chem. Soc.* **1991**, 113, 6689-6690.
3. (a) L. Ackermann, L. T. Kaspar, C. J. Gschrei. *Chem. Commun.* **2004**, 2824-2825. (b) J. Barluenga, M. A. Fernández, F. Aznar, C. Valdés. *Chem. Eur. J.* **2005**, 11, 2276-2283.
4. B. Z. Lu, W. Zhao, H. X. Wei, M. Dufour, V. Farina, C. H. Senanayake. *Organic Letters* **2006**, 8, 3271-3274.
5. (a) B. J. Stokes, H. Dong, B. E. Leslie, A. L. Pumphrey, T. G. Driver. *J. Am. Chem. Soc.* **2007**, 129, 7500-7501. (b) M. Shen, B. E. Leslie, T. G. Driver. *Angew. Chem. Int. Ed.* **2008**, 47, 5056-5059.
6. B. Lu, Y. Luo, L. Liu, L. Ye, Y. Wang, L. Zhang. *Angew. Chem. Int. Ed.* **2011**, 50, 8358-8362.
7. S. Jana, M. D. Clements, B. K. Sharp, N. Zheng. *Organic Letters* **2010**, 12, 3736-3739.
8. S. Würtz, S. Rakshit, J. J. Neumann, T. Dröge, F. Glorius. *Angew. Chem. Int. Ed.* **2008**, 47, 7230-7233.
9. Y. Tan, J. F. Hartwig. *J. Am. Chem. Soc.* **2010**, 132, 3676-3677.
10. (a) D. R. Stuart, M. Bertrand-Laperle, K. M. N. Burgess, K. Fagnou. *J. Am. Chem. Soc.* **2008**, 130, 16474-16475. (b) Z. Shi, C. Zhang, S. Li, D. Pan, S. Ding, Y. Cui, N. Jiao. *Angew. Chem. Int. Ed.* **2009**, 48, 4572-4576. (c) D. R. Stuart, P. Alsabeh, M. Kuhn, K. Fagnou. *J. Am. Chem. Soc.* **2010**, 132, 18326-18339.
11. F. Ragaini, A. Rapetti, E. Visentin, M. Monzani, A. Caselli, S. Cenini. *J. Org. Chem.* **2006**, 71, 3748-3753.
12. F. Ferretti, M. A. El-Atawy, S. Muto, M. Hagar, E. Gallo, F. Ragaini. *Eur. J. Org. Chem.* **2015**, 2015, 5712-5715.
13. N. Jana, F. Zhou, T. G. Driver. *J. Am. Chem. Soc.* **2015**, 137, 6738-6741.
14. P. Zardi, A. Savoldelli, D. M. Carminati, A. Caselli, F. Ragaini, E. Gallo. *ACS Catal.* **2014**, 4, 3820-3823.





# Chapter V

## C-N bond formations: Amines



*Parts of this chapter have been published and are reproduced here from:*

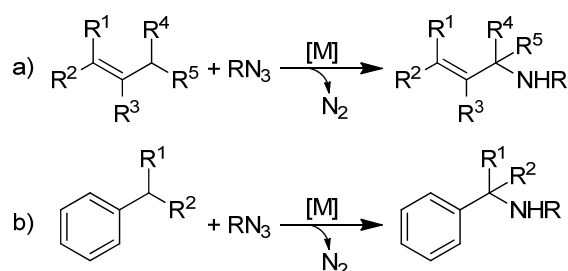
G. Manca, C. Mealli, D. M. Carminati, D. Intriery and E. Gallo. *Eur. J. Inorg. Chem* **2015**, 4885-4893.

D. Intriery, D. M. Carminati and E. Gallo. *J. Porphyrins Phthalocyanines* **2016**, 20, 190-203.

# 1. Introduction

Given the prevalence of nitrogen-containing compounds in functional materials, natural products and important pharmaceutical agents, the insertion of a nitrene functionality into a C-H bond is a synthetic procedure of enormous interest: it allows the conversion of low-cost materials, such as simple hydrocarbons, into high added-value nitrogen-containing molecules. In addition, the ubiquity of C-H functionalities in almost every molecular scaffold further expands the synthetic applicability of the procedure, which can also be stereoselective when promoted by a chiral catalyst.

In this context, the transition metal-catalysed C-H amination protocol using organic azides as the amino source is one of the most efficient methodology to produce aza-compounds, and metal-porphyrin complexes show very good activity in the synthesis of allylic and benzylic amines (Scheme 53)



**Scheme 53.** Allylic (a) and Benzylic (b) amination reaction by using organic azides.

## 1.1. Group 8 porphyrin-catalysed amination reactions by organic azides

Iron porphyrin complexes represent a class of sustainable catalysts due to the combination of an active, low-toxicity and cheap iron centre with an environmentally benign porphyrin ligand. In 2010, Liu and Che published the first example of amination reaction catalysed by iron porphyrin complex, in particular Fe(F<sub>20</sub>TPP)Cl.<sup>1</sup> The authors reported the good catalytic activity of Fe(F<sub>20</sub>TPP)Cl in the intramolecular amination of substituted styrenes by the use of methansulfonyl azide (MsN<sub>3</sub>), tosyl azide (TsN<sub>3</sub>), 4-acetamidobenzenesulfonyl azide (p-ABSA) and 4-nitrophenyl azide as nitrene sources (Figure 30). Interestingly, allylic amination of styrenes occurred without the formation of aziridine, whereas, when terminal non-activated alkenes were employed, they gave aziridines as the major products without the formation of any allylic amination products. The catalytic activity of Fe(F<sub>20</sub>TPP)Cl was also tested in the amination reaction of hydrocarbons by 4-nitrophenyl azide. Reactions of substrates containing benzylic C-H bonds gave amination products in 71-80% yield with complete conversion of the azide, instead unactivated aliphatic C-H bonds formed the corresponding amines in lower yields with an incomplete azide consumption (Figure 30). Reactions generally required long reaction times, but microwave irradiation reduced reaction times without sacrificing yield.

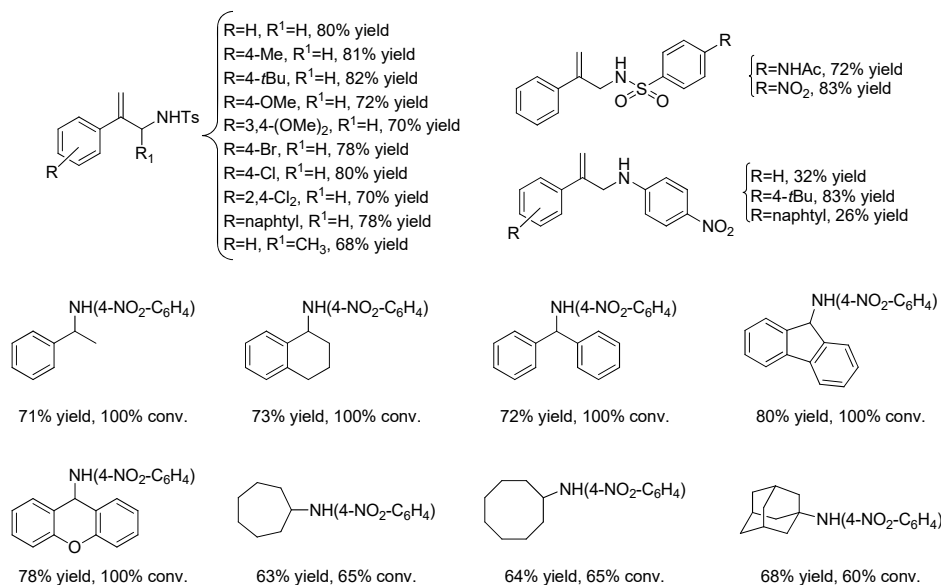
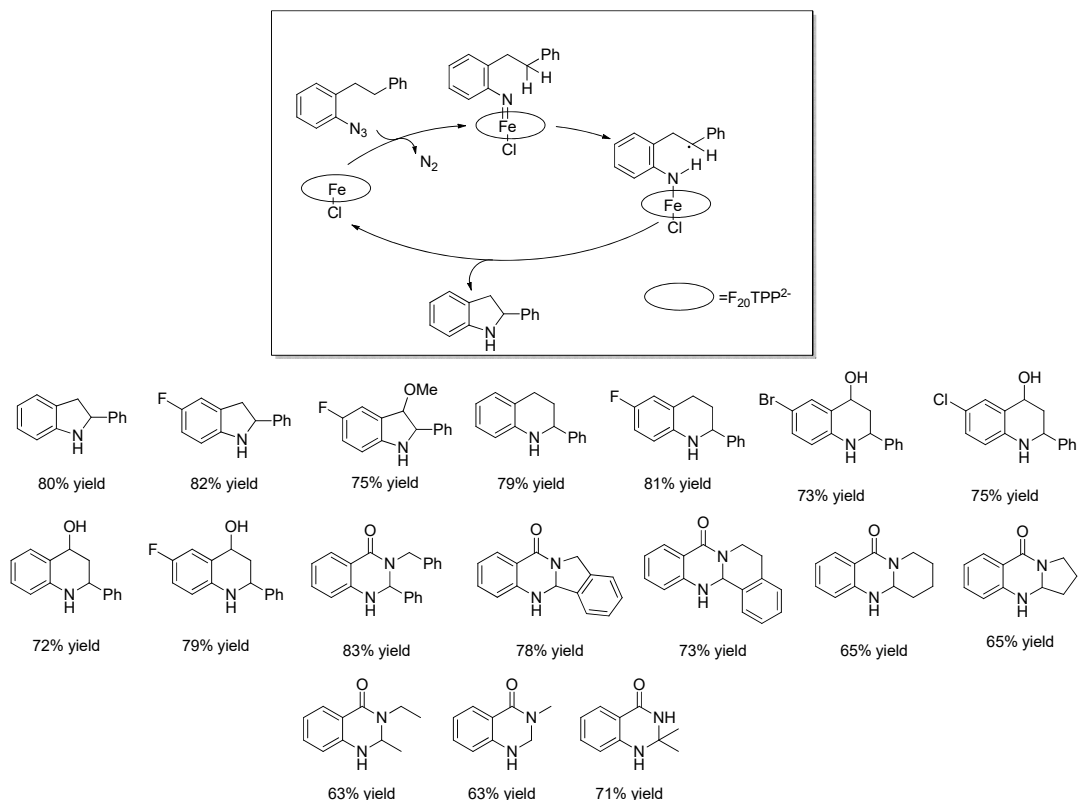


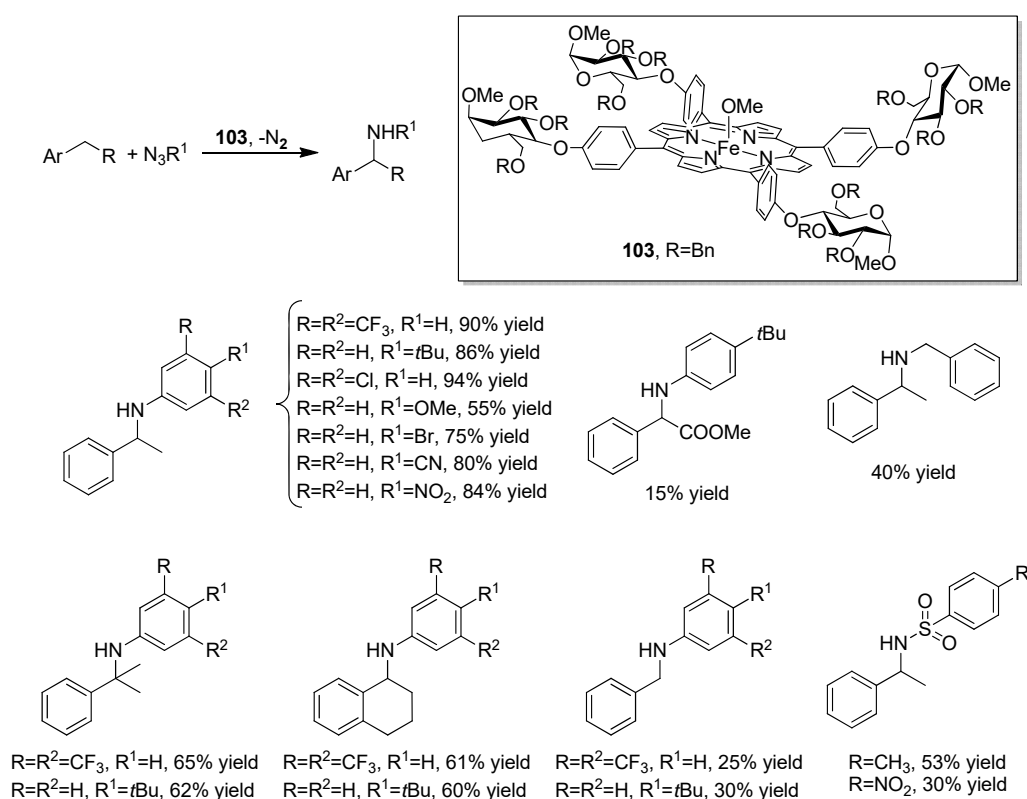
**Figure 30.** Styrenes and saturated C-H bond amination.

Moreover, Liu and Che reported the catalytic efficiency of the commercially-available and air-stable Fe(F<sub>20</sub>TPP)Cl complex in the synthesis of indolines, tetrahydroquinolines and dihydroquinazolinone via intramolecular amination of sp<sup>2</sup> and sp<sup>3</sup> C-H bonds with aryl azides (Scheme 54).<sup>2</sup> The authors proposed a hydrogen atom abstraction mechanism for the Fe(F<sub>20</sub>TPP)Cl-catalysed amination of sp<sup>3</sup> C-H bonds. First, Fe(F<sub>20</sub>TPP)Cl catalyses the decomposition of aryl azide to give an iron-nitrene/imido complex **A**. Then, a benzyl radical intermediate **B** is generated by an intramolecular hydrogen atom abstraction pathway and it undergoes a ring-close reaction to form the C-N bond and therefore the product (Scheme 54).



**Scheme 54.** Synthesis of indolines, tetrahydroquinolines and dihydroquinazolinone via intramolecular amination and proposed mechanism.

To improve the eco-tolerability of iron porphyrin complexes, in 2015 Gallo, Lay and co-workers synthesised a new iron glycoporphyrin, **103**, in which four glycoside groups were introduced onto the porphyrin skeleton to modulate the chemophysical characteristics of the catalyst.<sup>3</sup> The iron complex **103** showed a good catalytic activity in the intermolecular amination of C-H bonds using organic azides as aminating species (Scheme 55). The reaction worked well using aryl azides while, when benzylic or sulfonyl azides were employed as the aminating agents, the corresponding amines were isolated in moderate yields. Considering that the reaction sustainability also depends on the catalyst recyclability, it is important to say that catalyst **103** was used for three consecutive runs in the benzylic amination of ethylbenzene by 3,5-bis-trifluoromethylphenyl azide. Also, the formation of the desired amine with the final yield of 90% for each run indicated a very good chemical stability of iron catalyst **103**.

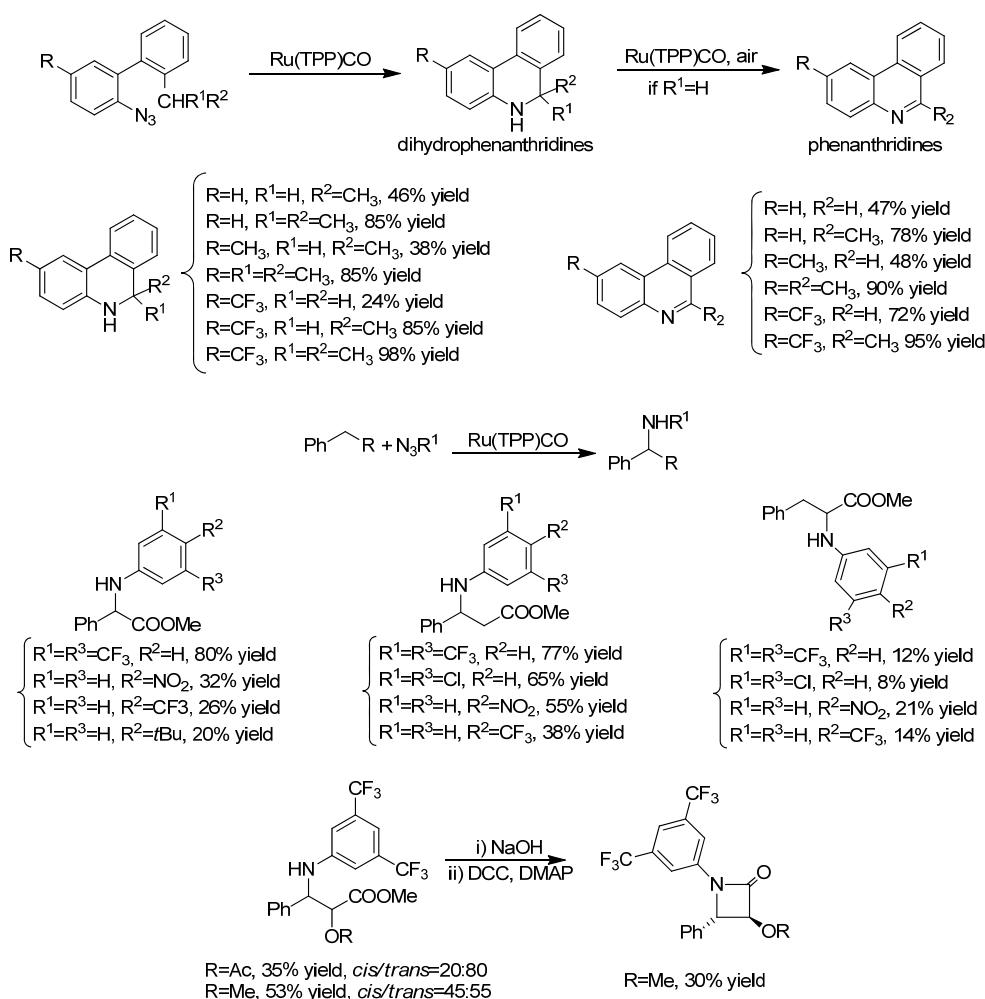


**Scheme 55.** Synthesis of benzylic amines promoted by complex **103**.

Being very similar to natural systems, the application of iron porphyrin-based catalytic processes is becoming more and more appealing to the scientific community, that is constantly working to develop new sustainable synthetic methods. For this reason enzymes have been used to promote amination reactions by using biochemically compatible azides as aminating agents. During the last five years, several papers have been published about the intramolecular and intermolecular amination catalysed by active enzymes, which have formed products from moderate to good yields and excellent enantioselectivities.<sup>4</sup> It is important to underline that, conversely to classical catalytic procedures, enzyme-based catalytic aminations require the presence of a reducing agent to indicate the involvement of an iron(II) reduced species, which is transformed into the active iron(IV) imido intermediate by reaction with the azide substrate.

Ruthenium porphyrin derivatives have been largely used to promote amination reactions due to their high catalytic reactivity and good chemical stability. In 2010, Gallo and co-workers reported the first benzylic amination catalysed by Ru(TPP)CO using aryl azides as nitrene source. Products were obtained from moderate to good yields using a catalytic ratio of Ru(TPP)CO/azide 4:50 and hydrocarbons as solvent at 100°C. Better results were obtained when the reactions were carried out with a lower catalyst loading (1:50) and a higher temperature. Comparing the aminations by 3,5-bis(trifluoromethyl)phenyl azide and 4-nitrophenyl azide, we can note that, in case of the 3,5-bis(trifluoromethyl)phenyl azide, the reactions occurred with an improvement of the yields, on the contrary when 4-nitrophenyl azide was used the yields were lower. This result is justified by the different thermal stability of the two aryl azides: the presence of two electron withdrawing groups (trifluoromethyl groups) conferred a major stability preserving the thermal decomposition. After this pioneering work, Ru(TPP)CO-aryl azides catalytic system has been extensively studied.

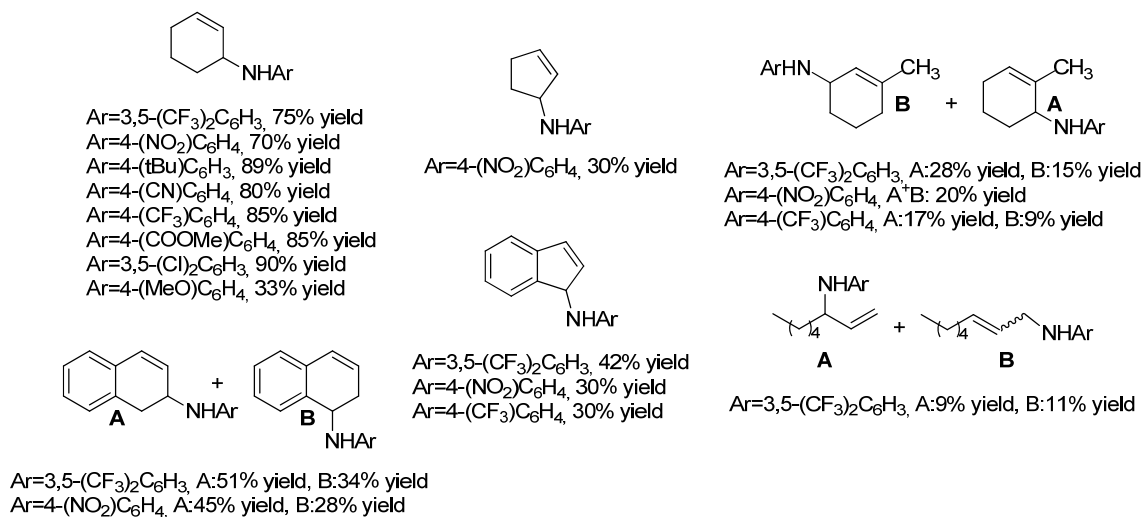
The benzylic amination reaction, intramolecular or intermolecular, is an interesting strategy to obtain compounds which show biological and/or pharmaceutical features such as phenanthridines and amino acids. The intramolecular amination of 2-azido biaryls mediated by Ru(TPP)CO resulted in dihydrophenanthridines and phenanthridines instead of yielding the usual carbazole molecule (Scheme 56).<sup>5</sup> To have a complete conversion of dihydrophenanthridines into phenanthridines it is necessary to irradiate the reaction mixture with a halogen lamp in presence of oxygen.



**Scheme 56.** Synthesis of dihydrophenanthridines, phenanthridines,  $\alpha$ - and  $\beta$ -amino esters and  $\beta$ -lactams.

Gallo *et al* also reported the synthesis of  $\alpha$ -aminoesters and  $\beta$ -lactams by the amination of a benzylic C-H bond placed in  $\alpha$  or  $\beta$  positions to an ester group.<sup>6</sup> Even if the benzylic positions of the substrates are electron deficient, products were obtained in good yields especially when very electron-withdrawing azides were employed (Scheme 56).

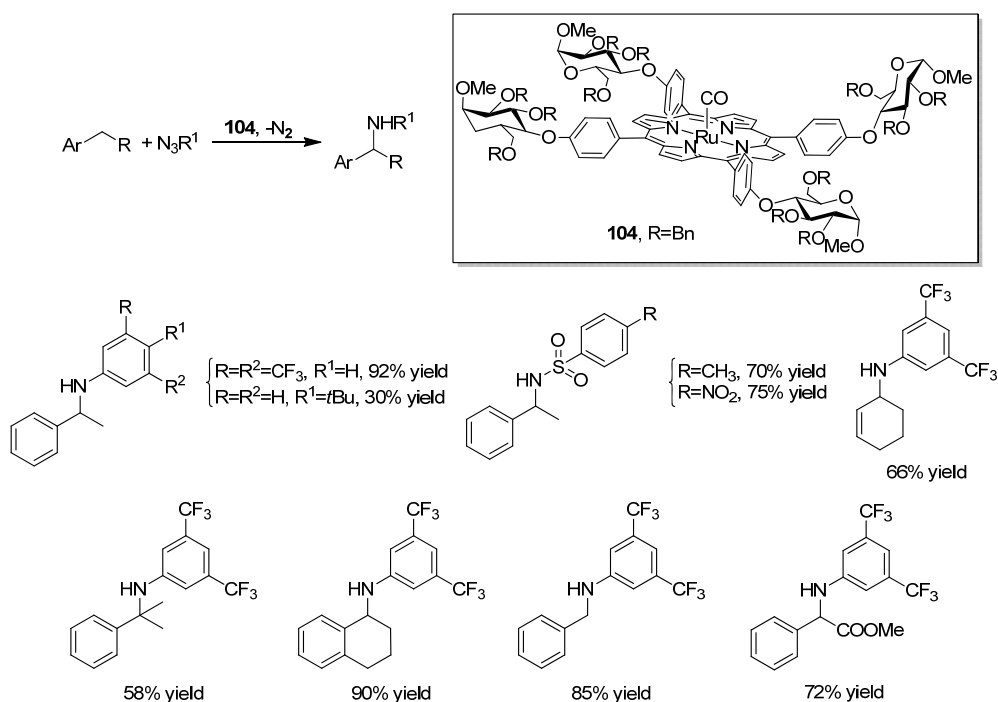
Ru(TPP)CO was also a good catalyst of allylic amination giving compounds reported in Scheme 57.<sup>7</sup>



**Scheme 57.** Allylic amination catalysed by Ru(TPP)CO.

In the previous chapter we reported the use of complexes **55** and **56**, synthesised by Che, as catalysts in the aziridination reaction, but these two complexes also showed a very high catalytic activity in the amination reaction of several alkenes by pentafluorophenyl azide. Amines were obtained in good yields and when the reaction of ethylbenzene was catalysed by chiral complex **54** the product was formed in high yield and enantioselectivity.<sup>8</sup>

The amines bearing EDGs were also synthesised by ruthenium glycoporphyrin complex **104**, which was more efficient in the activation of the electron-deficient aryl azides compared to those electron-rich (Scheme 58).<sup>3</sup>

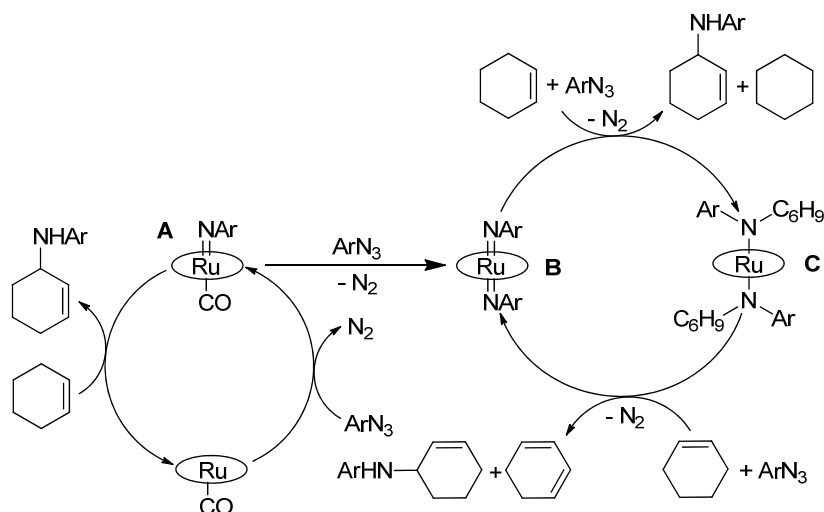


**Scheme 58.** Ruthenium glycoporphyrin-catalysed benzylic amination.

### 1.1.1. Proposed mechanism for the ruthenium porphyrin-catalysed amination reaction of hydrocarbons by aryl azides

The mechanism of ruthenium porphyrin-catalysed amination reaction was investigated for several systems and especially Gallo and co-authors devoted many efforts in studying the reaction in which aryl azides are used as nitrene sources. Kinetic, DFT studies and the isolation of intermediate compounds were fundamental to suggest the catalytic cycle reported in Scheme 59, where imido complex is the active intermediate. The studies were performed using the allylic amination of cyclohexene by 3,5-bis(trifluoromethyl)phenyl azide promoted by Ru(TPP)CO as model reaction.

The proposed mechanism shows the coexistence of two independent catalytic cycles based on two different active species: *mono*-imido complex **A** (Scheme 59), which was neither isolated or spectroscopically detected, and *bis*-imido complex **B** (Scheme 59).<sup>7</sup> The first step of both cycles is the reaction between ArN<sub>3</sub> and Ru(TPP)CO forming the *mono*-imido intermediate which reacts with cyclohexene, yielding the final allylic amine (path *b*) when a high concentration of hydrocarbons is employed. On the contrary, at low hydrocarbon concentration, the *mono*-imido complex immediately reacts with another molecule of aryl azide forming a *bis*-imido complex. Intermediate **B** then reacts with cyclohexene obtaining the product and another active species, the *bis*-amido complex **C**, which restores the *bis*-imido complex by reaction with the substrate.



**Scheme 59.** Mechanism of Ru(TPP)CO-catalysed allylic amination.

Complex **71** Ru(TPP)(NAr)<sub>2</sub> (Ar=3,5-bis(trifluoromethyl)phenyl), obtained by reaction between Ru(TPP)CO and 3,5-bis(trifluoromethyl)phenyl azide, was isolated and fully characterised, also by X-ray analysis, and was the first reported ruthenium *bis*-imido complex catalytically active in nitrene transfer reactions.<sup>9</sup>

As previously reported, Manca, Gallo *et al* also performed DFT calculations. The results support the hypothesis of the two catalytic cycles and reveal that they occur via a radical pathway.<sup>10</sup> In order to simplify the calculations, the ruthenium porphine complex is used as the catalyst and MeN<sub>3</sub> is used instead of ArN<sub>3</sub> (Figure 31). The first step is the coordination of the azide to the ruthenium porphyrine giving the complex (Ru)(porphine)(MeN<sub>3</sub>)(CO). Then, the complex releases a nitrogen molecule forming the intermediate **A**, thanks to the folding of the N<sub>α</sub>-N<sub>β</sub>-N<sub>γ</sub> bonds from a linear angle to 136° and a decrease of the distance between N<sub>β</sub>-N<sub>γ</sub>. Intermediate **A** is obtained as a singlet species, and this undergoes a singlet→triplet interconversion acquiring a diradical character. At this point two possibilities can occur: i) the *mono*-imido complex **A<sub>T</sub>** reacts with the cyclohexene or ii) complex **A<sub>T</sub>** loses the CO ligand forming the *bis*-imido complex, which also undergoes a singlet→triplet interconversion forming **B<sub>T</sub>**. In any case, when the reactive species, *mono*- or *bis*-

imido, is formed, the activation of the allylic C-H bond of cyclohexene occurs by abstraction of the allylic hydrogen through a C-H••N adduct, detected as a transition state.

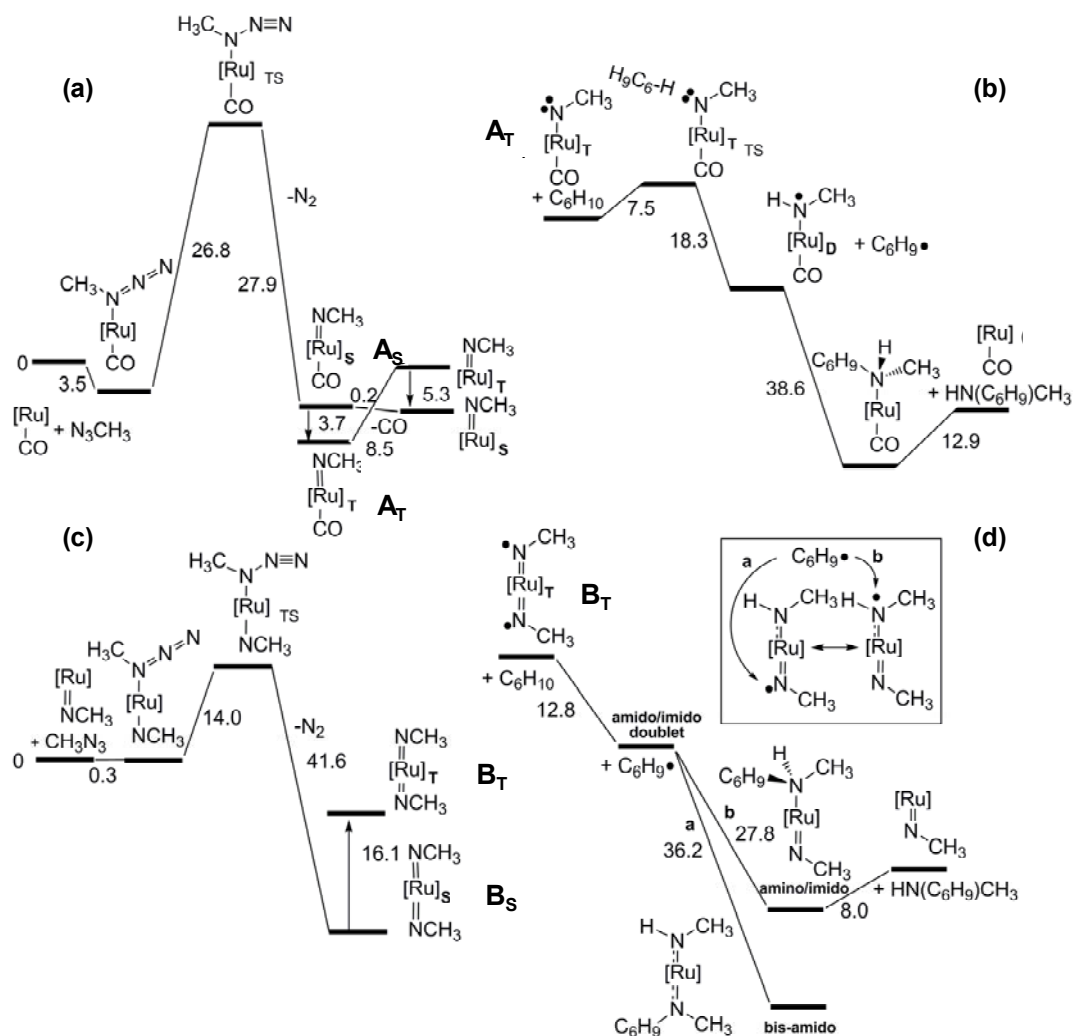


**Figure 31.** Calculated pathway for the ‘mono-imido based catalytic cycle’ (a and b) and ‘bis-imido based catalytic cycle’ (c and d).

The formation of amine occurs by a ‘rebound’ mechanism in which the nitrogen and carbon radicals couple together. Then, the release of the product restores the initial catalyst. DFT analysis disclosed that both the interconnected cycles have similarly high exergonic balances, while the radical nature of the reaction was experimentally proven by observing the reaction rate decrease when the amination was performed in presence of radical traps such as TEMPO ((2,2,6,6-tetramethylpiperidin-1-yl)oxyl).

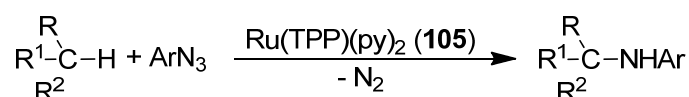


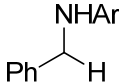
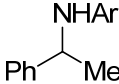
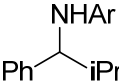
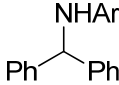
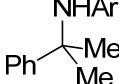
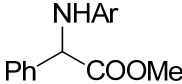
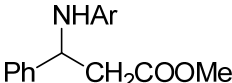
## 2. Discussion

One of the most extensively used amination catalyst is the five-coordinate complex Ru(TPP)(CO) which presents the  $\pi$ -acceptor CO ligand in one axial position, and a vacant coordination site on the other axial position for the azide activation. As reported in the previous chapter, the proposed mechanism of Ru(TPP)CO-catalysed allylic amination involves the formation of two different active species: *mono*-imido complex **A**, Ru(porphine)(CO)(NAr) (Scheme 59, Chap. 1.2.1) and *bis*-imido complex **B**, Ru(porphine)(NAr)<sub>2</sub> (Scheme 59, Chap. 1.2.1).<sup>7</sup> Both CO and NR ligands, placed *trans* to the vacant coordination site where the azide is activated, combine  $\pi$ -acceptor and  $\sigma$ -donor abilities. To analyse the catalytic influence of the axial ligand electronic features we decided to investigate the catalytic behaviour of Ru(TPP)(py)<sub>2</sub> (py=pyridine), **105**, both from an experimental and theoretical (DFT study) point of view.

Ru(TPP)(py)<sub>2</sub> results a good catalyst in the amination of benzylic and allylic C-H bonds using an electron-deficient azide such as 3,5-*bis*(trifluoromethyl)phenyl azide (table 5). All products were obtained in good yields (up to 85%) and short reaction times. Moreover, complex **105** catalysed the reaction between 3,5-*bis*(trifluoromethyl)phenyl azide and methyl hydrocinnamate to synthesise the biological active  $\beta$ -amino ester **113**. Product **113**, 3-[3,5-*bis*(trifluoromethyl)phenylamino]-3-phenylpropanoate, was obtained in good yield (82%) (table 5, entry 7).

**Table 5.** Synthesis of amines catalyzed by Ru(TPP)(py)<sub>2</sub> (**105**).<sup>a</sup>

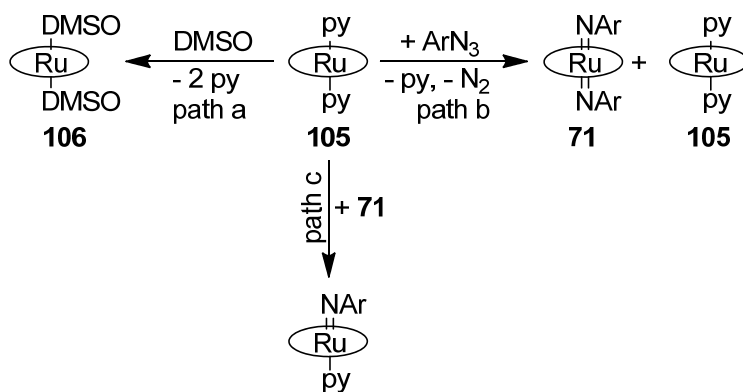


Entry	Product	Ar	t (h) <sup>b</sup>	yield (%) <sup>c</sup>
1		3,5-(CF <sub>3</sub> ) <sub>2</sub> C <sub>6</sub> H <sub>3</sub>	0.5 (1) <sup>d</sup>	<b>106</b> , 62 (66) <sup>d</sup>
2		3,5-(CF <sub>3</sub> ) <sub>2</sub> C <sub>6</sub> H <sub>3</sub> 4- <i>t</i> BuC <sub>6</sub> H <sub>4</sub>	0.6 (4) <sup>d</sup> 0.5	<b>107</b> , 85 (85) <sup>d</sup> <b>108</b> , 3
3		3,5-(CF <sub>3</sub> ) <sub>2</sub> C <sub>6</sub> H <sub>3</sub>	0.5 (1) <sup>d</sup>	<b>109</b> , 50 (75) <sup>d</sup>
4 <sup>e</sup>		3,5-(CF <sub>3</sub> ) <sub>2</sub> C <sub>6</sub> H <sub>3</sub>	0.3 (0.4) <sup>d</sup>	<b>110</b> , 65 (65) <sup>d</sup>
5		3,5-(CF <sub>3</sub> ) <sub>2</sub> C <sub>6</sub> H <sub>3</sub>	0.25 (1.15) <sup>d</sup>	<b>111</b> , 61 (90) <sup>d</sup>
6 <sup>f</sup>		3,5-(CF <sub>3</sub> ) <sub>2</sub> C <sub>6</sub> H <sub>3</sub>	12 (6) <sup>g</sup>	<b>112</b> , 56 (60) <sup>g</sup>
7 <sup>f</sup>		3,5-(CF <sub>3</sub> ) <sub>2</sub> C <sub>6</sub> H <sub>3</sub>	8 (10) <sup>g</sup> 1.3	<b>113</b> , 55 (77) <sup>g</sup> 82

<sup>a</sup>Reaction conditions:  $6.8 \cdot 10^{-3}$  mmol of the catalyst (2% with respect to ArN<sub>3</sub>) in 15.0 mL of refluxing hydrocarbon substrate as the reaction solvent. <sup>b</sup>Time required for complete azide conversion, determined by IR spectroscopic monitoring of the decrease in N<sub>3</sub> absorbance at about 2115 cm<sup>-1</sup>. <sup>c</sup>Yields based on ArN<sub>3</sub> and determined by <sup>1</sup>H NMR spectroscopy (2,4-dinitrotoluene as the internal standard). <sup>d</sup>Reaction catalysed by Ru(TPP)CO. <sup>e</sup>Reaction run at 150 °C. <sup>f</sup>Reaction run at 80 °C. <sup>g</sup>Reaction catalysed by Ru(TPP)CO. <sup>h</sup>6% of **105** was used.

As reported in table 5, the catalytic efficiency of Ru(TPP)(py)<sub>2</sub> is comparable to that of Ru(TPP)CO. This result indicates the low dependence of the ruthenium(II) porphyrin complexes' catalytic activity on the axial ligands nature and this is somewhat surprising, because, differently from Ru(TPP)CO, **105** needs first to vacate one coordination site for azide activation.

To obtain more experimental information on the strength of the Ru-py bond in Ru(TPP)(py)<sub>2</sub>, we also studied the substitution of pyridine by dimethyl sulfoxide (DMSO) by treating Ru(TPP)(py)<sub>2</sub> with a DMSO excess. The quantitative formation of Ru(TPP)(DMSO)<sub>2</sub> reveals that the two pyridine ligands are not irreversibly coordinated to the metal centre and they can be easily displaced by another 2e<sup>-</sup> donor ligand (Scheme 60, path a). In view of this result, we treated **105** with an equimolar amount of ArN<sub>3</sub> to substitute pyridine by an azide ligand to give the *mono*-imido complex Ru(TPP)(py)(NAr). Unfortunately, we did not observe the coordination of one imido ligand to the metal centre, in fact the NMR analysis of the crude reaction product revealed the presence of an equimolar mixture of **105** and *bis*-imido complex **71** (Scheme 60, path b). This suggests that even if the *mono*-imido complex is momentarily formed, it is too elusive to be experimentally detected and quickly forms the thermodynamically stable product **71**. Moreover, we tried to detect the formation of the key intermediate Ru(TPP)(py)(NAr) in the reaction of equimolar amounts of **105** and **71** (Scheme 60, path c). Unfortunately, the desired nitrene-transfer reaction from **71** to **105** did not occur, and the formation of the elusive *mono*-imido intermediate was not observed.

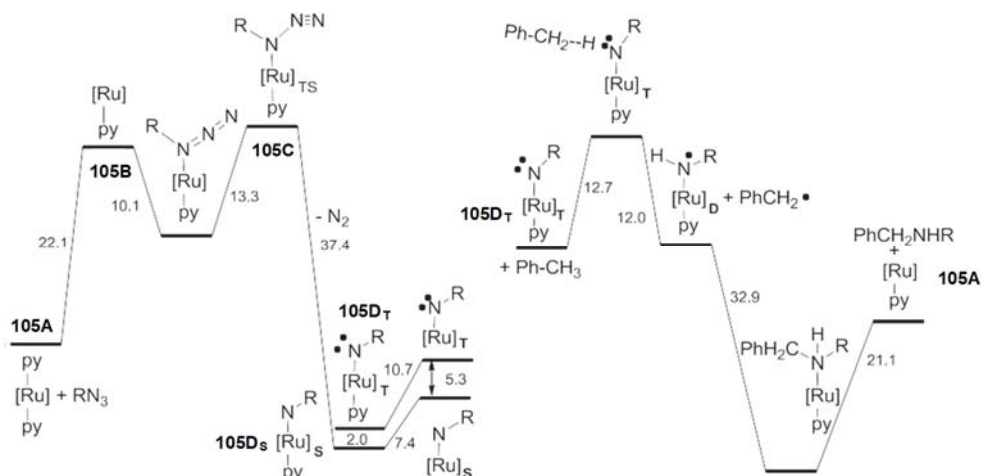


**Scheme 60.** The reactivity of complex **105**.

Experimental results were supported by DFT analyses which were elaborated by Dr. G. Manca and Dr. C. Mealli of ICCOM-CNR, Florence. DFT analyses contributed to rationalise some key aspects of the catalytic mechanism, also through the elaboration of a previously developed cyclohexene Ru(TPP)CO-catalysed allylic amination model. DFT calculations were performed by using Ru(porphine)(py)<sub>2</sub>, **105A**, which has to be considered a pre-catalyst. Complex **105A**, by losing one pyridine ligand, yields the unsaturated species Ru(porphine)(py) (**105B**) able to coordinate another aryl azide molecule forming the Ru(porphine)(N<sub>3</sub>Ar)(py) complex (Scheme 61, intermediate **105C**). The Ru(porphine)(N<sub>3</sub>Ar)(py) complex has a higher stabilisation energy than the corresponding carbonylated complex Ru(porphine)(CO)(N<sub>3</sub>Ar): -10.1 versus -3.5 kcalmol<sup>-1</sup>. The better stabilisation of complex **105C** is reflected in the shorter Ru-N<sub>azide</sub> coordination bond compared to that in Ru(porphine)(CO)(N<sub>3</sub>Ar) (2.17 vs. 2.31 Å) due to the stronger CO trans influence. At this point, diatomic N<sub>2</sub> is released by the formation of *mono*-imido complex **105D** which is initially formed as a singlet. Then its transformation into the diradical triplet species provokes the radical homolytic activation of one benzylic C-H bond, with the consequent formation of the desired benzylic amine. Concerning the overall free-energy balance of the process, the benzylic amination described, catalysed by the Ru(porphine)(py)<sub>2</sub> complex, is more exergonic than that promoted by the corresponding Ru(porphine)(CO) catalyst (-43.3 vs. -37.2

kcalmol<sup>-1</sup>, respectively). However, when Ru(porphine)(CO) is directly available for azide activation, Ru(porphine)(py) needs to be generated first from the bis-pyridine precursor **105A**, which has a high energy cost of +22.1 kcalmol<sup>-1</sup>. Alternatively, the mono-imido complex **105D** may lose the apical pyridine ligand leaving a vacant coordination site to another azide molecule to form a bis-imido complex Ru(TPP)(NAr)<sub>2</sub>. This complex undergoes a singlet→triplet interconversion and then the radical activation of the benzylic substrate occurs forming the benzylic amine through the known rebound mechanism.

These theoretical results reveal that the Ru(porphyrin)(L)-catalysed amination mechanism is independent from the ruthenium porphyrin's axial ligand nature, along with confirming the catalytic results.



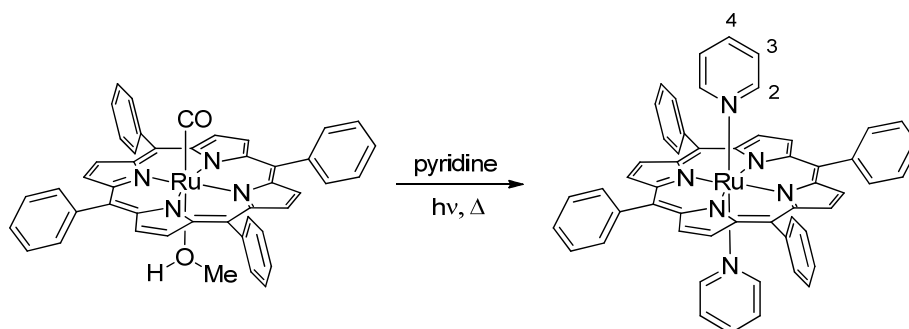
**Scheme 61.** Energy profile of the Ru(TPP)(py)<sub>2</sub> (**105**)-catalysed benzylic amination.

## 3. Experimental Section

**General conditions:** Unless otherwise specified, all reactions were carried out under nitrogen or argon atmosphere employing standard Schlenk techniques and magnetic stirring. Dichloromethane, benzene, cumene, toluene and pyridine were purified by using standard methods and stored under nitrogen atmosphere. All other starting materials were commercial products used as received. NMR spectra were recorded at room temperature on a Bruker Avance 300-DRX, operating at 300 MHz for  $^1\text{H}$ , at 75 MHz for  $^{13}\text{C}$  and 282 MHz for  $^{19}\text{F}$ , or on a Bruker Avance 400-DRX spectrometer, operating at 400 MHz for  $^1\text{H}$ , at 100 MHz for  $^{13}\text{C}$  and at 376 MHz for  $^{19}\text{F}$ . Chemical shifts (ppm) are reported relative to TMS. The  $^1\text{H}$  NMR signals of the compounds described in the following were identified by 2 D NMR techniques. Assignments of the resonance in  $^{13}\text{C}$  NMR were made using the APT pulse sequence and HSQC and HMBC techniques. GC-MS analyses were performed on Shimadzu QP5050A instrument. Infrared spectra were recorded on a Varian Scimitar FTS 1000 spectrophotometer. UV/Vis spectra were recorded on an Agilent 8453E instrument. Elemental analyses and mass spectra were recorded in the analytical laboratories of Milan.

### 3.1. Synthesis of ruthenium porphyrin complexes

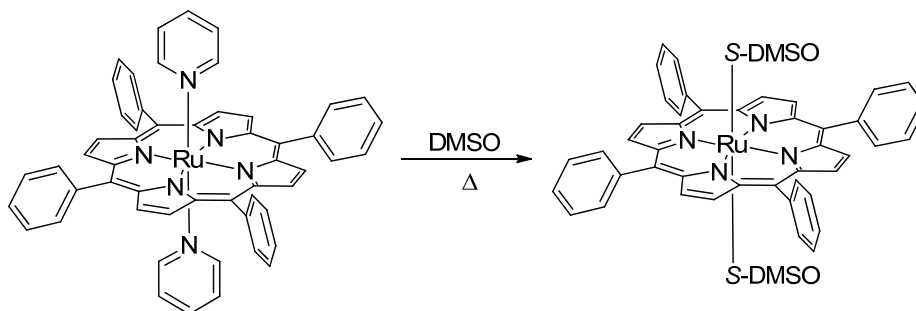
#### 3.1.1. Synthesis of Ru(TPP)(py) $_2$ (105)



Ru(TPP)(CO)(MeOH) (0.100 g,  $1.29 \cdot 10^{-4}$  mol) was dissolved in 25.0 mL of freshly distilled pyridine. The sample was refluxed for 1 hour and then irradiated by a low-pressure Hg lamp for 72 hours. The pyridine was removed under reduced pressure and the brownish, purple solid was redissolved in a mixture of  $\text{CH}_2\text{Cl}_2/\text{MeOH}$  1:1. Dichloromethane was removed under reduced pressure and the precipitate, formed in the remaining methanol, was filtered and washed with hexane (0.187 g, 50%).

$^1\text{H}$  NMR (300 MHz,  $\text{CDCl}_3$ ):  $\delta$  7.95 (s, 8H,  $\text{H}_\beta$ ), 7.67-7.58 (m, 20H,  $\text{H}_{\text{Ar}}$ ), 5.92 (t, 2H,  $J=6.2$  Hz,  $\text{H}^4$ ), 5.33 (t, 4H,  $J=6.4$  Hz,  $\text{H}^3$ ), 2.37 ppm (d, 4H,  $J=5.2$  Hz,  $\text{H}^2$ ).

### 3.1.2. Synthesis of Ru(TPP)(S-DMSO)<sub>2</sub>



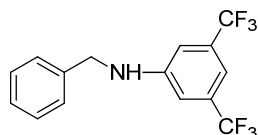
Ru(TPP)(py)<sub>2</sub> complex (13.7 mg,  $1.54 \cdot 10^{-5}$  mol) was suspended in 2.00 mL of DMSO and the resulting solution was heated at 110°C for 4 hours. The solution was evaporated to dryness and the crystalline violet solid was dried *in vacuo* (0.134 g, 99%).

<sup>1</sup>H NMR (300 MHz, CDCl<sub>3</sub>):  $\delta$  8.59 (s, 8H, H <sub>$\beta$</sub> ), 8.13 (m, 8H, H<sub>o</sub>), 7.78-7.74 (m, 12H, H<sub>m</sub> and H<sub>p</sub>), -1.64 ppm (s, 12H, H<sub>CH<sub>3</sub></sub>).

## 3.2. Amination reaction catalysed by Ru(TPP)(py)<sub>2</sub>

**General catalytic procedure:** In a typical run, the aryl azide ( $3.40 \cdot 10^{-4}$  mol) and Ru(TPP)(py)<sub>2</sub> (**105**) (6.00 mg,  $6.80 \cdot 10^{-6}$  mol) were dissolved in the hydrocarbon (15.0 mL). The resulting mixture was heated until complete consumption of the azide. The catalytic reaction was monitored by IR spectroscopy by measuring the characteristic N<sub>3</sub> absorbance at  $\approx 2100$  cm<sup>-1</sup>. The reaction was considered finished when the absorbance value of the azide was less than 0.01 (by using a 0.1 mm-thick cell). The solvent was evaporated to dryness and the residue analysed by <sup>1</sup>H NMR analysis with 2,4-dinitrotoluene as the internal standard.

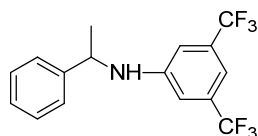
### 3.2.1. *N*-benzyl-3,5-bis(trifluoromethyl)benzenamine (**106**)



Compound **106** was obtained from toluene and 3,5-bis(trifluoromethyl)phenyl azide. The collected data are in accord with those reported in literature.<sup>11</sup>

<sup>1</sup>H NMR (300 MHz, CDCl<sub>3</sub>):  $\delta$  7.43-7.31 (m, 5H, H<sub>Ar</sub>), 7.19 (s, 1H, H<sub>Ar</sub>), 6.99 (s, 2H, H<sub>Ar</sub>), 4.56 (br, 1H, H<sub>NH</sub>), 4.39 ppm (s, 1H, H<sub>CH<sub>2</sub></sub>). <sup>19</sup>F NMR (282 MHz, CDCl<sub>3</sub>):  $\delta$  -63.53 ppm (6F, CF<sub>3</sub>).

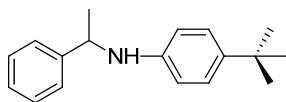
### 3.2.2. *N*-(1-phenylethyl)-3,5-bis(trifluoromethyl)benzenamine (**107**)



Compound **107** was obtained from ethylbenzene and 3,5-bis(trifluoromethyl)phenyl azide. The collected data are in accord with those reported in literature.<sup>3</sup>

<sup>1</sup>H NMR (300 MHz, CDCl<sub>3</sub>):  $\delta$  7.39-7.16 (m, 5H, H<sub>Ar</sub>), 7.09 (s, 1H, H<sub>Ar</sub>), 6.87 (s, 2H, H<sub>Ar</sub>), 4.53 (m, 2H, H<sub>NH</sub> and H<sub>CH</sub>), 1.59 ppm (d, 3H,  $J=5.9$  Hz, H<sub>CH<sub>3</sub></sub>).

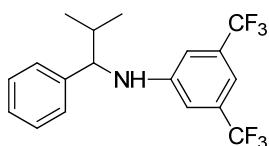
### 3.2.3. *N*-(1-phenylethyl)-4-*t*butylbenzenamine (108)



Compound **108** was obtained from ethylbenzene and 4-*t*butylphenyl azide. The collected data are in accord with those reported in literature.<sup>12</sup>

<sup>1</sup>H NMR (400 MHz, CDCl<sub>3</sub>): δ 7.24-7.21 (m, 2H, H<sub>Ar</sub>), 7.17-7.14 (m, 2H, H<sub>Ar</sub>), 7.08-7.04 (m, 1H, H<sub>Ar</sub>), 6.98-6.94 (m, 2H, H<sub>Ar</sub>), 6.33-6.29 (m, 2H, H<sub>Ar</sub>), 4.28 (q, 1H, *J*=6.8 Hz, H<sub>CH</sub>), 3.76 (br, 1H, *H*NH), 1.33 (d, 3H, *J*=6.7 Hz, H<sub>CH<sub>3</sub></sub>), 1.07 ppm (s, 9H, H<sub>CH<sub>3</sub></sub>).

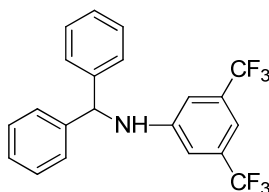
### 3.2.4. *N*-(2-methyl-1-phenylpropyl)-3,5-bis(trifluoromethyl)benzenamine (109)



Compound **109** was obtained from isobutylbenzene and 3,5-*bis*(trifluoromethyl)phenyl azide. The collected data are in accord with those reported in literature.<sup>9</sup>

<sup>1</sup>H NMR (300 MHz, CDCl<sub>3</sub>): δ 7.35-7.27 (m, 5H, H<sub>Ar</sub>), 7.08 (s, 1H, H<sub>Ar</sub>), 6.88 (s, 2H, H<sub>Ar</sub>), 4.58 (d, 1H, *J*=5.7 Hz, *H*NH), 4.15 (pst, 1H, *J*=6.3 Hz, *H*NH), 2.12-2.05 (m, 1H, H<sub>CH</sub>), 1.06 (d, 3H, *J*=6.9 Hz, H<sub>CH<sub>3</sub></sub>), 0.94 ppm (d, 3H, *J*=6.9 Hz, H<sub>CH<sub>3</sub></sub>).

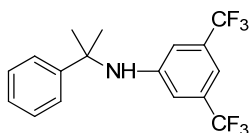
### 3.2.5. *N*-benzhydryl-3,5-bis(trifluoromethyl)benzenamine (110)



Compound **110** was obtained from diphenylmethane and 3,5-*bis*(trifluoromethyl)phenyl azide. The collected data are in accord with those reported in literature.<sup>9</sup>

<sup>1</sup>H NMR (300 MHz, CDCl<sub>3</sub>): δ 7.37-7.31 (m, 6H, H<sub>Ar</sub>), 7.26-7.22 (m, 4H, H<sub>Ar</sub>), 7.19 (s, 1H, H<sub>Ar</sub>), 6.93 (s, 2H, H<sub>Ar</sub>), 5.60 (m, 1H, H<sub>CH</sub>), 4.72 ppm (br, 1H, *H*NH).

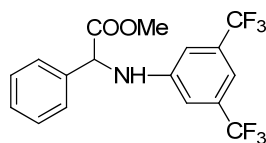
### 3.2.6. *N*-(2-phenylpropan-2-yl)-3,5-bis(trifluoromethyl)benzenamine (111)



Compound **111** was obtained from cumene and 3,5-*bis*(trifluoromethyl)phenyl azide. The collected data are in accord with those reported in literature.<sup>9</sup>

<sup>1</sup>H NMR (400 MHz, CDCl<sub>3</sub>): δ 7.48 (d, 2H, *J*=7.3 Hz, H<sub>Ar</sub>), 7.38 (pst, 2H, *J*=7.3 Hz, H<sub>Ar</sub>), 7.29 (t, 1H, *J*=7.3 Hz, H<sub>Ar</sub>), 7.06 (s, 1H, H<sub>Ar</sub>), 6.68 (s, 2H, H<sub>Ar</sub>), 4.56 (br, 1H, *H*NH), 1.71 ppm (6H, s, H<sub>CH<sub>3</sub></sub>).

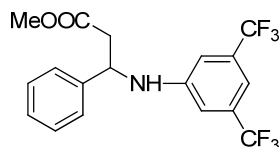
### 3.2.7. Methyl (3,5-bis(trifluoromethyl)phenylamino)phenylacetate (112)



Compound **112** was obtained from methyl phenylacetate and 3,5-bis(trifluoromethyl)phenyl azide. The collected data are in accord with those reported in literature.<sup>6</sup>

<sup>1</sup>H NMR (300 MHz, CDCl<sub>3</sub>): δ 7.48-7.34 (m, 5H, H<sub>Ar</sub>), 7.15 (s, 1H, H<sub>Ar</sub>), 6.90 (s, 2H, H<sub>Ar</sub>), 5.48 (br, 1H, H<sub>NH</sub>), 5.09 (s, 1H, H<sub>CH</sub>), 3.76 ppm (s, 3H, H<sub>OCH<sub>3</sub></sub>).

### 3.2.8. Methyl (3,5-bis(trifluoromethyl)phenylamino)-3-phenylpropanoate (113)



Compound **113** was obtained from methyl methyl dihydrocinnamate and 3,5-bis(trifluoromethyl)phenyl azide. The collected data are in accord with those reported in literature.<sup>6</sup>

<sup>1</sup>H NMR (300 MHz, CDCl<sub>3</sub>): δ 7.38-7.27 (m, 5H, H<sub>Ar</sub>), 7.12 (s, 1H, H<sub>Ar</sub>), 6.90 (s, 2H, H<sub>Ar</sub>), 5.17 (br, 1H, H<sub>NH</sub>), 4.85 (dd, 1H, *J*=7.7, 5.3 Hz, H<sub>CH</sub>), 3.67 (s, 3H, H<sub>OCH<sub>3</sub></sub>), 2.90 (dd, 1H, <sup>2</sup>*J*=15.2 Hz, *J*=5.2 Hz, H<sub>CH<sub>2</sub>A</sub>), 2.82 (dd, 1H, <sup>2</sup>*J*=15.2 Hz, *J*=7.8 Hz, H<sub>CH<sub>2</sub>B</sub>).

## 4. References

1. Y. Liu, C. M. Che. *Chem. Eur. J.* **2010**, 16, 10494-10501.
2. Y. Liu, J. Wei, C. M. Che. *Chem. Commun.* **2010**, 46, 6926-6928.
3. G. Tseberlidis, P. Zardi, A. Caselli, D. Cancogni, M. Fusari, L. Lay, E. Gallo. *Organometallics* **2015**, 34, 3774-3781.
4. (a) J. A. McIntosh, P. S. Coelho, C. C. Farwell, Z. J. Wang, J. C. Lewis, T. R. Brown, F. H. Arnold. *Angew. Chem. Int. Ed.* **2013**, 52, 9309-9312. (b) M. Bordeaux, R. Singh, R. Fasan. *Bioorg. Med. Chem.* **2014**, 22, 5697-5704. (c) T. K. Hyster, C. C. Farwell, A. R. Buller, J. A. McIntosh, F. H. Arnold. *J. Am. Chem. Soc.* **2014**, 136, 15505-15508.
5. D. Intriери, M. Mariani, A. Caselli, F. Ragaini, E. Gallo. *Chem. Eur. J.* **2012**, 18, 10487-10490.
6. P. Zardi, A. Caselli, P. Macchi, F. Ferretti, E. Gallo. *Organometallics* **2014**, 33, 2210-2218.
7. D. Intriери, A. Caselli, F. Ragaini, P. Macchi, N. Casati, E. Gallo. *Eur. J. Inorg. Chem.* **2012**, 2012, 569-580.
8. K. H. Chan, X. Guan, V. K. Y. Lo, C. M. Che. *Angew. Chem. Int. Ed.* **2014**, 53, 2982-2987.
9. S. Fantauzzi, E. Gallo, A. Caselli, F. Ragaini, N. Casati, P. Macchi, S. Cenini. *Chem. Commun.* **2009**, 3952-3954.
10. G. Manca, E. Gallo, D. Intriери, C. Mealli. *ACS Catal.* **2014**, 4, 823-832.
11. D. Intriери, A. Caselli, F. Ragaini, S. Cenini, E. Gallo. *J. Porphyrins Phthalocyanines* **2010**, 14, 732-740.
12. S. Zhou, S. Fleischer, H. Jiao, K. Junge, M. Beller. *Adv. Synt. Catal.* **2014**, 356 (16), 3451-3455.



# Summary

**Chapter I** gives an overview on the synthesis of porphyrins and metal porphyrin complexes. Porphyrins, thanks to the highly stable macrocycle ring and the rigid structure, are a unique class of ligands. They are able to coordinate the majority of elements in the periodic table. Moreover, chapter I describes the catalytic activity of metal porphyrin complexes in Nature where the most important metal porphyrin complex is the iron complex of protoporphyrin IX, known as Heme. Heme and its derivatives play a vital role for many crucial biological processes because they are the prosthetic group in a wide range of active proteins. Among heme-containing enzymes, the cytochromes P450 occupy a prominent role and are present in many monooxygenase. This class of enzymes catalyses a series of oxidative reactions by the insertion of an activated oxygen atom; in particular, they promote the oxidation of nonactivated hydrocarbons at physiological temperature. Inspired by the outstanding catalytic activity of heme-containing enzymes, many efforts have been made to synthesise metal porphyrin complexes as artificial counterparts of these biological systems. Thanks to the relationship to the iron atom (same periodic group and electronic structure in the outer shell), ruthenium porphyrins have shown high activity in the oxygen activation and they are able to oxidize many compounds such as amines, thioethers, phosphines etc.

Moreover, iron and ruthenium porphyrins have been studied in other atom/group transfer reactions, such as carbene and nitrene transfer reactions, in which they show a unique catalytic activity producing important compounds such as cyclopropanes, amines, aziridines and indoles in good yield and stereoselectivity.

**Chapter II** describes our efforts to synthesis new chiral iron(III) porphyrin complexes to promote cyclopropanation reactions. In 2014, Gallo and co-authors reported the synthesis and full characterisation of new  $C_2$ -symmetrical binap-*bis*-strapped porphyrin **17** and its iron(III) complex **Fe(17)OMe**.

**Fe(17)OMe** catalysed the cyclopropanation of several aromatic alkenes by diazoacetates and desired products were obtained in good yields, excellent *trans*-diastereo- and enantioselectivities, except when very sterically hindered reagents were employed. For this reason, we decided to study the steric effect of the chiral group on the catalytic activity of complex **Fe(17)OMe** by synthesising the iron(III) complex **Fe(18)OMe** in which ligand **17** was replaced by the less sterically encumbered ligand **18** (precursor of **17**). Complex **Fe(18)OMe** results a good catalyst also when very hindered diazocompounds were employed giving cyclopropanes in good yields and good *trans*-diastereoselectivities.

Data collected up to now on the catalytic activity of complexes **Fe(18)OMe** and **Fe(17)OMe**, have suggested that porphyrin **17** shows a ‘Totem’ structure which is formed by three different and independent elements (Figure 1). The first element is the tetrapyrrolic core where the metal centre is placed and it is responsible for the EDA activation, the second element is constituted by the benzoyl group which is responsible for the diastereoselectivity, and the last element is formed by the chiral ‘hat’ which is responsible for the enantioselectivity. These three independent elements can be replaced to obtain a library of ‘Totem porphyrin ligands’ showing different chemical features.

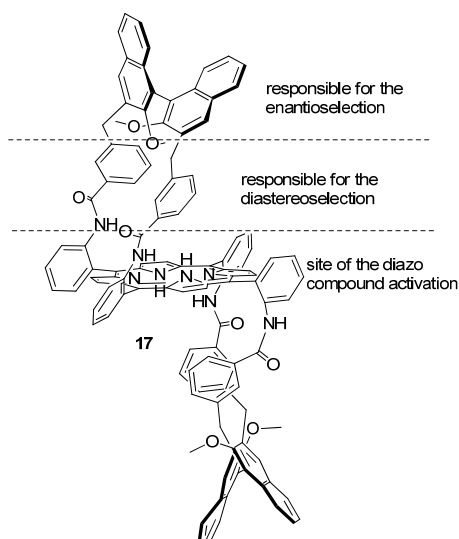
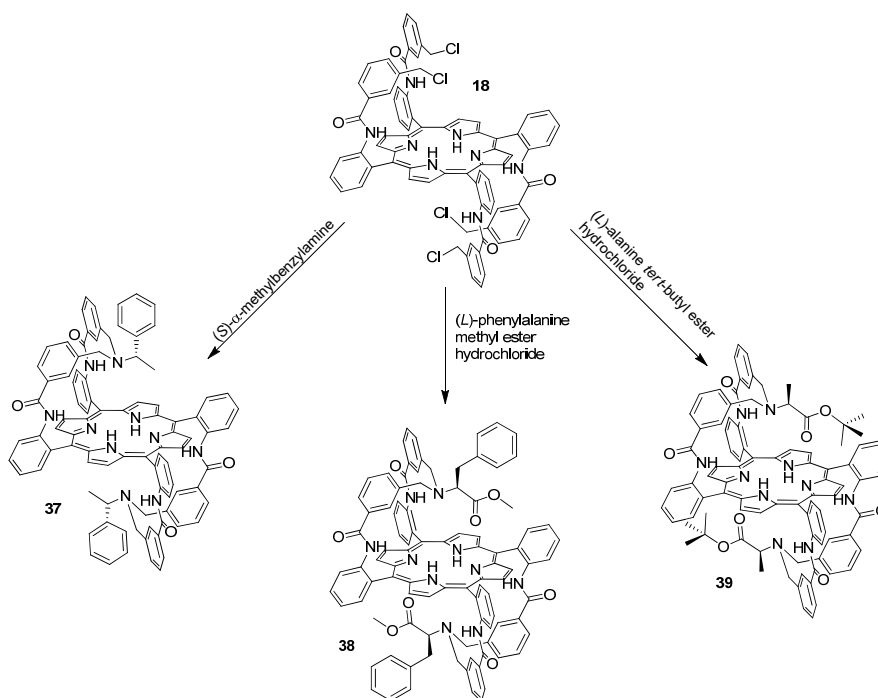


**Figure 1.** Totem structure of chiral porphyrin **17**.

Furthermore, in collaboration with Dr. B. Boitrel (Université de Rennes 1, France), we synthesised new porphyrin ligands by replacing the chiral binaphthyl group of porphyrin **17** with more biocompatible groups such as glycoside groups or amino acids. Therefore, we synthesised three new chiral porphyrins: porphyrin **37** with a (*S*)-methyl benzyl amino group, porphyrin **38** with (*L*)-phenylalanine methyl ester group and porphyrin **39** with (*L*)-alanine tert-butyl ester group (Scheme 1). All porphyrins were fully characterised including the X-ray analysis of **38**. In addition, we synthesised a glycoporphyrin ligand **40** by using  $\alpha$ -trehalose, which was synthesised by prof. L. Lay's group (Università degli Studi di Milano, Italy), as the chiral glycoside 'hat' of the Totem structure. The reaction of **37**, **38**, **39** and **40** with  $\text{FeBr}_2$  afforded respectively **Fe(37)OMe**, **Fe(38)OMe**, **Fe(39)OMe** and **Fe(40)OMe** in a quantitative yield. All iron complexes were tested in cyclopropanation reactions and even if short reaction times, good yields and trans-diastereoselectivities were achieved, very low enantioselectivities were observed.



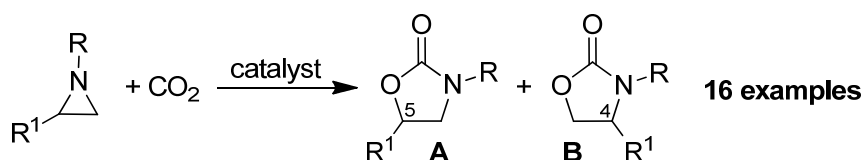
**Scheme 1.** Synthesis of porphyrin **37**, **38** and **39**.

DFT study suggested that the lack of the enantiocontrol was probably due to the long distance between the chiral bulk and the active metal centre, thus we decided to synthesise a new class of ‘Totem’ porphyrins which show a three-dimensional conformation similar to those observed for other porphyrin ligands, but with a chiral moiety closer to the porphyrin core to better discriminate an enantio-pathway. First, we synthesised porphyrin **44** and its iron(III) complex **Fe(44)OMe** which promoted the synthesis of ethyl-2-methyl-2-phenylcyclopropanecarboxylate in a very short time, good yield and *trans*-diastereoselectivity but low enantioselectivity. Therefore, to increase the catalyst’s enantiocontrol, we decided to functionalise the pickets with a naphthyl group and the new *bis*-strapped porphyrin **48** was synthesised by using  $\alpha_2\beta_2$ -tetra[(2-acetoxy-2-phenyl)acetamide] phenyl] porphyrin **45** as started material.

Finally, we decided to synthesise a water soluble ‘Totem’ ligand by modifying the porphyrin scaffold of porphyrin **17**. Therefore, we synthesised the new porphyrin **52** which shows four hydroxy groups on the porphyrin scaffold. Unfortunately, porphyrin **52** was obtained in a very low yield due to the formation of porphyrin’s polymers in the last step of its synthesis.

**Chapter III** describes the synthesis and reactivity of aziridines. Ruthenium porphyrin complexes are extensively used to promote aziridination reactions by a nitrene transfer reaction from organic azides ( $\text{ArN}_3$ ) to alkenes. In order to develop a simple and safe synthesis of aziridines, we investigated in collaboration with Prof. M. Benaglia group the Ru(TPP)CO-catalysed aziridination of styrenes by aryl azides in mesoreactors under continuous flow conditions. The reactions were carried out in a two-syringe flow system, using a 500 mL PTFE microreactor where several aryl azides and alkenes were tested. Aziridines were obtained in good yields and selectivities and achieved results were comparable with those obtained in batch reactions, with the undeniable advantage of operating with smaller reaction volumes.

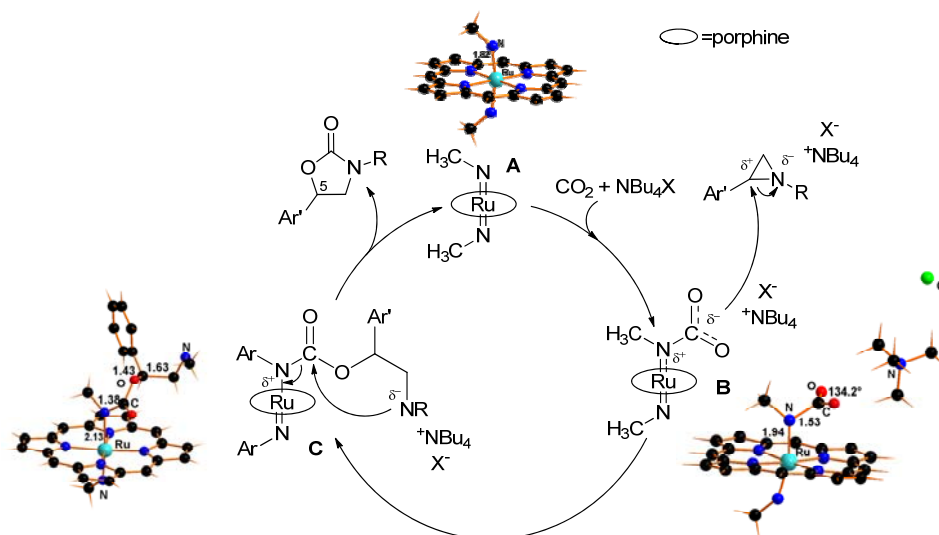
Then, we studied the reactivity of aziridines with carbon dioxide to obtain oxazolidinones. The coupling reaction between aziridines and carbon dioxide represents an attractive route to synthesis oxazolidinones due to the 100% atom efficiency and the use of the most abundant greenhouse gas (Scheme 2).



**Scheme 2.** Coupling reaction between aziridines and carbon dioxide.

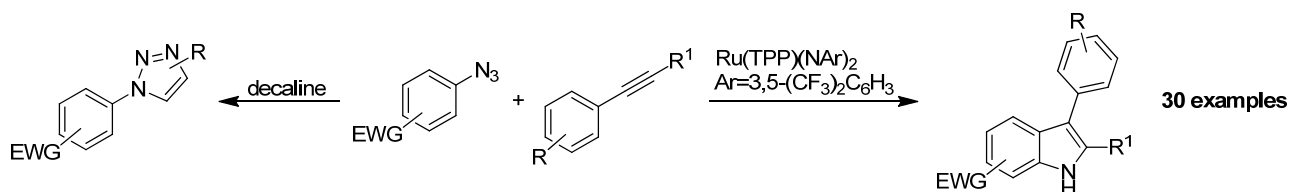
We started our work by studying the coupling reaction between 1-butyl-2-phenyl aziridine and carbon dioxide in presence of several catalysts and co-catalysts: Ru(TPP)(NAr)<sub>2</sub> (Ar=3,5-(CF<sub>3</sub>)<sub>2</sub>C<sub>6</sub>H<sub>3</sub>)/TBACl resulted the best catalytic system which was employed to optimise the experimental conditions. Then, we performed a screening of aziridines and a series of *N*-substituted-5-phenyl oxazolidinones was obtained with yields (up to 96%) and high regioselectivities (up to A/B=99:1).

In collaboration with Dr. G. Manca and Dr. C. Mealli, who performed DFT studies by using a simplified model of ruthenium *bis*-imido catalyst, we proposed the reaction mechanism which is reported in Scheme 3. The first step is the polarization of a molecule of carbon dioxide and the formation of intermediate **B** where carbon dioxide is bonded to the imido moiety of the catalyst. Then the intermediate **B** attacks the aziridine three-membered ring, in which bonds are polarized by the interaction with tetrabutyl ammonium salt, forming intermediate **C**. Intermediate **C** undergoes a cyclization to give the 5-oxazolidinone as a product and regenerates the catalytic species **A**.



**Scheme 3.** Proposed mechanism for ruthenium porphyrin-catalysed aziridines/ $\text{CO}_2$  coupling.

**Chapter IV** describes our efforts to synthesis indoles. In 2014 our research group reported the first synthetic strategy to obtain indoles by an intermolecular reaction between aryl azides and aryl alkynes using ruthenium *bis*-imido complex  $\text{Ru}(\text{TPP})(\text{NAr})_2$  ( $\text{Ar}=3,5\text{-(CF}_3)_2\text{C}_6\text{H}_3$ ) as the catalyst (Scheme 4). The catalytic reaction occurred in the presence of 2% of  $\text{Ru}(\text{TPP})(\text{NAr})_2$  and C3-functionalised indoles were obtained with yields up to 95% and with complete regioselectivity.

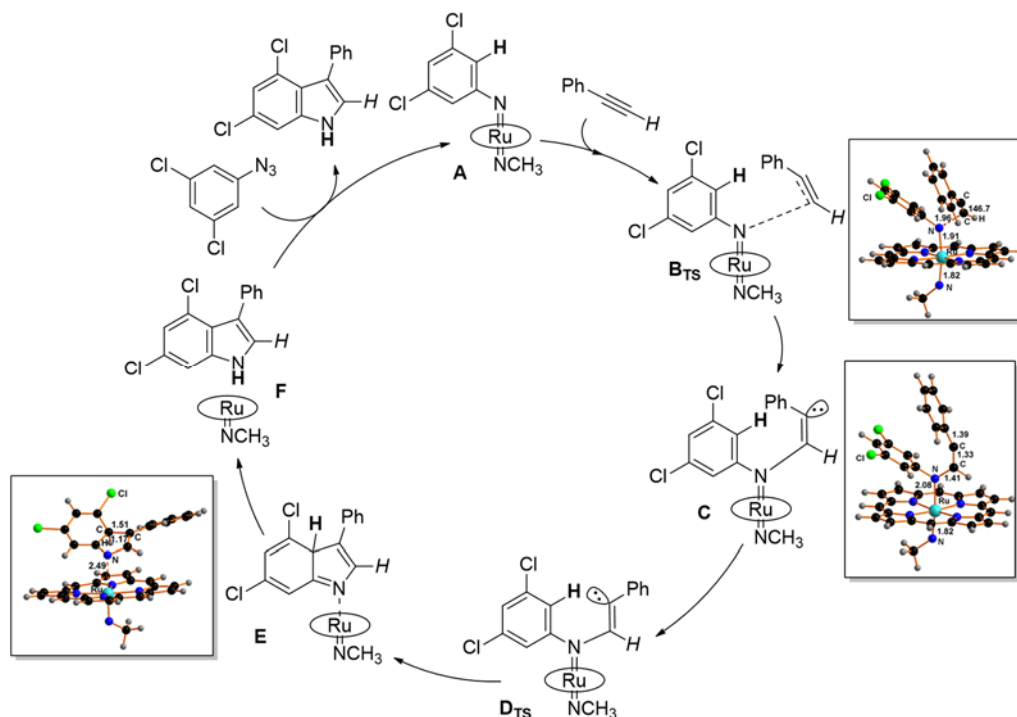


**Scheme 4.** Synthesis of indoles by intermolecular reaction between aryl azides and aryl alkynes.

To improve the generality of the reaction, other indoles were synthesised using 3,5-dinitrophenyl azide and several alkynes. The use of 3,5-dinitrophenyl azide allowed the simple recovery of 3-aryl-4,6-dinitroindoles by a simple filtration because they are insoluble in the reaction medium. Data showed a very good catalytic activity of ruthenium complexes and indoles were obtained in good yields by using both electron poor and electron rich alkynes (Figure 4).

Based on kinetic and DFT studies, we proposed the mechanism reported in Scheme 5. DFT calculations were performed by using a  $\text{Ru}(\text{porphine})(\text{NC}_6\text{H}_3\text{Cl}_2)(\text{NCH}_3)$ , **A**, as catalyst to speed up the calculations. The first step of the catalytic cycle is the approach of the phenylacetylene to the imido moiety of complex **A** forming the transition state **B<sub>TS</sub>**. Then, the transition state **B<sub>TS</sub>** forms the amido-imido species  $\text{Ru}(\text{porphine})(\text{N}(\text{C}_6\text{H}_3\text{Cl}_2)(\text{CH}=\text{CC}_6\text{H}_5))(\text{NCH}_3)$ , **C**, with the formation of the N-C bond (1.41 Å). Since intermediate **C** shows the lone pair on the distal carbon oriented far away from the imido-ligand aryl moiety, a rotation around the C-N bond is fundamental to orient the lone pair towards the aryl moiety, allowing the close-ring reaction and the formation of the indole. The energy cost associated to the rotation is very low and, as soon as the rotation happens, the formation of the C-C bond occurs between the distal carbon atom of the alkyne moiety and the one in *ortho* to the aryl's chloride atom (intermediate **D<sub>TS</sub>**, Scheme 5).

At this point, thanks to the ring closure reaction, the distance between the ruthenium atom and the nitrogen atom increases by promoting the rearrangement toward the indole and the dismissal of the product from the ruthenium complex.



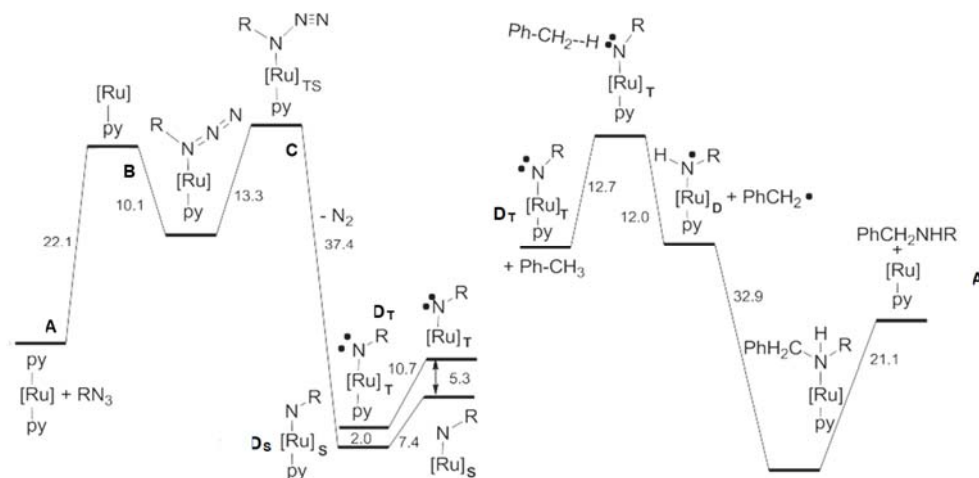
**Scheme 5.** Proposed mechanism for the synthesis of indoles.

**Chapter V** describes our efforts to study the influence of the axial ligand nature on the catalytic activity of ruthenium porphyrin complexes in amination reaction. Metal porphyrin complexes efficiently promote amination reactions of saturated and unsaturated hydrocarbons by aryl azides. One of the most extensively used amination catalyst is the five-coordinate complex  $\text{Ru}(\text{TPP})(\text{CO})$  which presents the  $\pi$ -acceptor CO ligand in one axial position, and a vacant coordination site on the other axial position for the azide activation. In order to study the catalytic influence of the axial ligand electronic features, we investigated the catalytic behaviour of  $\text{Ru}(\text{TPP})(\text{py})_2$  ( $\text{py}=\text{pyridine}$ ) complex, both from an experimental and theoretical (DFT study) point of view.  $\text{Ru}(\text{TPP})(\text{py})_2$  results a good catalyst of C-H aminations using an electron-deficient azide such as 3,5-bis(trifluoromethyl)phenyl azide. All products were obtained in good yields and short reaction times. The catalytic efficiency of  $\text{Ru}(\text{TPP})(\text{py})_2$  was comparable to that of  $\text{Ru}(\text{TPP})\text{CO}$  and this result indicates the low dependence of the catalytic activity of ruthenium(II) porphyrin complexes on the nature of axial ligands.

To obtain experimental information on the strength of the Ru–py bond in  $\text{Ru}(\text{TPP})(\text{py})_2$ , we also studied the substitution of pyridine by dimethyl sulfoxide (DMSO) by treating  $\text{Ru}(\text{TPP})(\text{py})_2$  with a DMSO excess. The quantitative formation of  $\text{Ru}(\text{TPP})(\text{DMSO})_2$  revealed that the two pyridine ligands are not irreversibly coordinated to the metal centre and they can be easily displaced by another  $2e^-$  donor ligand.

Experimental results were supported by DFT analyses which were elaborated by Dr. G. Manca and Dr. C. Mealli. DFT calculations were performed by using  $\text{Ru}(\text{porphine})(\text{py})_2$ , **A** (Scheme 6), which has to be considered a pre-catalyst. The overall free-energy balance of the process, the benzylic amination described, catalysed by the  $\text{Ru}(\text{porphine})(\text{py})_2$  complex, is more exergonic than that promoted by the corresponding  $\text{Ru}(\text{porphine})(\text{CO})$  catalyst (-43.3 vs. -37.2 kcalmol<sup>-1</sup>, respectively). However, when  $\text{Ru}(\text{porphine})(\text{CO})$  is directly available for azide activation,  $\text{Ru}(\text{porphine})(\text{py})$  needs to be generated first from the bis-pyridine

precursor **A**, which has a high energy cost of +22.1 kcalmol<sup>-1</sup>. These theoretical results reveal that the Ru(porphyrin)(L)-catalysed amination mechanism is independent from the ruthenium porphyrin's axial ligand nature, along with confirming the catalytic results.



**Scheme 6.** Energy profile of the Ru(TPP)(py)<sub>2</sub>-catalysed benzylic amination.

# List of publications

1. D. M. Carminati, D. Intrieri, G. Manca, C. Mealli and E. Gallo. 'Ruthenium porphyrin-catalysed CO<sub>2</sub>/aziridines coupling reaction'. Manuscript in preparation.
2. D. M. Carminati, D. Intrieri, P. Zardi, G. Manca, C. Mealli and E. Gallo. 'Indoles from Alkynes and Aryl Azides. Scope and Mechanism of the Ruthenium Porphyrin-Catalyzed Reaction'. Manuscript in preparation.
3. D. M. Carminati, D. Intrieri, S. Le Gac, T. Roisnel, B. Boitrel, L. Toma, L. Legnani and E. Gallo. 'Synthesis, Characterisation and Catalytic Use of Iron Porphyrin Amino Ester Conjugates'. *New J. Chem.* **2017**, 41, 5950-5959.
4. D. Intrieri, D. M. Carminati and E. Gallo. 'Iron-catalyzed Cyclopropanation of Alkenes by Carbene Transfer Reactions' in book 'Non-Noble Metal Catalysis: Molecular Approaches and Reactions', Wiley, in press.
5. P. Zardi, D. Intrieri, D. M. Carminati, F. Ferretti, P. Macchi and E. Gallo. 'Synthesis and Catalytic Activity of m-oxo Ruthenium (IV) Porphyrin Species to Promote Amination Reactions'. *J. Porphyrins Phthalocyanines* **2016**, 20, 1156-1165.
6. D. M. Carminati, D. Intrieri, A. Caselli, S. Le Gac, B. Boitrel, L. Toma, L. Legani and E. Gallo. 'Designing 'Totem' C<sub>2</sub>-Symmetrical Iron Porphyrin Catalysts for Stereoselective Cyclopropanations'. *Chem. Eur. J.* **2016**, 22, 13599-13612.
7. D. Intrieri, D. M. Carminati and E. Gallo. 'The ligand influence in stereoselective carbene transfer reactions promoted by chiral metal porphyrin catalysts'. *Dalton Transaction* **2016**, 45, 15746-15761. Cover.
8. D. Intrieri, D. M. Carminati and E. Gallo. 'Recent advanced in C-H bond aminations catalyzed by ruthenium porphyrin complexes'. *J. Porphyrins Phthalocyanines* **2016**, 20, 190-203.
9. S. Rossi, A. Puglisi, M. Benaglia, D. M. Carminati, D. Intrieri and E. Gallo. 'Synthesis in mesoreactors: 'Ru(porphyrin)CO-catalyzed aziridination of olefins under continuous flow conditions'. *Catal. Sci. Technol.* **2016**, 6, 4700-4704.
10. D. Intrieri, D. M. Carminati and E. Gallo, E. 'Recent Advances in Metal Porphyrinoid-Catalyzed Nitrene and Carbene Transfer Reactions' in Handbook of Porphyrin Science; eds. Kadish, K. M.; Smith, K. M.; Guillard, R.; World Scientific Publishing Co. Pte. Ltd.: Set 8, Volume 38.
11. G. Manca, C. Mealli, D. M. Carminati, D. Intrieri and E. Gallo. 'Comparative Study of the Catalytic Amination of Benzylic C-H Bonds Promoted by Ru(TPP)(py)<sub>2</sub> vs Ru(TPP)(CO)'. *Eur. J. Inorg. Chem* **2015**, 4885-4893.
12. P. Zardi, A. Savoldelli, D. M. Carminati, A. Caselli, F. Ragaini and E. Gallo. 'Indoles Rather than Triazoles from the Ruthenium Porphyrin-Catalysed Reaction of Alkynes with Aryl Azides'. *ACS catalysis* **2014**, 4, 3820-3823.